

Syntheses of Peptidic, Natural Product-inspired, and Heterocyclic Molecules as Biological Probes

by

Jared T. Hammill

BA, Franklin & Marshall College, 2007

Submitted to the Graduate Faculty of

The Kenneth P. Dietrich School of Arts and Sciences in partial fulfillment

of the requirements for the degree of

Doctor of Philosophy

University of Pittsburgh

2012

UNIVERSITY OF PITTSBURGH
THE KENNETH P. DIETRICH SCHOOL OF ARTS AND SCIENCES

This thesis was presented

by

Jared T. Hammill

It was defended on

November 19th, 2012

and approved by

Paul Floreancig, Professor, Department of Chemistry

Billy Day, Professor, Department of Chemistry

Donna Hurn, Professor, Department of Pharmaceutical Sciences

Thesis Director: Peter Wipf, Distinguished University Professor, Department of Chemistry

Copyright © by Jared Hammill

2012

Syntheses of Peptidic, Natural Product-inspired, and Heterocyclic Molecules as Biological Probes

Jared T. Hammill, PhD

University of Pittsburgh, 2012

The first section of this thesis describes the solid phase peptide synthesis of scotophobin, a small peptide thought to be responsible for the transference of a learned response between mammals, and several related peptides. The synthetic peptides were tested against an array of G protein-coupled receptors. Although interesting activity was observed, these studies failed to provide closure to the storied past of scotophobin. We were able to demonstrate that the small peptide possesses *in vitro* activity.

The second section describes the optimization of the thiol-mediated epoxide opening and intramolecular aldol reaction of epoxyketones. This methodology provided access to a variety of densely functionalized bicyclo[3.3.1]non-3-en-2-ones in moderate to good yield (64-88%). The newly synthesized bicyclo[3.3.1]non-3-en-2-ones were shown by a ChemGPS-NP analysis to occupy novel regions of chemical space. In addition, they exhibited moderate activity in several assays.

The third section describes our efforts toward the total synthesis of chrysopaentin A. Although the synthesis of the natural product has yet to be achieved, the convergent synthesis of the monomeric C₁-C₁₆ tetraphenol of chrysopaentin A was completed in 10 steps (longest linear sequence) and 24% overall yield. The collaborative biological evaluation of two monomeric chrysopaentin A fragments revealed that they retained the potent antimicrobial activity of the parent natural product.

The final section of this thesis describes the synthesis of three peptide-like inhibitors as well as several non-peptidic small-molecule inhibitors of botulinum neurotoxin serotype A light chain (BoNT/A LC). In collaborative work, all three peptidic inhibitors were found to possess sub- μ M activity. X-ray crystallography was used to document the binding mode of one of the peptidic inhibitors on BoNT/A LC.

TABLE OF CONTENTS

LIST OF ABBREVIATIONS	XIX
1.0 THE SYNTHESIS OF SCOTOPHOBIN AND ANALOGOUS PEPTIDES VIA MICROWAVE ASSISTED SOLID PHASE PEPTIDE SYNTHESIS	1
1.1 INTRODUCTION	1
1.2 SYNTHESIS OF SCOTOPHOBIN AND RELATED ANALOGUES	6
1.3 FIRST GENERATION APPROACH TOWARDS SCOTOPHOBIN	12
1.3.1 Optimization of the Coupling Reaction	13
1.3.1.1 Synthesis of the Goodman Reagent.....	14
1.3.2 Optimization of Cleavage and Global Deprotection.....	15
1.3.3 Final Optimization	17
1.4 BIOLOGICAL RESULTS.....	23
1.5 CONCLUSIONS.....	27
1.6 EXPERIMENTAL	28
1.6.1 General Procedure A: Solid Phase Peptide Synthesis.	30
1.6.2 SPPS Experimental Procedures.....	31
2.0 LIBRARY SYNTHESIS OF BICYCLO[3.3.1]NONANES	51
2.1 INTRODUCTION	51
2.2 LIBRARY SYNTHESIS OF BICYCLO[3.3.1]NONANES.....	58
2.2.1 First Generation Approach.....	58

2.2.2	Second Generation Approach.....	61
2.2.3	Attempts to Directly Epoxidize Dienone 2.14.....	64
2.2.4	Model System Investigations.....	66
2.3	CONCLUSIONS.....	85
2.4	EXPERIMENTAL	86
2.4.1	General Procedure A: Addition/Rearrangement to Afford the Bicyclo[3.3.1]nonane Scaffold.	87
2.4.2	General Procedure B: Microwave Assisted Addition/Rearrangement to Afford the Bicyclo[3.3.1]nonane Scaffold.	87
3.0	EFFORTS TOWARD THE TOTAL SYNTHESIS OF CHRYSOPHAENTIN A	123
3.1	INTRODUCTION	123
3.2	1 ST GENERATION SYNTHESIS OF CHRYSOPHAENTIN A	128
3.3	2 ND GENERATION SYNTHESIS OF CHRYSOPHAENTIN A.....	134
3.4	CONCLUSIONS.....	156
3.5	EXPERIMENTAL	157
4.0	SYNTHESIS OF BONT/A LC INHIBITORS	187
4.1	INTRODUCTION	187
4.2	DESIGN OF INHIBITORS.....	191
4.3	SYNTHESIS OF INHIBITORS.....	199
4.4	RESULTS AND DISCUSSION.....	203
4.5	CONCLUSIONS.....	208
4.6	DEVELOPMENT OF SMALL MOLECULE INHIBITORS OF BONT/A LC209	
4.7	CONCLUSIONS AND FUTURE DIRECTIONS	218

4.8	EXPERIMENTAL FOR PEPTIDIC INHIBITORS.....	219
4.8.1	General Procedure A: Solid Phase Peptide Synthesis.	221
4.9	EXPERIMENTAL FOR SMALL-MOLECULE INHIBITORS.....	233
APPENDIX A	249
APPENDIX B	263
APPENDIX C	272
5.0	REFERENCES.....	331

LIST OF TABLES

Table 1. Comparison of sequence homology between scotophobin and several known neuroactive peptides.....	11
Table 2. Screen of activating agents for synthesis of scotophobin.....	14
Table 3. Optimization of cleavage/global deprotection conditions and composition of the cocktails explored	16
Table 4. Synthesis of scotophobin and related analogues.....	19
Table 5. Agonist/antagonist activity of JTH-NB72-40 and JTH-NB72-60 against several metabotropic glutamate receptors at 10 μ M	27
Table 6. ^1H and ^{13}C NMR Data for JTH-NB72-40	32
Table 7. ^1H and ^{13}C NMR Data for JTH-NB72-41	37
Table 8. ^1H and ^{13}C NMR Data for JTH-NB72-42	42
Table 9. ^1H and ^{13}C NMR Data for JTH-NB72-60	47
Table 10. Solvent screen for addition/rearrangement reaction	64
Table 11. Attempts at direct bisepoxidization of dienone 2.22	65
Table 12. Optimization of addition/rearrangement reaction.....	68
Table 13. Scope and limitations of the addition/rearrangement reaction	70
Table 14. Attempt to expand the reaction scope to include heterocyclic and alkyl thiols.....	73
Table 15. Attempt to expand the reaction scope to include non-thiol nucleophiles	74

Table 16. Selected physiochemical properties of the newly synthesized bicyclo[3.3.1]non-3-en-2-ones	81
Table 17. Nucleophilic displacement of 3.3 with 3.4	130
Table 18. Nucleophilic coupling to synthesize 3.10	133
Table 19. Iodochlorination of alkynes 3.13 and 3.18	136
Table 20. Optimization of Negishi coupling in model system	140
Table 21. Optimization of Negishi coupling of 3.28a/3.28b and 3.25	142
Table 22. Final optimization of the Negishi coupling	144
Table 23. Optimization of methyl deprotection	145
Table 24. Summary of antibacterial activity of chrysopaentin A, 3.36 , and 3.1 against five diverse strains of <i>Staphylococcus aureus</i>	146
Table 25. Attempted oxidative dimerization of 3.1	147
Table 26. Attempt to dimerize 3.1	148
Table 27. Preparation and attempted Ullmann coupling of 3.56	154
Table 28. Investigation of the effect of increasing complexity on the intermolecular Ullmann coupling	155
Table 29. BoNT/A LC inhibitor summary	204
Table 30. Attempts to synthesize 4.5 via direct de-sulfurization of 4.2	217
Table 31. ¹ H and ¹³ C NMR Data for JTH-NB72-35	223
Table 32. ¹ H and ¹³ C NMR Data for JTH-NB72-38	227
Table 33. ¹ H and ¹³ C NMR Data for JTH-NB72-39	231
Table 34. Crystal data and structure refinement for 2.3	249

Table 35. Atomic coordinates ($\times 10^4$) and equivalent isotropic displacement parameters ($\text{\AA}^2 \times 10^3$)	251
Table 36. Bond lengths [\AA] and angles [$^\circ$] for 2.3	253
Table 37. Anisotropic displacement parameters ($\text{\AA}^2 \times 10^3$) for 2.3	260
Table 38. Hydrogen coordinates ($\times 10^4$) and isotropic displacement parameters ($\text{\AA}^2 \times 10^3$)	262
Table 39. Crystal data and structure refinement for 2.37	263
Table 40. Atomic coordinates ($\times 10^4$) and equivalent isotropic displacement parameters ($\text{\AA}^2 \times 10^3$).....	265
Table 41. Bond lengths [\AA] and angles [$^\circ$] for 2.37	266
Table 42. Anisotropic displacement parameters ($\text{\AA}^2 \times 10^3$) for 2.37	270
Table 43. Hydrogen coordinates ($\times 10^4$) and isotropic displacement parameters ($\text{\AA}^2 \times 10^3$)	271

LIST OF FIGURES

Figure 1. Chemical structure of oxytocin	1
Figure 2. Structure of scotophobin.....	10
Figure 3. Rink amide resin (polystyrene (1% cross-linked with DVB) shown as gray sphere)...	12
Figure 4. Commonly used activating reagents and additives	14
Figure 5. HPLC traces of crude peptide resulting from the evaluation of the different cleavage cocktails	17
Figure 6. Comparison of crude peptide purity when using the unoptimized microwave conditions and Reagent A (left) and the fully optimized procedure (right)	19
Figure 7. Secondary radioligand binding inhibition assay results for JTH-NB72-42	24
Figure 8. Secondary radioligand binding inhibition assay results for JTH-NB72-40	25
Figure 9. Secondary radioligand binding inhibition assay results for JTH-NB72-60	26
Figure 10. Diagram of assembled 25 mL polypropylene reaction vessel.....	29
Figure 11. CD Spectrum of JTH-NB72-40 (0.5 mmol) in MeOH.....	35
Figure 12. Analytical HPLC trace of JTH-NB72-40	36
Figure 13. CD spectrum of JTH-NB72-41 (0.5 mmol) in MeOH	40
Figure 14. Analytical HPLC trace of JTH-NB72-41	41
Figure 15. CD spectrum of JTH-NB72-42 (0.5 mmol) in MeOH	45
Figure 16. Analytical HPLC trace of JTH-NB72-42	46

Figure 17. CD spectrum of JTH-NB72-60 (0.5 mmol) in MeOH	48
Figure 18. Analytical HPLC trace of JTH-NB72-60	49
Figure 19. Major epimer of aranorosin.....	51
Figure 20. NOE correlations used to assign the relative stereochemistry of the epoxidation product	53
Figure 21. Potential sites of nucleophilic attack	54
Figure 22. Structure of gymnastatin F and gymnastatin Q.....	57
Figure 23. Diversification points of the bicyclo[3.3.1]nonane scaffold	57
Figure 24. X-ray structure of diepoxy spirolactone 2.3	61
Figure 25. (A) X-ray structure of <i>o</i> -bromo-bicyclo[3.3.1]nonane 2.37 generated using the Mercury software package (B) Structures of both the equatorial and axial diastereomers used for molecular modeling calculations	71
Figure 26. Attempt to use a chloride to elicit the addition/rearrangement reaction	75
Figure 27. ChemGPS-NP coordinates of the synthesized bicyclononanes (in blue) and bicyclononanes in the MLSMR library (X's). Also shown is the new products lacking hydroxyl groups (yellow boxes).....	79
Figure 28. ChemGPS-NP coordinates of the bicyclo[3.3.1]nonenones (blue boxes) in the MLMSR library (crosses). (a) Graph of PC1 and PC4, which represent the principle component dervied from molecular size and flexibility respectively. (b) Graph of PC5 and PC6 which represent the principle components dervied from electronegativity and electropositive atom content, respectively	80

Figure 29. Structure of 2.33 and the most potent inhibitors of the interaction of the lipase co-activator protein, abhydrolase domain containing 5 (ABHD5) with perilipin-5 (MDLDP; PLIN5)	82
Figure 30. Structure of 2.35 and some of the most potent inhibitors of ataxin-2 protein (ATXN2) expression	83
Figure 31. Structure of 2.35 and some other potent antagonists of the human trace amine associated receptor 1 (TAAR1)	84
Figure 32. Cartoon representation of bacterial cell division and ribbon representation of the FtsZ protein adapted from PDB structure 3VPA	124
Figure 33. Natural product inhibitors of FtsZ.....	125
Figure 34. Small molecule inhibitors of FtsZ.....	126
Figure 35. Structure of chrysopaentins A-H.....	127
Figure 36. 1st Generation retrosynthetic analysis of chrysopaentin A.....	128
Figure 37. Revised synthesis of 3.10	131
Figure 38. Chrysopaentin A ring labeling.....	149
Figure 39. Attempted Ullmann coupling of 3.41 with several phenols	151
Figure 40. Ribbon representation of the three domains of botulinum neurotoxin serotype A adapted from PDB structure 3BTA.....	188
Figure 41. Cartoon representation of I) Normal neurotransmitter release. II) Individual stages of BoNT-intoxication including: A) neurotoxin binding to cell-surface receptors, B) endocytosis into an intracellular vesicle, C) HC-mediated translocation of the LC into the cytosol, and D) proteolytic cleavage of specific SNARE proteins	189
Figure 42. Small molecule inhibitors of the BoNT/A LC	193

Figure 43. Structure of the 7-residue sequence of SNAP-25 and its peptidomimetic inhibitor I1	194
Figure 44. Coordination of the zinc ion bound to the I1 inhibitor.....	195
Figure 45. Crystal structure of previously synthesized inhibitor I1 (left), and polar interactions of the DNP-DAB residue bound within the active site (right, I1 shown in magenta, H-bonding shown in yellow, and the Zn ion shown in red).....	196
Figure 46. Trp residue bound in the active site (the I1 inhibitor is shown in purple)	197
Figure 47. Polar contacts of the Thr residue of I1 (magenta) with Asp307 of BoNT/A LC	198
Figure 48. Structure of I1 and analogous PLM structures.....	199
Figure 49. Crystal structure with JTH-NB72-35 (in magenta) bound to the BoNT/A LC	205
Figure 50. Comparison of I1 (top left) and JTH-NB72-39 (top right) bound to the active site of BoNT/A LC as well as both a front (bottom left) and back (bottom right) view of an overlay (JTH-NB72-39 carbons are magenta while I1 carbons are green)	206
Figure 51. Panoramic view of the JTH-NB72-39 inhibitor bound to BoNT/A LC active site..	207
Figure 52. Refined pharmacophore for BoNT/A LC inhibition	210
Figure 53. (A) Structures of the four most potent BoNT/A LC inhibitors screened (B) Docking of NSC 240898 fit with good steric and hydrophobic complementarity in the BoNT/A LC substrate binding cleft	211
Figure 54. Structure of potent small-molecule inhibitors of BoNT/A LC and SAR studies of NSC240898 to yield CWD-021	212
Figure 55. Proposed rigidified small-molecule inhibitors of BoNT/A LC.....	212
Figure 56. Diagram of assembled 25 mL polypropylene reaction vessel.....	220
Figure 57. CD spectrum of JTH-NB72-35 (0.5 mmol) in MeOH	225

Figure 58. Analytical HPLC trace of JTH-NB72-35	226
Figure 59. CD spectrum of JTH-NB72-38 (0.5 mmol) in MeOH	229
Figure 60. Analytical HPLC trace of JTH-NB72-38	230
Figure 61. CD spectrum of JTH-NB72-39 (0.5 mmol) in MeOH	232
Figure 62. Analytical HPLC trace of JTH-NB72-39	233

LIST OF SCHEMES

Scheme 1. Merrifield's solid phase peptide synthesis.....	2
Scheme 2. Common mechanisms of epimerization of an activated amino acid.....	3
Scheme 3. Cartoon representation of Unger's transfer experiment	9
Scheme 4. Cartoon representation of SPPS	13
Scheme 5. Synthesis of the Goodman reagent.....	15
Scheme 6. Synthesis of scotphobin (SDNNQQGKSAQQGGY, JTH-NB72-40).....	20
Scheme 7. Synthesis of substance P precursor fragment (SDTKHRKHSLSQGHGY, JTH-NB72-41).....	21
Scheme 8. Synthesis of β -lipotropin fragment (VLPTQSKESTMFGGY, JTH-NB72-42)	22
Scheme 9. Synthesis of residues 8-15 of scotophobin (KSAQQGGY, JTH-NB72-60).....	23
Scheme 10. Key synthetic step in the Wipf group's synthesis of aranorosin.....	52
Scheme 11. Kinetic resolution resulting from steric congestion during the Henbest epoxidation	53
Scheme 12. Addition/rearrangement to access the bicyclo[3.3.1]nonane scaffold	55
Scheme 13. <i>In situ</i> NMR studies to gain mechanistic insight into the addition/rearrangement pathway.....	55
Scheme 14. Proposed mechanism for the conversion of the spirocyclic diepoxyketone to the bicyclo[3.3.1]nonane scaffold.....	56
Scheme 15. Retrosynthetic analysis of the diversified bicyclo[3.3.1]nonane scaffold	58

Scheme 16. Synthesis of 2.1	59
Scheme 17. Synthesis of BOMSnBu ₃	60
Scheme 18. First generation approach to the key intermediate 2.3	60
Scheme 19. Attempted deprotection/reprotection of bisepoxy spirolactone	61
Scheme 20. Revised protection scheme to access diepoxy spirolactone	62
Scheme 21. Improved synthesis of BOMSnBu ₃	62
Scheme 22. Preparation of key intermediate 2.13	63
Scheme 23. Preparation of bicyclic amide 2.26	63
Scheme 24. Rama Rao's bisepoxidation in his synthesis of aranorosin.....	65
Scheme 25. Access to bisepoxy ketone model system	66
Scheme 26. Proposed mechanism for the ring-opening and intermolecular aldol reaction of diepoxyketone 2.32 with thiophenol.....	72
Scheme 27. Synthesis of naphthyl derivative 2.48	76
Scheme 28. Synthesis and addition/rearrangement of 2.52	77
Scheme 29. Attempt to synthesize the 7-membered ring variant 2.57	78
Scheme 30. Synthesis of benzyl bromide 3.3	129
Scheme 31. Synthesis of alkyne 3.4	129
Scheme 32. Synthesis of benzyl bromide 3.13	132
Scheme 33. Synthesis of alkyne 3.13	132
Scheme 34. 2 nd Generation retrosynthetic analysis of chrysopaentin A.....	135
Scheme 35. Synthesis and iodochlorination of alkyne 3.27	137
Scheme 36. Synthesis of organo-zinc 3.25 and initial attempt at its Negishi coupling with 3.28	138

Scheme 37. Synthesis of model vinyl iodide 3.32	138
Scheme 38. Scale-up of intermediates 3.14 and 3.28a/3.28b	141
Scheme 39. Synthesis of 3.41	150
Scheme 40. Synthesis and Ullmann coupling of 3.46	152
Scheme 41. Synthesis and Ullmann coupling of 3.50	153
Scheme 42. Investigation of diaryl ether formation via hypervalent iodonium coupling	156
Scheme 43. Schematic representation of the proteolytic cleavage of the Gln197-Arg198 peptide bond in SNAP-25	192
Scheme 44. Synthesis of RR(1-Nap)(AIB)AML (JTH-NB72-35)	201
Scheme 45. Synthesis of RRW(AIB)AML (JTH-NB72-38)	202
Scheme 46. Synthesis of RRF(AIB)AML (JTH-NB72-39)	203
Scheme 47. Dr. Igor Opsenica's synthesis of 4.13	213
Scheme 48. Synthesis of thioamide 4.4	214
Scheme 49. Synthesis of the eight-membered lactam 4.25	215
Scheme 50. Completion of thioamide 4.2	216
Scheme 51. Attempted synthesis of 4.30	218

LIST OF ABBREVIATIONS

A.....	alanine
AA.....	amino acid
AIB.....	α -aminoisobutyric acid
Ala.....	alanine
Arg.....	arginine
Asn.....	asparagine
Asp.....	aspartic acid
Boc.....	<i>tert</i> -butyloxycarbonyl
BoNT.....	botulinum neurotoxin
Bn.....	benzyl
Bu.....	butyl
C.....	cysteine
Cbz.....	carboxybenzyl
CFU.....	colony forming units
COSY.....	correlation spectroscopy
Cys.....	cysteine
D.....	aspartic acid
DCC.....	dicyclohexylcarbodiimide
DDQ.....	2,3-dichloro-5,6-dicyano-1,4-benzoquinone
DEPBT.....	3-(diethoxy-phosphoryloxy)-3 <i>H</i> -benzo[<i>d</i>][1,2,3] triazin-4-one
DEPT.....	distortionless enhancement by polarization transfer
DIPEA.....	<i>N,N</i> -diisopropylethylamine
DMAC.....	dimethylacetamide
DMAP.....	4-dimethylaminopyridine

1,2-DME.....	1,2-dimethoxyethane
DMF.....	<i>N,N</i> -dimethylformamide
DMS.....	dimethyl sulfide
DMSO.....	dimethylsulfoxide
DNA.....	deoxyribonucleic acid
DVB.....	divinylbenzene
E.....	glutamic acid
EDCI.....	1-ethyl-3-(3-dimethylaminopropyl)carbodiimide
1,2-EDT.....	1,2-ethanedithiol
ESI.....	electrospray ionization
Et.....	ethyl
equiv.....	equivalent
FGI.....	functional group interconversion
FtsZ.....	filamenting temperature-sensitive mutant Z
Fmoc.....	fluorenylmethyloxycarbonyl
GABA.....	γ -aminobutyric acid
GDP.....	guanosine diphosphate
Gln.....	glutamine
Glu.....	glutamic acid
Gly.....	glycine
GPCR.....	G-protein coupled receptor
GTP.....	guanosine triphosphate
H.....	histidine
h.....	hour(s)
HC.....	heavy chain
His.....	histidine
HMBC.....	heteronuclear multiple bond correlation
HMPA.....	hexamethylphosphoramide
HMQC.....	heteronuclear multiple quantum coherence
HOAt.....	<i>N</i> -hydroxy-7-azabenzotriazole
HOBt.....	<i>N</i> -hydroxybenzotriazole

HPLC.....	high performance liquid chromatography
HRMS.....	high-resolution mass spectrometry
Hz.....	hertz
I.....	isoleucine
ICl.....	iodine monochloride
IR.....	infrared spectroscopy
<i>i</i> -PrOH.....	isopropanol
Ile.....	isoleucine
K.....	lysine
KHMDS.....	potassium bis(trimethylsilyl)amide
L.....	leucine or liter(s)
LAH.....	lithium aluminum hydride
LC.....	light chain
LCMS.....	liquid chromatography mass spectroscopy
LDA.....	lithium diisopropylamide
Leu.....	leucine
LHMDS.....	lithium bis(trimethylsilyl)amide
Lys.....	lysine
M.....	methionine
<i>m</i>	meta
MALDI.....	matrix-assisted laser desorption/ionization
MCPBA.....	3-chloroperbenzoic acid
Me.....	methyl
MeCN.....	acetonitrile
MeOH.....	methanol
Met.....	methionine
mGluR.....	metabotropic glutamate receptors
MHz.....	megahertz
min.....	minutes
mL.....	milliliter
MLSMR.....	Molecular Libraries Small Molecule Repository

mmol.....	millimole
mol.....	mole
1-Nal.....	1-naphthylalanine
MBC.....	minimum bactericidal concentration
MIC.....	minimum inhibitory concentration
MS.....	molecular sieves
N.....	asparagine
NCI.....	National Cancer Institute
NIH.....	National Institutes of Health
NIMH.....	National Institute of Mental Health
nm.....	nanometer
NMR.....	nuclear magnetic resonance
NMP.....	<i>N</i> -methyl-2-pyrrolidone
NOE.....	Nuclear Overhauser Effect
NSF.....	<i>N</i> -ethylmaleimide-sensitive fusion protein
OAc.....	acetate
OPiv.....	pivalate
P.....	proline
Pbf.....	2,2,4,6,7-pentamethyldihydrobenzofuran-5-sulfonyl
PDB.....	protein data bank
PG.....	protecting group
Phe.....	phenylalanine
PhOH.....	phenol
PhSCH ₃	thioanisole
PIDA.....	phenyliodine diacetate
PLM.....	peptide-like molecules
Pro.....	proline
Q.....	glutamine
R.....	arginine
RP.....	reverse phase
RT.....	retention time

S.....	serine
SAR.....	structure-activity relationship
Ser.....	serine
SFC.....	supercritical fluid chromatography
SNARE.....	soluble NSF-attachment protein receptors
SNAP-25.....	synaptosomal-associate protein-25 kD
SPPS.....	solid phase peptide synthesis
SM.....	starting material
SS.....	soft shell
T.....	threonine
TBAF.....	tetrabutylammonium fluoride
^t Bu.....	<i>tert</i> -butyl
TFA.....	trifluoroacetic acid
THF.....	tetrahydrofuran
Thr.....	threonine
TIPSH.....	triisopropylsilane
TLC.....	thin layer chromatography
TMHD.....	2,2,6,6-tetramethylheptanedione
Trp.....	tryptophan
Trt.....	triphenylmethyl
Tyr.....	tyrosine
V.....	valine
Val.....	valine
W.....	tryptophan
Y.....	tyrosine
Å.....	angstrom(s)
µm.....	micrometer
µM.....	micromolar

1.0 THE SYNTHESIS OF SCOTOPHOBIN AND ANALOGOUS PEPTIDES VIA MICROWAVE ASSISTED SOLID PHASE PEPTIDE SYNTHESIS

1.1 INTRODUCTION

Peptides play a pivotal role in the fundamental physiological and biochemical functions of life, making them crucial to biological, medical, and pharmaceutical research; as such, they have been a major focus of synthetic chemistry for over a century.¹ The first coupling of two amino acids was reported by Emil Fischer in 1901; however, the paucity of amino-protecting groups prohibited the synthesis of longer sequences.² Over the course of the next fifty years, advancements in protecting groups and coupling agents led to synthesis of longer and more complicated peptides. In 1954, du Vigneaud successfully synthesized the disulfide containing neurohypophysial nonapeptide hormone, oxytocin (Figure 1), an effort for which he later received the Nobel prize (1955).³

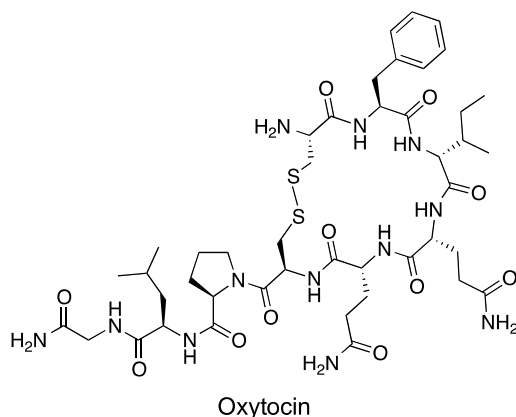
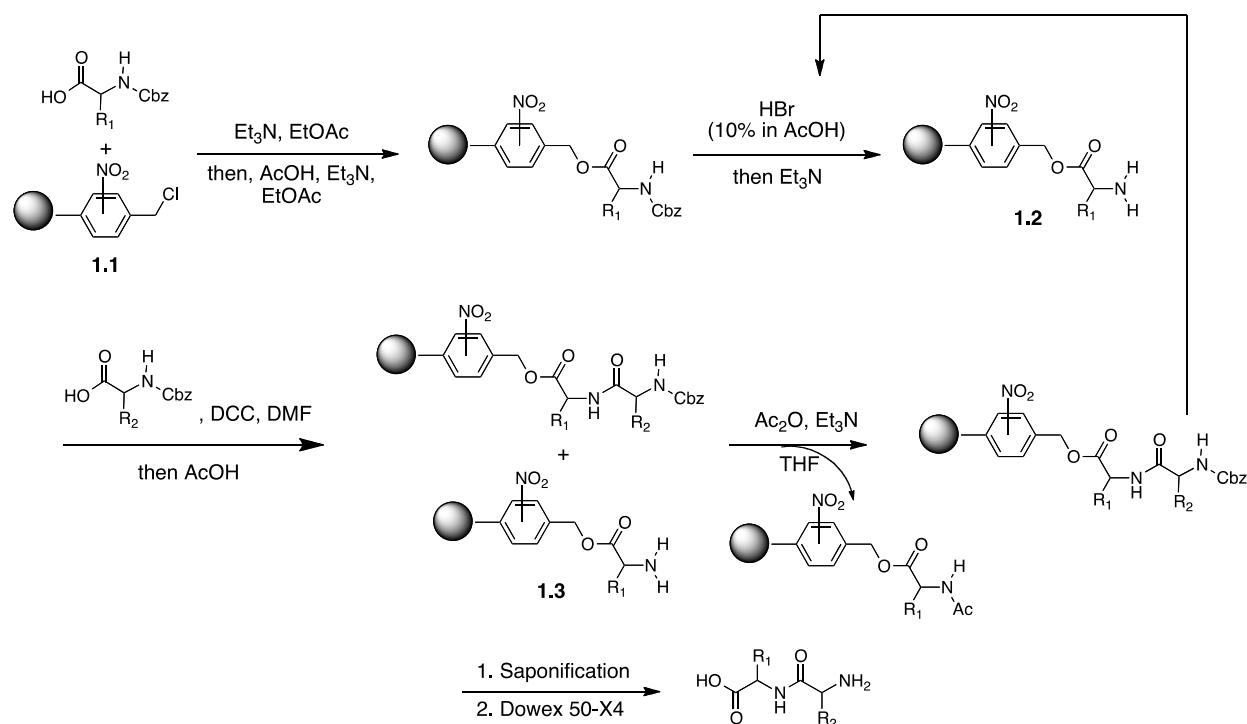


Figure 1. Chemical structure of oxytocin.

The solution phase synthesis of oxytocin and larger peptides consisted of a series of repetitive coupling and deprotection steps, which required isolation and purification of each intermediate. These endeavors proved to be both labor and time intensive. In addition, solubility

and aggregation problems of growing peptide chains led to reduced coupling efficiency in the synthesis of longer peptides. In 1963, Merrifield addressed some of these problems by reporting a new method for peptide synthesis, which employed the use of an insoluble support (Scheme 1).⁴



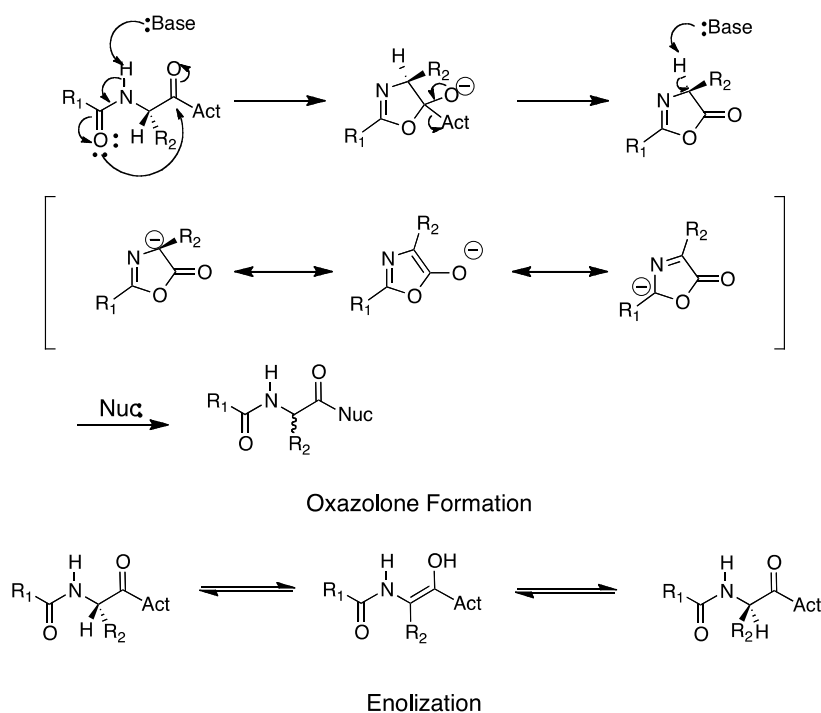
Scheme 1. Merrifield's solid phase peptide synthesis

Merrifield found that a chloromethylated copolymer of styrene and divinylbenzene possessed the requisite solubility and porous gel structure, which allowed penetration of reagents, especially in the presence of swelling solvents. The copolymer (**1.1**) could be functionalized via a S_N2 displacement of chloride with the corresponding triethylammonium salt of the first carbobenzyloxy (Cbz)-protected amino acid. The amino protecting group was removed in the presence of hydrogen bromide (10% in glacial acetic acid) and converted to the free base (**1.2**) with triethylamine. The free amine was then coupled to the subsequent amino acid using *N,N'*-dicyclohexylcarbodiimide (DCC) in DMF.⁵ The unwanted byproducts were effectively removed via thorough washing of the polymer, and the residual unreacted amine (**1.3**) was acetylated with acetic anhydride to reduce the level of free amine to <0.1%. The process of coupling and deprotection was repeated until the full-length peptide was bound to the polymer, at which point cleavage from the resin was accomplished by saponification. Purification of the peptide was

accomplished via chromatography on a Dowex 50-X4 column using a pyridinium acetate buffer (0.1 M, pH=4.0).⁴

Solid phase peptide synthesis (SPPS) offers several important advantages over solution phase synthesis. A large excess of activated amino acid and high reaction concentration allow the coupling to proceed more rapidly and nearly to completion. Since excess reagents are removed by simple filtration and washing steps, SPPS eliminates the need for isolation and purification of intermediates. In addition, due to the ease of purification, reaction vessels have been developed such that the entire synthesis can be completed in the same vessel without the need for transfer, saving both time and material.

Despite its advantages, SPPS presented some interesting challenges in the form of undesired side reactions during its infancy. In addition, SPPS still suffered from epimerization problems. Activation of the acid can be accomplished through a variety of pathways (*e.g.*, conversion to the acid halide, (mixed) anhydride, or activated ester).^{6,7} The increased acidity and electrophilicity of the activated amino acid however, promote both enolization and oxazolone formation (Scheme 2), which are the two most common causes of epimerization in peptide synthesis.⁸ Although a variety of coupling reagents and additives have been described to minimize epimerization and oxazolone formation,^{6,7} they have yet to be completely eliminated from peptide synthesis.



Scheme 2. Common mechanisms of epimerization of an activated amino acid

A major breakthrough in peptide synthesis was the evolution of protecting groups. One year after reporting his first protocol for SPPS, Merrifield introduced the use of the *tert*-butoxycarbonyl (Boc)/Cbz protecting group scheme in a revised procedure.⁹ First introduced by the Carpino group in 1957,¹⁰ the Boc functionality served as an ideal temporary protecting group for the *N*-terminal amine. *N*-Boc protected peptides allow for deacylation to occur under milder conditions (*e.g.*, neat TFA), and thus decrease the loss of peptide from the resin.⁹ More permanent protection of side-chain functionality is accomplished using Cbz protecting groups, which are cleaved in the presence of stronger acids (*e.g.*, anhydrous hydrofluoric acid).

By incorporation of milder deprotection steps, changing the coupling solvent from THF to DMF, and altering the cleavage conditions, Merrifield's revised protocol eliminated the need for the acetylation step, thereby dramatically decreasing the total reaction time for one cycle from over 24 h to 4 h with improved yields.^{9,11,12} These advancements allowed him to synthesize the octapeptide Bradykinin in an overall 68% yield in only 8 days.¹¹ This was a substantial improvement, considering that only 10 years earlier, the synthesis of a nonapeptide was considered worthy of a Nobel prize.

Although the Boc/Cbz protecting scheme was widely used to synthesize a number of peptides, it requires the use of HF. Due to the extreme toxicity of HF as well as the requirement for HF-resistant equipment (*e.g.*, polytetrafluoroethylene-lined) this method was and continues to be limited to specialists in the field.

In 1970, Carpino *et al.* described the use of the 9-fluorenylmethoxycarbonyl (Fmoc) functionality as an acid stable amino protecting group which could be readily removed in the presence of mild base.¹³ This led to its incorporation into SPPS in 1978.¹⁴ The use of the orthogonal Fmoc/*t*-Bu protecting scheme allows for cleavage of the temporary Fmoc group under mild base conditions (20% piperidine in DMF). In contrast, removal of the acid labile *t*-Bu protecting groups and cleavage from the resin can be accomplished simultaneously in the presence of TFA. The main advantage of the Fmoc/*t*-Bu protecting scheme is that the orthogonal protecting groups are removed by different mechanisms; thus a milder acid may be used in the final deprotection step.¹⁵ Due to the mild reagents used, the Fmoc/*t*-Bu protecting scheme is more broadly applicable and has become the method of choice for most non-specialized laboratories.

Another major advancement in SPPS was the use of the microwave. Microwaves first appeared in the organic synthesis literature around 1986, with the pioneering work of Gedye¹⁶ and Giguere¹⁷ who reported comparable or better yields and significantly reduced reaction times compared to conventional thermal conditions. These early works were carried out in domestic kitchen microwave ovens. Over the course of the last 30 years, laboratory-grade microwaves have become commercially available. This new generation of single-mode microwave reactors provide built-in direct temperature control, magnetic stirring, and software for temperature and pressure control, which minimize the formation of local hot spots and has made the microwave a more viable option for a wide range of organic reactions.¹⁸

It was not until 1991 that Wang *et al.* described the first use of microwave irradiation to increase the efficiency and reduce the reaction times associated with SPPS.^{19,20} This initial protocol proved to be difficult to reproduce as it called for the use of a modified commercial microwave.²⁰ Today, commercially available microwave reactors, specifically designed for peptide synthesis, allow for the reaction times of coupling and deprotection steps to be reduced to mere minutes. In addition, microwave irradiation reduces the amount of aggregation within the growing peptide chain, increasing the yields in longer sequences.

Although the use of microwaves have led to a significant improvement in the synthesis of milligram quantities of peptides, its viability for large-scale production of peptides remains unproven. One of the major challenges facing process scale-up of microwave technology is the transfer of heat to and from larger reaction vessels. The penetration depth of microwave irradiation, although dependent on the dielectric properties of the solvent, is usually only a few centimeters.²¹ As such, reaction vessels exceeding 500 mL require larger microwaves with more sophisticated cooling systems, which introduce added size, complexity, and cost to reactors. In addition, the efficiency of converting electricity into microwave power can be relatively low (70% or less) as well as the expense of the large excess of reagents, and resins generally used in SPPS, makes the use of microwaves less attractive for large scale preparation of peptides.

Microwave assisted SPPS also suffers from some more general challenges associated with solid-phase synthesis. While solid-phase synthesis methods are now considered well developed, a number of significant challenges still remain. Variability in the characteristics of the resin used, as well as the substitution levels and distribution of the sites for attachment of the peptide, can dramatically affect both the coupling and deprotection steps.²² Therefore, improved methods of synthesis and characterization of different resins are imperative to improving the reproducibility of SPPS. Furthermore, although several techniques to monitor the coupling and deprotection

steps during SPPS have been described, most are implemented qualitatively and suffer the requirement for irreversible consumption of material. This inevitably leads either to loss of peptide-resin during testing or the potential for incomplete reactions, which lead to the formation of deletion peptides and truncated sequences that complicate final product purification. In addition, the inability to isolate and purify intermediates and potential for several residue or sequence-specific side reactions (*i.e.*, diketopiperazine or aspartimide formation) further complicate the final purification process and can make the preparation of high-purity samples very challenging. Thus, although solid-phase peptide synthesis has evolved tremendously in the past 40 years, and the incorporation of microwaves has elevated it even further, it is clear a number of challenges still remain.

1.2 SYNTHESIS OF SCOTOPHOBIN AND RELATED ANALOGUES

The concept of memory transfer, or that a memory could be transferred from one organism to another, has been of great interest to scientists for decades. The first step towards the realization of this concept is to develop an understanding of how the brain stores information. In the 1950's, several theories emerged pertaining to the mechanism by which the brain processes and stores the rich variety of experiences we incur during the course of our lifetime.²³ One of the first detailed theories was proposed by Katz and Halstead.²⁴ They recognized several pieces of empirical evidence: neuronal membranes contain proteins, neurons have a high rate of protein synthesis, some protein denaturants stimulate neurons, specifically arranged proteins have the potential to conduct electricity, and finally that protein content is lower in people with mental disorders.²⁴ This empirical data led Katz and Halstead to conclude that proteins played a pivotal role in both axonal conduction and memory storage. Their theory postulated that neuronal proteins are arranged in rough lattices that, when induced by a stimulus, could undergo conformational changes which elicit downstream neurotransmitter release. Trans-synaptic transmission of these proteins establishes new neural networks and thus creates a "memory" of the stimulus. The theory also postulated that each new experience causes certain neurons to synthesize a novel protein, which acts as a template for self-replication. These new proteins can aggregate to form lattices each with a unique pattern of activation and propagation leading to the creation of new neural networks.²⁵ Although the empirical evidence in hand at the time would

seem to support this hypothesis, the scarcity of methods for further evaluation and testing required the development of new experimental techniques.

In 1962, McConnell provided empirical evidence in the form of a memory transfer experiment. In this experiment, he classically conditioned planaria, pulverized them and fed them to a second batch of planaria, which “subsequently showed a saving upon learning the same task” as compared to a control group.²⁵ However, this and other planarian experiments faced two major points of criticism: there was insufficient evidence to support the hypothesis that invertebrates could in fact learn, and no group had demonstrated specificity in their memory transfer experiments.²⁵ It was not until 1965 that the first examples of memory transfer in mammals appeared in the literature. Four different reports were published in 1965,²⁶⁻²⁹ in three of the four reports RNA was hypothesized to be the transfer unit, while in the study conducted by Unger and Oceaguera-Navarro a small peptide was hypothesized to conduct the transfer.²⁹ Being versed in stimulation-induced changes in protein structure and function in nerve proteins, Unger was most likely familiar with the hypotheses put forth by Katz and Halstead and very interested in contributing to the new memory transfer paradigm.

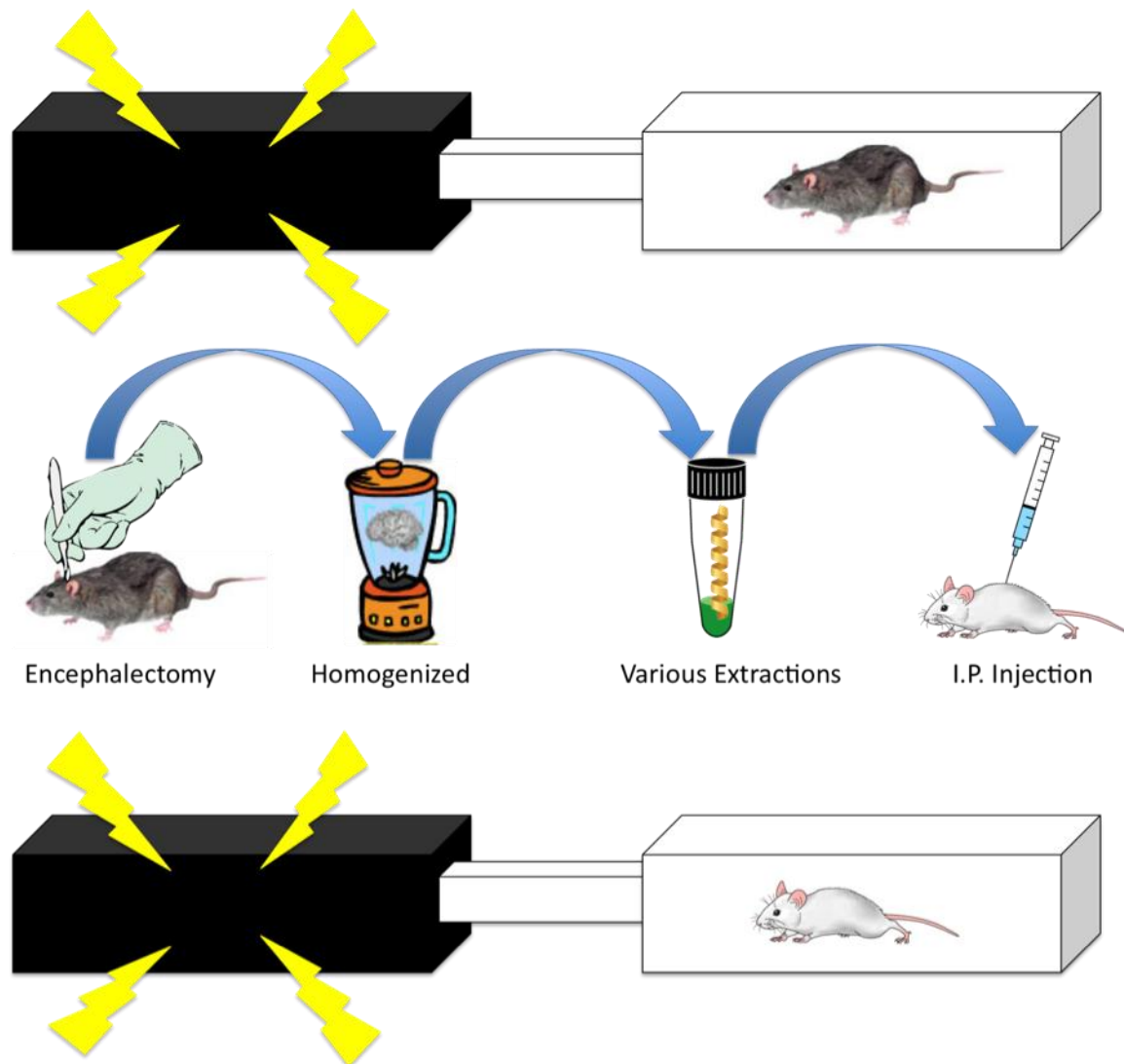
Unger’s early work in this area focused on the transfer of morphine tolerance in rats.²⁵ This initial success led him to attempt the transfer of a learned behavior, giving rise to his 1965 *Nature* publication²⁹ and fueling his interest in the subject. In this publication, Unger and Oceaguera-Navarro conditioned the startle response of rats by repeatedly exposing them to a loud noise. After several days of habituation, the rats’ brains were removed, homogenized, and injected intra-peritoneally into mice. These mice exhibited significantly faster habituation to the same noise as compared to a control group injected with the brains of untrained rats. The most important aspect of this work was that in direct contrast to the three other groups publishing memory transfer papers that year, Unger and Oceaguera-Navarro identified the transfer unit to be a protein. The authors demonstrated that the transfer effect was eliminated by incubating the brain homogenate in chymotrypsin, and it persisted when the brain homogenate was incubated in ribonuclease, clearly supporting the hypothesis that a protein or peptide, not RNA, was responsible for the transfer effect.²⁹ This and the other results published in 1965 prompted a flurry of attempts to repeat the memory transfer experiments. The majority of these attempts however, were met with very little success.

One of the main criticisms in this field was always the lack of specificity. Thus Unger, in a set of follow-up startle experiments, showed that mice receiving extracts from loud noise habituated rats showed faster habituation only to the sound and not to an air-puff, whereas the

opposite was true for those mice receiving the extracts of air-puff habituated rats.²⁵ These studies were quickly followed by two papers, one of which presented his theory on the molecular basis for memory and a second, which became the most well-known publication of his career.

In the first paper, Unger outlined his theory, which stated that when a pre-synaptic neuron fired it released a “connector” assumed to be a small peptide.³⁰ This peptide was then taken up by a nearby post-synaptic neuron establishing a unique connection between the two neurons and thus establishing a new neural network. Repeated connections between the neurons could strengthen the signaling pathway and each neural network in the brain (sensory, motor, etc.) had its own “connector”. If these connections were uniquely involved in specific behaviors, it follows that certain molecules could be specific to these circuits. Therefore, these molecules could essentially act as a code for the circuit and by extension the specific behavior.

The second paper, which Unger published in 1968 provided experimental evidence to support his hypothesis.³¹ Unger reported another set of memory transfer experiments, this time using a previously described³² dark avoidance task. In this experiment, rats were placed in a two-compartment apparatus (Scheme 3). One compartment remained illuminated while the other remained in darkness.



Scheme 3. Cartoon representation of Unger's transfer experiment

Upon entering the dark compartment, the rats received an electric shock, causing them to return to the lighted compartment. This training was repeated five times a day, for a varying number of days until the rats spent significantly less time in the dark compartment. Once “trained”, the rats’ brains were removed, homogenized, and subjected to various extractions before being intra-peritoneally injected into mice. Upon entering the same two-compartment apparatus, the mice that received extracts from the brains of trained rats spent significantly less time in the dark compartment than mice receiving extracts from the brain of an untrained rat.²⁹ In addition, the authors investigated the chemical composition of the extracts and identified a small peptide as being responsible for the transfer effect. This was an astounding feat since at the time the origin of the transfer effect was being debated at the macroscopic level between peptides and RNA. Meanwhile, Unger had not only provided empirical evidence supporting his hypothesis that

peptides were the transfer unit, he went further to propose that a single peptide was responsible. This result received much attention in both the scientific and public communities as evident by a *Time* magazine article describing Unger and his work.²⁵

Over the course of the next several years, a number of attempts to reproduce Unger's results were published with mostly negative or inconclusive outcome. However, approximately five years after his initial study, Unger revealed the identity of his peptide to be a pentadecamer, which he named scotophobin (derived from the ancient Greek terms *skotos* and *phobos* meaning fear and darkness).²⁵ Subsequently, several isolation, characterization, and synthetic studies led to the confirmation of the final pentadecamer structure (Figure 2).

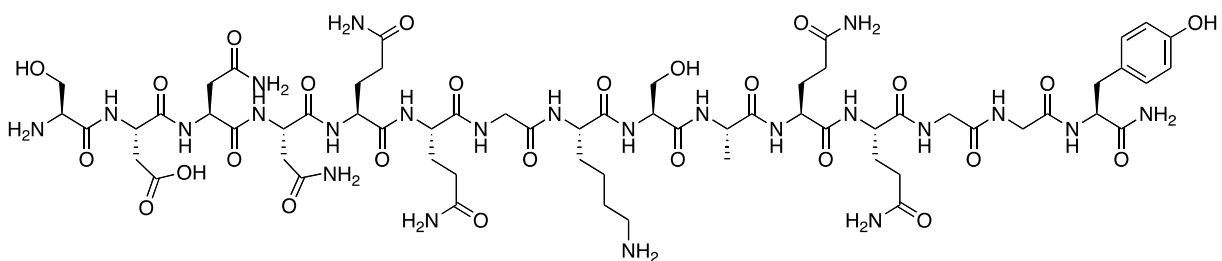


Figure 2. Structure of scotophobin

Unger willingly provided samples of the peptide to a variety of groups for testing with mixed results in different animal models.³³⁻³⁵ Scotophobin has been synthesized both by traditional solution phase organic chemistry and utilizing Merrifield's SPPS techniques. Problems with reproducibility caused the topic, which had thrived in the 50's-70's, to quickly vanish. The last study involving scotophobin was published in 1979, one year after Unger's death. In a 1978 article,³⁶ Irwin, a former co-worker and colleague, observed "in the long run it was not confusion over the biochemical identity of the transfer factors... which most damaged the credibility of the transfer paradigm, but simply the unreliability of the phenomenon."

Later, in a 1986 scientific correspondence published in *Science*, Irwin noted the sequence homology scotophobin shares with several known neuropeptides or their precursors (Table 1). In particular, scotophobin shares sequence homology with MSEL-neurophysin, which is known to be associated with two hormones, oxytocin and vasopressin.³⁷ Oxytocin and vasopressin are associated with female reproduction and the body's retention of water, respectively.

Table 1. Comparison of sequence homology between scotophobin and several known neuroactive peptides.

Molecule	Amino terminal substituent	Sequence (C to N Termini)
Scotophobin	(NH ₂)	YGGQQASKGQQNND S
Enkephalins	(NH ₂)	YGGFM or YGGFL
MSEL-neurophysin	(63)	SGGRCAAFGVCCNDE
Substance P precursor	(88)	YGHGQLSHKRHKTDS
β-Lipotropin	(61)	YGGFMTSEKSQTPLV

*Numbers in parentheses give the number of residues along polypeptide chain from amino terminal end. “NH₂” indicates an amino terminal end. Bold amino acids indicate sequence homology with scotophobin.

Interestingly, the pentadecamer scotophobin has an amino-terminal peptide triplet that is identical to the enkephalins. The enkephalins are naturally occurring pentameric peptides known as endogenous opioids, which have potent painkilling effects and are released by neurons in the central nervous system and by the cells in the adrenal medulla.³⁸ Sequence homology is also observed with β-lipotropin, which is part of a family of closely related peptides that exert modulatory effects on the neuromuscular function, including important components of motor pathways.³⁹ Interestingly, Irwin notes that there appears to be an evolutionary relationship between substance P precursor and scotophobin, as judged by the stability of the sequence similarity under simulated evolutionary change.⁴⁰ Substance P is an important element in pain perception, and has been associated with the regulation of mood disorders, anxiety, and stress.⁴¹

It is interesting to note the sequence homology scotophobin shares with these particular neuropeptides. Considering scotophobin is associated with rats that were trained by undergoing an extended and stressful training, including footshock, one could expect certain structural similarities with related known neuropeptides and their precursor fragments associated with the processing of information concerning pain in the nervous system. In light of the observed sequence homology and the now widely accepted view that certain neuropeptides play important roles as neurotransmitters and as modulators of brain function and behavior,⁴⁰ our group decided to reassess scotophobin's potential as a neuroactive peptide.

Considering the major advancements in peptide synthesis, purification and characterization since the final experiments with scotophobin in 1979,²⁵ we felt that we would be able to provide peptide samples of superior quality. Furthermore, by testing the synthetic scotophobin and analogous portions of known neuroactive peptides against an array of G-protein coupled receptors (GPCRs,) through a collaboration with Dr. Bryan Roth and the NIMH

Psychoactive Drug Screening Program at the University of North Carolina at Chapel Hill, we hoped to avoid the irreproducibility problems exhibited in various animal models.

G-protein coupled receptors (GPCRs) are the largest family of cell-surface receptors, and transduce signals mediated by a wide variety of both endogenous and exogenous signalling molecules, including peptides, to mediate alterations of intracellular function.⁴² These receptors control key physiological functions, including neurotransmission, hormone and enzyme release from endocrine and exocrine glands, cardiac and smooth muscle contraction, and nociception, or perception of a painful stimulus to name a few.⁴³ GPCRs have also been associated with the modulation of anxiolytic activity. Thus, one would expect scotophobin, a molecule proposed to be responsible for the transference of a conditioned response to an extended stressful and painful training, could stimulate one or more GPCRs.

1.3 FIRST GENERATION APPROACH TOWARDS SCOTOPHOBIN

Initial attempts to synthesize scotophobin utilized manual microwave assisted solid phase peptide synthesis conditions previously optimized by a former post-doctoral researcher, Dr. Abhisek Banerjee. These conditions exploited the use of Fmoc protected amino acids, Rink amide SS resin⁴⁴ (Figure 3), and the combination of PyBOP⁴⁵ and HOBT⁴⁶ for activation of the acid. Cleavage from the resin was accomplished using a modified version of Reagent K⁴⁷ (89.5% TFA, 3.0% thioanisole, 2.5% phenol, 0.5% H₂O, 4% triisopropylsilane) and after work-up the crude peptides were purified by preparative RP HPLC. Using these conditions, scotophobin was successfully synthesized, as confirmed by Edman degradation; unfortunately this method of preparation resulted in an unacceptable 3% overall yield. Therefore, further optimization of the synthesis was required.

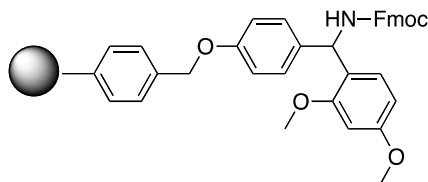
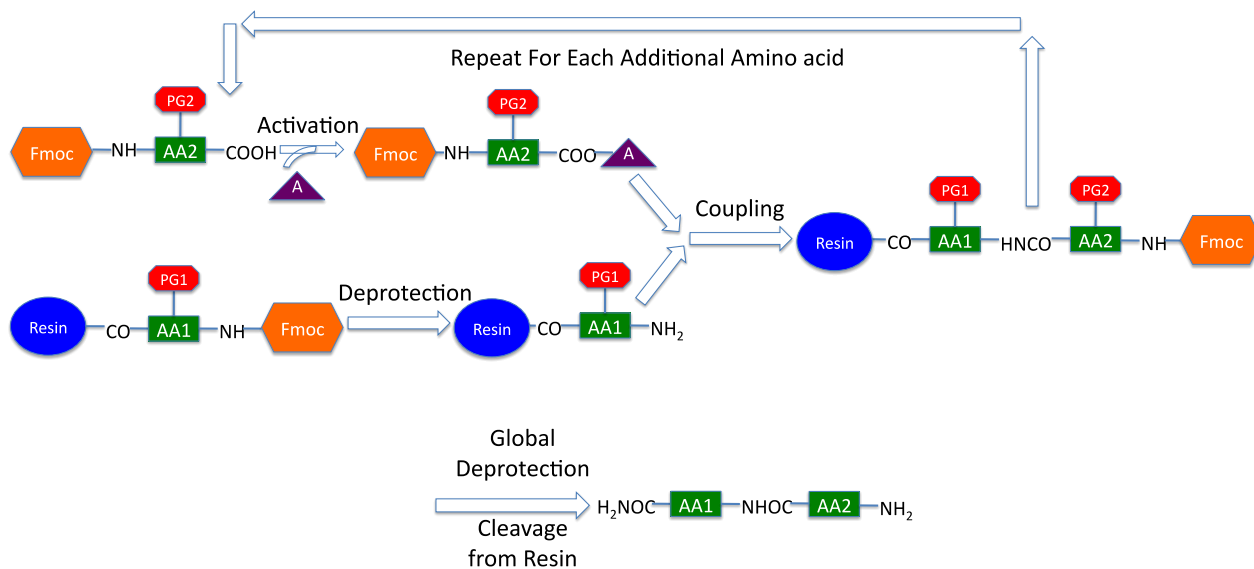


Figure 3. Rink amide resin (polystyrene (1% cross-linked with DVB) shown as gray sphere).⁴⁴

SPPS consists of three different types of reactions: deprotection, coupling, and cleavage/global deprotection (Scheme 4). As most publications describe the use of a 20% piperidine solution in DMF for the deprotection of the Fmoc protecting group,⁴⁷ we focused on the optimization of the coupling and cleavage/global deprotection steps.



Scheme 4. Cartoon representation of SPPS

1.3.1 Optimization of the Coupling Reaction

In SPPS, the preferred reagents for the *in situ* activation of a carboxylic acid are either phosphonium based salts such as PyBOP⁴⁵ and PyAOP⁴⁸, or uronium/aminium based salts such as HATU⁴⁹ or HBTU⁴⁹ (Figure 4).^{15,47} In addition, the use of additives such as HOBt or HOAt is known to enhance reactivity while decreasing the rate of epimerization via formation of the OBt/OAt ester, which stabilize the approach of the amine via H-bonding.^{6,7}

Since the application of Dr. Banerjee's conditions, utilizing PyBOP, in the presence of HOBt, provided an unacceptable yield, the use of the more active PyBrOP⁵⁰ was investigated. However, due to its reportedly higher rate of epimerization,⁶ HOBt was added to the reaction mixture, most likely leading to the *in situ* formation of PyBOP. Gratifyingly, the use of PyBrOP and HOBt increased the overall yield to 10%, but still left room for improvement. In 1999, the Goodman group described a new coupling reagent: 3-(diethoxyphosphoryloxy)-1,2,3-benzotriazin-4-(3*H*)-one (DEPBT) (Figure 4).⁵¹

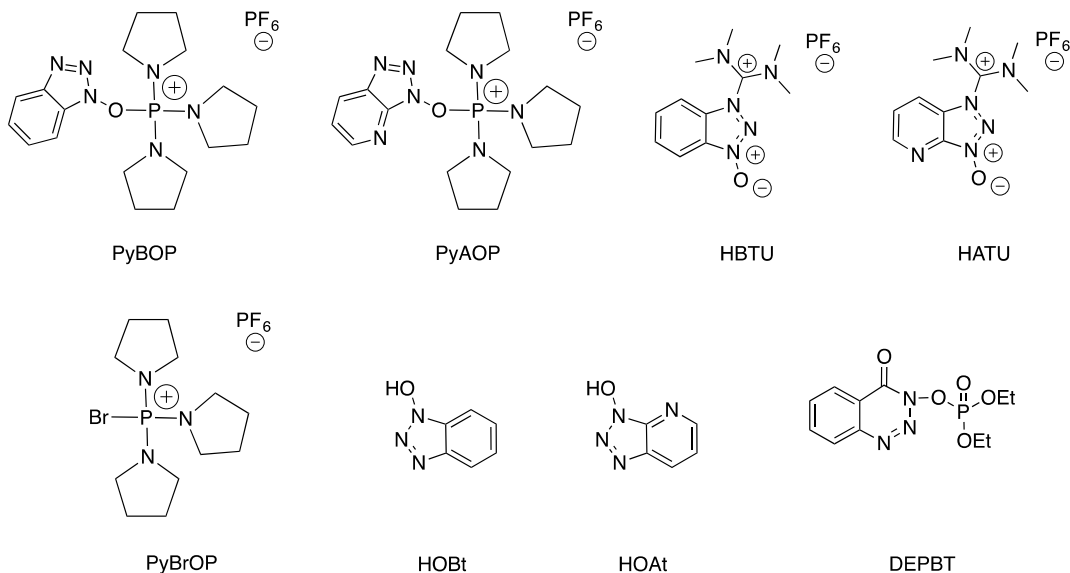


Figure 4. Commonly used activating reagents and additives.

In this initial report, Goodman *et al.* demonstrated the superiority of DEPBT as compared to PyBrOP, HATU, and HBTU in racemization studies, while exhibiting comparable or improved yields.⁵¹ Thus, employing DEPBT as the activating agent, in the absence of additives, increased the overall yield to 25% (Table 2). Satisfied with an almost 10-fold improvement in overall yield, DEPBT was used as the activating agent in all subsequent couplings.

Table 2. Screen of activating agents for synthesis of scotophobin.^a

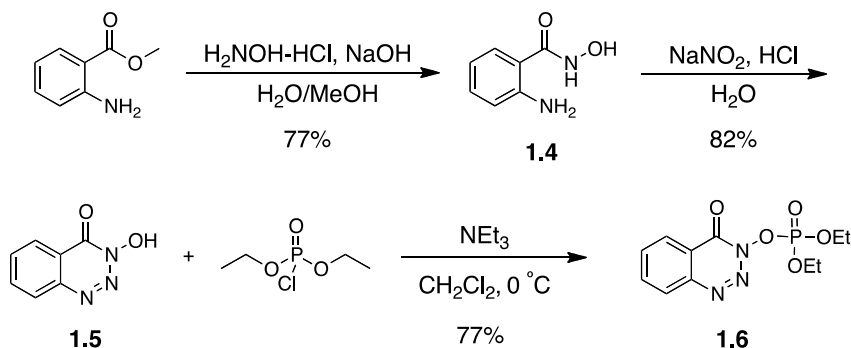
Entry	Coupling Agent	Additive	Isolated Product (mg)	*Overall Yield (%)
1	PyBOP	HOBt	5	3
2	PyBrOP	HOBt	15	10
3	DEPBT	None	39	25

^aAll syntheses were completed using 3.5 equiv of both the coupling reagent and the additive. Final deprotection was accomplished via stirring in a modified version of Reagent K (89.5% TFA, 3.0% thioanisole, 2.5% phenol, 0.5% H₂O, 4% triisopropylsilane) for 2 h at rt. The crude peptides were purified via RP HPLC. *Yields are determined assuming the initial loading of the resin to be 0.7 mmol/g.

1.3.1.1 Synthesis of the Goodman Reagent

Although initially purchased from a commercial vendor, the Goodman reagent was subsequently synthesized according to a known protocol (Scheme 5).⁵¹ The commercially

available methyl anthranilate was treated with hydroxylamine hydrochloride and sodium hydroxide in methanol/water to afford hydroxamic acid **1.4** in 77% yield. Treatment of **1.4** with sodium nitrite and hydrochloric acid in water provided 3-hydroxy-1,2,3-benzotriazin-4 (3*H*)-one (**1.5**) in 82% yield. **1.5** was subsequently converted to DEPBT (**1.6**) in the presence of ethyl chlorophosphate and triethylamine in CH₂Cl₂ in 77% yield.



Scheme 5. Synthesis of the Goodman reagent

1.3.2 Optimization of Cleavage and Global Deprotection

Next, attention was directed toward the optimization of the cleavage and global deprotection steps. The treatment of a peptidyl resin with a cleavage cocktail is not one simple reaction, but a series of competing reactions. Unless suitable reagents and reaction conditions are selected the peptide will be irreversibly modified or damaged. The overall nature of the cleavage cocktail is dependent on the linker. The Rink Amide SS resin requires the use of high concentration TFA solutions. Cleavages in these solutions lead to the formation of carbonium ions and other reactive intermediates. Hence, the appropriate mixture of scavengers is critical for the minimization of undesired side reactions, and has been shown to have a large effect on the purity of the isolated peptides.⁵² A variety of widely used TFA cleavage cocktails were investigated (Table 3).^{47,52} In addition, Dr. Banerjee's optimized cocktail, herein referred to as Reagent A, was examined. This cocktail is a modified version of Reagent K and possess a slightly different ratio of reagents, as well as the exclusion of the malodorous 1,2-ethanedithiol (1,2-EDT), and addition of triisopropylsilane (TIS), which has been shown to be especially useful in the presence of more sensitive peptides.⁵³

Scotophobin was synthesized according to the Fmoc/*t*-Bu protecting scheme and utilizing DEPBT as the activating agent. Following the final deprotection of the Fmoc group, the resin was dried, split into four batches, and subjected to a specific cleavage cocktail for 2 h at rt. Purification was accomplished via RP HPLC and yields were determined assuming a homogenous peptide distribution on the resin (Table 3).

Table 3. Optimization of cleavage/global deprotection conditions and composition of the cocktails explored^a

Cocktail	*Overall Yield	TFA	PhSCH ₃	PhOCH ₃	1,2-EDT	PhOH	H ₂ O	DMS	NH ₄ I	TIS
Reagent R	3.4%	90	5	2	3	-	-	-	-	-
Reagent K	2.6%	82.5	5	-	2.5	5	5	-	-	-
Reagent H	3.3%	82	5	-	2.5	5	3	2	1.5	-
Reagent A*	23%	89.5	3	-	-	2.5	0.5	-	-	4
Reagent J*	22%	87.5	3.5	-	2	3.5	2	-	-	1

^aRows correspond to the ratio of components. Peptide synthesis was accomplished using DEPBT (3.5 equiv) as the activating agent. Following the final deprotection of the Fmoc group, the resin was dried, split into four batches, and subjected to the specific cleavage cocktail for 2 h at rt. Purification was accomplished via RP HPLC. *Yields are determined assuming the peptide is homogeneously dispersed on the resin and an initial loading of 0.7 mmol/g. *Reagent A refers to a modified version of the Reagent K, which was optimized by Dr. Banerjee.

Examination of the data revealed that Reagent A gave superior yields. Although, significant improvement in isolated yield was observed, examination of the HPLC traces (Figure 5) following cleavage/global deprotection revealed a large number of side products or deletion sequences. Thus, the coupling and deprotection reactions were not proceeding smoothly and further optimization was required.

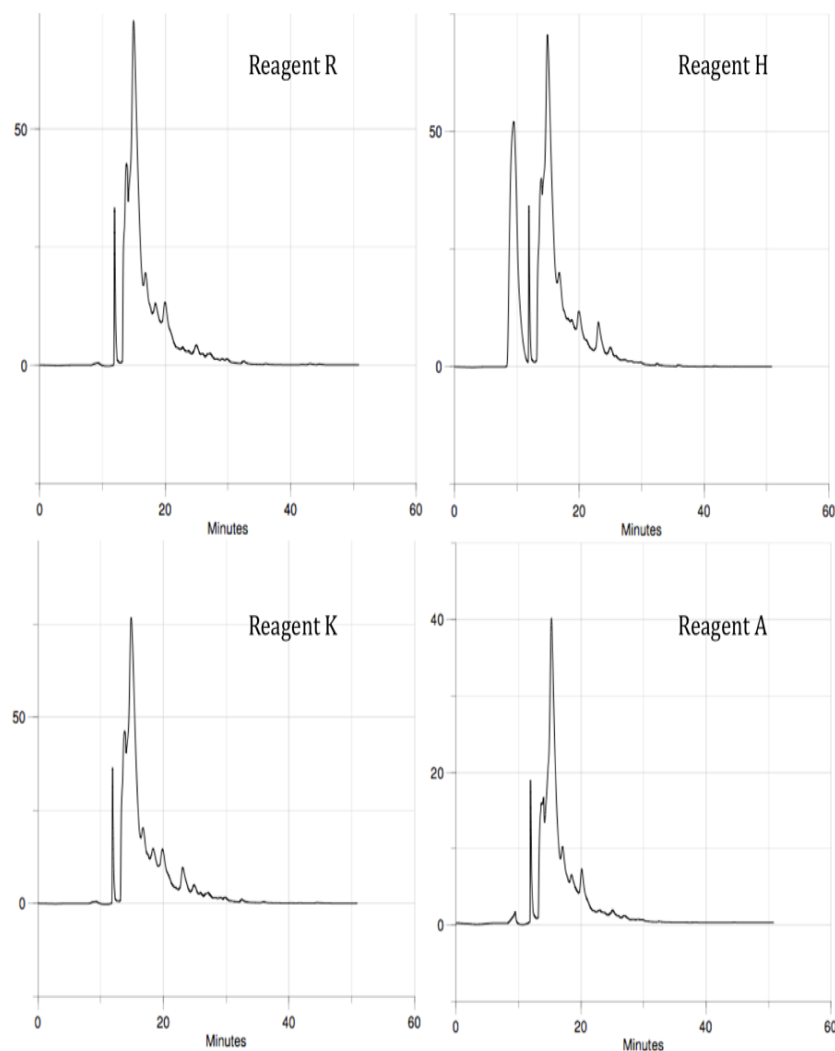


Figure 5. HPLC traces of crude peptide resulting from the evaluation of the different cleavage cocktails using a linear gradient of 30-80% buffer B in A (A: water containing 0.1% TFA, B: acetonitrile containing 0.1% TFA) over 45 min with UV detection at 220 nm at a flow rate of 2 mL/min.

1.3.3 Final Optimization

After optimizing the coupling and cleavage/global deprotection steps, focus turned to the refinement of the microwave conditions. The microwave conditions used to this point had been optimized by Dr. Banerjee for the solid phase synthesis of hybrid molecules containing both a trimeric peptide and a spiroketal modified steroid.⁵⁴ Although these conditions afforded high yields during the synthesis of the hybrid molecules, the low yield observed for the synthesis of the pentadecameric scotophobin, suggested further refinement was needed. After a series of discussions with Dr. Kazi Islam of the Peptide Synthesis Core of the Clinical and Translational

Science Institute of the University of Pittsburgh, the use of a new set of microwave conditions, which had proven successful in his laboratory, were investigated.

These new conditions involved modification of both the coupling and deprotection reactions. Starting from the the previously optimized microwave conditions (40 W, 70 °C, 5 min), it was discovered that decreasing the wattage to 25 W significantly reduced the propensity for temperature spikes during the course of the reaction. Thus, the formation of unwanted side-products was diminished. However, in order to maintain coupling efficiency, the reaction temperature was increased to 80 °C. The wattage for the deprotection step was also reduced from 50 W to 35 W in an effort to decrease potential epimerization and other side reactions which can take place under the basic deprotection conditions. However, as with the coupling, in order to ensure complete deprotection the temperature was increased from 50 °C to 78 °C.

The composition of final cleavage cocktail was also further refined. An examination of the literature revealed that the presence of sulfur containing residues can lead to the formation of disulfide bonds or sulfoxides.⁵² Thus, in an effort to make Reagent A more generally applicable, it was slightly modified to include 1,2-EDT.⁵² Therefore, the final cleavage cocktail consisted of TFA (87.5%), PhSCH₃ (3.5%), 1,2-EDT (2%), PhOH (3.5%), H₂O (2%), and TIS (1%).

Applying the fully optimized conditions to the synthesis of scotophobin, the crude peptide was obtained in considerably higher purity (Figure 6). It should be noted that direct comparison of the HPLC traces is not possible, as the two runs were performed under different conditions. The fully optimized procedure required a more shallow gradient to obtain a significant degree of separation.

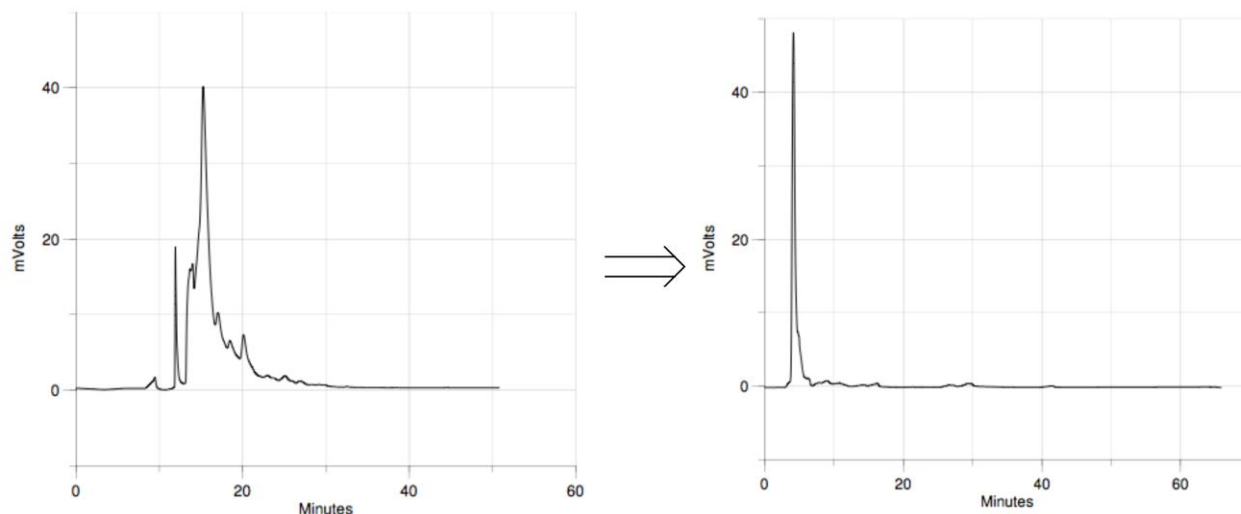


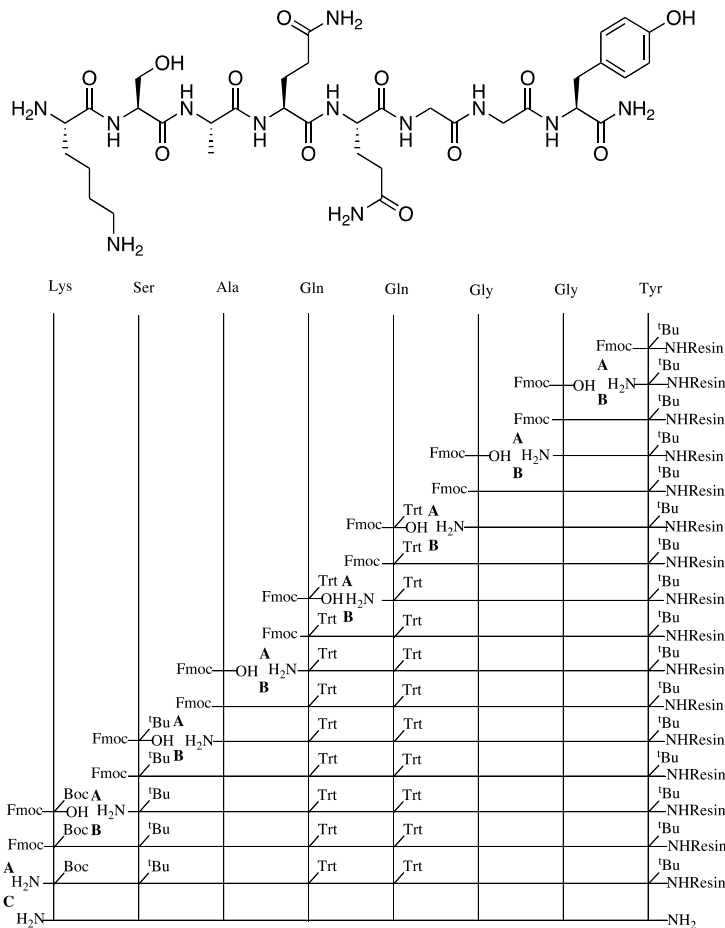
Figure 6. Comparison of crude peptide purity when using the unoptimized microwave conditions and Reagent A (left) and the fully optimized procedure (right). Note: direct comparisons cannot be made since analyses used slightly different conditions: Left conditions: a gradient from 30% Organic (0.1% TFA in CH₃CN) and 70% Aqueous (0.1% TFA in H₂O) to 80% Organic (0.1% TFA in CH₃CN) and 20% Aqueous (0.1% TFA in H₂O) over 45 minutes. Right: a gradient from 30% Organic (0.1% TFA in CH₃CN) and 70% Aqueous (0.1% TFA in H₂O) to 60% Organic (0.1% TFA in CH₃CN) and 40% Aqueous (0.1% TFA in H₂O) over 60 minutes.

Scotophobin, and fragments of both β -lipotropin and substance P precursor were synthesized using the optimized SPPS conditions (Table 4). In addition, a fourth analogue composed of residues 8-15 of scotophobin was synthesized to aid in characterization as well as to help identify the active portion of scotophobin. The structure of the newly synthesized peptides was confirmed by 1D and 2D NMR experiments as well as HRMS analysis.

Table 4. Synthesis of scotophobin and related analogues.

Analogue	Sequence (C to N Termini)	Isolated Product (mg) ^a	Overall Yield (%) ^b
Scotophobin	YGGQQASKGQQNDS	34.0	22
Scotophobin 8-15	YGGQQASK	46.5	55
Substance P Precursor	YGHGQLSHKRHKTDS	14	9
β -Lipotropin	YGGFMTSEKSQTPLV	19.1	11

^aAll peptide synthesis was completed on 0.100 mmol scale. ^bYields were determined assuming an initial loading of 0.7 mmol/g.



A: Piperidine, DMF, 35 W, 78 °C, 3 min B: DEPBT, DMF, DIPEA, 25 W, 80 °C, 5 min C: TFA, PhSCH₃, PhOH, TIPS, H₂O, EDT, rt, 2 h

Scheme 9. Synthesis of residues 8-15 of scotophobin (KSAQQGGY, **JTH-NB72-60**)

1.4 BIOLOGICAL RESULTS

Approximately 10 mg of scotophobin and the other analogues (Table 4) were sent to our collaborator Dr. Bryan Roth of the Pharmacology department at the University of North Carolina School of Medicine. Each compound was screened for radioligand binding inhibition of approximately 50 different G-protein coupled receptors (GPCRs). The primary assays were conducted at 10 μ M and the data represents a mean percent inhibition of radioligand binding (N=4 determination) for compound tested at the receptor subtypes. Radioligand binding inhibition is considered significant in primary assays exhibiting 50% or greater inhibition of radioligand binding to the receptor. If significant binding inhibition was observed during the primary assay, a second, dose-response radioligand binding inhibition assay was used to determine the substrate's binding affinity (K_i). Although each peptide was tested against

approximately 50 GPCRs, only results that exhibited significant radioligand binding inhibition in primary assays will be discussed herein.

The portion of the substance P precursor peptide (**JTH-NB72-41**) exhibited no activity against any of the screened receptors. The portion of β -lipotropin, **JTH-NB72-42**, exhibited 56% inhibition of radioligand binding to the kappa opioid receptor at 10 μ M. The kappa opioid receptors are widely distributed throughout the brain, spinal cord, and in pain neurons and are associated primarily with nociception, or perception of a painful stimulus.⁵⁵ A secondary assay confirmed its activity and determined **JTH-NB72-42**'s K_i to be 2.7 μ M (Figure 7). In addition, **JTH-NB72-42** exhibited 54% inhibition of radioligand binding to the opioid Sigma 2 receptor at 10 μ M. The function of the sigma receptors are not yet clearly defined, however, they have been shown to be involved in neurotransmitter release, modulation of neurotransmitter receptor function, learning and memory processes, and regulation of movement and posture.⁵⁶ A secondary binding assay revealed that **JTH-NB72-42** possessed a K_i of 6.7 μ M (Figure 7).

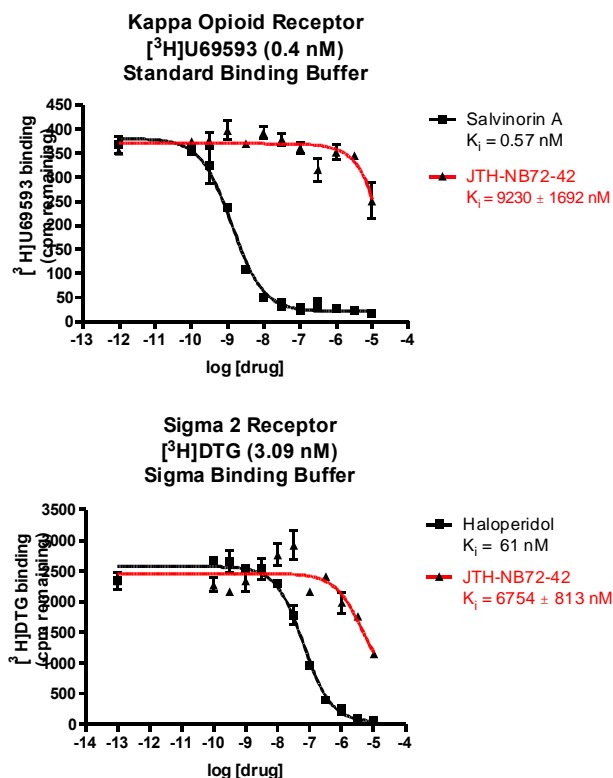


Figure 7. Secondary radioligand binding inhibition assay results for **JTH-NB72-42** (shown in red).⁵⁷

In a primary assay, synthetic scotophobin (**JTH-NB72-40**) exhibited 76% inhibition of radioligand binding to the serotonin (5-hydroxytryptamine) receptor 5-HT_{1A} at 10 μ M. 5-HT_{1A} is

known to be expressed in regions of the brain (*e.g.*, cerebral cortex, hippocampus, amygdala, etc.) that are associated with the limbic system and are known to support a variety of functions including emotion, behavior, and memory.⁵⁵ In addition, agonists of the 5-HT_{1A} receptor (*i.e.*, buspirone, flesinoxan, etc.) have been shown to exhibit anxiolytic and antidepressant activity.⁵⁵ A secondary binding assay however, revealed that the K_i of synthetic scotophobin was in fact greater than 10 μM (Figure 8).

In another primary assay, **JTH-NB72-40** exhibited 67% inhibition of radioligand binding to the adrenergic Alpha_{1D} receptor at 10 μM. The adrenergic receptors mediate the diverse effects of the neurotransmitters of the sympathetic nervous system, norepinephrine, and epinephrine, at virtually all sites throughout the body.⁵⁵ Specifically, the Alpha_{1D} receptor is associated with smooth muscle contraction. A secondary assay revealed confirmed this activity and revealed synthetic scotophobin possessed a sub-micromolar K_i of 0.7 μM (Figure 8).

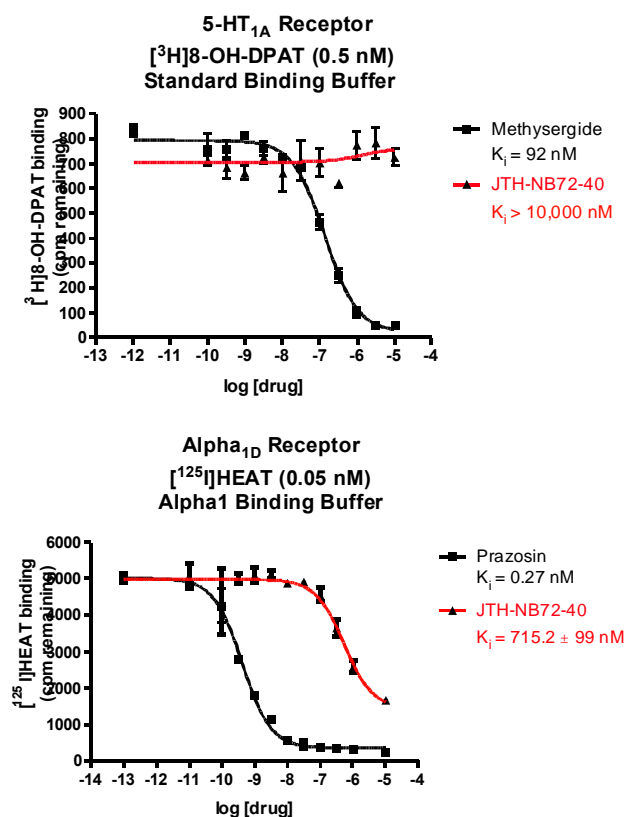


Figure 8. Secondary radioligand binding inhibition assay results for **JTH-NB72-40** (shown in red).⁵⁸

Interestingly, the truncated version of scotophobin (**JTH-NB72-60**) also demonstrated inhibitory activity against 5-HT_{1A} in a primary binding assay (69% inhibition of radioligand

binding at 10 μ M). Once again, a secondary assay revealed that **JTH-NB72-60** possessed a K_i greater than 10 μ M (Figure 9). **JTH-NB72-60** exhibited 62% inhibition of radioligand binding to the kappa opioid receptor at 10 μ M. The secondary assay however, revealed **JTH-NB72-60**'s K_i to be greater than 10 μ M (Figure 9).

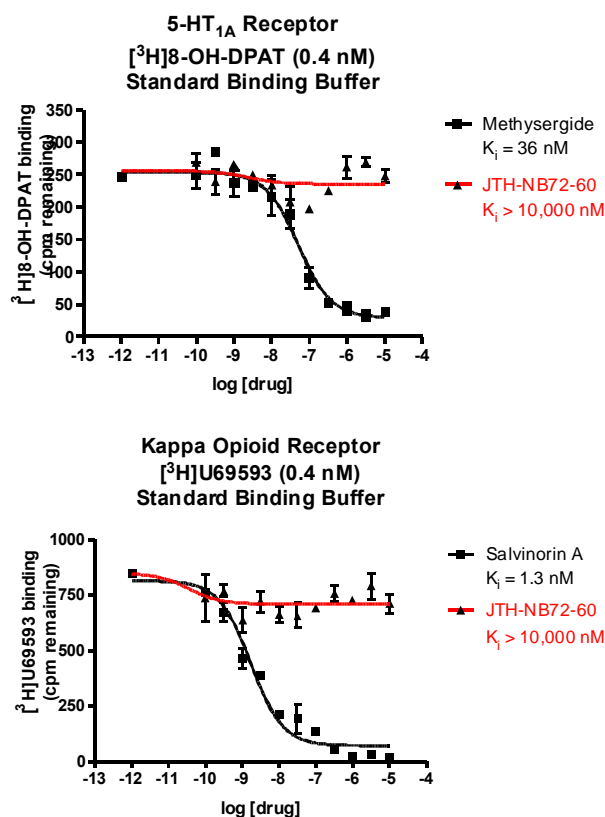


Figure 9. Secondary radioligand binding inhibition assay results for **JTH-NB72-60** (shown in red).⁵⁹

In addition to screening their binding affinities, both **JTH-NB72-40** and **JTH-NB72-60** were screened for agonist/antagonist activity at 10 μ M against several metabotropic glutamate receptors (mGluRs) (Table 5). The reported results for each compound are calculated for agonists as the percent of maximal activity (as obtained with maximal agonist concentrations) and for antagonist as the percent of inhibition of receptor activity (in presence of an EC_{50} concentration of the agonist). mGluRs are generally involved in the tuning of glutamatergic synapses, GABA-ergic, dopaminergic, and serotonergic synapses. As such, these receptors are common targets for therapeutic drugs associated with anxiety, pain, ischaemia, Parkinson's disease, epilepsy, and schizophrenia.

Both **JTH-NB72-40** and **JTH-NB72-60** exhibited antagonistic activity of mGluR₅ (68% and 67% inhibition respectively), which is associated with increasing neuronal excitability, pain sensitivity, anxiolytic activity, and even nootropic (cognitive enhancing) effects.^{55,60} **JTH-NB72-60** also exhibited agonistic activity of mGluR₆, which is exclusively located in a single cell type of the retina. The receptor is responsible for the hyperpolarization of the these cells in the dark, when glutamate is released from the rod or cone photoreceptor.⁵⁵ Most intriguingly, both **JTH-NB72-40** and **JTH-NB72-60** exhibited antagonist activity against mGluR₈ (74% and 76% inhibition respectively). Recently activation of mGluR₈ has been shown to provide powerful inhibitory control of synaptic transmission within the lateral amygdala, with the ability to reduce activity in such a way that the expression and the acquisition of a learned fear become strongly impaired in vivo.⁶¹

Table 5. Agonist/antagonist activity of **JTH-NB72-40** and **JTH-NB72-60** against several metabotropic glutamate receptors at 10 μ M.⁶²

Compound	mGluR1a	mGluR2	mGluR4
JTH-NB72-40	AGO-%MAX :-3 ANT-%INH: 92	AGO-%MAX :-2 ANT-%INH: 90	AGO-%MAX :-28 ANT-%INH: 100
JTH-NB72-60	AGO-%MAX :0 ANT-%INH: 108	AGO-%MAX :8 ANT-%INH: 90	AGO-%MAX :7 ANT-%INH: 107

Compound	mGluR5	mGluR6	mGluR8
JTH-NB72-40	AGO-%MAX :-10 ANT-%INH: 68	AGO-%MAX :21 ANT-%INH: 116	AGO-%MAX :-15 ANT-%INH: 74
JTH-NB72-60	AGO-%MAX :-2 ANT-%INH: 67	AGO-%MAX :28 ANT-%INH: 128	AGO-%MAX :4 ANT-%INH: 76

Legend:

0-50% Inhibition	51-75% Inhibition	25-49% Activation	50-100% Activation
------------------	-------------------	-------------------	--------------------

The reported results for each compound are calculated for agonists as the percent of maximal activity (as obtained with maximal agonist concentrations) and for antagonist as the percent of inhibition of receptor activity (in presence of an EC₅₀ concentration of the agonist).

1.5 CONCLUSIONS

Starting from the previously optimized conditions, improvement of the coupling and cleavage/global deprotection steps, as well as refinement of the microwave irradiation conditions led to almost a 10-fold improvement in overall yield of the pentadecameric scotophobin as well as a dramatic increase in crude peptide purity. The optimized protocol was successfully applied to the synthesis of scotophobin as well as several other analogues. Through a collaboration with Dr. Byran Roth's lab and the NIMH Psychoactive Drug Screening Program, these compounds were tested for radioligand binding inhibition against an array of GPCRs as well as agonist/antagonist modulation of several mGluRs.

Considering scotophobin's association with rats that have undergone an extended and stressful training, including footshock, one might expect the observed activity in relation to known modulators of anxiolytic and antidepressant activity. In addition, the activity observed with modulators of pain sensitivity and even receptors specifically associated with the acquisition of a learned fear is very intriguing. Although the data does not confirm the hypothesis that the transfer of a learned response exhibited in Unger's studies was a result of the administration of scotophobin, it demonstrates that a pure synthetic sample of scotophobin does possess *in vitro* neuropeptidic activity.

1.6 EXPERIMENTAL

N,N-Diisopropylethylamine was sequentially distilled from ninhydrin then KOH and stored under argon. Piperidine was distilled from CaH₂ and stored under argon. Phenol was purified by dissolving the solid in diethyl ether, washing with a saturated aqueous solution of NaHCO₃ (3x), extracting with aqueous NaOH (0.1 M) (3x), acidifying with 0.1 N HCl, extracting with Et₂O (3x), concentrating under reduced pressure, and the dry solid was stored under argon. *N,N*-dimethylformamide was purchased from Alfa Aesar as anhydrous and amine free in 4 L quantities and stored in 1 L amber bottles (dried overnight in an oven at 140 °C) over activated 4 Å molecular sieves and under argon. Trifluoroacetic acid (biochemical grade, 99.5+% pure) was purchased from Alfa Aesar and used as received. Methanol (HPLC grade), water (HPLC grade), and thioanisole (99% purity) were purchased from Aldrich and used as received. Triisopropylsilane (99% pure) was purchased from Acros and used as received. 1,2-ethanedithiol (>98% pure) was purchased from Fluka and used as received. All natural Fmoc-protected amino acids and 3-(diethoxy-phosphoryloxy)-3*H*-benzo[*d*][1,2,3] triazin-4-one were purchased from either Peptides International or Advanced Automated Peptide Protein Technologies (AAPPTEC) and used as received. Unnatural Fmoc protected amino acids and Rink Amide Resin SS, 100-200 mesh, 1% DVB (catalogue #: SA5030) were purchased from Advanced Chemtech and used as received. BD Falcon BlueMax 50 mL Graduated tubes and 25 mm syringe filters with a 0.45 µm nylon frit were purchased from Fischer Scientific.

The Fmoc-solid phase peptide syntheses were performed on a CEM Discover manual microwave peptide synthesizer fitted with a fiber-optic temperature probe. Solid phase peptide

syntheses were performed in a 25 mL polypropylene reaction vessel. The 25 mL polypropylene reaction vessel was constructed by inserting a Teflon ring (0.4 mm height, 2.1 mm outer diameter, 1.8 mm inner diameter) into a capped 25 mL SPE reservoir purchased from Grace Davison Discovery Science (Catalogue #: 210425) containing a frit purchased from Grace Davison Discovery Science (Catalogue #: 211416) (Figure 10).

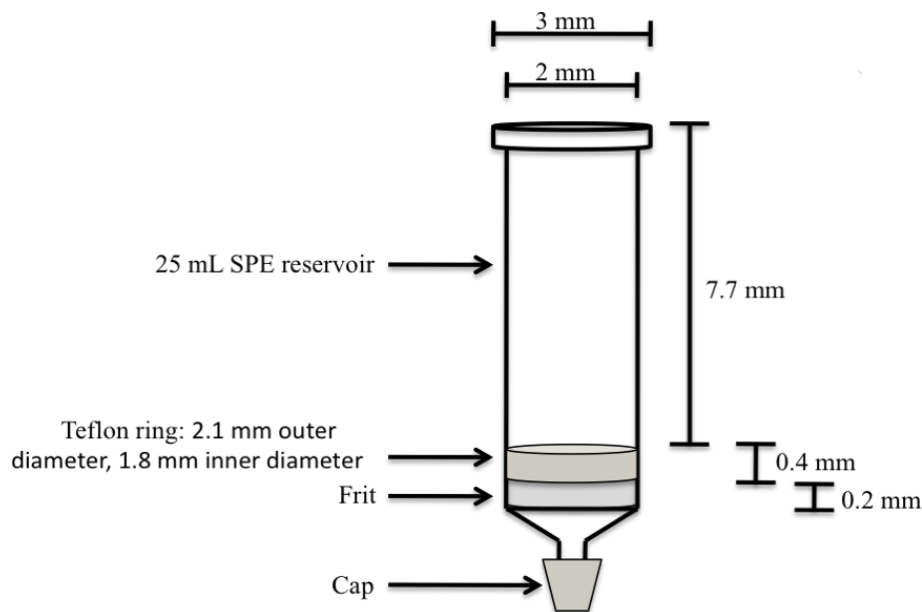


Figure 10. Diagram of assembled 25 mL polypropylene reaction vessel.

Preparative reverse phase HPLC purifications were performed on a Gilson HPLC system with 220 and 254 nm UV detection, using a Phenomenex Luna 5 μ C18(2) 100 Å, AX (75 x 30.0 mm) column at a flow rate of 10 mL/min. Unless otherwise noted, all preparative runs used linear gradients of 30-60% buffer B in A (A: water containing 0.1% TFA, B: CH₃CN containing 0.1% TFA) over 30 min. Analytical HPLC traces of final products were performed on a Gilson HPLC system with 220 and 254 nm UV detection, using a Varian Microsorb 100-3 C18 (100 x 4.6 mm) column at a flow rate of 0.7 mL/min. Unless otherwise noted, all analytical runs used linear gradients of 30-100% buffer B in A (A: water containing 0.1% TFA, B: MeOH) over 70 min. CD Spectra were recorded on a Jasco J-815 Circular Dichroism Spectrometer. Unless otherwise noted, all CD spectra were recorded in MeOH at a concentration of 0.5 mmol, at 298 K, over a range of 300-200 nm, at a scan rate of 50 nm/min. Mass spectra were obtained using an ABI 4800 MALDI TOF/TOF instrument with 2,5-dihydroxybenzoic acid as the matrix in the

positive ion mode. Lyophilization was accomplished using a Labconco FreeZone 4.5 liter benchtop freeze dry system.

Proton and carbon NMR spectra were recorded using a Bruker Avance spectrometer at 600 MHz/150 MHz (^1H NMR/ ^{13}C NMR) in D_2O (298 K), unless otherwise noted. Chemical shifts (δ) are reported in parts per million (ppm) using MeOH solvent peaks as an internal reference (referenced to 3.34 ppm (^1H) and 49.5 ppm (^{13}C)). ^1H NMR data are reported as follows: chemical shift, multiplicity (s = singlet, d = doublet, t = triplet, q = quartet, m = multiplet, dd = doublet of doublets, dt = doublet of triplets, td = triplet of doublets, qd = quartet of doublets), coupling constants (J) in Hertz (Hz), and integration. ^{13}C NMR spectra were obtained using a proton-decoupled pulse sequence with d1 of 6 sec, and are tabulated by observed peak.

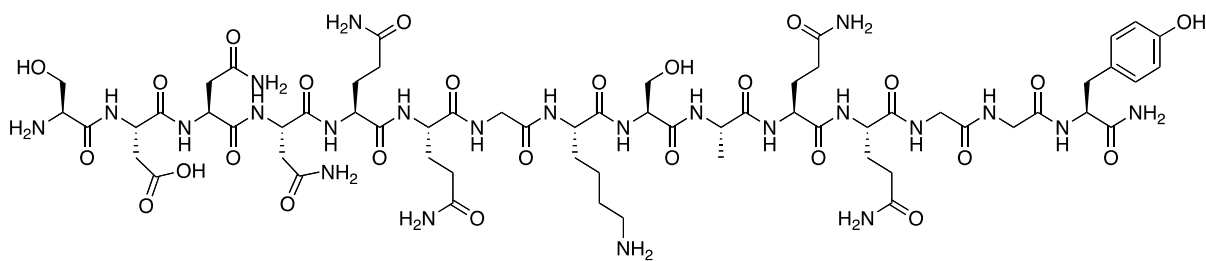
A stock solution of the coupling base was prepared by dissolving DIPEA (1.74 mL, 1.00 mmol) in DMF (5.00 mL) to give a 0.148 M solution. A stock solution of the Fmoc-cleavage base was prepared by dissolving piperidine (1.00 mL, 10.1 mmol) in DMF (4.00 mL) to give a 2.02 M solution. A stock solution of the resin cleavage cocktail was prepared by combining TFA (5.07 g, 44.5 mmol), PhSCH_3 (0.210 g, 1.69 mmol), PhOH (0.215 g, 2.28 mmol), TIPS H (0.0620 g, 0.392 mmol), 1,2-EDT (0.135 g, 1.43 mmol) and H_2O (0.100 g, 5.56 mmol). All stock solutions were freshly prepared prior to use.

1.6.1 General Procedure A: Solid Phase Peptide Synthesis.

To a polypropylene reaction vessel (25 mL) charged with a Teflon stir bar (10 x 3 mm) was added the Rink Amide resin (0.143 g, 0.100 mmol, loading 0.700 mmol/g, 1.00 equiv). The resin was washed with MeOH (2 x 5 mL), CH_2Cl_2 (3 x 10 mL) and DMF (3 x 10 mL), suspended in CH_2Cl_2 (5 mL) and allowed to swell at room temperature for 20 min. The resin was filtered and washed with DMF (3 x 10 mL). The reaction vessel was fitted with the fiber optic temperature probe and the Fmoc group was cleaved by heating the resin in the Fmoc-cleavage base stock solution (1 mL) in the microwave (35 W, 78 °C, 3 min). The resin was filtered and washed with DMF (3 x 10 mL), CH_2Cl_2 (3 x 10 mL) and DMF (3 x 10 mL). The first Fmoc protected amino acid was coupled to the resin by heating in a pre-mixed solution of amino acid (0.350 mmol, 3.50 equiv), DEPBT (0.105 g, 0.350 mmol, 3.50 equiv), DMF (0.800 mL), and Fmoc-coupling base stock solution (0.750 mL) in the microwave (25 W, 80 °C, 5 min). The resin was filtered and washed with DMF (3 x 10 mL), CH_2Cl_2 (3 x 10 mL) and DMF (3 x 10 mL). The

Fmoc group was cleaved by heating the resin in Fmoc-cleavage base stock solution (1 mL) in the microwave (35 W, 78 °C, 3 min). The resin was filtered and washed with DMF (3 x 10 mL), CH₂Cl₂ (3 x 10 mL) and DMF (3 x 10 mL). The second Fmoc protected amino acid was coupled to the resin by heating in a pre-mixed solution of amino acid (0.350 mmol, 3.50 equiv), DEPBT (0.105 g, 0.350 mmol, 3.50 equiv), DMF (0.800 mL), and Fmoc-coupling base stock solution (0.750 mL) in the microwave (25 W, 80 °C, 5 min). This process of Fmoc cleavage and amino acid coupling was repeated for each additional amino acid. After the final Fmoc cleavage, the resin was washed with DMF (30 mL) and CH₂Cl₂ (20 mL). The protecting groups were cleaved by treatment of the dry resin with the resin cleavage cocktail stock solution (2.50 mL) for 2 h at room temperature with vigorous stirring. The resin was filtered and rinsed with the remaining resin cleavage cocktail stock solution (1.50 mL) and TFA (1.50 mL), collecting the filtrate and rinses in a BD Falcon tube (50 mL). The sample was concentrated to a heterogeneous mixture (approximately 0.2 mL) under a stream of argon for 30 min. Cold diethyl ether (45 mL) was added to precipitate the crude peptide. The sample was centrifuged (3200 rpm, -8 °C, 15 min) and the supernatant was discarded. The crude peptide was transferred to a scintillation vial (20 mL) with approximately 5 mL of a mixture of H₂O/CH₃CN (9:1) and lyophilized overnight. The crude peptide was dissolved in H₂O containing 0.1% TFA (5.00 mL) and filtered through a 0.45 μm nylon syringe filter. The filtrate was purified by preparative RP HPLC.

1.6.2 SPPS Experimental Procedures



JTH-NB72-40

SDNNQQGKSAQQGGY (JTH-NB72-40). Prepared according to general procedure A utilizing the following amino acid sequence: Fmoc-L-Tyr(tBu)-OH (0.161 g, 0.350 mmol, 3.50 equiv), Fmoc-L-Gly-OH (0.104 g, 0.350 mmol, 3.50 equiv), Fmoc-L-Gly-OH (0.104 g, 0.350 mmol, 3.50 equiv), Fmoc-L-Gln(Trt)-OH (0.214 g, 0.350 mmol, 3.50 equiv), Fmoc-L-Gln(Trt)-

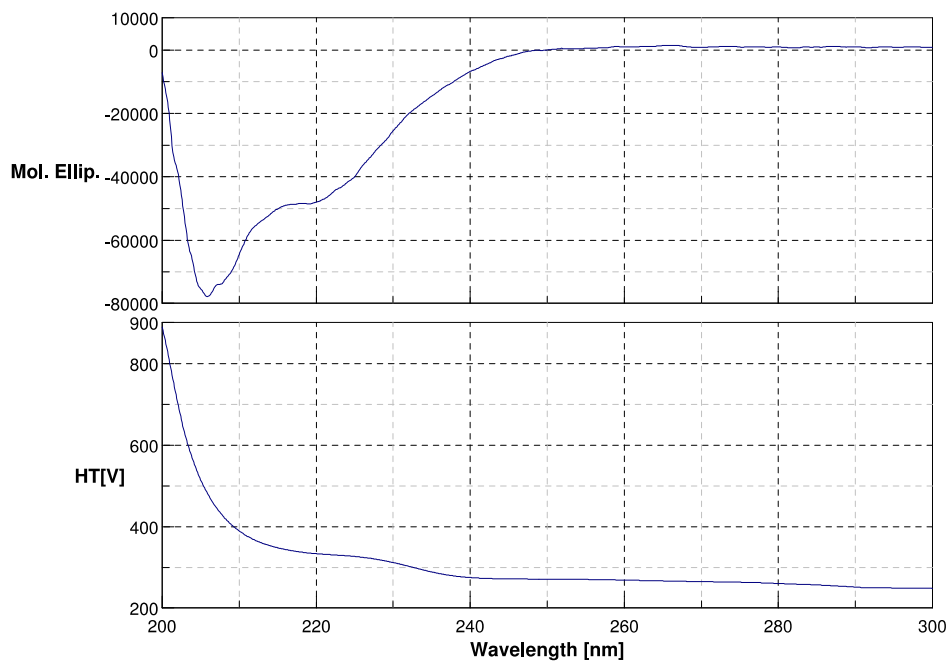
OH (0.214 g, 0.350 mmol, 3.50 equiv), Fmoc-L-Ala-OH (0.115 g, 0.350 mmol, 3.50 equiv), Fmoc-L-Ser(tBu)-OH (0.134 g, 0.350 mmol, 3.50 equiv), Fmoc-L-Lys(Boc)-OH (0.164 g, 0.350 mmol, 3.50 equiv), Fmoc-L-Gly-OH (0.104 g, 0.350 mmol, 3.50 equiv), Fmoc-L-Gln(Trt)-OH (0.214 g, 0.350 mmol, 3.50 equiv), Fmoc-L-Gln(Trt)-OH (0.214 g, 0.350 mmol, 3.50 equiv), Fmoc-L-Asn(OtBu)-OH (0.209 g, 0.350 mmol, 3.50 equiv), Fmoc-L-Asn(OtBu)-OH (0.209 g, 0.350 mmol, 3.50 equiv), Fmoc-L-Asp(OtBu)-OH (0.144 g, 0.350 mmol, 3.50 equiv), Fmoc-L-Ser(tBu)-OH (0.134 g, 0.350 mmol, 3.50 equiv). **JTH-NB72-40** (0.0342 g, 22%) was obtained as a white powder. The sample was subjected to HPLC purification twice using a linear gradient of 30-60% buffer B in A (A: water containing 0.1% TFA, B: MeOH) over 30 min. The product was characterized by ^1H NMR (Table 6); ^{13}C NMR (Table 6); COSY; HMBC; HMQC; HLC RT 4.3 min, HRMS (MALDI⁺) m/z calcd for $\text{C}_{62}\text{H}_{97}\text{N}_{23}\text{O}_{26}$ $[\text{M}+\text{H}]^+$ 1580.7053, Found 1580.7041.

Table 6. ^1H and ^{13}C NMR Data for **JTH-NB72-40** (700 MHz/176 MHz) in D_2O (298 K) with MeOH as an internal reference (referenced to 3.34 ppm (^1H) and 49.5 ppm (^{13}C)).

Residue #	Amino Acid (N->C)	Resonance	^1H δ [ppm]	^{13}C δ [ppm]
1	Serine	CO		168.5
		C_αH	4.18 (t, $J = 4.8$ Hz, 1 H)	55.1
		C_βH	3.90 (dd, $J = 5.6, 11.6$ Hz, 1 H) 3.85 (dd, $J = 5.0, 11.6$ Hz, 1 H)	60.8
2	Aspartic Acid	CO		174.8
		C_αH	4.81-4.74 (m, 1 H)	50.3
		C_βH	2.89 (dd, $J = 5.8, 12.9$ Hz, 2 H)	35.9
		C_γ		172.9
3	Asparagine	CO		175.1
		C_αH	4.71 (dd, $J = 6.0, 12.1$ Hz, 1 H)	51.3
		C_βH	2.87-2.82 (m, 2 H)	36.4
		C_γ		174.0
4	Asparagine	CO		175.0
		C_αH	4.70 (dd, $J = 6.5, 11.4$ Hz, 1 H)	51.3
		C_βH	2.81-2.73 (m, 2 H)	36.4
		C_γ		173.3
5	Glutamine	CO		174.4
		C_αH	4.34-4.29 (m, 1 H)	53.9
		C_βH	2.05-1.94 (m, 2 H)	27.2

		C _γ H	2.36 (dt, <i>J</i> = 15.6, 7.6 Hz, 2 H)	31.7
		C _δ		178.4
6	Glutamine	CO		174.4
		C _α H	4.34-4.29 (m, 1 H)	53.9
		C _β H	2.19-2.05 (m, 2 H)	27.2
		C _γ H	2.36 (dt, <i>J</i> = 15.6, 7.6 Hz, 2 H)	31.7
		C _δ		178.4
7	Glycine	CO		171.7
		C _α H	4.01-3.98 (m, 2 H)	43.0
8	Lysine	CO		174.7
		C _α H	4.38-4.34 (m, 1 H)	54.2
			1.89-1.80 (m, 1 H),	
		C _β H	1.79-1.71 (m, 1 H)	31
		C _γ H	1.49-1.41 (m, 2 H)	22.7
		C _δ H	1.70-1.61 (m, 2 H)	26.9
		C _ε H	2.97 (app t, <i>J</i> = 7.0 Hz, 2 H)	39.8
9	Serine	CO		172.5
		C _α H	4.43 (t, <i>J</i> = 5.3 Hz, 1 H)	56.3
		C _β H	4.01-3.92 (m, 2 H)	61.7
10	Alanine	CO		175.8
		C _α H	4.30 (q, <i>J</i> = 5.7 Hz, 1 H)	50.8
		C _β H	1.38 (d, <i>J</i> = 7.2 Hz, 3 H)	16.9
11	Glutamine	CO		174.4
		C _α H	4.34-4.29 (m, 1 H)	53.9
		C _β H	2.05-1.94 (m, 2 H)	27.2
		C _γ H	2.36 (dt, <i>J</i> = 15.6, 7.6 Hz, 2 H)	31.7
		C _δ		178.4
12	Glutamine	CO		174.4
		C _α H	4.34-4.29 (m, 1 H)	53.9
		C _β H	2.19-2.05 (m, 2 H)	27.2
		C _γ H	2.36 (dt, <i>J</i> = 15.6, 7.6 Hz, 2 H)	31.7
		C _δ		178.4
13	Glycine	CO		172.4
		C _α H	3.97-3.92 (m, 2 H)	43.2
14	Glycine	CO		172.4

		C _α H	3.87 (s, 2 H)	43.2
15	Tyrosine	CO		176.5
		C _α H	4.52 (dd, <i>J</i> = 5.9, 8.8 Hz, 1 H)	55.5
			3.09 (dd, <i>J</i> = 5.8, 14.1 Hz, 1 H),	
		C _β H	2.92 (dd, <i>J</i> = 9.0, 14.1 Hz, 1 H)	36.8
		C _γ		128.9
		C _δ H	7.14 (d, <i>J</i> = 8.4 Hz, 2 H)	131.2
		C _ε H	6.83 (d, <i>J</i> = 8.4 Hz, 2 H)	116.1
		C _ζ		155.1



Date	2/10/2009 9:07PM
File name	JTH_NB72_40_Standard_Sub_MeOH_Moll_Elip_Smooth.jws
Model	J-815
Serial No.	A019361168
Band width	1 nm
Response	1 sec
Sensitivity	Standard
Measurement range	300 - 200 nm
Data pitch	0.1nm
Scanning speed	50 nm/min
Accumulation	1
Cell Length	0.1 cm
Concentration	0.0005 mol/L
Temperature	Room Temperature
Sample name	MeOH
Operator	Jared Hammill
Comment	

Figure 11. CD Spectrum of **JTH-NB72-40** (0.5 mmol) in MeOH

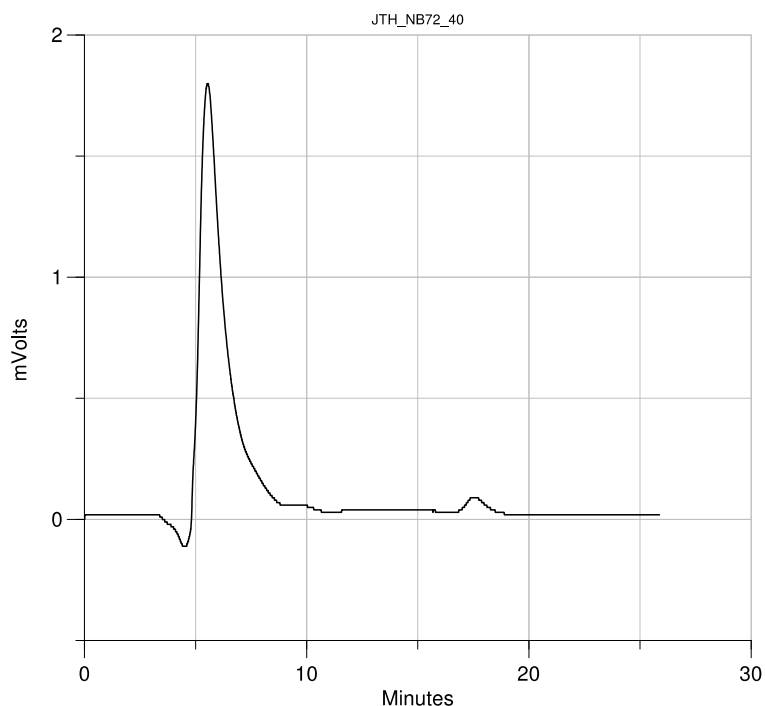
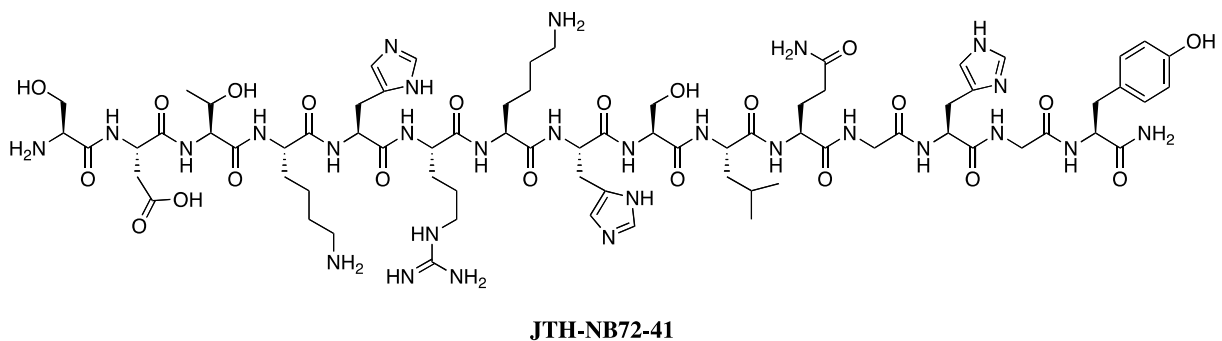


Figure 12. Analytical HPLC trace of **JTH-NB72-40** using a linear gradient of 30-50% buffer B in A (A: water containing 0.1% TFA, B: MeOH) over 20 min with UV detection at 220 nm at a flow rate of 0.5 mL/min.



SDTKHRKHSLQGHGY (JTH-NB72-41). Prepared according to general procedure A utilizing the following amino acid sequence: Fmoc-L-Tyr(tBu)-OH (0.161 g, 0.350 mmol, 3.50 equiv), Fmoc-L-Gly-OH (0.104 g, 0.350 mmol, 3.50 equiv), Fmoc-L-His(Trt)-OH (0.217 g, 0.350 mmol, 3.50 equiv), Fmoc-L-Gly-OH (0.104 g, 0.350 mmol, 3.50 equiv), Fmoc-L-Gln(Trt)-OH (0.214 g, 0.350 mmol, 3.50 equiv), Fmoc-L-Leu-OH (0.124 g, 0.350 mmol, 3.50 equiv), Fmoc-L-Ser(tBu)-OH (0.134 g, 0.350 mmol, 3.50 equiv), Fmoc-L-His(Trt)-OH (0.217 g, 0.350 mmol, 3.50 equiv), Fmoc-L-Lys(Boc)-OH (0.164 g, 0.350 mmol, 3.50 equiv), Fmoc-L-Arg(Pbf)-OH (0.227 g, 0.350 mmol, 3.50 equiv), Fmoc-L-His(Trt)-OH (0.217 g, 0.350 mmol, 3.50 equiv), Fmoc-L-Lys(Boc)-OH (0.164 g, 0.350 mmol, 3.50 equiv), Fmoc-L-Thr(tBu)-OH (0.139 g, 0.350 mmol, 3.50 equiv), Fmoc-L-Asp(OtBu)-OH (0.144 g, 0.350 mmol, 3.50 equiv), Fmoc-L-Ser(tBu)-OH (0.134 g, 0.350

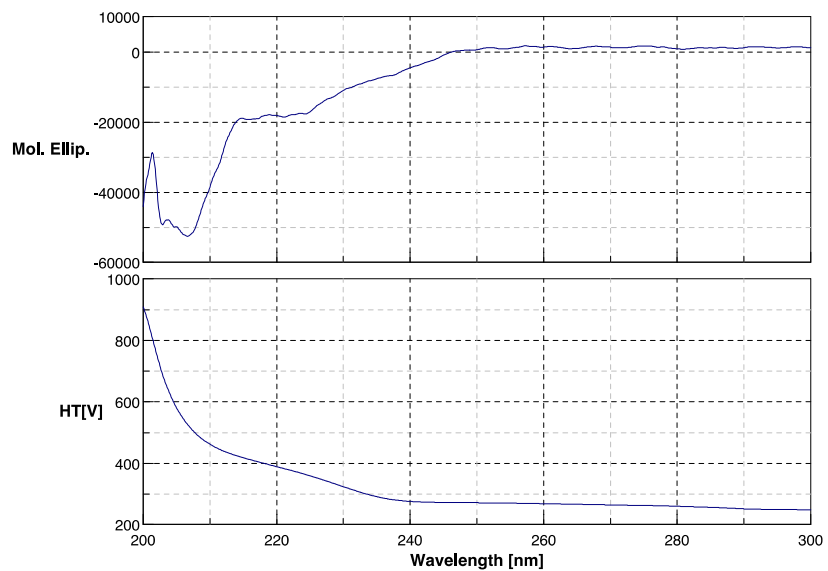
mmol, 3.50 equiv). **JTH-NB72-41** (0.0191 g, 11%) was obtained as colorless to white crystals. The sample was subjected to HPLC purification twice using a linear gradient of 30-60% buffer B in A (A: water containing 0.1% TFA, B: MeOH) over 30 min. The product was characterized by ^1H NMR (Table 7); ^{13}C NMR (Table 7); DEPT-135; COSY; HMBC; HMQC; HPLC RT 5.5 min. HRMS (MALDI $^+$) m/z calcd for $\text{C}_{74}\text{H}_{116}\text{N}_{28}\text{O}_{22}$ $[\text{M}+\text{Na}]^+$ 1749.8897, Found 1749.8827.

Table 7. ^1H and ^{13}C NMR Data for **JTH-NB72-41** (700 MHz/150 MHz) in D_2O (298 K) with MeOH as an internal reference (referenced to 3.34 ppm (^1H) and 49.5 ppm (^{13}C)).

Residue #	Amino Acid (N->C)	Resonance	^1H δ [ppm]	^{13}C δ [ppm]
1	Serine	CO		168.5
		C_αH	4.19 (t, $J = 4.9$ Hz, 1 H)	55.0
		C_βH	3.88-3.79 (m, 2 H)	60.8
2	Aspartic Acid	CO		173.1
		C_αH	4.88 (t, $J = 6.7$ Hz, 1 H)	50.8
		C_βH	2.96-2.91 (m, 1 H), 2.90-2.85 (m, 1 H)	36.3
		C_γ		175.0
3	Threonine	CO		172.1
		C_αH	4.27 (d, $J = 4.7$ Hz, 1 H)	60.0
		C_βH	4.21-4.16 (m, 1 H)	67.4
		C_γH	1.17 (d, $J = 6.4$ Hz, 3 H)	19.5
4	Lysine	CO		174.3
		C_αH	4.24 (dd, $J = 5.9, 8.3$ Hz, 1 H)	53.2
		C_βH	1.78-1.69 (m, 2 H)	30.5
		C_γH	1.48-1.39 (m, 2 H)	22.8
		C_δH	1.69-1.54 (m, 2 H)	26.8
		$\text{C}_\epsilon\text{H}$	3.00-2.93 (m, 2 H)	39.7
5	Histidine	CO		172.4
		C_αH	4.73-4.68 (m, 1 H)	53.0
		C_βH	3.31-3.22 (m, 1 H), 3.18-3.11 (m, 1 H)	27.0
		C_γ		128.9

		C _δ H	7.29 (s, 1 H)	117.9
		C _ε H	8.62 (d, <i>J</i> = 1.2 Hz, 1 H)	134.1
6	Arginine	CO		174.0
		C _α H	4.31 (app dd, <i>J</i> = 8.1, 14.1 Hz, 1 H)	54.4
		C _β H	1.85-1.77 (m, 2 H)	29.0
		C _γ H	1.69-1.54 (m, 2 H)	22.8
		C _δ H	3.22-3.15 (m, 2 H)	41.1
		C _ε		157.3
7	Lysine	CO		174.3
		C _α H	4.31 (dd, <i>J</i> = 8.1, 14.1 Hz, 1 H)	53.8
		C _β H	1.78-1.69 (m, 2 H)	31.0
		C _γ H	1.39-1.30 (m, 2 H)	22.8
		C _δ H	1.69-1.54 (m, 2 H)	26.9
		C _ε H	3.00-2.93 (m, 2 H)	39.8
8	Histidine	CO		172.7
		C _α H	4.73-4.68 (m, 1 H) 3.31-3.22 (m, 1 H),	53.1
		C _β H	3.18-3.11 (m, 1 H)	27.4
		C _γ		129.0
		C _δ H	7.30 (s, 1 H)	117.9
		C _ε H	8.63 (d, <i>J</i> = 1.1 Hz, 1 H)	134.1
9	Serine	CO		175.1
		C _α H	4.43 (t, <i>J</i> = 5.7 Hz, 1 H)	56.0
		C _β H	4.03-3.96 (m, 2 H)	61.7
10	Leucine	CO		172.0
		C _α H	4.36 (dd, <i>J</i> = 5.2, 9.4 Hz, 1 H)	54.3
		C _β H	1.78-1.69 (m, 2 H)	40.1
		C _γ H	1.69-1.54 (m, 1 H)	25.0
			0.89 (d, <i>J</i> = 5.8 Hz, 3 H),	22.8,
		C _δ H	0.84 (d, <i>J</i> = 5.8 Hz, 3 H)	21.3
11	Glutamine	CO		174.2
		C _α H	4.31 (dd, <i>J</i> = 8.1, 14.1 Hz, 1 H)	53.9
			2.08 (dt, <i>J</i> = 13.5, 7.4 Hz, 1 H),	
		C _β H	1.96 (dt, <i>J</i> = 7.4, 15.8, Hz, 1 H)	27.4
		C _γ H	2.33 (t, <i>J</i> = 7.5 Hz, 2 H)	31.6

		C _δ		178.4
12	Glycine	CO		171.6
		C _α H	3.86 (s, 2 H)	43.0
13	Histidine	CO		172.3
		C _α H	4.67 (dd, <i>J</i> = 5.7, 8.5 Hz, 1 H)	52.8
			3.31-3.22 (m, 1 H),	
		C _β H	3.18-3.11 (m, 1 H)	27.0
		C _γ		128.8
		C _δ H	7.26 (s, 1 H)	117.9
		C _ε H	8.61 (d, <i>J</i> = 1.2 Hz, 1 H)	134.1
14	Glycine	CO		171.8
		C _α H	3.93-3.89 (m, 2 H)	43.0
15	Tyrosine	CO		176.4
		C _α H	4.53 (dd, <i>J</i> = 5.9, 8.7 Hz, 1 H)	55.5
			3.08 (dd, <i>J</i> = 5.8, 14.1 Hz, 1 H),	
		C _β H	2.91 (dd, <i>J</i> = 8.9, 14.1 Hz, 1 H)	36.9
		C _γ		129.0
		C _δ H	7.12 (d, <i>J</i> = 8.4 Hz, 2 H)	131.2
		C _ε H	6.81 (d, <i>J</i> = 8.5 Hz, 2 H)	116.0
		C _ζ		155.0



Date 2/10/2009 8:27PM
 File name JTH_NB72_41_Standard_Subtracted_MeOH_MoL_ellip_Smooth.jws
 Model J-815
 Serial No. A019361168
 Band width 1 nm
 Response 1 sec
 Sensitivity Standard
 Measurement range 300 - 200 nm
 Data pitch 0.1nm
 Scanning speed 50 nm/min
 Accumulation 1
 Cell Length 0.1 cm
 Concentration 0.0005 mol/L
 Temperature Room Temperature

Figure 13. CD spectrum of JTH-NB72-41 (0.5 mmol) in MeOH

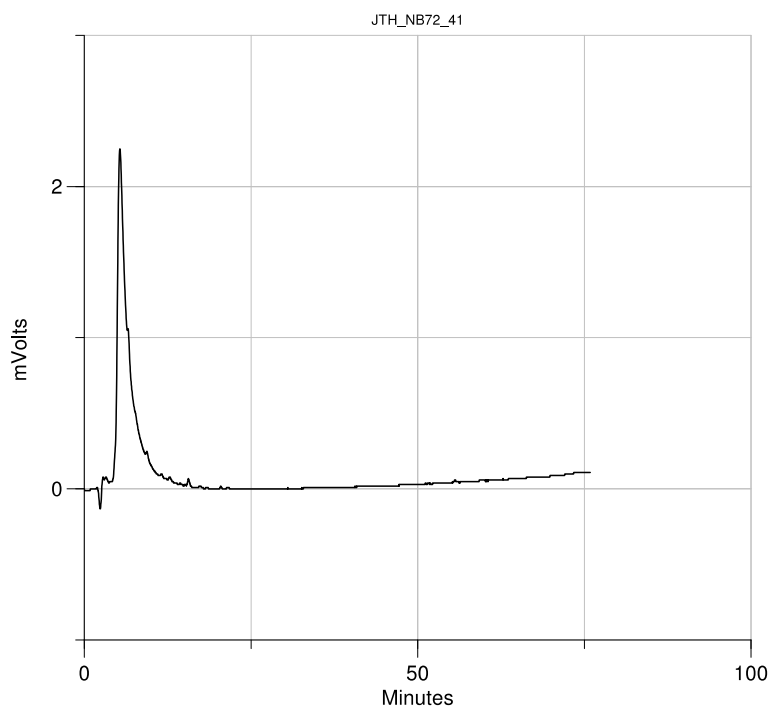
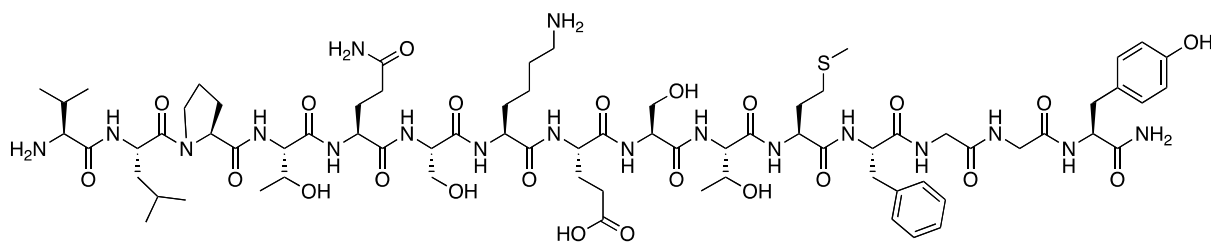


Figure 14. Analytical HPLC trace of **JTH-NB72-41** using a linear gradient of 30-100% buffer B in A (A: water containing 0.1% TFA, B: MeOH) over 70 min with UV detection at 220 nm at a flow rate of 0.7 mL/min.



JTH-NB72-42

VLPTQSKESTMFGGY (JTH-NB72-42). Prepared according to general procedure A utilizing the following amino acid sequence: Fmoc-L-Tyr(tBu)-OH (0.161 g, 0.350 mmol, 3.50 equiv), Fmoc-L-Gly-OH (0.104 g, 0.350 mmol, 3.50 equiv), Fmoc-L-Gly-OH (0.104 g, 0.350 mmol, 3.50 equiv), Fmoc-L-Phe-OH (0.136 g, 0.350 mmol, 3.50 equiv), Fmoc-L-Met-OH (0.130 g, 0.350 mmol, 3.50 equiv), Fmoc-L-Thr(tBu)-OH (0.139 g, 0.350 mmol, 3.50 equiv), Fmoc-L-Ser(tBu)-OH (0.134 g, 0.350 mmol, 3.50 equiv), Fmoc-L-Glu(tBu)-OH (0.149 g, 0.350 mmol, 3.50 equiv), Fmoc-L-Lys(Boc)-OH (0.164 g, 0.350 mmol, 3.50 equiv), Fmoc-L-Ser(tBu)-OH (0.134 g, 0.350 mmol, 3.50 equiv), Fmoc-L-Gln(Trt)-OH (0.214 g, 0.350 mmol, 3.50 equiv), Fmoc-L-Thr(tBu)-OH (0.139 g, 0.350 mmol, 3.50 equiv), Fmoc-L-Pro-OH (0.118 g, 0.350 mmol, 3.50 equiv), Fmoc-L-Leu-OH (0.124 g, 0.350 mmol, 3.50 equiv), Fmoc-L-Val-OH (0.119 g, 0.350 mmol, 3.50 equiv). **JTH-NB72-42** (0.0140 g, 9%) was obtained as a white powder. The sample was

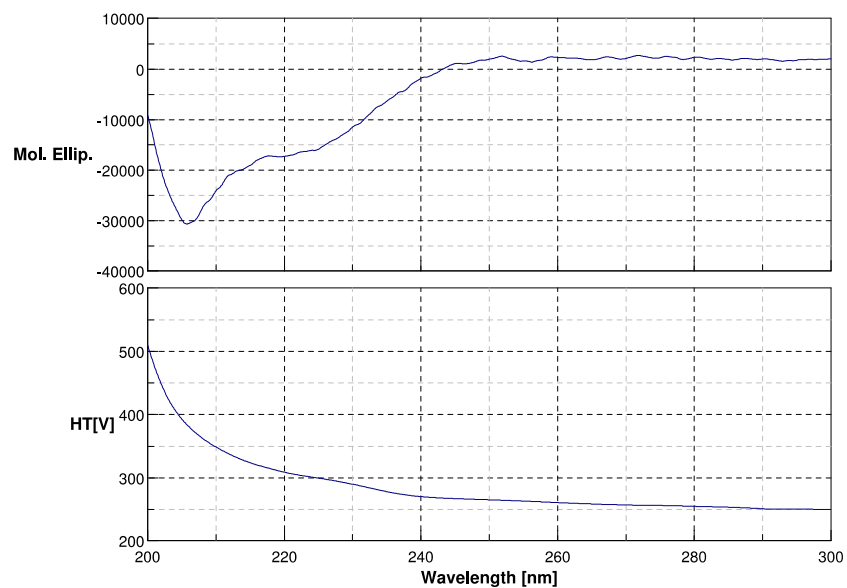
subjected to HPLC purification twice using a linear gradient of 30-70% buffer B in A (A: water containing 0.1% TFA, B: MeOH) over 40 min. The product was characterized by ^1H NMR (Table 8); ^{13}C NMR (Table 8); DEPT-135; COSY; HMBC; HMQC; HPLC RT 18.7 min, HRMS (MALDI⁺) m/z calcd for $\text{C}_{73}\text{H}_{114}\text{N}_{18}\text{O}_{23}\text{S}$ $[\text{M}+\text{H}]^+$ 1643.8103, Found 1643.8116.

Table 8. ^1H and ^{13}C NMR Data for **JTH-NB72-42** (600 MHz/150 MHz) in D_2O (298 K) with MeOH as an internal reference (referenced to 3.34 ppm (^1H) and 49.5 ppm (^{13}C)).

Residue #	Amino Acid (N->C)	Resonance	^1H δ [ppm]	^{13}C δ [ppm]
1	Valine	CO		169.9
		C_αH	3.83-3.78 (m, 1 H)	58.8
		C_βH	2.20 (qd, $J = 6.8, 13.6$ Hz, 1 H)	30.8
		C_γH	1.01 (d, $J = 6.9$ Hz, 3 H), 1.00 (d, $J = 6.9$ Hz, 3 H)	18.3, 17.4
2	Leucine	CO		172.6
		C_αH	4.69 (dd, $J = 10.2$ Hz, 1 H)	51.1
		C_βH	1.64-1.56 (m, 2 H)	39.7
		C_γH	1.74-1.67 (m, 1 H)	25.0
3	Proline	CO		174.9
		C_αH	4.50 (dd, $J = 6.0, 8.1$ Hz, 1 H)	61.1
		C_βH	2.34-2.29 (m, 1 H), 1.93-1.88 (m, 1 H)	30.0
		C_γH	2.05 (td, $J = 7.4, 14.7$, 2 H)	25.4
4	Threonine	CO		172.5
		C_αH	4.26 (d, $J = 4.8$ Hz, 1 H)	59.9
		C_βH	4.21-4.16 (m, 1 H)	67.4
		C_γH	1.16 (d, $J = 6.4$ Hz, 3 H)	19.5
5	Glutamic acid	CO		173.8
		C_αH	4.41-4.38 (m, 1 H)	53.6
		C_βH	2.16-2.08 (m, 2 H)	26.7
		C_γH	2.48 (t, $J = 7.5$ Hz, 1 H),	30.9

			2.48 (d, $J = 7.1$ Hz, 1 H)	
		C_{δ}		177.8
6	Serine	CO		173.1
		$C_{\alpha}H$	4.42 (t, $J = 5.7$ Hz, 1 H)	56.3
		$C_{\beta}H$	3.86-3.83 (m, 2 H)	61.5
7	Lysine	CO		174.2
		$C_{\alpha}H$	4.33-4.30 (m, 1 H)	54.5
			1.89-1.83 (m, 1 H),	
		$C_{\beta}H$	1.79-1.74 (m, 1 H)	30.8
		$C_{\gamma}H$	1.51-1.35 (m, 2 H)	22.7
		$C_{\delta}H$	1.70-1.65 (m, 2 H)	26.8
		$C_{\epsilon}H$	2.98 (t, $J = 7.5$ Hz, 2 H)	39.8
8	Glutamine	CO		176.3
		$C_{\alpha}H$	4.41-4.38 (m, 1 H)	53.6
		$C_{\beta}H$	2.02-1.97 (m, 2 H)	27.4
		$C_{\gamma}H$	2.39-2.34 (m, 2 H)	31.7
		C_{δ}		178.3
9	Serine	CO		174.6
		$C_{\alpha}H$	4.46 (t, $J = 5.5$ Hz, 1 H)	56.5
		$C_{\beta}H$	3.91-3.88 (m, 2 H)	61.7
10	Threonine	CO		172.8
		$C_{\alpha}H$	4.33-4.30 (m, 1 H)	59.9
		$C_{\beta}H$	4.25-4.21 (m, 1 H)	67.6
		$C_{\gamma}H$	1.22 (d, $J = 6.4$ Hz, 3 H)	19.6
11	Methionine	CO		174.9
		$C_{\alpha}H$	4.38 (dd, $J = 5.6, 8.8$ Hz, 1 H)	54.5
		$C_{\beta}H$	1.96-1.91 (m, 2 H)	30.7
			2.46-2.40 (m, 1 H),	
		$C_{\gamma}H$	2.35-2.29 (m, 1 H)	29.7
		$C_{\delta}H$	2.02 (s, 3 H)	14.7
12	Phenylalanine	CO		174.2
		$C_{\alpha}H$	4.63 (dd, $J = 7.3, 8.3$ Hz, 1 H)	55.7
			3.17 (dd, $J = 6.8, 13.9$ Hz, 1 H),	
		$C_{\beta}H$	3.04 (dd, $J = 8.8, 13.9$ Hz, 1 H)	37.3

		C _γ		127.8
		C _δ H	7.26 (d, <i>J</i> = 7.1 Hz, 2 H)	129.8
		C _ε H	7.34 (t, <i>J</i> = 7.6 Hz, 2 H)	129.4
		C _ζ H	7.26-7.23 (m, 1 H)	136.9
13	Glycine	CO		172.3
		C _α H	3.88 (s, 2 H)	43.2
14	Glycine	CO		171.5
		C _α H	3.82 (d, <i>J</i> = 6.0 Hz, 2 H)	42.9
15	Tyrosine	CO		176.3
		C _α H	4.53 (dd, <i>J</i> = 5.8, 9.0 Hz, 1 H)	55.5
			3.11 (dd, <i>J</i> = 5.7, 14.1 Hz, 1 H),	
		C _β H	2.92 (dd, <i>J</i> = 9.1, 14.1 Hz, 1 H)	36.8
		C _γ		128.9
		C _δ H	7.16 (d, <i>J</i> = 8.4 Hz, 2 H)	131.2
		C _ε H	6.85 (d, <i>J</i> = 8.4 Hz, 2 H)	116.1
		C _ζ		155.1



Date	2/10/2009 8:55PM
File name	JTH_NB72_42_Standard_Subtract_MeOH_Moll_Elip_Smooth.jws
Model	J-815
Serial No.	A019361168
Band width	1 nm
Response	1 sec
Sensitivity	Standard
Measurement range	300 - 200 nm
Data pitch	0.1nm
Scanning speed	50 nm/min
Accumulation	1
Cell Length	0.1 cm
Concentration	0.0005 mol/L
Temperature	Room Temperature

Figure 15. CD spectrum of **JTH-NB72-42** (0.5 mmol) in MeOH

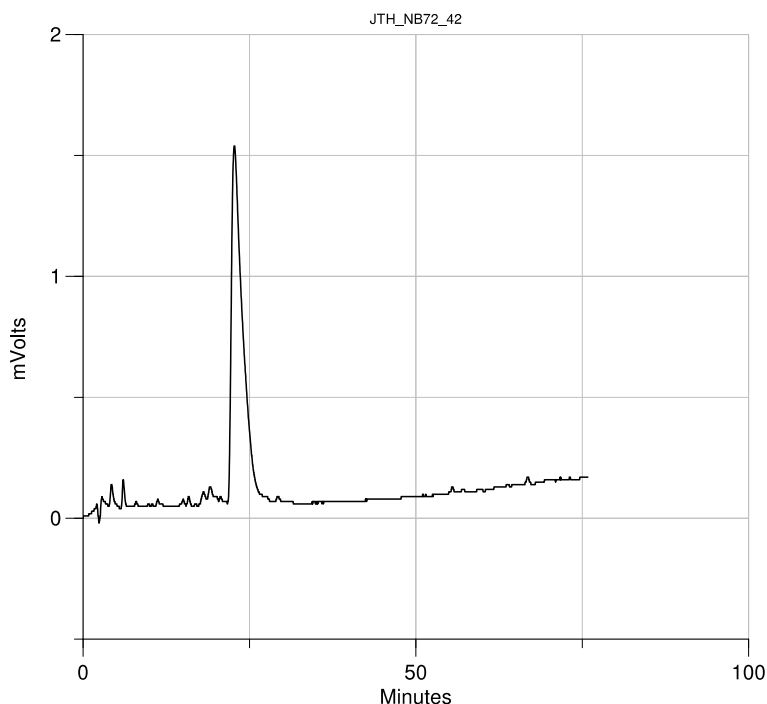
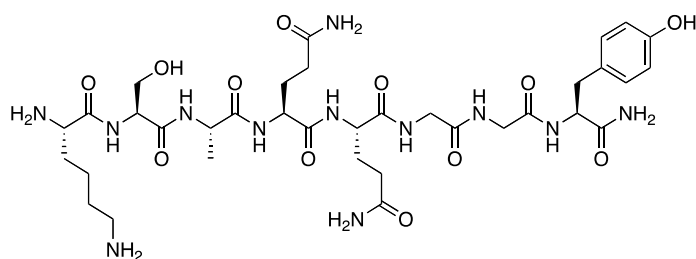


Figure 16. Analytical HPLC trace of **JTH-NB72-42** using a linear gradient of 30-100% buffer B in A (A: water containing 0.1% TFA, B: MeOH) over 70 min with UV detection at 220 nm at a flow rate of 0.7 mL/min.



JTH-NB72-60

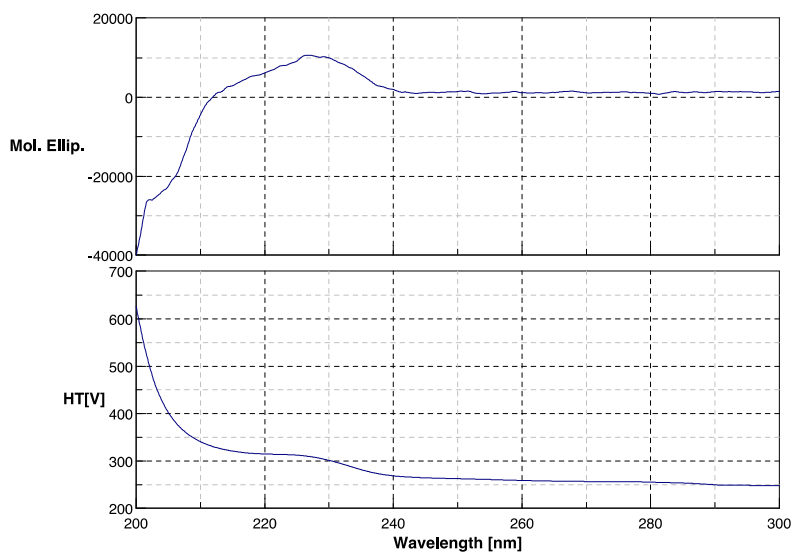
KSAQQGGY (JTH-NB72-60). Unlike the other syntheses presented, DEPBT used in this sequence was not purchased but synthesized according to literature protocols.⁵¹ **JTH-NB72-60** was prepared according to general procedure A utilizing the following amino acid sequence: Fmoc-L-Tyr(tBu)-OH (0.161 g, 0.350 mmol, 3.50 equiv), Fmoc-L-Gly-OH (0.104 g, 0.350 mmol, 3.50 equiv), Fmoc-L-Gly-OH (0.104 g, 0.350 mmol, 3.50 equiv), Fmoc-L-Gln(Trt)-OH (0.214 g, 0.350 mmol, 3.50 equiv), Fmoc-L-Gln(Trt)-OH (0.214 g, 0.350 mmol, 3.50 equiv), Fmoc-L-Ala-OH (0.115 g, 0.350 mmol, 3.50 equiv), Fmoc-L-Ser(tBu)-OH (0.134 g, 0.350 mmol, 3.50 equiv), Fmoc-L-Lys(Boc)-OH (0.164 g, 0.350 mmol, 3.50 equiv). **JTH-NB72-60** (0.0465 g, 56%) was obtained as colorless to white crystals: The sample was subjected to HPLC purification using a linear gradient of 30-50% buffer B in A (A: water containing 0.1% TFA, B: MeOH) over 20 min. The product was characterized by ¹H NMR (Table 9); ¹³C NMR (Table 9); DEPT-135; COSY;

HMBC; HMQC; HPLC RT 4.8 min, HRMS (MALDI⁺) *m/z* calcd for C₃₅H₅₆N₁₂O₁₂ [M+Na]⁺ 859.4039, Found 859.4034.

Table 9. ¹H and ¹³C NMR Data for **JTH-NB72-60** (600 MHz/150 MHz) in D₂O (298 K) with MeOH as an internal reference (referenced to 3.34 ppm (¹H) and 49.5 ppm (¹³C)).

Residue #	Amino Acid (N->C)	Resonance	¹ H δ [ppm]	¹³ C δ [ppm]
1	Lysine	CO		170.4
		C _α H	4.08 (t, <i>J</i> = 6.6 Hz, 1 H)	53.4
		C _β H	1.96-1.86 (m, 2 H)	31.0
		C _γ H	1.47 (dt, <i>J</i> = 7.6, 16.3 Hz, 2 H)	21.8
		C _δ H	1.70 (app td, <i>J</i> = 7.6, 15.2 Hz, 2 H)	27.0
		C _ε H	2.99 (t, <i>J</i> = 7.6 Hz, 2 H)	39.6
2	Serine	CO		171.7
		C _α H	4.51 (app dd, <i>J</i> = 5.5, 10.1 Hz, 1 H)	55.9
		C _β H	3.89 (dd, <i>J</i> = 5.9, 8.9 Hz, 2 H)	61.8
3	Alanine	CO		175.6
		C _α H	4.33-4.29 (m, 1 H)	50.6
		C _β H	1.39 (t, <i>J</i> = 9.9 Hz, 3 H)	17.0
4	Glutamine	CO		174.3
		C _α H	4.29 (dd, <i>J</i> = 6.5, 9.1 Hz, 1 H)	53.9
		C _β H	2.04-1.95 (m, 2 H)	27.3
		C _γ H	2.35 (dt, <i>J</i> = 15.3, 7.6 Hz, 2 H)	31.7
		C _δ		178.4
5	Glutamine	CO		173.9
		C _α H	4.34 (dd, <i>J</i> = 5.4, 8.9 Hz, 1 H)	53.8
		C _β H	2.14-2.05 (m, 2 H)	27.3
		C _γ H	2.35 (dt, <i>J</i> = 15.3, 7.6 Hz, 2 H)	31.6
		C _δ H		178.4
6	Glycine	CO		172.6
		C _α H	3.95 (d, <i>J</i> = 11.0 Hz, 2 H),	43.1
7	Glycine	CO		172.4

		C _α H	3.86 (s, 2 H)	42.9
8	Tyrosine	CO		176.4
		C _α H	4.51 (app dd, <i>J</i> = 5.5, 10.1 Hz, 1 H)	55.5
		C _β H	3.09 (dd, <i>J</i> = 5.8, 14.1 Hz, 1 H), 2.91 (dd, <i>J</i> = 8.9, 14.1 Hz, 1 H)	36.8
		C _γ		128.9
		C _δ H	7.14 (d, <i>J</i> = 8.4 Hz, 2 H)	131.4
		C _ε H	6.83 (d, <i>J</i> = 8.4 Hz, 2 H)	116.0
		C _ζ H		155.0



Date 2/10/2009 8:42PM
 File name JTH_NB72_60_Standard_Subtract_MeOH_Moll_Elipp_Smooth.jws
 Model J-815
 Serial No. A019361168
 Band width 1 nm
 Response 1 sec
 Sensitivity Standard
 Measurement range 300 - 200 nm
 Data pitch 0.1nm
 Scanning speed 50 nm/min
 Accumulation 1
 Cell Length 0.1 cm
 Concentration 0.0005 mol/L
 Temperature Room Temperature

Figure 17. CD spectrum of **JTH-NB72-60** (0.5 mmol) in MeOH

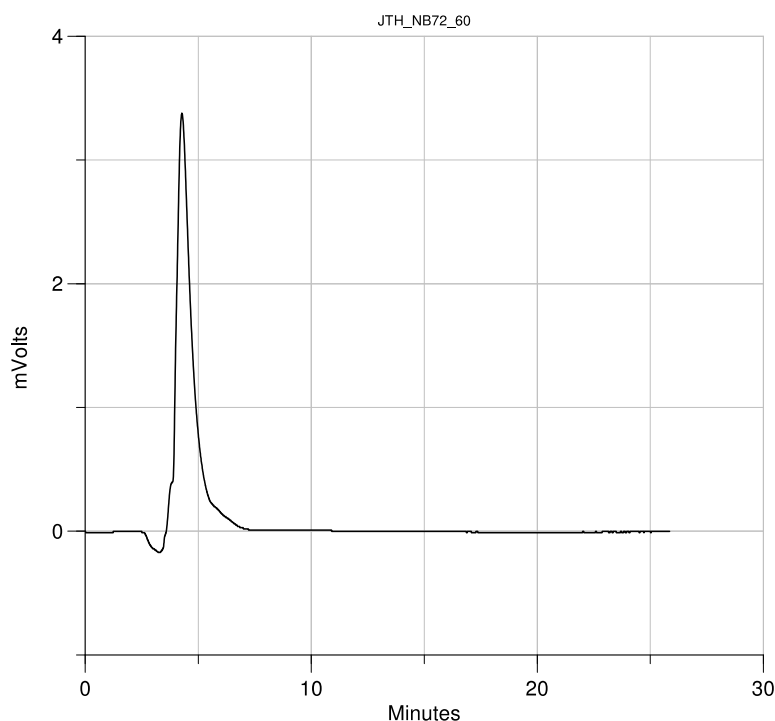
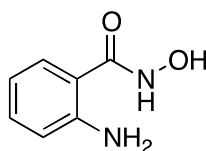
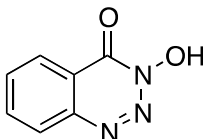


Figure 18. Analytical HPLC trace of **JTH-NB72-60** using a linear gradient of 30-50% buffer B in A (A: water containing 0.1% TFA, B: MeOH) over 20 min with UV detection at 220 nm at a flow rate of 0.5 mL/min.



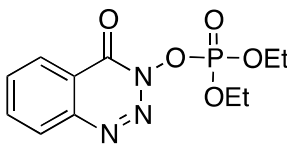
1.4

2-Amino-N-hydroxybenzamide (1.4).⁶³ To a stirred solution of NaOH (24.0 g, 0.600 mol, 4 equiv) in H₂O (150 mL) at 0 °C was slowly added hydroxylamine hydrochloride (20.8 g, 0.300 mol, 2 equiv). To the resulting solution was added methyl anthranilate (22.6 g, 0.150 mol, 1 equiv), followed by methanol (200 mL). The mixture was allowed to stir for 2 d under TLC control, and concentrated under reduced pressure until the sodium salt of the hydroxamic acid began to precipitate (~50 mL). The salt was filtered and washed with cold water. The pH of the filtrate was adjusted to 6 with conc. HCl and the free hydroxamic acid was precipitated. The precipitate was filtered, washed with cold water, the volume of the resulting filtrate was reduced *in vacuo*, the pH adjusted to 6 and the precipitate filtered. This process was repeated until no more precipitate was obtained to give **1.4** (17.6 g, 77%) as small white crystals: ¹H NMR (300 MHz, DMSO-*d*₆) 10.91 (bs, 1 H), 8.83 (s, 1 H), 7.30 (dd, 1 H, *J* = 1.5, 8.1 Hz), 7.12 (dt, 1 H, *J* = 1.5, 7.2 Hz), 6.69 (dd, 1 H, *J* = 1.2, 8.4 Hz), 6.47 (dt, 1 H, *J* = 1.2, 7.8 Hz), 6.22 (bs, 2 H); ¹³C NMR (75 MHz, DMSO-*d*₆) 167.0, 149.3, 131.6, 127.5, 116.2, 114.7, 113.1.



1.5

3-Hydroxybenzo-1,2,3-triazin-4(3H)-one (1.5).⁶³ A solution of **1.4** (10.5 g, 69.0 mmol, 1 equiv) in conc. HCl (18 mL) was diluted with H₂O (200 mL) and cooled to 0 °C. A pre-cooled (0 °C) solution of NaNO₂ (5.21 g, 75.6 mmol, 1.1 equiv) in H₂O (6.25 mL) was added slowly to the mixture at 0 °C. The resulting heterogeneous solution was allowed to stir at room temperature for 2 h. The precipitate was filtered and recrystallized from boiling ethanol to give **1.5** (9.26 g, 82%) as white crystals: ¹H NMR (300 MHz, DMSO-*d*₆); 12.9 (s, 1 H), 8.28 (d, 1 H, *J* = 3.6 Hz), 8.23 (d, 1 H, *J* = 3.5 Hz), 8.09 (t, 1 H, *J* = 3.3 Hz), 7.93 (t, 1 H, *J* = 3.3 Hz); ¹³C NMR (75 MHz, DMSO-*d*₆) 151.1, 143.9, 135.1, 132.5, 128.1, 124.8, 121.2.



1.6

3-(Diethoxyphosphoryloxy)-1,2,3-benzotriazin-4(3H)-one (1.6).⁵¹ To a solution of **1.5** (2.00 g, 12.3 mmol, 1 equiv) and triethylamine (1.71 mL, 12.3 mmol, 1 equiv) in CH₂Cl₂ (11.3 mL) at 0 °C was added a solution of freshly distilled diethyl chlorophosphate (2.02 mL, 14.0 mmol, 1.1 equiv) in CH₂Cl₂ (5.6 mL) was added dropwise over 1 h. The reaction was allowed to warm to rt and stirred for 3 h. The resulting heterogeneous mixture was filtered, and the filtrate was concentrated under reduced pressure. The resulting crude material was dissolved in EtOAc (30 mL), washed with water (x2), brine, dried (MgSO₄), and concentrated under reduced pressure. The resulting solid was recrystallized from EtOAc/hexanes to give **1.6** (2.74 g, 74%) as colorless to white crystals: *M*_p=73-73.5 °C; ¹H (600 MHz, CDCl₃) 8.38 (d, 1 H, *J* = 7.8 Hz), 8.22 (d, 1 H, *J* = 8.4 Hz), 8.00 (t, 1 H, *J* = 8.4 Hz), 7.84 (t, 1 H, 7.8 Hz) 4.57-4.47 (m, 4 H), 1.47 (t, 6 H, *J* = 3.6 Hz).

2.0 LIBRARY SYNTHESIS OF BICYCLO[3.3.1]NONANES

2.1 INTRODUCTION

Aranorosin was isolated from the fermentation broth of the fungal strain *Pseudoarachniotus roseus* by Fehlhaber *et al.* in 1988.^{64,65} It was found to possess antibiotic, antifungal, and antitumor properties.⁶⁴ Aranorosin's structure was assigned through extensive NMR studies and confirmed by synthesis in several groups, including our own.⁶⁴⁻⁶⁷ One of the most intriguing structural features of aranorosin is the *syn* orientation of the two epoxide oxygens and the spiro-ether oxygen. Aranorosin exists as a mixture of two epimeric hemiacetals, with the major isomer (Figure 19) orienting the amide and hydroxyl groups in a *syn* fashion comprising 75% of the mixture. At the time of our group's synthesis, the stereochemistry at the C(6') position had not been determined.

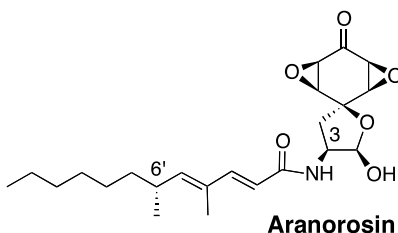
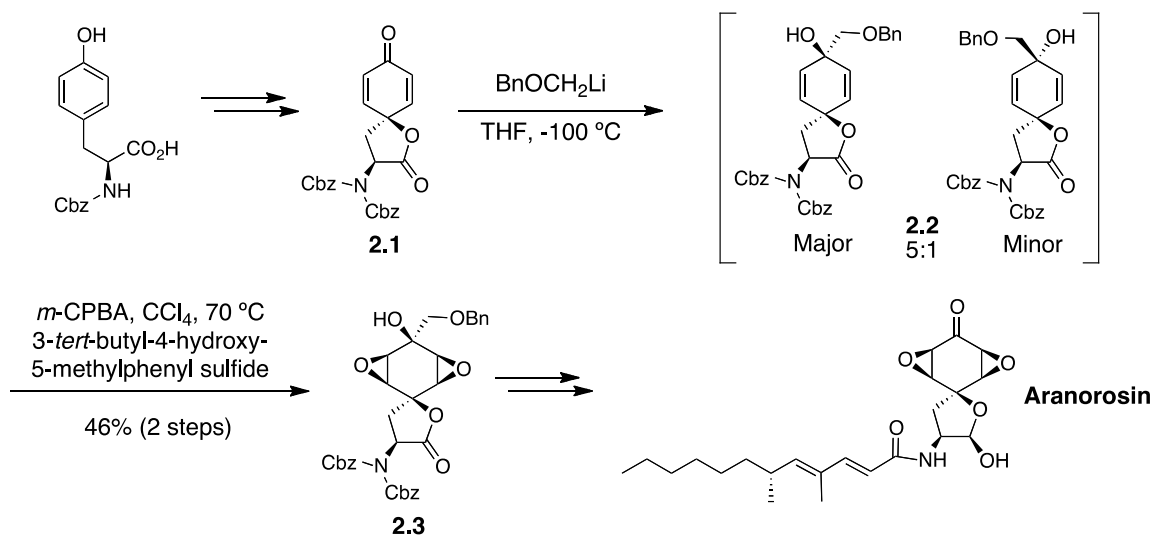


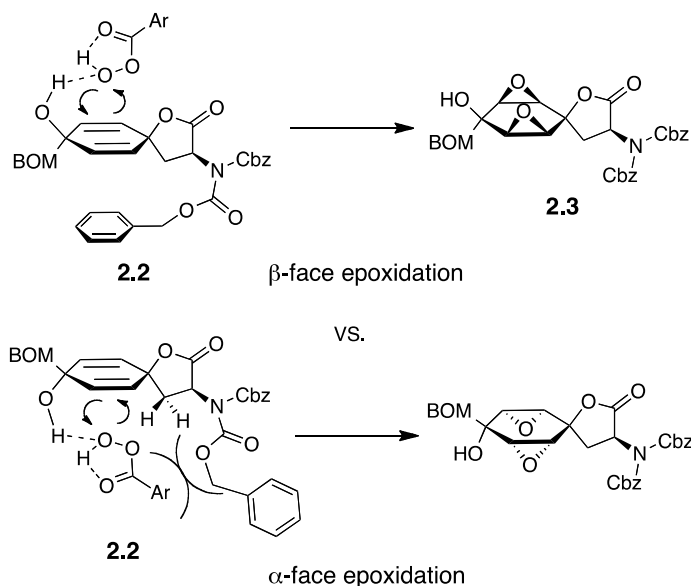
Figure 19. Major epimer of aranorosin

Our synthesis was successfully completed in 1993⁶⁶ and featured an elegant method to set the all *syn* oxygenation. A stereoselective addition of benzyloxy methyl lithium (BOMLi) to bis- α,β -unsaturated ketone **2.1**, followed by a Henbest epoxidation, directed by the newly formed tertiary alcohol **2.2**, gave the desired *syn* oxygenated product **2.3** in 46% yield (Scheme 10).⁶⁶



Scheme 10. Key synthetic step in the Wipf group's synthesis of aranorosin

An important aspect that had to be considered in the addition reaction was the π -facial selectivity of the nucleophile as it approached the dienone. Gratifyingly, addition of the BOMLi nucleophile occurred in a 5:1 ratio favoring the desired attack to the α -face of the ketone (Scheme 11). In subsequent work by Wipf and Kim, it was determined that the selectivity resulted from dipolar control. Hyperconjugative orbital stabilization in the transition state and orbital distortion effects appeared to be of secondary importance.⁶⁸ After addition of BOMLi, a Henbest epoxidation, in the presence of Kishi's radical inhibitor,⁶⁹ provided only the all *syn*-diepoxy (**2.3**). It was hypothesized that the observed selectivity during the epoxidation arises from a kinetic resolution. The steric congestion experienced by the peracid during its approach to the α -face of the dienone (**2.2**) (Scheme 11) caused the rate of α -face epoxidation to be slow enough that this reaction pathway was essentially inoperable under the reaction conditions. Therefore, although the reaction was performed on a crude mixture of isomeric addition products, only the desired *syn*-diepoxy **2.3** was isolated.



Scheme 11. Kinetic resolution resulting from steric congestion during the Henbest epoxidation

The authors did not report a crystal structure for **2.2**, but the relative stereochemistry of the product was supported by a weak (<1%) NOE between the BOM methylene protons and the methylene protons of the 5-membered spirocyclic ring (Figure 20). In addition, further support was derived from comparison to a model system in which a methyl Grignard reagent was used and a larger NOE (3%) was observed (Figure 20).⁷⁰

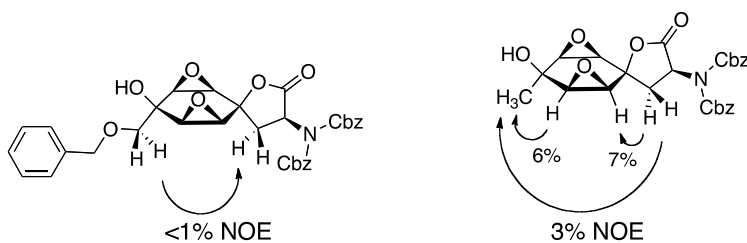


Figure 20. NOE correlations used to assign the relative stereochemistry of the epoxidation product

With the desired diepoxide **2.3** in hand, the synthesis continued via acylation with the unsaturated fatty acid side chain, followed by several functional group manipulations which led to both the natural product aranosin and its epimer at the C(6') position. Having successfully synthesized the target molecule and assigned the absolute stereochemistry of the remote C(6') stereocenter, our group sought to explore the natural product's reactivity toward biologically relevant nucleophiles.

Aranorosin possesses two characteristic segments: the oxaspiro[5.4]decane moiety and the unsaturated fatty acid chain. One could envision that both segments contain multiple sites that are susceptible to nucleophilic attack (Figure 21). Many examples demonstrate the potential reactivity between sulfhydryl groups from natural sources (*e.g.*, glutathione, cysteine) and α,β -unsaturated ketone functional groups of biologically active natural compounds.⁷¹⁻⁷³ Thus, Michael addition to the unsaturated fatty acid chain is likely to occur. In addition, Sharpless has done extensive studies of epoxide opening with thiol nucleophiles.^{74,75} Therefore, it became apparent that the compound may be readily intercepted by a thiol nucleophile such as glutathione or a cysteine.

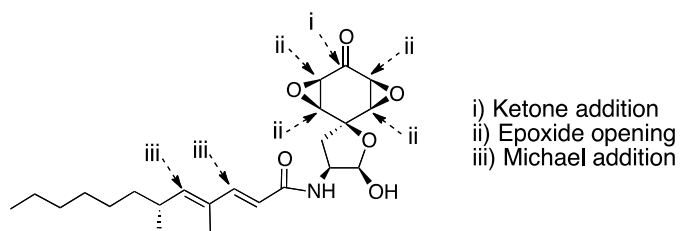
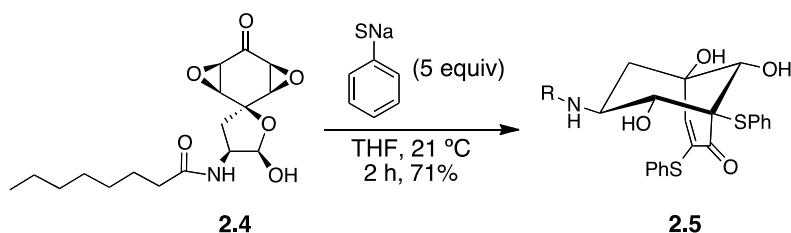


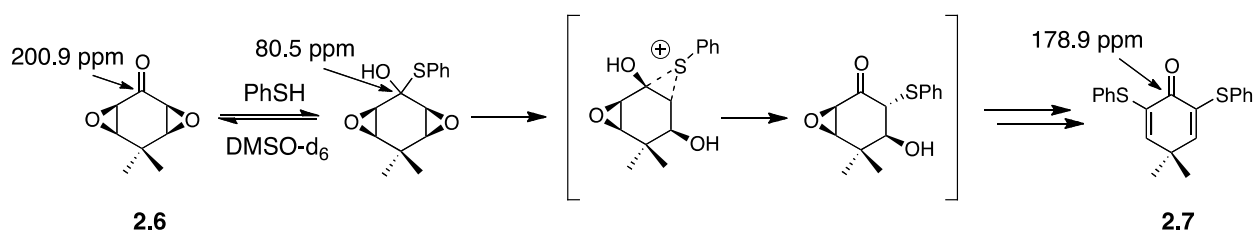
Figure 21. Potential sites of nucleophilic attack

Due to the large number of reactive sites, our group chose first to explore the reactivity of the oxaspiro[5.4]decane core of aranorosin, using the saturated side chain model system (**2.4**). This model removed the potential for Michael additions while allowing more rapid access to test material. Diepoxyketone **2.4** was treated with several nucleophiles containing either nucleophilic sulfur or nitrogen atoms. Interestingly, no reaction was observed with nitrogen containing nucleophiles such as dibenzylamine, pyrrole, or guanosine.⁷⁰ However, in the presence of sodium thiophenoxide, a substitute for glutathione, a novel reaction pathway led to the formation of bicyclo[3.3.1]nonane **2.5** (Scheme 12). The structure of the bicyclo[3.3.1]nonane **2.5** was rigorously elucidated via 1D and 2D NMR experiments.^{70,76}



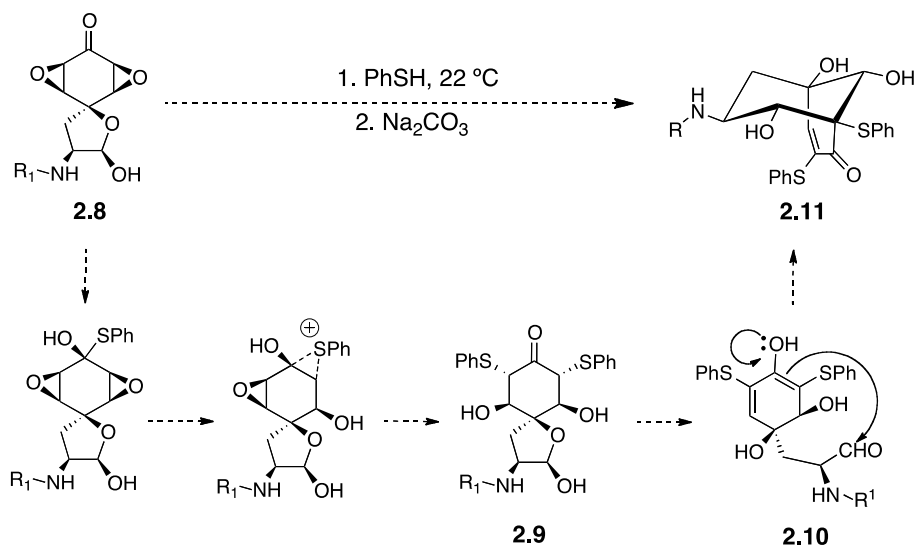
Scheme 12. Addition/rearrangement to access the bicyclo[3.3.1]nonane scaffold

Subsequent *in situ* NMR studies of ketone **2.6** revealed the initial conversion of the carbonyl carbon (200.9 ppm) to a hemithioacetal (80.5 ppm), followed by conversion to the bis- α,β -unsaturated ketone **2.7** (178.9 ppm) (Scheme 13).⁷⁶ Therefore, the first step is most likely the attack of the thiol nucleophile at the carbonyl group followed by a 1,2-migration and elimination.



Scheme 13. *In situ* NMR studies to gain mechanistic insight into the addition/rearrangement pathway

A hypothetical reaction mechanism was proposed (Scheme 14) in which an initial nucleophilic attack of thiophenol at the ketone **2.8**, followed by an irreversible 1,2-migration leads to opening of the epoxide. This sequence can be repeated to open the other epoxide and provide **2.9**. Sequential dehydration provided **2.10**, which underwent a base-catalyzed intramolecular aldol reaction to the lactol/aldehyde to furnish the bicyclo[3.3.1]nonane **2.11** (Scheme 14).⁷⁶ The intramolecular aldol reaction proceeded stereoselectively and only one diastereomer was observed.⁷⁷



Scheme 14. Proposed mechanism for the conversion of the spirocyclic diepoxyketone to the bicyclo[3.3.1]nonane scaffold

Based on this and similar results in closely related model systems, a new general reactivity pattern for the addition of thiol nucleophiles to diepoxyketones was elucidated.⁷⁶ Our group hypothesized that the intramolecular aldol reaction, which occurs in the lactol/aldehyde scaffold, could provide access to interesting derivatives, with stable carbon-sulfur linkages, for the diversity-oriented synthesis of libraries of bicyclic ring systems.

The National Institutes of Health have launched an ambitious Molecular Libraries Program whose goal is to enhance chemical biology efforts through high throughput screening. Our group has been interested in the development of new methodologies that can be applied to the syntheses of focused libraries of underrepresented chemotypes in the NIH libraries.⁷⁸ One of the most important questions that must be addressed before undertaking the synthesis of a focus library is how to design small-molecules possessing new structures and properties while populating the biologically relevant regions of chemical space.⁷⁸ One solution is to design natural product-like libraries.

Natural products have had a profound impact on both chemical biology and drug discovery. Over the last 70 years, out of the 155 small molecules approved for the treatment of cancer in humans, 47% were either natural products or derived from natural products.⁷⁹ Natural product-like libraries can be filed into three categories: 1) libraries based on the core scaffold of an individual natural product, 2) libraries based on structural motifs that are found across an entire class of natural products, and 3) libraries that more generally mimic the structural

characteristics of natural products.⁸⁰ Our strategy focused on using the novel addition/rearrangement methodology discovered during our study of aranorosin to synthesize a small library of highly functionalized bicyclo[3.3.1]nonanes which resemble the core of the interesting natural products gymnastatins F⁸¹ and Q (Figure 22).⁸²

Gymnastatins F and Q were isolated from the extract of the *Halichondria* sponge-derived fungus *Gymnascella dankaliensis*. Their relative configurations have been established on the basis of spectroscopic analyses using 1D and 2D NMR techniques. Both gymnastatin F and Q were found to exhibit potent growth inhibition against murine P388 lymphocytic leukemia and human cancer cell lines.⁸¹ Furthermore, gymnastatin Q showed appreciable growth inhibition against BSY-1 (breast) and MKN7 (stomach) human cancer cell lines.⁸²

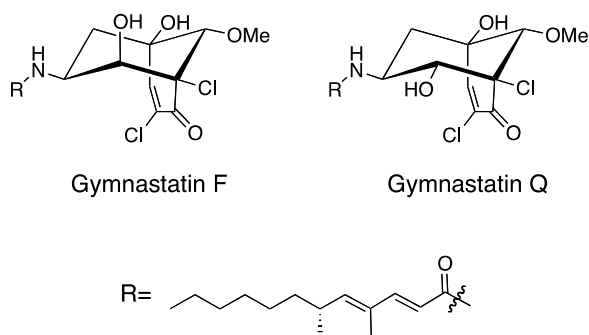


Figure 22. Structure of gymnastatin F and gymnastatin Q

We envisioned that our new reaction pathway could be utilized to offer intriguing analogues that possess the functionalized bicyclo[3.3.1]nonane core present in these natural products. By using a variety of thionucleophiles, and different acylating agents, diversity can be introduced at both the nitrogen and the carbon-sulfur linkages (Figure 23).

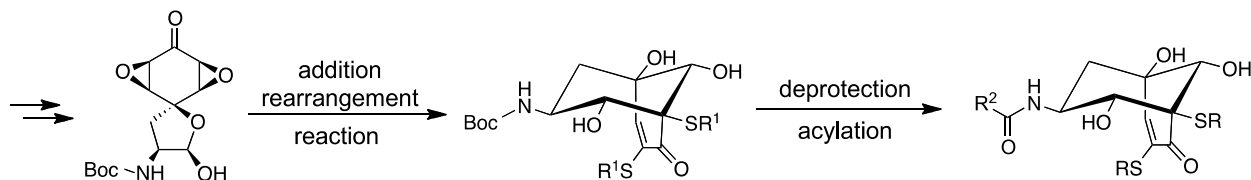
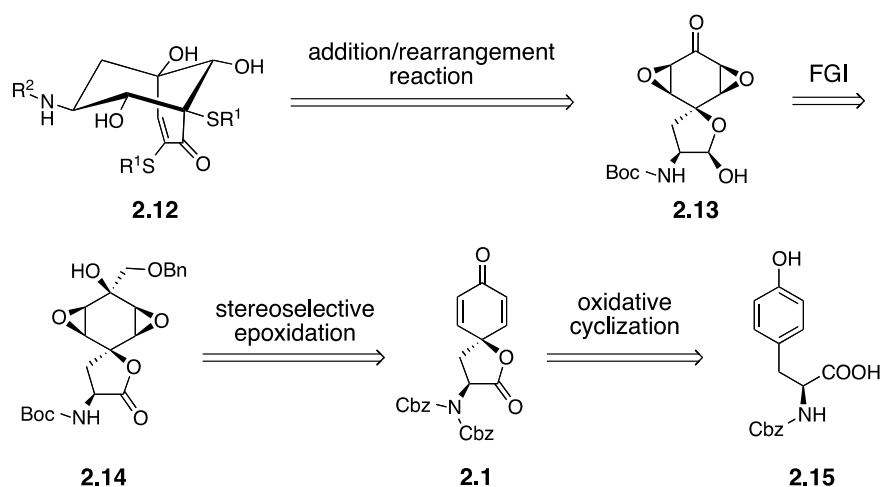


Figure 23. Diversification points of the bicyclo[3.3.1]nonane scaffold

2.2 LIBRARY SYNTHESIS OF BICYCLO[3.3.1]NONANES

2.2.1 First Generation Approach

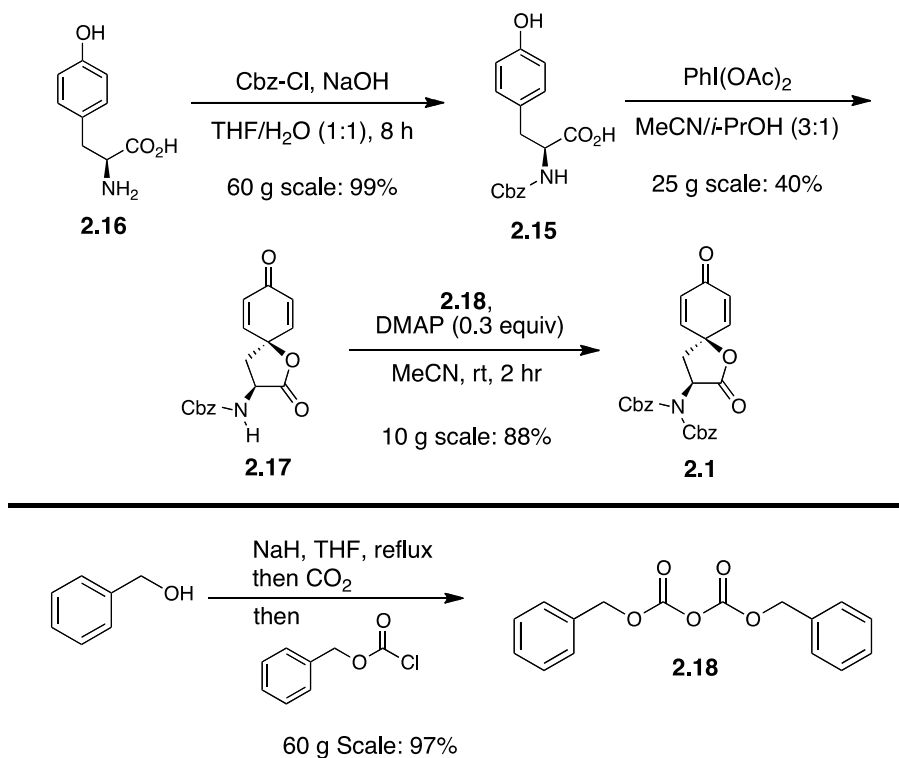
A retrosynthetic analysis of the functionalized scaffold is illustrated in Scheme 15. The diversified bicyclo[3.3.1]nonane scaffold **2.12** is accessed via the addition/rearrangement reaction from key intermediate **2.13**, followed by Boc removal and acylation. The use of different acylating as well as different thionucleophiles provides two points of diversification. The key intermediate **2.13** is closely related to an intermediate in the previously described synthesis of aranorosin (*vide supra*).⁶⁶ Therefore, in an analogous fashion the all *syn* oxygenation present in **2.14** will be set using addition of the BOMLi nucleophile to the corresponding dienone **2.1**, followed by a Henbest epoxidation. The dienone **2.1** can be readily accessed from Cbz-*L*-tyrosine **2.15** via oxidative cyclization methodology and a subsequent second Cbz protection.



Scheme 15. Retrosynthetic analysis of the diversified bicyclo[3.3.1]nonane scaffold

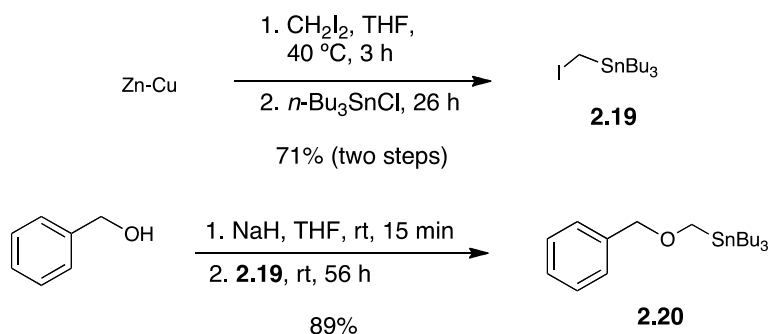
The synthetic route commenced with a scalable protection of *L*-tyrosine (**2.16**) with Cbz-Cl in a basic H₂O/THF medium to provide the protected amino acid **2.15** in quantitative yield. In a very scalable process (25 g), the Cbz-protected *L*-tyrosine was converted to the desired spirocycle **2.17** via an oxidative cyclization in the presence of iodobenzene diacetate (PIDA). Bis-protection of the amine with a second Cbz group proceeded to give **2.1** in good yield (88%)

in the presence of a catalytic amount of DMAP and Cbz₂O (**2.18**). Cbz₂O (**2.18**) was readily accessed on a 60 g scale in 97% yield via deprotonation of benzyl alcohol with NaH, trapping of the alkoxide with CO₂, followed by trapping of the resulting carbonate with Cbz-Cl. With the protected bis- α,β -unsaturated ketone **2.1** in hand, the key reaction to set the diepoxy function was investigated.



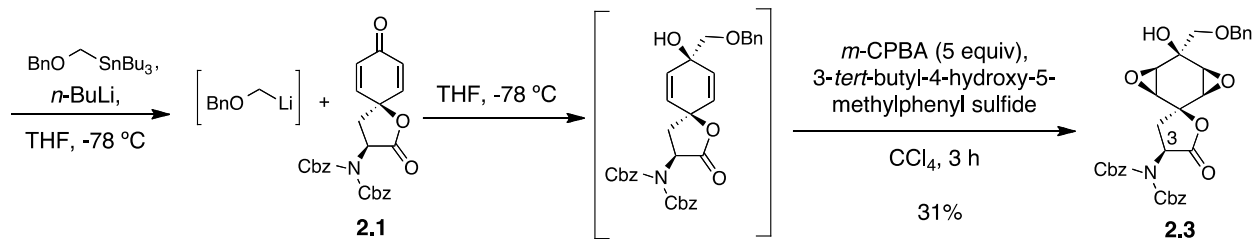
Scheme 16. Synthesis of **2.1**

Preparation of benzyloxymethyl stannane **2.20** (BOMSn(Bu)₃) was accomplished using a known procedure (Scheme 17).⁸³ Generation of a zinc-copper couple, followed by formation of iodomethylzinc iodide and transmetalation to tin provided iodomethylstannane **2.19** in 71% yield. Deprotonation of benzyl alcohol followed by S_N2 displacement of the iodide provided the desired benzyloxymethyl stannane **2.20** in 89% yield.



Scheme 17. Synthesis of BOMSnBu₃

Benzyloxymethyl lithium (BOMLi) was prepared *in situ* from the corresponding stannane with *n*-BuLi in THF at -78 °C and rapidly cannulated into a pre-cooled (-78 °C) solution of dienone **2.1** in THF. Due to the instability of the intermediate bis-allylic alcohol, the product was only partially purified and directly subjected to bis-epoxidation. Henbest epoxidation, directed by the newly formed tertiary alcohol, in the presence of *m*-CPBA and Kishi's radical inhibitor⁶⁹ in CCl₄ provided the desired diepoxy spirolactone **2.3** in 31% yield as a single diastereomer.



Scheme 18. First generation approach to the key intermediate **2.3**

Although the relative stereochemistry of diepoxy lactone **2.3** was previously assigned via a weak NOE correlation and comparison to model systems,^{70,76} the configuration could be unambiguously determined via single crystal X-ray analysis (Figure 24).

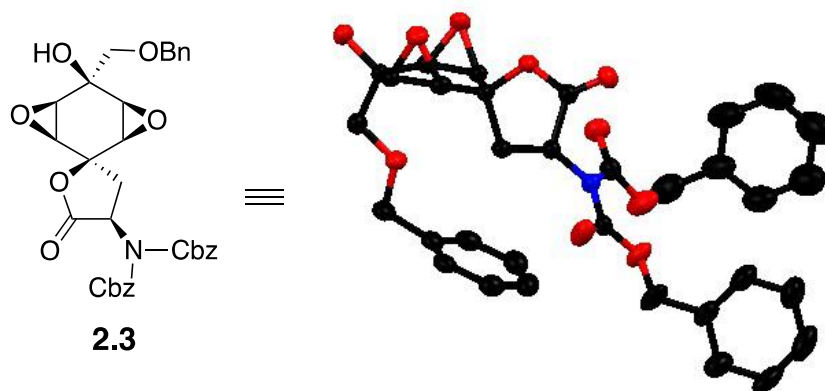
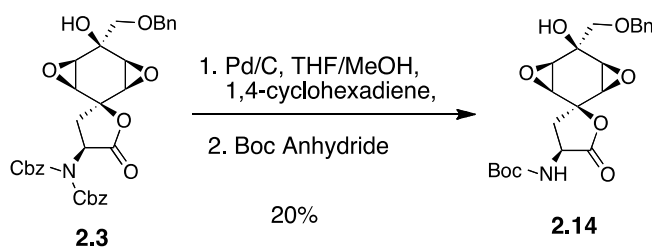


Figure 24. X-ray structure of diepoxy spirolactone **2.3** generated using the Mercury software package.⁸⁴

After confirming the relative stereochemistry of the desired diepoxy spirolactone **2.3**, the Cbz protecting groups were cleaved using Pd/C with 1,4-cyclohexadiene as a source of hydrogen in a 1:1 mixture of MeOH/THF. Protection of the resulting crude amine with Boc₂O proved to be a very low yielding process due to difficulties in purifying the desired product **2.14**.



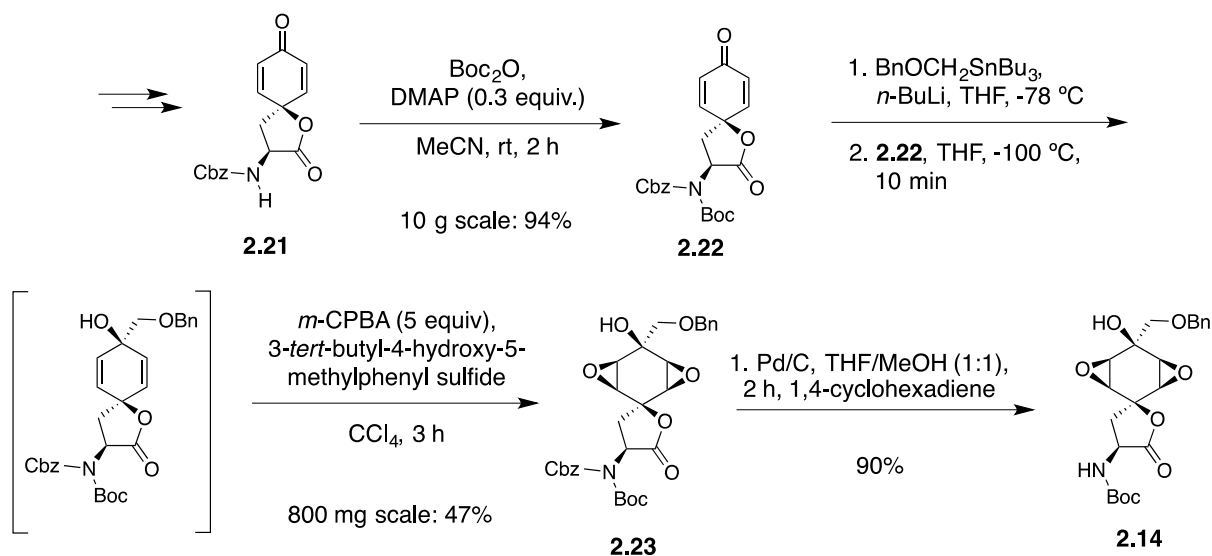
Scheme 19. Attempted deprotection/reprotection of bisepoxy spirolactone

In order to improve the possibility for a large scale production of the desired diepoxy ketone **2.14**, the protecting group scheme was altered so that the complete deprotection and reprotection of the amine was no longer required.

2.2.2 Second Generation Approach

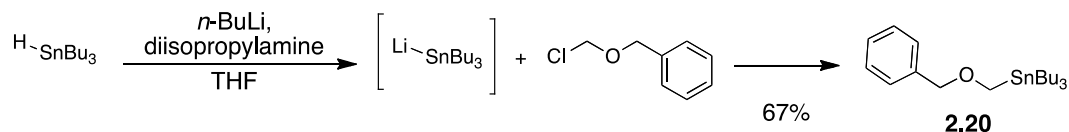
Starting from the dienone **2.21**, protection with Boc₂O proceeded smoothly in the presence of a catalytic amount of DMAP to give the desired bis-protected dienone **2.22** in 94% yield on 10 g scale. Gratifyingly, the addition/diepoxidation reaction of the Boc/Cbz-protected

spirolactone **2.22** proceeded at $-100\text{ }^{\circ}\text{C}$ to give **2.23** as a single diastereomer in an improved 47% yield. Selective Cbz removal in the presence of Pd/C with 1,4-cyclohexadiene in a 1:1 mixture of THF/MeOH provided the protected diepoxy spirolactone **2.14** in 90% yield.



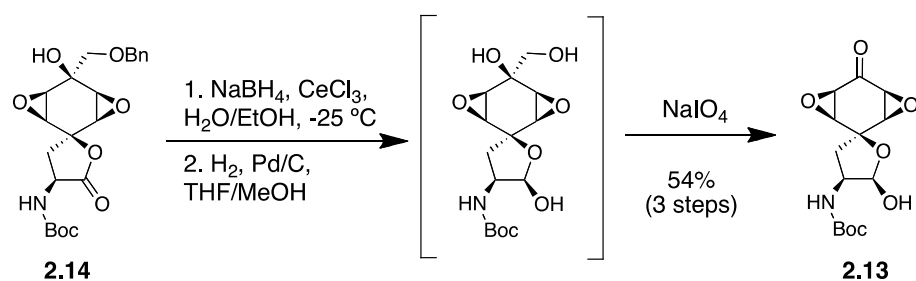
Scheme 20. Revised protection scheme to access diepoxy spirolactone

Upon scale-up of the route outlined in Scheme 20, it became apparent that the preparation of BOMSnBu_3 (**2.20**, Scheme 17) was experimentally challenging. A brief survey of the literature revealed that a more scalable procedure had been described.⁸⁵ Utilizing this new procedure BOMSnBu_3 **2.20** was prepared in one step in 67% yield (Scheme 21).



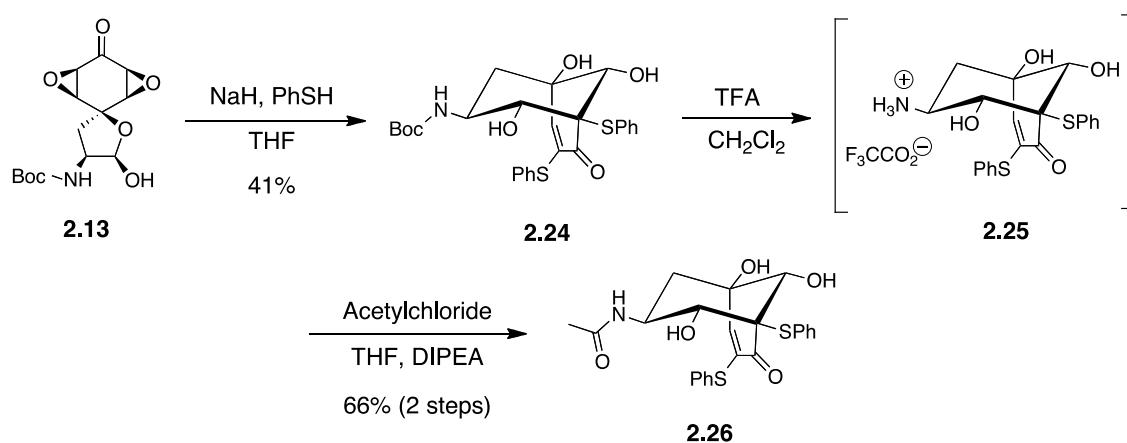
Scheme 21. Improved synthesis of BOMSnBu_3

With the diepoxy spirolactone **2.14** in hand, partial lactone reduction in the presence of sodium borohydride and cerium trichloride, benzyl removal with Pd/C and vigorously bubbling H_2 , and diol cleavage with sodium periodate provided the desired key intermediate **2.13** in 54% yield over 3 steps (Scheme 22).



Scheme 22. Preparation of key intermediate **2.13**

Replacement of the saturated alkyl side chain used in the previous study (Scheme 12) with a Boc group significantly decreased the yield of the thiol-mediated rearrangement. Using the reported procedure,⁷⁰ a solution of spirolactone **2.13** was treated with NaH (10 equiv) and thiophenol (5 equiv) in THF to afford the desired product **2.24** in 41% yield.



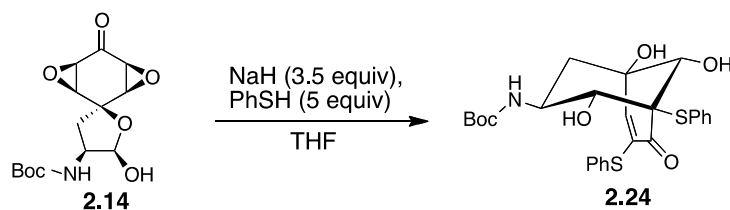
Scheme 23. Preparation of bicyclic amide **2.26**

The partially purified bicyclo[3.3.1]nonane **2.24** was deprotected in the presence of TFA in CH_2Cl_2 . A subsequent solvent swap, conversion to the free base with DIPEA, and addition of freshly distilled acetyl chloride afforded the acetylated bicyclo[3.3.1]nonane **2.26** along with an intractable impurity in a modest 66% yield.

It soon became clear that the addition/rearrangement sequence would need to be re-optimized in order to increase the yield. A solvent screen revealed that THF gave the highest, though still unacceptable, yield of 36% and the product always contained an intractable impurity (Table 10). In polar solvents such as acetonitrile, a decrease in yield to 23% was observed. Significant decomposition was observed in DMF and only 5% of the desired product was

isolated after purification. In 1,2-DME, the substrate quickly decomposed. In the non-polar solvent toluene, only 12% of the desired product was isolated due to the poor solubility of the substrate. Since THF produced the highest yield, the order of addition was explored in this solvent. Variation of addition sequence had little effect on the quantity of isolated product. In order to optimize the addition/rearrangement reaction a more readily accessible diepoxy ketone was needed.

Table 10. Solvent screen for addition/rearrangement reaction

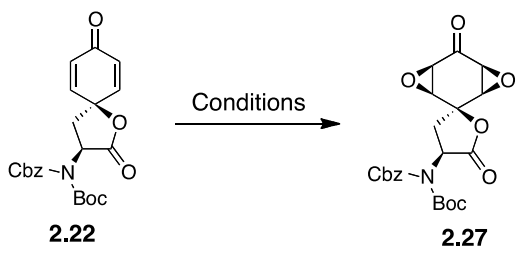


Entry	Solvent	Time	Yield of 2.24
1	ACN	18 h	23%
2 ^a	DMF	18 h	5%
3 ^b	1,2-DME	1 h	dec
4 ^c	THF	18 h	36%
5 ^d	Toluene	18 h	12 %

^aThe reaction immediately turned brown. ^bColor changed from clear to orange to brown. ^cAll orders of addition were explored with no improvement in yield. ^dThe reagents were not completely soluble in toluene.

2.2.3 Attempts to Directly Epoxidize Dienone 2.14

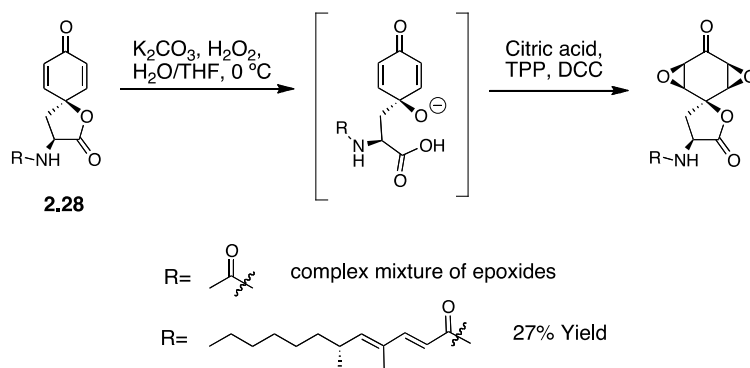
Next, the preparation of **2.27** by direct epoxidation of **2.22** was explored. Due to the electronic withdrawing nature of dienone **2.14**, it was expected that electrophilic epoxidizing agents such as *m*-CPBA would not react. The Weitz-Scheffer epoxidation however, utilizing alkaline H₂O₂, is known to epoxidize α,β-unsaturated ketones and has been well documented in the literature⁸⁶ along with several asymmetric versions.⁸⁷ A brief screening of basic epoxidation conditions provided only decomposition products (Table 11). This was surprising because other groups had utilized this methodology in the synthesis of aranorosin.^{67,88}

Table 11. Attempts at direct bisepoxidation of dienone **2.22**

Chemical reaction showing the conversion of dienone **2.22** to bisepoxide **2.27** under various conditions.

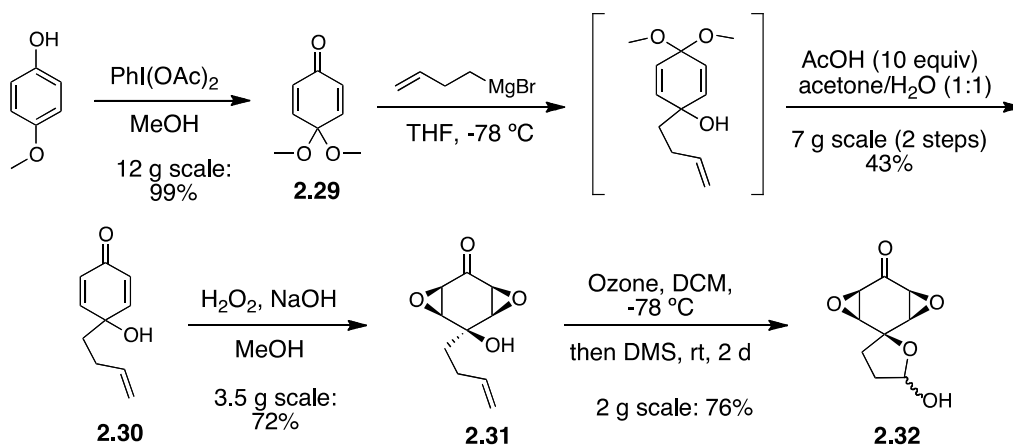
Entry	Conditions	Solvent	Result
1	H ₂ O ₂ (aq.), NaOH	MeOH	Decomp
2	H ₂ O ₂ (aq.), NaOH	<i>i</i> -PrOH	Decomp
3	<i>t</i> -BuOOH, NaOH	Toluene	Decomp
4	<i>t</i> -BuOOH, NaOH, BnNEt ₃ Cl	Toluene/H ₂ O	Decomp

In 1993, the McKillop group demonstrated the selective epoxidation of the lactol containing either a Boc or a Cbz amino protecting group in moderate yields, using the ethereal oxygen as a directing group.⁶⁷ The only example of epoxidation of a spiro lactone came from Rama Rao's group, who clearly stated the epoxidation proved to be quite difficult.⁸⁹ The authors found that treatment of the dienone spiro lactone **2.28** with potassium carbonate and hydrogen peroxide in methanol at 0 °C followed by acidification and careful quenching of excess peroxide with triphenylphosphine, and lactonization in the presence of DCC led to a mixture of epoxides (Scheme 24). They suggested the smaller acetyl amino protecting group was interfering with the directing ability of the newly formed tertiary alcohol. Upon switching to the full-length unsaturated fatty acid side chain, they were able to successfully arrive at the desired bis-epoxy dienone in a very modest 27% yield.

**Scheme 24.** Rama Rao's bisepoxidation in his synthesis of aranorosin

2.2.4 Model System Investigations

In order to simplify the synthesis of the bisepoxy ketone **2.14**, the preparation of a derivative lacking the amino functionality was explored. During the course of their investigation of the synthesis of aranorosin, the McKillop group synthesized such a substrate.^{90,91} Following this protocol, oxidative addition of MeOH in the presence of PIDA to *p*-methoxy phenol provided the desired quinone monoketal **2.29** in quantitative yield on 12 g scale (Scheme 25). *In situ* generation of butenylmagnesium bromide followed by addition to quinone monoacetal **2.29**, a solvent swap, and ketal hydrolysis, provided the desired bis- α,β -unsaturated ketone **2.30** in a very scalable process. Conversion of dienone **2.30** to the diepoxide **2.31** proceeded in slightly lower yields than reported (cf. 80%) to arrive at the desired *syn* oxygenated diepoxo ketone **2.31** in 72% yield. Ozonolysis in CH₂Cl₂ at -78 °C followed by stirring in an excess of DMS for several days to ensure decomposition of the unusually stable ozonide intermediate provided the desired model system **2.32** in 76% yield as a 1:1 mixture of lactols as determined by ¹H NMR.

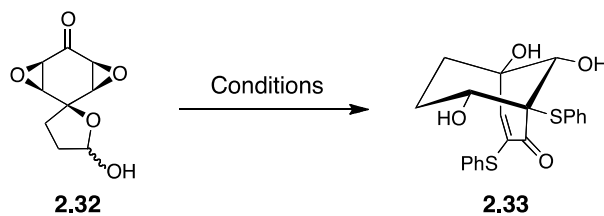


Scheme 25. Access to bisepoxy ketone model system

With a sufficient quantity of lactol **2.32** in hand, optimization of the addition/rearrangement reaction was performed. Under the previously reported conditions, spiro lactol **2.32** was treated with thiophenol (5 equiv) and sodium hydride (10 equiv) in THF. Surprisingly, only 28% of the desired compound **2.33** was isolated (Table 12, entry 1). An

increase in the equivalents of thiophenol and an initial survey of different orders of addition revealed no improvement in the reaction (Table 12, entry 2). Upon decreasing the temperature to $-78\text{ }^{\circ}\text{C}$, no increase in yield was observed. Next, a number of bases, ranging in strengths, were investigated. In the presence of *n*-BuLi, decomposition of the reaction mixture was observed, thus it was hypothesized a milder base may be necessary to effect the transformation. In the presence of triethylamine, an intractable mixture was formed. Na_2CO_3 , which was previously reported to effect the desired reaction in the system containing a saturated alkyl chain,⁷⁶ also led to the formation of a complex mixture. Switching to K_2CO_3 , the yield increased to 72% in 8 h at rt (Table 12, entry 7).

Next, the use of different solvents were investigated. The poor results exhibited by DMF, 1,2-DME, and toluene during the initial solvent screen (Table 10, *vide supra*) deterred their further use. The use of the polar protic solvent methanol, led to decomposition of the starting material. It was later determined that the starting material decomposes in methanol in the absence of the other reagents, likely due to the nucleophilicity of methanol. ^1H NMR analysis of the starting material after stirring overnight in methanol revealed a mixture of Michael addition products consistent with previous reports. The use of the polar aprotic solvent acetonitrile led to the formation of the product in 40% yield. Moving to more non-polar aprotic solvents provided markedly better results. Although the use of diethyl ether increased the isolated yield of **2.33** to 80% it noticeably slowed down the reaction. Methylene chloride was found to be the optimal solvent screened and provided the desired product in 84% yield in only 5 h at room temperature.

Table 12. Optimization of addition/rearrangement reaction

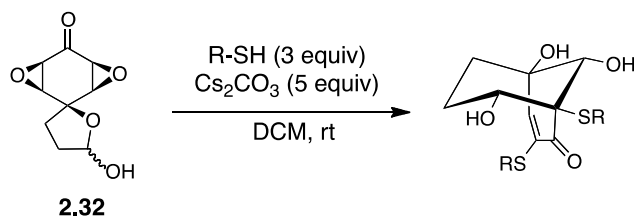
Entry	PhSH	Base (equiv)	Temperature	Solvent	Time	Result (Yield of 2.33)
1	5 equiv	NaH (10)	r.t.	THF	6 h	28%
2 ^a	10 equiv	NaH (10)	0 °C	THF	5 h	28-30%
3 ^b	10 equiv	NaH (10)	-78 °C	THF	24 h	28%
4 ^c	10 equiv	<i>n</i> -BuLi (10)	0 °C	THF	2 h	Decomp
5 ^c	10 equiv	NEt ₃ (10)	r.t.	THF	24 h	Complex Mixture
6 ^c	10 equiv	Na ₂ CO ₃ (10)	r.t.	THF	24 h	Complex Mixture
7	10 equiv	K ₂ CO ₃ (10)	r.t.	THF	8 h	72%
8 ^d	10 equiv	K ₂ CO ₃ (10)	r.t.	MeOH	2 h	Decomp
9	10 equiv	K ₂ CO ₃ (10)	r.t.	ACN	10 h	40%
10	10 equiv	K ₂ CO ₃ (10)	r.t.	Et ₂ O	23 h	84%
11	10 equiv	K ₂ CO ₃ (10)	r.t.	DCM	5 h	84%
12	10 equiv	(NH ₄) ₂ CO ₃ (10)	r.t.	DCM	24 h	50% Mono thiol addition
13	10 equiv	CaCO ₃ (10)	r.t.	DCM	20 h	37% Mono thiol addition
14	10 equiv	Li ₂ CO ₃ (10)	r.t.	DCM	24 h	24%
15	10 equiv	Cs ₂ CO ₃ (10)	r.t.	DCM	2 h	86%
16	3 equiv	Cs ₂ CO ₃ (5)	r.t.	DCM	1.5 h	83%
17	2 equiv	Cs ₂ CO ₃ (2)	r.t.	DCM	3 h	70%
18	3 equiv	Cs ₂ CO ₃ (5)	100 °C (MW)	DCM	5 min	Decomp
19	3 equiv	Cs ₂ CO ₃ (5)	80 °C (MW)	DCM	1 min	83%
20	3 equiv	Cs ₂ CO ₃ (5)	60 °C (MW)	DCM	2 min	88%
21	2 equiv	Cs ₂ CO ₃ (5)	60 °C (MW)	DCM	2 min	82%

^aThe range of yields listed represent the result obtained from all possible orders of addition. ^bThe reaction immediately turned black upon the addition of base. ^cThe reagents were added at 0 °C and the reaction mixture was allowed to warm to rt. ^dThe bisepoxy ketone starting material decomposed in MeOH.

Next, the effect of the counter cation on the carbonate base was screened. Both ammonium and calcium carbonate significantly reduced the rate of the reaction and after stirring overnight at room temperature none of the desired product was observed. Lithium carbonate provided bicyclo[3.3.1]non-3-en-2-one **2.33** in 24% yield. The use of cesium carbonate decreased the reaction time and afforded 86% of the desired product (**2.33**) in only 2 h (Table 12,

entry 15). The equivalents of thiol and base were also examined. Using 2 equivalents of both base and thiol decreased the yield to 70%. A slight excess of thiophenol (3 equiv) and base (5 equiv) gave an 83% yield. Heating the reaction mixture in CH₂Cl₂ at reflux led to formation of the desired product in only 15 min in 70% yield. This result prompted the exploration of microwave conditions. Initially, 100 °C for 5 min in CH₂Cl₂ led to decomposition. After decreasing the temperature to 80 °C, the reaction was complete in 1 min and provided the desired product in 83% yield; however, two unidentified side products were detected by TLC. Decreasing the reaction temperature further to 60 °C led to a slight increase in reaction time to two minutes but provided the desired product in a reproducibly higher yield and cleaner conversion (Table 12; entry 20). As observed previously, using stoichiometric amounts of thiol led to a slight decrease in yield (82%).

Satisfied with both the optimized room temperature and microwave conditions we focused on expanding the scope of the reaction. Specifically the use of aryl thiols containing electron donating, electron withdrawing, and sterically demanding substitution were evaluated under both the room temperature and microwave irradiation conditions. The electron donating *p*-methyl, *t*-butyl, and methoxy substitutions were well tolerated, affording the desired bicycles in good yields (entries 1-3, Table 13). Electron withdrawing substituents such as an *o*-bromo, *m*-fluoro, and *p*-trifluoromethyl groups also proved efficient, affording the corresponding bicyclo[3.3.1]nonenones in good yields (entries 5-7, Table 13). The use of 2-naphthyl thiophenol resulted in a slightly lower yield (57%); however, this decrease in yield can partly be explained by the reduced solubility of both the starting material and the product in dichloromethane (entry 8, Table 13). Gratifyingly, microwave irradiation successfully afforded the desired bicycles in 2 min at 60 °C in comparable yields to the thermal process. Most notably, the lowest yielding naphthyl derivative (**2.40**) performed well under microwave conditions to provide the desired product in 74% yield.

Table 13. Scope and limitations of the addition/rearrangement reaction

Entry	R-SH	Time	Product	% Yield ^a	Entry	R-SH	Time	Product	% Yield ^a
1		1 h	2.33	83% (88%)	5		1.5 h	2.37	87% (83%)
2		1 h	2.34	73% (74%)	6		1.5 h	2.38	72% (77%)
3		1 h	2.35	72% (84%)	7 ^b		1.5 h	2.39	78% (71%)
4		1 h	2.36	74% (80%)	8		1.5 h	2.40	57% (74%)

^aYields in parentheses correspond to microwave yields using R-SH (3 equiv), Cs₂CO₃ (5 equiv), in CH₂Cl₂ in the microwave for 2 min at 60 °C. All yields are for isolated product. ^bProduct contains a minor intractable aromatic impurity.⁷⁸

Unambiguous structure determination of bicyclo[3.3.1]non-3-en-2-one **2.37** was accomplished by X-ray crystallography (Figure 25). NMR analysis of **2.37**, revealed a single diastereomer was observed, which was determined by X-ray analysis to be the diastereomer placing the hydroxyl substituents on the chair in an equatorial orientation. Semi-empirical calculations (PM3) using the Spartan molecular modeling software⁹² revealed the observed equatorial diastereomer to be ~1.1 kcal/mol higher in energy than the axial diastereomer (Figure 25). Thus, the reaction does not appear to be under thermodynamic control.

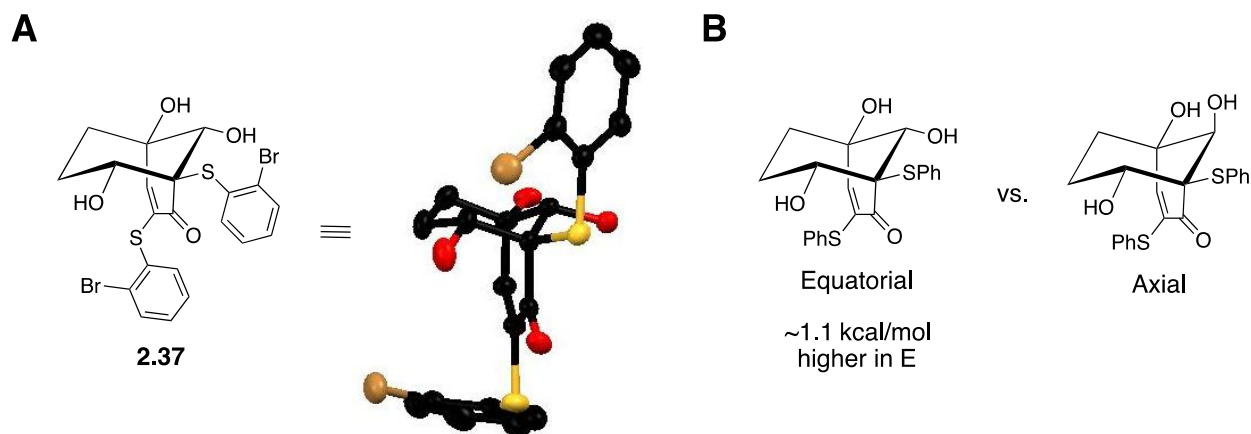
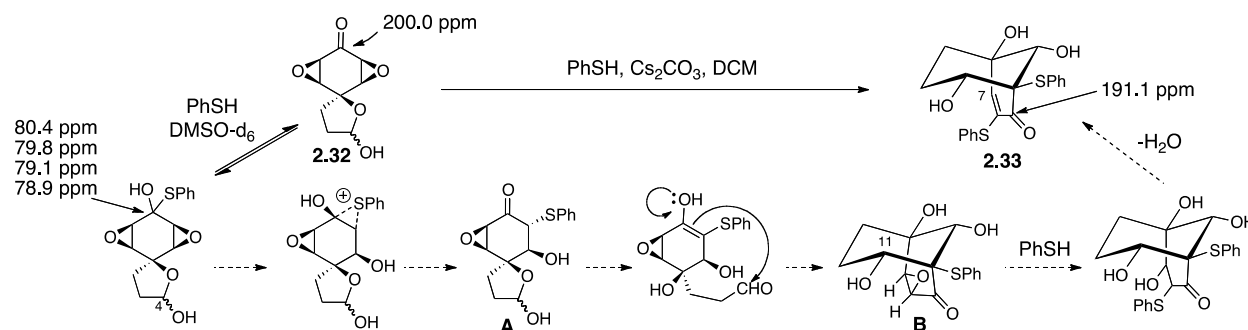


Figure 25. (A) X-ray structure of *o*-bromo-bicyclo[3.3.1]nonane **2.37** generated using the Mercury software package.⁸⁴ (B) Structures of both the equatorial and axial diastereomers used for molecular modeling calculations

Next, a combination of ^{13}C and ^1H NMR studies were used to refine our previous mechanistic hypothesis (Scheme 14).⁷⁶ *In situ* ^{13}C NMR studies conducted with spiro lactol **2.32** revealed that upon incubation with thiophenol (3 equiv) in DMSO-d_6 , reversible nucleophilic attack of thiophenol at the carbonyl carbon (200.0 ppm) occurred leading to formation of all four possible diastereomeric O,S-acetals (80.4, 79.8, 79.1, 78.9 ppm). Upon the addition of Cs_2CO_3 (5 equiv), these thioacetals were converted to the α,β -unsaturated carbonyl (191.1 ppm) corresponding to the bicyclo[3.3.1]non-3-en-2-one product **2.33**. In addition, monitoring the reaction by ^1H NMR revealed the accumulation of a defined intermediate prior to product formation. Upon the addition of base complete disappearance of the lactol hydrogen at C4 (5.76 ppm) and two of the epoxide hydrogens (3.40-3.36 ppm) from **2.32** were observed. However, prior to formation of bicyclo[3.3.1]non-3-en-2-one **2.33** (indicated by the alkene hydrogen at C7 of **2.33**, 5.96 ppm), an intermediate containing a doublet of doublets ultimately assigned to the C11 hydrogen of **B** (3.34 ppm) was observed. In order to confirm the identify of intermediate **B**, spiro lactol **2.32** was subjected to the optimized room temperature conditions and quenched after only 5 min to afford epoxyketone **B** in 18% yield along with 53% yield of **2.33**. As expected, upon resubmission of **B** to the reaction conditions, bicyclo[3.3.1]non-3-en-2-one **2.33** was formed in a comparable 77% yield. Based on these NMR studies, we refined our previously proposed mechanistic hypothesis (Scheme 14). Our refined mechanistic hypothesis (Scheme 26) postulates that after initial reversible addition of thiophenol, the resulting thioacetal undergoes an irreversible 1,2-migration to open the epoxide and afford intermediate **A**. Next, prior to the addition of a second equivalent of thiophenol, a base catalyzed intramolecular aldol reaction with

the hemiacetal proceeds to give intermediate **B** which, upon addition of a second equivalent of thiophenol and elimination, affords the observed bicyclo[3.3.1]non-3-en-2-one product **2.33**.



Scheme 26. Proposed mechanism for the ring-opening and intermolecular aldol reaction of diepoxyketone **2.32** with thiophenol. Reproduced with permission from ref.⁷⁸

Having refined our mechanistic hypothesis and shown that aryl thiols containing electron donating, electron withdrawing, and sterically demanding substituents are well-tolerated we focused on expanding the scope of the reaction to include heterocyclic and alkyl thiols (Table 14). Although six different heterocyclic thiols were subjected to the optimized room temperature reaction conditions, none of the desired bicyclo[3.3.1]non-3-en-2-ones were observed (entries 1-6, Table 14). In all of the heterocyclic thiol examples only complex mixtures containing either recovered heterocyclic thiol and several unidentified products or complete decomposition was observed. These results suggest that the addition/rearrangement reaction is intolerant of the tertiary Lewis basic amine functionality. This result was also observed during our optimization studies (Table 12). The use of triethylamine, a base of similar strength to the carbonate bases, provided a complex mixture like those observed during the screen of heterocyclic thiols.

Investigating the use of alkyl thiols for the addition/rearrangement reaction also provided none of the desired bicyclo[3.3.1]non-3-en-2-one products (entries 7-11, Table 14). The use of isopropyl 3-mercaptopropionate in the presence of cesium carbonate afforded an unexpected major product that was tentatively assigned by ¹H NMR to be addition of the thiol to both epoxides as well as the lactol to give **2.41** in 32% yield. Unfortunately, subjecting the reaction mixture to elongated reaction times or heating afforded only a complex mixture of products. One plausible explanation for the limited success of the alkyl thiols is that their decreased acidity may require the use of a stronger base. Under the optimized conditions the aryl thiols (pK_a ~ 7) should be completely deprotonated by cesium carbonate (pK_a ~ 10) while the alkyl thiols (pK_a ~

18) remain almost entirely protonated. This hypothesis is supported by our initial optimization studies (Table 12) that demonstrated the use of a number of bases, ranging in strength provided markedly different results.

Table 14. Attempt to expand the reaction scope to include heterocyclic and alkyl thiols

Reaction scheme showing the conversion of bicyclo[3.3.1]non-3-en-2-one derivative **2.32** to a bicyclic product with multiple hydroxyl and thiol groups. Reagents: R-SH (3 equiv), Cs₂CO₃ (5 equiv), CH₂Cl₂, rt.

Chemical structure of product **2.41**, a bicyclic molecule with multiple hydroxyl and thiol groups, and a defined R group.

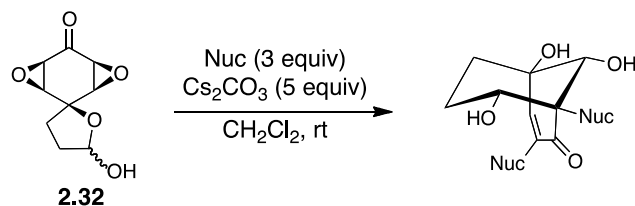
R =

Entry	R-SH	Time	Result	Entry	R-SH	Time	Result
1		18 h	complex mix	7		4 h	complex mix
2		18 h	dec.	8		16 h	dec.
3		18 h	dec.	9		3 h	32% of 2.41
4		18 h	complex mix	10		8 min ¹	dec.
5		3 h	only thiol rec.	11		4 min ¹	complex mix
6		8 min ¹	only thiol rec.				

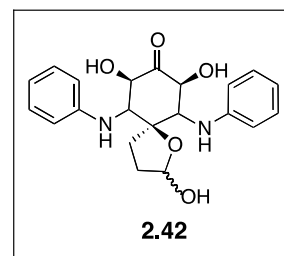
¹ Reaction run in μ W at 60 °C.

Next, the use of non-sulfur nucleophiles was investigated (Table 15). The use of three equivalents of a thioamide, phenol, or an aniline in the presence of base at room temperature proved inefficient and none of the corresponding bicyclo[3.3.1]non-3-en-2-ones were isolated. The use of aniline led to a product tentatively assigned by ¹H NMR to be **2.42**. Although opening of both epoxides was observed, elimination and intramolecular aldol reaction did not proceed and **2.42** was isolated in 45% yield.

Table 15. Attempt to expand the reaction scope to include non-thiol nucleophiles



Entry	Nuc	Time	% Yield
1		18 h	dec
2		4 h	dec
3		24 h	2.42 (45%)



Finally, in an attempt to synthesize the chlorinated core of the gymnastatins (Figure 22), focus was directed towards the use of chloride as a nucleophile (Figure 26). Stirring **2.32** with an excess (10 equiv) of lithium chloride (LiCl) in either CH₂Cl₂ or THF at room temperature overnight afforded only recovered starting material. The addition of either titanium tetrachloride or trifluoroacetic acid to a mixture of LiCl and **2.32** in THF led to complete consumption of the starting material, however only a complex mixture of unidentified products was observed. The use of either tetrabutylammonium chloride or hydrochloric acid as a chloride source returned, after stirring overnight with **2.32** in THF, only recovered starting material. These experiments suggest that the decreased nucleophilicity of the chloride relative to the thiolate requires the use of either Lewis or Bronsted acid catalysis to obtain reactivity with **2.32**. Unfortunately, these harsher conditions resulted in the formation of a complex mixture of products. Thus, further experimentation with chloride nucleophiles was not pursued.

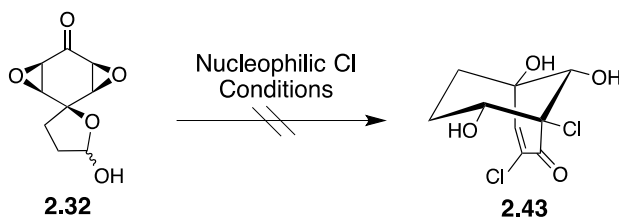
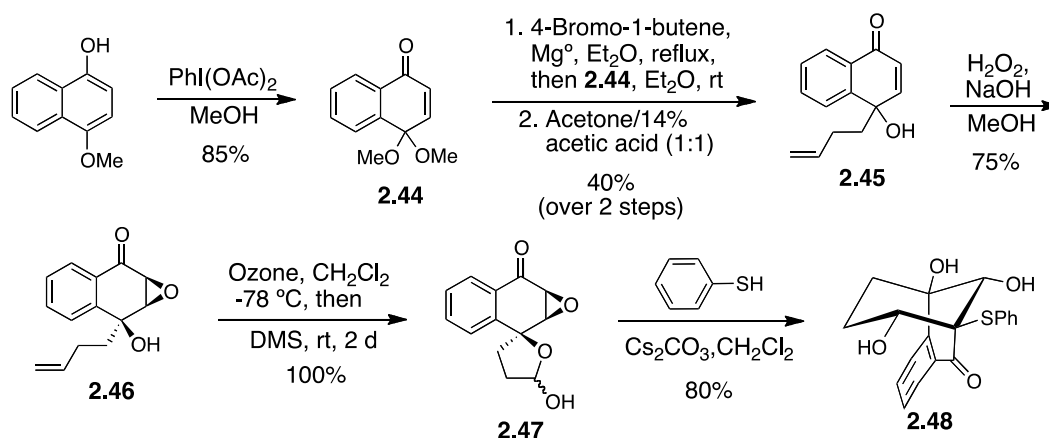


Figure 26. Attempt to use a chloride to elicit the addition/rearrangement reaction

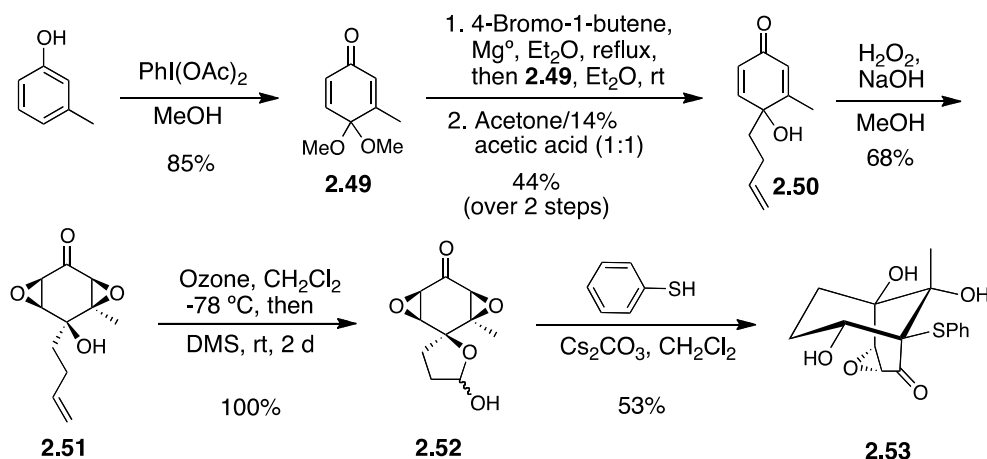
Unfortunately, heterocyclic thiols, alkyl thiols, and several other non-sulfur nucleophiles all proved to be ineffective substrates for the desired addition/rearrangement reaction under the optimized conditions. Although the lack of success observed with heterocyclic thiols was attributed to the presence of Lewis basic amine functionalities, the ineffectiveness of the alkyl thiols and non-sulfur nucleophiles is more likely a result of differences in their nucleophilic properties. Mechanistic studies have revealed that the reaction likely proceeds via initial attack of the thiol at the ketone to generate an intermediate hemithioacetal that undergoes an irreversible 1,2-migration to open the epoxide.⁹⁴

Next, several epoxy ketone cores were prepared and evaluated in the addition/rearrangement reaction (Scheme 27, Scheme 28, and Scheme 29). First, the use of a naphthyl derivative **2.47** was explored (Scheme 27). Oxidative addition of methanol to 4-methoxy-1-naphthol in the presence of PIDA afforded acetal **2.44** in 85% yield. *In situ* generation of butenylmagnesium bromide followed by addition to quinone monoacetal **2.44**, a solvent swap, and ketal hydrolysis, provided the desired α,β -unsaturated ketone **2.45** in 40% over two steps. Epoxidation of enone **2.45** in the presence of hydrogen peroxide and sodium hydroxide afforded the *syn* oxygenated epoxy ketone **2.46** in 75% yield. Ozonolysis in CH_2Cl_2 at $-78\text{ }^\circ\text{C}$ followed by stirring in an excess of DMS provided the desired naphthyl derivative **2.47** in quantitative yield as a 1:1 mixture of lactols as determined by ^1H NMR. Gratifyingly, subjection of epoxy-ketone **2.47** to the optimized conditions with thiophenol gave bicyclo[3.3.1]non-3-en-2-one **2.48** in 80% yield.



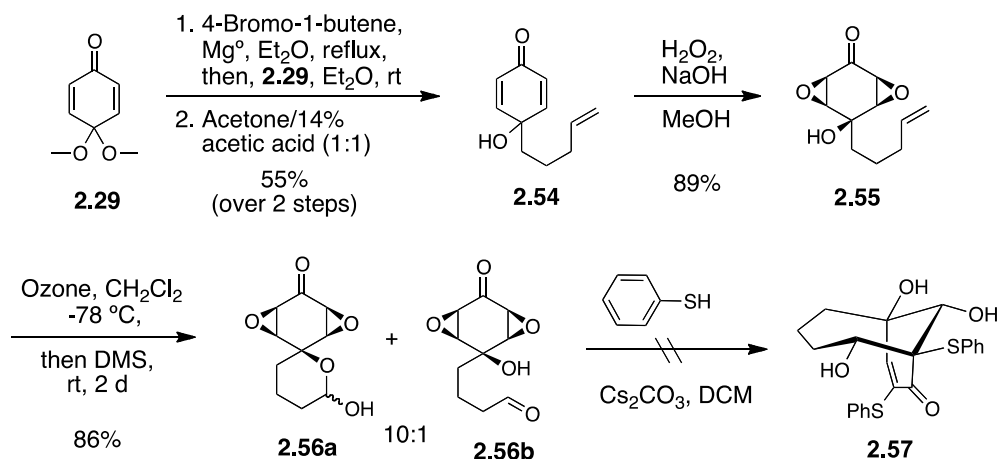
Scheme 27. Synthesis of naphthyl derivative **2.48**

Next, the effect of substitution of the enone was examined (Scheme 28). Oxidative addition of methanol to 3-methyl phenol gave **2.49**, which after addition of butenyl magnesium bromide and acetal deprotection provided bis- α,β -unsaturated ketone **2.50** in 37% yield over three steps. Epoxidation and ozonolysis of **2.50** proceeded smoothly to afford diepoxy spiro lactol **2.52** in 68% yield (two steps). Interestingly, reaction of **2.52** with thiophenol in the presence of base afforded the tricyclic epoxide **2.53** in 53% yield. Even under forcing microwave conditions (10 equiv of thiophenol, 10 equiv of base, 80 °C, 3 h) none of the expected bicyclo[3.3.1]non-3-en-2-one was observed. The presence of the axial methyl group is likely to sterically destabilize the transition state of the epoxide opening process. The observed stability of the epoxide in the presence of a large excess of nucleophile is promising for the potential use of more rigid epoxy-ketones in biological assays.



Scheme 28. Synthesis and addition/rearrangement of **2.52**

Finally, an attempt to extend the methodology to the formation of bicyclo[3.4.1]dec-3-en-2-ones proved unsuccessful (Scheme 29). *In situ* generation of the pentenylmagnesium bromide followed by addition to quinone monoketal **2.29** and ketal hydrolysis furnished **2.54** in 55% yield (two steps). Diepoxidation and ozonolysis proceeded smoothly to give a 10:1 mixture of spiro lactol **2.56a** and aldehyde **2.56b** as determined by ^1H NMR. Subjection of **2.56** to thiophenol and base afforded, after silica gel chromatography, an intractable mixture of products containing a major product and several unidentified by-products; however none of the desired bicycle **2.57** (as indicated by the characteristic alkene proton at 6 ppm) was observed. ^1H NMR analysis of the intractable mixture revealed that the major product contained protons corresponding to the incorporation of thiophenol (7-8 ppm) and a proton corresponding to an intact lactol (5.5 ppm). Therefore, it appears that although thiophenoxide addition occurred, intramolecular aldol reaction to form the seven-membered ring did not. The absence of intramolecular aldol product is most likely a result of the less favorable formation of the seven-membered ring as compared to six-membered ring formation.⁹³



Scheme 29. Attempt to synthesize the 7-membered ring variant **2.57**

Having demonstrated the scope and limitations of the addition/rearrangement and successfully preparing eleven new bicyclo[3.3.1]non-3-en-2-ones, we sought to compare the new products to the bicyclo[3.3.1]non-3-en-2-ones currently contained in the Molecular Libraries Small Molecule Repository (MLSMR) library (1907 compounds).

Through a collaboration with Dr. Beratan and coworkers at Duke University, the molecular diversity of the newly synthesized structures were analyzed using the ChemGPS-NP⁹⁴ map of chemical space. ChemGPS-NP is a software program that provides a coordinate system designed for exploration of biologically relevant compounds. It uses principle component analysis derived from the physiochemical properties of known bioactive natural products. The first four principles components account for roughly 77% of data variance. Principal Component 1 (PC1) represents size, shape and polarizability of a compound. PC2 corresponds to aromatic and conjugative properties, PC3 describes lipophilicity, polarity, and H-bond capacity, and PC4 expresses the flexibility and rigidity of a molecule.⁹⁴

Figure 27 illustrates a comparison of the polarity/lipophilicity and aromatic character of the newly synthesized bicyclo[3.3.1]non-3-en-2-ones (blue circles) and the bicyclononanes already present in the MLSMR (crosses). From Figure 27 it is clear that the newly synthesized bicyclo[3.3.1]non-3-en-2-ones occupy a novel region of the MLSMR chemical space. This novel space is primarily derived from the high levels of aromaticity and low lipophilicity relative to the bicyclononanes currently present in the MLSMR library. The increased aromaticity is derived from the aryl thiols, in particular the naphthyl derivate **2.40** shown as number 15 in

Figure 27 is far outside the previously prepared bicyclononanes. The low lipophilicity of the compounds is derived from the densely hydroxylated core the derivatives. This is demonstrated by the yellow boxes in Figure 27, which represent the newly synthesized compounds lacking hydroxyl groups.

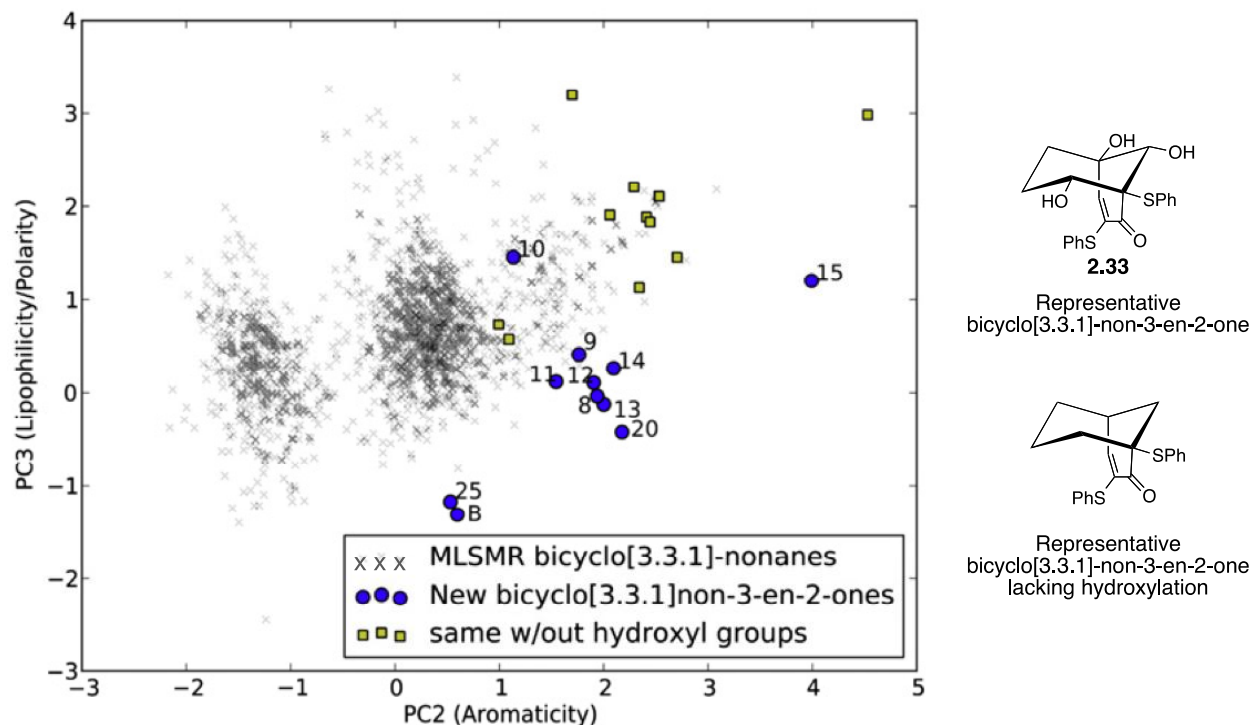


Figure 27. ChemGPS-NP coordinates of the synthesized bicyclononanes (in blue) and bicyclononanes in the MLSMR library (X's). Also shown are the new products lacking hydroxyl groups (yellow boxes). Figure reproduced with permission from ref.⁷⁸

Figure 28 (a) is a graph of PC4 and PC1, which represent the two principle components for molecular flexibility and size, respectively, and also compares the newly synthesized bicyclo[3.3.1]non-3-en-2-ones (blue boxes) to the bicyclononanes already in the MLSMR library (crosses). It is clear from Figure 28 (a) that the new compounds are not significantly different in molecular size relative to the previously prepared bicyclononanes; however, some of the newly prepared analogues are slightly larger than previously prepared compounds. In addition, the newly prepared analogues are generally less flexible than the previously prepared compounds. The relatively high polarity and structural rigidity of the new compounds are potentially attractive for their biological activity and make them less likely to exhibit non-specific ligand-receptor interactions.

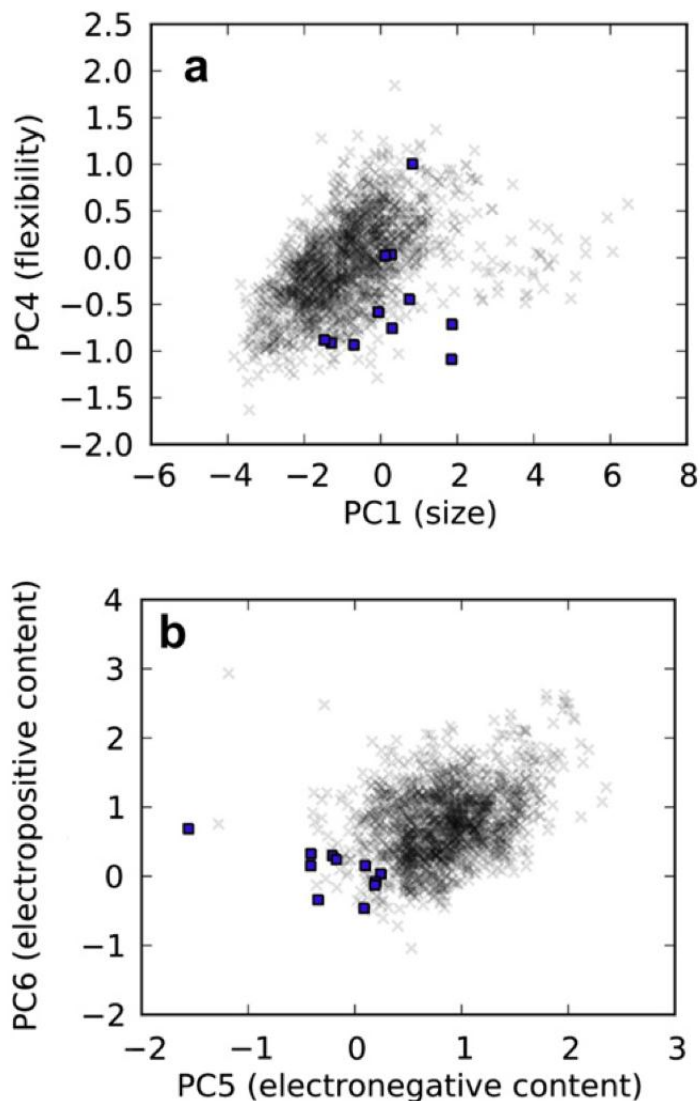


Figure 28. ChemGPS-NP coordinates of the bicyclo[3.3.1]non-3-en-2-ones (blue boxes) in the MLSMR library (crosses). (a) Graph of PC1 and PC4, which represent the principle component derived from molecular size and flexibility respectively. (b) Graph of PC5 and PC6 which represent the principle components derived from electronegativity and electropositive atom content, respectively. Figure was reproduced with permission for ref.⁷⁸

Figure 28 (b) is a graph of PC6 and PC5 which represent the principle components corresponding to electronegativity and electropositive atomic content respectively. Again this graph is a comparison of newly synthesized compounds (blue boxes) and those already in the MLSMR library (crosses). Figure 28 (b) illustrates that the new compounds are clustered around the origin of the PC6 axis and occupy the relatively empty negative PC5 axis.

In addition, the physiochemical descriptors of the newly synthesized bicyclo[3.3.1]non-3-en-2-ones were evaluated using the OpenEye toolkit as well as ChemAxon (Table 16). All but two of the new prepared bicyclic compounds obey Lipinski's rule of 5.⁹⁵ As these rules were generated to roughly correlate to the efficiency of drug transport across membranes, the fact that all compounds are well below the required <5 hydrogen bond donors (HBD) and <10 hydrogen bond acceptors (HBA) bodes well for their potential biological activity. In addition, most of the new compounds exhibit XlogP's <5, indicating low lipophilicity and promising bioavailability.

Table 16. Selected physiochemical properties of the newly synthesized bicyclo[3.3.1]non-3-en-2-ones

Product	MW	XLogP	Lipinski HBD	Lipinski HBA	Lipinski violations	Aryl rings
B	308.35	-0.27	3	5	0	1
2.33	400.51	3.06	3	4	0	2
2.34	428.56	3.65	3	4	0	2
2.35	512.72	6.20	3	4	2	2
2.36	460.56	2.77	3	6	0	2
2.37	558.30	4.66	3	4	1	2
2.38	436.49	3.33	3	4	0	2
2.39	536.51	4.87	3	4	1	2
2.40	500.63	5.16	3	4	2	4
2.48	342.41	1.92	3	4	0	2
2.53	322.38	0.12	3	5	0	1

The present ChemGPS-NP analysis demonstrates how the densely hydroxylated core and large aromatic character of the natural-product like bicyclo[3.3.1]non-3-en-2-ones allows them to access new regions of biologically relevant chemical space. The combination of ease of synthesis, limited flexibility, hydrophilic nature, and promising physiochemical properties suggests these compounds may be potential leads for the development of bioactive compounds.⁷⁸

The newly synthesized bicyclo[3.3.1]non-3-en-2-ones were submitted to the MLSMR in 50+ mg quantities. Since their submission, seven of the eleven newly synthesized bicyclo[3.3.1]non-3-en-2-ones have been evaluated in 58 different biological assays. The parent bicyclo[3.3.1]non-3-en-2-one, **2.33**, exhibited 33±2.6% (N = 3) inhibition at 4 μM in a luminescence-based high throughput assay for inhibitors of the interaction of the lipase co-

activator protein, abhydrolase domain containing 5 (ABHD5), with perilipin-5 (MDLDP; PLIN5).⁹⁶ ABHD5 is a protein that activates an enzyme, adipose triglyceride, which plays a role in breaking down triglycerides.⁹⁶ Structural comparison of **2.33** to some of the most potent interaction inhibitors (100% inhibition at 4 μ M) reported in PubChem⁹⁷ reveals that while a diverse set of structures have exhibited activity in this assay, **2.33** contains an unrepresented structure (Figure 29). A counterscreen for selective interaction inhibition of ABHD5 revealed **2.33** exhibited 43 \pm 2.5% (N = 3) inhibition at 4 μ M of hepatocyte nuclear factor 4 dimerization (HNF4).⁹⁶ HNF4 is a member of the nuclear receptor superfamily and binds DNA exclusively as a homodimer. Dimerization controls important aspects of receptor function, such as DNA binding, protein stability, ligand binding and interactions with co-activators.⁹⁶

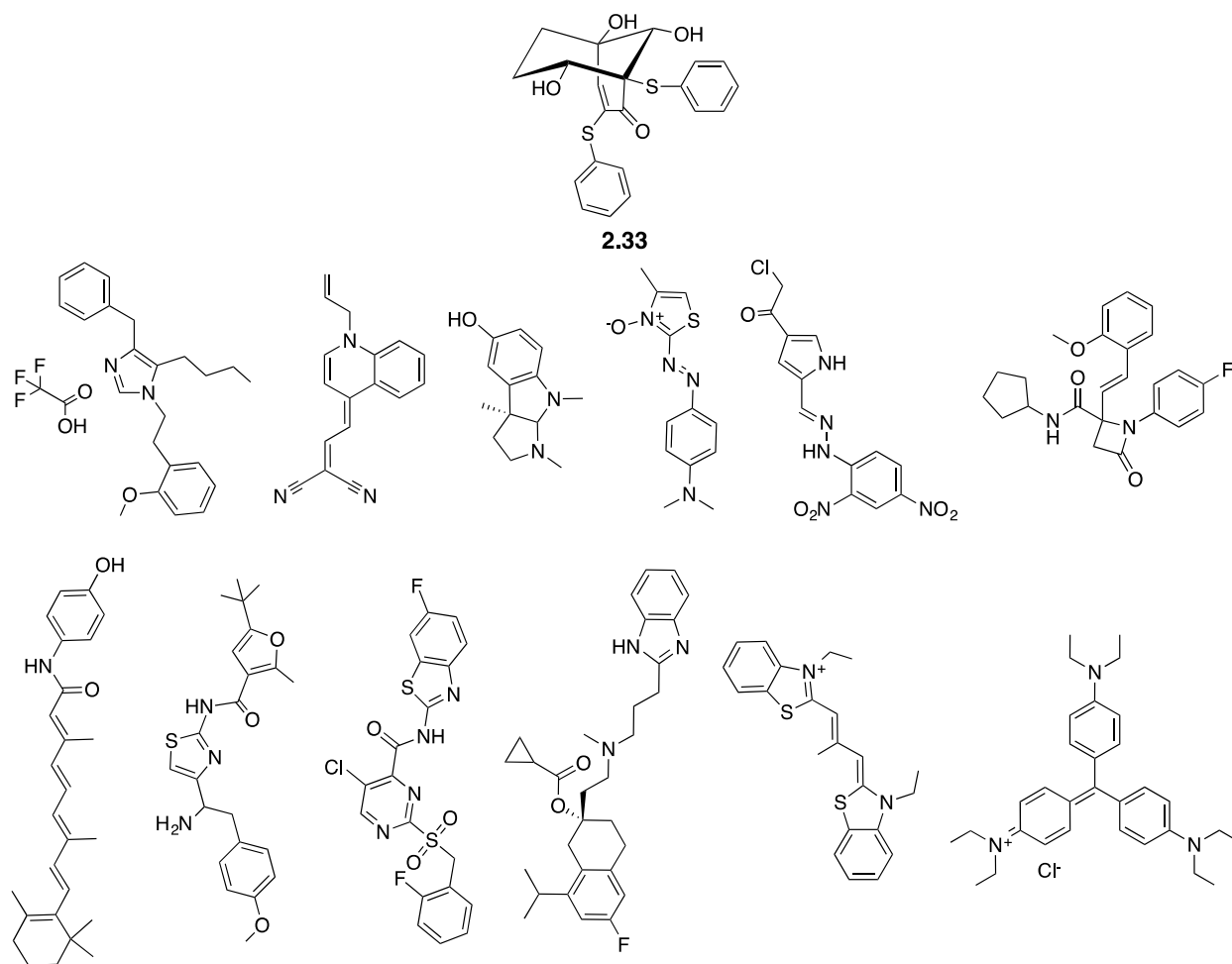


Figure 29. Structure of **2.33** and the most potent inhibitors of the interaction of the lipase co-activator protein, abhydrolase domain containing 5 (ABHD5) with perilipin-5 (MDLDP; PLIN5).⁹⁶

(TAAR1).⁹⁶ TAAR1 is a G protein-coupled receptor activated by trace amines, which has been shown to modulate the activity of neurotransmitters such as dopamine and γ -amino butyric acid and alterations in their brain levels are associated with schizophrenia and depression.⁹⁶ As a result, TAAR1 is an interesting target for the development of ligands to probe the role of this receptor in CNS function and disease.⁹⁶ While a diverse set of structures have exhibited activity in this assay, **2.35** contains a novel structure (Figure 31).

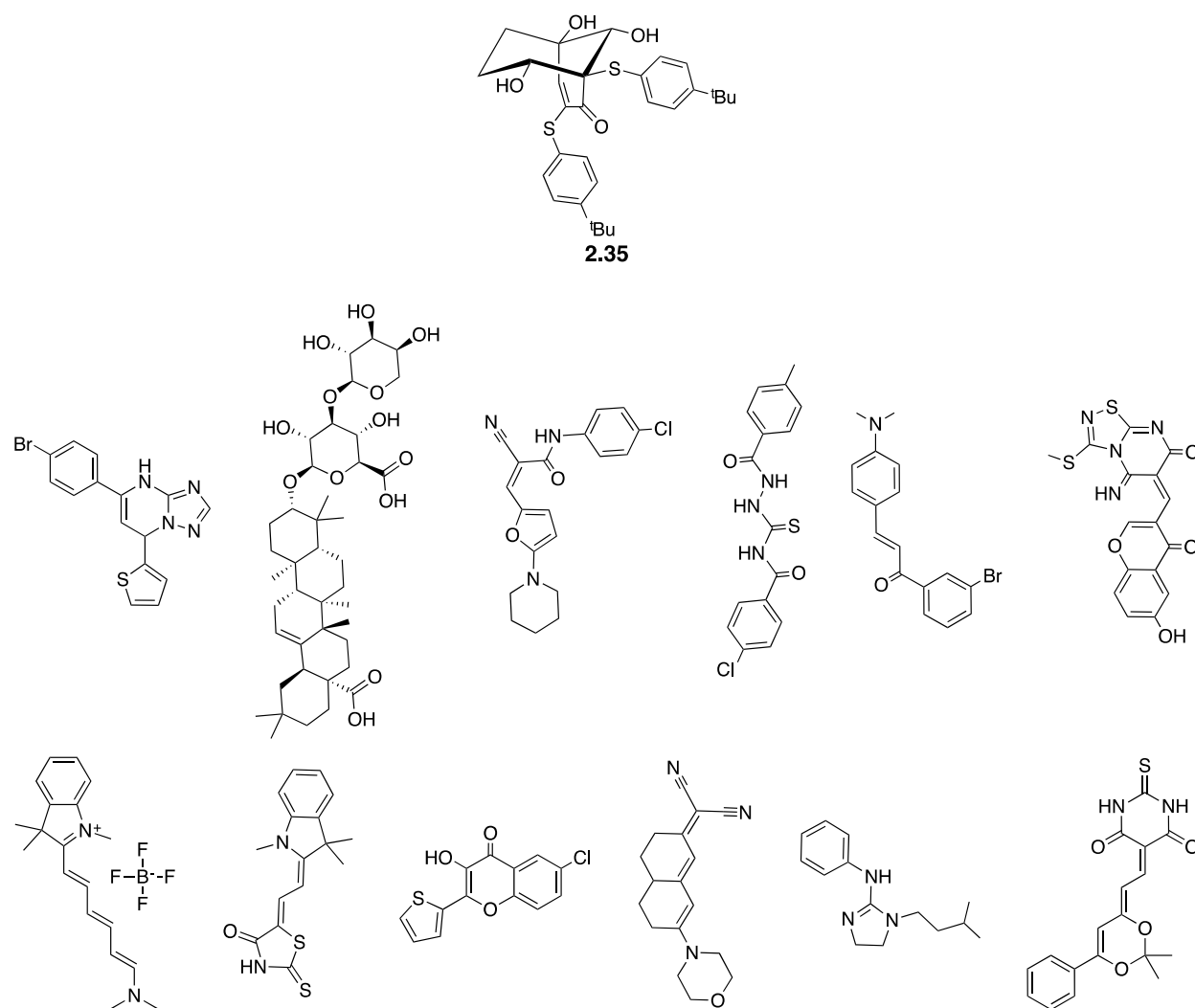


Figure 31. Structure of **2.35** and some other potent antagonists of the human trace amine associated receptor 1 (TAAR1).⁹⁷

A counterscreen for selective antagonists of TAAR1 revealed **2.35** exhibited $33 \pm 2.3\%$ ($N = 3$) inhibition at $3 \mu\text{M}$ in a fluorescence-based cell-based high throughput assay to identify antagonists of the G-protein alpha subunit, G-alpha-16 (Ga16).⁹⁶ Ga16 has been shown to play a

role in the formation of blood cellular components and its down-regulation is associated with leukemia.⁹⁶

2.3 CONCLUSIONS

The successful preparation of a single member of the fully functionalized bicyclo[3.3.1]non-3-en-2-one core containing the amino functionality presented here provides a proof of principle for the creation of a natural product-like small library based on this scaffold. Completion of the synthesis of a model system allowed rapid access to a precursor that was used to rigorously optimize conditions for the addition/rearrangement reaction. Two optimized procedures were realized. A more broadly applicable procedure at room temperature in CH₂Cl₂ provided the desired products in 1.5 h in 57-87% yield, and microwave conditions in CH₂Cl₂ shortened the reaction time to 2 min at 60 °C to provide the desired products in 64-88% yield.

Both sets of conditions were shown to tolerate electron-donating, electron-withdrawing, and sterically demanding substituents as well as several epoxy ketone starting materials. *In situ* NMR studies allowed for the refinement of our mechanistic hypothesis. The limitations of the methodology were explored and although a number of aryl thiols were converted, the use of heterocyclic and alkyl thiols as well as other non-sulfur based nucleophiles was unsuccessful. In addition, attempts to synthesize a bicyclo[3.4.1]decenone were unsuccessful.

The newly synthesized bicyclo[3.3.1]non-3-en-2-ones were shown via ChemGPS-NP analysis to occupy novel regions of chemical space when compared to the bicyclononanes currently present in the MLMSR. The unique hydrophilicity of the new analogues coupled with their structural rigidity and promising physiochemical properties make them prime candidates for lead compounds with decreased potential for non-specific binding. All of the newly synthesized compounds have passed quality control and have been submitted to the MLMSR in 50+ mg quantities for biological evaluation.

Seven of the eleven compounds submitted to the MLMSR were tested for activity in 58 different assays. Two of the bicyclo[3.3.1]non-3-en-2-ones, **2.33** and **2.35**, exhibited activity. Although neither compound proved to be the most potent inhibitor evaluated in these assays,

structural comparison to some of the most potent inhibitors revealed that the newly synthesized bicyclo[3.3.1]non-3-en-2-ones were structurally novel. These assays, in combination with the ChemGPS analysis, demonstrate that the goal of synthesizing a small natural product-like focus library containing a biologically relevant and currently underrepresented scaffold in the NIH libraries has been achieved.

2.4 EXPERIMENTAL

General. All moisture sensitive reactions were performed using syringe-septum techniques under an atmosphere of either dry N₂ or dry argon unless otherwise noted. All glassware was dried in an oven at 140 °C for a minimum of 6 h or flame-dried under an atmosphere of dry nitrogen prior to use. Reactions carried out at -78 °C employed a CO₂(s)/acetone bath. Diethyl ether and tetrahydrofuran were dried by distillation over sodium/benzophenone under an argon atmosphere. Dry methylene chloride was purified by filtration through an activated alumina column. Methylene chloride was degassed using the freeze/pump/thaw method (3x). Methanol was stored over molecular sieves (3Å). Deuterated chloroform was stored over anhydrous potassium carbonate. Reactions were monitored by TLC analysis (pre-coated silica gel 60 F₂₅₄ plates, 250 μm layer thickness) and visualized by using UV lamp (254 nm) or by staining with either Vaughn's reagent (4.8 g of (NH₄)₆Mo₇O₂₄•4 H₂O and 0.2 g of Ce(SO₄)₂ in 100 mL of a 3.5 N H₂SO₄) or a potassium permanganate solution (1.5 g of KMnO₄ and 1.5 g of K₂CO₃ in 100 mL of a 0.1% NaOH solution). Flash column chromatography was performed with 40-63 μm silica gel (Silicycle). Microwave reactions were performed on a Biotage Initiator microwave reactor. Infrared spectra were measured on a Smiths Detection IdentifyIR FT-IR spectrometer (ATR). Unless otherwise indicated, all NMR data were collected at room temperature in CDCl₃ on a 300, 500, 600, or 700 MHz Bruker instrument. Chemical shifts (δ) are reported in parts per million (ppm) with internal CHCl₃ (δ 7.26 ppm for ¹H and 77.00 ppm for ¹³C), internal acetone (δ 2.05 ppm for ¹H and 29.85 ppm for ¹³C), or internal DMSO (δ 2.50 ppm for ¹H and 39.52 for ¹³C) as the reference. ¹H NMR data are reported as follows: chemical shift, multiplicity (s = singlet, bs = broad singlet, d = doublet, t = triplet, q = quartet, m = multiplet, dd = doublet of

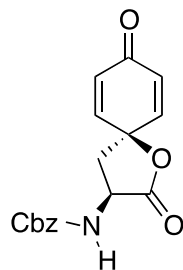
doublets, dt = doublet of triplets, td = triplet of doublets, qd = quartet of doublets, sep = septet), integration, and coupling constant(s) (J) in Hertz (Hz). HRMS analyses were obtained using either a Q-TOF Ultima API, Micromass UK Limited (ESI) or a VG Autospec, FISIONS instrument (EI).

2.4.1 General Procedure A: Addition/Rearrangement to Afford the Bicyclo[3.3.1]non-3-en-2-one Scaffold.

To a stirred solution of **2.32** (0.0500 g, 0.252 mmol, 1 equiv) in dry, degassed CH_2Cl_2 (12 mL) was added Cs_2CO_3 (0.411 g, 1.26 mmol, 5 equiv) and the thiol nucleophile (0.757 mmol, 3 equiv). The reaction mixture was allowed to stir at room temperature for 1-2 h, diluted with EtOAc (40 mL), and washed with brine. The organic layer was separated and the aqueous layer was extracted with EtOAc (2 x 10 mL). The combined organic layers were washed with brine, dried (MgSO_4), filtered, and concentrated under reduced pressure. The crude mixture was dissolved in CH_2Cl_2 and purified by chromatography on SiO_2 .

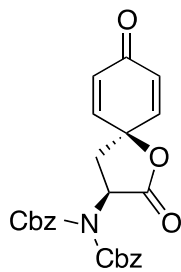
2.4.2 General Procedure B: Microwave Assisted Addition/Rearrangement to Afford the Bicyclo[3.3.1]non-3-en-2-one Scaffold.

To a stirred solution of **2.32** (0.0100 g, 0.0505 mmol, 1 equiv) in dry, degassed CH_2Cl_2 (2 mL) was added Cs_2CO_3 (0.0822 g, 0.252 mmol, 5 equiv) and the thiol nucleophile (0.151 mmol, 3 equiv). The reaction mixture was heated in the microwave reactor for 2 min at 60 °C, diluted with CH_2Cl_2 (10 mL), and washed with brine. The organic layer was separated and the aqueous layer was extracted with EtOAc (2 x 10 mL). The combined organic layers were washed with brine, dried (MgSO_4), filtered, and concentrated under reduced pressure. The crude mixture was dissolved in CH_2Cl_2 and purified by chromatography on SiO_2 .



2.17

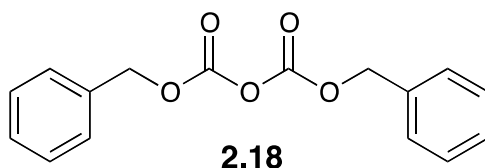
(3S)-3-[(Benzyloxycarbonyl)amino]-1-oxaspiro[4.5]deca-7,10-diene-2,8-dione (2.17).⁷⁰ To a stirred solution of iodobenzene diacetate (75.0 g, 228 mmol, 1.20 equiv) in MeCN/*i*-PrOH (3:1, 500 mL) was added a solution of **2.15** (60.0 g, 190 mmol, 1 equiv) in MeCN/*i*-PrOH (3:1, 400 mL) dropwise over 2 h. After the addition was complete, the mixture was allowed to stir at rt for 4 h open to the air, quenched with a saturated aqueous solution of NaHCO₃ (400 mL), and extracted with EtOAc (3 x 300 mL). The combined organic layers washed with a saturated aqueous solution of NaHCO₃, brine, dried (MgSO₄), filtered, and concentrated under reduced pressure. The crude residue was dissolved in EtOAc/hexanes (4:1, 300 mL) and passed through a pad of SiO₂. The resulting solution was concentrated and purified by chromatography on SiO₂ (EtOAc/hexanes, 1:4-1:1) to give **2.17** (24.0 g, 41%) as yellow powder: R_f 0.43 (EtOAc/hexanes, 1:1); Mp 104-106 °C (EtOAc); [α]_D -25.6 (*c* 1.04, CH₂Cl₂); IR (neat) 3336, 3034, 2971, 2935, 1761, 1711, 1675, 1634, 1258, 1211 cm⁻¹; ¹H NMR (700 MHz, CDCl₃) δ 7.32 (s, 5 H), 6.86 (s, 2 H), 6.24 (app t, 2 H, *J* = 11.9 Hz), 5.91 (d, 1 H, *J* = 4.9 Hz), 5.11 (d, 1 H, *J* = 12.6 Hz), 5.08 (d, 1 H, *J* = 12.6 Hz), 4.64 (d, 1 H, *J* = 8.4 Hz), 2.2263 (t, 1 H, *J* = 11.2 Hz), 2.48 (t, 1 H, *J* = 11.9 Hz); ¹³C NMR (176 MHz, CDCl₃) δ 184.0, 173.5, 155.9, 146.0, 144.1, 135.6, 129.6, 129.0, 128.5, 128.4, 128.1, 76.1, 67.5, 50.3, 37.9; HRMS (ESI⁺) *m/z* calcd for C₁₇H₁₅NO 313.0950, found 313.0946.



2.1

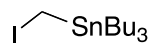
(3S)-3-[Bis(benzyloxycarbonyl)amino]-1-oxaspiro[4.5]deca-7,10-diene-2,8-dione (2.1).⁷⁰

To a stirred solution of **2.17** (8.90 g, 28.4 mmol, 1 equiv) in MeCN (90 mL) was added DMAP (1.04 g, 8.52 mmol, 0.3 equiv) and Cbz₂O (**2.18**) (32.5 g, 114 mmol, 4 equiv) in ten portions at 5 min intervals. The reaction mixture was allowed to stir at rt for 2 h, diluted with EtOAc (50 mL), washed with water and brine (x2), dried (MgSO₄), filtered, and concentrated under reduced pressure. The crude residue was purified by chromatography on SiO₂ (EtOAc/hexanes, 1:5 to 1:3) to give **2.1** (10.8 g, 85%) as white powder: R_f 0.66 (EtOAc/hexanes, 1:1); Mp 113-116 °C (CHCl₃); [α]_D -46.2 (*c* 1.02, CH₂Cl₂); IR (neat) 3060, 3032, 2982, 2973, 2953, 2894, 1772, 1709, 1670, 1629, 1297, 1226, 1187, 752, 695 cm⁻¹; ¹H NMR (300 MHz, CDCl₃) δ 7.43-7.27 (m, 10 H), 6.81 (dd, 1 H, *J* = 3.1, 10.1 Hz), 6.47 (dd, 1 H, *J* = 3.1, 10.1 Hz), 6.21 (dd, 1 H, *J* = 1.9, 10.1 Hz), 6.14 (dd, 1 H, *J* = 1.9, 10.1 Hz), 5.52 (t, 1 H, *J* = 10.2 Hz), 5.28 (d, 2 H, *J* = 12.0 Hz), 5.23 (d, 2 H, *J* = 12.0 Hz), 2.57 (dd, 2 H, *J* = 2.0, 10.2 Hz); ¹³C NMR (75 MHz, CDCl₃) δ 183.9, 171.4, 152.3, 146.0, 144.8, 134.0, 129.0, 128.7, 128.6, 128.5, 128.5, 75.5, 70.0, 54.3, 35.2; HRMS (ESI⁺) *m/z* calcd for C₂₅H₂₁NO₇Na 470.1216, found 470.1231.



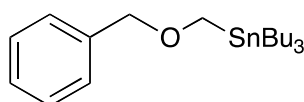
Dibenzyl Carbonate (2.18).⁷⁰ NaH (60% in mineral oil; 12.0 g, 300 mmol, 1.3 equiv) was washed with dry hexanes (30 mL), dried under vacuum, and resuspended in THF (60 mL). A solution of benzyl alcohol (25.0 g, 231 mmol, 1 equiv) in dry THF (450 mL) was added, via an addition funnel to the NaH slurry over 30 min. The reaction mixture was heated at reflux for 2 h and then cooled to 0 °C in an ice bath. Dry CO₂ was bubbled through the vigorously stirred solution for 1 h at 0 °C. To this very viscous slurry was added benzyl chloroformate (33.0 mL, 231 mmol, 1 equiv) dropwise via an addition funnel over 20 min. The reaction mixture was allowed to warm to rt, stirred for an additional 3 h, diluted with H₂O (200 mL), and extracted with Et₂O (2 x 100 mL). The combined organic layers were washed with brine, dried (Na₂SO₄), filtered, and concentrated under reduced pressure. The resulting oil was washed with hexanes, placed under vacuum for several minutes, and allowed to crystallize for 2 d to give **2.18** (64.5 g, 98%) as white solid (Note: yield was determined from NMR which showed THF and hexanes, which, using the molar ratio, were subtracted from the mass of the crude material): Mp 23 °C; ¹H NMR (300 MHz, CDCl₃) δ 7.42 (s, 10 H), 5.28 (s, 4 H); ¹³C NMR (75 MHz, CDCl₃) δ 148.2,

133.6, 128.8, 128.5, 128.5, 71.1.



2.19

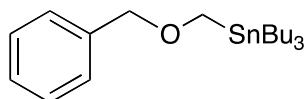
1st Generation approach to tri-*n*-butyliodomethylstannane (2.19).⁹⁸ In a 100 mL, three-neck, round bottomed flask, cupric acetate monohydrate (0.0400 g 0.200 mmol, 1 equiv) was dissolved in glacial acetic acid (4 mL) by heating in an oil bath. To the resulting greenish blue solution was added granular zinc (2.60 g, 40 mg atom, 1 equiv) and this mixture was stirred for 2 min while heating was continued. The acetic acid was decanted from the settled dark brown Cu/Zinc couple; a second batch of glacial acetic acid (4 mL) was added, stirred with heating for 2 min, and decanted. The metal couple was cooled to room temperature, washed with dry Et₂O (2 x 8 mL), and dried under an argon stream. After the addition of dry THF (7 mL), the reaction was initiated with several drops of diiodomethane. Upon appearance of a purple color, an additional portion of dry THF (13 mL) was added to the flask and a solution of diiodomethane (10.8 g, 40.2 mmol, 2 equiv) in THF (7 mL) was added dropwise at a rate which allowed the reaction mixture to maintain a temperature of *ca.* 40 °C. The stirring was continued for the first hour without heating but during the last two hours the temperature was maintained with an oil bath. The resulting dark purple slurry was cannulated to another 100 mL round-bottom flask through a glass filter. To the very pale yellow ICH₂ZnI solution was added tributyltin chloride (90%; 6.60 mL, 21.2 mmol, 1 equiv) dropwise over 10 min and the mixture was stirred for 26 h. The yellow reaction mixture was diluted with hexanes (150 mL), washed with water and brine, dried (MgSO₄), filtered, and concentrated under reduced pressure to give a pale yellow oil. The crude oil was purified by chromatography on SiO₂ (hexanes) to give **2.19** (6.20 g, 68%) as a colorless oil: R_f 0.87 (hexanes); ¹H NMR (300 MHz, CDCl₃) δ 1.95 (s, 2 H), 1.59-1.48 (m, 6 H), 1.39-1.27 (m, 6 H), 1.01-0.89 (m, 15 H).



2.20

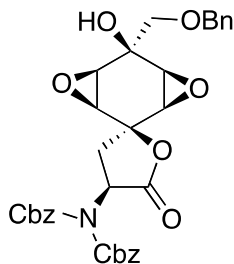
1st Generation approach to benzyloxymethyl tri-*n*-butylstannane (2.20).⁹⁸ To a slurry of NaH (60% in mineral oil; 0.746 g, 18.6 mmol, 1.4 equiv) in dry THF (35 mL) was added

dropwise at rt benzyl alcohol (1.72 mL, 18.6 mmol, 1.25 equiv). The reaction mixture was allowed to stir until H₂ evolution subsided (~15 min). To the resulting stirred solution was added **2.19** (6.20 g, 14.4 mmol, 1 equiv) in one portion and the mixture was stirred at rt for 64 h, diluted with hexanes (100 mL), washed with water and brine, dried (MgSO₄), filtered, and concentrated under reduced pressure. The resulting pale yellow oil was purified by chromatography on Si₂O (EtOAc/hexanes 0:1 to 1:50) to give **2.20** (4.86 g, 89%) as a colorless oil: ¹H NMR (300 MHz, CDCl₃) δ 7.33 (s, 5 H) 4.45 (s, 2 H), 3.78 (t, 2 H, *J* = 7.8 Hz), 1.60-1.40 (m, 6 H), 1.39-1.27 (m, 6 H), 0.97-0.89 (m, 15 H); ¹³C NMR (75 Hz, CDCl₃) δ 138.9, 128.2, 127.5, 127.3, 77.2, 61.5, 29.1, 27.3, 13.7, 9.0.



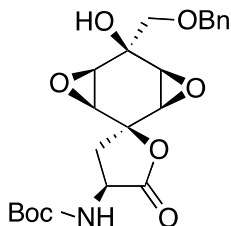
2.20

2nd Generation approach to benzyloxymethyl tri-*n*-butylstannane (2.20).⁸⁵ To a stirred solution of freshly distilled diisopropylamine (3.20 mL, 22.7 mmol, 1.1 equiv) in dry THF (40 mL) was added dropwise *n*-BuLi (1.6 M in hexanes; 12.9 mL, 20.6 mmol, 1 equiv) at -78 °C. After addition, the reaction mixture was allowed to warm to 0 °C for 30 min and Bu₃SnH (5.56 mL, 20.6 mmol, 1 equiv) was added. The resulting greenish solution was stirred at 0 °C for 30 min and then cooled to -78 °C. Freshly distilled chloromethyl benzyl ether (2.86 mL, 20.6 mmol, 1 equiv) was added and the solution was allowed to stirred for 30 min at -78 °C. The reaction mixture was allowed to warm to rt and stir for 6 h, diluted with hexanes (50 mL), washed with brine (x2), dried (MgSO₄), filtered, and concentrated under reduced pressure to give a yellow oil. The crude oil was purified by chromatography on SiO₂ (hexanes/CH₂Cl₂, 8:2) to give **2.20** (5.66 g, 67%) as a colorless oil: ¹H NMR (300 MHz, CDCl₃) δ 7.33 (s, 5 H) 4.45 (s, 2 H), 3.78 (t, 2 H, *J* = 7.80 Hz), 1.60-1.40 (m, 6 H), 1.39-1.27 (m, 6 H), 0.97-0.89 (m, 15 H); ¹³C NMR (75 MHz, CDCl₃) δ 138.9, 128.2, 127.5, 127.3, 77.2, 61.5, 29.1, 27.3, 13.7, 9.0.



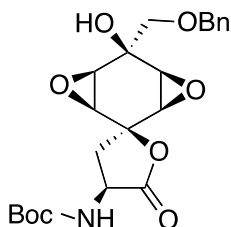
2.3

(3*S*,5*S*,6*S*,7*R*,8*S*,9*S*,10*R*)-3-[Bis(benzyloxycarbonyl)amino]-8-[(benzyloxy)-methyl]-6,7:9,10-diepoxy-8-hydroxy-1-oxaspiro[4.5]decan-2-one (2.3).⁷⁰ To a stirred solution of **2.20** (1.38 g, 3.35 mmol, 1.5 equiv) in dry THF (15 mL) was added *n*-BuLi (1.6 M in hexanes; 2.10 mL, 3.35 mmol, 1.5 equiv) dropwise at -78 °C. After 10 min, the deep yellow solution was cooled to -100 °C and rapidly cannulated to a pre-cooled (-100 °C) solution of **2.1** (1.00 g, 2.24 mmol, 1 equiv) in dry THF (10 mL). After 10 min, the mixture was quenched at -78 °C with NaHCO₃ (5% aqueous solution; 30 mL) under vigorous stirring, allowed to warm to rt and extracted with EtOAc (3 x 60 mL). The combined organic layers were washed with brine, dried (Na₂SO₄), filtered, and concentrated under reduced pressure to give a yellow-green oil. Upon addition of hexanes (5 mL) to the oily residue, two immiscible layers formed. The top layer was decanted, the remaining oil was diluted with CCl₄ (20 mL) and *m*-CPBA (1.75 g, 9.61 mmol, 4.3 equiv) and 3-tert-butyl-4-hydroxy-5-methylphenylsulfide (0.721 g, 2.01 mmol, 0.9 equiv) were added. The resulting slurry was heated at 70 °C for 3 h, at which point the solvent was removed under reduced pressure. The crude residue was dissolved in CH₂Cl₂ (5 mL) and purified by chromatography on SiO₂ (EtOAc/hexanes 1:5 to 1:1) to give **2.3** (0.300 g, 23%) as a white powder: R_f 0.16 (EtOAc/hexanes, 1:1); Mp 163-164 °C (CHCl₃); [α]_D -18.6 (*c* 1.00, CH₂Cl₂); IR (neat) 3513, 3060, 3030, 2965, 2855, 1781, 1729, 1688, 1339, 1231, 1120, 941, 760, 749, 697 cm⁻¹; ¹H NMR (300 MHz, CDCl₃) δ 7.36-7.3 (s, 10 H), 7.22-7.20 (m, 5 H), 5.30, 5.23 (AB, 2 H, *J* = 12.0 Hz), 5.27 (m, 1 H), 4.50, 4.44 (AB, 1 H, *J* = 11.0 Hz), 3.62, 3.56 (AB, 2 H, 9.0 Hz), 3.25 (dt, 2 H, *J* = 1.2, 3.9 Hz), 3.15 (dd, 1 H, *J* = 2.7, 4.2 Hz), 3.07 (dd, 1 H, *J* = 3.0, 3.9 Hz), 2.26 (dd, 1 H, *J* = 10.8, 13.8 Hz), 1.94 (dd, 1 H, *J* = 10.2, 14.1 Hz); ¹³C NMR (176 MHz, CDCl₃) δ 171.6, 152.4, 136.8, 134.2, 128.8, 128.7, 128.5, 128.5, 128.4, 128.3, 79.2, 74.1, 72.7, 69.9, 68.7, 59.1, 59.1, 58.7, 58.6, 54.0, 32.4; HRMS (ESI⁺) *m/z* calcd for C₃₃H₃₁NO₁₀Na 624.1846, found 624.1831.



2.14

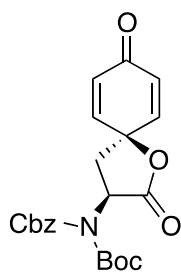
1st Generation approach to (3*S*,5*S*,6*S*,7*R*,8*S*,9*S*,10*R*)-3-[(*tert*-butoxy-carbonyl)amino]-8-[(benzyloxy)-methyl]-6,7:9,10-diepoxy-8-hydroxy-1-oxaspiro[4.5]decan-2-one (2.14).⁷⁰ To a stirred solution of **2.3** (0.150 g, 0.255 mmol, 1 equiv) in dry THF/absolute MeOH (1:1, 12 mL) was added 1,4-cyclohexadiene (0.938 mL, 9.91 mmol, 38.8 equiv) and Pd/C (10% w/w; 0.160 g). The reaction mixture was stirred at rt for 2 h, filtered through Celite and di-*tert*-butyl dicarbonate (0.167 g, 0.766 mmol, 3 equiv) was added to the filtrate. The mixture was stirred at rt for 30 min. The solvent was removed under reduced pressure and the crude residue was purified by chromatography on SiO₂ (EtOAc/hexanes, 1:1) to give **2.14** (0.0406 g, 38%) as a white solid: ¹H NMR (300 MHz, CDCl₃) δ 7.48 (s, 5 H), 5.72 (bs, 1 H), 4.68 (s, 3 H), 3.75 (s, 2 H), 3.58-3.47 (m, 4 H), 2.68 (t, 1 H, *J* = 11.0 Hz), 2.27 (dd, 1 H, *J* = 11.0 Hz), 1.61 (s, 9 H). For full characterization see 2nd generation approach.



2.14

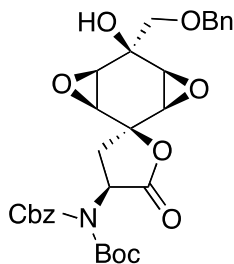
2nd Generation approach to (3*S*,5*S*,6*S*,7*R*,8*S*,9*S*,10*R*)-3-[(*tert*-butoxycarbonyl)amino]-8-[(benzyloxy)-methyl]-6,7:9,10-diepoxy-8-hydroxy-1-oxaspiro[4.5]decan-2-one (2.14).⁷⁰ To a stirred solution of **2.23** (0.430 g, 0.758 mmol, 1 equiv) in dry THF/absolute MeOH (1:1, 40 mL) was added 1,4-cyclohexadiene (3.13 mL, 33.1 mmol, 43.7 equiv) and Pd/C (10% w/w; 0.100 g). The reaction mixture was allowed to stir at rt for 2 h, an additional batch of Pd/C (10% w/w; 0.200 g) was added, and the mixture was allowed to stir at rt for an additional 5 h, filtered through Celite and purified by chromatography on SiO₂ (deactivated with Et₃N, EtOAc/hexanes,

1:1) to give **2.14** (0.234 g, 72%) as a white foam: R_f 0.58 (EtOAc/hexanes, 3:1); $[\alpha]_D +0.9$ (c 1.05, CH_2Cl_2); IR (neat) 3457, 3063, 2976, 2905, 1783, 1692, 1597, 1531, 1464, 1326, 1155, 1080, 989, 700 cm^{-1} ; ^1H NMR (300 MHz, CDCl_3) δ 7.39-7.28 (m, 5 H), 5.21 (bs, 1 H), 4.56 (d, 1 H, $J = 11.4$ Hz), 4.51 (d, 1 H, $J = 11.4$ Hz), 4.41 (q, 1 H, $J = 10.0$ Hz), 3.63 (d, 1 H, $J = 9.3$ Hz), 3.59 (d, 1 H, $J = 9.3$ Hz), 3.42-3.38 (m, 1 H), 3.30-3.27 (m, 3 H), 3.10 (bs, 1H), 2.59 (dd, 1 H, $J = 10.2$ Hz, 13.8 Hz), 2.06 (app t, 1 H, $J = 12$ Hz), 1.47 (s, 9 H); ^{13}C NMR (75 MHz, CDCl_3) δ 173.8, 155.1, 136.9, 128.6, 128.3, 128.2, 80.9, 79.5, 74.1, 72.7, 68.5, 59.4, 59.3, 59.3, 58.0, 49.8, 35.3, 28.3; HRMS (ESI⁺) m/z calcd for $\text{C}_{22}\text{H}_{27}\text{NO}_8\text{Na}$ 456.1634, found 456.1612.



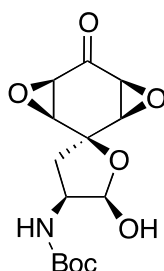
2.22

(3S)-3-[(Benzyloxycarbonyl)-(tert-butoxycarbonyl)amino]-1-oxaspiro[4.5]deca-7,10-diene-2,8-dione (2.22). To a stirred solution of **2.21** (7.84 g, 25.0 mmol, 1 equiv) in dry MeCN (125 mL) was added DMAP (0.917 g, 7.51 mmol, 1 equiv), followed by Boc_2O (6.55 g, 30.0 mmol, 1.2 equiv) in two portions at a 30 min interval. The resulting solution was allowed to stir at rt for 45 min, and concentrated under reduced pressure. The crude residue was dissolved in EtOAc/hexanes (3:1), passed through a plug of SiO_2 , and concentrated under reduced pressure to give **2.22** (9.73 g, 94%) as a white solid: R_f 0.40 (EtOAc/hexanes, 1:2); Mp 60-63 °C (EtOAc); $[\alpha]_D -26.7$ (c 0.99, CH_2Cl_2); IR 2976, 2935, 1785, 1731, 1694, 1671, 1634, 1347, 1226, 1142, 1107 cm^{-1} ; ^1H NMR (300 MHz, CDCl_3) δ 7.35-7.27 (m, 5 H), 6.84 (dd, 1 H, $J = 10.2$ Hz), 6.69 (dd, 1 H, $J = 3.2, 10.2$ Hz), 6.15 (dd, 1 H, $J = 3.2, 10.2$ Hz), 6.12 (dd, 1 H, $J = 1.8, 3.4$ Hz), 5.42 (t, 1 H, $J = 10.2$ Hz), 5.19 (d, 1 H, $J = 11.9$ Hz), 5.13 (d, 1 H, $J = 11.9$ Hz), 2.61-2.45 (m, 2 H), 1.38 (s, 9 H); ^{13}C NMR (75 MHz, CDCl_3) δ 183.8, 171.6, 152.5, 150.7, 146.1, 145.0, 134.1, 128.7, 128.5, 128.4, 128.3, 128.1, 84.9, 75.3, 69.4, 53.8, 35.1, 27.5; ESI-MS m/z 436.5 $[\text{M}+\text{Na}]^+$ 314.5 $[\text{M}-\text{Boc}]^+$.



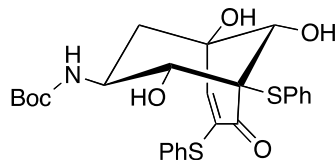
2.23

(3*S*,5*S*,6*S*,7*R*,8*S*,9*S*,10*R*)-3-[(*tert*-Butoxycarbonyl)(benzyloxycarbonyl)amino]-8-[(benzyloxy)-methyl]-6,7:9,10-diepoxy-8-hydroxy-1-oxaspiro[4.5]decan-2-one (2.23).⁷⁰ To a stirred solution of **2.20** (1.49 g, 3.63 mmol, 1.5 equiv) in dry, degassed THF (10 mL) was added dropwise at -78 °C of *n*-BuLi (2.27 mL, 1.6 M in hexanes; 3.63 mmol, 1.5 equiv). After 20 min, the deep yellow solution was cooled to -105 °C and rapidly cannulated to a pre-cooled (-105 °C) solution of the **2.22** (1.00 g, 2.42 mmol, 1 equiv) in dry, degassed THF (15 mL). After 45 min, the reaction was quenched at -105 °C with NaHCO₃ (3% aqueous solution; 15 mL) under vigorous stirring. The mixture was allowed to warm to rt and extracted with EtOAc (3 x 40 mL). The combined organic layers were washed with brine, dried (Na₂SO₄), filtered, and concentrated under reduced pressure to give an oil. Upon addition of hexanes (2 mL) to the oily residue, two immiscible layers formed. The top layer was decanted, the remaining oil was diluted with degassed CCl₄ (15 mL), and *m*-CPBA (2.20 g, 12.1 mmol, 5 equiv) and 3-*tert*-butyl-4-hydroxy-5-methylphenylsulfide (0.867 g, 2.42 mmol, 1 equiv) were added to the stirred solution. The resulting slurry was heated at 70 °C for 3 h, diluted with EtOAc (40 mL), and the solvent was removed under reduced pressure. The crude residue was dissolved in CH₂Cl₂, loaded onto SiO₂ and purified by chromatography on SiO₂ (deactivated with Et₃N; EtOAc/hexanes 4:1 to 2:1 to 1:1 to 1:2) to give **2.23** (0.798 g, 58%) as a colorless foam: *R*_f 0.16 (EtOAc/hexanes, 1:1); [α]_D -6.6 (*c* 0.68, CH₂Cl₂); IR (neat) 1787, 1731, 1696, 1349, 1230, 937, 698 cm⁻¹; ¹H NMR (300 MHz, CDCl₃) δ 7.42-7.35 (m, 5 H), 7.30-7.23 (m, 5 H), 5.26 (d, 1 H, *J* = 11.7 Hz), 5.22 (t, 1 H, *J* = 9.6 Hz), 5.20 (d, 1 H, *J* = 12 Hz), 4.52 (d, 1 H, *J* = 11.1 Hz), 4.47 (d, 1 H, *J* = 11.1 Hz), 3.62 (d, 1 H, *J* = 9.3 Hz), 3.58 (d, 1 H, *J* = 9.3 Hz), 3.31-3.24 (m, 3 H), 3.21 (dd, 1 H, *J* = 2.7, 3.9 Hz), 2.30 (dd, 1 H, *J* = 10.5, 13.8 Hz), 2.03 (dd, 1 H, *J* = 10.2, 13.8 Hz), 1.45 (s, 9 H); ¹³C NMR (125 MHz, CDCl₃) δ 171.9, 152.8, 151.0, 136.9, 134.5, 128.8, 128.8, 128.7, 128.5, 128.5, 128.3, 85.1, 79.0, 77.3, 74.1, 72.8, 69.7, 68.7, 59.1, 59.1, 58.9, 58.7, 53.7, 32.6, 30.9, 27.9; HRMS (ESI⁺) *m/z* calcd. for C₃₀H₃₃NO₁₀Na 590.2002, found 590.2019.



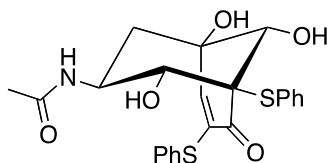
2.13

(2R,3S,5S,6S,7R,9S,10R)-3-[(*tert*-Butoxycarbonyl)amino]-6,7:9,10-diepoxy-2-hydroxy-1-oxaspiro[4.5]decan-8-one (2.13).⁷⁰ A solution of **2.14** (0.160 g, 0.369 mmol, 1 equiv) and CeCl₃·7H₂O (0.459 g, 1.85 mmol, 5 equiv) in EtOH/H₂O (2:1, 13 mL) was stirred for 10 min at rt until all solids had completely dissolved. The mixture was cooled to -25 °C, treated with NaBH₄ (0.084 g, 2.21 mmol, 6 equiv) in three portions at 30 min intervals, allowed to stir at -25 °C for an additional 30 min and quenched with several drops of acetone. The reaction mixture was diluted with EtOAc (150 mL), washed with brine, dried (MgSO₄), filtered, and concentrated under reduced pressure. The crude residue was dissolved in MeOH/THF (1:1, 16 mL) and of Pd/C (300 mg, 10% w/w) was added to the stirred solution. The reaction vessel was evacuated and back filled with H₂ three times. H₂ was vigorously bubbled through the solution at rt overnight. The mixture was filtered through a pad of Celite and concentrated under reduced pressure. The resulting yellow residue was dissolved in MeOH/THF (1:1, 10 mL) and a solution of NaIO₄ (0.395 g, 1.85 mmol, 5 equiv) in H₂O (2 mL) was added. After 1.5 h, a second solution of NaIO₄ (0.250 g) in H₂O (1 mL) was added to the reaction mixture. After an additional 1 h at rt, the reaction mixture was diluted with EtOAc (20 mL), washed with brine, dried (MgSO₄), filtered, and concentrated under reduced pressure. The crude residue was dissolved in CH₂Cl₂ (3 mL) purified by chromatography on SiO₂ (deactivated with Et₃N, EtOAc/hexanes, 1:1) to give **2.13** (0.0624 g, 54%) as a colorless film: R_f 0.78; [α]_D +2.3 (*c* 0.60, CH₂Cl₂); IR (CDCl₃) 3388, 2976, 1700, 1508, 1364, 1243, 1161, 1006, 926, 790 cm⁻¹; ¹H NMR (600 MHz, CDCl₃) δ 5.59 (s, 1 H), 5.15 (d, 1 H, *J* = 8.4 Hz), 4.59 (s, 1 H), 4.42 (s, 1 H), 3.68 (s, 1 H), 3.50 (s, 1 H), 3.43 (s, 2 H), 2.53 (t, 1 H, *J* = 11.4 Hz), 2.03 (t, 1 H, *J* = 12.0 Hz), 1.44 (s, 9 H); ¹³C NMR (150 MHz, CDCl₃) δ 198.3, 155.3, 96.4, 80.3, 78.6, 64.2, 62.9, 55.8, 55.5, 53.2, 35.9, 28.3; HRMS (ESI⁺) *m/z* calcd for C₁₄H₁₉NO₇Na 336.1059, found 336.1060.



2.24

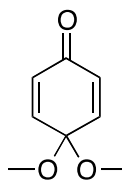
tert-Butyl-(1*S*,2*S*,3*R*,5*S*)-2,5,9-trihydroxy-8-oxo-1,7-bis(phenylthio)bicyclo[3.3.1]non-6-en-3-ylcarbamate (2.24). To a stirred solution of **2.13** (0.025 g, 0.0803 mmol, 1 equiv) in dry THF (3 mL) was added NaH (60% dispersion in mineral oil; 0.00963 g, 0.241 mmol, 3 equiv) and thiophenol (0.0442 g, 0.402 mmol, 5 equiv). The reaction mixture was allowed to stir at rt for 2 h, diluted with EtOAc (10 mL), washed with H₂O and brine, dried (Mg₂SO₄), filtered, and concentrated under reduced pressure. The residue was purified by chromatography on SiO₂ (EtOAc/hexane 1:5 to 1:1) to give **2.24** (0.0171 g, 41%) as a colorless film: R_f 0.26 (EtOAc/hexane, 1:1); ¹H NMR (300 MHz, CDCl₃) δ 7.59-7.27 (m, 10 H), 6.01 (s, 1 H), 4.59 (s, 1 H), 3.60 (bs, 1 H), 3.50 (bs, 1 H), 3.26 (s, 1 H), 3.24 (s, 1 H), 3.20 (s, 1 H), 3.13 (d, 1 H, *J* = 3.9 Hz), 2.14 (bs, 1 H), 1.70 (s, 1 H), 1.26 (s, 1H); ¹³C (75 MHz, CDCl₃) δ 189.0, 171.2, 155.7, 142.4, 139.6, 137.9, 134.8, 133.3, 132.1, 130.6, 129.9, 129.7, 129.5, 129.2, 126.4, 124.4, 123.6, 80.3, 75.7, 72.3, 72.0, 69.8, 51.0, 36.5, 29.7, 28.3.



2.26

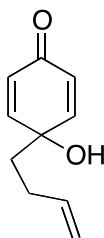
Acetyl-(1*S*,2*S*,3*R*,5*S*)-2,5,9-trihydroxy-8-oxo-1,7-bis(phenylthio)bicyclo[3.3.1]non-6-en-3-ylcarbamate (2.26). To a stirred solution of **2.24** (0.0182 g, 0.0353 mmol, 1 equiv) in CH₂Cl₂ (0.3 mL) was added trifluoroacetic acid (0.026 mL, 0.353 mmol, 10 equiv) and the mixture was allowed to stir at rt for 2.5 h. The solvent was removed with purging N₂. To the crude TFA salt (0.014 g, 0.0337 mmol, 1 equiv) was added DIPEA (0.234 mL, 1.15 mmol, 40 equiv) and the reaction mixture was allowed to stir for 10 min, and heated with a solution of freshly distilled acetyl chloride (0.00317 g, 0.0404 mmol, 1.2 equiv) in CH₂Cl₂ (0.060 mL). The mixture was allowed to stir at rt for 30 min, concentrated in a stream of N₂, washed with citric acid (1 M aqueous solution) (2 x 10 mL), saturated aqueous NaHCO₃ (2 x 10 mL), brine, dried (Na₂SO₄),

filtered, and concentrated under reduced pressure. The crude residue was purified by chromatography on SiO₂ (MeOH/ CH₂Cl₂, 3:97) to give **2.26** (0.0102 g, 66%) as a colorless film: R_f 0.62 (CH₂Cl₂/MeOH, 9:1); ¹H NMR (700 MHz, CDCl₃) δ 7.60-7.27 (m, 10 H), 6.00 (s, 1 H), 5.69 (s, 1 H), 3.90 (s, 2 H), 3.49 (s, 1 H), 3.28 (s, 1 H), 3.21 (d, 1 H, *J* = 9.8 Hz), 2.09 (dd, 1 H, *J* = 4.2, 12.6 Hz), 1.96 (s, 3 H), 1.34 (t, 1 H, *J* = 12.6 Hz); ¹³C NMR (176 MHz, CDCl₃) δ 189.3, 171.4, 142.3, 138.1, 134.8, 130.49, 130.0, 129.5, 129.2, 126.8, 123.5, 77.8, 75.7, 73.4, 72.2, 71.9.



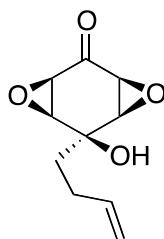
2.29

4,4-Dimethoxycyclohexa-2,5-dienone (2.29).^{91,99} To a stirred solution of 4-methoxyphenol (10.0 g, 80.6 mmol, 1 equiv) in dry MeOH (200 mL) at 0 °C under a nitrogen atmosphere was added phenyliodonium diacetate (PIDA; 25.9 g, 80.6 mmol, 1 equiv), and the resulting solution was stirred for 45 min. After 45 min, the mixture was quenched with a saturated aqueous solution of NaHCO₃ (300 mL) and extracted with Et₂O (3x). The combined organic layers were washed with brine, dried (MgSO₄), filtered, and concentrated under reduced pressure. The reaction mixture was purified by chromatography on SiO₂ (deactivated with 0.1% Et₃N; EtOAc/hexanes 1:5 to 1:1) to give **2.29** (12.3 g, 99%) as a colorless oil: R_f 0.41 (EtOAc/hexanes, 1:3); IR (neat) 2991, 2941, 2830, 1685, 1671, 1636, 1178, 1105, 1083, 1059, 1034, 1034, 958, 853 cm⁻¹; ¹H NMR (300 MHz, CDCl₃) δ 6.84-6.79 (m, 2 H), 6.29-6.24 (m, 2 H), 3.37 (s, 6 H); ¹³C NMR (75 Hz, CDCl₃) δ 185.1, 143.2, 130.0, 92.4, 50.4; HRMS (EI⁺) *m/z* calcd for C₈H₁₀O₃ 154.0630, found 154.0628.



2.30

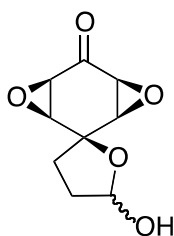
4-(But-3-enyl)-4-hydroxycyclohexa-2,5-dienone (2.30).⁹¹ To a dry, 100 mL, three-necked, round-bottom flask equipped with an addition funnel and reflux condenser was added magnesium turnings (2.27 g, 93.4 mmol, 1.2 equiv) and a crystal of iodine. Heat (Bunsen burner flame) was applied to the stirred turnings until a purple gas coated the interior of the flask. The sample was allowed to cool under argon and suspended in dry THF (30 mL). To the stirred solution was added via an addition funnel a solution of 4-bromo-1-butene (9.48 mL, 93.4 mmol, 1.2 equiv) in dry THF (10 mL) at a rate so that the solution maintained a gentle reflux. After the addition was complete, the reaction mixture was allowed to stir at reflux for 45 min, cooled to rt and cannulated over 30 min into a pre-cooled (-78 °C) solution of **2.29** (12.0 g, 77.8 mmol, 1 equiv) in dry THF (150 mL). The reaction mixture was allowed to stir at -78 °C for 3 h and quenched with a saturated aqueous solution of NH₄Cl, warmed to rt, and extracted with EtOAc (3 x 150 mL). The combined organic layers were washed with brine, dried (MgSO₄) and concentrated under reduced pressure. The resulting oil was diluted with H₂O/acetone (1:1, 500 mL) and glacial acetic acid (50 mL) was added. The reaction mixture was allowed to stir at rt for 3 h, and extracted with EtOAc (3 x 150 mL). The combined organic layers were washed with brine, dried (MgSO₄), filtered, and concentrated under reduced pressure to give a yellow oil which was purified by chromatography on SiO₂ (EtOAc/hexanes, 1:3) to give **2.30** (7.05 g, 43%) as a volatile pale yellow oil: R_f 0.24 (EtOAc/hexanes, 1:3); IR (neat) 3339, 3276, 2937, 1662, 1606, 1396, 1052, 1018, 991, 859, 716 cm⁻¹; ¹H NMR (300 MHz, CDCl₃) δ 6.86-6.81 (m, 2 H), 6.21-6.16 (m, 2 H), 5.77 (dddd, 1 H, *J* = 6.3, 6.3, 10.2, 16.5 Hz), 5.06-4.96 (m, 2 H), 2.52 (s, 1 H), 2.09-2.01 (m, 2 H), 1.88-1.83 (m, 2 H); ¹³C NMR (75 MHz, CDCl₃) δ 185.5, 150.9, 137.1, 128.4, 115.4, 69.8, 38.8, 27.8. HRMS (EI⁺) *m/z* calcd for C₁₀H₁₂O₂ 164.0837, found 164.0829.



2.31

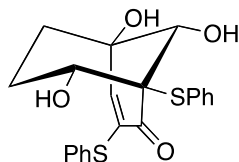
4-(But-3-enyl)-4-hydroxycyclohexa-2,5-dioxirane (2.31).⁹¹ To a stirred solution of enone **2.30** (4.25 g, 25.9 mmol, 1 equiv) in methanol (100 mL) and 30 % aq. hydrogen peroxide (7.93 mL,

77.6 mmol, 3 equiv) at 0 °C was added 6 M NaOH (2.16 mL, 7.00 mmol, 0.5 equiv) dropwise. The reaction mixture was allowed to stir at 0 °C for 2 h, poured onto DI water and thoroughly extracted with EtOAc (7 x 100 mL). The combined organic layers were washed with brine, poured onto activated 4 Å molecular sieves, and allowed to stir at rt for 3 h. The mixture was filtered and concentrated under reduced pressure to give **2.31** (3.68 g, 72%) as an off-white solid: R_f 0.62 (EtOAc/ CH₂Cl₂, 1:1); IR (neat) 3459, 3028, 2976, 2940, 1702, 1366, 1328, 1239, 1090, 1060, 1025, 926, 917 cm⁻¹; ¹H NMR (300 MHz, CDCl₃) δ 5.79 (ddd, 1 H, J = 6.6, 10.2, 16.8 Hz), 5.09-5.01 (m, 2 H), 3.50 (s, 4 H), 3.03 (s, 1 H), 2.27-2.15 (m, 2 H), 1.96-1.90 (m, 2 H); ¹³C NMR (75 MHz, CDCl₃) δ 198.9, 136.7, 115.9, 68.9, 63.9, 57.0, 35.6, 26.9. HRMS (ESI⁺) m/z calcd for C₁₀H₁₂O₄ 196.0736, found 196.0726.



2.32

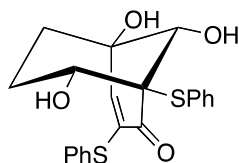
1-Oxaspiro[4.5]deca-6,9-diepoxy-2,8-lactol (2.32).⁹¹ A solution of **2.31** (1.00 g, 5.10 mmol, 1 equiv) in CH₂Cl₂ (30 mL) was cooled to -78 °C. Ozone was passed through the stirred solution for 3.5 h followed by purging with N₂ before the dropwise addition of DMS (7.54 mL, 102 mmol, 20 equiv) at -78 °C. The reaction mixture was allowed to stir at -78 °C for 1 h and then allowed to warm to rt and stirred at rt for 3 d. The solvent was removed under reduced pressure. The crude product was purified by chromatography on SiO₂ (EtOAc) to give **2.32** (0.962 g, 95%) as an off-white solid: R_f 0.45 (EtOAc); Mp 164-166 °C; IR (neat) 3369, 3440, 2965, 1722, 1459, 1431, 1349, 1243, 1202, 1038, 976, 919 cm⁻¹; ¹H NMR (500 MHz, acetone-*d*₆) δ 5.69 (d, 1 H, J = 1.8 Hz), 5.53 (bs, 1 H), 3.62 (t, 1 H, J = 2.4 Hz), 3.49 (t, 1 H, J = 2.1 Hz), 3.35 (t, 1 H, J = 2.4 Hz), 3.31 (t, 1 H, J = 2.4 Hz), 2.35-2.27 (m, 1 H), 2.19-2.11 (m, 2 H), 2.05-2.00 (m, 1 H); ¹³C NMR (125 MHz, acetone-*d*₆) δ 200.5, 100.6, 80.3, 65.2, 63.6, 56.1, 55.9, 33.9, 31.1; HRMS (EI⁺) m/z calcd for C₉H₁₀O₅ 198.0528, found 198.0523.



2.33

(1*S*,8*R*,9*S*)-5,8,9-Trihydroxy-1,3-bis(phenylthio)bicyclo[3.3.1]non-3-en-2-one (2.33).

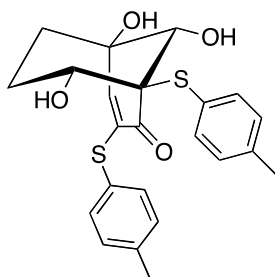
Prepared according to general procedure A utilizing **2.32** (0.025 g, 0.126 mmol, 1 equiv), Cs₂CO₃ (0.205 g, 0.631 mmol, 5 equiv), and thiophenol (0.039 mL, 0.38 mmol, 3 equiv). The crude mixture was purified by chromatography on SiO₂ (EtOAc/hexanes 1:2 to 1:1) to give **2.33** (0.0416 g, 83%) as a white solid: R_f 0.33 (EtOAc/hexanes, 1:1); Mp 185-188 °C; IR (neat) 3502, 3335, 3051, 2945, 2879, 1666, 1590, 1472, 1439, 1310, 1228, 1100, 1032, 954, 738, 689 cm⁻¹; ¹H NMR (500 MHz, CDCl₃) δ 7.52-7.51 (m, 2 H), 7.46-7.41 (m, 5 H), 7.33-7.32 (m, 3 H), 5.96 (d, 1 H, *J* = 0.9 Hz), 3.85-3.83 (m, 1 H), 3.48 (s, 1 H), 3.32 (s, 1 H), 3.24 (s, 1 H), 2.27 (s, 1 H), 2.06-2.03 (m, 1 H), 1.89 (dd, 1 H, *J* = 1.5, 6.6 Hz), 1.76 (dt, 1 H, *J* = 2.1, 8.1 Hz), 1.67 (s, 1 H), 1.38 (dq, 1 H, *J* = 3.0, 8.1 Hz); ¹³C NMR (125 MHz, CDCl₃) δ 193.0, 143.3, 141.9, 134.9, 133.4, 133.1, 130.1, 129.9, 129.5, 129.2, 128.4, 73.0, 69.9, 63.4, 58.4, 33.3, 29.1; HRMS (EI⁺) *m/z* calcd for C₂₁H₂₀O₄S₂ 400.0803, found 400.0822.



2.33

(1*S*,8*R*,9*S*)-5,8,9-Trihydroxy-1,3-bis(phenylthio)bicyclo[3.3.1]non-3-en-2-one (2.33).

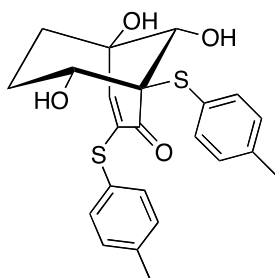
Prepared according to general procedure B utilizing **2.32** (0.0100 g, 0.0505 mmol, 1 equiv), Cs₂CO₃ (0.0822 g, 0.252 mmol, 5 equiv) and thiophenol (0.015 mL, 0.151 mmol, 3 equiv). The crude reaction mixture was purified by chromatography on SiO₂ (EtOAc/hexanes 1:2 to 1:1) to give **2.33** (0.0178 g, 88%) as a white solid: R_f 0.33 (EtOAc/hexanes, 1:1); ¹H NMR (300 MHz, acetone-*d*₆) δ 7.79-7.75 (m, 2 H), 7.52-7.39 (m, 8 H), 5.99 (d, 1 H, *J* = 2.4 Hz), 4.65 (bs, 1 H), 4.52 (bs, 1 H), 4.02 (d, 1 H, *J* = 1.8 Hz), 3.42-3.37 (m, 1 H), 3.19, (s, 1 H), 2.00-1.94 (m, 1 H), 1.62-1.54 (m, 1 H), 1.51-1.34 (m, 2 H). For full characterization see directly preceding experimental.



2.34

(1*S*,8*R*,9*S*)-5,8,9-Trihydroxy-1,3-bis(*p*-tolylthio)bicyclo[3.3.1]non-3-en-2-one (2.34).

Prepared according to general procedure A utilizing **2.32** (0.0500, 0.252 mmol, 1 equiv), Cs₂CO₃ (0.411 g, 1.26 mmol, 5 equiv), and *p*-thiocresol (0.0940 mL, 0.757 mmol, 3 equiv). The crude reaction mixture was purified by chromatography on SiO₂ (EtOAc/hexanes, 1:1) to give **2.34** (0.078.6 g, 73%) as a white solid: R_f 0.29 (EtOAc/hexanes, 1:1); Mp 191-193 °C; IR (neat) 3496, 3345, 3060, 2942, 1664, 1578, 1472, 1420, 1314, 1217, 1100, 1031, 868, 731 cm⁻¹; ¹H NMR (300 MHz, acetone-*d*₆) δ 7.64-7.62 (m, 2 H), 7.40-7.38 (m, 2 H), 7.28 (d, 2 H, *J* = 8.1 Hz), 7.23 (d, 2 H, *J* = 8.1 Hz), 5.84 (d, 1 H, *J* = 2.4 Hz), 4.44 (bs, 1 H), 3.99 (s, 1 H), 3.37 (dd, 1 H, *J* = 6.0, 10.8 Hz), 3.17 (d, 1 H, *J* = 2.4 Hz), 2.36 (s, 3 H), 2.35 (s, 3 H), 1.99-1.92 (m, 1 H), 1.58-1.51 (m, 1 H), 1.48-1.32 (m, 2 H); ¹³C NMR (75 MHz, acetone-*d*₆) δ 190.9, 143.1, 140.8, 140.0, 139.9, 139.1, 135.6, 131.4, 130.6, 128.1, 126.1, 77.5, 75.8, 74.2, 69.2, 31.4, 28.4, 21.2, 21.2; HRMS (EI⁺) *m/z* calcd for C₂₃H₂₄O₄S₂ 428.1116, found 428.1101

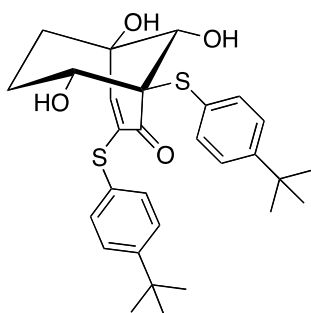


2.34

(1*S*,8*R*,9*S*)-5,8,9-Trihydroxy-1,3-bis(*p*-tolylthio)bicyclo[3.3.1]non-3-en-2-one (2.34).

Prepared corresponding to general procedure B utilizing **2.32** (0.0100 g, 0.0505 mmol, 1 equiv), Cs₂CO₃ (0.0822 g, 0.252 mmol, 5 equiv) and *p*-thiocresol (0.0188 g, 0.151 mmol, 3 equiv). The crude reaction mixture was purified by chromatography on SiO₂ (EtOAc/hexanes 1:2 to 1:1) to

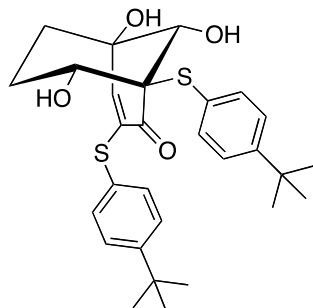
give **2.34** (0.0160 g, 74%) as a white solid: R_f 0.29 (EtOAc/hexanes, 1:1); $^1\text{H NMR}$ (300 MHz, acetone- d_6) δ 7.63 (dm, 2 H, $J = 8.1$ Hz), 7.39 (dm, 2 H, $J = 8.1$ Hz), 7.28 (d, 2 H, $J = 8.1$ Hz), 7.23 (d, 2 H, $J = 8.1$ Hz), 5.84 (d, 1 H, $J = 2.4$ Hz), 4.59 (bs, 1 H), 4.44 (d, 1 H, $J = 3.0$ Hz), 3.99 (d, 1 H, $J = 2.1$ Hz), 3.39-3.34 (m, 1 H), 3.17 (s, 1 H), 2.36 (s, 3 H), 2.35 (s, 3 H), 1.99-1.92 (m, 1 H), 1.58-1.51 (m, 1 H), 1.48-1.32 (m, 2 H). For full characterization see directly preceding experimental.



2.35

(1S,8R,9S)-1,3-Bis(4-*tert*-butylphenylthio)-5,8,9-trihydroxybicyclo[3.3.1]non-3-en-2-one

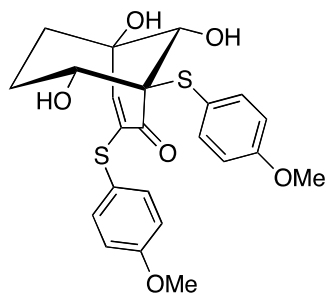
(2.35). Prepared according to general procedure A utilizing **2.32** (0.0500, 0.252 mmol, 1 equiv), Cs_2CO_3 (0.411 g, 1.26 mmol, 5 equiv), and 4-*tert*-butylthiophenol, (0.13 mL, 0.76 mmol, 3 equiv). The crude reaction mixture was purified by chromatography on SiO_2 (EtOAc/hexanes, 5:1 to 3:1) to give **2.35** (0.0935 g, 72%) as a white solid: R_f 0.86 (EtOAc/hexanes, 1:1); Mp 203-207 °C; IR (neat): 3475, 2956, 2902, 2866, 1674, 1591, 1489, 1265, 1099, 1034, 1012, 831, 729 cm^{-1} ; $^1\text{H NMR}$ (300 MHz, acetone- d_6) δ 7.71-7.69 (m, 1 H), 7.68-7.67 (m, 1 H), 7.52-7.41 (m, 6 H), 5.94 (d, 1 H, $J = 2.4$ Hz), 4.62 (bs, 1 H), 4.48 (bs, 1 H), 4.04 (d, 1 H, $J = 1.8$ Hz), 3.40 (dd, 1 H, $J = 6.0, 11.1$ Hz), 3.19 (d, 1 H, $J = 2.1$ Hz), 2.01-1.93 (m, 1 H), 1.61-1.54 (m, 1 H), 1.49-1.35 (m, 2 H), 1.33 (s, 9 H), 1.32 (s, 9 H); $^{13}\text{C NMR}$ (75 MHz, acetone- d_6) δ 190.9, 153.7, 152.8, 143.8, 139.5, 138.9, 134.9, 128.4, 127.6, 126.9, 126.1, 77.7, 75.8, 74.2, 69.3, 35.3, 28.3; HRMS (EI+) m/z calcd for $\text{C}_{29}\text{H}_{36}\text{O}_4\text{S}_2$ 512.2055, found 512.2076.



2.35

(1*S*,8*R*,9*S*)-1,3-Bis(4-*tert*-butylphenylthio)-5,8,9-trihydroxybicyclo[3.3.1]non-3-en-2-one

(2.35). Prepared corresponding to general procedure B utilizing **2.32** (0.0100 g, 0.0505 mmol, 1 equiv), Cs₂CO₃ (0.0822 g, 0.252 mmol, 5 equiv) and 4-*tert*-butyl-thiophenol (0.026 mL, 0.15 mmol, 3 equiv). The crude reaction mixture was purified by chromatography on SiO₂ (EtOAc/hexanes 1:5 to 1:2) to give **2.35** (0.0218 g, 84%) as an off-white solid: R_f 0.86 (EtOAc/hexanes, 1:1); ¹H NMR (300 MHz, acetone-*d*₆) δ 7.70-7.67 (m, 2 H), 7.52-7.41 (m, 6 H), 5.94 (d, 1 H, *J* = 2.4 Hz), 4.47 (bs, 1 H), 4.04 (bs, 1 H), 3.40 (dd, 1 H, *J* = 5.7, 10.8 Hz), 3.19 (d, 1 H, *J* = 2.7 Hz), 2.01-1.93 (m, 1 H), 1.61-1.54 (m, 1 H), 1.49-1.35 (m, 2 H), 1.33 (s, 9 H), 1.32 (s, 9 H). For full characterization see directly preceding experimental.

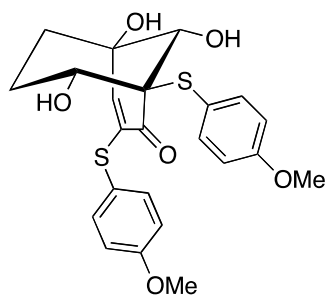


2.36

(1*S*,8*R*,9*S*)-5,8,9-Trihydroxy-1,3-bis(4-methoxyphenylthio)bicyclo[3.3.1]non-3-en-2-one

(2.36). Prepared according to general procedure A utilizing **2.32** (0.0500 g, 0.252 mmol, 1 equiv), Cs₂CO₃ (0.411 g, 1.26 mmol, 5 equiv), and 4-methoxythiophenol (0.093 mL, 0.76 mmol, 3 equiv). The crude reaction mixture was purified by chromatography on SiO₂ (EtOAc/hexanes, 1:1) to give **2.36** (0.0857 g, 74%) as a white solid. R_f 0.29 (EtOAc/hexanes, 1:1); Mp 105-107 °C; IR (neat) 3487, 2937, 2911, 2903, 1670, 1588, 1491, 1285, 1243, 1172, 1101, 1025, 950, 829 cm⁻¹; ¹H NMR (300 MHz, acetone-*d*₆) δ 7.69-7.65 (m, 2 H), 7.45-7.42 (m, 2 H), 7.06-7.02 (m, 2 H), 6.99-6.95 (m, 2 H), 5.70 (d, 1 H, *J* = 2.4 Hz), 4.55 (bs, 1 H), 4.37 (s, 1 H), 3.97 (d, 1 H *J* =

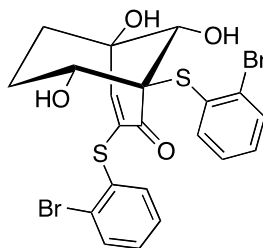
2.1 Hz), 3.85 (s, 3 H), 3.83 (s, 3 H), 3.36 (dd, 1 H, $J = 6.0, 10.8$ Hz), 3.15 (s, 1 H), 1.98-1.91 (m, 1 H), 1.56-1.50 (m, 1 H), 1.46-1.32 (m, 2 H); ^{13}C NMR (75 MHz, acetone- d_6) δ 191.1, 162.0, 161.7, 141.7, 140.9, 140.5, 137.9, 121.4, 119.9, 116.3, 115.4, 77.4, 75.8, 74.1, 69.1, 55.8, 55.7, 31.5, 28.3; HRMS (EI $^+$) m/z calcd for $\text{C}_{23}\text{H}_{24}\text{O}_6\text{S}_2$ 460.1014, found 460.1009.



2.36

(1S,8R,9S)-5,8,9-Trihydroxy-1,3-bis(4-methoxyphenylthio)bicyclo[3.3.1]non-3-en-2-one

(2.36). Prepared according to general procedure B utilizing **2.32** (0.0100 g, 0.0505 mmol, 1 equiv), Cs_2CO_3 (0.0822 g, 0.252 mmol, 5 equiv) and 4-methoxythiophenol (0.019 mL, 0.15 mmol, 3 equiv). The crude mixture was purified by chromatography on SiO_2 (EtOAc/hexanes 1:5 to 1:2) to give **2.36** (0.0186 g, 80%) as a white solid: R_f 0.29 (EtOAc/hexanes, 1:1); ^1H NMR (300 MHz, acetone- d_6) δ 7.66 (dm, 2 H, $J = 8.7$ Hz), 7.43 (dm, 2 H, $J = 9.0$ Hz), 7.04 (dm, 2 H, 9.0 Hz), 6.96 (dm, 2 H, $J = 8.7$ Hz), 5.69 (d, 1 H, $J = 2.4$ Hz), 4.38 (bs, 1 H), 3.98 (d, 1 H, $J = 2.1$ Hz), 3.85 (s, 3 H), 3.83 (s, 3 H), 3.35 (dd, 1 H, $J = 6.0, 10.8$ Hz), 3.15 (d, 1 H, $J = 2.4$ Hz), 1.98-1.91 (m, 1 H), 1.56-1.50 (m, 1 H), 1.46-1.32 (m, 2 H). For full characterization see directly preceding experimental.

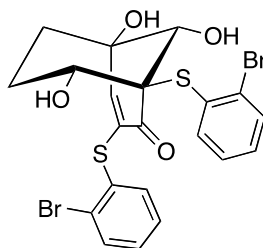


2.37

(1S,8R,9S)-1,3-Bis(2-bromophenylthio)-5,8,9-trihydroxybicyclo[3.3.1]non-3-en-2-one (2.37).

Prepared according to general procedure A utilizing **2.32** (0.0500, 0.252 mmol, 1 equiv), Cs_2CO_3

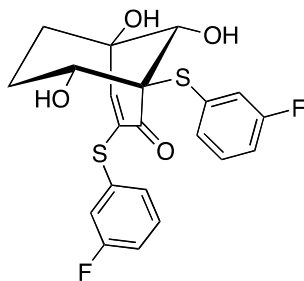
(0.411 g, 1.26 mmol, 5 equiv), and 2-bromobenzenethiol (0.091 mL, 0.76 mmol, 3 equiv). The crude reaction mixture was purified by chromatography on SiO₂ (EtOAc/hexanes 1:3 to 1:1) to give **2.37** (0.121 g, 87%) as a white solid. A small portion was recrystallized (acetone/Et₂O) to give colorless crystals for x-ray analysis: R_f 0.28 (EtOAc/hexanes, 1:1); Mp 171-173 °C; IR (neat) 3427, 3468, 2937, 2883, 2868, 1659, 1599, 1446, 1420, 1331, 1272, 1248, 1110, 1019, 954, 760, 732 cm⁻¹; ¹H NMR (300 MHz, acetone-*d*₆) δ 8.06 (dd, 1 H, *J* = 2.4, 7.2 Hz), 7.79 (dd, 1 H, 2.1, 7.2 Hz), 7.75 (dd, 1 H, *J* = 0.9, 8.1 Hz), 7.56 (dd, 1 H, *J* = 1.5, 7.8 Hz), 7.45-7.29 (m, 4 H), 6.19 (d, 1 H, *J* = 2.7 Hz), 4.86 (bs, 1 H), 4.63 (s, 1 H), 3.79 (d, 1 H, *J* = 2.1 Hz), 3.47 (dd, 1 H, *J* = 5.7, 10.2 Hz), 3.43 (d, 1 H, *J* = 2.1 Hz), 1.74-1.55 (m, 4 H); ¹³C NMR (75 MHz, acetone-*d*₆) δ 190.0, 148.5, 141.6, 135.8, 135.6, 134.5, 134.4, 134.3, 133.2, 132.4, 131.5, 130.8, 129.6, 129.1, 127.6, 78.1, 76.2, 70.0, 69.9, 31.3, 28.4; HRMS (ESI+) *m/z* calcd for C₂₁H₁₈O₄NaS₂Br₂ 578.8911, found 578.8945.



2.37

(1S,8R,9S)-1,3-Bis(2-bromophenylthio)-5,8,9-trihydroxybicyclo[3.3.1]non-3-en-2-one (2.37).

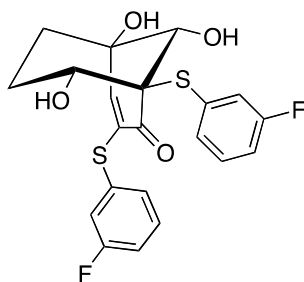
Prepared according to general procedure B utilizing **2.32** (0.0100 g, 0.0505 mmol, 1 equiv), Cs₂CO₃ (0.0822 g, 0.252 mmol, 5 equiv) and 2-bromothiophenol (0.018 mL, 0.15 mmol, 3 equiv). The crude reaction mixture was purified by chromatography on SiO₂ (EtOAc/hexanes, 2:1 to 1:1) to give **2.37** (0.0233 g, 83%) as a white solid: R_f 0.28 (EtOAc/hexanes, 1:1); ¹H NMR (300 MHz, acetone-*d*₆) δ 8.06 (dd, 1 H, *J* = 2.4, 7.2 Hz), 7.79 (dd, 1 H, 2.1, 7.2 Hz), 7.75 (dd, 1 H, *J* = 0.9, 8.1 Hz), 7.56 (dd, 1 H, *J* = 1.5, 7.8 Hz), 7.45-7.29 (m, 4 H), 6.19 (d, 1 H, *J* = 2.4 Hz), 4.86 (bs, 1 H), 4.69 (bs, 1 H), 3.80 (s, 1 H), 3.48 (dd, 1 H, *J* = 5.7, 10.2 Hz), 3.43 (d, 1 H, *J* = 2.4 Hz), 2.04-2.00 (m, 1 H), 1.74-1.55 (m, 3 H). For full characterization see directly preceding experimental.



2.38

(1*S*,8*R*,9*S*)-1,3-Bis(3-fluorophenylthio)-5,8,9-trihydroxybicyclo[3.3.1]non-3-en-2-one (2.38).

Prepared according to general procedure A utilizing **2.32** (0.0500, 0.252 mmol, 1 equiv), Cs₂CO₃ (0.411 g, 1.26 mmol, 5 equiv), and 3-fluorothiophenol (0.064 mL, 0.76 mmol, 3 equiv). The crude reaction mixture was purified by chromatography on SiO₂ (EtOAc/hexanes, 1:1) to give **2.38** (0.110 g, 74%) as a white solid: R_f 0.46 (EtOAc/hexanes, 1:1); Mp 190-192 °C; IR (neat) 3349, 3345, 3060, 2942, 2918, 1664, 1578, 1472, 1420, 1472, 1314, 1217, 1155, 1099, 868, 731 cm⁻¹; ¹H NMR (300 MHz, acetone-*d*₆) δ 7.63-7.56 (m, 2 H), 7.51-7.41 (m, 2 H), 7.30-7.21 (m, 3 H), 7.16-7.09 (m, 1 H), 6.39 (d, 1 H, *J* = 2.4 Hz), 4.76 (bs, 1 H), 4.19 (s, 1 H), 3.48 (dd, 1 H, *J* = 6.0, 11.1 Hz), 3.29 (d, 1 H, 2.4 Hz), 2.06-1.98 (m, 1 H), 1.72-1.63 (m, 1 H), 1.58-1.42 (m, 2 H); ¹³C NMR (75 MHz, acetone-*d*₆) δ 190.3, 165.1 (d, *J* = 48.8 Hz), 161.8 (d, *J* = 48.8 Hz), 149.3, 137.0, 135.9 (d, *J* = 8.3 Hz), 135.2 (d, *J* = 3.0 Hz), 132.3 (d, *J* = 7.5 Hz), 132.0 (d, *J* = 9.0 Hz), 131.3 (d, *J* = 8.3 Hz), 129.1 (d, *J* = 3.0 Hz), 125.5 (d, *J* = 21.0 Hz), 119.7 (d, *J* = 22.5 Hz), 117.6 (d, *J* = 21.0 Hz), 115.7 (d, *J* = 21.0 Hz), 77.8, 76.0, 74.7, 69.4, 31.2, 28.6; HRMS (EI⁺) *m/z* calcd for C₂₁H₁₉F₂O₄S₂ 436.0615, found 436.0633.

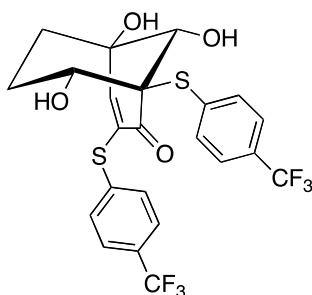


2.38

(1*S*,8*R*,9*S*)-1,3-Bis(3-fluorophenylthio)-5,8,9-trihydroxybicyclo[3.3.1]non-3-en-2-one (2.38).

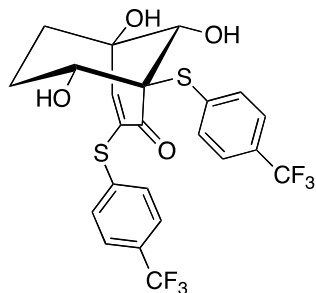
Prepared according to general procedure B utilizing **2.32** (0.0100 g, 0.0505 mmol, 1 equiv), Cs₂CO₃ (0.0822 g, 0.252 mmol, 5 equiv) and 3-fluorothiophenol (0.013 mL, 0.15 mmol, 3 equiv). The crude reaction mixture was purified by chromatography on SiO₂ (EtOAc/hexanes, 1:1) to

give **2.38** (0.017 g, 77%) as a white solid: R_f 0.46 (EtOAc/hexanes, 1:1); ^1H NMR (300 MHz, acetone- d_6) δ 7.63-7.56 (m, 2 H), 7.49-7.42 (m, 2 H), 7.30-7.22 (m, 3 H), 7.16-7.10 (m, 1 H), 6.38 (d, 1 H, $J = 2.4$ Hz), 4.76 (bs, 1 H), 4.19 (s, 1 H), 3.49 (dd, 1 H, $J = 6.0, 10.8$ Hz), 3.29 (d, 1 H, 2.4 Hz), 2.02-1.98 (m, 1 H), 1.72-1.63 (m, 1 H), 1.58-1.42 (m, 2 H). For full characterization see directly preceding experimental.



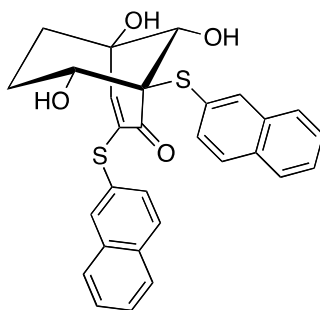
2.39

(1S,8R,9S)-5,8,9-Trihydroxy-1,3-bis(4-(trifluoromethyl)phenylthio)bicyclo[3.3.1]non-3-en-2-one (2.39). Prepared according to general procedure A utilizing **2.32** (0.0500, 0.252 mmol, 1 equiv), Cs_2CO_3 (0.411 g, 1.26 mmol, 5 equiv), and 4-trifluoromethylthiophenol (0.135 g, 0.757 mmol, 3 equiv). The crude reaction mixture was purified by chromatography on SiO_2 (EtOAc/hexane, 1:1) to give **2.39** (0.100 g, 74%) as a foam: R_f 0.21 (EtOAc/hexanes, 1:1); Mp 145-148 °C IR (neat) 3498, 1685, 1604, 1319, 1163, 1120, 1103, 1062, 1013, 839 cm^{-1} ; ^1H NMR (300 MHz, acetone- d_6) δ 8.00 (d, 2 H, $J = 8.1$ Hz), 7.74 (d, 2 H, $J = 8.1$ Hz), 7.69 (d, 2 H, $J = 8.4$ Hz), 7.60 (d, 2 H, $J = 8.4$ Hz), 6.69 (d, 1 H, $J = 2.7$ Hz), 4.84 (bs, 1 H), 4.28 (s, 1 H), 3.54 (dd, 1 H, $J = 5.7, 10.5$ Hz), 3.32 (d, 1 H, $J = 2.4$ Hz), 2.03-1.96 (m, 1 H), 1.80-1.47 (m, 3 H); ^{13}C NMR (75 MHz, acetone- d_6) δ 190.0, 152.8, 139.6, 135.8, 135.4, 131.9, 126.8 (q, $J = 3.75$ Hz), 126.4 (q, $J = 3.75$ Hz), 78.0, 76.0, 75.0, 69.6, 31.0, 28.8. HRMS (ESI+) m/z calcd for $\text{C}_{23}\text{H}_{18}\text{O}_4\text{F}_6\text{NaS}_2$ 559.0448, found 559.0490.



2.39

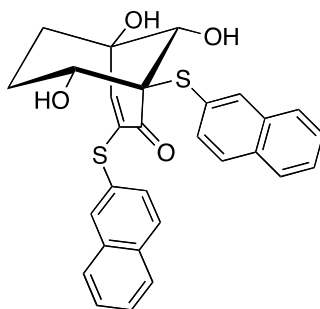
(1*S*,8*R*,9*S*)-5,8,9-Trihydroxy-1,3-bis(4-(trifluoromethyl)phenylthio)bicyclo[3.3.1]non-3-en-2-one (2.39). Prepared according to general procedure B utilizing **2.32** (0.0100 g, 0.0505 mmol, 1 equiv), Cs₂CO₃ (0.0822 g, 0.252 mmol, 5 equiv) and 4-trifluoromethylthiophenol (0.0207 g, 0.151 mmol, 3 equiv). The crude reaction mixture was purified by chromatograph on SiO₂ (EtOAc/hexanes, 1:1) to give **2.39** (0.0191 g, 71%) as a yellow film: R_f 0.21 (EtOAc/hexanes, 1:1); ¹H NMR (300 MHz, acetone-*d*₆) δ 8.00 (d, 1 H, *J* = 8.1 Hz), 7.75 (d, 1 H, *J* = 8.1 Hz), 7.68 (d, 1 H, *J* = 8.4 Hz), 7.60 (d, 1 H, *J* = 8.4 Hz) 6.69 (d, 1 H, *J* = 2.7 Hz), 4.28 (s, 1 H), 3.53 (dd, 1 H, *J* = 5.7, 10.5 Hz), 2.03-1.96 (m, 1 H), 1.80-1.47 (m, 3 H). For full characterization see directly preceding experimental.



2.40

(1*S*,8*R*,9*S*)-5,8,9-Trihydroxy-1,3-bis(naphthalen-2-ylthio)bicyclo[3.3.1]non-3-en-2-one (2.40). Prepared according to general procedure A utilizing **2.32** (0.0250, 0.126 mmol, 1 equiv), Cs₂CO₃ (0.206 g, 0.631 mmol, 5 equiv), and naphthalene-2-thiol (0.0606 g, 0.378 mmol, 3 equiv). The crude reaction mixture was purified by chromatography on SiO₂ (EtOAc/hexanes, 1:1) to give **2.40** (0.0357 g, 57%) as a white solid: R_f 0.44 (EtOAc/hexanes, 1:1); Mp 230-233 °C; IR (neat) 2509, 3351, 3047, 2984, 2871, 1662, 1584, 1129, 1099, 1032, 954, 857, 820, 745 cm⁻¹; ¹H NMR (300 MHz, DMSO-*d*₆) δ 8.39 (s, 1 H), 8.09 (s, 1 H), 8.00-7.88 (m, 6 H), 7.83 (d, 1 H, *J* =

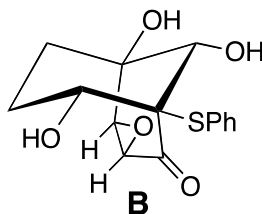
8.4 Hz), 7.59-7.57 (m, 4 H), 7.49 (d, 1 H, $J = 8.1$ Hz), 6.05 (d, 1 H, $J = 1.8$ Hz), 5.62 (d, 1 H, $J = 3.6$ Hz), 5.51 (s, 1 H), 5.22 (d, 1 H, $J = 3.9$ Hz), 3.03 (s, 1 H), 1.83-1.81 (m, 1 H), 1.46-1.38 (m, 2 H), 1.22-1.14 (m, 1 H); ^{13}C NMR (75 MHz, DMSO- d_6) δ 190.7, 146.7, 138.5, 136.0, 134.6, 133.5, 132.9, 132.4, 132.3, 129.8, 129.3, 128.7, 128.0, 127.9, 127.7, 127.6, 127.2, 127.0, 126.9, 126.5, 76.6, 74.7, 74.0, 68.1, 30.6, 28.4; HRMS (ESI+) m/z calcd for $\text{C}_{29}\text{H}_{24}\text{O}_4\text{NaS}_2$ 523.1014, found 523.1017.



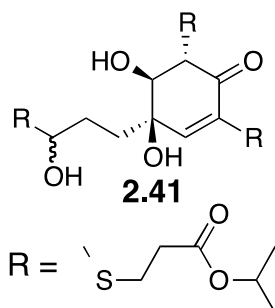
2.40

(1*S*,8*R*,9*S*)-5,8,9-Trihydroxy-1,3-bis(naphthalen-2-ylthio)bicyclo[3.3.1]non-3-en-2-one

(2.40). Prepared according to general procedure B utilizing **2.32** (0.0100 g, 0.0505 mmol, 1 equiv), Cs_2CO_3 (0.0822 g, 0.252 mmol, 5 equiv) and naphthalene-2-thiol (0.0242 g, 0.151 mmol, 3 equiv). The crude reaction mixture was purified by chromatograph on SiO_2 (EtOAc/hexanes, 1:1) to give **2.40** (0.0186 g, 74%) as a yellow film: R_f 0.44 (EtOAc/hexanes, 1:1); ^1H NMR (300 MHz, DMSO- d_6) δ 8.39 (s, 1 H), 8.09 (s, 1 H), 8.00-7.88 (m, 6 H), 7.83 (d, 1 H, $J = 8.4$ Hz), 7.59-7.57 (m, 4 H), 7.49 (dd, 1 H, $J = 1.5, 8.1$ Hz), 6.05 (d, 1 H, $J = 2.1$ Hz), 5.62 (d, 1 H, $J = 3.9$ Hz), 5.51 (s, 1 H), 5.22 (d, 1 H, $J = 3.6$ Hz), 3.35-3.30 (m, 1 H), 3.03 (m, 1 H), 1.83-1.81 (m, 1 H), 1.46-1.38 (m, 2 H), 1.22-1.14 (m, 1 H). For full characterization see directly preceding experimental.

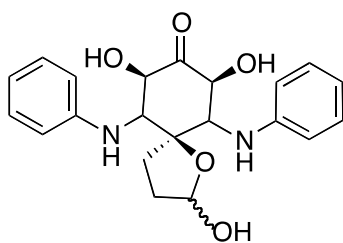


(1R,2R,4S,6S,7R,10S)-1,7,10-Trihydroxy-6-(phenylthio)-3-oxatricyclo[4.3.1.0^{2,4}]decan-5-one (B). To a stirred solution of **2.32** (0.250 g, 1.27 mmol, 1 equiv) in CH₂Cl₂ (25 mL) was added thiophenol (0.391 mL, 3.82 mmol, 3 equiv) and Cs₂CO₃ (3.46 g, 6.37 mmol, 5 equiv). The reaction mixture was allowed to stir at rt for 5 min then quenched with a saturated aqueous solution of NH₄Cl and extracted with EtOAc (3x). The combined organic layers were washed with brine, dried (MgSO₄), filtered, and concentrated under reduced pressure. The crude mixture was purified by chromatography on SiO₂ (EtOAc/hexanes, 1:1) to give **B** (0.070 g, 18%) as a colorless film: R_f 0.45 (EtOAc); IR (CDCl₃) 3465, 2943, 2877, 1709, 1274, 1437, 1326, 1111, 1085, 1025, 904, 729, 703 cm⁻¹; ¹H NMR (300 MHz, CDCl₃) δ 7.64 (d, 2 H, *J* = 7.5 Hz), 7.50-7.36 (m, 3 H), 3.69 (d, 1 H, *J* = 3.3 Hz), 3.62 (d, 1 H, *J* = 2.1 Hz), 3.47 (d, 2 H, *J* = 4.2 Hz), 3.36 (s, 1 H), 3.32 (s, 1 H), 2.92 (d, 1 H, *J* = 12.3 Hz), 2.14-2.07 (m, 2 H), 1.50-1.38 (m, 2 H); ¹³C NMR (75 MHz, CDCl₃) δ 198.3, 138.2, 130.4, 129.3, 126.0, 73.6, 71.7, 70.7, 70.6, 60.8, 56.6, 29.9, 27.7; HRMS (EI⁺) *m/z* calcd for C₁₅H₁₆O₅S 308.0718, found 308.0713.



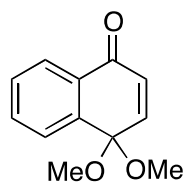
Diisopropyl-3,3'-(((1S,5S,8R,9S)-5,8,9-trihydroxy-2-oxobicyclo[3.3.1]non-3-ene-1,3-diyl)bis(sulfanediyl))dipropanoate (2.41). To a stirred solution of **2.32** (0.0500 g, 0.252 mmol, 1 equiv) in dry CH₂Cl₂ (12 mL) was added Cs₂CO₃ (0.411 g, 0.757 mmol, 5 equiv) and isopropyl 3-mercaptopropionate (0.112 g, 0.757 mmol, 3 equiv). The reaction mixture was allowed to stir at rt for 3 h. The reaction mixture was diluted with EtOAc, washed with brine, and the aqueous layer was extracted with EtOAc (x 2). The combined organic layers were washed with brine, dried (MgSO₄), filtered, and concentrated under reduced pressure. The reaction mixture was purified by chromatography on SiO₂ (EtOAc/hexanes 3:1 to 1:1) to give **2.41** (0.050 g, 32%) as a yellowish film: R_f 0.54 (EtOAc/hexanes, 1:1); ¹H NMR (300 MHz, Acetone-d₆) δ 6.40 (d, 1 H, *J* = 2.1 Hz), 4.96 (sep, 3 H, *J* = 6.3 Hz), 4.66 (s, 1 H), 4.47 (m, 1 H), 3.43 (d, 1 H, *J* = 2.1 Hz), 3.26

(ddd, 1 H, $J = 6.3, 7.2, 18.3$ Hz), 3.10-2.8 (m, 7 H), 2.75-2.48 (m, 7 H), 2.19 (dt, 1 H, $J = 4.2, 13.2$), 1.97 (dq, 1 H, $J = 15.0, 2.1$ Hz), 1.72 (ddd, 1 H, $J = 1.8, 4.8, 13.2$ Hz), 1.53-1.41 (m, 1 H), 1.22 (d, 6 H, $J = 6.0$ Hz), 1.21 (d, 12 H, $J = 6.3$ Hz); ^{13}C NMR (75 MHz, Acetone- d_6) δ 195.2, 172.5, 171.7, 171.3, 145.3, 136.7, 75.3, 69.4, 68.8, 63.2, 35.6, 34.6, 34.0, 31.5, 28.2, 26.3, 26.0, 22.0.



2.42

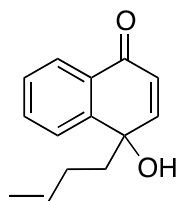
(5*r*,7*R*,9*S*)-2,7,9-Trihydroxy-6,10-bis(phenylamino)-1-oxaspiro[4.5]decan-8-one (2.42). To a stirred solution of **2.32** (0.0200 g, 0.101 mmol, 1 equiv) in CH_3CN (0.5 mL) was added aniline (0.030 mL, 0.30 mmol, 3 equiv) and ZnCl_2 (0.00687 g, 0.05 equiv). The reaction mixture was allowed to stir at rt for 24 h, diluted with EtOAc, washed with brine, dried (MgSO_4), filtered, and concentrated under reduced pressure. The crude mixture was purified by chromatography on SiO_2 (EtOAc/hexanes, 3:1 to 1:1) to give **2.42** (0.0174 g, 45%) as a 1:1 mixture of diastereomers: R_f 0.27 (EtOAc/hexanes); ^1H NMR (300 MHz, CDCl_3) δ 7.21 (t, 2 H, $J = 6.0$ Hz), 6.86 (d, 2 H, $J = 6.0$ Hz), 6.81 (t, 1 H, $J = 6.0$ Hz), 5.81 (d, 1 H, $J = 3.0$ Hz), 4.33 (bs, 1 H), 3.67 (s, 1 H), 3.57 (s, 1 H), 3.54 (s, 1 H), 3.48 (s, 1 H), 3.44 (s, 2 H), 3.39 (s, 2 H), 2.49-2.43 (m, 1 H), 2.36-2.02 (m, 4 H); ^{13}C NMR (75 MHz, CDCl_3) δ 199.3, 145.3, 129.3, 119.5, 114.5, 99.9, 88.0, 79.9, 64.3, 33.0, 29.7. Only NMR data for the major diastereomers is shown.



2.44

4,4-Dimethoxynaphthalen-1(4*H*)-one (2.44).¹⁵ To a stirred solution of 4-methoxynaphthol (5.00 g, 28.7 mmol, 1 equiv) in MeOH (150 mL) was added PIDA (11.1 g, 34.4 mmol, 1.2 equiv), and

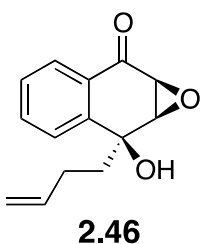
the resulting solution was stirred at rt for 1 h. The mixture was quenched with a saturated aqueous solution of NaHCO₃ and extracted with CH₂Cl₂ (3x). The combined organic layers were dried (MgSO₄), filtered, and concentrated under reduced pressure. The crude mixture was purified by chromatography on SiO₂ (deactivated with 0.1% Et₃N; EtOAc/hexanes, 1:3) to give **2.44** (5.00 g, 85%) as a blue semi-solid: R_f 0.52 (EtOAc/hexanes, 1:3); IR (CDCl₃) 2935, 2827, 1668, 1629, 1597, 1455, 1297, 1056, 974, 764 cm⁻¹; ¹H NMR (300 MHz, CDCl₃) 8.01 (d, 1 H, *J* = 7.5 Hz), 7.67 (d, 1 H, *J* = 7.2 Hz), 7.59 (t, 1 H, *J* = 8.1 Hz), 7.43 (t, 1 H, *J* = 8.1 Hz), 6.88 (d, 1 H, *J* = 10.5 Hz), 6.53 (d, 1 H, *J* = 10.5 Hz), 3.13 (s, 6 H); ¹³C NMR (75 Hz, CDCl₃) δ 183.6, 144.0, 139.5, 133.3, 132.4, 131.4, 129.1, 126.5, 126.1, 94.8, 51.0; HRMS (ESI⁺) *m/z* calcd for C₁₂H₁₃O₃ [M+H]⁺ 205.0865, found 205.0870.



2.45

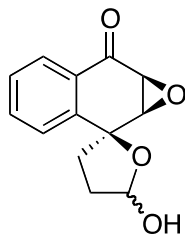
4-(But-3-enyl)-4-hydroxynaphthalen-1(4H)-one (2.45). To a dry, 250 mL round-bottom flask equipped with an addition funnel was added magnesium turnings (0.714 g, 29.4 mmol, 1.2 equiv) and a crystal of iodine. Heat (Bunsen burner flame) was applied to the stirred turnings until a purple gas coated the interior of the flask. The sample was allowed to cool under argon and suspended in dry ether (20 mL). To the stirred solution was added via an addition funnel a solution of 4-bromo-1-butene (2.98 mL, 29.4 mmol, 1.2 equiv) in dry ether (20 mL). The reaction mixture was allowed to stir at reflux for 1 h, allowed to cool to rt, and a solution of **2.44** (5.00 g, 24.5 mmol, 1 equiv) in dry ether (40 mL) was added and quantitatively transferred with dry ether (20 mL). The heterogeneous reaction mixture was allowed to stir at rt for 15 min, cooled to 0 °C, quenched with a saturated aqueous solution of NH₄Cl and extracted with ether (x3). The combined organic layers were washed with brine, dried (MgSO₄), filtered, and concentrated under reduced pressure. The crude oil was suspended in acetone/water (1:1, 200 mL) and glacial acetic acid (14 mL) was added. The reaction mixture was allowed to stir at 0 °C for 2 h and extracted with Et₂O (x2). The combined organic layers were washed with a saturated aqueous solution of NaHCO₃, brine, dried (MgSO₄), filtered, and concentrated under reduced

pressure. The crude mixture was purified by chromatography on SiO₂ (EtOAc/hexanes, 1:10 to 5:1 to 1:1) to give **2.45** (2.09 g, 40%) as a yellow oil: R_f 0.68 (EtOAc/hexanes, 1:1); IR (CDCl₃) 3407, 3066, 2937, 1657, 1597, 1456, 1297, 1150, 1051, 1014, 911, 762 cm⁻¹; ¹H NMR (300 MHz, CDCl₃) δ 7.99 (d, 1 H, *J* = 7.8 Hz), 7.70 (d, 1 H, *J* = 7.5 Hz), 7.60 (t, 1 H, 6.6 Hz), 7.40 (t, 1 H, 8.1 Hz), 6.92 (d, 1 H, *J* = 10.2 Hz), 6.31 (d, 1 H, *J* = 10.2 Hz), 5.62 (dddd, 1 H, *J* = 6.3, 6.3, 10.5, 12.6 Hz), 4.91-4.85 (m, 2 H), 2.81 (s, 1 H), 2.12-1.96 (m, 2 H), 1.96-1.82 (m, 1 H), 1.58-1.45 (m, 1 H); ¹³C NMR (75 Hz, CDCl₃) δ 184.6, 151.9, 146.0, 137.0, 133.4, 130.2, 128.4, 128.1, 126.3, 126.1, 115.0, 71.0, 42.0, 28.1; HRMS (ESI⁺) *m/z* calcd for C₁₄H₁₄O₂Na 237.0891, found 237.0900



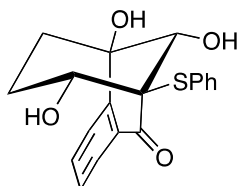
(1a*S*,7*S*,7a*R*)-7-(But-3-enyl)-7-hydroxy-7,7a-dihydronaphtho[2,3-*b*]oxiren-2(1a*H*)-one

(2.46). To a stirred solution of **2.45** (1.90 g, 8.87 mmol, 1 equiv) and 30% aq. hydrogen peroxide (2.72 mL, 1.3 mmol, 3 equiv) in methanol (80 mL) at 0 °C was added 6 M NaOH (0.74 mL, 4.4 mmol, 0.5 equiv) dropwise. The reaction mixture was allowed to stir at 0 °C for 2 h, poured onto a saturated aqueous NH₄Cl solution and extracted with EtOAc (x2). The combined organic layers were checked for peroxides, dried (MgSO₄), filtered, and concentrated under reduced pressure to give **2.46** (1.53 g, 75%) as a light green powder: R_f 0.73 (EtOAc/hexanes, 1:1); Mp 76-78 °C; IR (neat) 3437, 3004, 2953, 1675, 1597, 1452, 1334, 1293, 1062, 1010, 868, 773, 742 cm⁻¹; ¹H NMR (300 MHz, CDCl₃) δ 7.86-7.83 (m, 1 H), 7.69-7.62 (m, 2 H), 7.42 (td, 1 H, *J* = 2.7, 6.0 Hz) 5.71-5.58 (m, 1 H), 4.94-4.87 (m, 2 H), 3.79 (d, 1 H, *J* = 4.2 Hz), 3.75 (d, 1 H, *J* = 4.2 Hz), 2.75 (s, 1 H), 1.98-1.81 (m, 4 H); ¹³C NMR (75 MHz, CDCl₃) δ 193.5, 143.3, 136.9, 134.4, 128.5, 128.3, 126.7, 126.6, 115.2, 72.4, 58.8, 55.5, 40.6, 27.4; HRMS (EI⁺) *m/z* calcd for C₁₄H₁₄O₃Na 253.0841, found 253.0862.



2.47

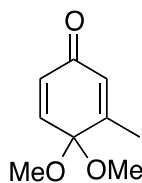
(1a'R,2S,7a'S)-5-Hydroxy-4,5-dihydro-1a'H,3H-spiro[furan-2,2'-naphtho[2,3-b]oxiren]-7'(7a'H)-one (2.47). A solution of **2.46** (1.10 g, 4.99 mmol, 1 equiv) in CH₂Cl₂ (40 mL) was cooled to -78 °C. Ozone was passed through the stirred solution for 1.5 h, which was then purged with N₂ before the dropwise addition of DMS (7.39 mL, 99.9 mmol, 20 equiv) at -78 °C. The reaction mixture was allowed to stir at -78 °C for 1 h and then allowed to warm to rt and stirred at rt for 3 d. The solvent was removed under reduced pressure and the crude mixture was purified by chromatography on SiO₂ (EtOAc/hexanes, 1:2 to 1:1) to give **2.47** (1.18 g, 100% yield) as a 2:1 mixture of diastereomers as an off-white solid: R_f 0.43 (EtOAc/hexanes, 1:1); IR (CDCl₃) 3446, 2984, 1685, 1599, 1456, 1338, 1297, 1047, 1027, 986, 755, 732 cm⁻¹; ¹H NMR (300 MHz, CDCl₃) δ 7.84 (d, 1 H, *J* = 7.5 Hz), 7.63 (d, 1 H, *J* = 9.0 Hz), 7.44-7.38 (m, 2 H), 6.02 (d, 1 H, *J* = 3.5 Hz), 4.04 (d, 1 H, *J* = 4.2 Hz), 3.79 (bs, 1 H), 3.74 (d, 1 H, *J* = 4.5 Hz), 2.55-2.45 (m, 1 H), 2.22-2.08 (m, 2 H), 1.77 (ddd, 1 H, *J* = 3.0, 8.1, 11.4 Hz); ¹³C NMR (75 Hz, CDCl₃) δ 194.2, 142.8, 134.4, 128.3, 127.2, 126.5, 125.2, 100.3, 82.8, 58.4, 54.1, 35.8, 32.0; HRMS (EI⁺) *m/z* calcd for C₁₃H₁₂O₄ 232.0736, found 232.0735. NMR data is for the major diastereomer only.



2.48

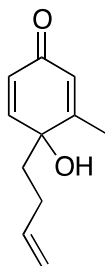
(5R,8S,9R,11R)-5,8,11-Trihydroxy-9-(phenylthio)-6,7,8,9-tetrahydro-5,9-methanobenzo[8]annulen-10(5H)-one (2.48). To a stirred solution of **2.47** (0.0500 g, 0.215 mmol, 1 equiv) in dry CH₂Cl₂ (5 mL) was added Cs₂CO₃ (0.351 g, 1.08 mmol, 5 equiv) and thiophenol (0.066 mL, 0.646 mmol, 3 equiv). The reaction was allowed to stir at rt for 1 h. The crude mixture was diluted with CH₂Cl₂ (4 mL), washed with brine, dried (MgSO₄), filtered, and

concentrated under reduced pressure. The residue was purified by chromatography on SiO₂ (EtOAc/hexanes, 10:1 to 1:1) to give **2.48** (59.0 mg, 80% yield) as a white solid. A small portion was recrystallized (acetone/Et₂O) to give colorless crystals for x-ray analysis: R_f 0.32 (EtOAc/hexanes, 1:1); Mp 180-182 °C; IR (CDCl₃) 3489, 1675, 1597, 1286, 1271, 1228, 1055, 1027, 760, 767 cm⁻¹; ¹H NMR (300 MHz, Acetone-d₆) δ 7.92 (d, 1 H, *J* = 7.8 Hz), 7.80 (d, 2 H, *J* = 7.8 Hz), 7.75 (s, 1 H), 7.71 (t, 1 H, *J* = 6.9 Hz), 7.54-7.42 (m, 4 H), 4.62 (bs, 1 H), 4.49 (s, 1 H), 4.04 (s, 1 H), 3.52 (dd, 1 H, *J* = 5.7, 11.7 Hz), 3.42 (s, 1 H), 1.89-1.83 (m, 1 H), 1.72-1.57 (m, 2 H), 0.99 (dq, 1 H, *J* = 5.7, 12.3 Hz); ¹³C NMR (75 MHz, Acetone-d₆) δ 193.9, 146.8, 139.2, 135.4, 133.5, 130.6, 129.9, 129.9, 128.2, 127.3, 125.8, 77.5, 75.2, 74.6, 69.8, 35.1, 28.6; HRMS (EI⁺) *m/z* calcd for C₁₉H₁₈O₄S 342.0926, found 342.0925.



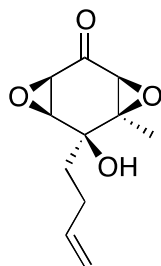
2.49

4,4-Dimethoxy-3-methylcyclohexa-2,5-dienone (2.49).¹⁴ To a stirred solution of *m*-cresol (9.67 mL, 92.5 mmol, 1 equiv) in MeOH (300 mL) at 0 °C was added PIDA (44.7 g, 139 mmol, 1.5 equiv). The reaction mixture was allowed to warm to rt and stirred for 1 h. At this point, an additional batch of PIDA (20.0 g, 64 mmol, 0.7 equiv) was added. The mixture was allowed to stir at rt for an additional 1 h, and quenched with a saturated aqueous solution of Na₂CO₃, and extracted with Et₂O (x2). The combined organic layers were washed with brine, dried (Na₂SO₄), filtered, and concentrated under reduced pressure. The crude residue was purified by chromatography on SiO₂ (deactivated with 0.1% Et₃N; EtOAc/hexanes, 1:4) to give **2.49** (13.1 g, 85% yield) as a yellow oil: R_f 0.38 (EtOAc/hexanes, 1:3); IR (CDCl₃) 2937, 1674, 1640, 1616, 1439, 1385, 1107, 1057, 965 cm⁻¹; ¹H NMR (300 MHz, CDCl₃) δ 6.62 (d, 1 H, *J* = 10.2 Hz), 6.23 (dd, 1 H, *J* = 1.8, 10.5 Hz), 6.06 (s, 1 H), 3.08 (s, 6 H), 1.78 (s, 3 H); ¹³C NMR (75 MHz, CDCl₃) δ 184.5, 155.6, 143.5, 131.9, 129.4, 95.0, 50.6, 16.3; HRMS (EI⁺) *m/z* calcd for C₉H₁₂O₃ 168.0786, found 168.0785.



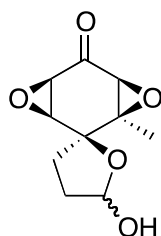
2.50

4-(But-3-en-1-yl)-4-hydroxy-3-methylcyclohexa-2,5-dienone (2.50). To a dry, 25 mL round-bottom flask equipped with an addition funnel was added magnesium turnings (0.0305 g, 1.26 mmol, 1.2 equiv) and a crystal of iodine. Heat (Bunsen burner flame) was applied to the stirred turnings until a purple gas coated the interior of the flask. The sample was allowed to cool under argon and suspended in dry ether (6 mL). To the stirred solution was added via an addition funnel a solution of 4-bromo-1-butene (0.13 mL, 1.26 mmol, 1.2 equiv) in dry ether (2 mL). The reaction mixture was allowed to stir at reflux for 40 min, allowed to cool to rt, and a solution of **2.49** (0.176 g, 1.05 mmol, 1 equiv) in dry ether (3 mL) was added. The heterogeneous mixture was allowed to stir at rt for 15 min, cooled to 0 °C and quenched with a saturated aqueous solution of NH₄Cl and extracted with Et₂O (x3). The combined organic layers were washed with brine, dried (MgSO₄), filtered, and concentrated under reduced pressure. The crude amber oil was suspended in acetone/water (1:1, 20 mL) and glacial acetic acid (1.4 mL) was added. The reaction mixture was allowed to stir at 0 °C for 4 h and extracted with Et₂O (x2). The combined organic layers were washed with a saturated aqueous solution of NaHCO₃, brine, dried (MgSO₄), filtered, and concentrated under reduced pressure. The crude mixture was purified by chromatography on SiO₂ (EtOAc/hexanes, 1:5 to 1:3) to give **2.50** (0.0813 g, 44%) as a yellow oil: R_f 0.35 (EtOAc/hexanes, 1:2); IR (CDCl₃) 3420, 2920, 1666, 1633, 1446, 1431, 1394, 1375, 1243, 1049, 1001, 893 cm⁻¹; ¹H NMR (300 MHz, CDCl₃) δ 6.76 (dd, 1 H, *J* = 3.0, 10.2 Hz), 6.57 (s, 1 H), 6.07 (d, 1 H, *J* = 9.9 Hz), 5.71 (dddd, 1 H, *J* = 6.0, 6.0, 10.2, 16.5 Hz), 4.98-4.90 (m, 2 H), 3.34 (s, 1 H) 2.00-1.92 (m, 2 H), 1.80 (s, 3 H), 1.80-1.74 (m, 2 H); ¹³C NMR (75 Hz, CDCl₃) δ 186.6, 151.4, 147.0, 137.3, 134.5, 127.8, 115.0, 69.8, 38.8, 27.8, 15.5; HRMS (EI⁺) *m/z* calcd for C₁₁H₁₄O₂ 178.0994, found 178.0994.



2.51

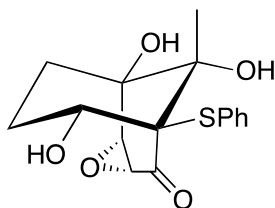
(1R,3S,5R,6S,7S)-6-(But-3-en-1-yl)-6-hydroxy-5-methyl-4,8-dioxatricyclo[5.1.0.0]octan-2-one (2.51). To a stirred solution of **2.50** (1.00 g, 5.61 mmol, 1 equiv) and 30 % aq. hydrogen peroxide (5.73 mL, 56.1 mmol, 10 equiv) in methanol 50 mL at rt was added 6 M NaOH (0.935 mL, 5.61 mmol, 1 equiv) dropwise. After 5 h, the reaction mixture was quenched with a saturated aqueous NH₄Cl solution and extracted with EtOAc (x2). The combined organic layers were checked for peroxides, dried (MgSO₄), filtered, and concentrated under reduced pressure. The crude residue was purified by chromatography on SiO₂ (EtOAc/hexanes, 1:2) to give **2.51** (0.800 g, 68% yield) as a pale yellow oil: R_f 0.66 (EtOAc/hexanes, 1:1); IR (CDCl₃) 3483, 2976, 2933, 2859, 1705, 1640, 1437, 1159, 1085, 1023, 919, 841 cm⁻¹; ¹H NMR (700 MHz, CDCl₃) δ 5.78 (dddd, 1 H, *J* = 6.3, 6.3, 10.5, 12.6 Hz), 5.06-5.01 (m, 2 H), 3.51 (d, 1 H, *J* = 4.2 Hz), 3.49 (t, 1 H, *J* = 4.2 Hz), 3.29 (d, 1 H, *J* = 3.5 Hz), 2.94 (bs, 1 H), 2.17-2.08 (m, 2 H), 1.96-1.89 (m, 2 H), 1.43 (s, 3 H); ¹³C NMR (176 Hz, CDCl₃) δ 199.9, 136.6, 116.0, 70.3, 69.0, 63.8, 62.3, 57.2, 35.6, 27.1, 15.7; HRMS (ESI⁺) *m/z* calcd for C₁₁H₁₄O₄Na 233.0790, found 233.0797.



2.52

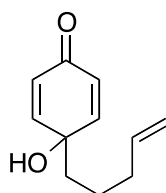
(1'R,2S,3'S,5'R,7'S)-5-Hydroxy-1'-methyldihydro-3H-4',8'-dioxaspiro[furan-2,2'-tricyclo[5.1.0.0^{3,5}]octan]-6'-one (2.52). A solution of **2.51** (0.0700 g, 0.333 mmol, 1 equiv) in CH₂Cl₂ (3 mL) was cooled to -78°C. Ozone was passed through the stirred solution for 1.5 h, which was then purged with N₂ before the dropwise addition of DMS (0.49 mL, 6.7 mmol, 20

equiv) at -78 °C. The reaction mixture was stirred at -78 °C for 1 h and then allowed to warm to rt and stirred for 3 d. The solvent was removed under reduced pressure and the crude mixture was purified by chromatography on SiO₂ (EtOAc/hexanes, 1:1) to give **2.52** (0.0710 g, 100% yield) as a colorless oil and as a 1:1 mixture of lactols: R_f 0.22 (EtOAc/hexanes, 1:1); IR (CDCl₃) 3496, 2976, 1705, 1442, 1457, 1204, 1159, 1094, 1034, 982, 915, 868, 795 cm⁻¹; ¹H NMR (300 MHz, CDCl₃) δ 5.82 (s, 1 H), 4.44 (bs, 1 H), 3.69 (t, 0.5 H, *J* = 3.6 Hz), 3.55 (d, 0.5 H, *J* = 3.3 Hz), 3.44-3.38 (m, 1.5 H), 3.21 (d, 0.5 H, *J* = 3.3 Hz), 2.37-1.95 (m, 4 H), 1.37 (s, 3 H); ¹³C NMR (75 Hz, CDCl₃) δ 200.1 (200.1), 99.8 (99.8), 79.6, (79.6), 70.6, (69.0), 64.3, (62.7), 61.1, (60.7), 55.9, (55.5), 33.0, (33.0), 30.5, (30.4), 15.5, (15.5); HRMS (EI⁺) *m/z* calcd for C₁₀H₁₂O₅ 212.0685, found 212.0680. ¹³C NMR data for the diastereomer are listed in parenthesis.



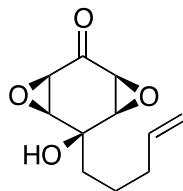
2.53

(1*S*,2*R*,4*S*,6*S*,7*R*,10*S*)-1,7,10-Trihydroxy-10-methyl-6-(phenylthio)-3-oxatricyclo[4.3.1.0^{2,4}]decan-5-one (2.53). To a stirred solution of **2.52** (0.0500 g, 0.236 mmol, 1 equiv) in dry CH₂Cl₂ (2 mL) was added Cs₂CO₃ (0.384 g, 1.18 mmol, 5 equiv) and thiophenol (0.072 mL, 0.707 mmol, 3 equiv). The reaction was stirred at rt for 2 h. The crude mixture was diluted with EtOAc, and washed with brine. The aqueous layer was extracted with EtOAc (x2), the organic layers were combined, washed with brine, dried (MgSO₄), filtered, and concentrated under reduced pressure. The crude mixture was purified by chromatography on SiO₂ (EtOAc/hexanes, 1:3 to 1:1) to give **2.53** (0.0400 g, 53% yield) as a colorless film: R_f 0.29 (EtOAc/hexanes, 1:1); IR (CDCl₃) 3476, 2933, 2877, 1720, 1437, 1426, 1360, 1113, 1081, 1032, 752, 729 cm⁻¹; ¹H NMR (300 MHz, CDCl₃) δ 7.65 (t, 1 H, *J* = 1.8 Hz), 7.63 (d, 1 H, *J* = 1.5 Hz), 7.48-7.35 (m, 3 H), 3.48-3.47 (m, 1 H), 3.42 (app t, 2 H, *J* = 2.4 Hz), 3.33 (dd, 1 H, *J* = 5.4, 11.7 Hz), 2.92 (dd, 1 H, *J* = 2.4 Hz, 12.3 Hz), 2.18-2.02 (m, 2 H), 1.54 (s, 3 H), 1.51-1.25 (m, 2 H); ¹³C NMR (75 MHz, CDCl₃) δ 199.0, 138.2, 130.2, 129.2, 126.4, 73.9, 72.1, 70.6, 70.6, 67.2, 62.3, 29.6, 27.6, 14.8; HRMS (EI⁺) *m/z* calcd for C₁₆H₁₈O₅S 322.0875, found 322.0880.



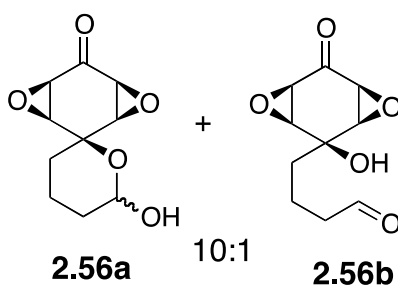
2.54

4-Hydroxy-4-(pent-4-enyl)cyclohexa-2,5-dienone (2.54). To a dry, 25 mL, two-necked, round-bottom flask equipped with an addition funnel was added magnesium turnings (0.341 g, 14.0 mmol, 1.2 equiv) and a crystal of iodine. Heat (Bunsen burner flame) was applied to the stirred turnings until a purple gas coated the interior of the flask. The sample was allowed to cool under argon and suspended in THF (4 mL). To the stirred solution was added via an addition funnel a solution of 5-bromo-1-pentene (1.7 mL, 14 mmol, 1.2 equiv) in THF (8 mL). The reaction mixture was allowed to stir at ca. 40 °C for 1 h, allowed to cool to rt, and added via dropwise addition to a solution of **2.29** (1.80 g, 11.7 mmol, 1 equiv) in THF (20 mL) at -78 °C. The reaction mixture was allowed to stir at -78 °C for 1 h and quenched with a saturated aqueous solution of NH₄Cl, warmed to rt, and extracted with EtOAc (x3). The combined organic layers were washed with brine, dried (MgSO₄) and concentrated under reduced pressure. The crude residue was suspended in acetone/water (1:1, 100 mL), glacial acetic acid (10 mL) was added, and the reaction mixture was allowed to stir at rt for 2 h. The reaction mixture was concentrated under reduced pressure. The remaining aqueous layer was extracted with EtOAc (x3) and the combined organic layers were washed with brine, dried (MgSO₄), and concentrated under reduced pressure. The crude residue was purified by chromatography on SiO₂ (EtOAc/hexanes, 1:5 to 1:3) to give **2.54** (1.14 g, 55% yield) as a yellow oil: R_f 0.2 (EtOAc/hexanes, 1:3); IR (neat) 3403, 2935, 2860, 1664, 1619, 1392, 1267, 1169, 1004, 859, 710 cm⁻¹; ¹H NMR (300 MHz, CDCl₃) δ 6.84-6.79 (m, 2 H), 6.19-6.14 (m, 2 H), 5.73 (dddd, 1 H, *J* = 6.6, 6.6, 10.2, 16.8 Hz), 5.02-4.94 (m, 2 H), 2.43 (s, 1 H), 2.04 (q, 2 H, *J* = 7.2 Hz), 1.78-1.73 (m, 2 H), 1.40-1.29 (m, 2 H); ¹³C NMR (75 MHz, CDCl₃) δ 185.7, 151.3, 137.7, 128.2, 115.3, 69.9, 39.1, 33.6, 22.8; HRMS (ESI⁺) *m/z* calcd for C₁₁H₁₄O₂K 217.0631, found 217.0639.



2.55

5-(Pent-4-enyl)-4-hydroxycyclohexa-2,5-dioxirane (2.55). To a stirred solution of **2.54** (1.00 g, 5.61 mmol, 1 equiv) and 30 % aq. hydrogen peroxide (1.72 mL, 16.8 mmol, 3 equiv) in methanol (50 mL) at 0 °C was added 6 M NaOH (0.467 mL, 2.81 mmol, 0.5 equiv) dropwise. The reaction mixture was allowed to stir at 0 °C for 2 h, poured onto a saturated aqueous NH₄Cl solution and extracted with EtOAc (x3). The combined organic layers were washed with brine, poured onto activated 4 Å molecular sieves, and allowed to stir at rt for 3 h. The mixture was filtered and concentrated under reduced pressure to give **2.55** (1.05 g, 89% yield) as a yellow oil: *R_f* 0.43 (EtOAc/hexanes, 1:1); IR (neat) 3481, 2935, 1702, 1638, 1435, 1435, 1239, 1084, 995, 926, 887, 788 cm⁻¹; ¹H NMR (300 MHz, CDCl₃) δ 5.75 (dddd, 1 H, *J* = 6.6, 6.6, 10.2, 13.5 Hz), 5.05-4.99 (m, 2 H), 3.50 (s, 4 H), 3.09 (s, 1 H), 2.11 (q, 2 H, *J* = 6.9 Hz), 1.84-1.78 (m, 2 H), 1.53-1.42 (m, 2 H); ¹³C NMR (75 MHz, CDCl₃) δ 199.0, 137.2, 115.8, 69.0, 64.0, 57.0, 35.8, 33.7, 21.9; HRMS (ESI⁺) *m/z* calcd for C₁₁H₁₄O₄Na 233.0790, found 233.0785.



(1'*R*,2_s,3'*S*,5'*R*,7'*S*)-6-Hydroxytetrahydro-4',8'-dioxaspiro[pyran-2,2'-tricyclo[5.1.0.0^{3,5}]octan]-6'-one (2.56). A solution of **2.55** (0.92 g, 4.38 mmol, 1 equiv) in CH₂Cl₂ (22 mL) was cooled to -78 °C. Ozone was passed through the stirred solution for 2 h, which was then purged with N₂ before the dropwise addition of DMS (6.47 mL, 87.5 mmol, 20 equiv) at -78 °C. The reaction mixture was allowed to stir at -78 °C for 1 h and then allowed to warm to rt and stirred at rt for 3 d. The solvent was removed under reduced pressure. The crude product was purified by chromatography on SiO₂ (EtOAc/hexanes, 1:2 to 1:1) to give **2.56**

(0.803 g, 86% yield) as a 10:1 mixture of the open and closed forms of the lactol, as an off-white solid: R_f 0.25 (EtOAc/hexanes, 1:1); Mp 112-115 °C; IR (CDCl₃) 3424, 2961, 2913, 1698, 1442, 1251, 1101, 1010, 988, 956, 902, 868, 788 cm⁻¹; ¹H NMR (600 MHz, CDCl₃) δ 5.60 (s, 1 H), 4.32 (bs, 1 H), 4.17 (t, 1 H, $J = 4.2$ Hz), 3.50 (t, 1 H, $J = 3.6$ Hz), 3.42-3.40 (m, 2 H), 2.14-2.06 (m, 1 H), 1.85-1.81 (m, 2 H), 1.79-1.71 (m, 3 H); ¹³C NMR (151 Hz, acetone-*d*₆) δ 199.1, 91.9, 69.7, 64.0, 62.9, 56.2, 55.5, 29.5, 29.3, 13.8; HRMS (EI⁺) m/z calcd for C₁₀H₁₂O₅ 212.0685, found 212.0691. Only the major lactol diastereomer is listed.

3.0 EFFORTS TOWARD THE TOTAL SYNTHESIS OF CHRYSOPHAENTIN A

3.1 INTRODUCTION

Infectious diseases, which include bacterial infections, are the leading cause of death worldwide.¹⁰⁰ The Center for Disease Control estimates that each year more than 90,000 people die in the United States from hospital acquired bacterial infections alone.¹⁰¹ The discovery, development, and clinical exploitation of antibiotics like penicillin, tetracycline and vancomycin were some of the greatest medical advances of the twentieth century. The development of drug-resistant bacterial strains however, documented as early as the 1930s, continues to pose a significant challenge.¹⁰² Since 1962, only three new classes of antibiotics have been approved for clinical use (an oxazolidinone, a cyclic lipopeptide, and a pleuromutilin derivative), and most “new” antibiotics are simply variants of older products.¹⁰¹⁻¹⁰³ Almost all of the approved antimicrobial drugs target one of four processes: cell wall synthesis, protein synthesis, DNA synthesis, or interruption of folic acid synthesis.¹⁰³ In addition, the long-term use of a single antibiotic (>10 days) promotes the growth of bacteria that are not only resistant to that antibiotic but also to other structurally unrelated antibiotics. Finally, while resistance in bacteria strains may appear rapidly, even in the absence of a selecting antibiotic they are slow to be lost, reflecting the minimal survival cost to the emerging resistance.¹⁰² The increase in multi-drug resistance, coupled with constantly emerging novel pathogens and potential bioterrorism, have created an urgent need for new antibiotics with novel mechanisms of action.

Bacterial cell division is an essential process that has yet to be targeted by a clinically approved antibiotic. Filamenting temperature-sensitive mutant Z (FtsZ) is an essential protein to bacterial cell division that is highly conserved in the bacterial kingdom and absent in the mitochondria of higher eukaryotes. Studies in *E. coli*, have shown that bacterial cell division takes place via a sequential protein assembly pathway: FtsZ > FtsA, Zap A, Zip A > FtsE, FtsX >

FtsK > FtsQ > FtsB, FtsL > FtsW > FtsI > FtsN > AmiC > EnvC.¹⁰³ FtsZ, after guanosine 5'-triphosphate (GTP) dependent polymerization, forms the contractile Z-ring. Upon moving to the mid-cell, FtsZ recruits other proteins, which gather to produce the new cell wall and septal ring. Contraction of the septal ring eventually leads to completion of the cell division (Figure 32). Therefore, the development of a small-molecule inhibitor of the FtsZ protein could provide a new antibiotic with a novel mechanism of action.

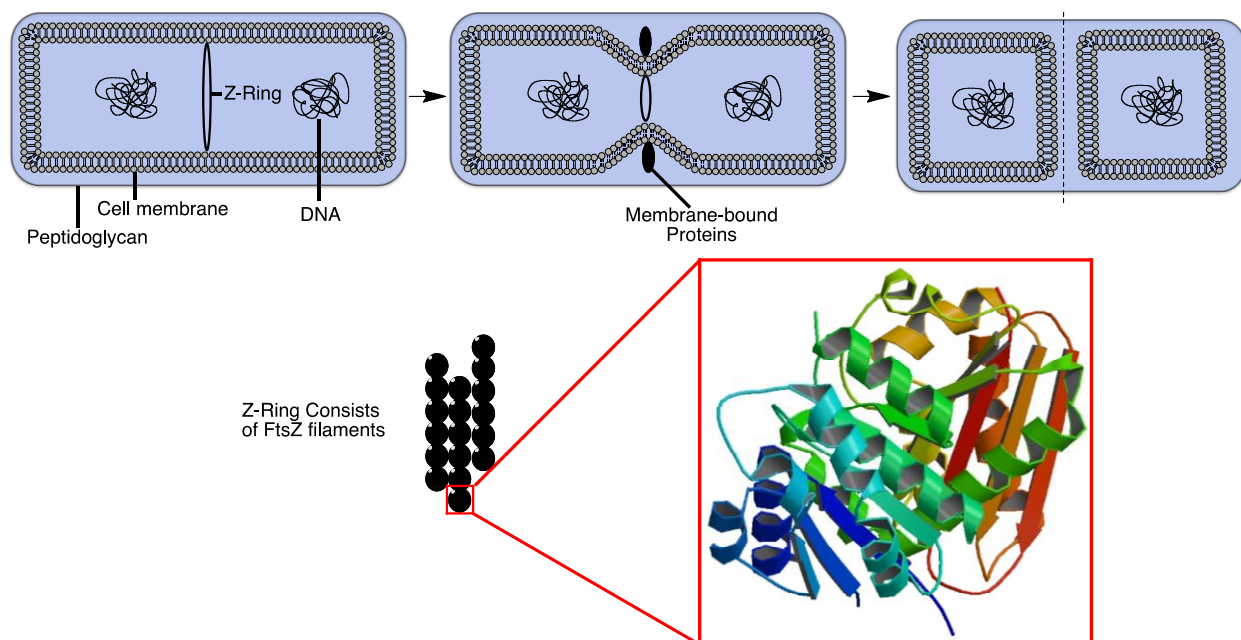


Figure 32. Cartoon representation of bacterial cell division and ribbon representation of the FtsZ protein adapted from PDB structure 3VPA.¹⁰⁴

FtsZ is a structural homologue of the mammalian β -tubulin. Similar to tubulin, FtsZ is a GTPase that polymerizes to generate dynamic structures that resemble microtubule protofilaments. GTP hydrolysis destabilizes the polymer, and once all of the GTP is converted to GDP the polymer completely disassembles into its individual monomers.¹⁰⁵ The successful targeting of β -tubulin in the treatment of cancer may suggest that the protein superfamily is a viable target for small-molecule modulation. In addition, targeting cell-division proteins, which are externally located, removes the need to optimize any small molecule inhibitors for entry into the cytoplasm. Although FtsZ and human tubulin share many structural and functional properties, none of the classical tubulin inhibitors exhibit significant inhibition of FtsZ

polymerization or GTPase activity *in vitro*. Thus, differentiation between inhibition of the two pathways should be plausible.¹⁰³

Several natural products have been isolated which modulate the activity of FtsZ polymerization (Figure 33). Viriditoxin, isolated from the venom of the prairie rattlesnake (*Crotalus viridis*),¹⁰⁶ was shown to inhibit FtsZ polymerization and concomitant GTPase inhibition with IC₅₀ values of 8.2 μg/mL and 7.0 μg/mL respectively.¹⁰⁷ Dichamanetin and 2''-hydroxy-5''-benzylisouvarinol-B (HBB), isolated independently by Hufford and Anam from *U. chamae* and *X. afticana* respectively and synthesized in the Shaw laboratory, exhibited FtsZ inhibition with IC₅₀ values of 12.5 and 8.3 μM respectively.¹⁰⁸⁻¹¹⁰ Another natural product, sanguinarine, induced cell filamentation in both Gram-positive and Gram-negative bacteria and was shown to act by inhibiting cytokinesis by perturbing formation of the Z-ring.¹¹¹ In addition to these natural products several small molecule modulators of the FtsZ protein have been reported (Figure 34).

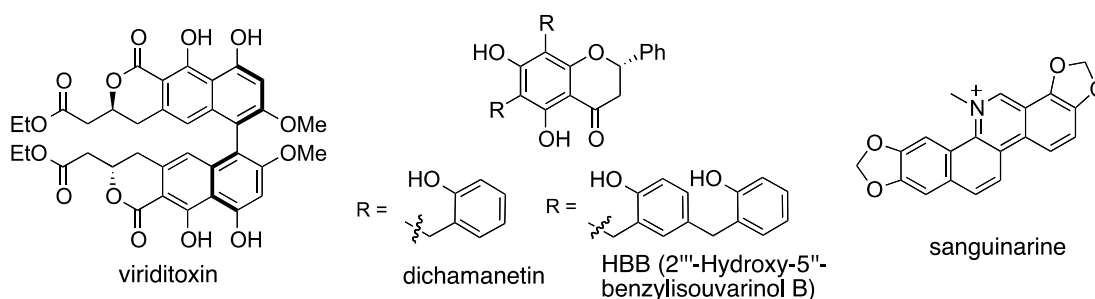


Figure 33. Natural product inhibitors of FtsZ

In 2004, RayChaudhuri and co-workers at Harvard reported the results of their efforts to identify small molecule inhibitors of the FtsZ protein. A screen of 18,320 compounds led to the isolation of five small molecules, which inhibited the polymerization-GTP hydrolysis-depolymerization cycle of FtsZ through distinct mechanisms.¹⁰⁵ Zantrin 4 and Zantrin 2 (Figure 34) exhibited FtsZ inhibition with IC₅₀ values of 25 μM and 10 μM respectively against several bacterial cell lines. Further mechanism of action studies revealed that while Zantrin 4 and Zantrin 2 acted by destabilizing polymer formation, other members of the five compounds acted by stabilization of the FtsZ assembly.¹⁰⁵ Each of the five identified inhibitors was structurally unrelated to GTP or each other. This study demonstrated that inhibition of cell division could be

achieved by either the stabilization or destabilization of the FtsZ assembly similar to the orthogonality between vinblastine and Taxol inhibition of microtubule function.

Czaplewski and co-workers at Begbroke Science Park in the United Kingdom, also seeking to identify small molecule inhibitors of cell division, developed a new cell-based microtiter plate assay to screen for inhibitors of cell division.¹¹² Using the very weak inhibitor 3-methoxybenzamide as a lead compound, they screened approximately 105,000 compounds. From this screen a new lead compound, PC170942, was identified and shown to inhibit the FtsZ protein in a dose-dependent manner with an IC_{50} of 10 μ M.¹¹² Several years and rounds of SAR later they identified the significantly more potent PC190723 that exhibited antibacterial activity against several bacterial cell lines as well as inhibited FtsZ with an IC_{50} value of 0.1 μ M.¹¹³ White and co-workers at the Southern Research Institute (SRI) have spent the last 30 years designing and preparing inhibitors of tubulin polymerization. Interestingly, a screen of over 200 compounds developed in their labs resulted in the identification of SRI-3072. SRI-3072 was shown to specifically target FtsZ with an IC_{50} of 52 μ M without inhibition of mammalian tubulin polymerization.¹¹⁴

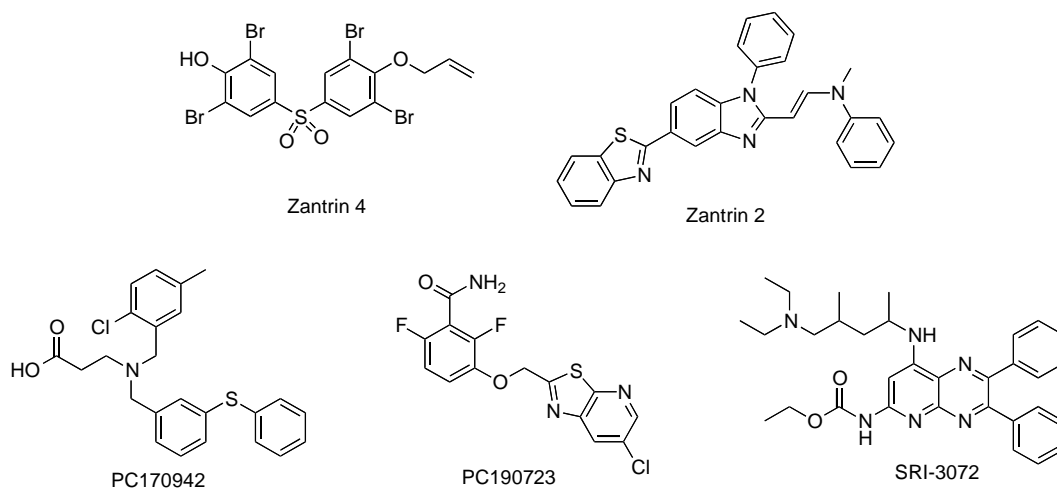


Figure 34. Small molecule inhibitors of FtsZ

The molecules discussed here comprise only a subset of the small molecule inhibitors of bacterial cell division that target the FtsZ protein. Examination of their structures reveals that a wide array of electronically and structurally diverse small molecules can be used to modulate the

FtsZ pathway in an orthogonal manner to FtsZ's eukaryotic homologue β -tubulin. These results coupled with the potential to modulate FtsZ via both stabilization and destabilization, and success of β -tubulin modulating therapies all serve to validate FtsZ modulation as a potential antimicrobial target.

Recently, Dr. Bewley and co-workers at the National Institutes of Health isolated eight new FtsZ modulating antimicrobial natural products, chrysophaentins A-H (Figure 35).¹¹⁵ The chrysophaentins were isolated from the marine chrysophyte alga *Chrysophaeum taylori* and are structurally characterized by the presence of two polyoxygenated, polyhalogenated ω,ω' -diarylbutene units connected by two ether bonds. While each member of the family exhibited antimicrobial activity, chrysophaentin A proved the most potent. Chrysophaentin A showed activity in resistant strains including methicillin-resistant *Staphylococcus aureus* ($MIC_{50} = 1.5 \pm 0.7 \mu\text{g/mL}$), multidrug resistant *S. aureus* ($1.4 \pm 0.4 \mu\text{g/mL}$), and vancomycin-resistant *Enterococcus faecium* ($2.9 \pm 0.8 \mu\text{g/mL}$).¹¹⁵ Limited access to the natural product led to a need for synthetic material for further biological evaluation. Accordingly, we devised a convergent synthetic strategy.

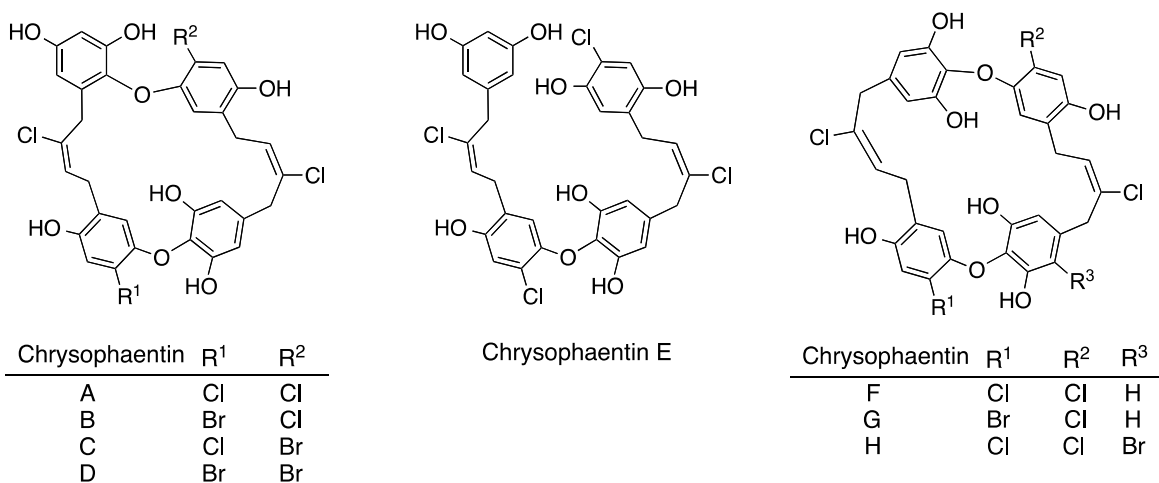


Figure 35. Structure of chrysophaentins A-H

3.2 1ST GENERATION SYNTHESIS OF CHRYSOPHAENTIN A

Our first generation retrosynthetic analysis of chrysophaentin A (Figure 36) begins with a potentially biomimetic oxidative dimerization of the C₁-C₁₆ fragment of chrysophaentin A **3.1**. Although a biosynthetic pathway for the chrysophaentins has yet to be elucidated, the isolation of the ring opened analogue chrysophaentin E (Figure 35) and the highly conserved oxygenation pattern suggests a laccase¹¹⁶ or other enzyme¹¹⁷ may form the diaryl ether linkages. In addition, the key oxidative dimerization would provide rapid access to chrysophaentin A and be amenable to the synthesis of the other chrysophaentins. Although oxidative diaryl ether formation has been well studied,¹¹⁸⁻¹²⁵ an asymmetric oxidative dimerization strategy has yet to be reported. Therefore, in order to rapidly access tetraphenol **3.1**, we envisioned its construction using a potential unselective hydrochlorination of alkyne **3.2**. Alkyne **3.2** could be accessed by nucleophilic displacement of benzyl bromide **3.3** with alkyne **3.4**. Finally, benzyl bromide **3.3** and alkyne **3.4** could be prepared using several functional group interconversions (FGIs) from the commercially available benzoic acid **3.5** and dimethyl hydroquinone **3.6** respectively.

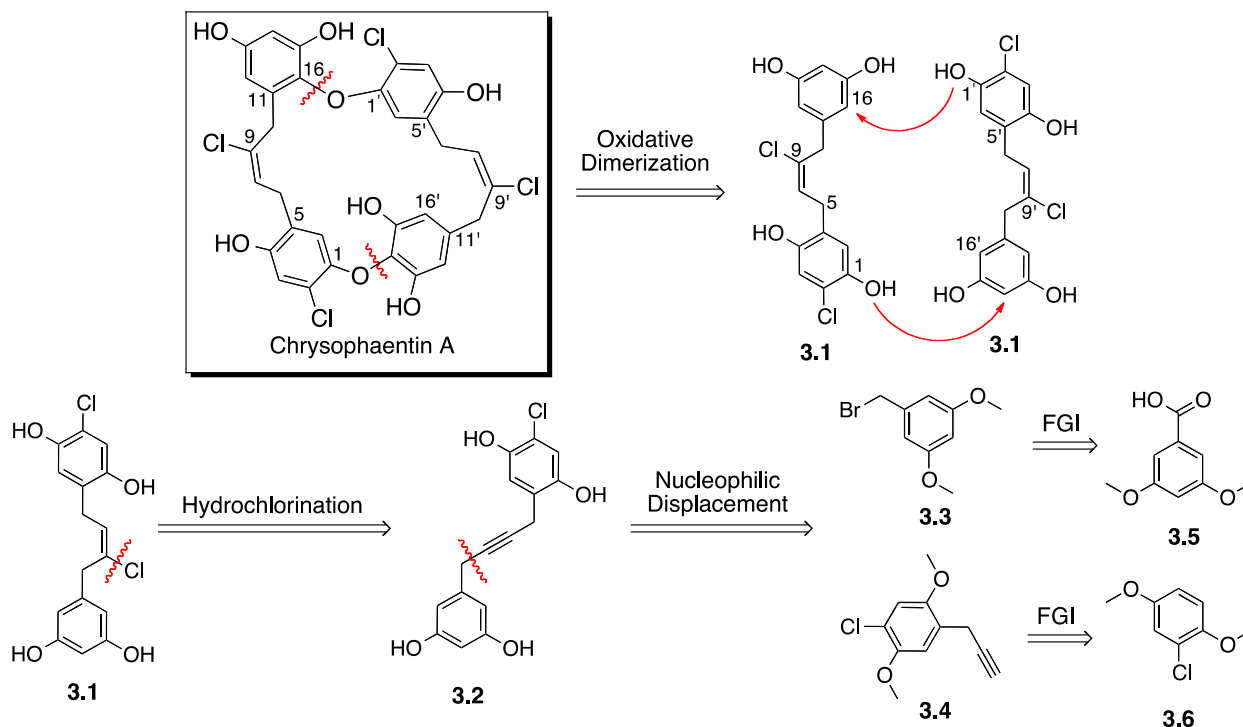
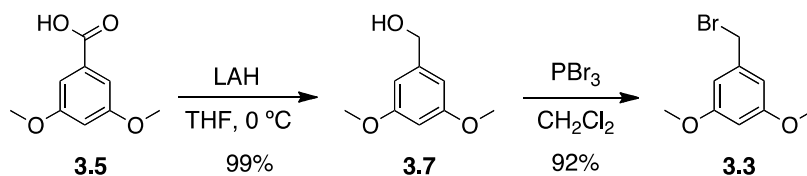


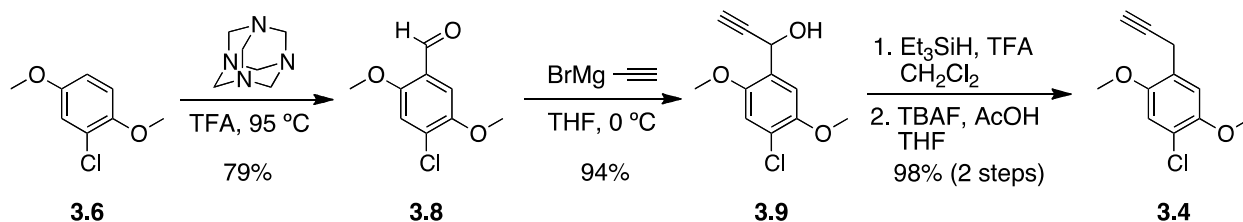
Figure 36. 1st Generation retrosynthetic analysis of chrysophaentin A

In the forward sense, our synthesis begins with preparation of benzyl bromide **3.3** (Scheme 30).¹²⁶ Reduction of the commercially available 3,5-dimethoxy benzoic acid (**3.5**) with lithium aluminum hydride (LAH) afforded benzyl alcohol **3.7** in excellent yield. Bromination using phosphorous tribromide (PBr₃) in dichloromethane gave benzyl bromide **3.3** in 92% yield. This route proved both efficient and scalable, permitting the preparation of 20 grams of **3.3**.



Scheme 30. Synthesis of benzyl bromide **3.3**.

Next, we focused on the synthesis of alkyne **3.4** (Scheme 31). Formylation of the commercially available dimethyl chlorohydroquinone **3.6** with hexamethylenetetramine in trifluoroacetic acid (TFA) at reflux afforded aldehyde **3.8** in good yield. Addition of ethynyl magnesium bromide to aldehyde **3.8** proceeded smoothly to afford alkyne **3.9** in 94% yield. Deoxygenation with TFA and triethylsilane yielded a mixture of the terminally silylated alkyne and alkyne **3.4** (~1:5 ratio). Desilylation of the crude mixture with tetrabutylammonium fluoride (TBAF) in the presence of acetic acid, afforded alkyne **3.4** in 98% yield over two steps. The addition of acetic acid proved crucial as in its absence allene formation predominated, most likely a result of trace ammonium hydroxide.

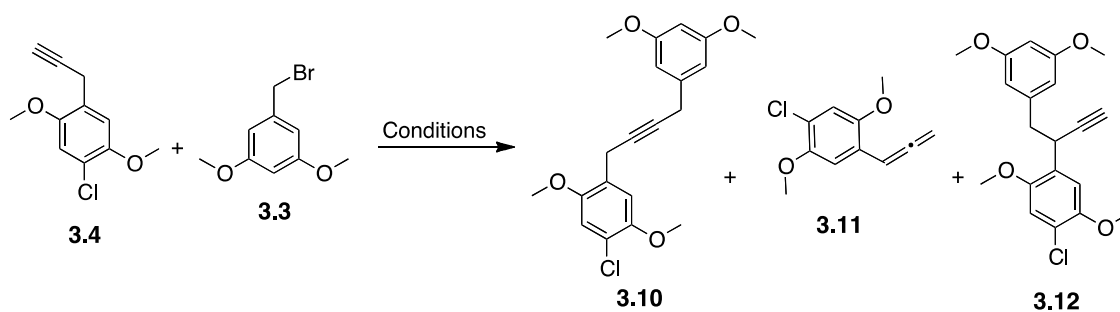


Scheme 31. Synthesis of alkyne **3.4**

Having synthesized both benzyl bromide **3.3** and alkyne **3.4**, their coupling in the presence of several bases was explored (Table 17). Addition of lithium hexamethyldisilazide

(LHMDS) to a mixture of **3.4** and **3.3** in THF at -78°C resulted in complete decomposition of alkyne **3.4** and only benzyl bromide **3.3** was isolated after purification (entry 1, Table 17). Treatment of alkyne **3.4** and benzyl bromide **3.3** with potassium hexamethyldisilazide in THF at -78°C (entry 2, Table 17) provided the unexpected benzylic substitution product tentatively assigned by ^1H NMR as **3.12**. Compound **3.12** potentially arises from formation of a benzylic anion followed by displacement of benzyl bromide **3.3**. This result contradicts a first order pka analysis, which suggests the terminal alkyne (pka ~ 25) should be selectively deprotonated in the presence of the less acidic benzylic position (pka ~ 32). This unusual reactivity was further demonstrated when switching to the stronger base *n*-BuLi. Addition of *n*-BuLi to a cooled (-78°C) mixture of **3.4** and **3.3** in THF led to the formation of a complex mixture, determined by ^1H NMR analysis to consist of benzyl bromide **3.3**, allene **3.11**, and the benzylic displacement product **3.12** (entry 3, Table 17).

Table 17. Nucleophilic displacement of **3.3** with **3.4**



Entry	Conditions	Result*
1	LHMDS, THF, -78°C	3.3 (50% rec.)
2	KHMDS (1.5 equiv), THF, -78°C	3.12 (56%)
3	<i>n</i> -BuLi, THF, $-78^{\circ}\text{C} \rightarrow \text{rt}$	crude mix of 3.3 , 3.11 , 3.12
4	<i>n</i> -BuLi, THF, HMPA, $-78^{\circ}\text{C} \rightarrow 0^{\circ}\text{C}$	complex mixture
5	CuI, K_2CO_3 , TBAI, MeCN	rec SM
6	3.4 (4 equiv), EtMgBr (4 equiv), CuBr (1 equiv), THF, reflux, 2 d	rec SM

One explanation for the unusually high reactivity of the benzylic position is that the *ortho*-methoxy group directs deprotonation and stabilizes the resulting benzylic anion via metal chelation. In order to break this potential chelation the use of hexamethylphosphoramide

(HMPA) was explored.¹²⁷ Treatment of a cooled (-78 °C) mixture of **3.4** and **3.3** in THF with *n*-BuLi and HMPA followed by warming to 0 °C resulted in the formation of a complex mixture of unidentifiable products (entry 4, Table 17). Next, activation of the alkyne with copper was investigated. The use of copper iodide, potassium carbonate, and tetrabutylammonium iodide¹²⁸ resulted in no reaction and only starting material was recovered (entry 5, Table 17). Moving to a stronger base, ethylmagnesium bromide, previously shown to provide superior yields in challenging alkyne couplings,¹²⁹ led to no observable reaction (entries 6, Table 17).

The unusual benzylic reactivity of alkyne **3.4** led us to reevaluate our displacement strategy. Therefore, a reversal of coupling partners was explored (Figure 37). This coupling reversal removes the potential for *o*-methoxy stabilization of the benzylic anion while decreasing the steric encumbrance of the terminal alkyne. In addition the *o*-methoxy substituent, now located on the benzyl bromide, can conjugatively stabilize the positive charge during the course of the reaction (Figure 37).

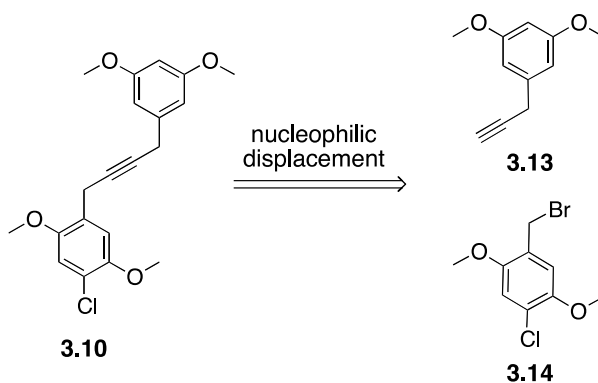
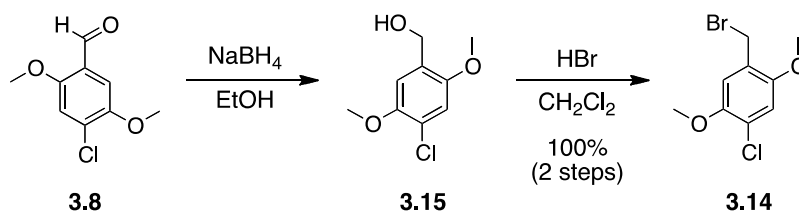


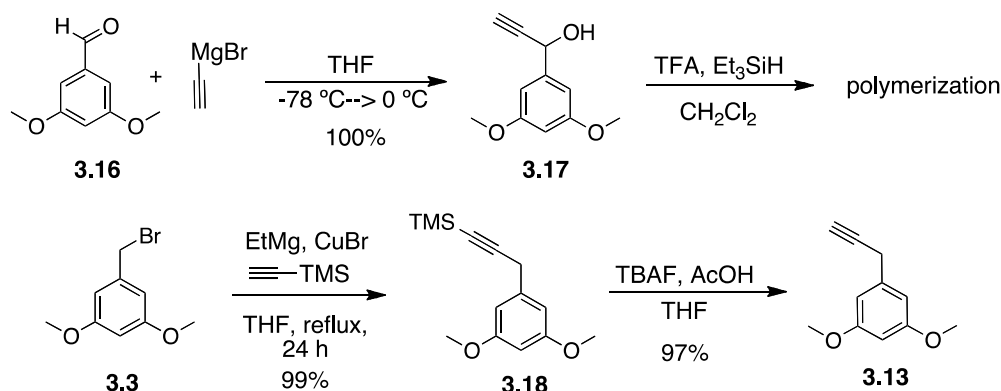
Figure 37. Revised synthesis of **3.10**

Benzyl bromide **3.14** was readily prepared from aldehyde **3.8** in two steps. Reduction of aldehyde **3.8** with sodium borohydride followed by a solvent swap and conversion to the bromide with hydrobromic acid afforded **3.14** in quantitative yield (Scheme 32).



Scheme 32. Synthesis of benzyl bromide **3.13**

Next, we focused on the synthesis of alkyne **3.13**. Addition of ethynyl magnesium bromide to aldehyde **3.16** afforded benzyl alcohol **3.17** in quantitative yield. Several attempts to deoxygenate **3.17** with TFA and triethylsilane as before were unsuccessful, furnishing only polymerized products (Scheme 33). Fortunately, an alternative approach published by the Wolff group¹³⁰ using the direct displacement of benzyl bromide **3.3** with trimethylsilyl ethynyl magnesium bromide in the presence of copper bromide afforded alkyne **3.18** in excellent yield. Desilylation with TBAF and acetic acid in THF gave the desired alkyne **3.13** in 97% yield.



Scheme 33. Synthesis of alkyne **3.13**

With a sufficient quantity of benzyl bromide **3.14** and alkyne **3.13** in hand, several basic coupling conditions were examined (Table 18). The use of *n*-BuLi in THF resulted in the isolation of a mixture of recovered starting material (**3.13** and **3.14**), benzylic homocoupling product **3.20**, and the benzylic displacement product **3.21**. The formation of the Wurtz coupling product **3.14** would suggest either an initial lithium halogen exchange followed by bromide displacement or single electron transfer mechanism occurred, not observed in the previous coupling studies. The addition of HMPA to the reaction mixture resulted in complete

consumption of the starting material to give a mixture of the homo-coupling product **3.20**, benzylic displacement product **3.21**, and allene **3.11**. Switching to copper-mediated conditions, a mixture of recovered starting materials (**3.13** and **3.14**), nucleophilic aromatic substitution to give **3.23**, and formation of the Glaser coupling product **3.24** was observed (Table 18). Investigating the use of a mesylate electrophile also afforded none of the desired product. Mesylate **3.19** proved unstable to isolation and after preparation by addition of methanesulfonyl chloride and triethylamine to benzyl alcohol **3.15** was directly subjected to the coupling conditions. In the presence of either KHMDS or *n*-BuLi, allene formation (**3.11**) and nucleophilic aromatic substitution (**3.22**) were observed. The structures of the side-products observed during the screen of basic coupling conditions and shown in Table 18 were tentatively assigned based solely on ¹H NMR analysis.

Table 18. Nucleophilic coupling to synthesize **3.10**

Conditions	Result
R=Br	
1. <i>n</i> -BuLi, THF, 0 °C-->rt, 12 h	3.13 (50%), 3.14 (35%), 3.20 (9%), 3.21 (6%)
2. <i>n</i> -BuLi, HMPA, THF, 0 °C	3.11 (80%), 3.20 (49%), 3.21 (20%)
3. 22 (4 equiv), EtMgBr (4 equiv) CuBr (1 equiv), THF, reflux, 48 h	3.13 (14%), 3.14 (35%), 3.23 (23%), 3.24 (4%)
R=OMs (Crude)	
1. KHMDS, THF, -78°C	3.11 (67%), 3.22 (31%), 3.15 (10%)
2. <i>n</i> -BuLi, THF, -78--> -50--> -20 --> 0 °C-- rt	mostly 3.11

The structures of the undesired side-products were tentatively assigned based ¹H NMR analysis.

3.20

3.21

3.11

3.19

3.15

3.22

3.23

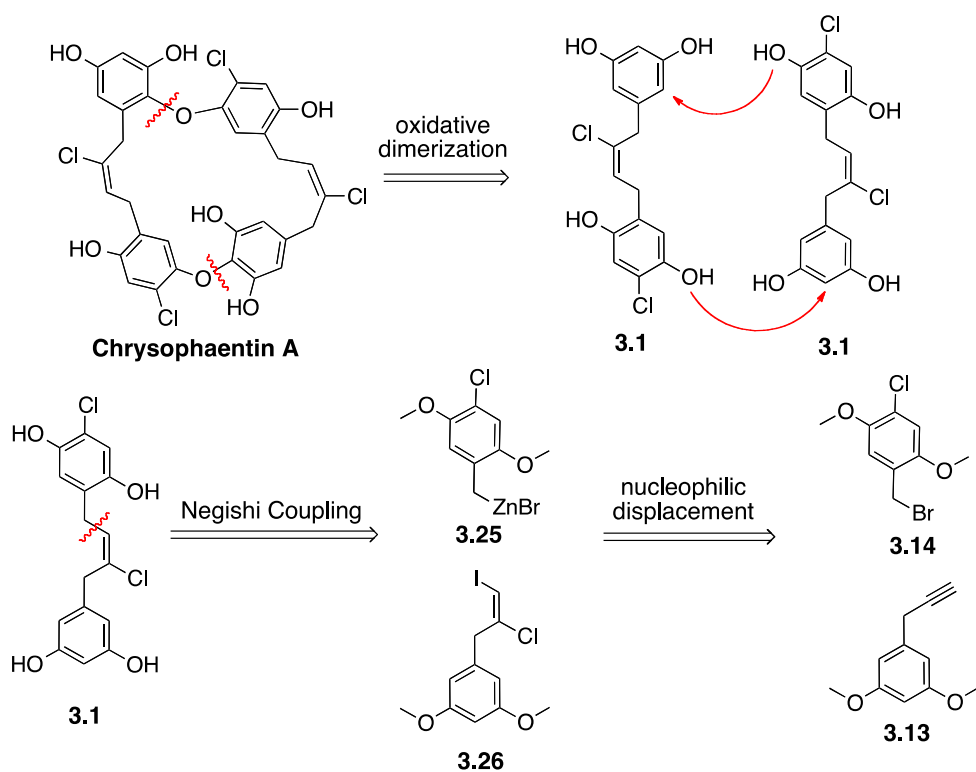
3.24

The unusual benzylic reactivity of the both alkyne **3.13** and alkyne **3.4** led us to reevaluate our initial retrosynthetic analysis. A key structural feature of the chrysophaentins is the presence of two *E*-chloroalkenes. Our initial retrosynthetic analysis proposed their installation using a potentially nonselective hydrochlorination. We envisioned the regiochemistry of the chloride would have little effect on the proposed oxidative dimerization and that this strategy would provide the most rapid access to tetraphenol **3.1**. Since access to the alkyne precursor using the outlined route (Figure 36) was complicated by the unusual benzylic reactivity of alkynes **3.13** and **3.4**, a different approach to the synthesis of fragment **3.1** was needed. Therefore, we decided to revise our synthetic strategy.

Interestingly, reports of the stereo- and regio-selective synthesis of dialkyl trisubstituted *E*-chloroalkenes are sparse and often complicated by preferential formation of the *Z*-chloroalkene.¹³¹⁻¹³³ A survey of the pertinent literature revealed that iodine monochloride (ICl) could be used for the stereo- and regio-selective selective iodochlorination of terminal alkynes.^{134,135} We envisioned that application of this selective iodochlorination to alkyne **3.13**, followed by a transition metal catalyzed coupling with benzyl bromide **3.14** would afford the desired *E*-chloroalkene. Therefore, our efforts were redirected towards the investigation of second-generation synthesis of chrysophaentin A.

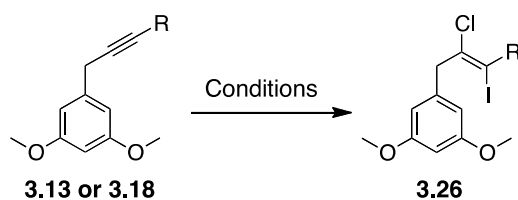
3.3 2ND GENERATION SYNTHESIS OF CHRYSOPHAENTIN A

As before, our 2nd generation retrosynthetic analysis (Scheme 34) of chrysophaentin A features a key oxidative dimerization of fragment **3.1** to give chrysophaentin A. Fragment **3.1** would now be prepared by a Negishi coupling of vinyl-iodide **3.25** and organo-zinc **3.26**. Iodo-chloroalkene **3.26** could be accessed using a regio- and stereo-selective iodochlorination of alkyne **3.13**. Finally, the benzylic zinc species **3.25** could be accessed via metalation of benzyl bromide **3.14** (Scheme 34). In fact, while some modification of protecting groups was required, the synthesis of fragment **3.1** could be readily realized employing this strategy.



Scheme 34. 2nd Generation retrosynthetic analysis of chrysopaentins A

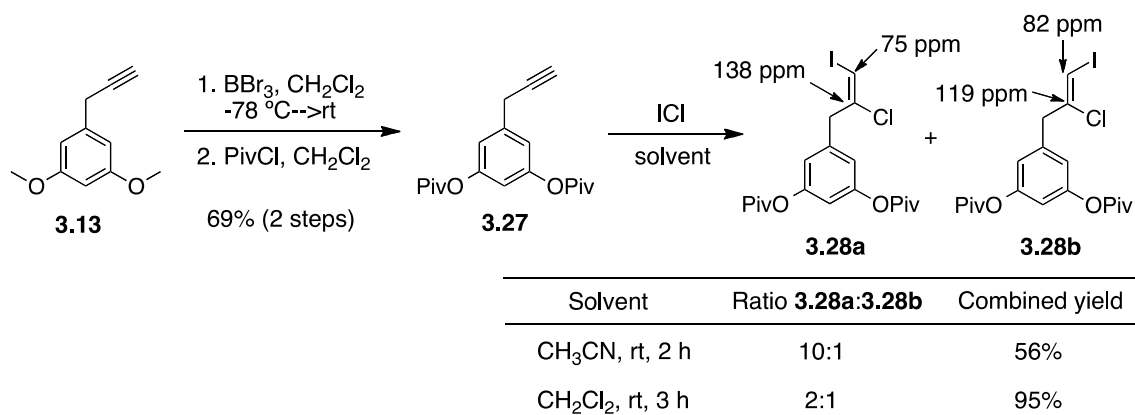
Our second-generation synthesis of chrysopaentins A begins with selective iodochlorination of alkyne **3.13**. Subjecting alkyne **3.13** to a small excess of iodine monochloride (ICl)¹³⁵ in a mixture of dichloromethane and 1,2-dichloroethane afforded 19% of the desired product **3.26** as an inseparable mixture with several over-iodinated products (Table 19). Screening varying equivalents of ICl, the addition of copper chloride,¹³⁴ and the use of different solvents, all led to formation of an inseparable mixture of compounds containing the iodochlorinated alkene as well as iodination of the aromatic ring (Table 19). Using the terminally silylated alkyne¹³⁶ **3.18** also resulted in non-selective iodination. The observed iodination of the aromatic ring likely results from the presence of two activating, electron donating methoxy groups. Therefore, the use of a different deactivating phenolic protecting group was investigated.

Table 19. Iodochlorination of alkynes **3.13** and **3.18**

Conditions	Result	Conditions	Result
R = H		R = TMS	
1. ICl, CH ₂ Cl ₂ /1,2-DCE, 3 h, rt	3.26 (19%) + Aryl iodination	1. ICl, CH ₂ Cl ₂ , rt, 6 h	rec 3.18 + Aryl iodination
2. ICl, CH ₃ CN, reflux, 18 h	Aryl iodination	2. ICl, CH ₃ CN, rt, 6 h	rec 3.18 + Aryl iodination
3. I ₂ , CuCl, CH ₃ CN, reflux, 3 h	Aryl iodination		
4. ICl, CH ₃ CN, rt, 24 h	rec 3.13 + Aryl iodination		
5. ICl CH ₃ CN, reflux, 24 h	rec 3.13 + Aryl iodination		
6. ICl (10 equiv), CH ₃ CN, 48 h	intractable mixture		

*Overiodinated products were identified by LCMS and crude ¹H NMR analysis.

In order to deactivate the aromatic ring both sterically and electronically, the methyl ethers were converted to the corresponding pivalate (Piv) protected phenols (Scheme 35). Deprotection of the methyl ethers with boron tribromide (BBr₃) in dichloromethane followed by re-protection with pivaloyl chloride (PivCl) afforded alkyne **3.27** in 69% yield (2 steps) (Scheme 35). Gratifyingly, alkyne **3.27** now underwent selective iodochlorination to provide an inseparable mixture of stereo-isomers, iodochloro-alkenes **3.28a** and **3.28b**. Changing the solvent from dichloromethane to acetonitrile increased stereoselectivity, favoring the desired product (**3.28a**); however, the significant decrease in reaction yield led to the use of dichloromethane in future reactions (Scheme 35). Although the observed improvement in stereo-selectivity could result from the increased polarity of acetonitrile relative to dichloromethane, the reduction in isolated yield may suggest it could also result from an increased rate of decomposition of **3.28b** relative to **3.28a**. It is unclear however, why the rate of decomposition of the undesired isomer would be preferentially accelerated in acetonitrile.

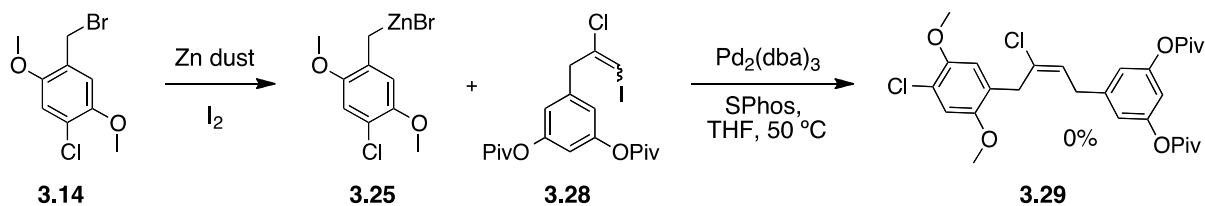


Scheme 35. Synthesis and iodochlorination of alkyne **3.27**

The assignment of both the regio- and stereo-chemistry of products **3.28a** and **3.28b** were based on NMR analysis and comparison to the literature.¹³⁵ The regiochemical outcome of the reaction corresponded to that predicted by the Markovnikov rule and was established based on the different effects exerted by a chlorine and an iodine atom on the chemical shift of the carbon to which they are directly bound. Although the chlorine atom induces a downfield shift due to its high electronegativity, the iodine atom induces an upfield shift due to the heavy atom effect (*i.e.*, increased diamagnetic shielding resulting from the large number electrons introduced by a heavy atom).¹³⁵ Attempts to elucidate the stereochemistry of the products by NOE analysis were inconclusive. Direct support for the assignment of stereochemistry can be made by comparison of the ¹³C alkene shifts of **3.28a** and **3.29b** to similar compounds in the literature.¹³⁴ Although only a small shift is observed for the terminal vinyl iodide carbon, the large shift of the vinyl chloride is consistent with previously reported values. The *trans*-substituted iodochloroalkenes generally exhibit a vinyl chloride carbon shift of 129-145 ppm depending on substitution while *cis*-substituted iodochloroalkenes exhibit a vinyl chloride carbon shift of 118-125 ppm (Scheme 35).^{134,135,137,138} Therefore, **3.28a**, with the chlorine and iodine *trans* to one another was assigned as the major product.

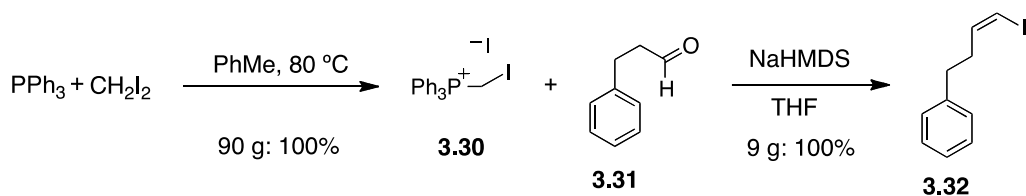
Next, the Negishi coupling of iodochloro-alkene **3.28** with benzylic organo-zinc **3.25** was investigated. Initially, conditions recently reported to give increased yields for the intermolecular Negishi coupling of alkyl substrates were evaluated.¹³⁹ Formation of organo-zinc **3.25** in THF with zinc dust and a catalytic amount of iodine, immediately followed by addition

of a mixture of **3.28a** and **3.28b**, tris(dibenzylideneacetone)dipalladium, and SPhos¹⁴⁰ in THF gave, after stirring overnight at 50 °C, none of the desired product (Scheme 36).



Scheme 36. Synthesis of organo-zinc **3.25** and initial attempt at its Negishi coupling with **3.28**

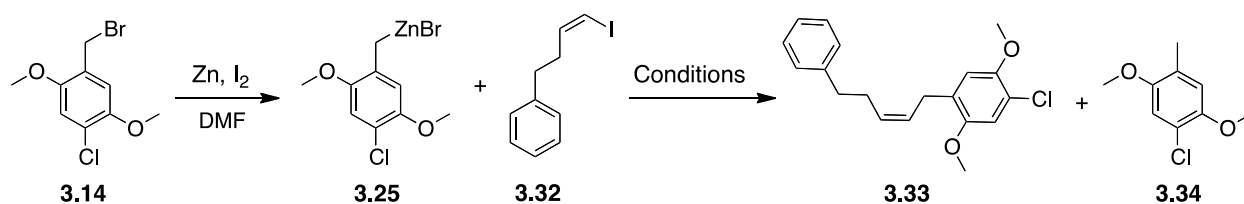
As Negishi couplings often rely on high sample concentrations (≥ 1 M), a model Z-vinyl iodide was generated in order to rapidly screen conditions while the synthesis of iodochloroalkene **3.28** was scaled-up. Generation of iodomethyltriphenylphosphonium iodide **3.30** from triphenylphosphine and diiodomethane proceeded in quantitative yield to give **3.30** on 90-gram scale.¹⁴¹ Z-selective Wittig reaction of iodomethyltriphenylphosphonium iodide (**3.30**) and the commercially available 3-phenyl propionaldehyde (**3.31**) afforded the desired *cis*-iodoalkene **3.32** in quantitative yield.



Scheme 37. Synthesis of model vinyl iodide **3.32**

With ample quantities of vinyl iodide **3.32** in hand, we optimized the Negishi coupling of organozinc **3.25** and vinyl iodide **3.32** (Table 20). Benzylic organozinc **3.25**, generated with zinc dust and catalytic iodine in DMF, was cannulated onto a stirred solution of SPhos, tris(dibenzylideneacetone)dipalladium, and **3.32** in THF. After stirring overnight at room temperature only starting material was recovered. Changing the solvent from THF to dimethylformamide (DMF),¹⁴² the desired product **3.33** was isolated in 43% yield along with recovered vinyl iodide (20%) and the proto-demetalated product **3.34** (5%) (entry 2, Table 20). Increasing the reaction temperature from room temperature to 60 °C had little effect on the

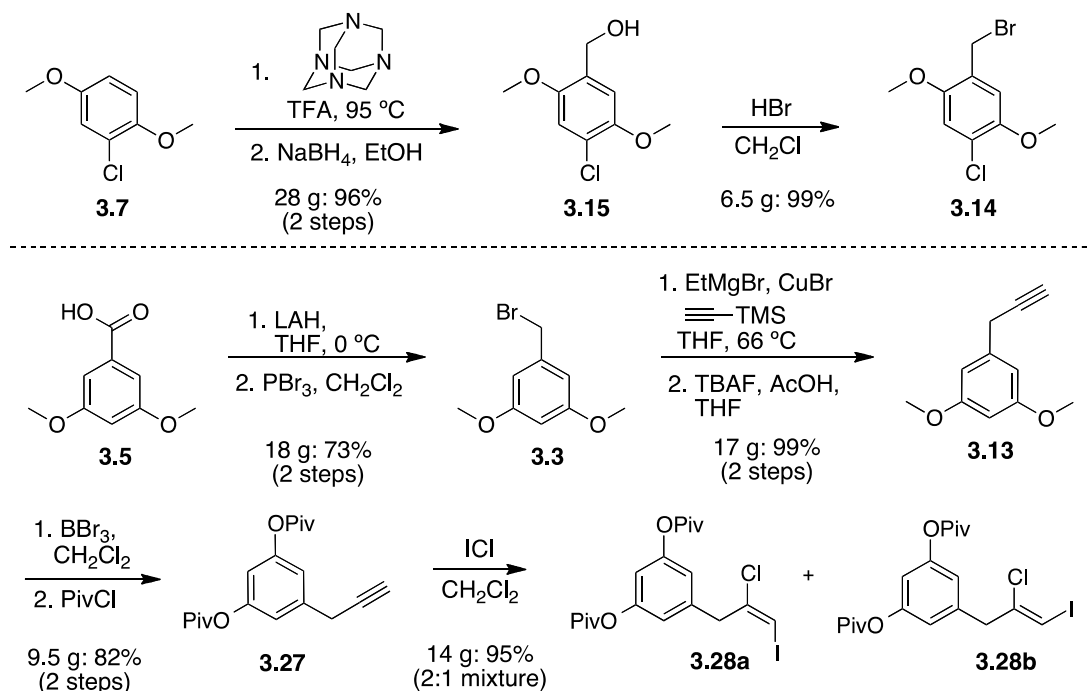
isolated yield of **3.33** however an increased yield of recovered vinyl iodide **3.32** (30%) and the proto-demetalated product **3.34** (15%) was observed. Next, several palladium catalysts systems were evaluated. Palladium acetate and tris(dibenzylideneacetone)dipalladium were screened using either SPhos or tri-*o*-tolyl phosphine (P(*o*-Tol)₃), which have been shown to improve yields in sterically hindered systems^{139,140} (entries 3-8, Table 20). Although the palladium source had little effect on isolated yield, the use of P(*o*-Tol)₃ provided slightly better yields than SPhos. In addition, the ratio of ligand:Pd, either 4:1 shown be optimal for the Negishi coupling of alkyl halides by Szczepankiewicz *et al.*¹⁴³ or 2:1 which proved optimal for Jackson *et al.*^{139,144} was investigated. Although varying the ligand:Pd ratio had little effect on the isolated yield of **3.33**, the isolated yield of recovered starting material **3.32** decreased. Finally, doubling the equivalents of organo-zinc **3.25** afforded a substantial increase in yield affording **3.33** in 68% isolated yield (entry 9, Table 20). Satisfied with the improvement in yield, the optimized conditions were applied to the Negishi coupling of benzyl bromide **3.14** and iodochloroalkenes **3.28a/3.28b**.

Table 20. Optimization of Negishi coupling in model system

Conditions	Result
1. 3.25 (1.5 equiv), Pd ₂ (dba) ₃ (2.5 mol%), SPhos (2.5 mol%), THF, rt, 1 d	3.32 (70%)
2. 3.25 (1.5 equiv), Pd ₂ (dba) ₃ (2.5 mol%), SPhos (2.5 mol%), DMF, rt, 2 d	3.33 (42%), 3.34 (5%), 3.32 (20%)
3. 3.25 (1.5 equiv), Pd ₂ (dba) ₃ (2.5 mol %), SPhos (10 mol %), DMF, 60 °C, 1 d	3.33 (42%), 3.34 (15%), 3.32 (30%)
4. 3.25 (1.5 equiv), Pd(OAc) ₂ (5 mol %), SPhos (10 mol %), DMF, rt, 1 d	3.33 (33%), 3.34 (20%), 3.32 (42%)
5. 3.25 (1.5 equiv), Pd ₂ (dba) ₃ (2.5 mol %), P(o-Tol) ₃ (10 mol%), DMF, rt, 1 d	3.33 (43%), 3.34 (15%), 3.32 (42%)
6. 3.25 (1.5 equiv), Pd(OAc) ₂ (5 mol %), P(o-Tol) ₃ (20 mol%), DMF, 60 °C, 1 d	3.33 (41%), 3.34 (17%), 3.32 (15%)
7. 3.25 (1.5 equiv), Pd ₂ (dba) ₃ (5 mol %), P(o-Tol) ₃ (20 mol%), DMF, rt, 1 d	3.33 (43%), 3.34 (18%),
8. ^a 3.25 (1.5 equiv), Pd ₂ (dba) ₃ (2.5 mol %), P(o-Tol) ₃ (10 mol%), DMF, rt, 1 d	3.33 (42%), 3.34 (21%),
9. 3.25 (3 equiv), Pd ₂ (dba) ₃ (2.5 mol %), P(o-Tol) ₃ (10 mol%), DMF, rt, 1 d	3.33 (68%), 3.34 (12%),

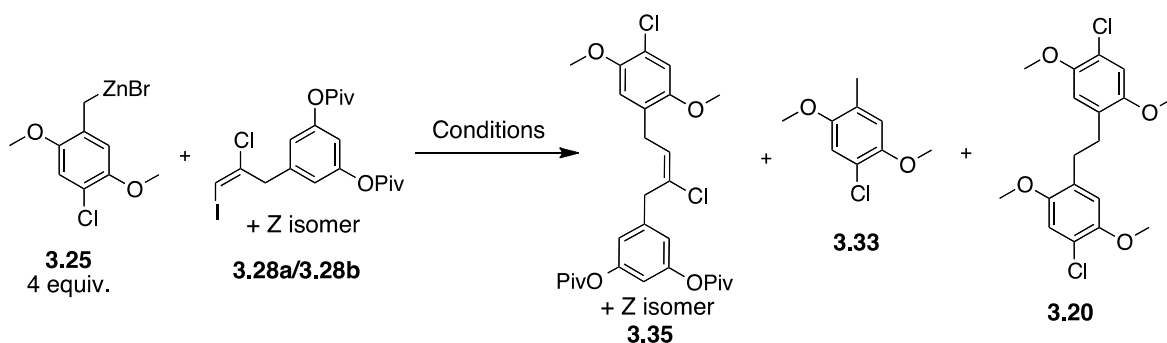
*Isolated Yields. ^a**3.25** was added via syringe pump over 90 min.

A multi-gram synthesis of benzyl bromide **3.14** and iodochloroalkenes **3.28a/3.28b** proceeded smoothly during the optimization studies (Scheme 38). Formylation of dimethyl hydroquinone **3.7** and subsequent reduction afforded benzylic alcohol **3.15** on 28-gram scale. Conversion to benzyl bromide **3.14**, as needed, proceeded quantitatively. The synthesis of **3.28a/3.28b** also proved quite scalable. Starting from benzoic acid **3.5**, reduction, bromination, displacement with trimethylsilylacetylene, and silyl deprotection afforded alkyne **3.13** on 17-gram scale in 72% yield (4 steps). Deprotection of the methyl ethers, reprotection with PivCl, and iodochlorination provided an inseparable mixture of **3.28a/3.28b** on a 14-gram scale in 78% yield over the three steps.



Scheme 38. Scale-up of intermediates **3.14** and **3.28a/3.28b**

With sufficient quantities of benzyl bromide **3.14** and iodochloroalkene **3.28** prepared, their Negishi coupling to furnish *E*-chloroalkene **3.35** was investigated (Table 21). In contrast to the model system, initial attempts to couple **3.14** and **3.28** revealed that the removal of excess zinc after generation of the organozinc reagent was critical prior to combination with **3.28a/3.28b**. Any residual zinc metal catalyzes the rapid *anti*-elimination of the *trans*-iodochloro alkene **3.28a**, thus returning alkyne **3.27**.¹³⁵ Therefore, **3.25** (4 equiv) was generated, rapidly filtered, and cannulated into a mixture of tris(dibenzylideneacetone)dipalladium, tri-*o*-tolyl phosphine, and a mixture of **3.28a/3.28b** in DMF. After stirring at room temperature overnight, desired product **3.35** (26%), benzylic homo-coupling product **3.20**, and the proto-demetalated product **3.33** were isolated.

Table 21. Optimization of Negishi coupling of **3.28a/3.28b** and **3.25**

Reaction conditions	Percent Yield (%)			
	3.28a/3.28b	3.35	3.33	3.20
1. Pd ₂ (dba) ₃ (2.5 mol %), P(<i>o</i> -tol) ₃ (10 mol %), DMF, rt, 16 h	-	26	7	17
2. Pd(OAc) ₂ (5 mol %), P(<i>o</i> -tol) ₃ (20 mol %), DMF, rt, 16 h	-	21	-	23
3. Pd ₂ (dba) ₃ (2.5 mol %), SPhos (5 mol %), DMF, rt, 16 h	25	22	11	12
4. Pd(OAc) ₂ (5 mol %), P(<i>o</i> -tol) ₃ (10 mol %), DMF, 50 °C, 16 h	14	29	7	13
5. Pd(OAc) ₂ (5 mol %), P(<i>t</i> -Bu) ₃ (5 mol %), DMF, rt, 16 h	-	9	-	33
6. Pd(OAc) ₂ (5 mol %), P(Bu) ₃ (5 mol %), DMF, rt, 16 h	-	33	-	28
7. Pd(OAc) ₂ (5 mol %), dppb (5 mol %), DMF, rt, 16 h	-	22	-	19
8. Ni(COD) ₂ (5 mol %), <i>i</i> -Pr PyBox (10 mol %), DMAC, 16 h	80	trace	-	-
9. NiCl ₂ (dppp) (5 mol %), DMAC, 16 h	80	-	-	-
10. Pd(OAc) ₂ (5 mol %), P(Bn) ₃ (10 mol %), DMAC, 16 h	85	trace	-	-
11. Pd(OAc) ₂ (40 mol %), P(Bu) ₃ (40 mol %), DMAC, 16 h	81	-	-	-
12. Pd(OAc) ₂ (5 mol %), P(<i>o</i> -tol) ₃ (10 mol %), DMF, μ W, 80 °C, 25 min	-	33	-	-

The use of the more air-stable palladium diacetate provided no significant drop in yield, thus it was selected for future optimization (entries 1, 2, Table 21). A screen of phosphine ligands revealed that tributyl phosphine and tri-*o*-tolyl phosphine provided superior yields. Again due to ease of handling, tri-*o*-tolyl phosphine was selected for future optimization (entries

3-7, 10, 11 Table 21). The use of either nickel (0) or nickel (II) catalysts in dimethyl acetamide (DMAC) resulted in no observable reaction and only starting material was recovered (entries 8, 9, Table 21). Due to the long reaction times associated with both the room temperature and conventional heating procedures (>12 h), microwave irradiation was explored. Gratifyingly, microwave irradiation (80 °C) of the reaction mixture in DMF afforded **3.35** in comparable yields after only 25 min. (Table 22).

Unfortunately, in several solvent systems, **3.35**, **3.33**, and **3.20** exhibited extremely similar retention factors (R_f 's) on silica gel, making reproducible levels of purity challenging to obtain. However, subjecting the impure Negishi coupling mixture to pivalate deprotection with cesium carbonate and methanol afforded the more readily separable diphenol **3.36**. Thus, in order to obtain more accurate yields, all future optimization studies used the two-step procedure of Negishi coupling and deprotection prior to purification.

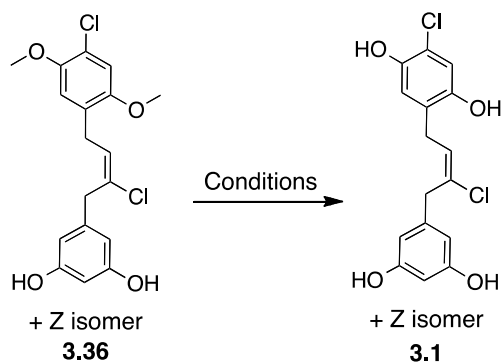
Final optimization of the Negishi coupling using microwave irradiation and immediate pivalate deprotection led to an optimized procedure (Table 22). Increasing the reaction temperature of the Negishi coupling from 80 °C to 140 °C reduced the reaction time from 25 min to 2 min, with no observable decrease in yield. The formation of palladium black during the course of the reaction led to the hypothesis that decomposition of the palladium catalyst was inhibiting further product formation. Decreasing the reaction temperature to 120 °C and sequential addition of the palladium catalyst led to an optimized procedure that afforded **3.36** as an inseparable mixture of *E*- and *Z*-isomers (4:1) in 51% (2 steps) in only 4 minutes.

Table 22. Final optimization of the Negishi coupling

<p>3.25 (4 equiv.)</p> <p>3.28a/3.28b + Z isomer</p> <p>1. Microwave Conditions 2. Cs₂CO₃, MeOH/CH₂Cl₂</p> <p>3.36 + Z isomer (4:1)</p>	<table border="1"> <thead> <tr> <th>Microwave conditions</th> <th>Yield (%) (2 steps)</th> </tr> </thead> </table>	Microwave conditions	Yield (%) (2 steps)
	Microwave conditions	Yield (%) (2 steps)	
	<table border="1"> <tbody> <tr> <td>1. Zn, DMF, Pd(OAc)₂ (0.05 equiv), P(<i>o</i>-Tol)₃ (0.1 equiv), 80 °C, 25 min</td> <td>30%</td> </tr> </tbody> </table>	1. Zn, DMF, Pd(OAc) ₂ (0.05 equiv), P(<i>o</i> -Tol) ₃ (0.1 equiv), 80 °C, 25 min	30%
	1. Zn, DMF, Pd(OAc) ₂ (0.05 equiv), P(<i>o</i> -Tol) ₃ (0.1 equiv), 80 °C, 25 min	30%	
	<table border="1"> <tbody> <tr> <td>2. Zn, DMF, Pd(OAc)₂ (0.05 equiv), P(<i>o</i>-Tol)₃ (0.1 equiv), 140 °C, 2 min</td> <td>30%</td> </tr> </tbody> </table>	2. Zn, DMF, Pd(OAc) ₂ (0.05 equiv), P(<i>o</i> -Tol) ₃ (0.1 equiv), 140 °C, 2 min	30%
2. Zn, DMF, Pd(OAc) ₂ (0.05 equiv), P(<i>o</i> -Tol) ₃ (0.1 equiv), 140 °C, 2 min	30%		
<table border="1"> <tbody> <tr> <td>3. Zn, DMF, Pd(OAc)₂ (0.05 equiv), P(<i>o</i>-Tol)₃ (0.1 equiv), 80 °C, 2 min then Pd(OAc)₂ (0.05 equiv) 120 °C, 2 min</td> <td>49%</td> </tr> </tbody> </table>	3. Zn, DMF, Pd(OAc) ₂ (0.05 equiv), P(<i>o</i> -Tol) ₃ (0.1 equiv), 80 °C, 2 min then Pd(OAc) ₂ (0.05 equiv) 120 °C, 2 min	49%	
3. Zn, DMF, Pd(OAc) ₂ (0.05 equiv), P(<i>o</i> -Tol) ₃ (0.1 equiv), 80 °C, 2 min then Pd(OAc) ₂ (0.05 equiv) 120 °C, 2 min	49%		
<table border="1"> <tbody> <tr> <td>4. Zn, DMF, Pd(OAc)₂ (0.05 equiv), P(<i>o</i>-Tol)₃ (0.1 equiv), 120 °C, 2 min then Pd(OAc)₂ (0.05 equiv) 120 °C, 2 min</td> <td>51%</td> </tr> </tbody> </table>	4. Zn, DMF, Pd(OAc) ₂ (0.05 equiv), P(<i>o</i> -Tol) ₃ (0.1 equiv), 120 °C, 2 min then Pd(OAc) ₂ (0.05 equiv) 120 °C, 2 min	51%	
4. Zn, DMF, Pd(OAc) ₂ (0.05 equiv), P(<i>o</i> -Tol) ₃ (0.1 equiv), 120 °C, 2 min then Pd(OAc) ₂ (0.05 equiv) 120 °C, 2 min	51%		
<p>Note: at concentrations of 3.25 > 1 M, the solution of 3.25 becomes too viscous to be rapidly filtered.</p>			

With an optimized procedure for the Negishi coupling obtained, attention was directed to deprotection of the methyl ethers of **3.36** and completion of key fragment **3.1** (Table 23). Deprotection of **3.36** (2:1 mixture of *E*- and *Z*-isomers) with boron tribromide in dichloromethane provided 27% of the desired product **3.1** as an inseparable mixture of *E*- and *Z*-stereoisomers (2:1). Several other nucleophilic deprotection conditions, as well as elevated reaction temperatures, led to decomposition of **3.36** (Table 23). Fortunately, decreasing the concentration of **3.36** (2:1 mixture of *E*- and *Z*-isomers) to 0.02 M in the presence of boron tribromide (BBr₃) afforded the desired tetraphenol **3.1** as an inseparable mixture of *E*- and *Z*-isomers (2:1) in quantitative yield. Therefore, the tetraphenolic C₁-C₁₆ monomer of chrysofaentin A **3.1** was synthesized in 10 steps (longest linear sequence) and 24% overall yield from commercially available starting materials.

100 mg of an analytically pure *E*-isomer of **3.36** was obtained by separation of the geometric isomers by supercritical fluid chromatography (SFC) using a semi-prep (250 × 10 mm) silica column (R_t 5.80 min, 10 mL/min, 15% methanol, 220 nm detection). Subjecting the pure *E*-isomer of **3.36** to the optimized deprotection conditions provided **3.1** as a single geometric isomer (*E*-isomer) in 96% yield. 40 mg of an analytically pure *E*-isomer of **3.1** was obtained by separation of the geometric isomers by SFC chromatography using a semi-prep (250 × 10 mm) silica column (R_t 4.68 min, 8 mL/min, 25% methanol, 220 nm detection).

Table 23. Optimization of methyl deprotection

Conditions	Result
1. BBr ₃ , -78 °C to 0 °C to rt, 0.2 M	27%
2. PhSH, K ₂ CO ₃ , DMF, 150 °C	complex mixture
3. EtSH, NaH, DMF, 100 °C	dec.
4. MeSi(Cl) ₃ , NaI, CH ₃ CN, rt, 24 h	dec.
5. Pyr·HCl, NMP, μ W, 220 °C	dec.
6. LiCl, DMF, 145 °C, 72 h	slow dec.
7. HBr, AcOH, 100 °C, 12 h	complex mixture
8. BBr ₃ , 0 °C to rt, 8 h, 0.02 M	100%
9. Pure <i>E</i> -isomer of 3.36 BBr ₃ , 0 °C to rt, 8 h, 0.02 M	96%

10 mg of pure *E*-isomer of both the dimethoxy monomer **3.36** and the tetraphenol **3.1** were sent to our collaborator Dr. Carole Bewley's lab at the NIH for evaluation of their antimicrobial activities. The synthesis of **3.36** and **3.1** discussed above and the biological evaluation discussed below were recently reported in the *Journal of Marine Drugs*¹⁴⁵ and are reproduced with permission.

“The antibacterial activity of the pure *E*-isomer of **3.36** and **3.1** were evaluated in a microbroth dilution assay. The minimum inhibitory concentration that led a 50% decrease in growth (MIC₅₀) was determined using a model curve fit to the data. The MIC₉₀ was determined as the lowest concentration where no visible growth was observed. The minimum bactericidal concentration (MBC) was determined as the lowest concentration where a plated aliquot of treated bacteria led to a three logarithmic decrease in colony forming units (CFU) per milliliter relative to the starting inoculum.” The antibacterial activity of both **3.36** and **3.1** were evaluated against five different strains of *Staphylococcus aureus* including a highly resistant strain, ATCC BAA-44 (Table 24).

Table 24. Summary of antibacterial activity of chrysopaentins A, **3.36**, and **3.1** against five diverse strains of *Staphylococcus aureus* (all values are in μM).

Compound	<i>S. aureus</i> 25923 (μM)			MRSA BAA-41 (μM)			MDRSA BAA-44(μM)		<i>S. aureus</i> UAMS-1 (μM)			CA-MRSA USA300-LAC (μM)		
	MIC ₅₀	MIC ₉₀	MBC	MIC ₅₀	MIC ₉₀	MBC	MIC ₅₀	MIC ₉₀	MIC ₅₀	MIC ₉₀	MBC	MIC ₅₀	MIC ₉₀	MBC
Chrysopaentins A	2.7 \pm 0.9	9.2 ^a	37 ^a	2.3 \pm 1.0	4.6 ^a	37 ^a	1.8 \pm 0.5	9.2 ^a	5.1 \pm 2.1	9.2 ^a	19 ^a	5.0 \pm 2.4	9.2 ^a	19 ^a
3.36	12 \pm 4.3	34 ^a	68 ^a	11 \pm 5.4	34 ^a	68 ^a	13 \pm 4.7	34 ^a	20 \pm 10	34 ^a	68 ^a	18 \pm 8.4	34 ^a	68 ^a
3.1	20 \pm 5.2	74 ^a	150 ^a	23 \pm 9.9	74 ^a	150 ^a	27 \pm 9.4	74 ^a	31 \pm 13	74 ^a	150 ^a	29 \pm 9.9	74 ^a	150 ^a

Strains used: *S. aureus* ATCC 25923, clinical isolate from Seattle, 1945; methicillin-resistant *S. aureus* ATCC BAA-41, a hospital-acquired strain isolated in New York City in 1994; multidrug-resistant *S. aureus* (MDRSA) ATCC BAA-44, a hospital-acquired strain isolated in Lisbon, Portugal, with resistance towards ampicillin, methicillin, oxacillin, penicillin, erythromycin, gentamicin, tetracycline, azithromycin, amikacin, clindamycin, cephalothin, ceftriaxone, imipenem, lincomycin, streptomycin, perfloracin, rifampin, and neomycin. *S. aureus* UAMS-1, a clinical osteomyelitis isolate; and community-associated methicillin-resistant *S. aureus*, USA300-LAC. ^aNote: MIC₉₀ and MBC values were determined using a microbroth dilution assay and represent the minimum concentration evaluated at which no visible growth of bacteria (MIC₉₀) or a three-fold logarithmic decrease in the number of viable bacteria relative to the starting inoculum (MBC) was observed; they are only approximate values.

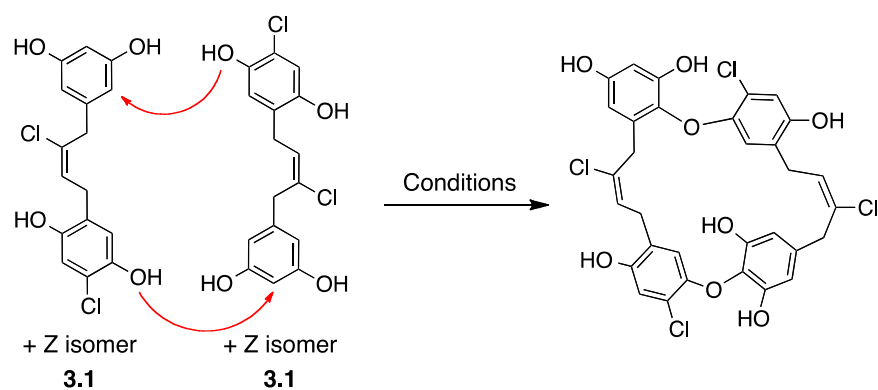
The monomeric units **3.36** and **3.1** retained the potent antibacterial activity of their parent natural product against all five strains of bacteria. In fact, compound **3.36** proved more potent than chrysopaentins D, E, and G. Since the acyclic variants were still approximately 10-fold less potent than chrysopaentins A, attention returned to the completion of the synthesis.

With a scalable route to monomer **3.1** in hand, investigation of the key oxidative dimerization to afford chrysopaentins A began. Although the desired oxidative addition requires the asymmetric formation of two diaryl ether bonds, small quantities of product should be identifiable by LCMS analyses. Isolation by either SFC or HPLC purification will provide access to chrysopaentins A, even if the efficiency of the reaction is poor. Therefore, all reactions were conducted using 20 mg of **3.1** and were monitored by LCMS. When major products were observed they were isolated and characterized by NMR analysis to provide insight into the inherent reactivity of fragment **3.1**.

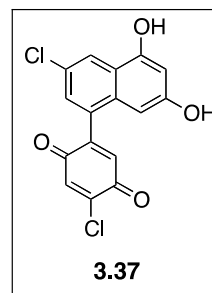
First, the use of iron catalysts was investigated (Table 25).^{123-125,146-148} Subjecting **3.1** to iron trichloride hexahydrate in either dichloromethane or toluene afforded no reaction after stirring at room temperature overnight. Upon heating the reaction mixtures to 60 °C, steady decomposition of **3.1** was observed. Switching to the more polar acetonitrile accelerated the decomposition process and after 2 h at room temperature only a small portion starting material

was recovered. Using DMF as the solvent led to the formation of an unexpected product in 2 h at room temperature. This product was purified by SFC and tentatively assigned based on ^1H NMR analysis to be tricycle **3.37**. Allowing the reaction mixture to stir for 3 d at room temperature afforded **3.37** along with a complex mixture of unidentified products. Increasing the temperature of the reaction led to decomposition of **3.1**. Although **3.37** is not a useful intermediate for the total synthesis of chrysopaentin A, this unusual cyclization may warrant further exploration in the future. The use of potassium ferricyanide was also explored (not shown). Unfortunately, in several solvents in the absence of base or in the presence of the weak base ammonium acetate no reaction was observed and only starting material was recovered. Switching to stronger carbonate bases or potassium hydroxide led to the decomposition of **3.1**.

Table 25. Attempted oxidative dimerization of **3.1**



Conditions ^a	Results
1. $\text{FeCl}_3 \cdot 6\text{H}_2\text{O}$, CH_2Cl_2 , rt, 24 h, then 60 °C 18 h	Dec
2. $\text{FeCl}_3 \cdot 6\text{H}_2\text{O}$, Tol, rt, 24 h, then 60 °C 18 h	Dec
3. $\text{FeCl}_3 \cdot 6\text{H}_2\text{O}$, CH_3CN , rt, 2 h	rec SM + Dec
4. $\text{FeCl}_3 \cdot 6\text{H}_2\text{O}$ DMF, rt, 2 h	3.37 (30%)
5. $\text{FeCl}_3 \cdot 6\text{H}_2\text{O}$, DMF, rt, 3 d	3.37 (33%) + complex
6. $\text{FeCl}_3 \cdot 6\text{H}_2\text{O}$, DMF, rt, 24 h, then 60 °C 18 h	complex mixture

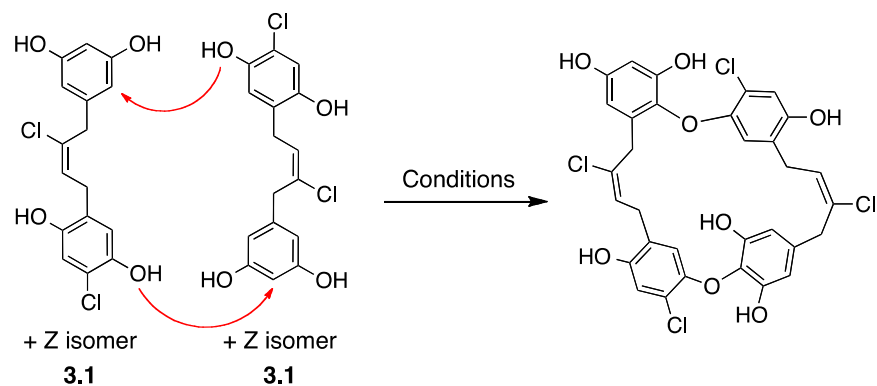


^aReaction were conducted on 20 mg and monitored by LCMS

Next, the use of copper catalysts was explored.¹⁴⁹⁻¹⁵² Subjecting **3.1** to copper chloride in acetonitrile at room temperature resulted in the formation of a small quantity of the oxidized

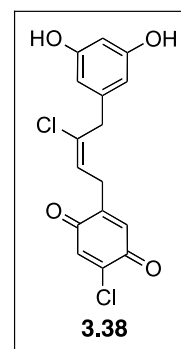
quinone **3.38** (20%) as well as some recovered starting material. Increasing the reaction temperature, only decomposition was observed. The use of phenyliodine diacetate (PIDA) was explored next.^{121,122,153,154} Subjecting to **3.1** to PIDA in acetonitrile provided a complex mixture of unidentified products. Although several other solvents were investigated, again only decomposition was observed. Next, the use of oxidative silver or manganese conditions to affect the desired oxidative dimerization were explored.^{125,148} The use of manganese dioxide resulted in no observable reaction and only starting material was recovered. Using freshly prepared silver oxide in diethyl ether led to the isolation of a major product, tentatively assigned by ¹H NMR analysis to be quinone **3.38**. Selective synthesis of quinone **3.38** using DDQ in diethyl ether afforded **3.38** in 99% yield. Attempts to functionalize the rapidly purified quinone **3.38** were met with decomposition. The instability of quinone **3.38** may suggest that some of the decomposition observed during the reaction screening was a result of initial formation of the quinone followed by a series of undesired side-reactions leading to the observed complex mixtures.

Table 26. Attempt to dimerize **3.1**



Conditions ^a	Results
1. CuCl, CH ₃ CN, 24 h	rec SM + 3.38 (20%)
2. PIDA, CH ₃ CN	complex mix
3. Ag ₂ O, Et ₂ O	3.38 (40%) + complex mix
4. Mn ₂ O, Et ₂ O, rt, 3 d	rec SM
5. DDQ, Et ₂ O	3.38 (99%)

^aReaction were conducted on 20 mg and monitored by LCMS



Finally we chose to investigate the use of enzymes for the desired oxidation dimerization.^{116,117,119,120,155-158} Initially we chose to investigate a commercially available laccase from *Trametes versicolor*. Laccases are copper-containing enzymes known to catalyze the single electron oxidation of variety of organic substrates including the oxidative dimerization of polyphenols to afford β -hydroxy diaryl ethers.^{116,155} Subjecting **3.1** to 10 units of the laccase in a 20 mM acetate buffer (pH = 4.3) afforded only decomposition. Next, we investigated the use of horseradish peroxidase (HRP), a hemoprotein known to oxidatively couple phenols in the presence of hydrogen peroxide.¹⁵⁹ Using a protocol recently used for the oxidative dimerization of 17-estradiol, **3.1** was subjected to HRP and hydrogen peroxide in a 0.1 mM phosphate buffer (pH = 7.4).¹⁶⁰ After stirring overnight, only decomposition was observed. These results led us to reevaluate our strategy for diaryl ether bond formation.

Examination of the literature revealed that although a number of different methods exist for diaryl ether bond formation, the Ullmann coupling has been refined over the last century and has one of the broadest applications of any methods reported so far.¹⁶¹⁻¹⁶⁴ Thus, we chose to investigate the Ullmann coupling of some simplified variants of chrysopaentins A.

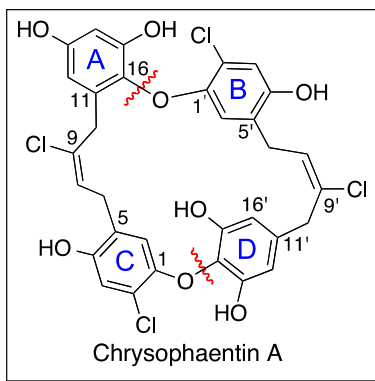
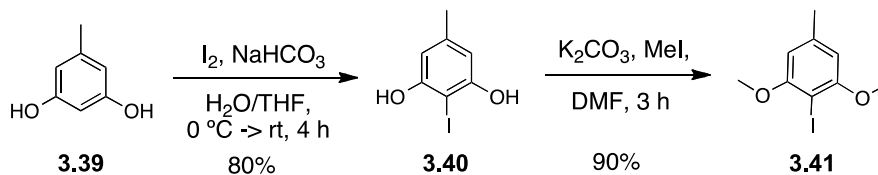


Figure 38. Chrysopaentins A ring labeling

Initially, the synthesis of both an aryl iodide and a phenol containing a similar substitution pattern to aryl rings **D** and **C** of chrysopaentins A was pursued (Figure 38). Starting from the commercially available 3,5-dihydroxy toluene (**3.39**), selective iodination with iodine and sodium bicarbonate in a mixture of THF and water afforded the desired aryl iodide **3.40** in

80% yield (Scheme 39). Protection of **3.40** with potassium carbonate and methyl iodide in DMF proceeded in 90% yield to provide aryl iodide **3.41**.



Scheme 39. Synthesis of **3.41**

With a sufficient quantity of **3.41** prepared, several Ullmann coupling conditions were investigated (Figure 39). 3,5-Dihydroxy toluene (**3.39**) was chosen as the first phenol as it contains a similar 1,3-dihydroxy substitution to the **A** and **D** rings of chrysopaentin A. 3,5-Dihydroxy toluene (**3.39**) and aryl iodide **3.41** were combined in the presence of copper iodide, cesium carbonate, and *N,N*-dimethylglycine¹⁶⁵ and the mixture was heated at 90 °C in dioxane overnight. Unfortunately, no reaction was observed and only starting material was recovered. 1,5-Dihydroxy toluene (**3.42**) was explored next as it contains a similar substitution pattern to the **A** and **C** rings of chrysopaentin A (Figure 38). Subjecting a mixture of dihydroxy toluene (**3.42**), aryl iodide **3.41**, copper iodide, cesium carbonate, and 1,10-phenanthroline¹⁶⁶ to either microwave irradiation or conventional heating again returned only starting material. Investigating the use of a copper triflate toluene complex, reported to provide superior yields than copper iodide in the Ullmann coupling,¹⁶⁷ once again afforded only unreacted starting material. Finally, in order to eliminate any potential steric and electronic effects of either the dihydroxy or methyl substituents, phenol (**3.43**) was evaluated in the Ullmann coupling with aryl iodide **3.41**. Screening the use of a copper bromide dimethylsulfide complex,¹⁶⁸ copper iodide and 1,10-phenanthroline, copper chloride and tetramethylheptanedione,¹⁶⁹ copper oxide in pyridine,¹⁶⁸ and copper iodide and picolinic acid¹⁷⁰ in the Ullmann coupling under conventional heating all returned only starting material. Based on these results, it was hypothesized that the electron rich nature and steric encumbrance of aryl iodide **3.41** was inhibiting oxidative insertion and therefore the success of the coupling.

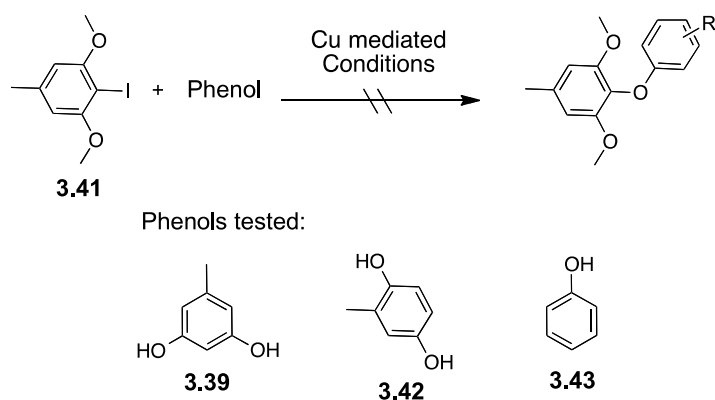
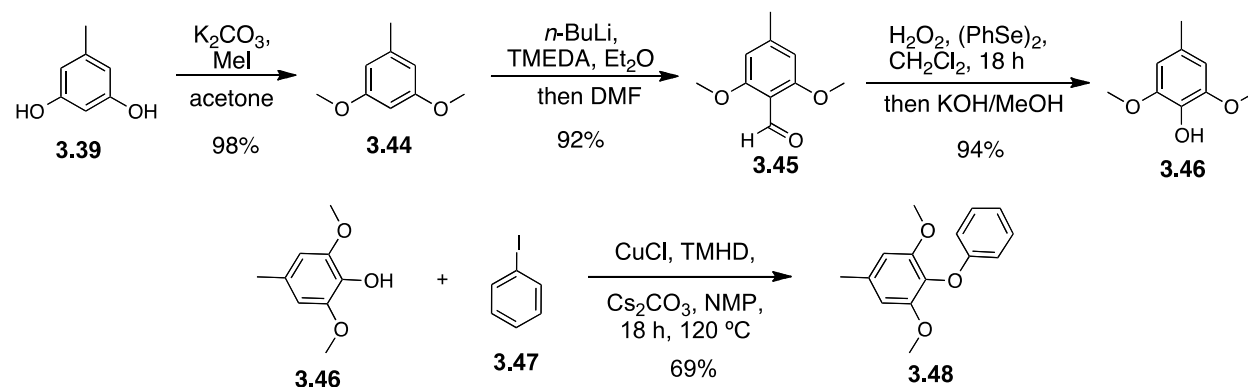


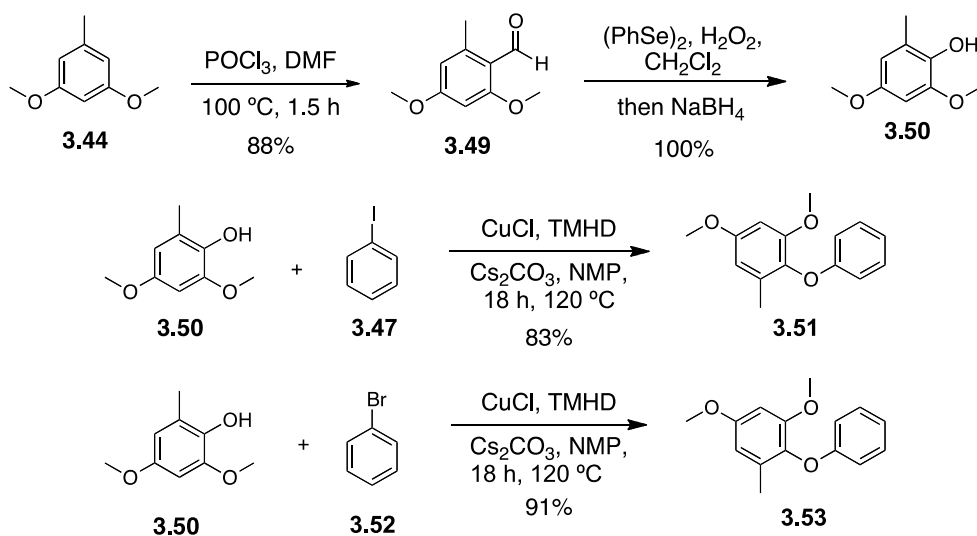
Figure 39. Attempted Ullmann coupling of **3.41** with several phenols

Since sterically hindered electron rich aryl iodides were found to be inefficient for the desired Ullmann coupling, the use of sterically encumbered electron rich phenols was evaluated. Selectively protected phenols with oxygenation patterns similar to the **D** ring of chrysopaentin A were prepared (Scheme 40, Scheme 41). Protection of 3,5-dihydroxy toluene (**3.39**) with potassium carbonate and methyl iodide gave 3,5-dimethoxy toluene **3.44** in 98% yield. Directed *ortho*-metalation¹⁷¹ of 3,5-dimethoxy toluene **3.44** with *n*-butyllithium in the presence of tetramethylethylenediamine followed by trapping with dimethylformamide gave aldehyde **3.45** in 92% yield. Although our initial attempt at the Dakin oxidation of **3.45** with *m*-CPBA provided a complex mixture, the use of hydrogen peroxide and catalytic diphenyl diselenide¹⁷² followed by methanolysis of the resulting ester intermediate afforded phenol **3.46** in 94% yield. Subjecting phenol **3.46** and iodobenzene to copper chloride, 2,2,6,6,-tetramethyl-3,5-heptanedione (TMHD), and cesium carbonate in NMP at 120 °C overnight provided diaryl ether **3.48** in 69% yield (Scheme 40).



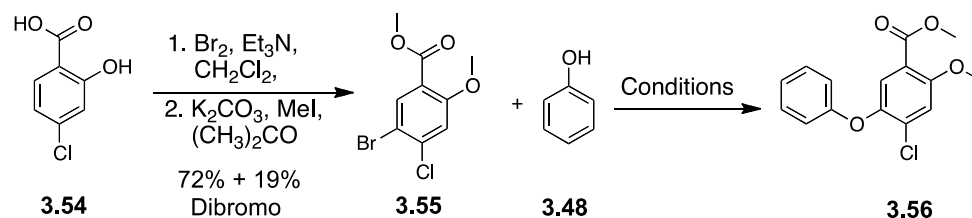
Scheme 40. Synthesis and Ullmann coupling of **3.46**

Next, the preparation and Ullmann coupling of phenol **3.50**, which contains the oxygenation present of the **A** ring of chrysopaentin A (Figure 38), was investigated (Scheme 41). Selective formylation of 3,5-dimethoxy toluene **3.44** with the Vilsmeier-Haack reagent, generated *in situ* from phosphorous oxychloride (POCl_3) and DMF, yielded aldehyde **3.49** in 88% yield. Dakin oxidation with hydrogen peroxide and catalytic diphenyl diselenide¹⁷² proceeded smoothly to give an intermediate ester which was reduced with sodium borohydride to provide phenol **3.50** in quantitative yield. Subjecting phenol **3.50** and iodobenzene (**3.47**) to the previously successful Ullmann conditions afforded the desired diaryl ether **3.51** in 83% yield. Bromobenzene (**3.52**) also proved competent in the Ullmann coupling to give the desired diaryl ether **3.51** in slightly improved 91% yield (Scheme 41).

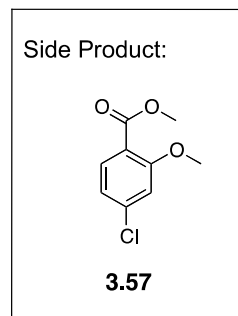


Scheme 41. Synthesis and Ullmann coupling of **3.50**

Having successfully coupled both **3.46** and **3.50**, the use of the fully functionalized **3.55** in the Ullmann coupling was explored (Table 27). Bromination of 2-hydroxy-4-chlorobenzoic acid (**3.54**) with bromine and triethylamine¹⁷³ followed by methylation of both the phenol and acid with methyl iodide provided aryl bromide **3.55** in 72% yield along with 19% of the dibrominated product. Ullmann coupling of **3.55** with copper iodide and TMHD in NMP overnight at 140 °C provided a complex mixture of products. Investigating different CuI ligands, *N,N*-dimethyl glycine¹⁶⁵ or 1,10-phenanthroline¹⁶⁶ afforded only recovered starting material. Varying the copper catalyst to either copper triflate¹⁶⁷ or copper oxide¹⁷⁴ resulted in no observable reaction and only starting material was recovered. Moving from conventional heating to microwave irradiation, the use of copper iodide and cesium carbonate at 200 °C for 20 minutes gave a complex mixture of unidentified products. Investigating the use of a recently reported copper thiophene complex^{175,176} in dimethylformamide under microwave irradiation (200 °C) afforded a mixture of recovered starting material (**3.59**), the proto-demetalated product (**3.62**), and decomposition. Decreasing the reaction temperature to 160 °C, approximately 20% of a product tentatively assigned as **3.56** was isolated along with an intractable impurity. Hoping to increase the reactivity of the aryl bromide, we also prepared and evaluated the aryl iodide (not shown). Unfortunately under a variety of copper mediated conditions, none of the desired product was isolated.

Table 27. Preparation and attempted Ullmann coupling of **3.56**

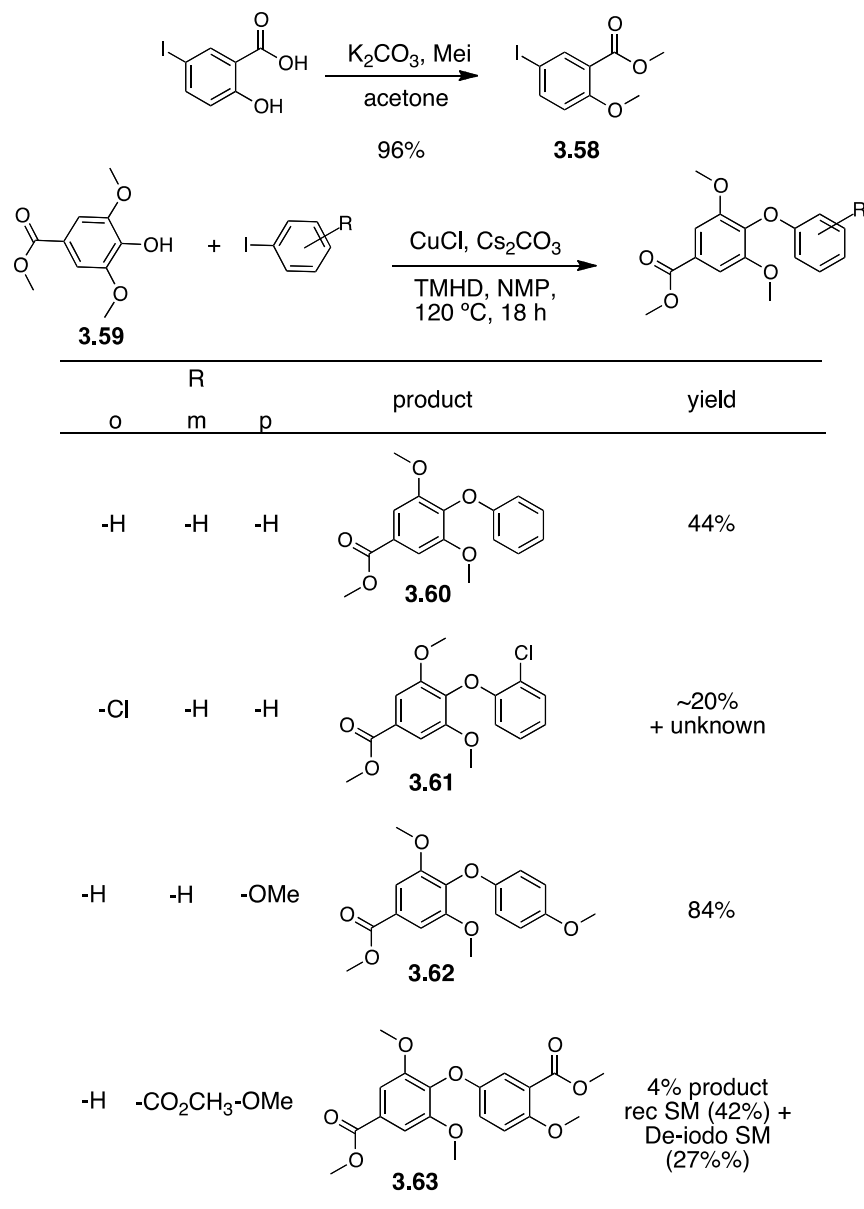
Conditions	Results
1. CuI, Cs ₂ CO ₃ , NMP, TMHD 18 h, 140 °C	complex mixture
2. CuI, Cs ₂ CO ₃ , N,N-dimethylglycine dioxane, 80 °C, 18 h	rec SM
3. CuI, Cs ₂ CO ₃ , N,N-dimethylglycine dioxane, 100 °C, 36 h	rec SM
4. CuI, Cs ₂ CO ₃ , Tol, 110 °C 1,10-phenanthroline, 18 h	rec SM
5. (CuOTf) ₂ PhMe, Cs ₂ CO ₃ Tol, 110 °C, 18 h	rec SM
6. Cu ₂ O, Pyr. 110 °C, 18 h	rec SM
7. CuI, Cs ₂ CO ₃ , DMF, μW, 200 °C, 20 min	complex mixture
8. CuTC, DMF, μW, 200 °C 20 min	rec SM + 3.57 and dec
9. CuTC, DMF, μW, 160 °C 1 h	<20% (3.56)



Based on the limited success of both the iodo and bromo derivatives, a series of aryl iodides were prepared to test which substitutions were inhibiting the Ullmann coupling. Using the commercially available methyl 3,5-dimethoxy-4-hydroxybenzoate, these aryl iodides were evaluated under the previously successful reaction conditions of copper chloride, cesium carbonate, and TMHD in NMP at 120 °C. Iodobenzene afforded the desired Ullmann coupling product **3.60** in 44% yield. Introduction of the *o*-chloride dramatically reduced the efficiency of the reaction and only 20% of a product tentatively assigned as **3.61** containing an intractable impurity was isolated. The presence of a *p*-methoxy substituent afforded the highest yield of the Ullmann coupling product **3.62** (84% yield). Introduction of a *m*-ester significantly decreased the efficiency of the reaction providing only 4% yield of **3.63**. Although several mechanisms have been postulated for the copper mediated Ullmann coupling, a mechanistic consensus has yet to be reached.^{161,177} Examination of Table 28 reveals that for the sterically hindered electron rich phenol **3.59** the combination of the *o*-chloride and *m*-ester are responsible for the

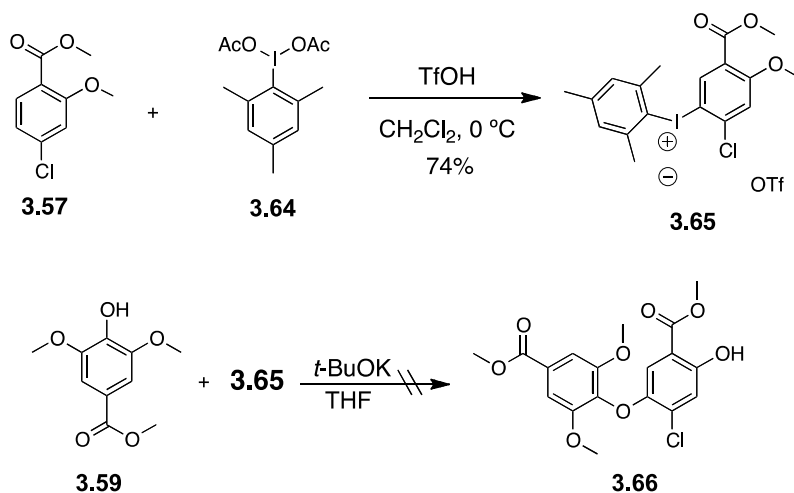
inefficiency of the Ullmann coupling. These studies led us to conclude that further optimization of the Ullmann coupling or its application to the fully functionalized fragment **3.1**, were not worth pursuing. Therefore, an alternative strategy for diaryl ether formation had to be explored.

Table 28. Investigation of the effect of increasing complexity on the intermolecular Ullmann coupling



In a final attempt to form the diaryl ether bond, a recently reported procedure for diaryl ether formation using diaryliodonium salts was investigated (Scheme 42).¹⁷⁸ Synthesis of diaryliodonium **3.65** from ester **3.57** was accomplished using the commercially available

iodomesitylene diacetate **3.64** in the presence of triflic acid in 74% yield.¹⁷⁹ Unfortunately, several attempts to synthesize diaryl ether **3.66** using *t*-butoxide in tetrahydrofuran failed to afford the desired product **3.66**.



Scheme 42. Investigation of diaryl ether formation via hypervalent iodonium coupling

3.4 CONCLUSIONS

Herein, the convergent synthesis of the C₁-C₁₆ tetraphenol of chrysopaentins A is reported in 10 steps (longest linear sequence) and 24% overall yield. Our synthetic strategy is highlighted by a regio and stereo-selective iodochlorination and subsequent Negishi cross-coupling to install the *E*-chloroalkene conserved throughout the chrysopaentins. After SFC separation of the *E*- and *Z*-stereoisomers, the pure *E*-isomer of both fragment **3.1** and the dimethyl variant **3.36** were submitted for biological evaluation.

Through a collaboration with Dr. Bewley and coworkers at the National Institutes of Health, the antibacterial activity of both **3.36** and **3.1** was evaluated. Gratifyingly, **3.36** and **3.1**, which comprise the conserved portions of the chrysopaentins, retained the potent growth inhibition exhibited by their parent natural product for several bacterial strains, including a highly drug resistant strain of *Staphylococcus aureus* (Table 24).¹⁴⁵

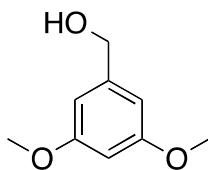
Although the formation of the diaryl ether linkages present in chrysopaentin A has yet to be realized, a series of oxidative, Ullmann, and hypervalent iodine conditions were examined and provided insight into the reactivity of the fully functionalized phenols. In particular, the fully functionalized fragment **3.1** exhibited a propensity to oxidize to the quinone, which could undergo a variety of undesired side reactions leading to a mixture of degradation products. The investigation of the Ullmann coupling of a series of model systems revealed that the presence of the *o*-chloride and a *m*-ester are primarily responsible for the decreased efficiency of the Ullmann coupling. Finally, the use of a hypervalent iodine derivative **3.65** proved inefficient for the S_NAr type coupling.

In the future, the formation of the diaryl ether bond must be addressed. Ideally, diaryl ether formation will be either the penultimate or final step affording the most convergent synthesis and allowing for full use of the described synthesis of fragment **3.1**. A major challenge associated with the total synthesis of the chrysopaentins, the installation of the dialkyl *E*-chloroalkene, has been addressed. The significant advances in metal mediated coupling made in the last 50 years make it likely that this strategy will be amenable to a large variety of substitution around the aryl rings. Therefore, it is likely that the Negishi coupling of fragments already containing the diaryl ether linkage will be successful.

3.5 EXPERIMENTAL

General. All moisture sensitive reactions were performed using syringe-septum techniques under an atmosphere of either dry N₂ or dry argon unless otherwise noted. All glassware was dried in an oven at 140 °C for a minimum of 6 h or flame-dried under an atmosphere of dry nitrogen prior to use. Reactions carried out at -78 °C employed a CO_{2(s)}/acetone bath. Et₂O and tetrahydrofuran were dried by distillation over sodium/benzophenone under an argon atmosphere. Dry methylene chloride was purified by filtration through an activated alumina column. All degassed solvents were prepared using the freeze/pump/thaw method (3×). Methanol, acetonitrile, and *N,N*-dimethylformamide were stored over molecular sieves (3 Å). Deuterated chloroform was stored over anhydrous potassium carbonate. Reactions were

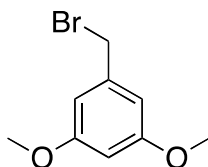
monitored by TLC analysis (pre-coated silica gel 60 F₂₅₄ plates, 250 μm layer thickness) and visualized by using UV lamp (254 nm) or by staining with either Vaughn's reagent (4.8 g of (NH₄)₆Mo₇O₂₄·4H₂O and 0.2 g of Ce(SO₄)₂ in 100 mL of a 3.5 N H₂SO₄) or a potassium permanganate solution (1.5 g of KMnO₄ and 1.5 g of K₂CO₃ in 100 mL of a 0.1% NaOH solution). Flash column chromatography was performed with 40–63 μm silica gel (Silicycle). Microwave reactions were performed on a Biotage Initiator microwave reactor. Infrared spectra were measured on a Smiths Detection IdentifyIR FT-IR spectrometer (ATR). Unless otherwise indicated, all NMR data were collected at room temperature in CDCl₃ or (CD₃)₂CO on a 300, 400, 500, 600, or 700 MHz Bruker instrument. Chemical shifts (δ) are reported in parts per million (ppm) with internal CHCl₃ (δ 7.26 ppm for ¹H and 77.00 ppm for ¹³C), or internal acetone (δ 2.05 ppm for ¹H and 29.85 ppm for ¹³C), as the reference. ¹H NMR data are reported as follows: chemical shift, multiplicity (s = singlet, bs = broad singlet, d = doublet, t = triplet, q = quartet, m = multiplet, dd = doublet of doublets, dt = doublet of triplets, td = triplet of doublets, qd = quartet of doublets, sep = septet), integration, and coupling constant(s) (*J*) in Hertz (Hz). HRMS analyses were obtained using either a Q-TOF Ultima API, Micromass UK Limited (ESI) or a VG Autospec, FISIONS instrument (EI).



3.7

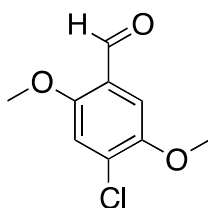
3,5-Dimethoxy benzyl alcohol (3.7). To a stirred suspension of lithium aluminum hydride (13.1 g, 329 mmol, 2 equiv) in dry THF (400 mL) at 0 °C was added a solution of 3,5-dimethoxybenzoic acid (30.0 g, 164 mmol, 1 equiv) in dry THF (400 mL) over 45 min. Upon completion of the addition, the reaction mixture was diluted with THF (300 mL), warmed to rt, stirred for 5 h, and slowly quenched with a saturated aqueous solution of Na/K tartrate. The resulting biphasic mixture was stirred at rt. for 1 h, the organic layer was separated, the remaining aqueous layer was extracted with EtOAc (x2), and the combined organic layers were dried (MgSO₄), filtered, and concentrated under reduced pressure to give **3.7** (27.0 g, 97%) as a

colorless oil: Rf 0.33 (EtOAc/hexanes, 1:2); IR (CDCl₃) 3390, 2937, 1594, 1456, 1428, 1318, 1294, 1202, 1146, 1057, 829 cm⁻¹; ¹H NMR (600 MHz, CDCl₃) δ 6.45 (d, 2 H, *J* = 2.4 Hz), 6.32 (d, 1 H, *J* = 2.4 Hz), 4.50 (d, 2 H, *J* = 5.4 Hz), 3.71 (s, 6 H), 3.49 (t, 1 H, *J* = 5.4 Hz); ¹³C NMR (150 MHz, CDCl₃) δ_C160.5, 143.3, 104.2, 99.2, 64.5, 55.0. Characterization matches that reported by Weist *et al.*¹⁸⁰



3.3

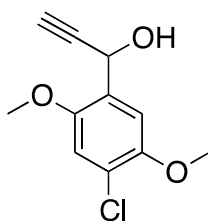
3,5-Dimethoxybenzyl bromide (3.3). To a stirred solution of **3.7** (17.5 g, 104 mmol, 1 equiv) in CH₂Cl₂ (500 mL) at 0 °C was added dropwise PBr₃ (12.1 mL, 125 mmol, 1.2 equiv). The reaction mixture was slowly warmed to rt, stirred for 3 h, quenched with a saturated aqueous solution of NaHCO₃, and stirred at rt. for 1 h. The organic layer was separated and the aqueous layer was extracted with Et₂O. The combined organic layers were dried (MgSO₄), filtered, and concentrated under reduced pressure to give **3.3** (22.2 g, 92%) as a white solid: Rf 0.75 (EtOAc/hexanes, 1:2); IR (CDCl₃) 2999, 2954, 1596, 1458, 1428, 1345, 1323, 1297, 1204, 1152, 1062, 930 cm⁻¹; ¹H NMR (400 MHz, CDCl₃) δ 6.54 (d, 2 H, *J* = 2.0 Hz), 6.39 (d, 1 H, *J* = 2.4 Hz), 4.42 (s, 2 H), 3.80 (s, 6 H); ¹³C NMR (150 MHz, CDCl₃) δ 160.9, 139.7, 107.0, 100.6, 55.4, 33.6; HRMS (ESI⁺) *m/z* calcd for C₉H₁₂O₂Br 231.0021, found 231.0038. Characterization matches that reported by Snyder, Scott A.¹⁸¹



3.8

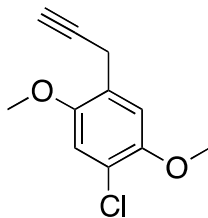
4-Chloro-2,5-dimethoxybenzaldehyde (3.8). To a stirred solution of 2-chloro-1,4-dimethoxybenzene (25.0 g, 0.145 mol, 1 equiv) and hexamethylenetetramine (20.5 g, 0.145 mol, 1 equiv) at rt. was carefully added TFA (250 mL). The resulting yellow suspension was heated to

95 °C, stirred for 5 h, and the hot brown solution was poured into a 2 L Erlenmeyer flask containing approximately 250 g of crushed ice. To the vigorously stirred mixture was slowly added solid NaHCO₃ (243 g, 2.90 mol, 20 equiv) in 5–10 g portions over two hours. The resulting yellow precipitate was filtered through a pad of Celite, washed with water, and dissolved in Et₂O. The organic layer was washed with water and brine, dried (MgSO₄), filtered, and concentrated under reduced pressure to give **3.8** yield (29.0 g, 100%) as an off-white solid: Rf 0.70 (EtOAc/hexanes, 3:7); IR (neat) 2941, 2874, 1664, 1601, 1575, 1497, 1478, 1461, 1389, 1269, 1213, 1023, 977 cm⁻¹; ¹H NMR (400 MHz, CDCl₃) δ 10.35 (s, 1 H), 7.33 (s, 1 H), 7.03 (s, 1 H), 3.87 (s, 6 H); ¹³C NMR (100 MHz, CDCl₃) δ 188.4, 156.1, 149.4, 130.4, 123.4, 114.5, 109.9, 56.5, 56.3; HRMS (EI⁺) *m/z* calcd for C₉H₉O₃Cl 200.0240, found 200.0238. Characterization matches that reported by Bloomer *et al.*¹⁸²



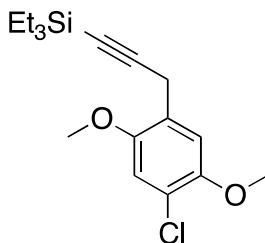
3.9

1-(4-Chloro-2,5-dimethoxyphenyl)prop-2-yn-1-ol (3.9).¹⁸³ To a stirred solution of **3.7** (2.50 g, 12.5 mmol, 1 equiv) in THF (20 mL) at 0 °C was added dropwise ethynyl magnesium bromide (0.5 M in THF; 49.8 mL, 24.9 mmol, 2.0 equiv). The reaction was allowed to stir at 0 °C for 30 min, quenched with a saturated aqueous solution of NH₄Cl, and extracted with Et₂O (x2). The combined organic layers were washed with brine, dried (MgSO₄), filtered, and concentrated under reduced pressure. The crude mixture was purified by chromatography on SiO₂ (EtOAc/hexanes, 1:3) to give **3.9** (2.64 g, 94% yield) as a white solid: Mp 80-81 °C; Rf 0.24 (EtOAc/hexanes, 1:3); IR (neat) 3282, 2958, 1491, 1463, 1441, 1388, 1206, 1178, 1031, 982, 740; ¹H NMR (300 MHz, CDCl₃) δ 7.21 (s, 1 H), 6.93 (s, 1 H), 5.66 (dd, 1 H, *J* = 2.1, 5.1 Hz), 3.87, (s, 3 H), 3.83 (s, 3 H), 3.06 (d, 1 H, *J* = 5.7 Hz), 2.62 (d, 1 H, *J* = 2.4 Hz); ¹³C NMR (75 MHz, CDCl₃) δ 150.5, 149.1, 127.5, 122.6, 113.5, 112.1, 82.6, 74.4, 60.1, 56.7, 56.3; HRMS (EI⁺) *m/z* calcd for C₁₁H₁₁O₃Cl 226.0397, found 226.0395.

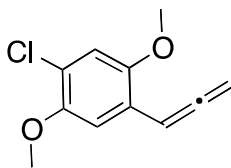


3.4

1-Chloro-2,5-dimethoxy-4-(prop-2-ynyl)benzene (3.4).¹⁸⁴ To a stirred solution of **3.9** (1.30 g, 5.74 mmol, 1 equiv) in CH₂Cl₂ (25 mL) was added triethylsilane (1.85 mL, 11.5 mmol, 2 equiv) followed by TFA (1.70 mL, 22.9 mmol, 4 equiv) under a N₂ atmosphere. The dark purple solution was stirred at rt for 20 min, quenched with a saturated aqueous solution of NaHCO₃, and extracted with Et₂O (x2). The combined organic layers were washed with brine, dried (MgSO₄), filtered, and concentrated under reduced pressure. The crude residue was dissolved in dry THF (20 mL) and AcOH (1 mL) and TBAF (1 M in THF; 11.5 mL, 11.5 mmol, 2 equiv) were added sequentially. The reaction mixture was stirred at rt under TLC control. Once complete, the reaction was diluted with Et₂O, washed with water (x2), brine, dried (MgSO₄), filtered, and concentrated under reduced pressure. The crude mixture was purified by chromatography on SiO₂ (hexanes/Et₂O, 9:1) to give **3.4** (1.18 g, 98% yield) as a colorless oil: R_f 0.66 (Et₂O/hexanes, 1:9); IR (neat) 3277, 2934, 2839, 1497, 1461, 1448, 1409, 1206, 1180, 1032, 818 cm⁻¹; ¹H NMR (300 MHz, CDCl₃) δ 7.17 (s, 1 H), 6.87 (s, 1 H), 3.89 (s, 6 H), 3.79 (s, 6 H), 3.54 (dd, 2 H, *J* = 0.6, 2.7 Hz), 2.21 (t, 1 H, *J* = 2.7 Hz); ¹³C NMR (75 MHz, CDCl₃) δ 150.8, 149.0, 123.9, 120.7, 113.7, 112.6, 81.4, 70.9, 56.9, 56.1, 29.7, 22.7, 19.2; HRMS (EI⁺) *m/z* calcd for C₁₁H₁₁O₂Cl 210.0448, found 210.0445.

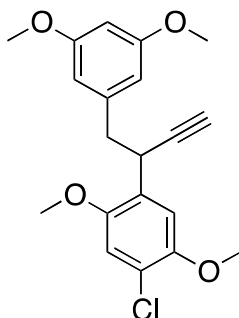


(3-(4-Chloro-2,5-dimethoxyphenyl)prop-1-ynyl)triethylsilane: ¹H NMR (300 MHz, CDCl₃) δ 7.27 (s, 1 H), 6.85 (s, 1 H), 3.88 (s, 1 H), 3.77 (s, 1 H), 3.60 (d, 2 H, *J* = 0.6 Hz), 1.02 (t, 9 H, *J* = 8.1 Hz), 0.63 (q, 6 H, *J* = 7.8, 15.6 Hz).



3.11

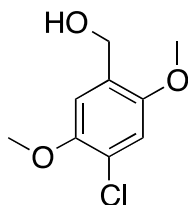
1-Chloro-2,5-dimethoxy-4-(propa-1,2-dienyl)benzene (3.11). To a stirred solution of **(3-(4-chloro-2,5-dimethoxyphenyl)prop-1-ynyl)triethylsilane** (mixture of product and SM, 0.113 g, 0.348 mmol, 1 equiv) in THF (2 mL) was added TBAF (1 M in THF; 0.696 mL, 0.696 mmol, 2 equiv). The reaction was stirred at rt for 1 h. The amber red reaction mixture was diluted with water and extracted with Et₂O (x3). The combined organic layers were washed with water (x2), brine, dried (MgSO₄), filtered, and concentrated under reduced pressure. The crude mixture was purified by chromatography on SiO₂ (EtOAc/hexanes, 1:9) to give undesired allene **3.11** (0.060 g, 82% yield): R_f 0.5 (EtOAc/hexanes, 1:9); ¹H NMR (300 MHz, CDCl₃) δ 6.97 (s, 1 H), 6.89 (s, 1 H), 6.51 (t, 1 H, *J* = 6.9 Hz), 5.14 (d, 2 H, *J* = 6.9 Hz), 3.85 (s, 3 H), 3.79 (s, 3 H).



3.12

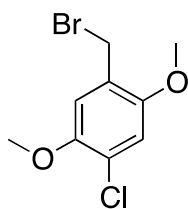
(5-Chloro-2-(1-(3,5-dimethoxyphenyl)but-3-yn-2-yl)-4-methoxyphenoxy)methylum (3.12). To a stirred solution of **3.4** (0.0500 g, 0.237 mmol, 1 equiv) and 3,5-dimethoxybenzyl bromide (0.0679 g, 0.284 mmol, 1.2 equiv) at -78 °C in THF (1 mL) was added dropwise a solution of KHMDS (0.0568 g, 0.284 mmol, 1.2 equiv) in THF (1 mL). The reaction was stirred at -78 °C for 4 h and quenched with a saturated solution of aqueous NH₄Cl. The aqueous solution was extracted with Et₂O (x2) and the combined organic layers were washed with brine, dried (MgSO₄), filtered, and concentrated under reduced pressure. The crude mixture was purified by chromatography on SiO₂ (EtOAc/hexanes, 1:9) to give **3.12** (0.0856 g, 56% yield) as an oil: R_f 0.5 (EtOAc/hexanes, 1:9); ¹H NMR (300 MHz, CDCl₃) δ 7.11 (s, 1 H), 6.89 (s, 1 H), 6.35 (s, 3

H), 4.33 (ddd, 1 H, $J = 2.4, 4.8, 11.1$ Hz), 3.83 (s, 3 H), 3.78 (s, 3 H), 3.75 (s, 3 H), 2.98 (dd, 1 H, $J = 4.8, 12.9$ Hz), 2.79 (s, 1 H, $J = 8.7, 13.2$ Hz), 2.27 (d, 1 H, $J = 2.4$ Hz); ^{13}C NMR (75 MHz, CDCl_3) δ 160.3, 150.1, 149.0, 141.1, 128.4, 120.9, 113.4, 112.9, 107.5, 98.4, 85.0, 71.9, 56.8, 56.1, 55.2, 42.7, 33.0.



3.15

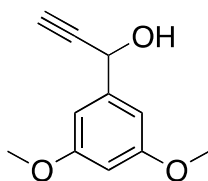
(4-Chloro-2,5-dimethoxyphenyl)methanol (3.15). To a stirred solution of **3.8** (29.0 g, 145 mmol, 1 equiv) in absolute ethanol (550 mL) was added sodium borohydride (27.3 g, 723 mmol, 5 equiv). The reaction mixture was stirred at rt for 6 h, quenched via dropwise addition of acetone, diluted with EtOAc, washed with brine (x2), dried (MgSO_4), filtered, and concentrated under reduced pressure. The crude residue was purified by chromatography on SiO_2 (EtOAc/hexanes, 1:1) to give **3.15** (28.0 g, 96%) as a white solid: Mp 89–90 °C; Rf 0.53 (EtOAc/hexanes, 1:1); IR (neat) 3258, 2958, 2915, 1495, 1461, 1392, 1204, 1061, 719 cm^{-1} ; ^1H NMR (300 MHz, CDCl_3) δ 6.90 (s, 1 H), 6.80 (s, 1 H), 4.55 (d, 2 H, $J = 4.2$ Hz), 3.77 (s, 3 H), 3.71 (s, 3 H), 3.10 (bs, 1 H); ^{13}C NMR (75 MHz, CDCl_3) δ 150.6, 148.7, 128.4, 120.8, 112.5, 112.4, 60.3, 56.5, 55.6; HRMS (ESI⁺) m/z calcd for $\text{C}_9\text{H}_{12}\text{O}_3\text{Cl}$ 203.0475, found 203.0465.



3.14

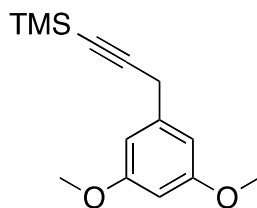
1-(Bromomethyl)-4-chloro-2,5-dimethoxybenzene (3.14).¹⁸⁵ To a stirred solution of **3.15** (5.00 g, 24.7 mmol, 1 equiv) in CH_2Cl_2 (125 mL) at 0 °C was added dropwise HBr (47–49% aqueous solution; 4.13 mL, 74.0 mmol, 3 equiv). The resulting solution was slowly warmed to rt and stirred overnight. The following morning a second batch of HBr (47–49% solution; 4.13 mL,

74.0 mmol, 3 equiv) was added to the reaction mixture, which was stirred at rt for an additional 4 h, extracted with Et₂O (×2), washed with water, a saturated aqueous solution of NaHCO₃, brine, dried (MgSO₄), filtered, and concentrated under reduced pressure to give **3.14** (6.55 g, 100%) as a white solid: Rf 0.31 (EtOAc/hexanes, 3:7); IR (neat) 2962, 2947, 2844, 1732, 1582, 1495, 1458, 1443, 1389, 1301, 1204, 1182, 1033, 882 cm⁻¹; ¹H NMR (400 MHz, CDCl₃) δ 6.91–6.90 (m, 2 H), 4.50 (s, 2 H), 3.84 (s, 3 H), 3.82 (s, 3 H); ¹³C NMR (75 MHz, CDCl₃) δ 151.3, 148.9, 125.1, 123.2, 114.6, 113.6, 56.6, 56.2, 28.2.



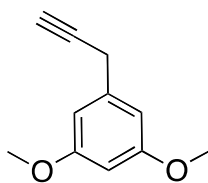
3.17

1-(3,5-Dimethoxyphenyl)prop-2-yn-1-ol (3.17).^{183,186} To a stirred solution of 3,5-dimethoxy benzaldehyde (0.521 g, 3.14 mmol, 1 equiv) in THF (5 mL) at -78 °C was added ethynylmagnesium bromide (0.5 M in THF; 12.5 mL, 6.27 mmol, 2.0 equiv) in two portions at a 30 min interval. After 1 h, the reaction was allowed to warm to 0 °C and stirred for an additional 30 min. The reaction was quenched with a saturated aqueous solution of NH₄Cl and extracted with Et₂O (x2). The combined organic layers were washed with brine, dried (MgSO₄), filtered, and concentrated under reduced pressure. The crude residue was purified by chromatography on SiO₂ (EtOAc/hexanes, 2:8) to give **3.17** (0.600 g, 100% yield) as a colorless oil: Rf 0.4 (EtOAc/hexanes, 3:7); IR (CDCl₃) 3416, 3278, 2937, 2836, 1595, 1457, 1427, 1314, 1292, 1202, 1150, 1055, 835, 727 cm⁻¹; ¹H NMR (300 MHz, CDCl₃) δ 6.69 (d, 2 H, *J* = 2.4 Hz), 6.40 (t, 1 H, *J* = 2.4 Hz), 5.36 (dd, 1 H, *J* = 2.1, 6.0 Hz), 3.77 (s, 6 H), 2.87 (d, 1 H, *J* = 6.3 Hz), 2.65 (d, 1 H, *J* = 2.4 Hz); ¹³C NMR (75 MHz, CDCl₃) δ 160.8, 142.4, 104.5, 100.4, 83.3, 74.6, 64.2, 55.3; HRMS (EI⁺) *m/z* calcd for C₁₁H₁₂O₃ 192.0786, found 192.0784. Characterization matches that reported by Trepanier *et al.*¹⁸³



3.18

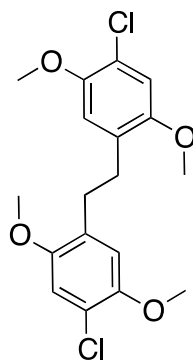
(3-(3,5-Dimethoxyphenyl)prop-1-ynyl)trimethylsilane (3.18). To a stirred solution of ethynyl trimethylsilane (39.1 mL, 277 mmol, 4 equiv) in THF (120 mL) at 0 °C was added ethylmagnesium bromide (3.16 M in Et₂O; 87.6 mL, 277 mmol, 4 equiv). After stirring for 30 min CuBr (9.93 g, 69.2 mmol, 1 equiv) followed 15 min later by 3,5-dimethoxybenzyl bromide (**3.3**, 16.0 g, 69.2 mmol, 1 equiv). The resulting mixture was heated to 66 °C, stirred overnight, diluted with Et₂O, slowly quenched with brine, and extracted with Et₂O (x2). The combined organic layers were washed with a saturated aqueous solution of NH₄Cl, brine, dried (MgSO₄), filtered, and concentrated under reduced pressure. The crude mixture was purified by chromatography on SiO₂ (EtOAc/hexanes, 1:10) to give **3.18** (17.2 g, 100%) as a pale yellow oil: Rf 0.41 (EtOAc/hexanes, 1:20); IR (neat) 2956, 2898, 2175, 1754, 1596, 1459, 1428, 1204, 1156, 1122, 1101, 839 cm⁻¹; ¹H NMR (400 MHz, CDCl₃) δ 6.53 (d, 2 H, *J* = 2.4 Hz), 6.34 (t, 1 H, *J* = 2.4 Hz), 3.79 (s, 6 H), 3.60 (s, 2 H), 0.19 (s, 9 H); ¹³C NMR (100 MHz, CDCl₃) δ 160.8, 138.7, 105.9, 104.0, 98.7, 87.1, 55.3, 26.3, 0.1; HRMS (ESI⁺) *m/z* calcd for C₁₄H₂₁O₂Si 249.1311, found 249.1287.



3.13

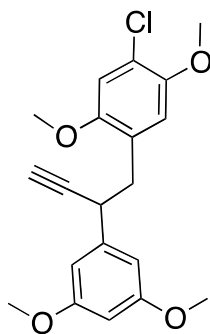
1,3-Dimethoxy-5-(prop-2-ynyl)benzene (3.13). To a stirred solution of **3.18** (5.37 g, 21.6 mmol, 1 equiv) and AcOH (4.99 mL, 86.5 mmol, 4 equiv) in THF (100 mL) was added dropwise TBAF (1 M in THF; 86.5 mL, 86.5 mmol, 4 equiv). The resulting reaction mixture was stirred at rt for 24 h, diluted with Et₂O, washed with brine (x2), dried (MgSO₄), filtered, and concentrated under reduced pressure. The crude mixture was purified by chromatography on SiO₂ (EtOAc/hexanes, 1:10) to give **3.13** (3.85 g, 100%) as a colorless oil: Rf 0.36 (EtOAc/hexanes, 1:10); IR (CDCl₃)

3286, 2999, 2954, 1593, 1457, 1428, 1344, 1323, 1288, 1204, 1154, 1064, 827; ^1H NMR (400 MHz, CDCl_3) δ 6.53 (d, 2 H, $J = 2.4$ Hz), 6.35 (t, 1 H, $J = 2.4$ Hz), 3.79 (s, 6 H), 3.56 (d, 2 H, $J = 2.8$ Hz), 2.20 (t, 1 H, $J = 2.8$ Hz); ^{13}C NMR (100 MHz, CDCl_3) δ 160.9, 138.3, 105.9, 98.7, 81.7, 70.6, 55.3, 25.0; HRMS (EI^+) m/z calcd for $\text{C}_{11}\text{H}_{12}\text{O}_2$ 176.0837, found 176.0834.



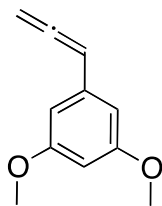
3.20

1,2-Bis(4-chloro-2,5-dimethoxyphenyl)ethane (3.20). ^1H NMR (400 MHz, CDCl_3) δ 6.86 (s, 1 H), 6.59 (s, 1 H), 3.78 (s, 3 H), 3.76 (s, 3 H), 2.82 (s, 2 H).



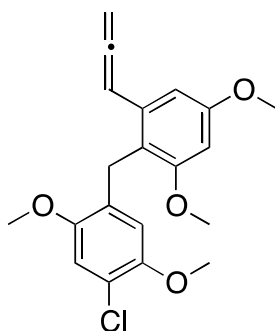
3.21

1-Chloro-4-(2-(3,5-dimethoxyphenyl)but-3-ynyl)-2,5-dimethoxybenzene (3.21). ^1H NMR (400 MHz, CDCl_3) δ 6.89 (s, 1 H), 6.67 (s, 1 H), 6.49 (d, 2 H, $J = 2.4$ Hz), 6.34 (t, 1 H, $J = 2.4$ Hz), 3.84 (d, 2 H, $J = 4$ Hz), 3.78 (s, 3 H), 3.77 (s, 9 H), 3.04 (dd, 1 H, $J = 6.4, 13.2$ Hz), 2.93 (dd, 1 H, $J = 8.8, 13.2$ Hz), 2.25 (d, 1 H, $J = 2.4$ Hz).



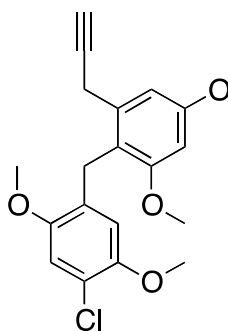
3.11

1,3-Dimethoxy-5-(propa-1,2-dienyl)benzene (3.11). ^1H NMR (400 MHz, CDCl_3) δ 6.47 (d, 2 H, $J = 2.4$ Hz), 6.33 (t, 1 H, $J = 2.4$ Hz), 6.10 (t, 1 H, $J = 6.8$ Hz), 5.16 (d, 2 H, $J = 6.8$ Hz), 3.79 (s, 6 H).



3.22

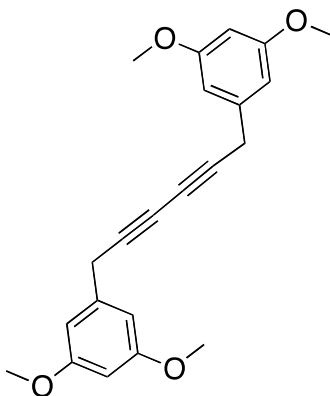
2-(4-Chloro-2,5-dimethoxybenzyl)-1,5-dimethoxy-3-(propa-1,2-dienyl)benzene (3.22). ^1H NMR (400 MHz, CDCl_3) δ 6.86 (s, 1 H), 6.51 (d, 1 H, $J = 2.4$ Hz), 6.39 (d, 1 H, $J = 2.4$ Hz), 6.39 (s, 1 H), 6.26 (t, 1 H, $J = 6.8$ Hz), 5.06 (d, 2 H, $J = 6.8$ Hz), 3.95 (s, 2 H), 3.84 (s, 3 H), 3.83 (s, 3 H), 3.76 (s, 3 H), 3.63 (s, 3 H).



3.23

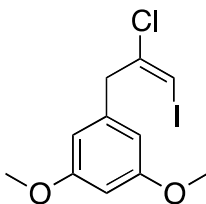
2-(4-Chloro-2,5-dimethoxybenzyl)-1,5-dimethoxy-3-(prop-2-ynyl)benzene (3.23). ^1H NMR (400 MHz, CDCl_3) δ 6.86 (s, 1 H), 6.77 (d, 1 H, $J = 2.4$ Hz), 6.44 (d, 1 H, $J = 2.4$ Hz), 6.35 (s, 1

H), 3.90 (s, 2 H), 3.85 (s, 3 H), 3.84 (s, 3 H), 3.76 (s, 3 H), 3.63 (s, 3 H), 3.44 (d, 2 H, $J = 2.8$ Hz), 2.13 (t, 1 H, $J = 2.8$ Hz).



3.24

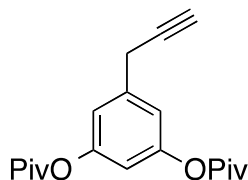
1,6-Bis(3,5-dimethoxyphenyl)hexa-2,4-diyne (3.24). ^1H NMR (400 MHz, CDCl_3) δ 6.48 (d, 2 H, $J = 2.4$ Hz), 6.34 (t, 1 H, $J = 2.4$ Hz), 3.79 (s, 6 H), 3.62 (s, 2 H).



3.26

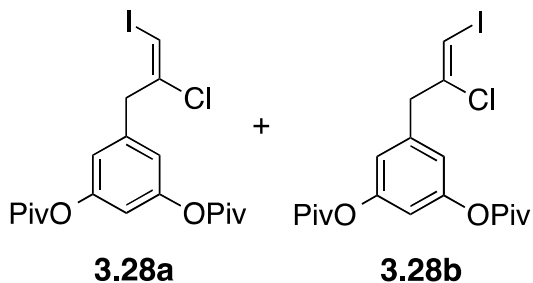
(E)-1-(2-Chloro-3-iodoallyl)-3,5-dimethoxybenzene (3.26). To a stirred solution of **3.13** (0.0500 g, 0.284 mmol, 1 equiv) in dry acetonitrile (3 mL) was added ICl (0.015 mL, 0.284 mmol, 1 equiv). The resulting mixture was heated to 80 °C in a sealed vial and stirred at 80 °C for 5 h. The reaction mixture was cooled, filtered, washing the solid with CH_2Cl_2 , and the filtrate was washed with a saturated aqueous solution of sodium thiosulfate, extracted with Et_2O , dried (MgSO_4), filtered, and concentrated under reduced pressure. The crude mixture was purified by chromatography on SiO_2 (EtOAc /hexanes, 1:10) to give **3.26** (0.053 g, 55% yield) as an impure colorless semi-solid. The impure solid was resubjected to chromatography on SiO_2 (EtOAc /hexanes, 1:10) to give 0.035 g of a mixture of *E*- and *Z*-isomers (3:1) of **3.26** and an intractable mixture of over-iodinated products as a semi-pure colorless solid: Characteristic signals for the major geometric isomer of **3.26**: ^1H NMR (300 MHz, CDCl_3) δ 6.48 (s, 1 H), 4.46

(d, 2 H, $J = 1.5$ Hz), 6.39 (t, 1 H, $J = 1.8$ Hz), 3.85 (s, 2 H), 3.79 (s, 6 H); ^{13}C NMR (75 MHz, CDCl_3) δ 160.9, 137.9, 136.4, 106.9, 98.9, 74.1, 55.3, 44.6. LCMS data was obtained using a Prevail C18-Select 3μ column (150 x 4.6 mm) ($R_t = 13.5$ min, 0.50 mL/min, 50% to 80% MeCN/ H_2O with 0.1% TFA, over 30 min): ESI m/z 339 $[\text{M}+\text{H}]^+$.

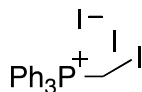


3.27

5-(Prop-2-ynyl)-1,3-phenylene bis(2,2-dimethylpropanoate (3.27)). To a stirred solution of **3.13** (6.50 g, 36.9 mmol, 1 equiv) in CH_2Cl_2 (1200 mL) at 0°C was added BBr_3 (1 M in CH_2Cl_2 ; 92.2 mL, 92.2 mmol, 5 equiv) over 1 h via an addition funnel. The reaction mixture was warmed to rt and stirred overnight. The reaction mixture was slowly quenched with a saturated aqueous solution of NaHCO_3 (500 mL) and stirred at rt for 4 h. The solution was acidified with HCl, extracted with CH_2Cl_2 and EtOAc, and the combined organic layers were dried (MgSO_4), filtered, and concentrated under reduced pressure. The crude mixture was dissolved in CH_2Cl_2 (180 mL), and triethylamine (20.9 mL, 148 mmol, 4 equiv) and PivCl (11.6 mL, 92.2 mmol, 2.5 equiv) were added. The resulting solution was stirred at rt for 90 min, diluted with brine, the organic layer was separated, and the aqueous layer was extracted with EtOAc. The combined organic layers were dried (MgSO_4), filtered, and concentrated under reduced pressure. The crude mixture was purified by chromatography on SiO_2 (EtOAc/hexanes, 1:10) to give **3.27** (9.6 g, 82%) as a colorless oil: R_f 0.85 (EtOAc/hexanes, 3:7); IR (neat) 3293, 2973, 1806, 1750, 1414, 1452, 1396, 1366, 1269, 1118, 1098, 1031, 1003 cm^{-1} ; ^1H NMR (300 MHz, CDCl_3) δ 6.95 (d, 2 H, $J = 1.8$ Hz), 6.76 (t, 1 H, $J = 1.8$ Hz), 3.61 (d, 2 H, $J = 2.4$ Hz), 2.21 (t, 1 H, $J = 2.4$ Hz); ^{13}C NMR (75 MHz, CDCl_3) δ 176.6, 151.5, 138.3, 118.3, 113.8, 80.7, 71.2, 39.1, 27.1, 24.5; HRMS (EI^+) m/z calcd for $\text{C}_{19}\text{H}_{24}\text{O}_4$ 316.1675, found 316.1670.

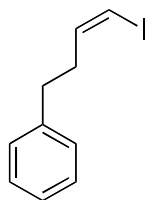


(E)-5-(2-Chloro-3-iodoallyl)-1,3-phenylene bis(2,2-dimethylpropanoate (3.28a) and (Z)-5-(2-Chloro-3-iodoallyl)-1,3-phenylene bis(2,2-dimethylpropanoate (3.28b). To a stirred solution of **3.27** (9.50 g, 30.0 mmol, 1 equiv) in dry CH₂Cl₂ (150 mL) at 0 °C was added ICl (1 M in CH₂Cl₂; 30.0 mL, 30.0 mmol, 1 equiv). The reaction mixture was warmed to rt, stirred protected from light (enclosed in aluminum foil) for 3 h, diluted with Et₂O, washed with Na₂SO₄ (×2), brine, dried (MgSO₄), filtered, and concentrated under reduced pressure. The crude mixture was purified by chromatography on SiO₂ (EtOAc/hexanes, 1:10) to give an inseparable 2:1 mixture of **3.28a** and **3.28b** (13.7 g, 95%) as a colorless oil: R_f 0.54 (EtOAc/hexanes, 1:10); IR (neat) 3277, 2934, 2872, 1746, 1592, 1497, 1461, 1409, 1269, 1207, 1122, 1103, 1032, 975, 723 cm⁻¹; HRMS (ESI⁺) *m/z* calcd for C₁₉H₂₄O₄NaClI 501.0306, found 501.0308. Characteristic data for the major, desired isomer **3.28a**: ¹H NMR (300 MHz, CDCl₃) δ 6.87 (d, 2 H, *J* = 1.5 Hz), 6.80 (t, 1 H, *J* = 2.1 Hz), 6.62 (s, 1 H), 3.90 (s, 2 H), 1.35 (s, 18 H); ¹³C NMR (100 MHz, CDCl₃) δ 176.6, 151.6, 137.9, 135.6, 119.0, 114.2, 74.8, 44.2, 39.1, 27.1. Characteristic signals for **3.28b**: ¹H NMR (300 MHz, CDCl₃) δ 7.06 (s, 1 H), 3.92 (s, 2 H).



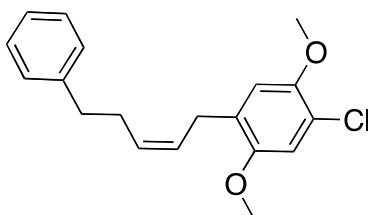
(Iodomethyl)triphenylphosphonium iodide (3.31).^{141,187} To a mechanically stirred solution of triphenylphosphine (60.0 g, 229 mmol, 1 equiv) in anhydrous toluene (120 mL) was added diiodomethane (23.4 mL, 297 mmol, 1.3 equiv). The reaction was heated to 80 °C and stirred under N₂ overnight (~20 h). The reaction mixture was filtered and washed with anhydrous toluene (1 L) until the filtrate was no longer yellow. The white solid was collected and further dried under vacuum to give **3.31** (92 g, 100% yield) as a white solid: ¹H NMR (400 MHz,

CDCl₃) δ 7.94-7.77 (m, 15 H), 5.05 (d, 2 H, $J = 8.4$ Hz); ¹³C NMR (100 MHz, CDCl₃) δ 135.2, 135.1, 133.8, 133.8, 130.2, 118.8, 117.9.



3.32

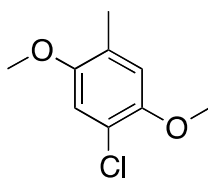
(Z)-(4-Iodobut-3-enyl)benzene (3.32).¹⁸⁸ To a stirred solution of **3.31** (26.6 g, 50.3 mmol, 1.5 equiv) in anhydrous THF (100 mL) at rt was added dropwise a solution of NaHMDS (9.71 g, 50.3 mmol, 3 equiv) in THF (25 mL) over 15 min. The reaction was stirred at rt for 10 min, cooled to -78 °C, and a solution of hydrocinnamaldehyde (4.93 mL, 33.5 mmol, 1 equiv) in THF (20 mL) was added dropwise over 20 min. The reaction mixture was stirred at -78 °C under N₂, protected from light, for an additional 10 min, quenched with brine, and allowed to warm to rt. The mixture was thoroughly extracted with EtOAc (4 x 250 mL) and the combined organic layers were dried (MgSO₄), filtered, and concentrated under reduced pressure to give a reddish semi-solid. The semi-solid was dissolved in CH₂Cl₂ and purified by chromatography on SiO₂ (CH₂Cl₂) to give **3.32** (8.7 g, 100%) as a colorless oil: R_f 0.67 (EtOAc/hexanes, 1:10); IR (neat) 3277, 2965, 2841, 1497, 1463, 1448, 1418, 1437, 1387, 1208, 1033, 846, 818, 688 cm⁻¹; ¹H NMR (400 MHz, CDCl₃) δ 7.33-7.29 (m, 2 H), 7.24-7.20 (m, 3 H), 6.26-6.19 (m, 2 H), 2.76 (t, 2 H, $J = 8.0$ Hz), 2.51-2.46 (m, 2 H); ¹³C NMR (100 MHz, CDCl₃) δ 141.0, 140.2, 128.4, 126.1, 83.1, 36.3, 34.0; HRMS (EI⁺) m/z calcd for C₁₀H₁₁I 257.9906, found 257.9907.



3.33

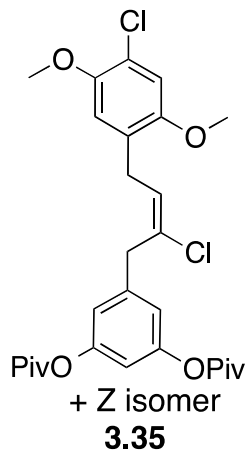
(Z)-1-Chloro-2,5-dimethoxy-4-(5-phenylpent-2-enyl)benzene (3.33). To a dry flask was added zinc dust (1.01 g, 15.5 mmol, 5 equiv) and iodine (0.118 g, 0.464 mmol, 0.15 equiv). Heat (Bunsen burner flame) was applied until a purple gas coated the interior of the flask. The sample

was allowed to cool under argon and suspended in dry, degassed DMF (1.5 mL). To the stirred solution was added **3.14** (1.24 g, 4.64 mmol, 1.5 equiv) and a second batch of iodine (0.118 g, 0.464 mmol, 0.15 equiv). The reaction was stirred at rt for 15 min. Meanwhile, in a separate, dry flask, **3.32** (0.200 g, 0.775 mmol, 1 equiv), Pd₂(dba)₃ (0.0178 g, 0.0194 mmol, 0.025 equiv) and P(*o*-Tol)₃ (0.0243, 0.0775 mmol, 0.1 equiv) were dissolved in dry, deoxygenated DMF (0.4 mL) and allowed to stir at rt for 10 min. The activated zinc reagent was then syringed off the excess zinc, rinsing with DMF (0.5 mL), and 1 mL of the heterogeneous mixture was added dropwise to the stirred solution of vinyl iodide. The reaction was allowed to stir at rt overnight (~16 h) and directly applied to SiO₂ for purification by chromatography (EtOAc/hexanes, 1:50) to give **3.33** (0.168 g, 68% yield) as well as the quenched organo zinc (0.056 g, 12% yield) and P(*o*-Tol)₃ (0.011 g) as an intractable mixture: R_f 0.18 (EtOAc/hexanes, 1:10); Characteristic signals for **3.33**: ¹H NMR (400 MHz, CDCl₃) δ 7.37 (d, 2 H, *J* = 7.2 Hz), 7.30 (t, 3 H, *J* = 6.4 Hz), 6.96 (s, 1 H), 6.82 (s, 1 H), 5.72-5.62 (m, 2 H), 3.83 (s, 6 H), 3.42 (d, 2 H, *J* = 6.0 Hz), 2.82 (t, 2 H, *J* = 7.2 Hz) 2.60 (t, 2 H, *J* = 8.4 Hz); ¹³C NMR (100 MHz, CDCl₃) δ 151.3, 148.8, 141.7, 130.1, 128.3, 128.1, 127.6, 125.7, 114.0, 112.6, 56.6, 55.8, 35.7, 28.9, 27.4.

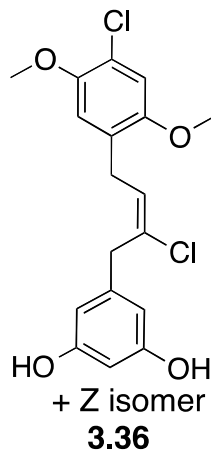


3.34

1-Chloro-2,5-dimethoxy-4-methylbenzene (3.34). R_f 0.18 (EtOAc/hexanes, 1:10); ¹H NMR (400 MHz, CDCl₃) δ 6.94 (s, 1 H), 6.85 (s, 1 H), 3.90 (s, 6 H), 2.31 (s, 3 H). Characterization matches that reported by Green *et al.*¹⁸⁹



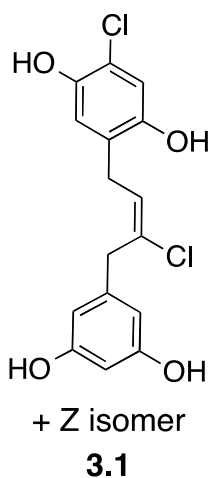
(E)-5-(2-Chloro-4-(4-chloro-2,5-dimethoxyphenyl)but-2-enyl)-1,3-phenylene-bis(2,2-dimethylpropanoate) (3.35). A flame-dried flask was charged with a catalytic amount of iodine and activated zinc (0.513 g, 7.69 mmol, 8 equiv). The flask was heated (Bunsen burner) until a purple gas coated the interior of the flask. The flask was allowed to cool to rt and dry degassed DMF (1 mL) was added followed by **3.14** (1.02 g, 3.84 mmol, 4 equiv) followed by a second catalytic amount of iodine the reaction was allowed to stir at rt for 15 min. A separate dry flask was charged with **3.28a/3.28b** (0.460 g, 0.961 mmol, 1 equiv), Pd(OAc)₂ (0.0108 g, 0.0480 mmol, 0.05 equiv), dry deoxygenated DMF (0.8 mL), and P(*o*-Tol)₃ (0.0301 g, 0.0961 mmol, 0.1 equiv). The mixture was allowed to stir at rt for 10 min. The activated organo-zinc reagent was then syringed off the excess Zn, filtered to removed any remaining solid zinc, and cannulated onto the vinyl iodide solution mixture. The resulting solution was heated in the microwave (80 °C for 25 min). The resulting solution was allowed to cool to rt and directly purified by chromatography on SiO₂ (EtOAc/hexanes, 1:20 to 1:10) to give **3.35** (0.16 g, 33% yield) as a colorless oil and an inseparable mixture with the Wurtz coupling product: R_f 0.37 (EtOAc/hexanes, 1:10); Characteristic signals for **3.35**: ¹H NMR (600 MHz, CDCl₃) δ 6.89 (s, 1 H), 6.87 (s, 1 H), 6.80 (d, 2 H, *J* = 2.4 Hz), 6.76 (t, 1 H, *J* = 2.4 Hz), 5.94 (t, 1 H, *J* = 7.8 Hz), 3.80 (s, 3 H), 3.78 (s, 3 H), 3.74 (s, 2 H), 3.43 (d, 2 H, *J* = 14.4 Hz), 1.33 (s, 18 H).



(E)-5-(2-Chloro-4-(4-chloro-2,5-dimethoxyphenyl)but-2-enyl)benzene-1,3-diol (3.36). A flame-dried microwave vial was charged with a 2:1 mixture of **3.28a** and **3.28b** (0.520 g, 1.08 mmol, 1 equiv), Pd(OAc)₂ (0.0122 g, 0.0543 mmol, 0.05 equiv), P(*o*-Tol)₃ (0.0341 g (0.109 mmol, 0.1 equiv), and freshly distilled, dry, degassed DMF (0.8 mL). The reaction mixture was stirred at rt. for 10 min. In a separate dry flask, a catalytic amount of iodine (~20 mg) and zinc (0.362 g, 5.43 mmol, 5 equiv) were heated (Bunsen burner) until a purple gas coated the interior of the flask. The flask was cooled to rt, charged with distilled, dry, degassed DMF (1 mL), and benzyl bromide **3.14** (1.15 g, 4.34 mmol, 4 equiv). The mixture was allowed to stir at rt. under argon for 6 min. The activated organozinc reagent was filtered through an oven dried fritted funnel under an atmosphere of argon and cannulated into the stirred solution of **3.28a** and **3.28b**. The resulting solution was heated in a microwave reactor (2 min, 120 °C), treated with a second batch of Pd(OAc)₂ (0.0122 g, 0.0543 mmol, 0.05 equiv) and resubjected to the microwave conditions (2 min, 120 °C). The crude reaction mixture was directly purified by chromatography on SiO₂ (EtOAc/hexanes, 1:20) to give a crude yellow oil, which was immediately dissolved in MeOH/CH₂Cl₂ (4 mL, 2:1), and Cs₂CO₃ (1.67 g, 5.08 mmol, 5 equiv) was added. The reaction mixture was stirred at rt. for 6 h, diluted with EtOAc, and acidified with conc. HCl. The organic layer was separated, and the acidified aqueous solution was extracted with EtOAc. The combined organic layers were washed with brine, dried (MgSO₄), filtered, and concentrated under reduced pressure. The crude mixture was purified by chromatography on SiO₂ (chloroform/acetone, 8:2) to give a 4:1 mixture (0.192 g, 51%) of **3.36a** and the undesired regioisomer **3.36b** as a yellow oil. Characteristic signals for **3.36a**: ¹H NMR (600 MHz (CD₃)₂CO) δ 8.20 (bs, 2 H), 7.02 (d, 2 H, *J* = 3.6 Hz), 6.45 (t, 1 H, *J* = 7.8 Hz), 6.26 (s, 3 H), 3.84

(app s, 5 H), 3.81 (s, 3 H), 3.50 (d, 2 H, $J = 7.8$ Hz); ^{13}C NMR (150 MHz, CDCl_3) δ 159.5, 152.3, 150.0, 141.5, 140.7, 127.7, 120.9, 115.6, 113.8, 108.1, 101.9, 101.7, 56.9, 56.5, 45.1.

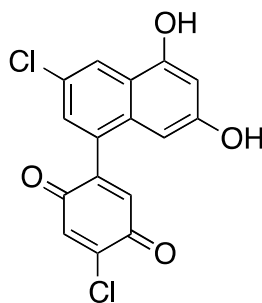
An analytically pure sample of **3.36** for biological evaluation and characterization was obtained via SFC chromatography using a semi-prep (250 \times 10 mm) silica column (Rt 5.80 min, 10 mL/min, 15% methanol, 220 nm detection): Rf 0.48 (acetone/chloroform, 2:8); IR (acetone) 3375, 3001, 2952, 1696, 1599, 1495, 1463, 1387, 1212, 1156, 1034, 1010 cm^{-1} ; ^1H NMR (600 MHz (CD_3) $_2\text{CO}$) δ 8.18 (bs, 2 H), 7.02 (s, 1 H), 6.99 (s, 1 H), 6.30 (s, 2 H), 6.25 (s, 1 H), 5.88 (t, 1 H, $J = 7.8$ Hz), 3.84 (s, 3 H), 3.81 (s, 3 H), 3.73 (s, 2 H), 3.51 (d, 2 H, $J = 7.8$ Hz); ^{13}C NMR (150 MHz, CDCl_3) δ 159.5, 152.3, 150.0, 140.6, 133.7, 128.1, 128.1, 120.8, 115.5, 113.8, 108.0, 101.8, 56.9, 56.5, 40.2, 29.5; HRMS (ES^-) $[\text{M} + \text{Cl}]^-$ m/z calcd for $\text{C}_{18}\text{H}_{18}\text{O}_4\text{Cl}_3$ 403.0271, found 403.0295.



(E)-5-(2-Chloro-4-(4-chloro-2,5-dihydroxyphenyl)but-2-enyl)benzene-1,3-diol (3.1). A stirred solution of **3.36** (pure *E*-isomer; 0.0500 g, 0.135 mmol, 1 equiv) in CH_2Cl_2 (7 mL) was enclosed in aluminum foil and cooled to 0 $^\circ\text{C}$. To the stirred solution was added dropwise BBr_3 (1 M in CH_2Cl_2 ; 0.677 mL, 0.677 mmol, 5 equiv). The resulting solution was slowly warmed to rt. and stirred overnight. The reaction mixture was quenched with a saturated aqueous solution of NaHCO_3 (8 mL) and stirred at rt. for an additional hour. The solution was acidified with HCl , extracted with EtOAc (x2) and the combined organic layers were dried (MgSO_4), filtered, and concentrated under reduced pressure. The crude product was purified by chromatography on SiO_2 (chloroform/acetone, 3:1) to give a single geometric isomer of **3.1** (0.0462 g, 96%) as a slightly yellow film. Before submission for biological testing, a sample of **3.1** was further

purified via SFC chromatography using a semi-prep (250 × 10 mm) silica column (R_t 4.68 min, 8 mL/min, 25% methanol, 220 nm detection): R_f 0.15 (acetone/chloroform, 2:8); IR (neat) 3343, 1692, 1599, 1495, 1417, 1329, 1184, 1143, 1005, 822 cm^{-1} ; ^1H NMR (600 MHz $(\text{CD}_3)_2\text{CO}$) δ 8.17 (bs, 4 H), 6.86 (s, 1 H), 6.84 (s, 1 H), 6.29 (d, 2 H, $J = 2.4$ Hz), 6.24 (t, 1 H, $J = 2.4$ Hz), 5.89 (t, 1 H, $J = 7.8$ Hz), 3.69 (s, 2 H), 3.47 (d, 2 H, $J = 7.8$ Hz); ^{13}C NMR (150 MHz, CDCl_3) δ 159.5, 149.0, 146.9, 140.5, 133.8, 128.0, 127.0, 118.5 (2C), 116.7, 108.0, 101.8, 40.2, 29.5; HRMS (ES^-) [$2\text{M} - \text{H}$] $^-$ m/z calcd for $\text{C}_{32}\text{H}_{27}\text{O}_8\text{Cl}_4$ 679.0460, found 679.0482.

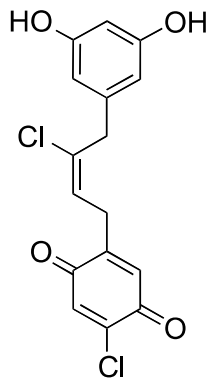
The demethylation reaction was also performed on a 2:1 mixture of **3.36a** and **3.36b**, resulting in a 2:1 mixture of **3.1** and its (*Z*)-diastereomer. Characteristic signals for the (*Z*)-diastereomer: ^1H NMR (400 MHz $(\text{CD}_3)_2\text{CO}$) δ 6.85 (s, 1 H), 6.48 (t, 1 H, $J = 7.6$ Hz), 3.81 (s, 2 H), 3.46 (d, 2 H, $J = 7.6$ Hz).



3.37

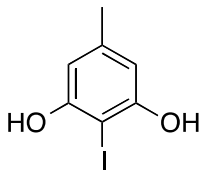
2-Chloro-5-(3-chloro-5,7-dihydroxynaphthalen-1-yl)cyclohexa-2,5-diene-1,4-dione (3.37).

To a stirred solution of **3.1** (0.0300 g, 0.0879 mmol, 1 equiv) in dry DMF (0.90 mL) was added ferric chloride hexahydrate (0.119 g, 0.440 mmol, 5 equiv). The reaction mixture was stirred at rt for 3 d and then heated to 60 °C for 18 h. The reaction mixture was allowed to cool to rt, diluted with EtOAc, washed with brine, dried (MgSO_4), filtered, and concentrated under reduced pressure. The crude mixture was purified by chromatography on SiO_2 (EtOAc/hexanes, 1:20) to give a semi-pure compound. An analytically pure sample was obtained via SFC chromatography using the semi-prep (250 × 10 mm) silica column ($R_T = 6.48$ min, 9 mL/min, 15% methanol, 220 nm detection) to give 0.010 g (40%) of the unexpected ring system **3.37**: ^1H NMR (400 MHz, CD_3OD) δ 7.36 (d, 1 H, $J = 1.6$ Hz), 7.31 (s, 1 H), 7.26 (d, 1 H, $J = 1.6$ Hz), 6.60 (d, 1 H, $J = 2.0$ Hz), 6.50 (d, 1 H, $J = 2.0$ Hz).



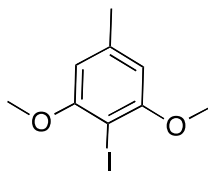
3.38

(E)-2-Chloro-5-(3-chloro-4-(3,5-dihydroxyphenyl)but-2-en-1-yl)cyclohexa-2,5-diene-1,4-dione (3.38). To a stirred solution **3.1** (0.0150 g, 0.0440 mmol, 1 equiv) in Et₂O (0.5 mL) was added DDQ (0.0130 g, 0.0571 mmol, 1.3 equiv). The reaction was stirred at rt for 5 min, diluted with Et₂O, washed with sodium thiosulfate (x2), dried (MgSO₄), filtered, and concentrated under reduced pressure to give **3.38** (0.012 g, 80%) as a reddish yellow film: R_f = 0.5 (EtOAc/hexanes, 1:1); ¹H NMR (400 MHz, (CD₃)₂CO) δ 8.16 (s, 1 H), 7.18 (s, 1 H), 6.81 (t, 1 H, *J* = 1.6 Hz), 6.25 (d, 2 H, *J* = 2.0 Hz), 5.85 (t, 1 H, *J* = 8.0 Hz), 3.66 (s, 2 H), 3.40 (dd, 2 H, *J* = 1.2, 7.6 Hz).



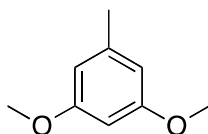
3.40

2-Iodo-5-methylresorcinol (3.40).¹⁹⁰ To a vigorously stirred solution of 3,5-dihydroxytoluene (2.00 g, 16.1 mmol, 1 equiv) and I₂ (4.09 g, 16.1 mmol, 1 equiv) in a mixture of THF/H₂O (1:1, 200 mL) at 0 °C was slowly added NaHCO₃ (1.35 g, 16.1 mmol, 1 equiv) in portions. The reaction mixture was warmed to rt, stirred for 10 min, diluted with EtOAc, washed with brine, dried (MgSO₄), filtered, and concentrated under reduced pressure. The crude mixture was purified by chromatography on SiO₂ (EtOAc/hexanes, 1:9 to 2:8) to give **3.40** (3.2 g, 79%) along with recovered starting material (0.3 g, 15%): R_f = 0.24 (EtOAc/hexanes, 1.5:8.5); Characteristic signals for **3.40**: ¹H NMR (400 MHz, CDCl₃) δ 6.40 (s, 2 H), 5.41 (bs, 2 H), 2.40 (s, 3 H). Characterization matches that reported by Srebniak *et al.*¹⁹⁰



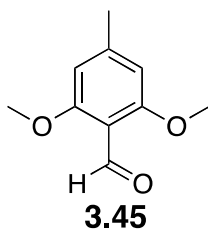
3.41

1,3-Dihydroxy-2-iodo-5-methylbenzene (3.41).¹⁹⁰ To a stirred solution of 2-iodo-5-methylresorcinol (0.100 g, 0.400 mmol, 1 equiv) in DMF (2 mL) was added K_2CO_3 (0.276 g, 2.00 mmol, 5 equiv) and MeI (0.124 mL, 2.00 mmol, 5 equiv). The reaction mixture was stirred at rt for 3 h, diluted with EtOAc, washed with brine, dried ($MgSO_4$), filtered, and concentrated under reduced pressure. The crude mixture was purified by chromatography on SiO_2 (EtOAc/hexanes, 1.5:8.5) to give **3.41** (0.102 g, 92%) as a pale yellow oil: $R_f = 0.66$ (EtOAc/hexanes, 1.5:8.5); 1H NMR (400 MHz, $CDCl_3$) δ 6.40 (s, 2 H), 3.87 (s, 6 H), 2.35 (s, 3 H); ^{13}C NMR (100 MHz, $CDCl_3$) δ 159.2, 140.4, 105.2, 73.6, 56.5, 22.0. Characterization matches that reported by Srebnik *et al.*¹⁹⁰

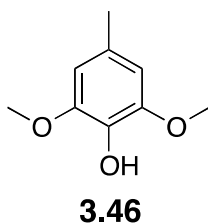


3.44

1,3-Dimethoxy-5-methylbenzene (3.44).¹⁹¹ To a stirred heterogeneous solution of 3,5-dihydroxytoluene (2.00 g, 16.1 mmol, 1 equiv) and 3 Å molecular sieves in acetone (30 mL) was added K_2CO_3 (22.3 g, 161 mmol, 10 equiv) and MeI (10.0 mL, 161 mmol, 10 equiv). The reaction mixture was stirred at 60 °C overnight, diluted with EtOAc, washed with 1 M aqueous NaOH (x3), dried ($MgSO_4$), filtered, and concentrated under reduced pressure to give **3.44** (2.40 g, 98%) as a pale yellow oil: $R_f = 0.58$ (EtOAc/hexanes, 1:10); IR ($CDCl_3$) 2995, 2937, 1593, 1458, 1424, 1320, 1202, 1146, 1068 cm^{-1} ; 1H NMR (400 MHz, $CDCl_3$) δ 6.36 (bs, 2 H), 6.31 (bs, 1 H), 3.79 (s, 6 H), 2.33 (s, 3 H); ^{13}C NMR (100 MHz, $CDCl_3$) δ 160.7, 140.2, 107.0, 97.5, 55.2, 21.8; HRMS (ESI⁺) m/z calcd for $C_9H_{12}O_2$ 152.0837, found 152.0878.

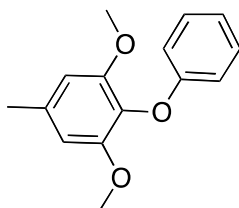


2,6-Dimethoxy-4-methylbenzaldehyde (3.45).¹⁷¹ To a stirred solution of **3.44** (0.600 g, 3.94 mmol, 1 equiv) in Et₂O (10 mL) at 0 °C was added TMEDA (1.19 mL, 7.88 mmol, 2 equiv) and *n*-butyllithium (1.4 M in hexanes; 4.22 mL, 5.91 mmol, 1.5 equiv). The resulting yellow slurry was heated at reflux for 3 h, cooled to 0 °C, and DMF (1.85 mL, 19.7 mmol, 5 equiv) was added. The reaction mixture was slowly warmed to rt, stirred for an additional 2 h, quenched with water (10 mL), and extracted with EtOAc (3 x 50 mL). The combined organic extracts were dried (MgSO₄), filtered, and concentrated under reduced pressure. The crude mixture was purified by chromatography on SiO₂ (EtOAc/hexanes, 2:8 to 1:1) to give **3.45** (0.65 g, 92%) as a white solid: R_f = 0.42 (EtOAc/hexanes, 1:1); ¹H NMR (400 MHz, CDCl₃) δ 10.44 (s, 1 H), 6.38 (s, 2 H), 3.87 (s, 6 H), 2.37 (s, 3 H). Characterization matches that reported by Trost *et al.*¹⁷¹



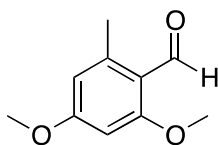
2,6-Dimethoxy-4-methylphenol (3.46). To a stirred solution of **3.45** (0.540 g, 3.00 mmol, 1 equiv) in CH₂Cl₂ (24 mL) was added (PhSe)₂ (0.0266 g, 0.120 mmol, 0.04 equiv), and H₂O₂ (30% aqueous solution; 0.918 mL, 8.99 mmol, 3 equiv). The reaction mixture was stirred at rt for 18 h, diluted with EtOAc, washed with brine, dried (MgSO₄), filtered, and concentrated under reduced pressure. The crude oil was resuspended in MeOH (25 mL) and KOH (0.841 g, 15.0 mmol, 5 equiv) was added. The reaction mixture was stirred at rt for 3 h, acidified with HCl, extracted with EtOAc, washed with brine, dried (MgSO₄), filtered, and concentrated under reduced pressure. The crude reaction mixture was purified by chromatography on SiO₂ (EtOAc/hexanes, 4:6) to give **3.46** (0.475 g, 94%) as a yellow oil: R_f = 0.27 (EtOAc/hexanes, 2:8); IR (CDCl₃) 3502, 2937, 2857, 1608, 1515, 1463, 1327, 1211, 1111 cm⁻¹; ¹H NMR (400 MHz, CDCl₃) δ 6.39 (s, 2 H), 5.37 (s, 1 H), 3.86 (s, 6 H), 2.29 (s, 3 H); ¹³C NMR (100 MHz,

CDCl₃) δ 146.8, 132.3, 128.7, 105.5, 56.1, 21.5; HRMS (ESI⁺) m/z calcd for C₉H₁₃O₃ [M+H]⁺ 169.0865, found 169.0889. Characterization matches that reported by Steinbess.¹⁹²



3.48

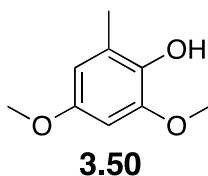
1,3-Dimethoxy-5-methyl-2-phenoxybenzene (3.48). To a stirred solution of **3.46** (0.100 g, 0.595 mmol, 1 equiv), iodobenzene (0.135 mL, 1.19 mmol, 2 equiv), Cs₂CO₃ (0.387 g, 1.19 mmol, 2 equiv), and THMD (0.0125 mL, 0.0595 mmol, 0.1 equiv) in dry, degassed NMP (1 mL) was added CuCl (0.0310 g, 0.297 mmol, 0.5 equiv). The reaction mixture was stirred overnight at 120 °C, diluted with EtOAc, washed with 1 M aqueous NaOH (x2), dried (MgSO₄), filtered, and concentrated under reduced pressure. The crude mixture was purified by chromatography on SiO₂ (EtOAc/hexanes, 1:10) to give **3.48** (0.092 g, 63%) as a white solid: Mp = 93.5-94.2 °C; Rf = 0.35 (EtOAc/hexanes, 1:10); IR (CDCl₃) 2935, 2839, 1590, 1488, 1463, 1336, 1228, 1126, 749 cm⁻¹; ¹H NMR (400 MHz, CDCl₃) δ 7.52 (t, 2 H, J = 7.6 Hz), 7.24 (t, 1 H, J = 7.2 Hz), 7.17 (d, 2 H, J = 8.4 Hz), 6.76 (s, 2 H), 4.02 (s, 6 H), 2.66 (s, 3 H); ¹³C NMR (100 MHz, CDCl₃) δ 158.5, 153.0, 135.4, 129.6, 129.1, 121.2, 114.6, 106.0, 56.0, 21.9; HRMS (ESI⁺) m/z calcd for C₁₅H₁₆O₃, 244.1099 found 244.1118.



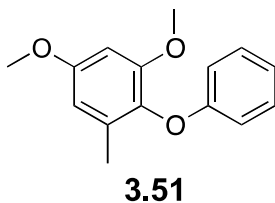
3.49

2,4-Dihydroxy-6-methylbenzaldehyde (3.49).¹⁹³ To a stirred solution of DMF (0.5 mL) at 0 °C was added POCl₃ (0.147 mL, 1.58 mmol, 1.2 equiv), the reaction mixture was warmed to rt and stirred for 15 min. In a separate flask, **3.44** (0.200 g, 1.31 mmol, 1 equiv) was dissolved in DMF (2.5 mL) and warmed to 120 °C. The Vilsmeier-Hack reagent was added dropwise to the stirred solution of **3.44** at 120 °C and allowed to stir at 120 °C for 2 h. The reaction mixture was cooled to rt, quenched with a saturated aqueous solution of NaHCO₃, extracted with EtOAc, dried

(MgSO₄), filtered, and concentrated under reduced pressure. The crude mixture was purified by chromatography on SiO₂ (EtOAc/hexanes, 1:9) to give **3.49** (0.208 g, 87%) as a white solid: R_f = 0.37 (EtOAc/hexanes, 2:8); ¹H NMR (400 MHz, CDCl₃) δ 10.49 (s, 1 H), 6.33 (s, 2 H), 3.88 (s, 3 H), 3.86 (s, 3 H), 2.59 (s, 3 H). Characterization matches that reported by Wang *et al.*¹⁹³

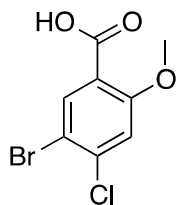


2,4-Dimethoxy-6-methylphenyl (3.50).¹⁹⁴ To a stirred solution of **3.49** (0.200 g, 1.11 mmol, 1 equiv) in CH₂Cl₂ (12 mL) was added (PhSe)₂ (0.0246 g, 0.111 mmol, 0.1 equiv), and H₂O₂ (30% aqueous solution; 0.340 mL, 3.33 mmol, 3 equiv). The reaction mixture was stirred at rt for 18 h, diluted with EtOAc, washed with 1 M aqueous NaOH, brine, dried (MgSO₄), filtered, and concentrated under reduced pressure. A portion of the crude formate (50 mg) was dissolved in EtOH (1 mL) and sodium borohydride (0.210 g, 5.55 mmol, 5 equiv) was added. The reaction mixture was stirred at rt for 5 h, diluted with EtOAc, quenched with 1 M aqueous HCl, extracted with EtOAc, dried (MgSO₄), filtered, and concentrated under reduced pressure to give **3.50** (0.0465 g, 100%) as an off-white solid: M_p = 102-103 °C; R_f = 0.41 (EtOAc/hexanes, 2:8); IR (CDCl₃) 3431, 2956, 1614, 1499, 1451, 1427, 1234, 1199, 1150, 1089, 1055, 913, 831 cm⁻¹; ¹H NMR (400 MHz, CDCl₃) δ 6.37 (d, 1 H, *J* = 2.4 Hz), 6.30 (d, 1 H, *J* = 2.0 Hz), 5.37 (s, 1 H), 3.85 (s, 3 H), 3.76 (s, 3 H), 2.26 (s, 3 H); ¹³C NMR (100 MHz, CDCl₃) δ 152.6, 146.6, 137.8, 123.7, 106.5, 96.7, 55.9, 55.7, 15.7; HRMS (ESI⁺) *m/z* calcd for C₉H₁₂O₃ 168.0786, found 168.0806.

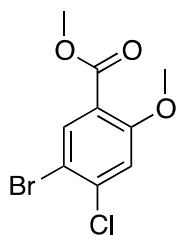


1,5-Dimethoxy-3-methyl-2-phenoxybenzene (3.51). To a stirred solution of **3.50** (0.0600 g, 0.357 mmol, 1 equiv), iodobenzene (0.0811 mL, 0.713 mmol, 2 equiv), Cs₂CO₃ (0.232 g, 0.713 mmol, 2 equiv), and THMD (0.00750 mL, 0.0357 mmol, 0.1 equiv) in dry, degassed NMP (1

mL) was added CuCl (0.0372 g, 0.357 mmol, 1 equiv). The reaction mixture was stirred overnight at 120 °C, diluted with EtOAc, washed with brine, dried (MgSO₄), filtered, and concentrated under reduced pressure. The crude mixture was purified by chromatography on SiO₂ (EtOAc/hexanes, 1:20) to give **3.51** (0.0725 g, 83%) as a colorless oil: R_f = 0.46 (EtOAc/hexanes, 1:10); IR (CDCl₃) 2950, 2837, 1601, 1487, 1348, 1219, 1200, 1150, 1094, 854 cm⁻¹; ¹H NMR (400 MHz, CDCl₃) δ 7.28 (t, 2 H, *J* = 7.6 Hz), 7.00 (t, 1 H, *J* = 7.2 Hz), 6.86 (d, 2 H, *J* = 8.0 Hz), 6.47 (d, 1 H, *J* = 2.0 Hz), 6.42 (d, 1 H, *J* = 2.0 Hz), 3.85 (s, 3 H), 3.77 (s, 3 H), 2.18 (s, 3 H); ¹³C NMR (100 MHz, CDCl₃) δ 158.5, 157.0, 153.1, 135.3, 133.0, 129.3, 121.2, 114.5, 106.2, 97.9, 55.8, 55.4, 16.4; HRMS (ESI⁺) *m/z* calcd for C₁₅H₁₇O₃ [M+H]⁺ 245.1178, found 245.1201.

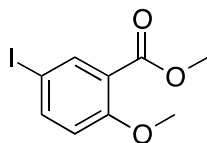


5-Bromo-4-chloro-2-methoxy-benzoic acid. To a stirred solution of 4-chlorosalicylic acid (10.0 g, 58.0 mmol, 1 equiv) in CH₂Cl₂ (250 mL) was added triethylamine (9.77 mL, 69.5 mmol, 1.2 equiv). The mixture was cooled to -78 °C and bromine (2.98 mL, 69.5 mmol, 1 equiv) was added to the solution. The reaction mixture was stirred at -78 °C for 5 h, quenched with a saturated aqueous solution of NaHCO₃ (70 mL), acidified with 1 M aqueous HCl, extracted with Et₂O, dried (MgSO₄), filtered, and concentrated under reduced pressure to give **5-Bromo-4-chloro-2-methoxy-benzoic acid** (15.0 g of an inseparable mixture (9:1 ratio of the desired product and the undesired debrominated compound)). The reaction mixture was directly carried onto the next step without further purification. Characteristic signals for the desired product: ¹H NMR (400 MHz, (CD₃)₂CO) δ 8.20 (s, 1 H), 7.23 (s, 1 H); Characteristic data for the undesired debrominated product: 7.90 (d, 1 H, *J* = 8.0 Hz), 7.1-6.9 (m, 2 H). The characterization matches that reported by Mizufune *et al.*¹⁷³



3.55

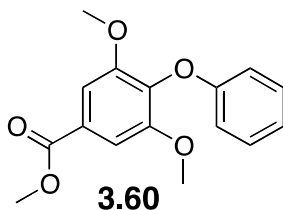
Methyl 5-bromo-4-chloro-2-methoxybenzoate (3.55). To a stirred solution of 5-Bromo-4-chloro-2-methoxybenzoic acid (15.0 g, 59.6 mmol, 1 equiv) in acetone (200 mL) was added K_2CO_3 (82.4 g, 597 mmol, 10 equiv) and MeI (26.0 mL, 417 mmol, 7 equiv). The reaction mixture was stirred at 60 °C overnight (~16 h), cooled to rt, diluted with EtOAc, washed with brine, dried ($MgSO_4$), filtered, and concentrated under reduced pressure. The crude mixture was purified by chromatography on SiO_2 (EtOAc/hexanes, 1:10 to 2:8) to give **3.55** (12.0 g, 72%) as an inseparable mixture (4:1 ratio of the desired product to the undesired debrominated product) as a white solid: Mp = 86-87 °C; Rf = 0.51 (EtOAc/hexanes, 2:8); IR ($CDCl_3$) 2947, 1728, 1709, 1586, 1552, 1478, 1431, 1368, 1234, 1090, 900 cm^{-1} ; HRMS (ESI^+) m/z calcd for $C_9H_9O_3ClBr$ $[M+H]^+$ 278.9424, found 278.9463; Characteristic data for **3.55**: 1H NMR (400 MHz, $CDCl_3$) δ 8.01 (s, 1 H), 7.05 (s, 1 H), 3.88 (s, 3 H), 3.86 (s, 3 H); ^{13}C NMR (100 MHz, $CDCl_3$) δ 164.4, 158.6, 139.3, 136.0, 119.7, 114.2, 112.4, 56.4, 52.3; Characteristic data for the undesired debrominated product: 1H NMR (400 MHz, $CDCl_3$) δ 7.72 (d, 1 H, $J = 8.8$ Hz), 6.94-6.92 (m, 2 H); ^{13}C NMR (100 MHz, $CDCl_3$) δ 165.6, 159.7, 134.1, 132.7, 120.3, 118.2, 112.6, 56.2, 52.0.



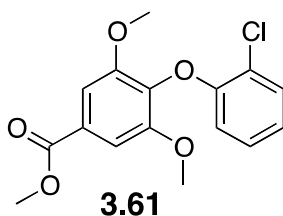
3.58

Methyl 5-iodo-2-methoxybenzoate (3.58). To a stirred solution of 5-iodosalicylic acid (1.00 g, 3.78 mmol, 1 equiv) in dry acetone (40 mL) was added K_2CO_3 (4.19 g, 30.3 mmol, 8 equiv) and MeI (1.18 mL, 18.9 mmol, 5 equiv). The reaction mixture was heated to 56 °C, stirred overnight, filtered through a pad of Celite, concentrated under reduced pressure, and purified by chromatography on SiO_2 (EtOAc/hexanes, 2:8) to give **3.58** (1.06 g, 96%) as a white solid: Rf = 0.16 (EtOAc/hexanes, 1:9); 1H NMR (400 MHz, $CDCl_3$) δ 8.07 (d, 1 H, $J = 2.0$ Hz), 7.72 (dd, 1

H, $J = 2.0, 8.8$ Hz) 6.75 (d, 1 H, $J = 8.8$ Hz), 3.88 (s, 6 H); ^{13}C NMR (100 MHz, CDCl_3) δ 165.1, 158.9, 141.9, 140.0, 122.1, 114.3, 81.7, 56.1, 52.2. Characterization matches reported data.¹⁹⁵

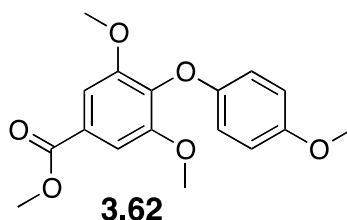


Methyl 3,5-dimethoxy-4-phenoxybenzoate (3.60). To a stirred solution of methyl 3,5-dimethoxy-4-hydroxybenzoate (0.100 g, 0.471 mmol, 1 equiv), iodobenzene (0.105 mL, 0.943 mmol, 2 equiv), Cs_2CO_3 (0.307 g, 0.942 mmol, 2 equiv), and THMD (0.00970 mL, 0.0471 mmol, 0.1 equiv) in dry, degassed NMP (1 mL) was added CuCl (0.0233 g, 0.236 mmol, 0.5 equiv). The reaction mixture was heated to 120 °C, stirred overnight, diluted with EtOAc, washed with 1 M NaOH (x2), brine, dried (MgSO_4), filtered, and concentrated under reduced pressure. The crude mixture was purified by chromatography on SiO_2 (EtOAc/hexanes, 2:8) to give **3.60** (0.060 g, 44%) as an inseparable mixture with methylated methyl 3,5-dimethoxy-4-hydroxybenzoate (5:1): $R_f = 0.51$ (EtOAc/hexanes, 3:7); Characteristic data for the **3.60**: ^1H NMR (400 MHz, CDCl_3) δ 7.33 (s, 2 H), 7.30 (t, 2 H, $J = 7.6$ Hz), 6.95 (t, 1 H, $J = 7.2$ Hz), 6.80 (d, 2 H, $J = 8.0$ Hz), 3.90 (s, 3 H), 3.78 (s, 6 H); ^{13}C NMR (100 MHz, CDCl_3) δ 166.5, 157.9, 153.2, 129.3, 127.1, 121.8, 114.8, 106.8, 55.3, 52.3; HRMS (ESI+) m/z calcd for $\text{C}_{16}\text{H}_{16}\text{O}_5$, 288.0998 found 288.1001.

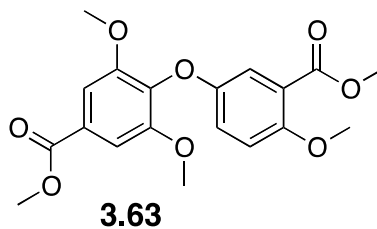


Methyl 4-(2-chlorophenoxy)-3,5-dimethoxybenzoate (3.61). To a stirred solution of methyl 3,5-dimethoxy-4-hydroxybenzoate (0.100 g, 0.471 mmol, 1 equiv), 2-chloro-iodobenzene (0.115 mL, 0.943 mmol, 2 equiv), Cs_2CO_3 (0.307 g, 0.942 mmol, 2 equiv), and TMHD (0.00970 mL, 0.0471 mmol, 0.1 equiv) in dry, degassed NMP (1 mL) was added CuCl (0.02330 g, 0.236 mmol, 0.5 equiv). The reaction mixture was heated to 120 °C, stirred overnight, diluted with

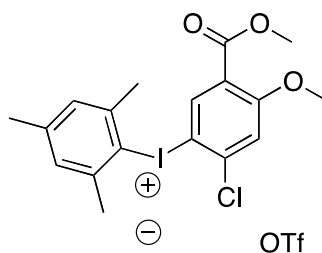
EtOAc, washed with 1 M NaOH (x2), brine, dried (MgSO₄), filtered, and concentrated under reduced pressure. The crude mixture was purified by chromatography on SiO₂ (EtOAc/hexanes, 2:8) to give **3.61** (0.030 g, 20%) as an inseparable mixture: R_f = 0.21 (EtOAc/hexanes, 3:7); **3.61** was tentatively assigned based on the following data: ¹H NMR (400 MHz, CDCl₃) δ 7.81 (dd, 2 H, *J* = 1.6, 8.0 Hz), 7.41 (dd, 2 H, *J* = 1.2, 8.0 Hz), 7.22 (s, 2 H), 3.90 (s, 3 H), 3.78 (s, 6 H); ¹³C NMR (100 MHz, CDCl₃) δ 166.7, 153.0, 152.9, 140.3, 129.4, 127.9, 127.3, 125.2, 122.6, 106.8, 56.2, 52.2; HRMS (ESI+) *m/z* calcd for C₁₆H₁₅O₅Cl, 322.0608 found 322.0658.



Methyl 3,5-dimethoxy-4-(4-methoxyphenoxy)benzoate (3.62). To a stirred solution of methyl 3,5-dimethoxy-4-hydroxybenzoate (0.120 g, 0.565 mmol, 1.2 equiv), 4-iodoanisole (0.221, 0.942 mmol, 2 equiv), Cs₂CO₃ (0.307 g, 0.942 mmol, 2 equiv), and TMHD (0.0970 mL, 0.471 mmol, 1 equiv) in dry, degassed NMP (1 mL) was added CuCl (0.0233 g, 0.236 mmol, 0.5 equiv). The reaction mixture was heated to 120 °C, stirred overnight, diluted with EtOAc, washed with 1 M NaOH (x2), brine, dried (MgSO₄), filtered, and concentrated under reduced pressure. The crude mixture was purified by chromatography on SiO₂ (EtOAc/hexanes, 1:10 to 2:8) to give **3.62** (0.166 g, 84%) as an inseparable mixture of and methylated methyl 3,5-dimethoxy-4-hydroxybenzoate (5:1): Mp = 92-99 °C; R_f = 0.46 (EtOAc/hexanes, 3:7); IR (neat) 2947, 2835, 1711, 1590, 1499, 1433, 1336, 1215, 1128, 1109, 999 cm⁻¹; Characteristic data for **3.62**: ¹H NMR (400 MHz, CDCl₃) δ 7.36 (s, 2 H), 6.78 (s, 4 H), 3.92 (s, 3 H), 3.82 (s, 6 H), 3.74 (s, 3 H); ¹³C NMR (100 MHz, CDCl₃) δ 160.5, 154.5, 153.2, 152.9, 152.1, 125.1, 115.6, 114.3, 106.8, 56.3, 55.6, 52.1.



Methyl 3,5-dimethoxy-4-(4-methoxy-3-(methoxycarbonyl)phenoxy)benzoate (3.63). To a stirred solution of methyl 3,5-dimethoxy-4-hydroxybenzoate (0.100 g, 0.471 mmol, 1 equiv), **3.63** (0.138, 0.943 mmol, 2 equiv), Cs₂CO₃ (0.307 g, 0.942 mmol, 2 equiv), and TMHD (0.00970 mL, 0.0471 mmol, 0.1 equiv) in dry, degassed NMP (1 mL) was added CuCl (0.0233 g, 0.236 mmol, 0.5 equiv). The reaction mixture was heated to 120 °C, stirred overnight, diluted with EtOAc, washed with 1 M NaOH (x2), brine, dried (MgSO₄), filtered, and concentrated under reduced pressure. The crude mixture was purified by chromatography on SiO₂ (EtOAc/hexanes, 2:8) to give **3.63** (0.0063 g, 4%) as a colorless film: R_f = 0.37 (EtOAc/hexanes, 2:8); ¹H NMR (400 MHz, CDCl₃) δ 7.37 (s, 2 H), 7.26 (d, 1 H, *J* = 3.2 Hz), 7.00 (dd, 1 H, *J* = 3.2, 9.2 Hz), 6.87 (d, 1 H, *J* = 9.2 Hz), 3.94 (s, 3 H), 3.86 (s, 3 H), 3.84 (s, 3 H), 3.83 (s, 6 H); HRMS (ESI+) *m/z* calcd for C₁₉H₂₁O₈ [M+H]⁺ 377.1236 found 377.1242.



3.65

(2-Chloro-4-methoxy-5-(methoxycarbonyl)phenyl)(mesityl)iodonium (3.65). To a stirred solution of iodomesitylene diacetate (3.20 g, 8.79 mmol, 1 equiv) and **3.57** (3.52 g, 17.6 mmol, 2 equiv) in CH₂Cl₂ (20 mL) at 0 °C was added triflic acid (0.936 mL, 10.5 mmol, 1.2 equiv). The reaction mixture was slowly warmed to rt, stirred overnight, concentrated under reduced pressure, resuspended in dry Et₂O and placed in the -20 °C freezer overnight. The reaction mixture was filtered and the precipitate was washed with cold Et₂O (x3) to give **3.65** (2.90 g, 74%) as an off-white (tannish) solid: Mp = 170-172 °C; IR (neat) 1743, 1730, 1577, 1549, 1461, 1352, 1284, 1230, 1168, 1092, 1020 cm⁻¹; ¹H NMR (400 MHz, CDCl₃) δ 7.95 (s, 1 H), 7.19 (s, 1 H), 7.10 (s, 2 H), 3.93 (s, 3 H), 3.84 (s, 3 H), 2.65 (s, 6 H), 2.35 (s, 3 H); ¹³C NMR (100 MHz, CDCl₃) δ 163.4, 162.4, 144.6, 142.4, 141.6, 138.6, 130.6, 122.0, 121.8, 114.9, 101.6, 56.9, 52.7, 26.9, 21.0; HRMS (ESI+) *m/z* calcd for C₁₈H₁₉O₃ClI [M-OTf]⁺ 445.0067 found 445.0066.

4.0 SYNTHESIS OF BONT/A LC INHIBITORS

4.1 INTRODUCTION

Botulinum neurotoxins (BoNTs) are the most toxic proteins known.¹⁹⁶ First described in the 1820's as "sausage poisoning", the term botulinum is derived from the Latin word *botulus*, meaning sausage. In 1895, Emile Pierre Marie van Ermengem discovered the bacteria responsible for the production of the toxin.¹⁹⁷ Today, seven biochemically and serologically distinct botulinum neurotoxins (designated BoNT/A to BoNT/G) have been characterized from the anaerobic spore-forming bacteria of the genus *Clostridium*.¹⁹⁶ Of the seven, BoNT A, B, E, and rarely F are responsible for human intoxication. The most lethal, BoNT/A, exhibits an LD₅₀ in humans of approximately 1 ng kg⁻¹ of body mass, approximately one hundred thousand times more potent than sarin and one hundred billion times more potent than cyanide.¹⁹⁸

BoNTs exist as progenitor toxins composed of inactive chains and accessory proteins. The accessory proteins protect the toxin as it passes through the digestive system to the small intestine where it is absorbed into the blood stream, subsequently making its way to the cholinergic presynaptic terminals.¹⁹⁸ The active form of BoNT consists of three domains: the C-terminal domain, which is responsible for specific synaptic binding, the N-terminal domain, a zinc dependent endopeptidase, and the middle domain, which mediates translocation into the cytosol of the nerve. The C-terminal and middle domains combine to make a 100 kD subunit known as the heavy-chain (HC), which is connected to the N-terminal domain, a 50 kD subunit, known as the light chain (LC), via a disulfide bond (Figure 40).

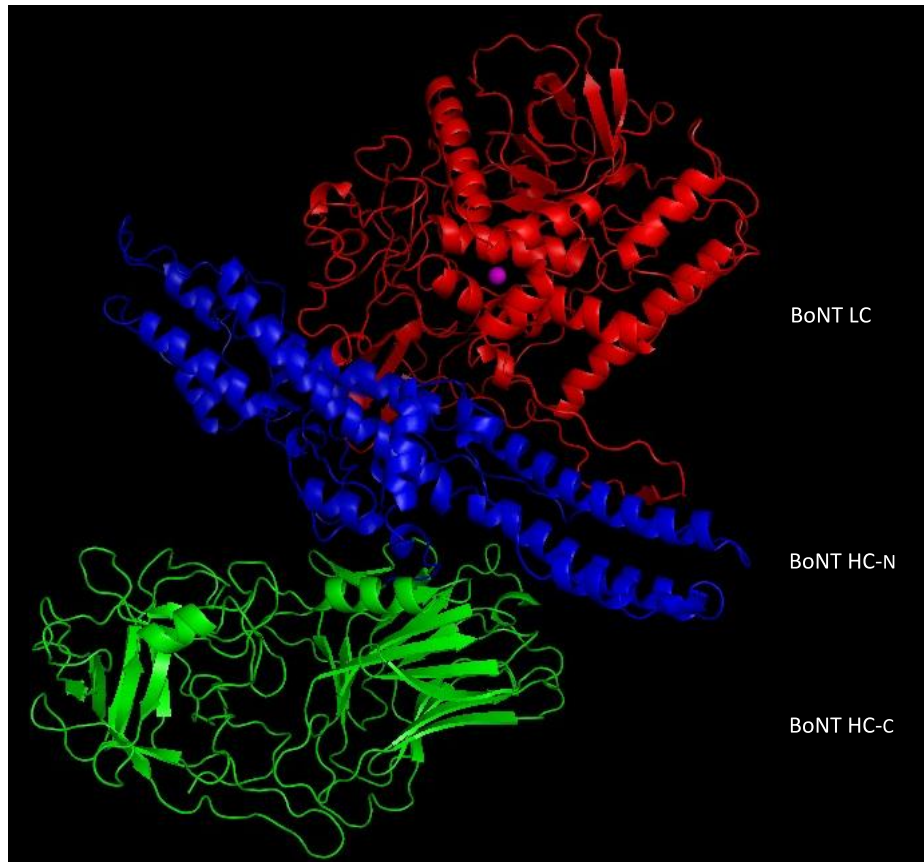


Figure 40. Ribbon representation of the three domains of botulinum neurotoxin serotype A adapted from PDB structure 3BTA¹⁹⁹ (The N-terminal domain (BoNT LC) is represented in red with the catalytic Zn ion in magenta, the middle domain (BoNT HC-N) is represented in blue, and the C-terminal domain (BoNT HC-C) is represented in green).

When an action potential from motor neurons arrives at the neuromuscular junction, the entry of calcium through a voltage-gated channel triggers the fusion of synaptic vesicles containing acetylcholine to the presynaptic membrane. Acetylcholine is subsequently released into the synaptic cleft and diffuses to the acetylcholine receptors located on the surface of the muscle fiber. Once bound, the acetylcholine causes a depolarization and the action potential travels throughout the length of the muscle cell triggering muscle contraction.¹⁹⁸ This union of the synaptic vesicles to the presynaptic membrane is mediated by several proteins, which act together to form a synaptic fusion complex. These proteins are collectively known as SNARE (soluble NSF-attachment protein receptors; NSF is *N*-ethylmaleimide-sensitive fusion protein) proteins and include SNAP-25 (synaptosomal-associate protein-25 kD), syntaxin, and synaptobrevin. BoNTs act by disrupting the fusion complex, thereby inhibiting the release of acetylcholine into the presynaptic cleft.

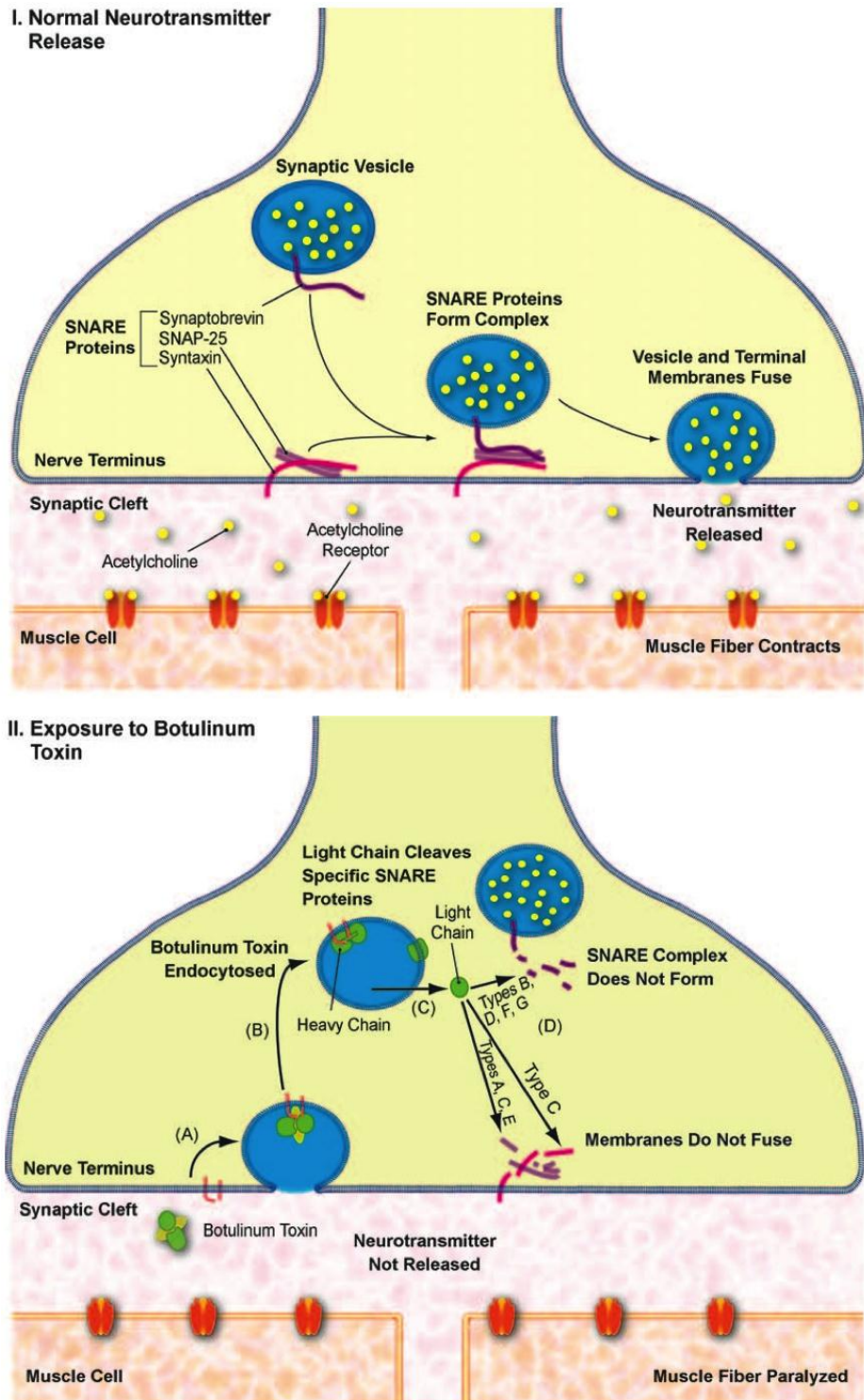


Figure 41. Cartoon representation of I) Normal neurotransmitter release. II) Individual stages of BoNT-intoxication including: A) neurotoxin binding to cell-surface receptors, B) endocytosis into an intracellular vesicle, C) HC-mediated translocation of the LC into the cytosol, and D) proteolytic cleavage of specific SNARE proteins. BoNT/B, /D, /F, and /G cleave synaptobrevin; BoNT/A, /C, and /E cleave SNAP25; BoNT/C also cleaves syntaxin. Reproduced with permission from ref.²⁰⁰

BoNT's mechanism of action consists of four sequential steps (Figure 41).²⁰⁰ The first stage involves binding to the specific cholinergic nerve terminal membrane followed by internalization inside a vesicle endowed with an ATPase proton pump. Membrane translocation is triggered by acidification of the vesicular lumen, which causes a structural rearrangement, insertion of the toxin, and translocation of the light chain into the cytosol. Finally, expression of the light chain and proteolytic activity leads to disruption of the fusion complex. Consequently, the toxins interfere with the transmission of nerve impulse and cause muscle paralysis. The different BoNTs target different proteins in the complex (Figure 41); however, the most lethal, BoNT/A, targets the SNAP-25 protein.¹⁹⁶

Once intoxicated, the facial and throat muscles are the first to become progressively paralyzed, causing diplopia, ptosis, dysphagia, and facial paralysis. The paralysis gradually descends to affect muscles of the trunk, including the respiratory and cardiac muscles. Death usually results from either respiratory failure or cardiac arrest. Concurrently, dysfunctions of the autonomic nervous systems develop, which result in reduced salivation, lacrimation, nausea, vomiting, and abdominal pain.¹⁹⁶

Interestingly, due its ability to decrease muscle activity, BoNT/A has received attention in the medical community. A localized injection of BoNT/A, known as BOTOX, renders muscles unable to contract for approximately 3-4 months. As such, BOTOX is commonly used to treat a variety of disorders associated with the hyperactivity of specific muscles, as well as for cosmetic purposes. The increasingly widespread use of BoNT as therapeutic and cosmetic agents is paralleled by an increased risk of accidental overdosing. Additionally, BoNT's ease of production, potent toxicity, ubiquitous nature, chemical and physical resistance, as well as their ability to be delivered via aerosol medium, has caused them to be considered Category A bioterror agents by the Center for Disease Control and Prevention.²⁰¹

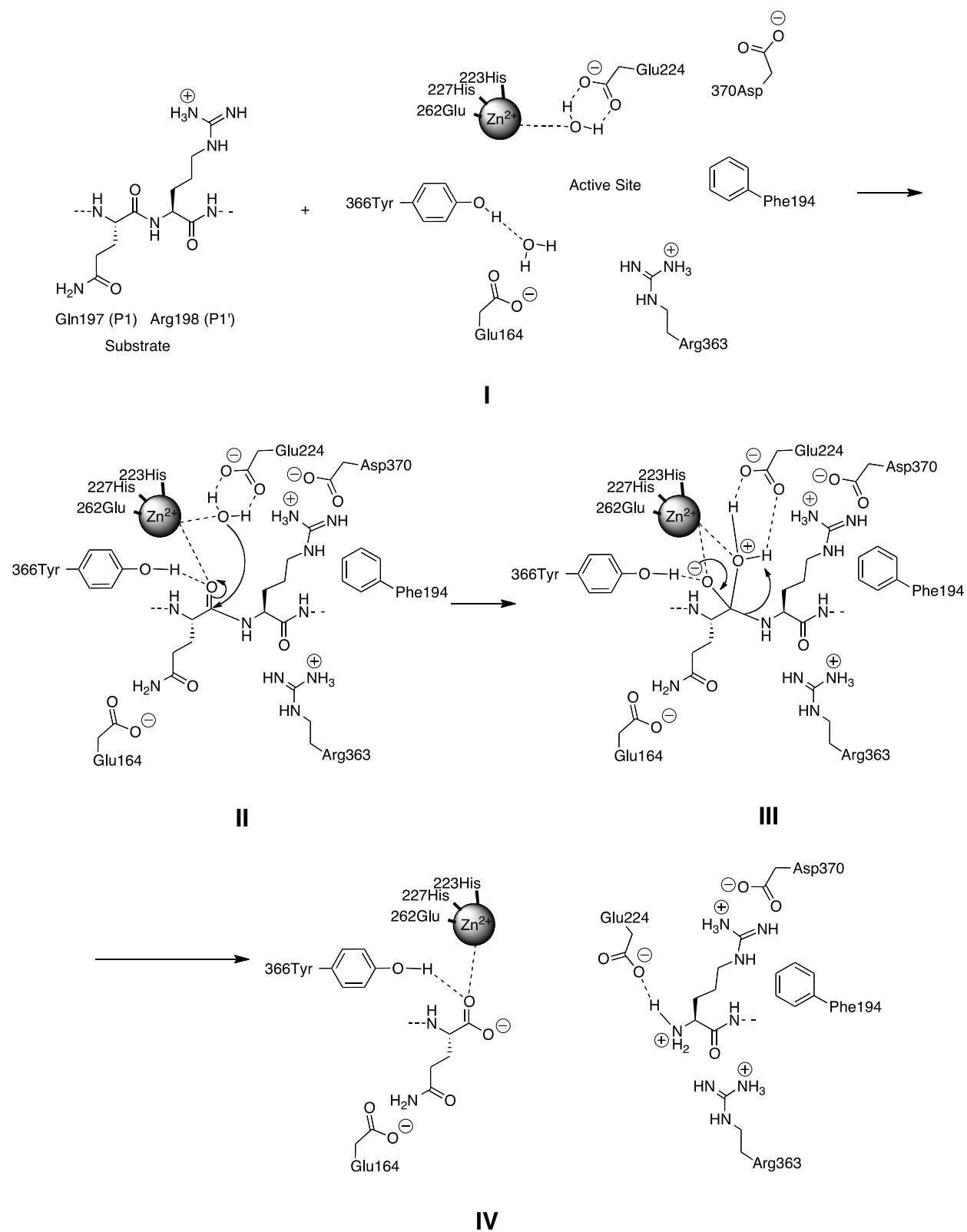
Current treatment involves passive administration of equine antibodies. Although broadly effective, administration of the antibodies can cause sickness or anaphylaxis. Additionally, these antitoxins are only capable of sequestering freely circulating BoNT, rendering them useless once the toxin has entered the neuronal cells. The onset of botulism is very rapid with initial symptoms appearing within two hours of ingestion; thus current therapeutics have a very short window of application. In most cases, even with therapeutic

intervention, intubation and mechanical respiration of patients is required for upwards of 6 months. Currently there are no drugs approved for the treatment of botulism.²⁰² Therefore, there is an urgent need for therapeutic strategies to counter BoNT intoxication.

4.2 DESIGN OF INHIBITORS

The structural basis for the rational design of BoNT/A inhibitors can be better understood in the context of the current model for its proteolytic activity, as well as through the examination of other known inhibitors. Thus, one must focus on the details of the proteolytic interaction of BoNT/A with SNAP-25 and the different mechanisms of inhibition that have previously been described.

The proteolytic cleavage of the Gln197-Arg198 peptide bond in SNAP-25 involves four distinct stages (Scheme 43). In the first stage, prior to entrance of the substrate, the catalytic zinc ion of BoNT/A is tetraordinated to Glu262, His223, His227, and Glu224 via H-bonding through a water molecule (Scheme 43, panel I). As the substrate enters the active site, the Michaelis complex is formed via anchoring of the P1' (Arg198) residue of SNAP-25 into the active site. Upon entering, the substrate elicits a conformational change of Asp370 with a concomitant formation of a salt bridge, along with cation- π interactions with Phe194 of the toxin. Further stabilization is achieved through polar contacts, via the displacement of a water molecule on Tyr363 by the carbonyl oxygen of P1 (Gln197) as well as favorable ionic interactions with Glu164 and Arg363 of the toxin (Scheme 43, panel II). Ionization of the catalytic water molecule H-bonded to Glu224, followed by nucleophilic attack at the P1 carbonyl leads to the formation of the tetrahedral intermediate. The resulting oxyanion is stabilized by both H-bonding interactions with Tyr366 and coordination to the zinc ion (Scheme 43, panel III). Breakdown of the tetrahedral intermediate is facilitated by the transfer of two protons by Glu224 to the P1' residue in the substrate. Thus, the stabilized amino group leaves the catalytic site of the BoNT/A LC and proteolysis is complete (Scheme 43, panel IV). Because of its crucial role in channeling these protons from the nucleophilic water molecule to the substrate, Glu224 in BoNT/A LC is often described as the general base or "proton shuttle".



Non-peptidic inhibitors of both BoNT/A HC and LC have been identified. In 2003, the first small molecule inhibitors (Michellamine B, Q2-12 and NSC 357736; Figure 42) were reported.²⁰³ In addition, zinc-coordinating hydroxamic acids (2,4-dichlorocinnamoyl-hydroxamic acid; Figure 42) represent another class of LC inhibitors.

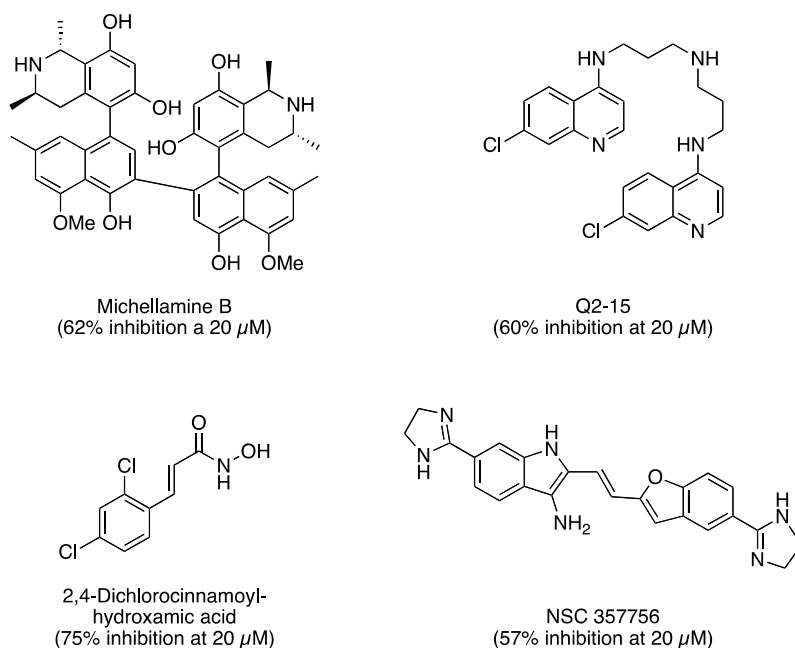


Figure 42. Small molecule inhibitors of the BoNT/A LC

These and other inhibitors containing zinc-coordinating moieties tend to exhibit mediocre selectivity, making them poor therapeutic leads.²⁰⁴ More recently, the Wipf group has focused on elaborating the indole bis-amidine containing compounds (NSC 357756; Figure 42) and through collaborations have successfully elucidated some structural requirements for binding.²⁰⁵ A more in depth discussion of the development of small-molecule inhibitors is included immediately preceding the discussion of our own work in this area.

Another approach to address the need for potent and effective inhibitors is the use of peptide-like molecules (PLMs). Over the past decade, a large number of PLM inhibitors have been investigated and have provided valuable information regarding substrate specificity, substrate recognition, and structural requirements.²⁰² Therefore, in parallel to our exploration of small molecule inhibitors of BoNT/A, we sought to expand our investigation to include PLM inhibitors.

Most PLM inhibitors share some fundamental contacts. All non-zinc-chelating BoNT/A peptide inhibitors reported to date orient their amino terminal group to contact the Glu224 carboxylate group, effectively displacing the catalytic water molecule and shutting down the “proton shuttle”. In addition, all of these structures exhibit substrate-like interactions between the P1 carbonyl and both the Tyr366 residue as well as the zinc ion of BoNT/A LC.

In 2008, Zuniga *et al.* published a series of SAR studies that led to the discovery of a potent PLM inhibitor, **I1** (Figure 43), along with a crystal structure of the **I1** inhibitor bound to the active site of BoNT/A.²⁰⁴ The **I1** inhibitor is the most-potent non-zinc chelating, non-hydroxamate based antagonist reported to date with a $K_i = 41$ nM.²⁰⁴ This inhibitor mimics the 7-residue QRATKML sequence of the native 206-residue, SNAP-25 protein (Figure 43).

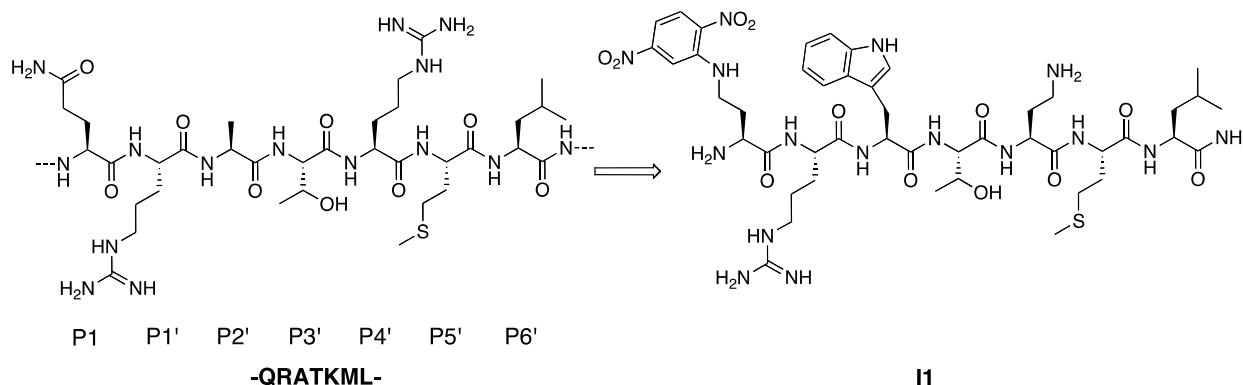


Figure 43. Structure of the 7-residue sequence of SNAP-25 and its peptidomimetic inhibitor **I1**

Examination of the crystal structure containing the bound inhibitor revealed **I1** inhibited protease activity via displacement of the catalytic water molecule on Glu224 with the terminal amine group of **I1** (Figure 44), as observed in previous non-zinc chelating PLM inhibitors.²⁰⁴

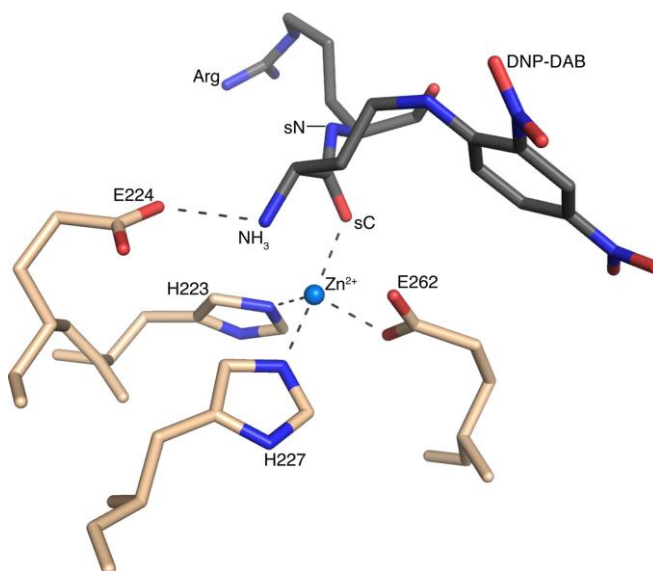


Figure 44. Coordination of the zinc ion bound to the **II** inhibitor²⁰⁴

Zuniga *et al.*'s SAR studies revealed that replacement of the P1, P2', and P4' residues of the native 7-residue QRATKML sequence had the greatest effect on inhibitor binding affinity.²⁰⁴ Specifically, replacing the native P1 arginine with 4-(2,4-dinitrophenylamino)-2-aminobutanoate (DNP-DAB) provided a 10-fold increase in the binding affinity of the inhibitor relative to an identical inhibitor containing a phenylalanine at the P1 position.²⁰⁴ The increased potency is primarily attributed to the polar nitro and butanoic acid groups of the DNP-DAB residue, which play a critical role in stabilizing the bound inhibitor via a network of polar interactions (Figure 45). Replacing the native P2' alanine with a tryptophan residue also significantly reduced the inhibitor's K_i , suggesting favorable hydrophobic interactions were effectively "locking" the inhibitor into place. Finally, the P4' (Arg) position was replaced with 2,4-diaminobutanoic acid (DAB), which crystal structural analysis revealed provided a strong hydrogen bonding interaction of its free terminal amine with Q162 of BoNT/A LC. Examination of the crystal structure revealed that when bound to the active site, the C-terminal residues of the **II** inhibitor adopt a 3_{10} -helical conformation (Figure 45).

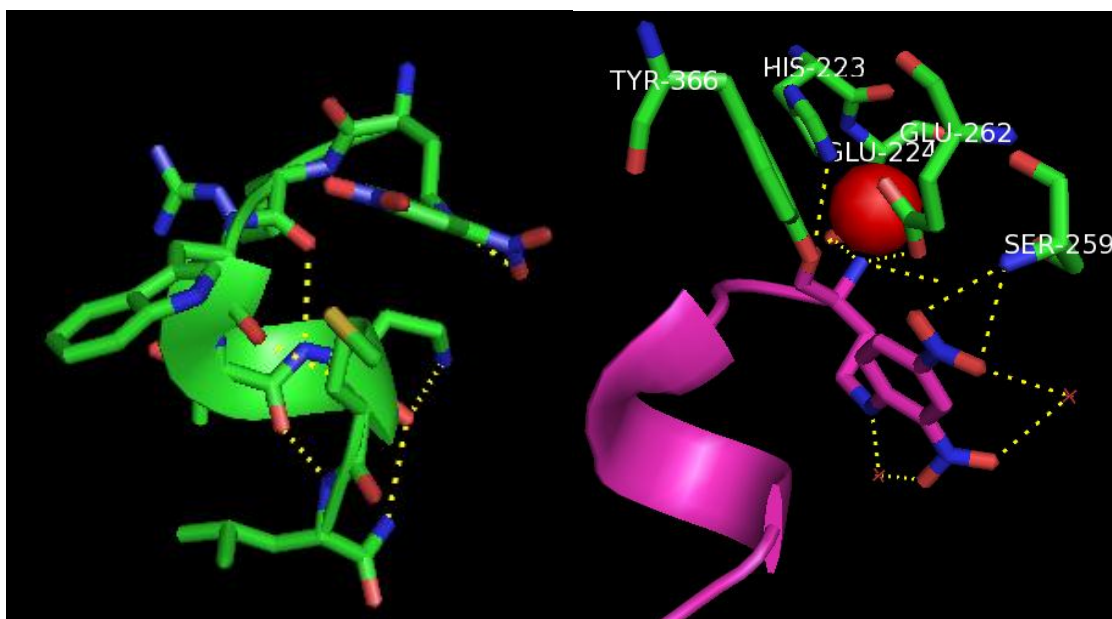


Figure 45. Crystal structure of previously synthesized inhibitor **II** (left), and polar interactions of the DNP-DAB residue bound within the active site (right, **II** shown in magenta, H-bonding shown in yellow, and the Zn ion shown in red).

The goal of our study was to further refine the **II** inhibitor to increase its drug-like character while retaining potency and its 3_{10} -helical conformation. Replacing the redox-active DNP-DAB group was instrumental to our goal in moving toward a more drug-like compound. Thus, in order to maintain potency, new electrostatic interactions must be accessed. In 2008, Kumaran *et al.* described four tetrameric peptide inhibitors (RRGC, RRGL, RRG1, and RRG2) with submicromolar activity.²⁰¹ The authors were able to obtain crystallographic data for each of the four tetrapeptides individually bound to the BoNT/A LC. In each of these structures, the guanidinium group of the P1 Arg exhibited strong electrostatic interactions with the toxin, while maintaining the previously described mechanism of inhibition.²⁰¹ Substituting the redox active DNP-DAB group with an arginine should allow access to these electrostatic interactions, thus compensating for the loss of the DNP-DAB residue.

The importance of an Arg at the P1' position has been established and is hypothesized to be necessary for efficient docking into the S1' pocket of the toxin.²⁰⁶ Zuniga *et al.*'s SAR revealed that the presence of a large aromatic residue at the P2' position induced a conformation of the active site, which provided favorable hydrophobic interactions as well as potential π -stacking interactions (Figure 46). In addition, the presence of an aromatic residue directly preceding the N-terminus of a 3_{10} -helix is known to have a stabilizing effect.²⁰⁷ Consequently,

we sought to further probe the effects of substitution of different aromatic residues at this position. Initially, three variants at the P2' were proposed to modulate the aromatic hydrophobic interactions by generating the sterically and electronically diverse benzyl, CH₂-naphthyl, and CH₂-indolyl analogues.

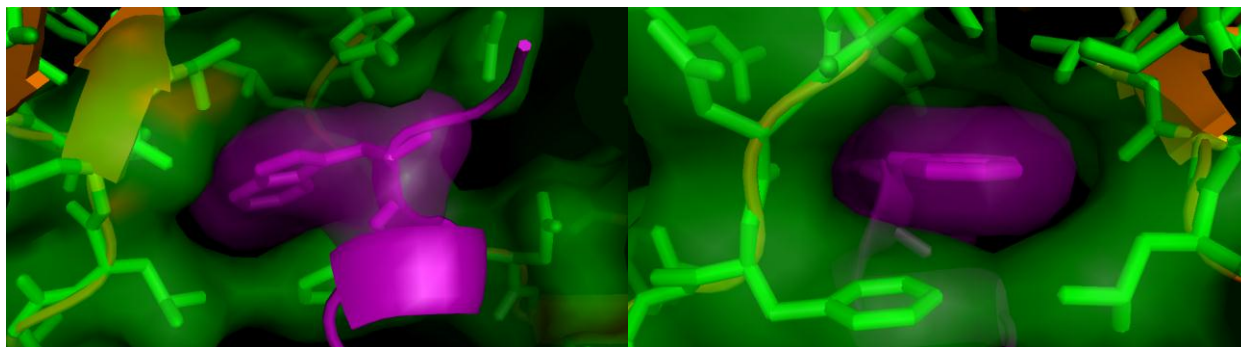


Figure 46. Trp residue bound in the active site (the **II** inhibitor is shown in purple)

Moreover, to further stabilize the 3₁₀-helical nature of the C-terminus of the inhibitor, an α -aminoisobutyric acid (AIB) residue, known to strongly favor the 3₁₀-helix^{208,209} was incorporated. Based on the chemical and electronic environments of the remaining amino acids, it became apparent that the Thr position immediately following the aromatic P2' residue would be the best site for replacement. The Thr residue benefits from favorable electrostatic interactions with both the backbone nitrogen and carboxylic acid side chain of Asp307 (Figure 47), however it exhibits no strong hydrophobic interactions.

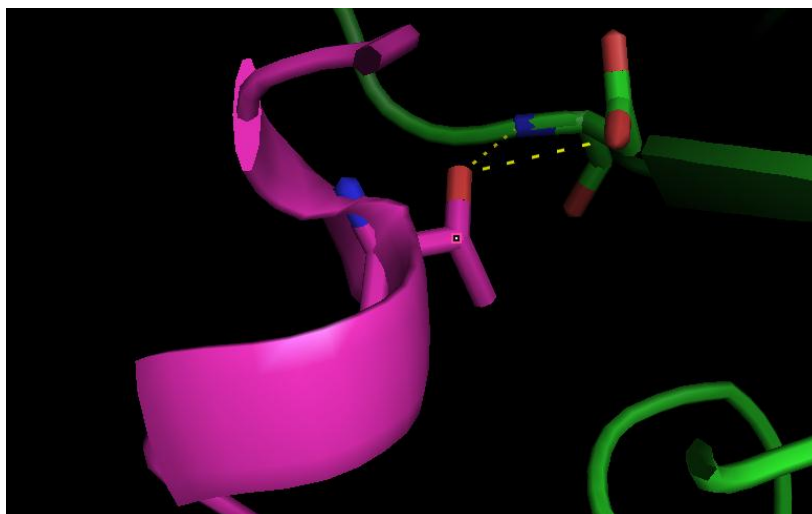


Figure 47. Polar contacts of the Thr residue of **II** (magenta) with Asp307 of BoNT/A LC

Low level (PM5) CACHE calculations for the heat of formation revealed that by replacing the Thr residue with an AIB residue in the conformation exhibited in the crystal structure, an increase in thermodynamic stability was observed (-240.799 kJ/mol for the structure containing the Thr residue vs. -342.1377 kJ/mol for the structure containing the AIB replacement).

The next residue in the **II** inhibitor, a DAB, exhibits favorable electrostatic interactions and previous SAR analysis revealed that replacement with other residues led to a decreased K_i .²⁰⁴ However, to increase the hydrophobicity of the C-terminus, the DAB residue was replaced with an Ala, which is commonly overrepresented in the 3_{10} -helix.²⁰⁷

The final two residues of the inhibitor, which correspond to the native substrate are located in a more solvent exposed cavity and do not exhibit strong electrostatic or hydrophobic interactions in the crystal structure of the bound inhibitor. As such, they were left as Met and Leu, respectively. Therefore, three PLMs were selected for an initial screening (**JTH-NB72-35**, **JTH-NB72-38**, **JTH-NB72-39**; Figure 48) and were synthesized via the previously optimized microwave solid phase peptide synthesis protocol (*vide supra*).

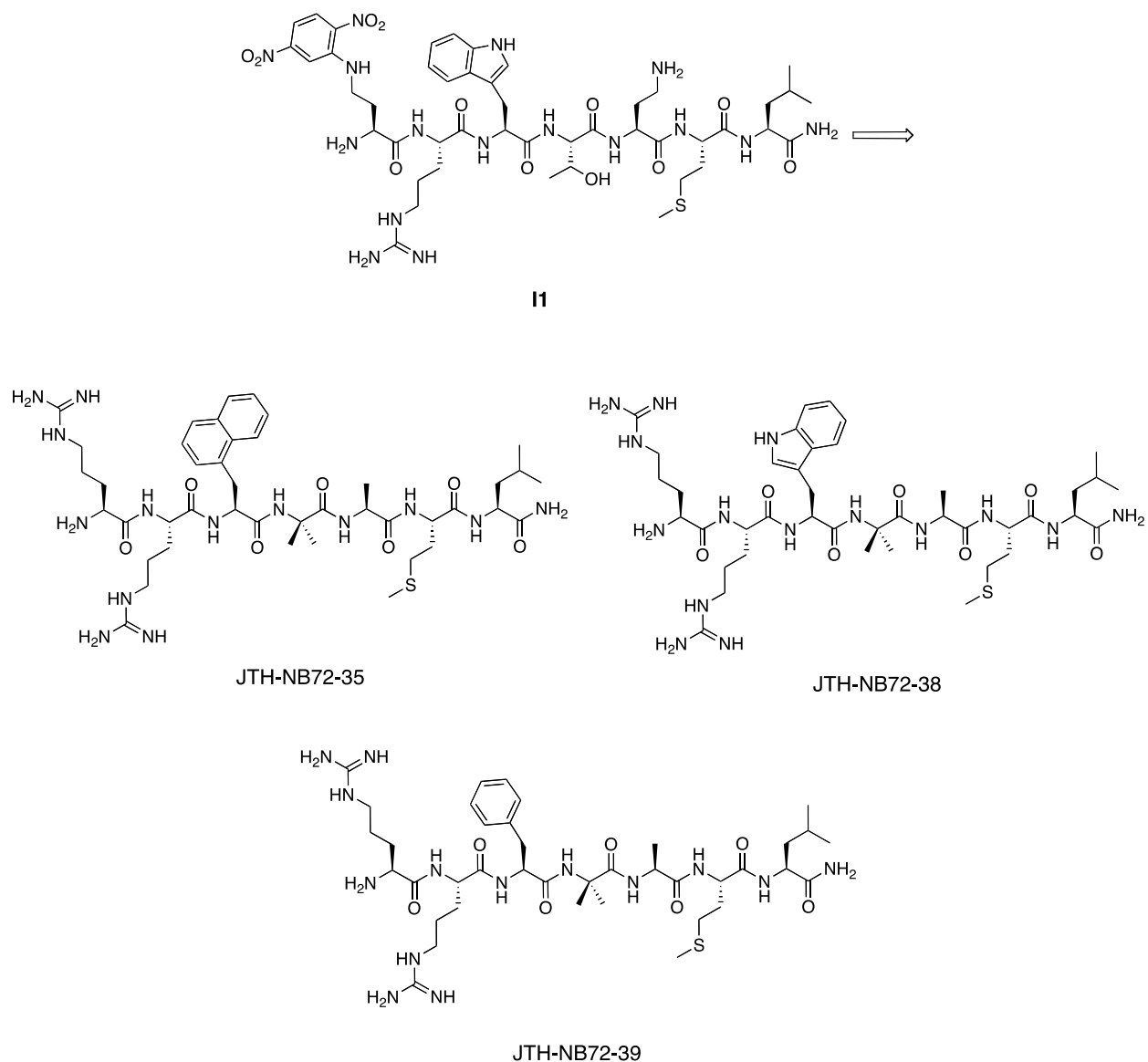
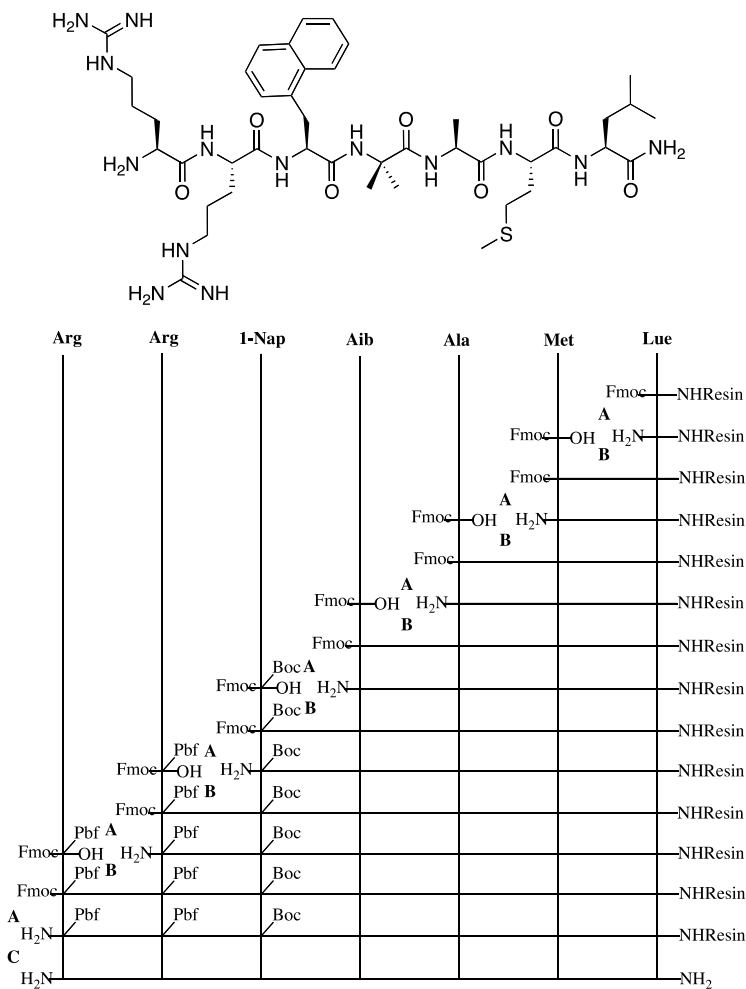


Figure 48. Structure of **I1** and analogous PLM structures

4.3 SYNTHESIS OF INHIBITORS

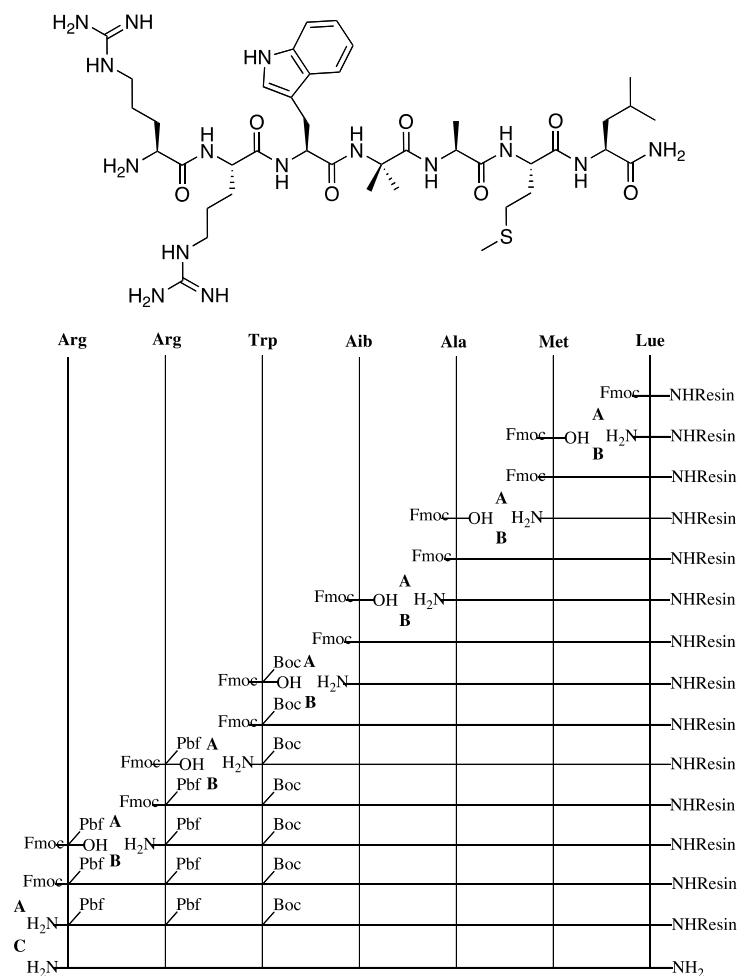
The desired heptameric peptides were synthesized via microwave assisted solid phase peptide synthesis using Fmoc protected amino acids and Rink amide SS resin (Figure 3). After swelling the resin in CH_2Cl_2 for 30 min, the synthesis was initiated by removal of the Fmoc protecting group from the Rink amide resin with a solution of 20% piperidine in DMF. The newly afforded free amine was then coupled to the protected amino acid, which had been

preactivated with the Goodman reagent (DEPBT), corresponding to the C-terminus of the desired heptamer. With the first amino acid successfully coupled to the Rink resin, the Fmoc group was once again removed and the subsequent activated amino acid was coupled to the freshly deprotected growing peptide chain. This process of deprotection and coupling was repeated until the *N*-terminal residue of the desired heptamer had been coupled (Scheme 44, Scheme 45, and Scheme 46). Following the final Fmoc deprotection, the peptide was cleaved from the solid support by stirring in a modified version of Reagent K, (87.5% TFA, 3.6% thioanisole, 2.3% EDT, 3.7% phenol, 1.8% H₂O, 1.1% triisopropylsilane) for 2 h at rt. The resin was filtered and washed with a small quantity of cleavage cocktail. The crude peptide was precipitated with ice-cold diethyl ether, collected via centrifugation, dissolved in deionized water, and lyophilized. The crude peptides were purified by preparative RP HPLC to afford approximately 35 mg of each of the desired peptides (**JTH-NB72-35**, **JTH-NB72-38**, and **JTH-NB72-39**; Figure 48).



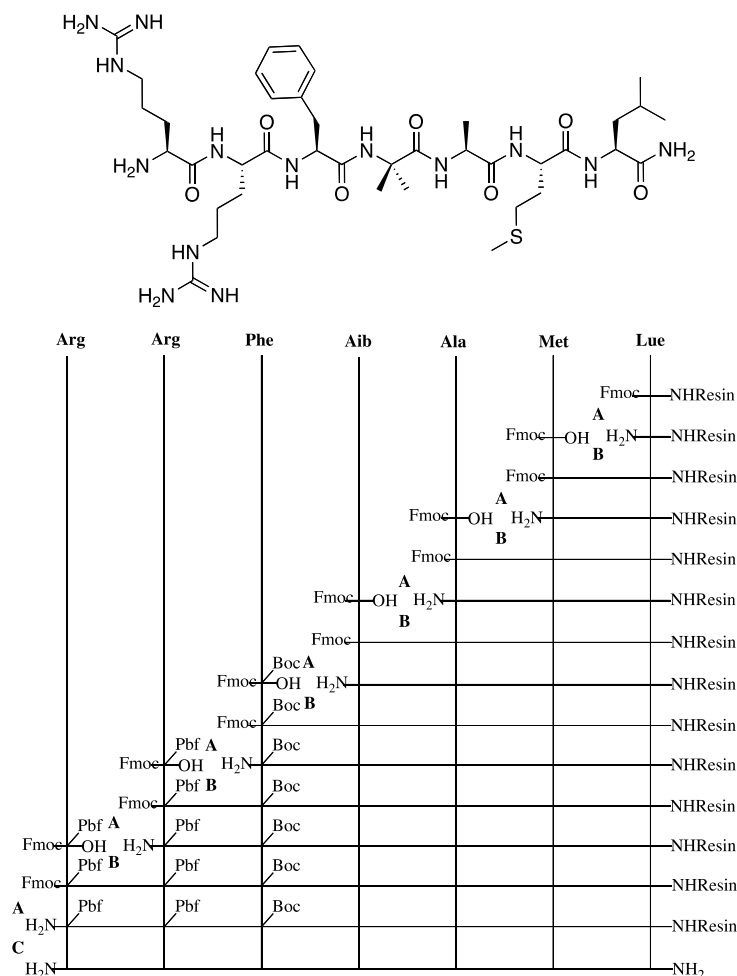
A: Piperidine, DMF, 35 W, 78 °C, 3 min B: DEPBT, DMF, DIPEA, 25 W, 80 °C, 5 min C: TFA, PhSCH₃, PhOH, TIPS, H₂O, EDT, rt, 2 h

Scheme 44. Synthesis of RR(1-Nap)(AIB)AML (**JTH-NB72-35**)



A: Piperidine, DMF, 35 W, 78 °C, 3 min B: DEPBT, DMF, DIPEA, 25 W, 80 °C, 5 min C: TFA, PhSCH₃, PhOH, TIPS, H₂O, EDT, rt, 2 h

Scheme 45. Synthesis of RRW(AIB)AML (JTH-NB72-38)



A: Piperidine, DMF, 35 W, 78 °C, 3 min B: DEPBT, DMF, DIPEA, 25 W, 80 °C, 5 min C: TFA, PhSCH₃, PhOH, TIPS, H₂O, EDT, rt, 2 h

Scheme 46. Synthesis of RRF(AIB)AML (JTH-NB72-39)

4.4 RESULTS AND DISCUSSION

The desired peptides were successfully synthesized in moderate yields (34-41%) after purification by reverse phase HPLC (Table 29). 25 mg of each of the newly synthesized peptides were sent to our collaborators Dr. Johnathan Nuss and Dr. Sina Bavari of the Department of Immunology, Target Identification, and Translational Research, Division of Bacteriology, at the United States Army Medical Research Institute of Infectious Diseases, for BoNT/A LC inhibition studies and all three compounds were found to possess sub- μ M activity (Table 29). Although the inhibitors did not possess the potency of **II**, the overall drug-like

nature of the molecule was increased both by removing the redox-active DNP-DAB group as well as increasing by the overall hydrophobicity of the molecule (Table 29) while maintaining sub μM potency.

Table 29. BoNT/A LC inhibitor summary.

Inhibitor	Sequence (C to N Termini)	Isolated Product (mg)	Overall Yield (%) ^a	K _i (nM) ^b	cLogP ^c
JTH-NB72-35	LMA(AIB)(1-Nal)RR	39.9	40	314.5±28.6	-1.442
JTH-NB72-38	LMA(AIB)WRR	41.5	41	990.5±116.9	-1.656
JTH-NB72-39	LMA(AIB)FRR	31.8	34	638.1±92.0	-2.008
I1	LM(DAB)TWR(DNP-DAB)	-	-	41	-2.346

^aYields are determined assuming the initial loading of the resin to be 0.7 mmol/g. ^bAll kinetic analysis was obtained through a collaboration with Dr. Johnathan Nuss and Dr. Sina Bavari at the Department of Immunology, Target Identification, and Translational Research, Division of Bacteriology, United States Army Medical Research Institute of Infectious Diseases using previously described assays.²⁰⁴ ^ccLogP data was generated using QikProp software from Schrödinger.

In addition, through the tireless efforts of our collaborators Jorge Zuniga and Dr. Axel Brunger of the Howard Hughes Medical Institute and Departments of Molecular and Cellular Physiology, Neurology, and Neurological Science, Structural Biology, and Photon Science, at Stanford University, the three dimensional structure of the BoNT/A LC:**JTH-NB72-39** complex was solved at 2.4 Å resolution by X-ray crystallography (Figure 49).



Figure 49. Crystal structure with **JTH-NB72-35** (in magenta) bound to the BoNT/A LC.

Structural comparison of the bound **I1** inhibitor and bound **JTH-NB72-39** revealed that although substantial replacements were made to the **I1** inhibitor, the overall conformation of the molecule as well as integrity of 3₁₀-helix were successfully maintained (Figure 50).

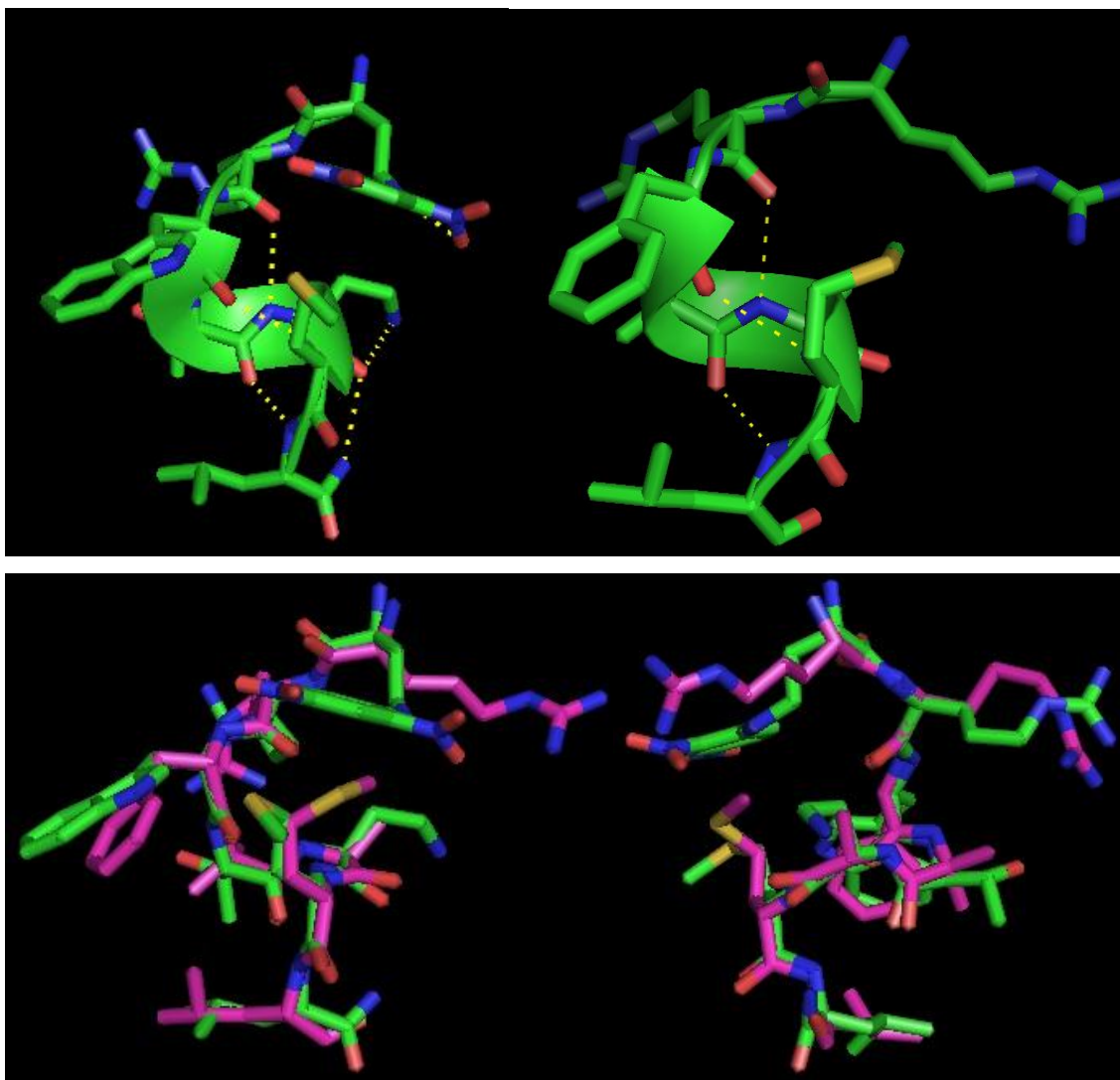


Figure 50. Comparison of **II** (top left) and **JTH-NB72-39** (top right) bound to the active site of BoNT/A LC as well as both a front (bottom left) and back (bottom right) view of an overlay (**JTH-NB72-39** carbons are magenta while **II** carbons are green).

Further examination of the crystal structure revealed that the majority of the toxin:inhibitor interactions occur along residues 1 through 4 (P1-P3'), while the last three residues have a less conspicuous electron density indicating the disordered nature of their binding. True to its design, **JTH-NB72-39** was able to exploit the electrostatic surface and hydrophobic interactions that had been previously established as binding surfaces for two different kinds of inhibitors.^{201,204}

In the BoNT/A LC:**JTH-NB72-39** complex, the backbone groups in the P1 Arg in the inhibitor established two crucial interactions that effectively impair the catalytic machinery of

the BoNT/A LC; first, the terminal amino group of the P1 Arg has displaced the catalytic water molecule normally observed at H-bond distance from Glu224, and second, this amino group is associated with the negative head group of the Glu224 side chain. In this way, the catalytic center of BoNT/A is deprived of the nucleophilic water molecule necessary for proteolytic bond-cleavage. Concurrently, **JTH-NB72-39** is exerting a “lock” effect in this “proton shuttle” of the active site. The inhibitor also displays substrate-like interactions by placing the carbonyl group of P1 2.4 Å away from the zinc ion and forming a H-bond with Tyr366 (Figure 51).

Although removing the DNP-DAP residue led to the loss of several strong electrostatic interactions, its replacement in **JTH-NB72-39** with an Arg led to the formation of new electrostatic interactions. The Arg (P1) of **JTH-NB72-39** forms a salt bridge with Glu164 and an H-bond with the carbonyl group of Cys165 in the toxin. The P1' Arg also possesses a salt bridge with the carboxylate group of Asp370 as well as cation- π interactions of the guanidinium with Phe194 of the toxin (Figure 51), as previously described.²⁰¹

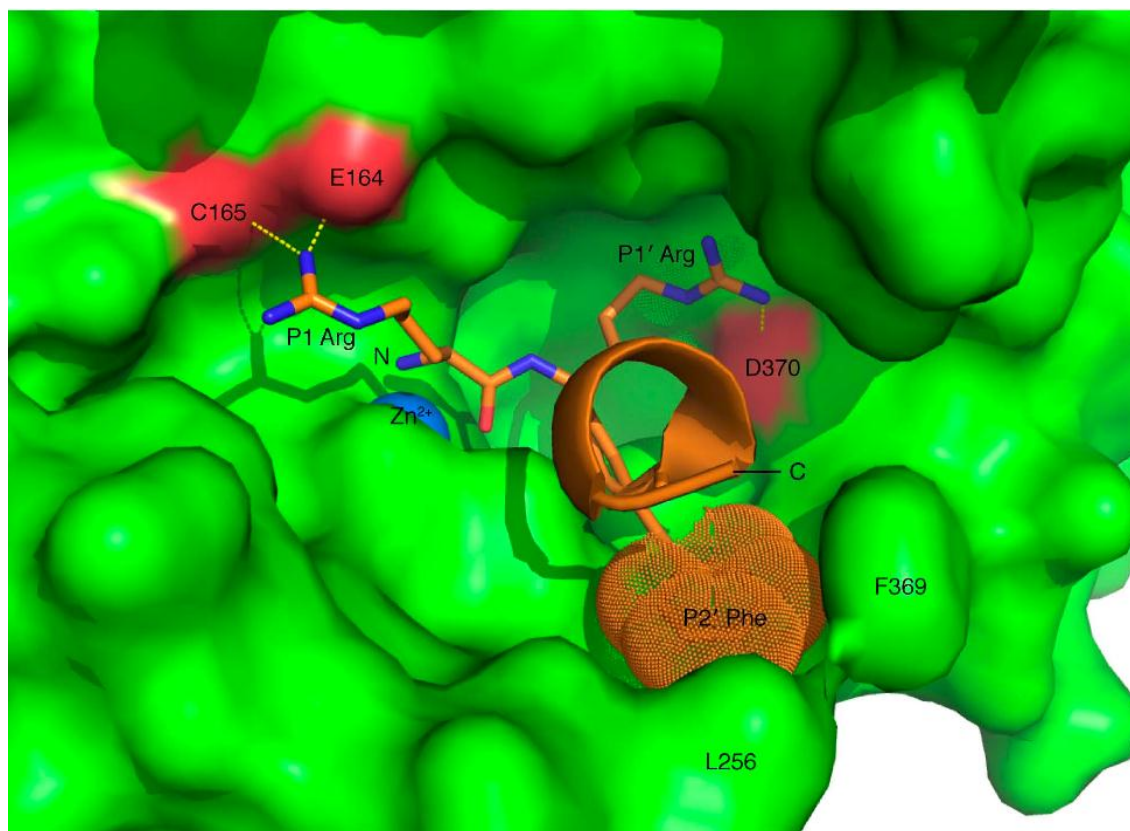


Figure 51. Panoramic view of the **JTH-NB72-39** inhibitor bound to BoNT/A LC active site²¹⁰

The P2' residue, a Phe, successfully exploits the hydrophobic interactions described as crucial for proper “locking” of the **II** inhibitor.²⁰⁴ Phe369 and Leu367 are responsible for the bulk of the hydrophobic interactions and have undergone a significant reorientation as compared to the free form of BoNT/A LC. However, both Phe369 and Leu367 exhibit stronger hydrophobic interactions with previously described **II** inhibitor, which may suggest that Trp is a better anchor than Phe in this inhibitor. Interestingly, the inhibitor containing the larger Trp residue at the P2' position (**JTH-NB72-38**) exhibited the highest K_i (990.5 ± 116.9 nM). One explanation is that due to the different mode of binding exhibited by **JTH-NB72-39**, the ability for electrostatic interactions of the indole nitrogen described by Zuniga *et al.* has been removed and the presence of a polar atom decreases the residue's overall affinity toward the hydrophobic pocket. This theory is supported by the increase in the activity of the analogue containing the 1-naphthyl residue. It is clear that hydrophobic interactions play a large role in modulating the affinity of the BoNT inhibitors and hydrophobicity is an important interaction that could be further optimized in future inhibitors.

Incorporation of the AIB residue successfully stabilized the 3_{10} -helix; however, AIB did not participate in any strong hydrophobic or electrostatic interactions. As previously mentioned, the last three residues are not as tightly bound to the toxin as the first four. Although several hydrophobic interactions are observed, they are likely transient.

4.5 CONCLUSIONS

The rational design and synthesis of three PLM inhibitors of BoNT/A LC have been described. Through collaboration with Dr. Johnathan Nuss and Dr. Sina Bavari of the Department of Immunology, Target Identification, and Translational Research, Division of Bacteriology, at the United States Army Medical Research Institute of Infectious Diseases, all three compounds have been tested in a biological assay for inhibition of BoNT/A LC, and found to possess sub- μ M activity (Table 29). The drug-like character of **II** was increased by removing the redox active DNP-DAB residue and increasing the hydrophobic nature of the C-terminus by replacing Thr with AIB and DAB with Ala residues, while maintaining the 3_{10} -helix. In addition, through a collaboration with Jorge Zuniga and Dr. Axel Brunger of the Howard Hughes

Medical Institute and Departments of Molecular and Cellular Physiology, Neurology, and Neurological Science, Structural Biology, and Photon Science, at Stanford University, the BoNT/A LC:**JTH-NB72-39** complex was solved at 2.4 Å resolution by X-ray crystallography. This crystal structure revealed that, true to its design, the inhibitor exhibited hydrophobic and electrostatic interactions previously described for two different inhibitors.^{201,204} Thus, the next stage of this project would be to use the information gained from the crystal structure to develop an even more drug-like molecule by decreasing the size of the inhibitor as well as removing the peptide bonds, which lead to the short *in vivo* lifetimes exhibited by peptidic inhibitors.

4.6 DEVELOPMENT OF SMALL MOLECULE INHIBITORS OF BONT/A LC

In addition to PLM inhibitors of BoNT/A LC, our group has focused on the identification and preparation of small-molecule inhibitors. Our collaborators, Gussio and coworkers conducted a high-throughput screen of the National Cancer Institute's (NCI) diversity set, which identified several non-peptidic small-molecule inhibitors of the BoNT LC.²¹¹ In particular this screen led to the identification of Michellamine B, Q2-15, and NSC 357736 (Figure 42). Based on the newly identified inhibitors, iterative conformational analyses, and molecular docking studies, the authors were able to develop a refined pharmacophore (Figure 52).^{211,212}

The refined pharmacophore, shown in Figure 52, is composed of two planar components (**A** and **B**), one of which contains a heteroatom atom thought to engage with the catalytic zinc either through direct contacts or by replacing the water molecule responsible for hydrolysis of the substrate peptide. Components **C** and **D** represent lipophilic portions of the inhibitors, which are placed into hydrophobic pockets of the active site. Finally, Component **E** represents the the polar, ionizable center, thought to be involved with electrostatic or water mediated interactions with the polar residues of the active site.²¹²

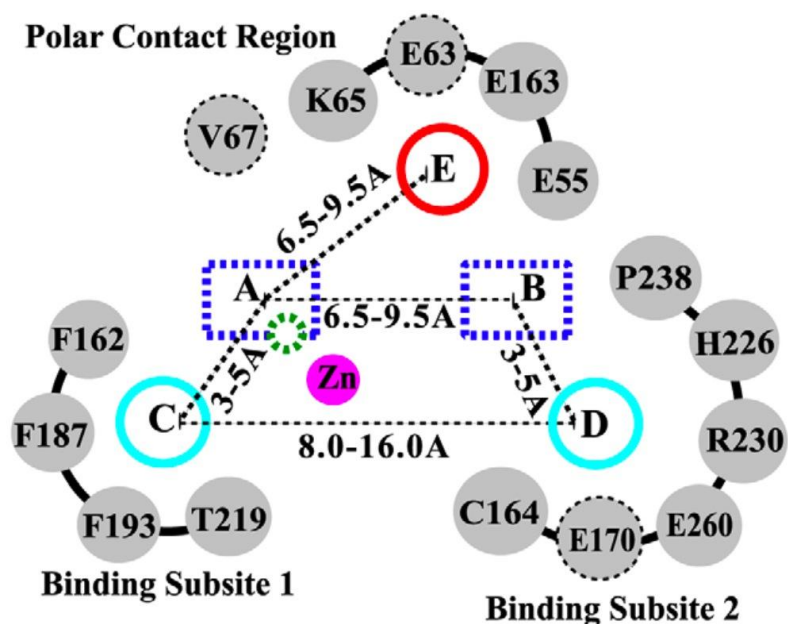


Figure 52. Refined pharmacophore for BoNT/A LC inhibition. Planar components **A** and **B** are represented as blue dashed rectangles. The dashed circle in plane **A** represents a heteroatom. Hydrophobic components **C** and **D** are shown as light blue circles. The positive ionizable component of **E** of the pharmacophore is shown as a red circle. Residues that remained consistent when docking inhibitors predicted binding subsites of both dynamic and molecular mechanics “only” refined models are shown as grey spheres. Residues E36, V67, and E170 are shown as gray spheres with dashed black borders—to indicate that these amino acids were found to participate when docking inhibitors in dynamic structures. Note this figure and caption were reproduced with permission from Burnett and coworkers.²¹²

Based on this pharmacophore as well as data generated from some peptidic inhibitors, Burnett and coworkers generated a series of queries searching the NCI’s Open Repository.²¹³ This set of queries led to the identification of several hits, which were assayed for inhibition of BoNT/LC A. These inhibition studies led to the identification of four potent inhibitors (Figure 53). Of the four newly identified inhibitors, NSC 240898 showed a dose-dependant inhibition of SNAP-25 proteolysis and displayed no cellular toxicity up to 40 μM concentration.²¹³ The molecular docking study for NSC 240898, shown in Figure 53, revealed that the indole nitrogen is positioned to interfere with the catalytic zinc in the active site while maintaining several stabilizing polar and hydrophobic contacts.²¹³ The potent activity and limited toxicity of NSC 240898 led our group to choose it as a lead for a structure-activity relationship (SAR) study aimed at generating more potent analogues (Figure 54).²⁰⁵

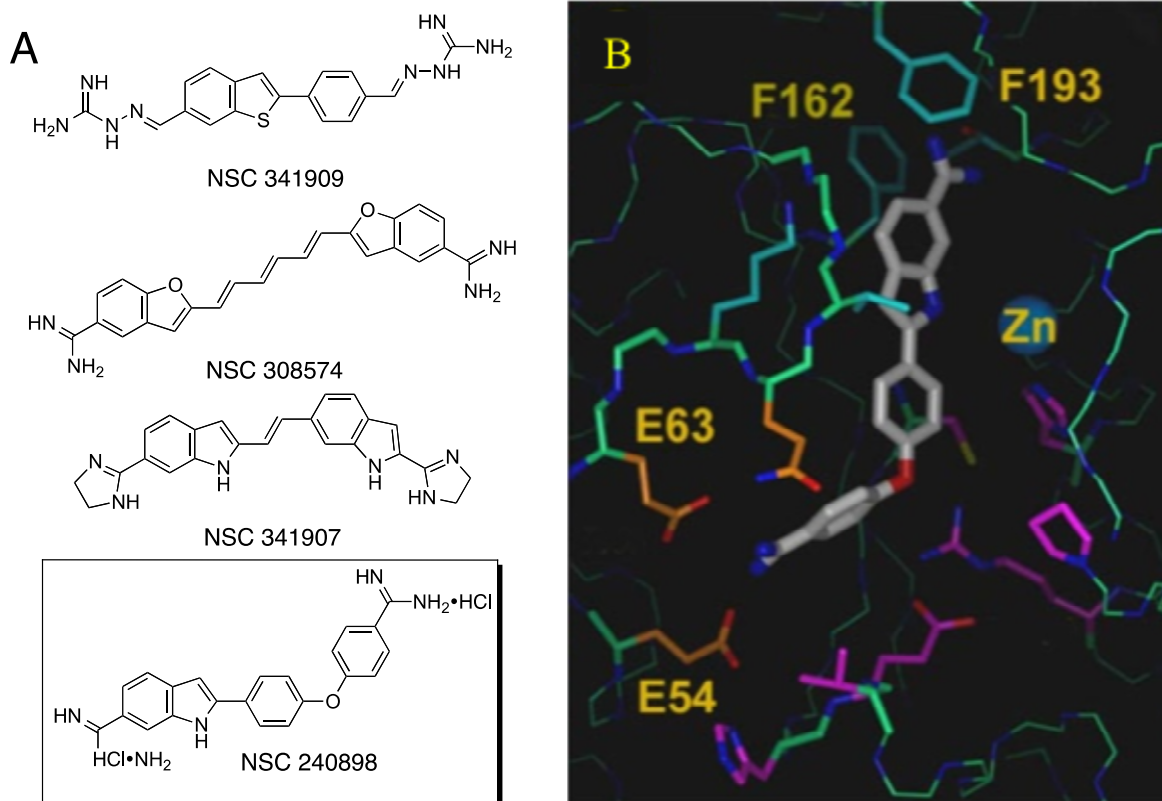


Figure 53. (A) Structures of the four most potent BoNT/A LC inhibitors screened. (B) Docking of NSC 240898 fit with good steric and hydrophobic complementarity in the BoNT/A LC substrate binding cleft. Reproduced with permission from ref.²¹³

The synthetic modifications made during our initial SAR study are highlighted in Figure 54.²⁰⁵ Specifically our SAR studies focused on replacing the two polar terminal amidines, moving the indole amidine from the indole C5 to the indole C6 carbon, and a variety of substitutions. The incorporation of heteroarenes (pink Z) were investigated to improve solubility properties while decreasing the potential for metabolism. Different heteroatomic linkers (X = O, N, S) were also investigated. Finally, substitution of the central phenyl ring was done to explore the electronic and steric requirements of the active site. These SAR studies revealed that substitution of the bis-amidines with imidazolines led to more pharmacologically relevant inhibitors without a significant decrease in potency. In addition, the SAR revealed the presence of additional polar atoms led to decreased potency, however switching to a softer sulfur linker improved activity. Ultimately our SAR studies led to the identification of CWD-021, a more potent NSC 240989 analogue.²⁰⁵

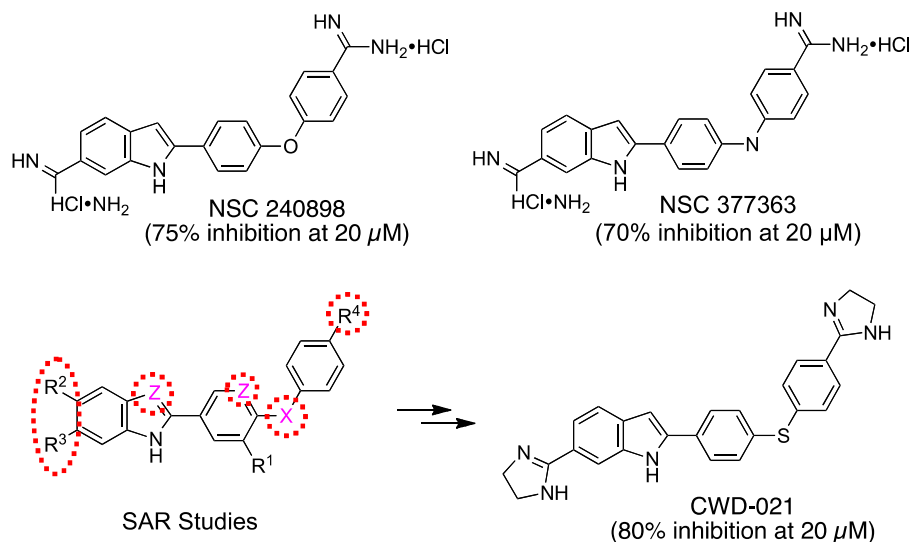


Figure 54. Structure of potent small-molecule inhibitors of BoNT/A LC and SAR studies of NSC240898 to yield CWD-021

As a part of an ongoing research program seeking to further elucidate the SAR of the BoNT/A LC small-molecule inhibitors, the synthesis of a set of structurally rigidified eight-membered ring analogues containing either an amide or amine was pursued (**4.1-4.5**, Figure 55).

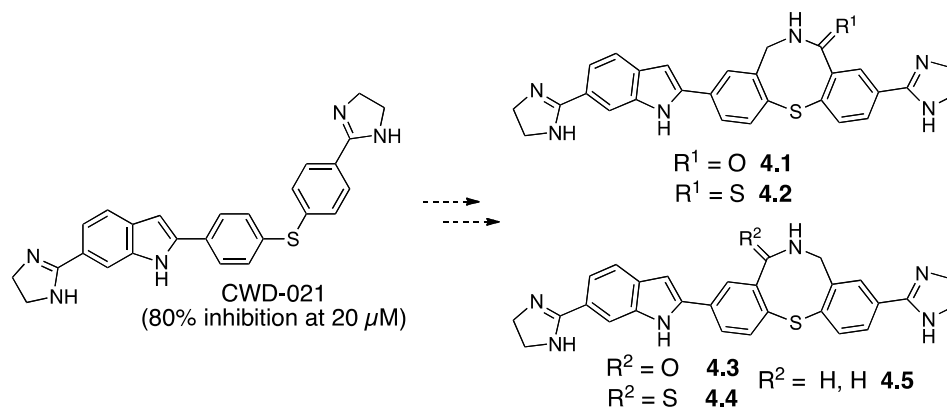
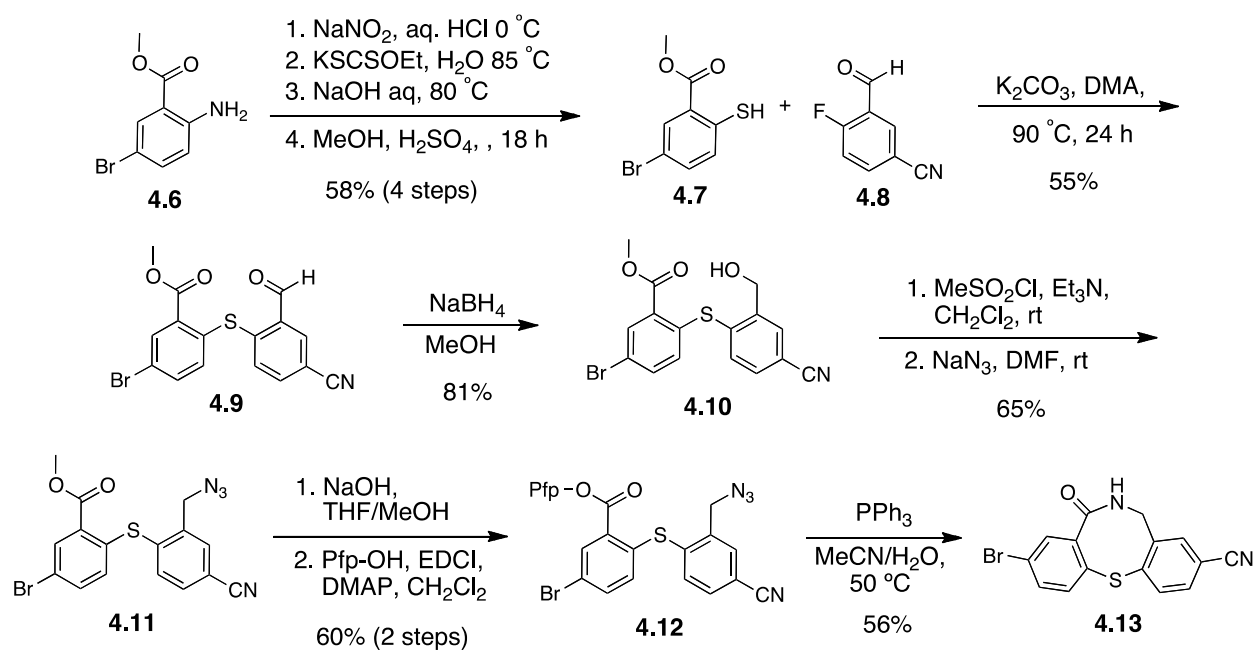


Figure 55. Proposed rigidified small-molecule inhibitors of BoNT/A LC

I was charged with continuing the efforts of a former postdoctoral scholar in our group, Dr. Igor Opsenica. Dr. Opsenica had successfully prepared both the amide derivatives **4.1** and **4.3** however, was unable to complete the thioamides **4.2** and **4.4**, as well as the amine derivative **4.5** prior to completion of his postdoctoral studies. My own synthetic work started from intermediate **4.13**, which was prepared by Dr. Opsenica according to the sequence outlined in

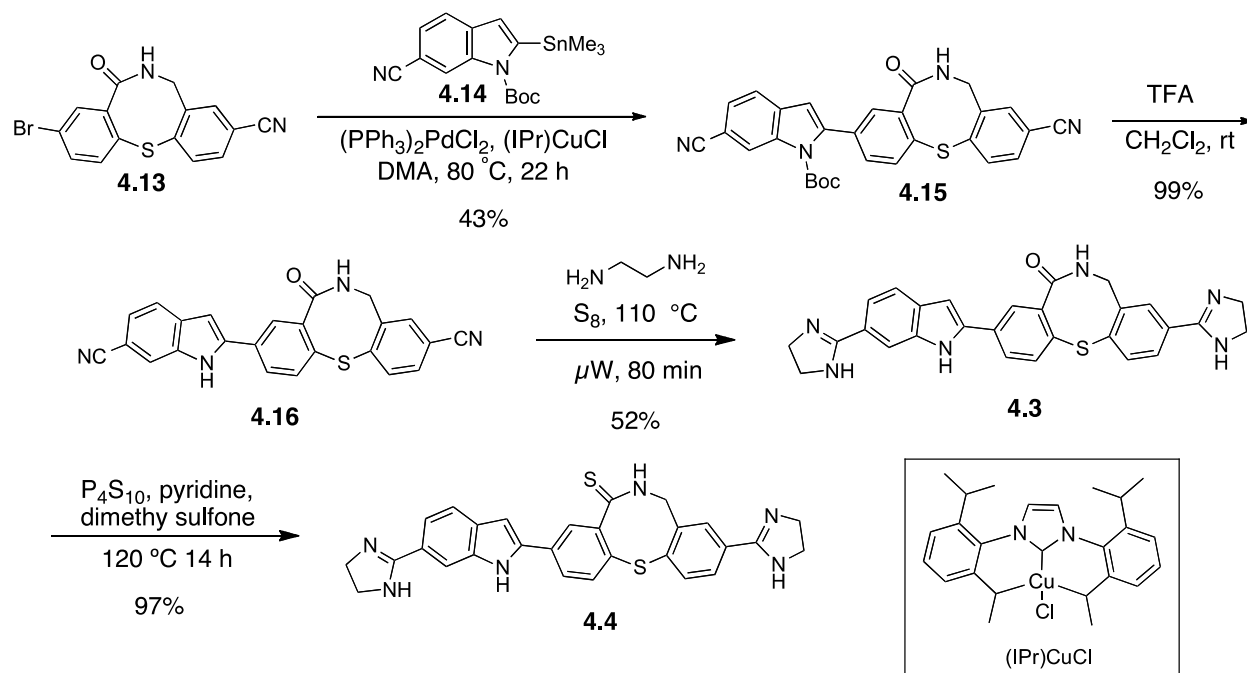
Scheme 47. Dr. Opsenica's synthesis of **4.13** began from aniline **4.6**. Diazotization of **4.6**, displacement with thioacetate, hydrolysis with sodium hydroxide, and conversion to the methyl ester in acidic methanol afforded **4.7** in 58% yield over the four steps. Thiophenol **4.7** was coupled with the commercially available 2-fluoro-5-cyano-benzaldehyde **4.8** in the presence of potassium carbonate to yield diaryl thiol **4.9** in 55% yield. Selective reduction of the aldehyde with sodium borohydride, followed by conversion to the meslate and displacement with sodium azide afforded the benzyl azide **4.11** in 53% yield over three steps. Hydrolysis of the ester followed by 1-ethyl-3-(3-dimethylaminopropyl)carbodiimide (EDCI) mediated pentafluorophenol (Pfp) ester formation afforded **4.12** in 60% yield over two steps. Staudinger reduction and subsequent amide formation provided **4.13** in moderate yield.



Scheme 47. Dr. Igor Opsenica's synthesis of **4.13**

Following Dr. Opsenica's previously optimized procedures, my own synthetic work began with the Stille coupling of the eight-membered lactam **4.13** with the readily available stannane **4.14**. The Stille coupling proceeded smoothly in the presence of an N-heterocyclic carbene copper chloride catalyst ((IPr)CuCl)²¹⁴ and bis(triphenylphosphine)palladium(II) chloride to afford **4.15** in 43% yield. Removal of the indole *t*-butyloxycarbonyl (Boc) protecting group with TFA in dichloromethane gave the free indole **4.16** in good yield. Conversion of the nitriles to

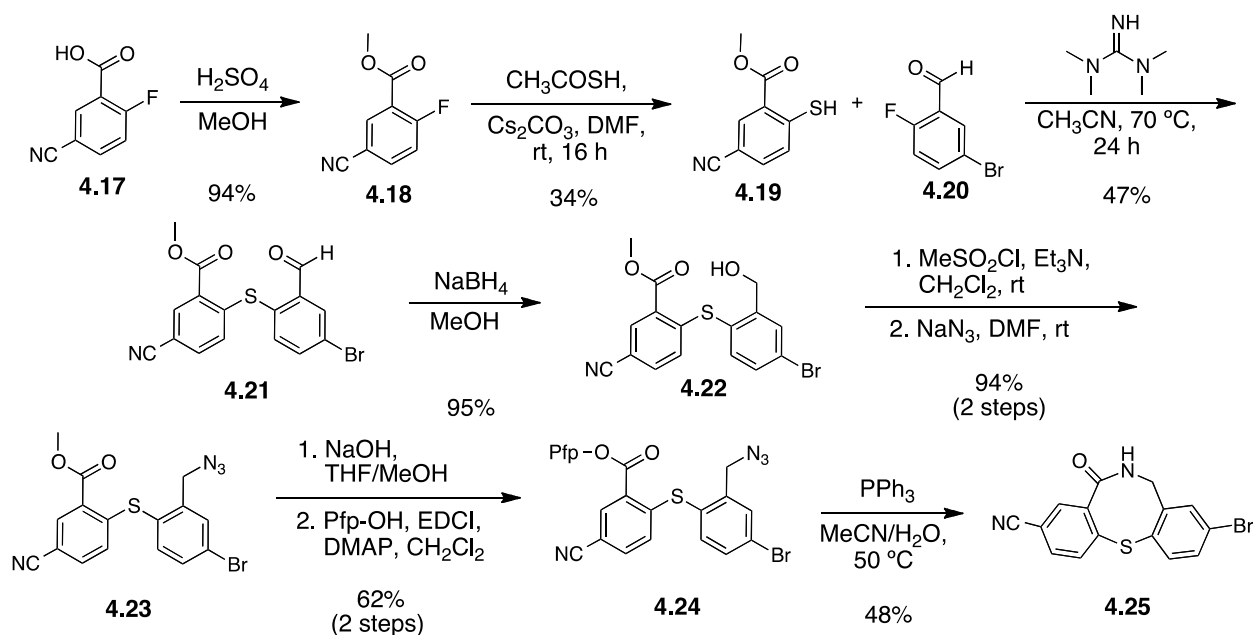
imidazolines was accomplished using 1,2-diaminoethane in the presence of sulfur to give **4.3** in 52% yield. After some optimization, it was found that heating **4.3** with phosphorous pentasulfide and pyridine in dimethyl sulfone overnight at 120 °C provided the desired thioamide **4.4** in excellent yield (Scheme 48). The use of dimethyl sulfone, which remains a solid below 110 °C, proved crucial for solubilizing **4.3** and providing reproducible levels of reactivity.



Scheme 48. Synthesis of thioamide **4.4**

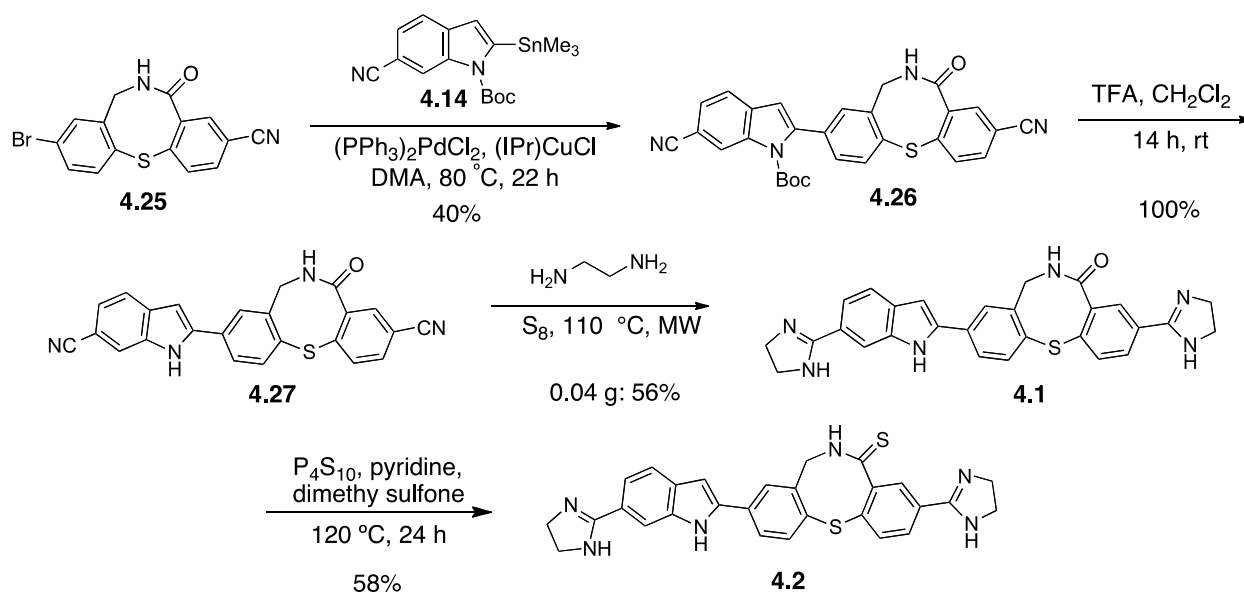
Next, we focused on the preparation of thiomide **4.2** (Scheme 49, Scheme 50). Starting from the commercially available 2-fluoro-5-cyanobenzoic acid **4.17**, Fischer esterification proceeded smoothly to afford methyl ester **4.18** in good yield. Nucleophilic aromatic substitution with thioacetic acid and subsequent hydrolysis afforded thiophenol **4.19** in 34% yield. Unfortunately, attempts to increase the yield of the substitution using different thiol sources as well as screening several bases proved unsuccessful. Thiophenol **4.19** was coupled with the commercially available 2-fluoro-5-bromo-benzaldehyde **4.20** in the presence of tetramethyl guanidine, which proved superior to potassium carbonate, to yield diaryl thiol **4.21** in 47%. Selective reduction of the aldehyde with sodium borohydride afforded benzyl alcohol **4.22**. Conversion to the meslate and displacement with sodium azide proceeded in excellent

yield to afford the benzyl azide **4.23**. Saponification of the methyl ester followed by formation of the penta-fluorophenol (Pfp) ester afforded **4.24** in 62% yield over two steps. Staudinger reduction and subsequent amide formation provided the eight-membered lactam **4.25** in 48% yield.



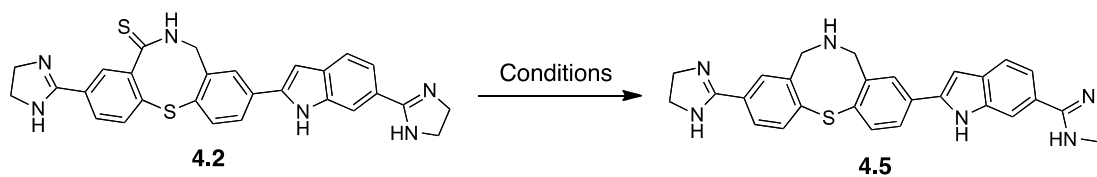
Scheme 49. Synthesis of the eight-membered lactam **4.25**

Completion of thioamide **4.2** following a similar sequence used in the preparation of thioamide **4.4** proceeded in comparable yields (Scheme 50). Stille coupling of eight-membered lactam **4.25** with the readily accessible cyano-indole **4.14** gave **4.26** in 40% yield. Removal of the *t*-butyloxycarbonyl (Boc) group with TFA proceeded in quantitative yield to afford the free indole **4.27**. Conversion of both nitriles to imidazolines in the microwave with 1,2-diaminoethane and sulfur provided **4.1** in 56% yield. Thioamide formation proceeded this time in moderate yield in the presence of phosphorous pentasulfide and pyridine in dimethyl sulfone to give thioamine **4.2** in 58% yield.



Scheme 50. Completion of thioamide **4.2**

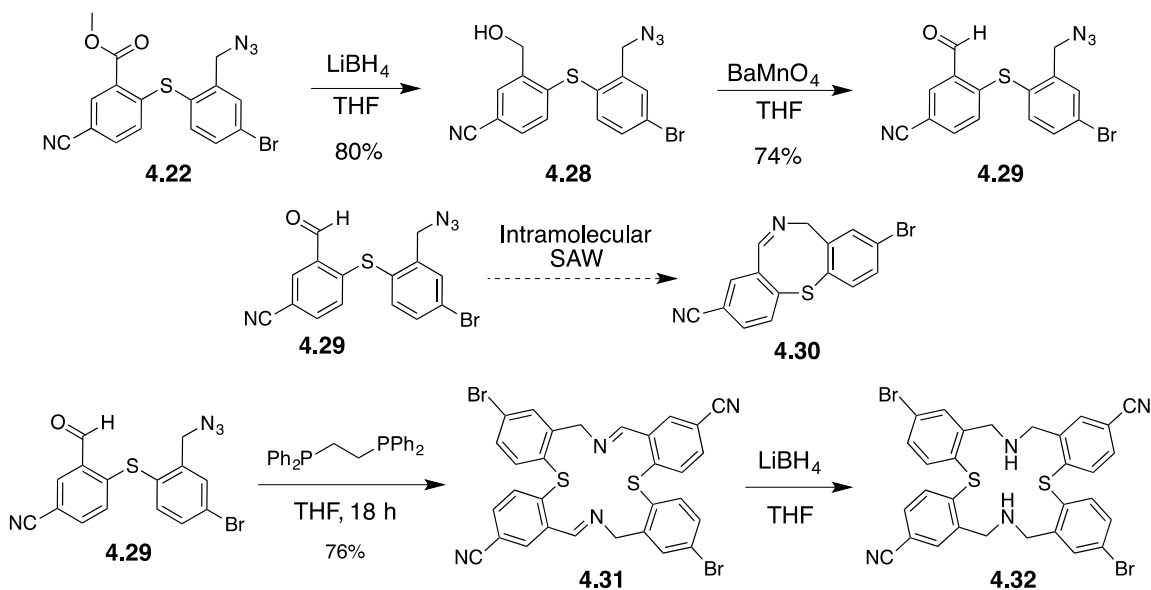
Next, the preparation of the final amino analogue **4.5** was investigated. Initial attempts to de-sulfurize thioamide **4.2** to give the desired product directly were unsuccessful (Table 30). The use of various equivalents of Raney-Ni in several solvent systems provided no reaction and only starting material was observed by LCMS analysis. The observed lack of reactivity is most likely a result of the poor solubility of **4.2** even in DMSO at elevated temperatures. Consumption of **4.2** was only observed with *in situ* prepared nickel borohydride and with Schwartz reagent (Cp_2ZrHCl); however in neither case was the desired product observed by LCMS analysis. These initial attempts to directly reduce the thioamide present in **4.2** were not promising and when coupled with a rapidly diminishing supply of **4.2** led us to re-evaluate our synthetic strategy. Therefore, focus was shifted to the installation of the amine prior to Stille coupling.

Table 30. Attempts to synthesize **4.5** via direct de-sulfurization of **4.2**

Conditions	Result
1. Raney-Ni (40 equiv), THF, 70 °C, 1 h	rec SM
2. Raney-Ni (160 equiv), THF, 16 h	rec SM
3. Raney-Ni (80 equiv), EtOH,)) , 1 h	rec SM
4. Raney-Ni (330 equiv), 16 h, rt	rec SM
5. H ₂ O/solutol, Raney-Ni (100 equiv), 14 h, rt	mostly SM
6. NiCl ₂ , NaBH ₄ , MeOH/THF, 16 h, rt	rec SM
7. NiCl ₂ , NaBH ₄ , EtOH (preform), 14 h	complex mixture
8. Cp ₂ ZrHCl (4 equiv), rt, overnight	SM + mass @ 493 + 466

Reactions were conducted on 2.0 mg scale monitoring by LCMS.)) indicates sonication.

Next, the intramolecular Staudinger-aza-Wittig (SAW) reaction to close the eight-membered ring was investigated (Scheme 51). To this end azido-ester **4.22** was reduced with lithium borohydride to provide benzyl alcohol **4.28** in 80% yield. Oxidation of **4.28** with MnO₂ provided unsatisfactorily low yields; however, switching to barium permanganate afforded the desired benzyl aldehyde **4.29** in 74% yield. Subjecting **4.29** to triphenylphosphine in THF, either at room temperature or 66 °C overnight, proved ineffective and only starting material was recovered. Switching to 1,2-bis(diphenylphosphino)ethane, after stirring with **4.29** in THF overnight at room temperature afforded a product tentatively assigned as **4.30** in 76% yield. Reduction of the product tentatively assigned as **4.30** with lithium borohydride, however, yielded a product assigned by HRMS analysis to be the dimeric product **4.32** (Scheme 51). Based on this result it is apparent that the desired intermolecular SAW reaction to form the eight-membered had not occurred; instead a bimolecular SAW reaction to form the symmetric dimer **3.31** had proceeded. Investigating more dilute conditions (c = 0.005 M) afforded none of the desired imine **4.30**, and only the dimeric **4.32** was observed. Therefore, an alternative approach to the synthesis of the amino derivative **4.5** is needed.



Scheme 51. Attempted synthesis of **4.30**

4.7 CONCLUSIONS AND FUTURE DIRECTIONS

Herein, the synthesis of several non-peptidic small-molecule inhibitors of BoNT/A LC is described. Successful preparation of amides **4.1** and **4.3** according to Dr. Igor Opsenica's previously optimized route allowed for the syntheses of the corresponding thioamides **4.2** and **4.4**. All four eight-membered ring analogues were sent to our collaborators Dr. Johnathan Nuss and Dr. Sina Bavari of the Department of Immunology, Target Identification, and Translational Research, Division of Bacteriology, at the United States Army Medical Research Institute of Infectious Diseases, for BoNT/A LC inhibition assays. Attempts to synthesize **4.5** by either desulfurization of **4.2** or an intramolecular Staudinger-aza-Wittig reaction of **4.29** proved unsuccessful. The future goal of this project is the completion of the amino derivative. We envision that selective reduction of the amide of **4.25** to the amine, followed by protection and an analogous reaction sequence used in the preparation of **4.1** and **4.3** will afford access to the desired amino derivative **4.5**.

4.8 EXPERIMENTAL FOR PEPTIDIC INHIBITORS

N,N-Diisopropylethylamine was sequentially distilled from ninhydrin then KOH and stored under argon. Piperidine was distilled from CaH₂ and stored under argon. Phenol was purified by dissolving the solid in diethyl ether, washing with a saturated aqueous solution of NaHCO₃ (3x), extracting with aqueous NaOH (0.1 M) (3x), acidifying with 0.1 N HCl, extracting with Et₂O (3x), concentrating under reduced pressure, and the dry solid was stored under argon. *N,N*-dimethylformamide was purchased from Alfa Aesar as anhydrous and amine free in 4 L quantities and stored in 1 L amber bottles (dried overnight in an oven at 140 °C) over activated 4 Å molecular sieves and under argon. Trifluoroacetic acid (biochemical grade, 99.5+% pure) was purchased from Alfa Aesar and used as received. Methanol (HPLC grade), water (HPLC grade), and thioanisole (99% purity) were purchased from Aldrich and used as received. Triisopropylsilane (99% pure) was purchased from Acros and used as received. 1,2-ethanedithiol (>98% pure) was purchased from Fluka and used as received. All natural Fmoc-protected amino acids and 3-(diethoxy-phosphoryloxy)-3*H*-benzo[d][1,2,3] triazin-4-one were purchased from either Peptides International or Advanced Automated Peptide Protein Technologies (AAPPTEC) and used as received. Unnatural Fmoc protected amino acids and Rink Amide Resin SS, 100-200 mesh, 1% DVB (catalogue #: SA5030) were purchased from Advanced Chemtech and used as received. BD Falcon BlueMax 50 mL Graduated tubes and 25 mm syringe filters with a 0.45 µm nylon frit were purchased from Fischer Scientific.

The Fmoc-solid phase peptide syntheses were performed on a CEM Discover manual microwave peptide synthesizer fitted with a fiber-optic temperature probe. Solid phase peptide syntheses were performed in a 25 mL polypropylene reaction vessel. The 25 mL polypropylene reaction vessel was constructed by inserting a Teflon ring (0.4 mm height, 2.1 mm outer diameter, 1.8 mm inner diameter) into a capped 25 mL SPE reservoir purchased from Grace Davison Discovery Science (Catalogue #: 210425) containing a frit purchased from Grace Davison Discovery Science (Catalogue #: 211416) (Figure 56).

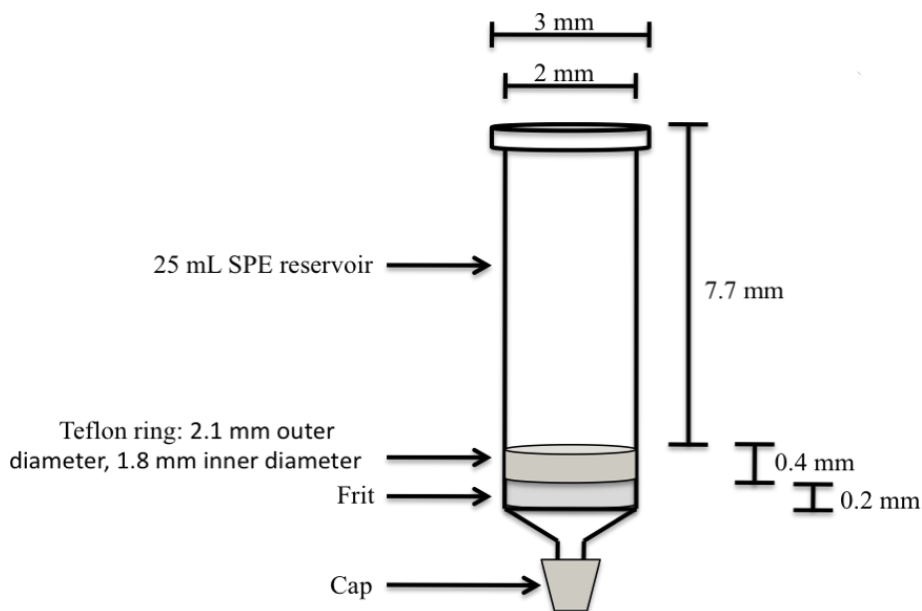


Figure 56. Diagram of assembled 25 mL polypropylene reaction vessel

Preparative reverse phase HPLC purifications were performed on a Gilson HPLC system with 220 and 254 nm UV detection, using a Phenomenex Luna 5 μ C18(2) 100 Å, AX (75 x 30.0 mm) column at a flow rate of 10 mL/min. Unless otherwise noted, all preparative runs used linear gradients of 30-60% buffer B in A (A: water containing 0.1% TFA, B: CH₃CN containing 0.1% TFA) over 30 min. Analytical HPLC traces of final products were performed on a Gilson HPLC system with 220 and 254 nm UV detection, using a Varian Microsorb 100-3 C18 (100 x 4.6 mm) column at a flow rate of 0.7 mL/min. Unless otherwise noted, all analytical runs used linear gradients of 30-100% buffer B in A (A: water containing 0.1% TFA, B: MeOH) over 70 min. CD Spectra were recorded on a Jasco J-815 Circular Dichroism Spectrometer. Unless otherwise noted, all CD spectra were recorded in MeOH at a concentration of 0.5 mmol, at 298 K, over a range of 300-200 nm, at a scan rate of 50 nm/min. Mass spectra were obtained using an ABI 4800 MALDI TOF/TOF instrument with 2,5-dihydroxybenzoic acid as the matrix in the positive ion mode. Lyophilization was accomplished using a Labconco FreeZone 4.5 liter benchtop freeze dry system.

Proton and carbon NMR spectra were recorded using a Bruker Avance spectrometer at 600 MHz/150 MHz (¹H NMR/¹³C NMR) in D₂O (298 K), unless otherwise noted. Chemical shifts (δ) are reported in parts per million (ppm) using MeOH solvent peaks as an internal reference (referenced to 3.34 ppm (¹H) and 49.5 ppm (¹³C)). ¹H NMR data are reported as

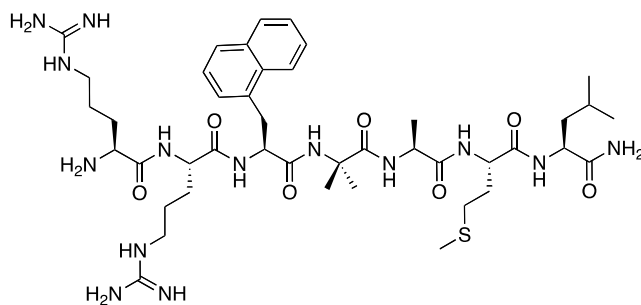
follows: chemical shift, multiplicity (s = singlet, d = doublet, t = triplet, q = quartet, m = multiplet, dd = doublet of doublets, dt = doublet of triplets, td = triplet of doublets, qd = quartet of doublets), coupling constants (J) in Hertz (Hz), and integration. ^{13}C NMR spectra were obtained using a proton-decoupled pulse sequence with d1 of 6 sec, and are tabulated by observed peak.

A stock solution of the coupling base was prepared by dissolving DIPEA (1.74 mL, 1.00 mmol) in DMF (5.00 mL) to give a 0.148 M solution. A stock solution of the Fmoc-cleavage base was prepared by dissolving piperidine (1.00 mL, 10.1 mmol) in DMF (4.00 mL) to give a 2.02 M solution. A stock solution of the resin cleavage cocktail was prepared by combining TFA (5.07 g, 44.5 mmol), PhSCH₃ (0.210 g, 1.69 mmol), PhOH (0.215 g, 2.28 mmol), TIPSH (0.0620 g, 0.392 mmol), 1,2-EDT (0.135 g, 1.43 mmol) and H₂O (0.100 g, 5.56 mmol). All stock solutions were freshly prepared prior to use.

4.8.1 General Procedure A: Solid Phase Peptide Synthesis.

To a polypropylene reaction vessel (25 mL) charged with a Teflon stir bar (10 x 3 mm) was added the Rink Amide resin (0.143 g, 0.100 mmol, loading 0.700 mmol/g, 1.00 equiv). The resin was washed with MeOH (2 x 5 mL), CH₂Cl₂ (3 x 10 mL) and DMF (3 x 10 mL), suspended in CH₂Cl₂ (5 mL) and allowed to swell at room temperature for 20 min. The resin was filtered and washed with DMF (3 x 10 mL). The reaction vessel was fitted with the fiber optic temperature probe and the Fmoc group was cleaved by heating the resin in the Fmoc-cleavage base stock solution (1 mL) in the microwave (35 W, 78 °C, 3 min). The resin was filtered and washed with DMF (3 x 10 mL), CH₂Cl₂ (3 x 10 mL) and DMF (3 x 10 mL). The first Fmoc protected amino acid was coupled to the resin by heating in a pre-mixed solution of amino acid (0.350 mmol, 3.50 equiv), DEPBT (0.105 g, 0.350 mmol, 3.50 equiv), DMF (0.800 mL), and Fmoc-coupling base stock solution (0.750 mL) in the microwave (25 W, 80 °C, 5 min). The resin was filtered and washed with DMF (3 x 10 mL), CH₂Cl₂ (3 x 10 mL) and DMF (3 x 10 mL). The Fmoc group was cleaved by heating the resin in Fmoc-cleavage base stock solution (1 mL) in the microwave (35 W, 78 °C, 3 min). The resin was filtered and washed with DMF (3 x 10 mL), CH₂Cl₂ (3 x 10 mL) and DMF (3 x 10 mL). The second Fmoc protected amino acid was

coupled to the resin by heating in a pre-mixed solution of amino acid (0.350 mmol, 3.50 equiv), DEPBT (0.105 g, 0.350 mmol, 3.50 equiv), DMF (0.800 mL), and Fmoc-coupling base stock solution (0.750 mL) in the microwave (25 W, 80 °C, 5 min). This process of Fmoc cleavage and amino acid coupling was repeated for each additional amino acid. After the final Fmoc cleavage, the resin was washed with DMF (30 mL) and CH₂Cl₂ (20 mL). The protecting groups were cleaved by treatment of the dry resin with the resin cleavage cocktail stock solution (2.50 mL) for 2 h at room temperature with vigorous stirring. The resin was filtered and rinsed with the remaining resin cleavage cocktail stock solution (1.50 mL) and TFA (1.50 mL), collecting the filtrate and rinses in a BD Falcon tube (50 mL). The sample was concentrated to a heterogeneous mixture (approximately 0.2 mL) under a stream of argon for 30 min. Cold diethyl ether (45 mL) was added to precipitate the crude peptide. The sample was centrifuged (3200 rpm, -8 °C, 15 min) and the supernatant was discarded. The crude peptide was transferred to a scintillation vial (20 mL) with approximately 5 mL of a mixture of H₂O/CH₃CN (9:1) and lyophilized overnight. The crude peptide was dissolved in H₂O containing 0.1% TFA (5.00 mL) and filtered through a 0.45 μm nylon syringe filter. The filtrate was purified by preparative RP HPLC.



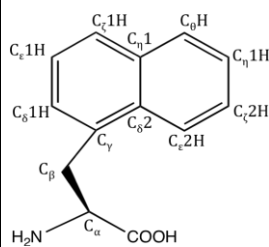
JTH-NB72-35

RR(1-Nal)(AIB)AML (JTH-NB72-35). Prepared according to general procedure A utilizing the following amino acid sequence: Fmoc-L-Leu-OH (0.124 g, 0.350 mmol, 3.50 equiv), Fmoc-L-Met-OH (0.130 g, 0.350 mmol, 3.50 equiv), Fmoc-L-Ala-OH (0.115 g, 0.350 mmol, 3.50 equiv), Fmoc-AIB-OH (0.114 g, 0.350 mmol, 3.50 equiv), Fmoc-L-1-Nal-OH (0.153 g, 0.350 mmol, 3.50 equiv), Fmoc-L-Arg(Pbf)-OH (0.227 g, 0.350 mmol, 3.50 equiv), Fmoc-L-Arg(Pbf)-OH (0.227 g, 0.350 mmol, 3.50 equiv). **JTH-NB72-35** (0.0399 g, 40%) was obtained as a white powder: The product was characterized by ¹H NMR (Table 31); ¹³C NMR (Table 31); DEPT-

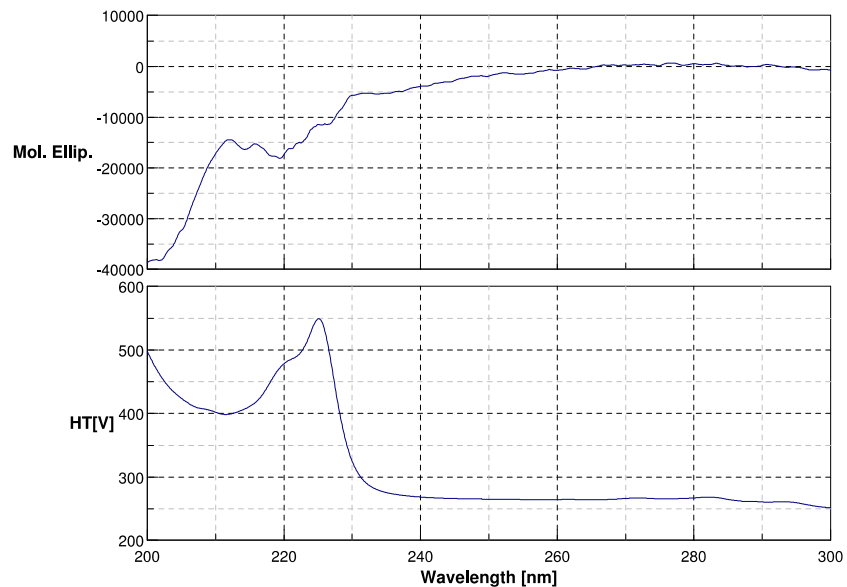
135; COSY; HMBC; HMQC; HPLC RT 5.7 min, HRMS (MALDI⁺) m/z calcd for C₄₃H₇₁N₁₄O₇S
[M+H]⁺ 927.5351, Found 927.5355.

Table 31. ¹H and ¹³C NMR Data for **JTH-NB72-35** (600 MHz/150 MHz) in D₂O (298 K) with MeOH as an internal reference (referenced to 3.34 ppm (¹H) and 49.5 ppm (¹³C)).

Residue #	Amino Acid (N->C)	Resonance	¹ H δ [ppm]	¹³ C δ [ppm]
1	Arginine	CO		169.7
		C _α H	3.97 (t, $J = 6.4$ Hz, 1 H)	53.1
		C _β H	1.86-1.76 (m, 2 H)	28.7
		C _γ H	1.51-1.42 (m, 2 H)	23.8
			3.03 (dt, $J = 6.3, 12.7$ Hz, 1 H),	
		C _δ H	3.00 (dt, $J = 6.3, 12.7$ Hz, 1 H)	41.0
2	Arginine	CO		173.3
		C _α H	4.35 (t, $J = 7.2$ Hz, 1 H)	53.8
		C _β H	1.72-1.62 (m, 2 H)	28.9
		C _γ H	1.62-1.53 (m, 2 H)	25.2
			3.14 (dt, $J = 6.7, 13.8$ Hz, 1 H),	
		C _δ H	3.1 (dt, $J = 6.7, 13.8$ Hz, 1 H)	41.2
3	3-(1-Naphthyl)-alanine	CO		172.7
		C _α H	4.73 (t, $J = 7.8$ Hz, 1 H)	55.2
			3.59 (dd, $J = 7.1, 14.1$ Hz, 1 H),	
		C _β H	3.50 (dd, $J = 8.6, 14.1$ Hz, 1 H)	34.5
		C _γ		132.7
		C _δ 1H	7.42 (d, $J = 6.9$ Hz, 1 H)	128.6
		C _δ 2		132.1
		C _ε 1H	7.48 (t, $J = 7.6$ Hz, 1 H)	126.4
		C _ε 2H	8.15 (d, $J = 8.5$ Hz, 1 H)	124.0
		C _ζ 1H	7.86 (d, $J = 8.2$ Hz, 1 H)	128.5
		C _ζ 2H	7.63 (t, $J = 7.6$ Hz, 1 H)	127.3
		C _η 1		134.2



		C _η 2H	7.57 (t, <i>J</i> = 7.5 Hz, 1 H)	126.8
		C _θ H	7.95 (d, <i>J</i> = 8.1 Hz, 1 H)	129.5
4	α-Aminoisobutyric acid	CO		177.7
		C _α		57.2
		C _β H	1.31 (s, 3 H), 1.28 (s, 3 H)	24.6, 25.0
5	Alanine	CO		176.2
		C _α H	4.22 (q, <i>J</i> = 7.3 Hz, 1 H)	51.1
		C _β H	1.38 (d, <i>J</i> = 7.3 Hz, 3 H)	16.8
6	Methionine	CO		174.3
		C _α H	4.35 (dd, <i>J</i> = 4.8, 9.6 Hz, 1 H)	52.8
		C _β H	2.12-1.95 (m, 2 H)	30.0
		C _γ H	2.57-2.45 (m, 2 H)	30.6
		C _δ H	2.02 (s, 3 H)	14.8
7	Leucine	CO		178
		C _α H	4.28 (dd, <i>J</i> = 3.9, 10.3 Hz, 1 H)	53.7
		C _β H	1.72-1.62 (m, 2 H)	40.2
		C _γ H	1.63-1.58 (m, 1 H)	24.6
			0.89 (d, <i>J</i> = 5.8 Hz, 3 H),	22.9
		C _δ H	0.83 (d, <i>J</i> = 5.7 Hz, 3 H)	21.0



Date 2/10/2009 5:24PM
 File name JTH_NB72_35_Standard_Subtracted_MeOH_Converted2Mol_ellip_Smoothed.jws
 Model J-815
 Serial No. A019361168
 Band width 1 nm
 Response 1 sec
 Sensitivity Standard
 Measurement range 300 - 200 nm
 Data pitch 0.1nm
 Scanning speed 50 nm/min
 Accumulation 1
 Cell Length 0.1 cm
 Concentration 0.0005 mol/L
 Temperature Room Temperature

Figure 57. CD spectrum of **JTH-NB72-35** (0.5 mmol) in MeOH.

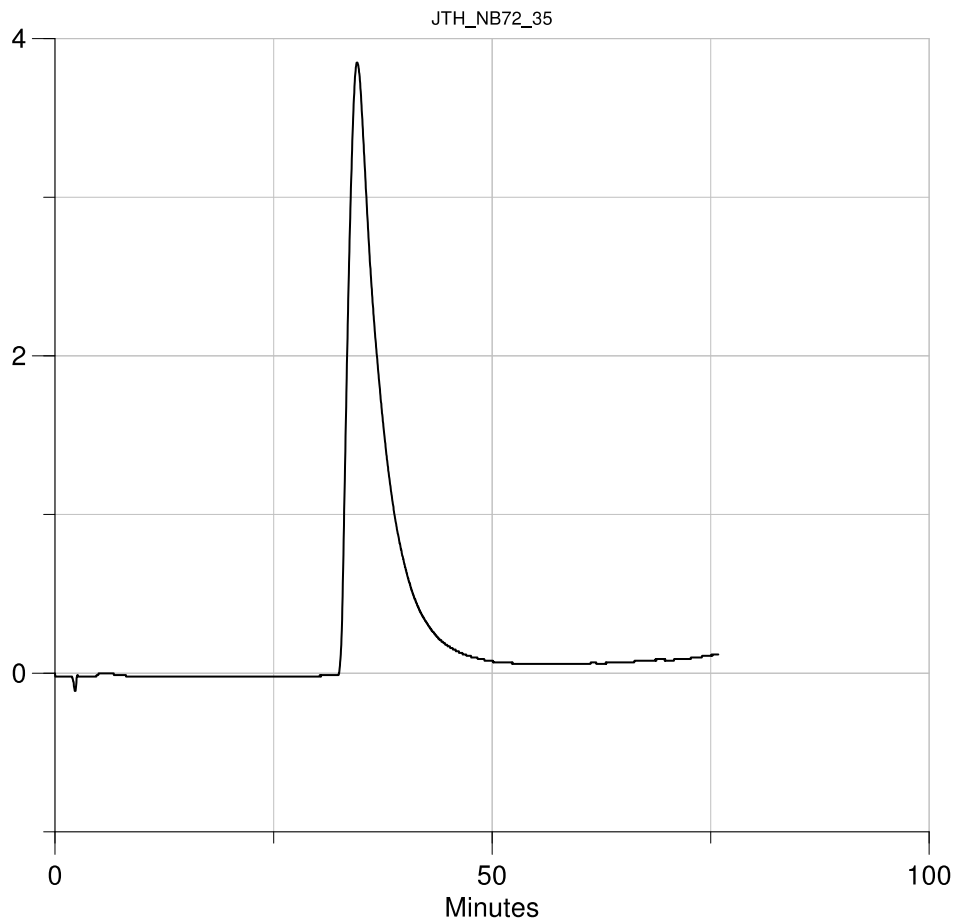
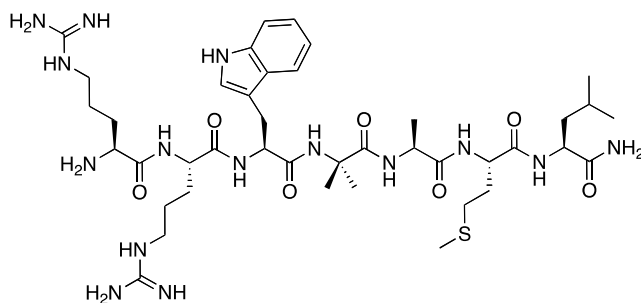


Figure 58. Analytical HPLC trace of **JTH-NB72-35** using a linear gradient of 30-100% buffer B in A (A: water containing 0.1% TFA, B: MeOH) over 70 min with UV detection at 220 nm.



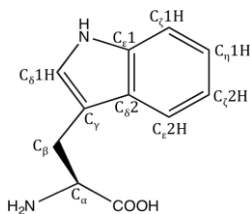
JTH-NB72-38

RRW(AIB)AML (JTH-NB72-38). Prepared according to general procedure A utilizing the following amino acid sequence: Fmoc-L-Leu-OH (0.124 g, 0.350 mmol, 3.50 equiv), Fmoc-L-Met-OH (0.130 g, 0.350 mmol, 3.50 equiv), Fmoc-L-Ala-OH (0.115 g, 0.350 mmol, 3.50 equiv), Fmoc-AIB-OH (0.114 g, 0.350 mmol, 3.50 equiv), Fmoc-L-Trp(Boc)-OH (0.185 g, 0.350 mmol, 3.50 equiv), Fmoc-L-Arg(Pbf)-OH (0.227 g, 0.350 mmol, 3.50 equiv), Fmoc-L-Arg(Pbf)-OH

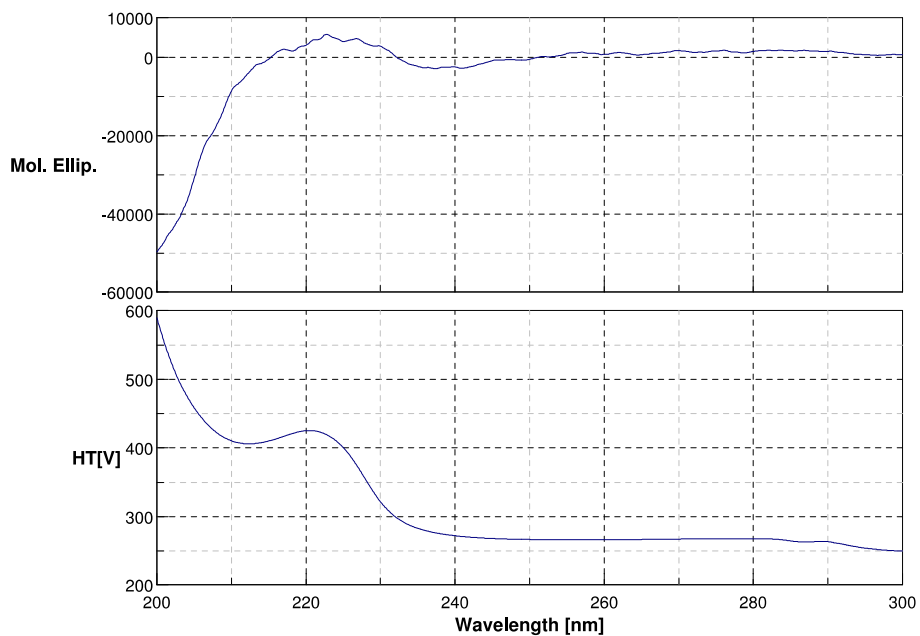
(0.227 g, 0.350 mmol, 3.50 equiv). **JTH-NB72-38** (0.0415 g, 41%) was obtained as a white powder: The product was characterized by ^1H NMR (Table 32); ^{13}C NMR (Table 32); DEPT-135; COSY; HMBC; HMQC; HPLC RT 5.7 min, HRMS (MALDI $^+$) m/z calcd for $\text{C}_{41}\text{H}_{70}\text{N}_{15}\text{O}_7\text{S}$ $[\text{M}+\text{H}]^+$ 916.5303, Found 916.5461.

Table 32. ^1H and ^{13}C NMR Data for **JTH-NB72-38** (600 MHz/150 MHz) in D_2O (298 K) with MeOH as an internal reference (referenced to 3.34 ppm (^1H) and 49.5 ppm (^{13}C)).

Residue #	Amino Acid (N->C)	Resonance	^1H δ ppm	^{13}C δ ppm
1	Arginine	CO		169.8
		C_αH	3.99 (t, $J = 6.5$ Hz, 1 H)	53.1
		C_βH	1.88-1.77 (m, 2 H)	28.7
		C_γH	1.52-1.42 (m, 2 H)	23.9
		C_δH	3.05 (dt, $J = 7.1, 13.5$ Hz, 1 H), 3.00 (dt, $J = 7.1, 13.6$ Hz, 1 H)	41.0
		C_ζ		157.2
2	Arginine	CO		173.3
		C_αH	4.40 (t, $J = 7.3$ Hz, 1 H)	53.8
		C_βH	1.75-1.64 (m, 2 H)	28.9
		C_γH	1.52-1.42 (m, 2 H)	25.1
		C_δH	3.15 (dt, $J = 6.8, 13.5$ Hz, 1 H), 3.11 (dt, $J = 6.9, 13.5$ Hz, 1 H)	41.2
		C_ζ		157.3
3	Tryptophan	CO		173.2
		C_αH	4.64 (t, $J = 7.5$ Hz, 1 H)	55.2
		C_βH	3.29 (dd, $J = 7.0, 14.6$ Hz, 1 H), 3.22 (dd, $J = 8.0, 14.7$ Hz, 1 H)	27.5
		C_γ		109.4
		$\text{C}_\delta\text{1H}$	7.26 (s, 1 H)	125
		$\text{C}_\delta\text{2}$		127.4
		C_ϵ		136.8
		$\text{C}_\epsilon\text{2H}$	7.66 (d, $J = 7.9$ Hz, 1 H)	119.1
		$\text{C}_\zeta\text{1H}$	7.48 (d, $J = 8.2$ Hz, 1 H)	112.5



		C _ε 2H	7.15 (t, <i>J</i> = 7.4 Hz, 1 H)	120.0
		C _η H	7.23 (t, <i>J</i> = 7.6 Hz, 1 H)	122.7
4	α-Aminoisobutyric acid	CO		178.0
		C _α		57.2
		C _β H	1.31 (s, 6 H)	24.7, 24.5
5	Alanine	CO		176.2
		C _α H	4.19 (q, <i>J</i> = 7.3 Hz, 1 H)	51.1
		C _β H	1.33 (d, <i>J</i> = 7.3 Hz, 3 H)	16.7
6	Methionine	CO		174.3
		C _α H	4.34 (dd, <i>J</i> = 9.3, 5.0 Hz, 1 H)	53.9
		C _β H	2.10-2.0 (m, 2 H)	30.7
		C _γ H	2.60-2.55 (m, 1 H), 2.53-2.49 (m, 1 H)	30.0
		C _δ H	2.05 (s, 3 H)	14.7
7	Leucine	CO		177.8
		C _α H	4.28 (dd, <i>J</i> = 10.5, 3.9 Hz, 1 H)	52.9
		C _β H	1.75-1.53 (m, 2 H)	40.2
		C _γ H	1.75-1.53 (m, 1 H)	25.1
			0.90 (d, <i>J</i> = 5.9 Hz, 3 H),	22.9
		C _δ H	0.84 (d, <i>J</i> = 5.9 Hz, 3 H)	21.0



Date 2/10/2009 8:09PM
 File name JTH_NB72_38_Standard_Mol_Elip_minus_MeOH_Smooth.jws
 Model J-815
 Serial No. A019361168
 Band width 1 nm
 Response 1 sec
 Sensitivity Standard
 Measurement range 300 - 200 nm
 Data pitch 0.1nm
 Scanning speed 50 nm/min
 Accumulation 1
 Cell Length 0.1 cm
 Concentration 0.0005 mol/L
 Temperature Room Temperature

Figure 59. CD spectrum of JTH-NB72-38 (0.5 mmol) in MeOH

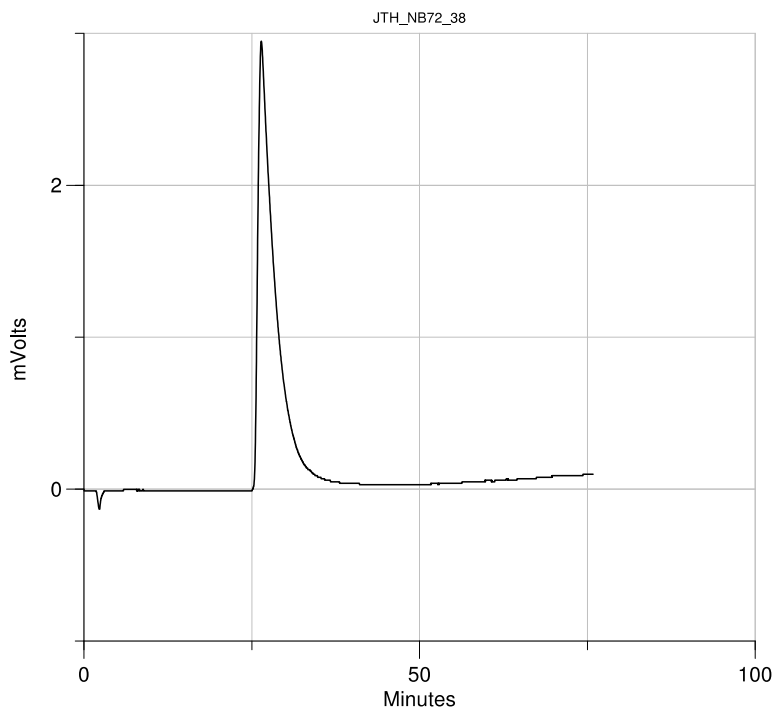
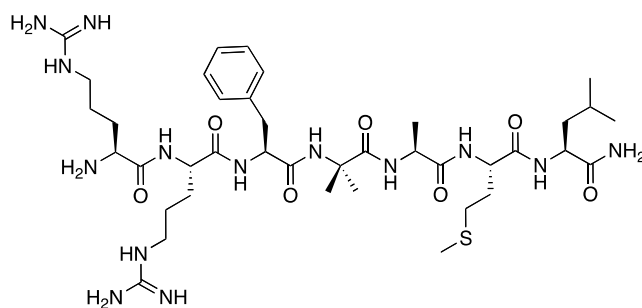


Figure 60. Analytical HPLC trace of **JTH-NB72-38** using a linear gradient of 30-100% buffer B in A (A: water containing 0.1% TFA, B: MeOH) over 70 min with UV detection at 220 nm at a flow rate of 0.7 mL/min.



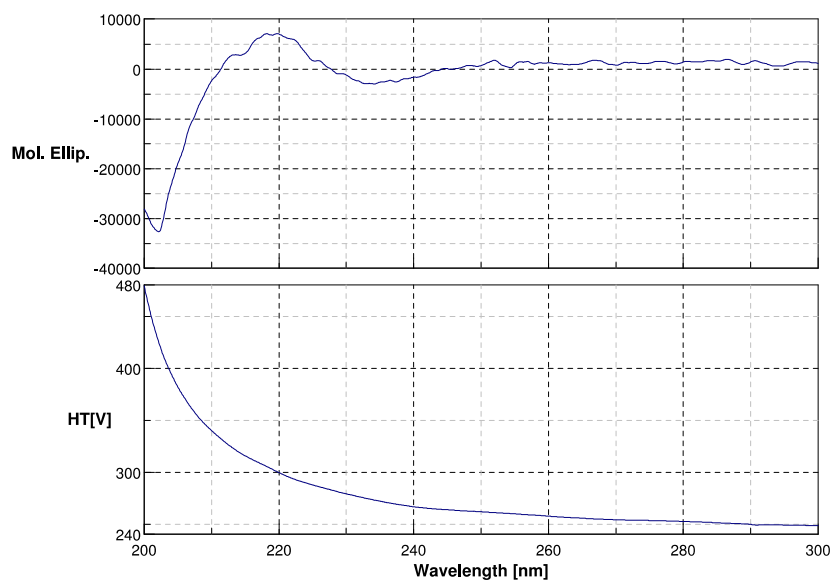
JTH-NB72-39

RRF(AIB)AML (JTH-NB72-39). Prepared according to general procedure A utilizing the following amino acid sequence: Fmoc-L-Leu-OH (0.124 g, 0.350 mmol, 3.50 equiv), Fmoc-L-Met-OH (0.130 g, 0.350 mmol, 3.50 equiv), Fmoc-L-Ala-OH (0.115 g, 0.350 mmol, 3.50 equiv), Fmoc-AIB-OH (0.114 g, 0.350 mmol, 3.50 equiv), Fmoc-L-Phe-OH (0.136 g, 0.350 mmol, 3.50 equiv), Fmoc-L-Arg(Pbf)-OH (0.227 g, 0.350 mmol, 3.50 equiv), Fmoc-L-Arg(Pbf)-OH (0.227 g, 0.350 mmol, 3.50 equiv). **JTH-NB72-39** (0.0318 g, 34%) was obtained as a white powder: The product was characterized by ^1H NMR (Table 33); ^{13}C NMR (Table 33); DEPT-135; COSY; HMBC; HMQC; HPLC RT 5.6 min, HRMS (MALDI $^+$) m/z calcd for $\text{C}_{39}\text{H}_{68}\text{N}_{14}\text{NaO}_7\text{S}$ $[\text{M}+\text{Na}]^+$ 899.5014, Found 899.5021.

Table 33. ^1H and ^{13}C NMR Data for **JTH-NB72-39** (600 MHz/150 MHz) in D_2O (298 K) with MeOH as an internal reference (referenced to 3.34 ppm (^1H) and 49.5 ppm (^{13}C)).

Residue #	Amino Acid (N->C)	Resonance	^1H δ [ppm]	^{13}C δ [ppm]
1	Arginine	CO		169.1
		C_αH	4.00 (t, $J = 6.5$ Hz, 1 H)	53.1
		C_βH	1.90-1.83 (m, 2 H)	29.0
		C_γH	1.60-1.47 (m, 2 H)	24.1
		C_δH	3.16 (t, $J = 6.8$ Hz, 2 H)	41.1
		C_ζ		157.3
2	Arginine	CO		173.3
		C_αH	4.29 (dd, $J = 7.5, 10.7$ Hz, 1 H)	53.9
		C_βH	1.77-1.65 (m, 2 H)	28.7
		C_γH	1.60-1.47 (m, 2 H)	25.1
		C_δH	3.16 (t, $J = 6.8$ Hz, 2 H)	41.2
		C_ζ		157.3
3	Phenylalanine	CO		172.8
		C_αH	4.55 (t, $J = 7.6$ Hz, 1 H)	55.7
		C_βH	3.11 (dd, $J = 7.0, 13.9$ Hz, 1 H), 3.05 (dd, $J = 8.3, 13.8$ Hz, 1 H)	37.5
		C_γ		136.7
		C_δH	7.36 (t, $J = 7.4$ Hz, 2 H)	129.4
		$\text{C}_\epsilon\text{H}$	7.28 (d, $J = 7.5$ Hz, 2 H)	130.0
		C_ζH	7.31 (t, $J = 7.4$ Hz, 1 H)	127.8
4	α -Aminoisobutyric acid	CO		178
		C_α		57.3
		C_βH	1.35 (s, 3 H), 1.34 (s, 3 H)	25.0, 24.3
5	Alanine	CO		176.1
		C_αH	4.22 (q, $J = 7.2$ Hz, 1 H)	51.0
		C_βH	1.37 (d, $J = 7.3$ Hz, 3 H)	16.8

6	Methionine	CO		174.2
		C _α H	4.39 (dd, <i>J</i> = 7.5, 9.3 Hz, 1 H)	52.9
		C _β H	2.18-1.99 (m, 2 H)	30.1
		C _γ H	2.65-2.51 (m, 2 H)	30.7
		C _δ H	2.10 (s, 3 H)	14.9
7	Leucine	CO		177.7
		C _α H	4.36 (t, <i>J</i> = 7.4 Hz, 1 H)	53.7
		C _β H	1.75-1.59 (m, 2 H)	40.3
		C _γ H	1.75-1.59 (m, 1 H)	25.0
		C _δ H	0.92 (d, <i>J</i> = 5.8 Hz, 3 H), 0.86 (d, <i>J</i> = 5.6 Hz, 3 H)	22.9, 21.0



Date 2/10/2009 9:18PM
 File name JTH_NB72_37_Standard_Sub_MeOH_Moll_ellip_Smooth.jws
 Model J-815
 Serial No. A019361168
 Band width 1 nm
 Response 1 sec
 Sensitivity Standard
 Measurement range 300 - 200 nm
 Data pitch 0.1nm
 Scanning speed 50 nm/min
 Accumulation 1
 Cell Length 0.1 cm
 Concentration 0.0003 mol/L
 Temperature Room Temperature

Figure 61. CD spectrum of **JTH-NB72-39** (0.5 mmol) in MeOH.

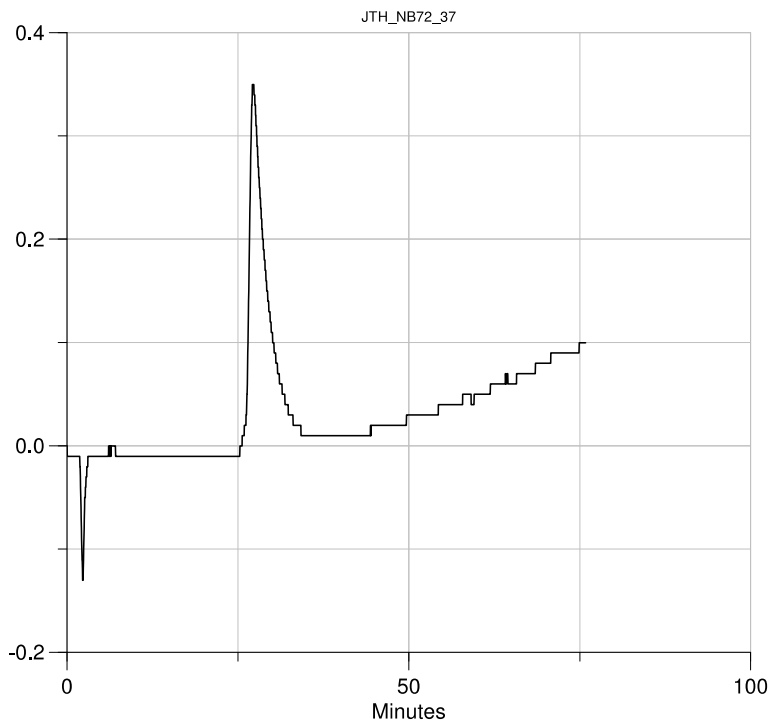
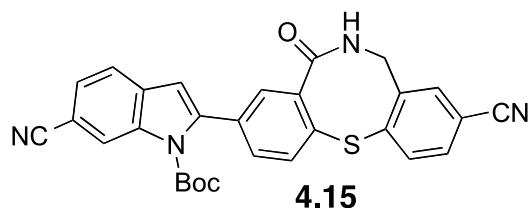


Figure 62. Analytical HPLC trace of **JTH-NB72-39** using a linear gradient of 30-100% buffer B in A (A: water containing 0.1% TFA, B: MeOH) over 70 min with UV detection at 220 nm at a flow rate of 0.7 mL/min.

4.9 EXPERIMENTAL FOR SMALL-MOLECULE INHIBITORS

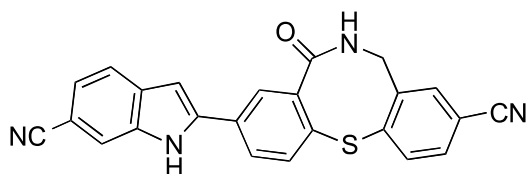
General. All moisture sensitive reactions were performed using syringe-septum techniques under an atmosphere of either dry nitrogen or dry argon unless otherwise noted. All glassware was dried in an oven at 140 °C for a minimum of 6 h or flame-dried under an atmosphere of dry nitrogen prior to use. Reactions carried out at -78 °C employed a CO_{2(s)}/acetone bath. Et₂O and tetrahydrofuran were dried by distillation over sodium/benzophenone under an argon atmosphere. Dry methylene chloride was purified by filtration through an activated alumina column. All degassed solvents were prepared using the freeze/pump/thaw method (3x). Methanol, acetonitrile, and *N,N*-dimethylformamide were stored over molecular sieves (3Å). Deuterated chloroform was stored over anhydrous potassium carbonate. Reactions were monitored by TLC analysis (pre-coated silica gel 60 F₂₅₄ plates, 250 μm layer thickness) and

visualized by using UV lamp (254 nm) or by staining with either Vaughn's reagent (4.8 g of $(\text{NH}_4)_6\text{Mo}_7\text{O}_{24}\cdot 4 \text{H}_2\text{O}$ and 0.2 g of $\text{Ce}(\text{SO}_4)_2$ in 100 mL of a 3.5 N H_2SO_4) or a potassium permanganate solution (1.5 g of KMnO_4 and 1.5 g of K_2CO_3 in 100 mL of a 0.1% NaOH solution). Flash column chromatography was performed with 40-63 μm silica gel (Silicycle). Microwave reactions were performed on a Biotage Initiator microwave reactor. Infrared spectra were measured on a Smiths Detection IdentifyIR FT-IR spectrometer (ATR). Unless otherwise indicated, all NMR data was collected at room temperature in CDCl_3 , $(\text{CD}_3)_2\text{SO}$, or $(\text{CD}_3)_2\text{CO}$ on a 300, 400, 500, 600, or 700 MHz Bruker instrument. Chemical shifts (δ) are reported in parts per million (ppm) with internal CHCl_3 (δ 7.26 ppm for ^1H and 77.00 ppm for ^{13}C), internal acetone (δ 2.05 ppm for ^1H and 29.85 ppm for ^{13}C), or internal DMSO (δ 2.50 ppm for ^1H and 39.52 for ^{13}C) as the reference. ^1H NMR data are reported as follows: chemical shift, multiplicity (s = singlet, bs = broad singlet, d = doublet, t = triplet, q = quartet, m = multiplet, dd = doublet of doublets, dt = doublet of triplets, td = triplet of doublets, qd = quartet of doublets, sep = septet), integration, and coupling constant(s) (J) in Hertz (Hz). HRMS analyses were obtained using either a Q-TOF Ultima API, Micromass UK Limited (ESI) or a VG Autospec, FISIONS instrument (EI).



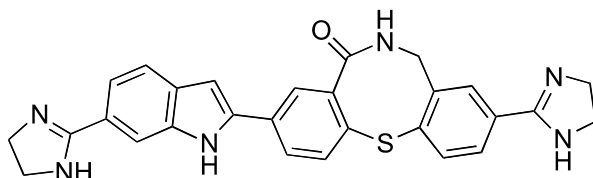
***tert*-Butyl-6-cyano-2-(9-cyano-5-oxo-6,7-dihydro-5H-dibenzo[*b,g*][1,5]thiazocin-3-yl)-1H-indole-1-carboxylate (4.15).** To a stirred solution of **4.13** (0.250 g, 0.724 mmol, 1 equiv) and **4.14** (0.352 g, 0.869 mmol, 1.2 equiv) in sparged (30 min) DMA (3 mL) at rt was added $\text{Pd}(\text{Ph}_3\text{P})_2\text{Cl}_2$ (0.0254 g, 0.0362 mmol, 0.05 equiv) and $(\text{IPr})\text{CuCl}$ (0.0265 g, 0.0543 mmol, 0.075 equiv). The reaction was heated to 80 °C and monitored by TLC. Upon completion of the reaction (22 h), the reaction was diluted with ethyl acetate (100 mL), washed with water (x2), brine, dried (Na_2SO_4), filtered, and concentrated under reduced pressure. The crude residue was purified by chromatography on SiO_2 (acetone/ CH_2Cl_2 , 5:95) to give **4.15** (0.195 g, 43%) as a pale yellow solid: Mp 215 °C (decomp.); IR (ATR): 3176, 3057, 2982, 2937, 2222, 1737, 1655, 1474, 1424, 1316, 1297, 1226 cm^{-1} ; ^1H NMR (400 MHz, DMSO) δ 8.50-8.45 (m, 1 H), 8.48-

8.42 (m, 1 H), 7.90-7.65 (m, 8 H), 7.07-7.02 (m, 1 H), 4.22 (bs, 2 H), 1.33 (s, 9 H); ^{13}C NMR (125 MHz, DMSO) δ 170.8, 148.6, 142.1, 141.6, 139.9, 137.1, 136.4, 136.0, 135.8, 134.1, 132.1, 131.7, 131.7, 130.7, 127.3, 126.2, 124.2, 122.3, 119.7, 119.0, 118.2, 110.9, 109.5, 106.4, 85.3, 45.0, 26.9. Note: characterization taken from Igor Opsenica's final postdoctoral report.



4.16

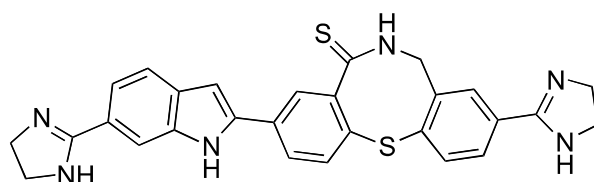
9-(6-Cyano-1H-indol-2-yl)-7-oxo-6,7-dihydro-5H-dibenzo[b,g][1,5]thiazocine-3-carbonitrile (4.16). To a solution of **4.15** (0.180 g, 0.355 mmol, 1 equiv) in degassed CH_2Cl_2 (3.5 mL) at rt was added TFA (0.792 mL, 10.7 mmol, 30 equiv). The reaction was stirred at rt for 14 h, poured onto a saturated aqueous solution of NaHCO_3 , and extracted with EtOAc (600 mL). The organic layer was washed with brine, dried (Na_2SO_4), filtered, and concentrated under reduced pressure to give **4.16** (0.144 g, 100%) as a white solid. The crude reaction mixture was directly used in next reaction: Mp >250 $^\circ\text{C}$; IR (ATR): 3334, 2231, 2209, 1650, 1618, 1594, 1472, 1452, 1418, 1385, 1355, 1340, 1320, 1282 cm^{-1} ; ^1H NMR (400 MHz, DMSO) δ 12.39 (s, 1 H), 8.50-8.45 (m, 1 H), 8.16-8.10 (m, 2 H), 7.90-7.88 (m, 1 H), 7.84 (d, $J = 8.0$ Hz, 1 H), 7.79-7.72 (m, 3 H), 7.69 (d, $J = 8.0$ Hz, 1 H), 7.38 (dd, 1 H, $J = 8.4, 1.2$ Hz), 7.33-7.30 (m, 1 H), 4.25-4.20 (m, 2 H); ^{13}C NMR (100 MHz, DMSO) δ 171.0, 143.2, 140.1, 139.7, 137.2, 136.9, 136.2, 134.2, 134.2, 131.7, 131.5, 130.5, 128.3, 123.9, 123.8, 122.4, 121.6, 120.5, 118.2, 116.2, 109.5, 103.5, 101.5, 45.1. Note: characterization taken from Igor Opsenica's final postdoctoral report.



4.3

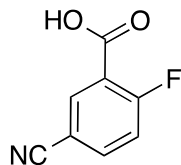
9-(4,5-Dihydro-1H-imidazol-2-yl)-3-(6-(4,5-dihydro-1H-imidazol-2-yl)-1H-indol-2-yl)-6,7-dihydro-5H-dibenzo[b,g][1,5]thiazocin-5-one (4.3). To a stirred solution of **4.16** (0.0800 g, 0.197 mmol, 1 equiv) in ethylenediamine (2 mL) was added sulfur (0.126 g, 0.394 mmol, 2

equiv) in one portion. The reaction was irradiated in the microwave (110 °C, 80 min), poured onto water, filtered, and the resulting solid was washed with water and toluene to give **4.3** (0.050 g, 52% yield) as a brown solid: Mp >250 °C; IR (ATR): 3258, 2932, 2863, 1636, 1599, 1554, 1443, 1334, 1273 cm⁻¹; ¹H NMR (400 MHz, DMSO) δ 12.00 (s, 1 H), 8.50-8.44 (m, 1 H), 8.10-8.05 (m, 2 H), 7.92-7.88 (m, 1 H), 7.81-7.77 (m, 1 H), 7.73-7.70 (m, 1 H), 7.67-7.64 (m, 1 H), 7.60-7.55 (m, 2 H), 7.54 (d, *J* = 8.0 Hz, 1 H), 7.17 (s, 1 H), 4.20 (bs, 2 H), 3.65 (s, 4 H), 3.60 (s, 4 H), 3.36 (bs, 2 H); ¹³C NMR (125 MHz, DMSO) δ 171.2, 164.6, 162.6, 143.5, 137.6, 136.9, 136.7, 135.7, 135.5, 134.5, 129.9, 129.6, 129.5, 129.4, 127.6, 126.7, 124.4, 123.8, 123.2, 119.9, 119.2, 110.6, 100.9, 49.3, 45.9; HRMS (ESI) *m/z* calcd for C₂₈H₂₅N₆OS [M+H]⁺ 493.1811, found 493.1828. LC-MS Purity: >95%. Note: characterization taken from Igor Opsenica's final postdoctoral report.



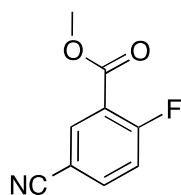
4.4

9-(4,5-Dihydro-1H-imidazol-2-yl)-3-(6-(4,5-dihydro-1H-imidazol-2-yl)-1H-indol-2-yl)-6,7-dihydro-5H-dibenzo[*b,g*][1,5]thiazocine-5-thione (4.4). To a stirred solution of **4.3** (0.0220 g, 0.0447 mmol, 1 equiv) in distilled pyridine (4 mL) was added P₄S₁₀ (0.198 g, 0.447 mmol, 10 equiv). The reaction was stirred at 120 °C for 1 h, Dimethyl sulfone (12 g) was added and stirring was continued overnight at 120 °C. The reaction mixture was cooled to rt, aqueous NaHCO₃ was added, and the yellow solution was stirred 3 h at rt. The resulting precipitate was filtered, washed with water (30 mL), toluene (20 mL), CH₂Cl₂ (20 mL), and THF (20 mL) to give **4.4** (0.022 g, 97%) as a yellow solid: Mp = >260 °C; IR (neat) 3105, 2974, 1597, 1545, 1366, 1137, 1012, 701; ¹H NMR (700 MHz, DMSO) δ 12.22 (s, 1 H), 10.85 (s, 1 H), 8.07 (s, 2 H), 7.98 (s, 1 H), 7.75-7.66 (m, 4 H), 7.55 (bs, 2 H), 7.19 (s, 1 H), 4.34 (bs, 2 H), 3.80 (s, 4 H), 3.60 (s, 4 H); ¹³C NMR (176 MHz, DMSO) δ 200.3, 165.2, 162.5, 148.6, 139.0, 136.8, 136.7, 136.2, 134.1, 133.3, 131.3, 130.0, 129.6, 129.0, 127.8, 127.0, 124.1, 121.9, 120.4, 119.2, 111.7, 101.1, 67.0, 50.3; HRMS (ESI⁺) *m/z* calcd for C₂₈H₂₅N₆S₂ [M+H]⁺ 509.1577, found 509.1563.



4.17

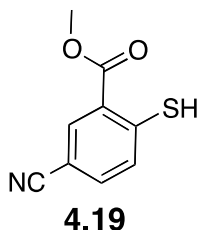
Methyl 5-cyano-2-fluorobenzoate (4.17). To a stirred solution of 5-cyano-2-fluorobenzoic acid (15.0 g, 89.0 mmol, 1 equiv) in MeOH (125 mL) was added 96% H₂SO₄ (4.96 mL, 89.0 mmol, 1 equiv). The reaction mixture was stirred at reflux overnight, the solvent was evaporated, and the crude residue was diluted with water (100 mL) and EtOAc (150 mL). The aqueous layer was separated and extracted with EtOAc (2 x 50 mL). The combined organic phases were washed with a saturated aqueous solution of NaHCO₃ (2 x 100 mL), dried (Na₂SO₄), filtered, and concentrated under reduced pressure to give **4.17** (15.0 g, 94%) as a white solid. The crude product was carried onto the next reaction without further purification: Mp 76-77 °C; IR (ATR): 3116, 3088, 3068, 3059, 3021, 2962, 2237, 1724, 1715, 1607, 1491, 1444, 1435, 1407, 1308, 1288, 1252, 1236, 1198, 1187, 1174, 1141, 1092, 982, 937, 842 cm⁻¹; ¹H NMR (400 MHz, CDCl₃) δ 8.30 (dd, 1 H, *J* = 6.4, 2.0 Hz), 7.83 (ddd, 1 H, *J* = 8.4, 4.0, 2.0 Hz), 7.29 (dd, 1 H, *J* = 9.6, 8.8 Hz), 3.98 (s, 3 H); ¹³C NMR (100 MHz, CDCl₃) δ 164.0 (d, *J* = 268 Hz), 162.8 (d, *J* = 4 Hz), 137.9 (d, *J* = 10 Hz), 136.8 (d, *J* = 2 Hz), 120.2 (d, *J* = 11 Hz), 118.7 (d, *J* = 24 Hz), 117.0, 108.9 (d, *J* = 4 Hz), 52.9; HRMS (ESI) *m/z* calcd for C₉H₇FNO₂ [M+H]⁺ 180.0461, found 180.0434. Note: characterization taken from Igor Opsenica's final postdoctoral report.



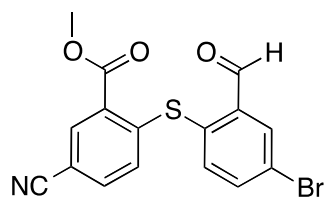
4.18

Methyl 5-cyano-2-mercaptopbenzoate (4.18). To a stirred solution of thioacetic acid (6.82 mL, 93.5 mmol, 2.5 equiv) in dry DMF (130 mL) at rt was added cesium carbonate (30.8 g, 93.5 mmol, 2.5 equiv). After 10 min, a solution of the **4.17** (6.7 g, 37.4 mmol, 1 equiv) in dry DMF (40 mL) was added dropwise (over the course of 45 min using a syringe pump) and the reaction mixture was stirred at rt for 14 h. The reaction mixture was diluted with H₂O (300 mL), carefully adjusted to a pH~1.0 with conc. HCl (~14 mL) and stirred at rt for 10 min. The

aqueous layer was extracted with EtOAc (300 mL x 3) and the combined organic layers were dried (MgSO₄), filtered, and concentrated under reduced pressure. The crude mixture was purified by chromatography on SiO₂ (EtOAc/hexanes, 2:8 to 3:7) to give **4.18** (3.06 g, 34%) as a brown solid: Mp 114-115 °C; IR (ATR): 3098, 3059, 2954, 2473, 2227, 1715, 1690, 1597, 1543, 1469, 1431, 1316, 1247, 1213, 1195, 1111, 1059, 964, 898, 889, 848, 839, 781 cm⁻¹; ¹H NMR (500 MHz, CDCl₃) δ 8.32 (d, 1 H, *J* = 2.0 Hz), 7.54 (dd, 1 H, *J* = 8.0, 2.0 Hz), 7.42 (d, 1 H, *J* = 8.0 Hz), 5.19 (s, 1 H), 3.97 (s, 3 H); ¹³C NMR (125 MHz, CDCl₃) δ 165.5, 145.7, 135.5, 134.3, 131.5, 126.2, 117.7, 108.4, 52.8; HRMS (ESI) *m/z* calcd for C₉H₈NO₂S [M+H]⁺ 194.0276, found 194.0268. Note: characterization taken from Igor Opsenica's final postdoctoral report.

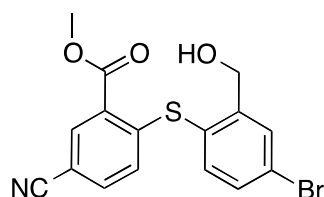


Methyl 5-cyano-2-mercaptobenzoate (4.19). To a stirred solution of thioacetic acid (6.82 mL, 93.5 mmol, 2.5 equiv) in dry DMF (130 mL) at rt was added cesium carbonate (30.8 g, 93.5 mmol, 2.5 equiv). After stirring at rt for 10 min, a solution of the **4.18** (6.7 g, 37.4 mmol, 1 equiv) in dry DMF (40 mL) was added dropwise (over 45 min using a syringe pump) and the reaction mixture was stirred at rt for 14 h. The reaction mixture was diluted with H₂O (300 mL), the pH was carefully adjusted to a ~1.0 with conc. HCl (~14 mL) and stirred at rt for 10 min. The mixture was extracted with EtOAc (300 mL x 3) and the combined organic layers were dried (MgSO₄), filtered, and concentrated under reduced pressure. The crude mixture was purified by chromatography on SiO₂ (EtOAc/hexanes, 2:8 to 3:7) to give **4.19** (3.06 g, 34%) as a brown solid: Mp 114-115 °C; IR (ATR): 3098, 3059, 2954, 2473, 2227, 1715, 1690, 1597, 1543, 1469, 1431, 1316, 1247, 1213, 1195, 1111, 1059, 964, 898, 889, 848, 839, 781 cm⁻¹; ¹H NMR (500 MHz, CDCl₃) δ 8.32 (d, 1 H, *J* = 2.0 Hz), 7.54 (dd, 1 H, *J* = 8.0, 2.0 Hz), 7.42 (d, 1 H, *J* = 8.0 Hz), 5.19 (s, 1 H), 3.97 (s, 3 H); ¹³C NMR (125 MHz, CDCl₃) δ 165.5, 145.7, 135.5, 134.3, 131.5, 126.2, 117.7, 108.4, 52.8; HRMS (ESI) *m/z* calcd for C₉H₈NO₂S [M+H]⁺ 194.0276, found 194.0268. Note: characterization taken from Igor Opsenica's final postdoctoral report.



4.21

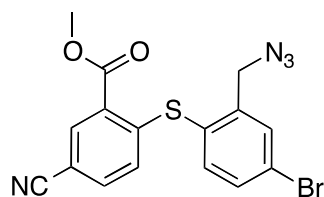
Methyl 2-((4-bromo-2-formylphenyl)thio)-5-cyanobenzoate (4.21). To a stirred solution of **4.19** (0.200 g, 1.04 mmol, 1 equiv) and 5-bromo-2-fluorobenzaldehyde (0.147 mL, 1.24 mmol, 1.2 equiv) in degassed CH₃CN (3 mL) was added TMG (0.156 mL, 1.24 mmol, 1.2 equiv). The reaction mixture was stirred overnight (~16 h) at 70 °C, cooled to rt, and diluted with EtOAc. The organic layer was washed with 1 M aqueous HCl, saturated aqueous NaHCO₃, dried (MgSO₄), filtered, and concentrated under reduced pressure. The crude mixture was purified by chromatography on SiO₂ (EtOAc/hexanes, 2:8) to give **4.21** (0.23 g, 80% pure; 47%) as a foam: IR (ATR): 3072, 3001, 2950, 2852, 2227, 1713, 1689, 1594, 1569, 1547, 1461, 1456, 1433, 1377, 1308, 1284, 1243, 1195, 1182, 1107, 1083, 1042, 973, 893, 874, 826 cm⁻¹; ¹H NMR (400 MHz, CDCl₃) δ 10.35 (s, 1 H), 8.34 (d, 1 H, *J* = 1.6 Hz), 8.21 (d, 1 H, *J* = 2.4 Hz), 7.84 (dd, 1 H, *J* = 8.4, 2.0 Hz), 7.52 (d, 1 H, *J* = 8.0 Hz), 7.50 (dd, 1 H, *J* = 8.4, 2.0 Hz), 6.72 (d, 1 H, *J* = 8.8 Hz), 4.02 (s, 3 H); ¹³C NMR (100 MHz, CDCl₃) δ 189.8, 164.8, 148.4, 139.1, 139.0, 138.3, 135.1, 135.1, 132.8, 132.7, 127.6, 127.0, 126.0, 117.4, 108.9, 53.0; HRMS (ESI) *m/z* calcd for C₁₆H₁₀BrNO₃S [M]⁺ 374.9565, found 374.9602. Note: characterization taken from Igor Opsenica's final postdoctoral report.



4.22

Methyl 2-((4-bromo-2-(hydroxymethyl)phenyl)thio)-5-cyanobenzoate (4.22). To a stirred solution of **4.19** (impure from last reaction; 1.00 g, 2.66 mmol, 1 equiv) in dry MeOH (30 mL) was added NaBH₄ (0.201 mg, 5.32 mmol, 2 equiv). The reaction mixture was stirred at rt for 2 h, the solvent was removed and the residue was diluted with EtOAc. The organic layer was washed with 1M aqueous HCl, brine, dried (NaSO₄), filtered, and concentrated under reduced pressure. The crude mixture was purified by chromatography on SiO₂ (EtOAc/hexanes, 8:2) to

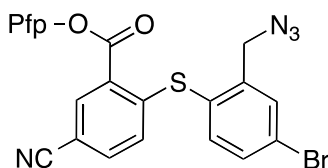
give **4.22** (0.780 g, 78% yield) as a slightly off-white foam: IR (ATR): 3493, 3424, 3079, 2949, 2921, 2848, 2229, 1715, 1594, 1575, 1551, 1461, 1435, 1310, 1282, 1245, 1197, 1107, 1085, 1060, 1048, 1034, 975, 852 cm^{-1} ; ^1H NMR (400 MHz, CDCl_3) δ 8.32 (d, 1 H, $J = 1.6$ Hz), 7.90-7.86 (m, 1 H), 7.55 (dd, 1 H, $J = 8.4, 2.0$ Hz), 7.45 (dd, 1 H, $J = 8.4, 2.0$ Hz), 7.41 (d, 1 H, $J = 8.4$ Hz), 6.69 (d, 1 H, $J = 8.8$ Hz), 4.72 (d, 2 H, $J = 5.6$ Hz), 4.01 (s, 3 H), 2.10-2.00 (m, 1 H); ^{13}C NMR (100 MHz, CDCl_3) δ 165.0, 149.0, 147.3, 138.6, 135.1, 134.8, 132.3, 131.9, 126.6, 126.6, 126.0, 117.7, 108.2, 62.4, 52.8; ^{13}C NMR (125 MHz, CDCl_3) δ 165.0, 149.0, 147.3, 138.6, 135.1, 134.8, 132.3, 131.9, 126.8, 126.7, 126.0, 117.7, 108.2, 62.4, 52.8; HRMS (ESI) m/z calcd for $\text{C}_{16}\text{H}_{12}\text{BrNO}_3\text{S}$ $[\text{M}]^+$ 376.9721, found 376.9762. Note: characterization taken from Igor Opsenica's final postdoctoral report.



4.23

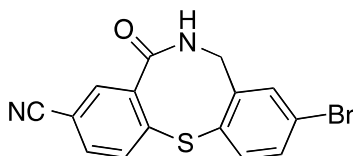
Methyl 2-((2-(azidomethyl)-4-bromophenyl)thio)-5-cyanobenzoate (4.23). To a stirred solution of the **4.22** (0.760 g, 2.01 mmol, 1 equiv) in CH_2Cl_2 (30 mL) at 0 °C was added triethylamine (0.570 mL, 4.02 mmol, 2 equiv) and methanesulfonyl chloride (0.234 mL, 3.01 mmol, 1.5 equiv). The reaction mixture was stirred at 0 °C for 10 min, warmed to rt, and stirred for 1 h. The reaction mixture was diluted with CH_2Cl_2 , washed with brine, and the aqueous layer was extracted with CH_2Cl_2 . The combined organic layers were dried (Na_2SO_4), filtered, and concentrated under reduced pressure to give a slight off-white solid. The crude mesylate was dissolved in DMF (5 mL) and sodium azide (0.660 g, 9.91 mmol, 5 equiv) was added. The reaction mixture was stirred at rt for 1.5 h, diluted with EtOAc, washed with brine, dried (Na_2SO_4) and concentrated under reduced pressure. The crude mixture was purified by chromatography on SiO_2 (EtOAc/hexanes, 15:85) to give **4.23** (0.746 g, 92%) as a yellow oil: IR (ATR): 2950, 3094, 3074, 2229, 2101, 1715, 1596, 1577, 1551, 1461, 1435, 1387, 1338, 1308, 1284, 1245, 1195, 1107, 1088, 1053, 1044, 826, 783 cm^{-1} ; ^1H NMR (400 MHz, CDCl_3) δ 8.34 (d, 1 H, $J = 2.0$ Hz), 7.79-7.76 (m, 1 H), 7.61 (dd, 1 H, $J = 8.0, 2.0$ Hz), 7.50-7.45 (m, 2 H), 6.64 (d, 1 H, $J = 8.4$ Hz), 4.51 (s, 2 H), 4.02 (s, 3 H); ^{13}C NMR (100 MHz, CDCl_3) δ 164.9, 148.8,

142.5, 139.1, 135.2, 134.9, 133.1, 133.1, 128.2, 126.7, 126.6, 126.0, 117.7, 108.4, 52.9, 52.2; HRMS (ESI) m/z calcd for $C_{16}H_{12}BrN_2O_2S$ ($M-N_2+H$) 374.9803, found 374.9835. Note: characterization taken from Igor Opsenica's final postdoctoral report.



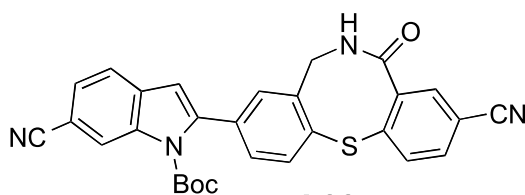
4.24

Perfluorophenyl 2-((2-(azidomethyl)-4-bromophenyl)thio)-5-cyanobenzoate (4.24). To a stirred solution of **4.23** (0.900 g, 2.23 mmol, 1 equiv) in MeOH/THF (1:1, 50 mL) was added 1M aqueous NaOH (23 mL). The solution was stirred at rt for 4 h and concentrated under reduced pressure. The remaining aqueous solution was acidified (pH~2) with 1M aqueous HCl, extracted with EtOAc (100 mL), dried (Na_2SO_4), and concentrated under reduced pressure. To a stirred solution of crude acid (0.800 g, 2.06 mmol, 1 equiv) in CH_2Cl_2 (125 mL) at 0 °C was added EDCI (0.591 g, 3.08 mmol, 1.5 equiv), Pfp-OH (0.378 g, 2.05 mmol, 1 equiv), and DMAP (0.00254 g, 0.206 mmol, 0.1 equiv). The mixture was warmed to rt, stirred for 2 h, poured onto water and extracted with CH_2Cl_2 . The organic layer was washed with brine, dried (Na_2SO_4), and concentrated under reduced pressure. The crude mixture was purified by chromatography on SiO_2 (EtOAc/hexanes, 1:9) to give **4.24** (0.71 g, 62%): IR (ATR): 2231, 2106, 1754, 1519, 1459, 1294, 1286, 1228, 1182, 1087, 1077, 1031, 1008, 995, 986 cm^{-1} ; 1H NMR (400 MHz, $CDCl_3$) δ 8.59 (d, 1 H, $J = 2.0$ Hz), 7.82-7.78 (m, 1 H), 7.64 (dd, 1 H, $J = 8.4, 2.0$ Hz), 7.61 (dd, 1 H, $J = 8.8, 2.0$ Hz), 7.50 (d, 1 H, $J = 8.4$ Hz), 6.75 (d, 1 H, $J = 8.4$ Hz), 4.52 (s, 2 H); ^{19}F NMR (376 MHz, $CDCl_3$) δ -152.4 (d, $J = 19$ Hz), -156.9 (t, $J = 23$ Hz), -162.0 (t, $J = 19$ Hz); ^{13}C NMR (125 MHz, $CDCl_3$) δ 160.2, 151.1, 142.6, 142.3 (m, C-F coupling), 141.0 (m, C-F coupling), 140.3 (m, C-F coupling), 139.1, 139.0 (C-F coupling), 137.0 (m, C-F coupling), 136.2, 136.2, 133.4, 133.4, 127.2, 127.1, 126.5, 124.6 (m, C-F coupling), 123.3, 117.2, 108.9, 52.3; HRMS (ESI) m/z calcd for $C_{21}H_9BrF_5N_4O_2S$ $[M+H]^+$ 554.9550, found 554.9520. Note: characterization taken from Igor Opsenica's final postdoctoral report.



4.25

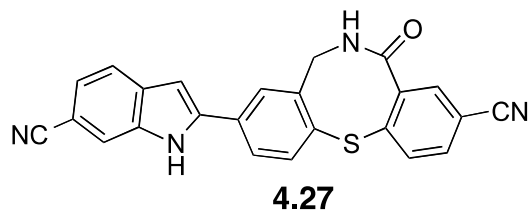
9-Bromo-5-oxo-6,7-dihydro-5H-dibenzo[*b,g*][1,5]thiazocine-3-carbonitrile (4.25). To a stirred solution of **4.24** (0.700 g, 1.26 mmol, 1 equiv) in CH₃CN/H₂O (4:1, 80 mL) at rt was added PPh₃ (0.401 g, 1.51 mmol, 1.2 equiv). The mixture was stirred at 50 °C for 6 h, filtered, and the solid product separated. The filtrate was diluted with EtOAc (100 mL), washed with brine, dried (Na₂SO₄), filtered, and concentrated under reduced pressure. The crude mixture was purified by chromatography on SiO₂ (acetone/CH₂Cl₂, 5:95) to give 0.125 g as a white solid which was combined with the filtered product (85 mg) to give **4.25** (0.21 g, 48% yield) as a white solid: Mp >250 °C; IR (ATR): 3290, 3277, 3202, 3081, 2930, 2229, 1653, 1594, 1452, 1416, 1366, 1342, 1284, 1269, 1202, 1184, 1102, 1087, 1046, 958, 900 cm⁻¹; ¹H NMR (400 MHz, DMSO) δ 8.55-8.48 (m, 1 H), 8.06-8.01 (m, 2 H), 7.92-7.88 (m, 1 H), 7.55-7.42 (m, 3 H), 4.15-4.05 (m, 2 H); ¹³C NMR (125 MHz, DMSO) δ 169.7, 143.9, 138.4, 137.1, 135.1, 133.4, 132.3, 131.5, 131.2, 130.6, 130.4, 120.6, 117.6, 114.2, 44.9; HRMS (ESI) *m/z* calcd for C₁₅H₉BrN₂OS [M]⁺ 343.9619, found 343.9645. Note: characterization taken from Igor Opsenica's final postdoctoral report.



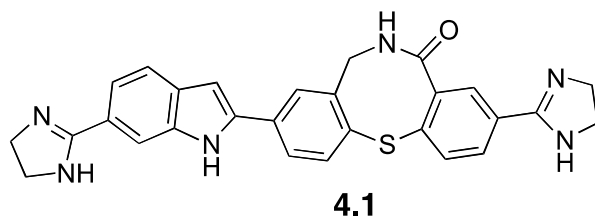
4.26

tert-Butyl 6-cyano-2-(9-cyano-7-oxo-6,7-dihydro-5H-dibenzo[*b,g*][1,5]thiazocin-3-yl)-1H-indole-1-carboxylate (4.26). To a stirred solution of **4.25** (0.120 g, 0.348 mmol, 1 equiv) and **4.8** (0.169 g, 0.417 mmol, 1.2 equiv) in degassed DMA (1.5 mL) at rt was added Pd(Ph₃P)₂Cl₂ (0.0122 g, 0.0174 mmol, 0.05 equiv) and (IPr)CuCl (0.0127 g, 0.0261 mmol, 0.075 equiv). The reaction was heated to 80 °C and monitored by TLC. Upon completion (22 h), the reaction was diluted with ethyl acetate (100 mL), washed with water (x2), brine, dried (Na₂SO₄), and concentrated under reduced pressure. The crude residue was purified by chromatography on SiO₂

(acetone/CH₂Cl₂, 3:97) to give **4.26** (0.070 g, 40%) as a off-white film: IR (ATR): 3215, 3088, 2982, 2932, 2222, 1735, 1670, 1472, 1458, 1435, 1370, 1361, 1325, 1294, 1228, 1161, 1150, 1133, 1053, 1042, 1029, 846, 833, 839 cm⁻¹; ¹H NMR (400 MHz, DMSO) δ 8.68-8.62 (m, 1 H), 8.44 (s, 1 H), 8.08-8.01 (m, 2 H), 7.91 (d, 1 H, *J* = 8.0 Hz), 7.84 (d, 1 H, *J* = 8.0 Hz), 7.69 (dd, 1 H, *J* = 8.0, 1.6 Hz), 7.61 (d, 1 H, *J* = 8.4 Hz), 7.46 (dd, 1 H, *J* = 8.0, 2.0 Hz), 7.40-7.38 (m, 1 H), 6.88 (s, 1 H), 4.18 (bs, 2 H), 1.29 (s, 9 H); ¹³C NMR (125 MHz, DMSO) δ 169.9 148.7, 144.0, 142.4, 136.9, 135.7, 135.7, 135.0, 132.5, 132.2, 132.2, 130.9, 130.8, 130.7, 130.3, 128.6, 126.2, 122.1, 119.8, 118.9, 117.7, 114.1, 109.9, 106.1, 84.9, 45.4, 27.0. Note: characterization taken from Igor Opsenica's final postdoctoral report.

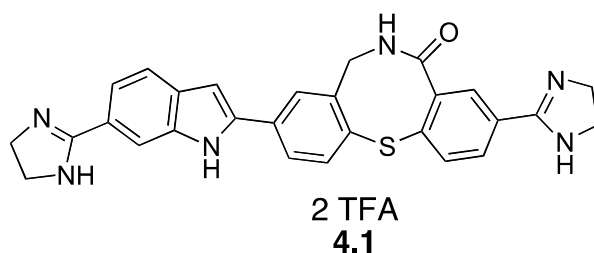


9-(6-Cyano-1H-indol-2-yl)-5-oxo-6,7-dihydro-5H-dibenzo[*b,g*][1,5]thiazocine-3-carbonitrile (4.27). To a stirred solution of **4.26** (0.0650 g, 0.128 mmol) in CH₂Cl₂ (4 mL, degassed) at rt was added TFA (0.286 mL, 1.53 mmol, 30 equiv). The reaction was stirred at rt for 14 h, carefully poured onto saturated aqueous NaHCO₃, and extracted with EtOAc (50 mL). The organic layer was washed with brine, dried (Na₂SO₄), filtered, and concentrated under reduced pressure to give 0.053 g (100%) of **4.27**. The crude compound was used in next reaction.



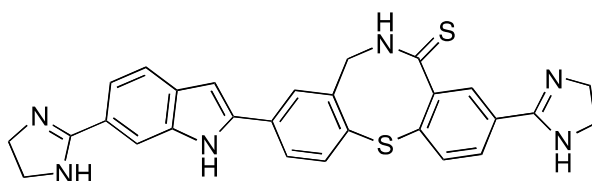
3-(4,5-Dihydro-1H-imidazol-2-yl)-9-(6-(4,5-dihydro-1H-imidazol-2-yl)-1H-indol-2-yl)-6,7-dihydro-5H-dibenzo[*b,g*][1,5]thiazocin-5-one (4.1). To a stirred solution of crude **4.21** (0.0600 g, 0.148 mmol, 1 equiv) in ethylenediamine (4 mL) was added sulfur (0.00947 g, 0.295 mmol, 2 equiv). The reaction was irradiated in the microwave (110 °C, 80 min), poured onto water, and filtered. The solid was washed with water, toluene, THF, and CH₂Cl₂ to give **4.1** (0.041 g, 56% yield): Compound is partially soluble (suspension) in DMSO (<1 mg/0.6 mL). Better solubility

(partially suspension) in the presence of d_3 -AcOH. ^1H NMR (400 MHz, DMSO) δ 11.84 (s, 1 H), 8.52-8.47 (m, 1 H), 8.02-7.98 (m, 1 H), 7.97-7.95 (m, 1 H), 7.88 (s, 1 H), 7.86-7.82 (m, 1 H), 7.81-7.77 (m, 1 H), 7.76-7.73 (m, 1 H), 7.60-7.54 (m, 3 H), 7.02-7.00 (m, 1 H), 4.20-4.17 (m, 2 H), 3.90-3.60 (m, 8 H). ^1H NMR (400 MHz, DMSO+ d_3 -AcOH) δ 8.16-8.13 (m, 1 H), 8.13-8.09 (m, 1 H), 8.06-8.02 (m, 2 H), 7.94-7.90 (m, 1 H), 7.83 (s, 1 H), 7.80-7.75 (m, 1 H), 7.68-7.64 (m, 1 H), 7.59-7.55 (m, 1 H), 7.13 (s, 1 H), 4.23 (bs, 2 H), 4.05-4.02 (m, 8 H). HRMS (ESI⁺) m/z calcd for $\text{C}_{28}\text{H}_{25}\text{ON}_6\text{S}$ $[\text{M}+\text{H}]^+$ 493.1805, found 493.1805. Note: characterization taken from Igor Opsenica's final postdoctoral report.



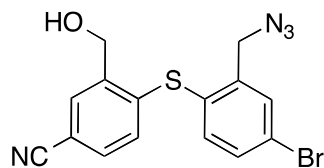
3-(4,5-Dihydro-1H-imidazol-2-yl)-9-(6-(4,5-dihydro-1H-imidazol-2-yl)-1H-indol-2-yl)-6,7-dihydro-5H-dibenzo[*b,g*][1,5]thiazocin-5-one-bis(2,2,2-trifluoroacetate) (IMO-27). A solution of TFA in THF (100 μL , 3.20 M) was added to a stirred suspension of **4.1** (40.0 mg, 0.0812 mmol) in THF (0.5 mL) and the reaction mixture was vigorously stirred over night at rt. The reaction mixture was evaporated to dryness, and co-evaporated with PhMe to provide the bis-TFA salt of **4.1** (0.0560 g, 96%) as a yellow solid: Mp >250 $^\circ\text{C}$; IR (ATR): 3184, 3114, 2969, 2919, 2718, 1763, 1672, 1616, 1599, 1459, 1413, 1364, 1288, 1167, 1124, 1031, 814 cm^{-1} ; ^1H NMR (500 MHz, DMSO) δ 12.38-12.34 (m, 1 H), 10.78 (s, 2 H), 10.40 (s, 2 H), 8.74-8.68 (m, 1 H), 8.15-8.13 (m, 1 H), 8.13-8.10 (m, 1 H), 8.08-8.05 (m, 1 H), 8.04 (s, 1 H), 7.96-7.92 (m, 1 H), 7.87-7.85 (m, 1 H), 7.80-7.77 (m, 1 H), 7.68-7.65 (m, 1 H), 7.59-7.55 (m, 1 H), 7.17-7.15 (m, 1 H), 4.23 (bs, 2 H), 4.06 (s, 4 H), 4.04 (s, 4 H), 3.64-3.60 (m, 2 H, 0.5 eq THF), 1.79-1.76 (m, 2 H, 0.5 eq THF); ^{13}C NMR (125 MHz, DMSO, without TFA peaks) δ 170.2, 165.8, 163.7, 143.7, 141.4, 137.1, 136.6, 136.2, 133.0, 132.3, 131.8, 131.1, 131.0, 130.4, 128.9, 128.2, 128.1, 127.0, 124.8, 120.7, 114.5, 112.4, 100.2, 67.0 (THF), 45.7, 44.6, 44.2, 25.1 (THF); HRMS (ESI) m/z calcd for $\text{C}_{28}\text{H}_{25}\text{N}_6\text{OS}$ $[\text{M}+\text{H}]^+$ 493.1811, found 493.1802. LC-MS Purity: $>95\%$. According to ^1H NMR there is 0.5 molecule of THF (complex).

Sample (5 mg) was dissolved in MeOH, and evaporated. NMR was taken in CD₃OD. ¹H NMR (400 MHz, CD₃OD) δ 8.07-8.04 (m, 3 H), 8.01-7.99 (m, 1 H), 7.87-7.83 (m, 1 H), 7.80-7.76 (m, 1 H), 7.74-7.71 (m, 1 H), 7.69-7.65 (m, 1 H), 7.53-7.48 (m, 1 H), 7.07 (s, 1 H), 4.36 (s, 2 H), 4.18 (s, 4 H), 4.13 (s, 4 H); ¹³C NMR (125 MHz, CD₃OD) δ 174.3, 169.7, 167.6, 145.9, 144.1, 139.6, 138.9, 138.2, 136.2, 135.7, 135.0, 133.5, 133.4, 133.3, 130.1, 128.7, 127.6, 127.4, 123.1, 120.8, 116.7, 114.1, 102.3, 48.4, 47.1, 46.6. Note: characterization taken from Igor Opsenica's final postdoctoral report.



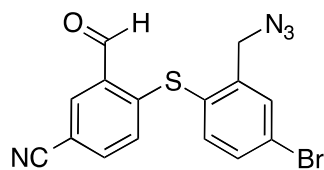
4.2

3-(4,5-Dihydro-1H-imidazol-2-yl)-9-(6-(4,5-dihydro-1H-imidazol-2-yl)-1H-indol-2-yl)-6,7-dihydro-5H-dibenzo[*b,g*][1,5]thiazocine-5-thione (4.2). To a stirred solution of **4.1** (0.0280 g, 0.0568 mmol, 1 equiv) in distilled pyridine (4 mL) was added P₄S₁₀ (0.253 g, 0.568 mmol, 10 equiv). The reaction was stirred at 110 °C for 1 h, dimethyl sulfone (12 g) was added and the mixture was stirred overnight at 120 °C. The reaction mixture was cooled to rt, diluted with a saturated aqueous solution of NaHCO₃ (60 mL), and the yellow solution was stirred at rt for 2 h. The reaction mixture was filtered (slowly), washed with water (5 mL), toluene (5 mL), and CH₂Cl₂ (5 mL). This provided a brown solid (0.023 g, 80%), which did not meet purity standards, thus the solid was washed with CH₂Cl₂ (15 mL), toluene (15 mL), and CH₂Cl₂ (15 mL) to give **4.2** (0.0168 g, 58%) as slightly green solid: Mp >260 °C; IR (neat) 3269, 2898, 1597, 1539, 1361, 1172, 815 cm⁻¹; ¹H NMR (600 MHz, DMSO) δ 11.80 (s, 1 H), 10.88 (dd, 1 H, *J* = 4.8, 8.4 Hz), 8.01 (d, 1 H, *J* = 1.8 Hz), 7.93 (dd, 1 H, *J* = 2.4, 8.4 Hz), 7.86-7.84 (m, 2 H), 7.77 (s, 1 H), 7.74 (d, 1 H, *J* = 8.4 Hz), 7.59 (d, 1 H, 8.4 Hz), 7.53 (s, 2 H), 7.15 (bs, 1 H), 6.99 (s, 1 H), 4.36 (dd, 1 H, *J* = 4.8, 16.2 Hz), 4.30 (dd, 1 H, *J* = 9.0, 15.6 Hz), 3.84 (bs, 2 H), 3.70-3.50 (m, 4 H), 3.50-3.41 (m, 2 H); ¹³C NMR (176 MHz, DMSO) δ 199.7, 165.6, 162.9, 148.2, 141.1, 136.5, 136.3, 134.2, 133.0, 132.7, 130.6, 130.3, 130.1, 128.4, 126.8, 126.6, 125.7, 120.3, 118.8, 114.3, 113.6, 99.7, 50.2, 44.3; HRMS (ESI⁺) *m/z* calcd for C₂₈H₂₅N₆S₂ [M+H]⁺ 509.1577, found 509.1571. Determined to be 99.1% pure by ELS.



4.28

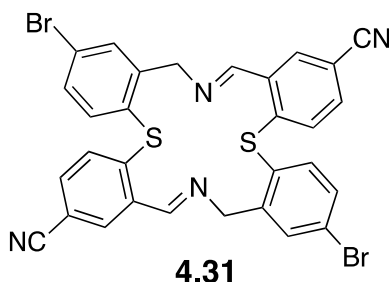
4-((2-(Azidomethyl)-4-bromophenyl)thio)-3-(hydroxymethyl)benzonitrile (4.28). To a stirred solution of **4.22** (0.100 g, 0.248 mmol, 1 equiv) in THF (2 mL) was added LiBH_4 (2 M in THF; 0.0620 mL, 0.124 mmol, 0.5 equiv). After stirring at rt for 5 h, a second batch of LiBH_4 (2 M in THF; 0.0620 mL, 0.124 mmol, 0.5 equiv) was added and the reaction was stirred at rt overnight. The reaction mixture was carefully quenched with sequential addition of EtOAc, acetone, and 1 M aqueous HCl. The quenched mixture was diluted with EtOAc, washed with 1 M aqueous HCl, dried (MgSO_4), filtered, and concentrated under reduced pressure. The crude mixture was purified by chromatography on SiO_2 (EtOAc/hexanes, 3:7) to give **4.28** (0.060 g, 64%) as a colorless film: $R_f = 0.16$ (EtOAc/hexanes, 2:8); IR (CDCl_3) 3464, 2918, 2227, 2101, 1593, 1459, 1338, 1087, 1036 cm^{-1} ; ^1H NMR (400 MHz, CDCl_3) δ 7.80 (s, 1 H), 7.69 (d, 1 H, $J = 2.0$ Hz), 7.51 (dd, 1 H, $J = 2.0, 8.4$ Hz), 7.38 (dd, 1 H, $J = 1.2, 8.0$ Hz), 7.30 (d, 1 H, $J = 8.4$ Hz), 6.79 (d, 1 H, $J = 8.4$ Hz), 4.82 (s, 2 H), 4.46 (s, 2 H); ^{13}C NMR (100 MHz, CDCl_3) δ 140.9, 140.8, 139.2, 133.0, 132.9, 131.4, 130.7, 128.8, 127.8, 124.66, 118.5, 109.8, 61.8, 52.3; HRMS (ESI) [$\text{M}-\text{N}_2+\text{H}$] m/z calcd for $\text{C}_{15}\text{H}_{12}\text{N}_2\text{OSBr}$ calcd 346.9854, found 346.9871.



4.29

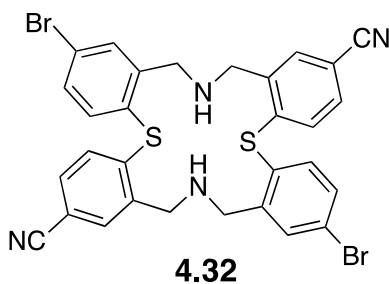
4-((2-(Azidomethyl)-4-bromophenyl)thio)-3-formylbenzonitrile (4.29). To a stirred solution of **4.28** (0.110 g, 0.293 mmol, 1 equiv) in CH_2Cl_2 (3 mL) was added BaMnO_4 (0.376 g, 1.47 mmol, 5 equiv). The reaction mixture was stirred overnight at rt, diluted with CH_2Cl_2 , filtered, washing the solid with CH_2Cl_2 . The filtrate was concentrated under reduced pressure and purified by chromatography on SiO_2 (EtOAc/hexanes, 2:8) to give **4.29** (0.021 g, 74%) as a colorless film: $R_f = 0.45$ (EtOAc/hexanes, 2:8); IR (CDCl_3) 3090, 2849, 2229, 2102, 1696, 1681, 1597, 1459, 1286, 1219, 1089, 762 cm^{-1} ; ^1H NMR (400 MHz, CDCl_3) δ 10.2 (s, 1 H), 8.1 (d, 1

H, $J = 1.2$ Hz), 7.75 (d, 1 H, $J = 1.6$ Hz), 7.60 (dd, 1 H, $J = 2.0, 8.0$ Hz), 7.54 (dd, 1 H, $J = 1.6, 8.4$ Hz), 7.44 (d, 1 H, $J = 8.4$ Hz), 6.72 (d, 1 H, $J = 8.4$ Hz), 4.49 (d, 2 H); ^{13}C NMR (100 MHz, CDCl_3) δ 189.3, 147.9, 142.1, 138.6, 137.5, 135.9, 133.2, 133.2, 132.2, 127.2, 127.0, 125.9, 117.3, 109.0, 52.2; HRMS (ESI) $[\text{M}-\text{N}_2+\text{H}] m/z$ calcd for $\text{C}_{15}\text{H}_{10}\text{N}_2\text{OSBr}$ 344.9697, found 344.9714.



(11E,23E)-8,20-Dibromo-10H,22H-

tetrabenzo[*b,g,j,o*][1,9]dithia[5,13]diazacyclohexadecine-2,14-dicarbonitrile (4.31). To a stirred solution of **4.29** (0.0200 g, 0.0534 mmol, 1 equiv) in THF (2 mL) was added DPPE (0.0427 g, 0.107 mmol, 2 equiv). The reaction mixture was stirred at rt for 18 h, diluted with EtOAc, washed with 1 M KOH, dried (MgSO_4), filtered, and concentrated under reduced pressure. The crude mixture was purified by chromatography on SiO_2 (0.5% MeOH/ CH_2Cl_2) to give **4.31** (0.0134 g, 76%) as a white solid: $R_f = 0.23$ (0.5% MeOH/ CH_2Cl_2); ^1H NMR (300 MHz, CDCl_3) δ 8.86 (s, 1 H), 7.49 (d, 2 H, $J = 1.8$ Hz), 7.71 (s, 1 H), 7.58 (dd, 1 H, $J = 2.1, 8.4$ Hz), 7.42 (dd, 1 H, $J = 1.8, 8.4$ Hz), 7.33 (d, 1 H, $J = 8.4$ Hz), 6.86 (d, 1 H, 8.4 Hz), 4.83 (s, 2 H); HRMS (ESI) $[(\text{M}+2\text{H}_2\text{O})/2+\text{H}] m/z$ calcd for $\text{C}_{15}\text{H}_{12}\text{N}_2\text{OSBr}$ 346.9848, found 346.9837.



8,20-Dibromo-11,12,23,24-tetrahydro-10H,22H-

tetrabenzo[*b,g,j,o*][1,9]dithia[5,13]diazacyclohexadecine-2,14-dicarbonitrile (4.32). To a stirred solution of **4.31** (0.0100 g, 0.0304 mmol, 1 equiv) in dry THF (3 mL) was added LiBH_4 (2

M in THF; 0.0228 mL, 0.0456 mmol, 1.5 equiv). The reaction mixture was stirred overnight at room temperature, quenched sequentially with EtOAc, acetone, and 1 M aqueous HCl. The reaction mixture was diluted with EtOAc, washed with 1 M aqueous HCl, dried (MgSO₄), filtered, and concentrated under reduced pressure. Analysis of the crude mixture by HRMS revealed the presence of **4.32**: HRMS (ESI) [(M+H) *m/z* calcd for C₃₀H₂₃Br₂N₄S₂ 660.9731, found 660.9723.

APPENDIX A

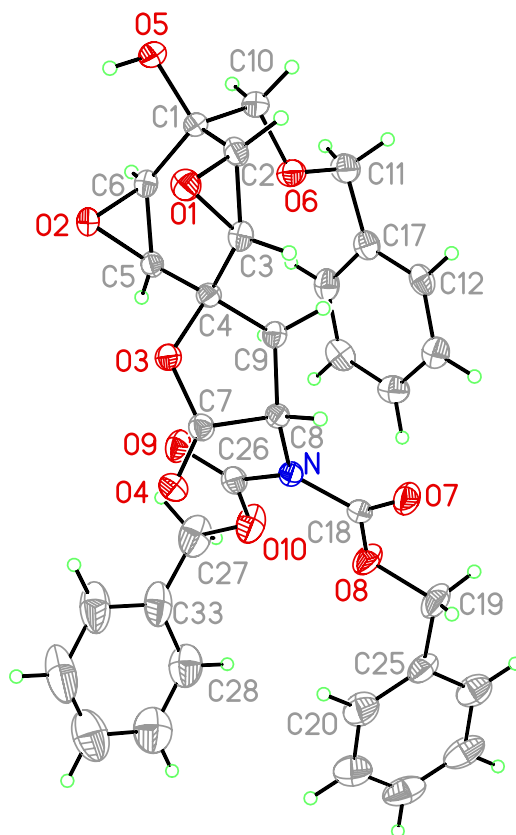


Table 34. Crystal data and structure refinement for **2.3**

Identification code	2.3	
Empirical formula	$C_{33}H_{31}NO_{10}$	
Formula weight	601.59	
Temperature	203(2) K	
Wavelength	0.71073 Å	
Crystal system	Orthorhombic	
Space group	P2(1)2(1)2(1)	
Unit cell dimensions	$a = 8.4680(10)$ Å	$a = 90^\circ$.

	$b = 10.7412(12) \text{ \AA}$	$b = 90^\circ$.
	$c = 32.884(4) \text{ \AA}$	$g = 90^\circ$.
Volume	$2991.0(6) \text{ \AA}^3$	
Z	4	
Density (calculated)	1.336 Mg/m^3	
Absorption coefficient	0.099 mm^{-1}	
F(000)	1264	
Crystal size	$0.35 \times 0.08 \times 0.04 \text{ mm}^3$	
Theta range for data collection	$1.99 \text{ to } 25.00^\circ$.	
Index ranges	$-10 \leq h \leq 10, -12 \leq k \leq 12, -39 \leq l \leq 38$	
Reflections collected	20924	
Independent reflections	3015 [R(int) = 0.0642]	
Completeness to theta = 25.00°	100.0 %	
Absorption correction	None	
Refinement method	Full-matrix least-squares on F^2	
Data / restraints / parameters	3015 / 0 / 401	
Goodness-of-fit on F^2	0.896	
Final R indices [I > 2sigma(I)]	$R1 = 0.0371, wR2 = 0.0954$	
R indices (all data)	$R1 = 0.0504, wR2 = 0.1026$	
Absolute structure parameter	-0.1(12)	
Largest diff. peak and hole	$0.173 \text{ and } -0.157 \text{ e.\AA}^{-3}$	

Table 35. Atomic coordinates ($\times 10^4$) and equivalent isotropic displacement parameters ($\text{\AA}^2 \times 10^3$) for **2.3**. $U(\text{eq})$ is defined as one third of the trace of the orthogonalized U^{ij} tensor.

	x	y	z	$U(\text{eq})$
N	1108(3)	7423(2)	8622(1)	31(1)
C(1)	1683(4)	7095(2)	6681(1)	32(1)
O(1)	-1180(2)	7124(2)	6887(1)	38(1)
C(2)	257(4)	7823(2)	6819(1)	33(1)
O(2)	860(3)	5119(2)	7043(1)	36(1)
C(3)	-399(3)	7682(3)	7229(1)	32(1)
O(3)	-834(2)	6171(2)	7757(1)	33(1)
C(4)	399(3)	6855(3)	7535(1)	28(1)
O(4)	-1670(3)	5901(2)	8392(1)	39(1)
C(5)	1482(3)	5893(2)	7360(1)	29(1)
O(5)	1471(3)	6691(2)	6269(1)	42(1)
C(6)	2092(4)	6006(2)	6948(1)	31(1)
O(6)	3356(2)	8274(2)	7094(1)	40(1)
C(7)	-826(4)	6431(2)	8157(1)	31(1)
O(7)	186(3)	9319(2)	8809(1)	51(1)
C(8)	250(3)	7532(2)	8237(1)	28(1)
O(8)	1774(3)	8295(2)	9227(1)	48(1)
C(9)	1253(3)	7655(3)	7855(1)	31(1)
O(9)	1932(3)	5530(2)	8404(1)	42(1)
C(10)	3112(4)	7962(3)	6680(1)	36(1)
O(10)	2904(3)	6306(2)	8988(1)	58(1)
C(11)	4664(4)	9062(3)	7174(1)	45(1)
C(12)	3908(4)	10016(3)	7846(1)	38(1)
C(13)	3851(4)	9993(3)	8266(1)	42(1)
C(14)	4647(4)	9077(3)	8478(1)	44(1)
C(15)	5514(4)	8197(3)	8267(1)	45(1)
C(16)	5577(4)	8221(3)	7847(1)	40(1)
C(17)	4769(3)	9137(3)	7631(1)	37(1)
C(18)	972(4)	8430(3)	8890(1)	32(1)
C(19)	1609(6)	9299(3)	9520(1)	61(1)
C(20)	1454(6)	7661(4)	10060(1)	66(1)
C(21)	1759(6)	7239(4)	10447(1)	74(1)

C(22)	2618(5)	7946(5)	10710(1)	68(1)
C(23)	3178(5)	9080(5)	10590(1)	65(1)
C(24)	2884(5)	9509(4)	10198(1)	58(1)
C(25)	2010(5)	8800(3)	9933(1)	47(1)
C(26)	2004(4)	6330(3)	8659(1)	36(1)
C(27)	3777(5)	5146(3)	9065(1)	67(1)
C(28)	3040(6)	4558(4)	9771(1)	74(1)
C(29)	2212(7)	3853(5)	10051(2)	90(2)
C(30)	1168(7)	2958(4)	9922(2)	95(2)
C(31)	993(8)	2764(4)	9516(2)	111(2)
C(32)	1841(7)	3458(4)	9233(2)	92(2)
C(33)	2881(5)	4365(3)	9360(1)	63(1)

Table 36. Bond lengths [Å] and angles [°] for **2.3**.

N-C(18)	1.399(3)
N-C(26)	1.403(4)
N-C(8)	1.463(3)
C(1)-O(5)	1.432(3)
C(1)-C(6)	1.504(4)
C(1)-C(2)	1.508(4)
C(1)-C(10)	1.526(4)
O(1)-C(3)	1.435(3)
O(1)-C(2)	1.448(3)
C(2)-C(3)	1.465(4)
C(2)-H(2A)	0.9900
O(2)-C(5)	1.433(3)
O(2)-C(6)	1.448(3)
C(3)-C(4)	1.504(4)
C(3)-H(3A)	0.9900
O(3)-C(7)	1.344(3)
O(3)-C(4)	1.471(3)
C(4)-C(5)	1.497(4)
C(4)-C(9)	1.539(4)
O(4)-C(7)	1.197(3)
C(5)-C(6)	1.456(4)
C(5)-H(5A)	0.9900
O(5)-H(5O)	0.87(4)
C(6)-H(6A)	0.9900
O(6)-C(11)	1.419(4)
O(6)-C(10)	1.419(3)
C(7)-C(8)	1.516(4)
O(7)-C(18)	1.194(3)
C(8)-C(9)	1.522(4)
C(8)-H(8A)	0.9900
O(8)-C(18)	1.311(3)
O(8)-C(19)	1.451(4)
C(9)-H(9A)	0.9800
C(9)-H(9B)	0.9800
O(9)-C(26)	1.202(3)

C(10)-H(10A)	0.9800
C(10)-H(10B)	0.9800
O(10)-C(26)	1.322(3)
O(10)-C(27)	1.471(4)
C(11)-C(17)	1.506(4)
C(11)-H(11A)	0.9800
C(11)-H(11B)	0.9800
C(12)-C(13)	1.381(4)
C(12)-C(17)	1.387(4)
C(12)-H(12A)	0.9400
C(13)-C(14)	1.381(4)
C(13)-H(13A)	0.9400
C(14)-C(15)	1.384(4)
C(14)-H(14A)	0.9400
C(15)-C(16)	1.380(4)
C(15)-H(15A)	0.9400
C(16)-C(17)	1.394(4)
C(16)-H(16A)	0.9400
C(19)-C(25)	1.499(4)
C(19)-H(19A)	0.9800
C(19)-H(19B)	0.9800
C(20)-C(25)	1.376(5)
C(20)-C(21)	1.378(5)
C(20)-H(20A)	0.9400
C(21)-C(22)	1.360(6)
C(21)-H(21A)	0.9400
C(22)-C(23)	1.365(6)
C(22)-H(22A)	0.9400
C(23)-C(24)	1.390(5)
C(23)-H(23A)	0.9400
C(24)-C(25)	1.375(5)
C(24)-H(24A)	0.9400
C(27)-C(33)	1.492(6)
C(27)-H(27A)	0.9800
C(27)-H(27B)	0.9800
C(28)-C(33)	1.372(5)
C(28)-C(29)	1.383(7)

C(28)-H(28A)	0.9400
C(29)-C(30)	1.373(7)
C(29)-H(29A)	0.9400
C(30)-C(31)	1.358(7)
C(30)-H(30A)	0.9400
C(31)-C(32)	1.392(8)
C(31)-H(31A)	0.9400
C(32)-C(33)	1.378(6)
C(32)-H(32A)	0.9400
C(18)-N-C(26)	129.5(2)
C(18)-N-C(8)	116.2(2)
C(26)-N-C(8)	114.3(2)
O(5)-C(1)-C(6)	110.2(2)
O(5)-C(1)-C(2)	110.0(2)
C(6)-C(1)-C(2)	114.3(2)
O(5)-C(1)-C(10)	106.4(2)
C(6)-C(1)-C(10)	107.0(2)
C(2)-C(1)-C(10)	108.6(2)
C(3)-O(1)-C(2)	61.08(17)
O(1)-C(2)-C(3)	59.01(17)
O(1)-C(2)-C(1)	116.8(2)
C(3)-C(2)-C(1)	121.9(2)
O(1)-C(2)-H(2A)	115.7
C(3)-C(2)-H(2A)	115.7
C(1)-C(2)-H(2A)	115.7
C(5)-O(2)-C(6)	60.71(17)
O(1)-C(3)-C(2)	59.90(17)
O(1)-C(3)-C(4)	119.0(2)
C(2)-C(3)-C(4)	120.5(2)
O(1)-C(3)-H(3A)	115.4
C(2)-C(3)-H(3A)	115.4
C(4)-C(3)-H(3A)	115.4
C(7)-O(3)-C(4)	112.2(2)
O(3)-C(4)-C(5)	106.3(2)
O(3)-C(4)-C(3)	108.0(2)
C(5)-C(4)-C(3)	115.1(2)
O(3)-C(4)-C(9)	105.85(19)

C(5)-C(4)-C(9)	111.2(2)
C(3)-C(4)-C(9)	109.9(2)
O(2)-C(5)-C(6)	60.16(16)
O(2)-C(5)-C(4)	117.1(2)
C(6)-C(5)-C(4)	121.2(2)
O(2)-C(5)-H(5A)	115.6
C(6)-C(5)-H(5A)	115.6
C(4)-C(5)-H(5A)	115.6
C(1)-O(5)-H(5O)	106(2)
O(2)-C(6)-C(5)	59.13(16)
O(2)-C(6)-C(1)	118.2(2)
C(5)-C(6)-C(1)	121.8(2)
O(2)-C(6)-H(6A)	115.3
C(5)-C(6)-H(6A)	115.3
C(1)-C(6)-H(6A)	115.3
C(11)-O(6)-C(10)	115.7(2)
O(4)-C(7)-O(3)	122.0(3)
O(4)-C(7)-C(8)	128.1(2)
O(3)-C(7)-C(8)	109.6(2)
N-C(8)-C(7)	112.7(2)
N-C(8)-C(9)	116.3(2)
C(7)-C(8)-C(9)	105.0(2)
N-C(8)-H(8A)	107.4
C(7)-C(8)-H(8A)	107.4
C(9)-C(8)-H(8A)	107.4
C(18)-O(8)-C(19)	115.4(3)
C(8)-C(9)-C(4)	104.7(2)
C(8)-C(9)-H(9A)	110.8
C(4)-C(9)-H(9A)	110.8
C(8)-C(9)-H(9B)	110.8
C(4)-C(9)-H(9B)	110.8
H(9A)-C(9)-H(9B)	108.9
O(6)-C(10)-C(1)	105.0(2)
O(6)-C(10)-H(10A)	110.8
C(1)-C(10)-H(10A)	110.8
O(6)-C(10)-H(10B)	110.8
C(1)-C(10)-H(10B)	110.8

H(10A)-C(10)-H(10B) 108.8
C(26)-O(10)-C(27) 116.6(2)
O(6)-C(11)-C(17) 105.2(2)
O(6)-C(11)-H(11A) 110.7
C(17)-C(11)-H(11A) 110.7
O(6)-C(11)-H(11B) 110.7
C(17)-C(11)-H(11B) 110.7
H(11A)-C(11)-H(11B) 108.8
C(13)-C(12)-C(17) 121.1(3)
C(13)-C(12)-H(12A) 119.5
C(17)-C(12)-H(12A) 119.5
C(14)-C(13)-C(12) 120.0(3)
C(14)-C(13)-H(13A) 120.0
C(12)-C(13)-H(13A) 120.0
C(13)-C(14)-C(15) 119.5(3)
C(13)-C(14)-H(14A) 120.2
C(15)-C(14)-H(14A) 120.2
C(16)-C(15)-C(14) 120.5(3)
C(16)-C(15)-H(15A) 119.7
C(14)-C(15)-H(15A) 119.7
C(15)-C(16)-C(17) 120.3(3)
C(15)-C(16)-H(16A) 119.8
C(17)-C(16)-H(16A) 119.8
C(12)-C(17)-C(16) 118.5(3)
C(12)-C(17)-C(11) 120.9(3)
C(16)-C(17)-C(11) 120.0(3)
O(7)-C(18)-O(8) 124.4(3)
O(7)-C(18)-N 121.7(2)
O(8)-C(18)-N 113.9(2)
O(8)-C(19)-C(25) 108.2(3)
O(8)-C(19)-H(19A) 110.0
C(25)-C(19)-H(19A) 110.0
O(8)-C(19)-H(19B) 110.0
C(25)-C(19)-H(19B) 110.0
H(19A)-C(19)-H(19B) 108.4
C(25)-C(20)-C(21) 120.6(4)
C(25)-C(20)-H(20A) 119.7

C(21)-C(20)-H(20A) 119.7
C(22)-C(21)-C(20) 120.3(4)
C(22)-C(21)-H(21A) 119.9
C(20)-C(21)-H(21A) 119.9
C(21)-C(22)-C(23) 120.0(4)
C(21)-C(22)-H(22A) 120.0
C(23)-C(22)-H(22A) 120.0
C(22)-C(23)-C(24) 120.1(4)
C(22)-C(23)-H(23A) 119.9
C(24)-C(23)-H(23A) 119.9
C(25)-C(24)-C(23) 120.1(4)
C(25)-C(24)-H(24A) 120.0
C(23)-C(24)-H(24A) 120.0
C(24)-C(25)-C(20) 119.0(3)
C(24)-C(25)-C(19) 120.0(3)
C(20)-C(25)-C(19) 121.0(3)
O(9)-C(26)-O(10) 125.8(3)
O(9)-C(26)-N 120.7(3)
O(10)-C(26)-N 113.6(2)
O(10)-C(27)-C(33) 109.4(3)
O(10)-C(27)-H(27A) 109.8
C(33)-C(27)-H(27A) 109.8
O(10)-C(27)-H(27B) 109.8
C(33)-C(27)-H(27B) 109.8
H(27A)-C(27)-H(27B) 108.2
C(33)-C(28)-C(29) 121.5(4)
C(33)-C(28)-H(28A) 119.2
C(29)-C(28)-H(28A) 119.2
C(30)-C(29)-C(28) 120.2(5)
C(30)-C(29)-H(29A) 119.9
C(28)-C(29)-H(29A) 119.9
C(31)-C(30)-C(29) 118.8(5)
C(31)-C(30)-H(30A) 120.6
C(29)-C(30)-H(30A) 120.6
C(30)-C(31)-C(32) 121.2(5)
C(30)-C(31)-H(31A) 119.4
C(32)-C(31)-H(31A) 119.4

C(33)-C(32)-C(31)	120.3(5)
C(33)-C(32)-H(32A)	119.8
C(31)-C(32)-H(32A)	119.8
C(28)-C(33)-C(32)	117.9(5)
C(28)-C(33)-C(27)	120.4(4)
C(32)-C(33)-C(27)	121.6(4)

Symmetry transformations used to generate equivalent atoms

Table 37. Anisotropic displacement parameters ($\text{\AA}^2 \times 10^3$) for **2.3**. The anisotropic displacement factor exponent takes the form: $-2p^2 [h^2 a^* 2U^{11} + \dots + 2 h k a^* b^* U^{12}]$

	U ¹¹	U ²²	U ³³	U ²³	U ¹³	U ¹²
N 39(1)	26(1)	26(1)	1(1)	-3(1)	1(1)	
C(1)43(2)	28(1)	24(1)	-1(1)	0(1)	-5(1)	
O(1)36(1)	39(1)	39(1)	1(1)	-8(1)	-6(1)	
C(2)38(2)	25(1)	36(2)	4(1)	-8(1)	-4(1)	
O(2)50(1)	25(1)	35(1)	-3(1)	0(1)	-5(1)	
C(3)31(2)	28(1)	36(1)	-4(1)	-2(1)	2(1)	
O(3)35(1)	34(1)	30(1)	-3(1)	1(1)	-11(1)	
C(4)29(2)	30(1)	26(1)	-1(1)	2(1)	-6(1)	
O(4)44(1)	37(1)	38(1)	3(1)	6(1)	-8(1)	
C(5)36(2)	23(1)	29(1)	1(1)	-6(1)	-2(1)	
O(5)60(2)	39(1)	27(1)	-3(1)	-2(1)	-11(1)	
C(6)33(2)	26(1)	33(1)	-3(1)	0(1)	1(1)	
O(6)41(1)	46(1)	33(1)	-3(1)	0(1)	-16(1)	
C(7)32(2)	28(1)	32(2)	1(1)	1(1)	2(1)	
O(7)85(2)	33(1)	36(1)	-4(1)	-10(1)	15(1)	
C(8)31(1)	26(1)	27(1)	2(1)	-2(1)	2(1)	
O(8)66(2)	46(1)	31(1)	-11(1)	-13(1)	13(1)	
C(9)33(2)	29(1)	31(1)	-3(1)	-1(1)	-4(1)	
O(9)50(1)	31(1)	46(1)	-7(1)	-7(1)	9(1)	
C(10)41(2)	34(2)	32(1)	0(1)	3(1)	-2(1)	
O(10)71(2)	45(1)	57(1)	-8(1)	-31(1)	19(1)	
C(11)43(2)	48(2)	43(2)	1(1)	-2(2)	-18(2)	
C(12)34(2)	31(2)	50(2)	6(1)	-9(2)	-6(1)	
C(13)35(2)	41(2)	49(2)	-6(1)	1(2)	-1(2)	
C(14)38(2)	54(2)	41(2)	4(2)	-2(2)	-7(2)	
C(15)35(2)	44(2)	57(2)	9(2)	-5(2)	-1(2)	
C(16)30(2)	35(2)	56(2)	-5(1)	2(2)	-3(1)	
C(17)29(2)	37(2)	45(2)	0(1)	-1(1)	-8(1)	
C(18)41(2)	29(2)	26(1)	3(1)	1(1)	0(1)	
C(19)99(3)	48(2)	36(2)	-17(1)	-15(2)	13(2)	
C(20)89(3)	70(3)	40(2)	-7(2)	-16(2)	-4(3)	
C(21)102(3)	78(3)	42(2)	4(2)	2(2)	-1(3)	
C(22)68(3)	100(3)	35(2)	0(2)	-2(2)	31(3)	

C(23)53(2)	103(3)	39(2)	-24(2)	-13(2)	7(3)
C(24)53(2)	73(3)	47(2)	-13(2)	-5(2)	-2(2)
C(25)57(2)	52(2)	33(2)	-12(2)	-3(2)	10(2)
C(26)39(2)	30(2)	38(2)	3(1)	-1(1)	4(1)
C(27)75(3)	53(2)	74(2)	-4(2)	-31(2)	31(2)
C(28)74(3)	62(3)	85(3)	-5(2)	-28(3)	1(2)
C(29)91(4)	78(3)	101(4)	1(3)	-24(3)	7(3)
C(30)91(4)	61(3)	133(4)	22(3)	-31(4)	2(3)
C(31)140(5)	50(3)	144(5)	16(3)	-65(4)	-25(3)
C(32)128(5)	45(2)	102(3)	4(2)	-64(3)	0(3)
C(33)70(3)	35(2)	84(3)	-1(2)	-41(2)	16(2)

Table 38. Hydrogen coordinates ($\times 10^4$) and isotropic displacement parameters ($\text{\AA}^2 \times 10^3$) for **2.3**

	x	y	z	U(eq)
H(2A)	121	8652	6693	39
H(3A)	-917	8433	7341	38
H(5A)	2187	5473	7557	35
H(5O)	830(50)	6060(40)	6278(11)	75(13)
H(6A)	3153	5644	6903	37
H(8A)	-424	8283	8255	33
H(9A)	2325	7345	7903	37
H(9B)	1313	8525	7767	37
H(10A)	4040	7539	6567	43
H(10B)	2898	8709	6518	43
H(11A)	4494	9890	7057	53
H(11B)	5635	8710	7060	53
H(12A)	3354	10637	7704	46
H(13A)	3271	10601	8407	50
H(14A)	4599	9051	8763	53
H(15A)	6065	7577	8410	54
H(16A)	6168	7617	7707	48
H(19A)	523	9615	9518	73
H(19B)	2322	9985	9449	73
H(20A)	861	7166	9880	79
H(21A)	1372	6460	10531	89
H(22A)	2827	7653	10974	81
H(23A)	3763	9571	10772	78
H(24A)	3283	10285	10115	70
H(27A)	4824	5340	9175	81
H(27B)	3918	4688	8809	81
H(28A)	3727	5183	9864	88
H(29A)	2365	3986	10330	108
H(30A)	585	2488	10110	114
H(31A)	287	2149	9425	133
H(32A)	1703	3308	8954	110

APPENDIX B

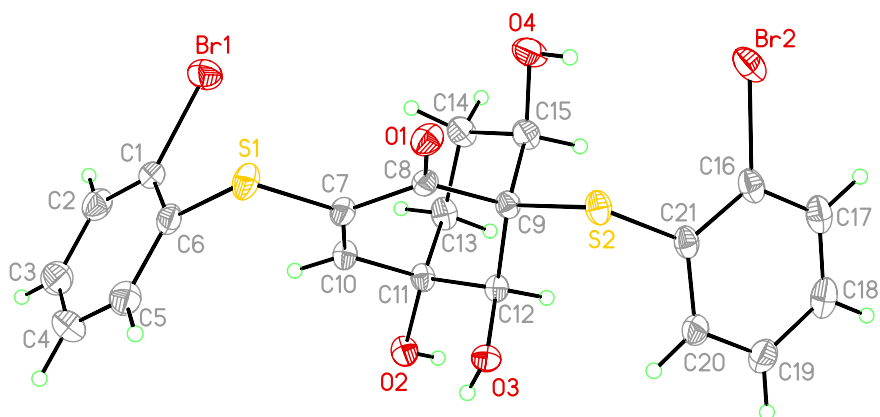


Table 39. Crystal data and structure refinement for **2.37**

Identification code	2.37	
Empirical formula	$C_{21}H_{18}Br_2O_4S_2$	
Formula weight	558.29	
Temperature	203(2) K	
Wavelength	0.71073 Å	
Crystal system	Monoclinic	
Space group	Cc	
Unit cell dimensions	$a = 15.9415(18)$ Å	$\langle = 90^\circ$.

	$b = 14.7510(17) \text{ \AA}$	$\beta = 99.907(2)^\circ$
	$c = 9.2139(11) \text{ \AA}$	$\gamma = 90^\circ$
Volume	$2134.4(4) \text{ \AA}^3$	
Z	4	
Density (calculated)	1.737 Mg/m^3	
Absorption coefficient	4.019 mm^{-1}	
F(000)	1112	
Crystal size	$0.28 \times 0.23 \times 0.20 \text{ mm}^3$	
Theta range for data collection	1.89 to 32.24°	
Index ranges	$-23 \leq h \leq 22$, $-21 \leq k \leq 21$, $-13 \leq l \leq 13$	
Reflections collected	12944	
Independent reflections	6478 [R(int) = 0.0214]	
Completeness to theta = 32.24°	94.7 %	
Absorption correction	multi-scan	
Max. and min. transmission	0.5003 and 0.3991	
Refinement method	Full-matrix least-squares on F^2	
Data / restraints / parameters	6478 / 3 / 275	
Goodness-of-fit on F^2	0.668	
Final R indices [I > 2sigma(I)]	R1 = 0.0304, wR2 = 0.0792	
R indices (all data)	R1 = 0.0380, wR2 = 0.0849	
Absolute structure parameter	0.000(6)	
Largest diff. peak and hole	0.832 and $-0.304 \text{ e. \AA}^{-3}$	

Table 40. Atomic coordinates ($\times 10^4$) and equivalent isotropic displacement parameters ($\text{\AA}^2 \times 10^3$) for **2.37**. $U(\text{eq})$ is defined as one third of the trace of the orthogonalized U^{ij} tensor

	x	y	z	$U(\text{eq})$
Br(1)	3894(1)	1914(1)	8392(1)	46(1)
Br(2)	-1565(1)	2296(1)	8844(1)	46(1)
S(1)	3281(1)	3720(1)	10086(1)	34(1)
S(2)	-88(1)	3919(1)	9128(1)	29(1)
O(1)	1555(1)	3478(1)	10525(2)	33(1)
O(2)	1757(1)	4484(1)	5024(2)	32(1)
O(3)	924(1)	5092(1)	7274(2)	27(1)
O(4)	558(2)	1956(1)	8675(3)	42(1)
C(1)	4378(2)	3076(2)	8275(3)	30(1)
C(2)	5016(2)	3162(2)	7432(3)	40(1)
C(3)	5384(2)	4007(3)	7330(4)	52(1)
C(4)	5122(2)	4745(2)	8049(5)	52(1)
C(5)	4482(2)	4655(2)	8883(4)	44(1)
C(6)	4096(2)	3809(2)	9010(3)	32(1)
C(7)	2377(2)	3715(2)	8664(3)	27(1)
C(8)	1570(1)	3583(2)	9223(3)	25(1)
C(9)	745(1)	3560(2)	8079(3)	24(1)
C(10)	2377(2)	3840(2)	7230(3)	28(1)
C(11)	1578(2)	3856(2)	6084(3)	26(1)
C(12)	821(1)	4186(2)	6778(2)	24(1)
C(13)	1371(2)	2916(2)	5434(3)	33(1)
C(14)	1209(2)	2233(2)	6597(3)	35(1)
C(15)	556(2)	2575(2)	7502(3)	32(1)
C(16)	-1658(2)	3337(2)	7616(3)	33(1)
C(17)	-2406(2)	3430(2)	6597(4)	40(1)
C(18)	-2517(2)	4171(3)	5673(4)	46(1)
C(19)	-1880(2)	4840(2)	5788(4)	42(1)
C(20)	-1140(2)	4749(2)	6816(3)	34(1)
C(21)	-1005(2)	3981(2)	7739(3)	29(1)

Table 41. Bond lengths [Å] and angles [°] for **2.37**

Br(1)-C(1)	1.891(3)
Br(2)-C(16)	1.898(3)
S(1)-C(6)	1.770(3)
S(1)-C(7)	1.773(2)
S(2)-C(21)	1.772(3)
S(2)-C(9)	1.849(2)
O(1)-C(8)	1.214(3)
O(2)-C(11)	1.411(3)
O(2)-H(2O)	0.75(4)
O(3)-C(12)	1.413(3)
O(3)-H(3O)	0.71(4)
O(4)-C(15)	1.415(4)
O(4)-H(4O)	0.77(2)
C(1)-C(2)	1.387(4)
C(1)-C(6)	1.390(4)
C(2)-C(3)	1.387(5)
C(2)-H(2A)	0.9400
C(3)-C(4)	1.377(6)
C(3)-H(3A)	0.9400
C(4)-C(5)	1.385(5)
C(4)-H(4A)	0.9400
C(5)-C(6)	1.406(4)
C(5)-H(5A)	0.9400
C(7)-C(10)	1.334(3)
C(7)-C(8)	1.480(3)
C(8)-C(9)	1.538(3)
C(9)-C(12)	1.534(3)
C(9)-C(15)	1.558(3)
C(10)-C(11)	1.508(3)
C(10)-H(10A)	0.9400
C(11)-C(13)	1.523(4)
C(11)-C(12)	1.539(3)
C(12)-H(12A)	0.9900
C(13)-C(14)	1.525(4)

C(13)-H(13A)	0.9800
C(13)-H(13B)	0.9800
C(14)-C(15)	1.528(4)
C(14)-H(14A)	0.9800
C(14)-H(14B)	0.9800
C(15)-H(4O)	1.72(5)
C(15)-H(15A)	0.9900
C(16)-C(17)	1.392(4)
C(16)-C(21)	1.399(4)
C(17)-C(18)	1.378(5)
C(17)-H(17A)	0.9400
C(18)-C(19)	1.407(5)
C(18)-H(18A)	0.9400
C(19)-C(20)	1.386(4)
C(19)-H(19A)	0.9400
C(20)-C(21)	1.410(4)
C(20)-H(20A)	0.9400
C(6)-S(1)-C(7)	99.63(12)
C(21)-S(2)-C(9)	102.42(11)
C(11)-O(2)-H(2O)	105(3)
C(12)-O(3)-H(3O)	110(3)
C(15)-O(4)-H(4O)	99(5)
C(2)-C(1)-C(6)	122.1(3)
C(2)-C(1)-Br(1)	117.4(2)
C(6)-C(1)-Br(1)	120.5(2)
C(1)-C(2)-C(3)	118.7(3)
C(1)-C(2)-H(2A)	120.7
C(3)-C(2)-H(2A)	120.7
C(4)-C(3)-C(2)	120.7(3)
C(4)-C(3)-H(3A)	119.6
C(2)-C(3)-H(3A)	119.6
C(3)-C(4)-C(5)	120.3(3)
C(3)-C(4)-H(4A)	119.9
C(5)-C(4)-H(4A)	119.9
C(4)-C(5)-C(6)	120.5(3)
C(4)-C(5)-H(5A)	119.8
C(6)-C(5)-H(5A)	119.8

C(1)-C(6)-C(5)	117.8(3)
C(1)-C(6)-S(1)	123.1(2)
C(5)-C(6)-S(1)	119.1(2)
C(10)-C(7)-C(8)	120.8(2)
C(10)-C(7)-S(1)	126.37(19)
C(8)-C(7)-S(1)	112.83(17)
O(1)-C(8)-C(7)	121.8(2)
O(1)-C(8)-C(9)	121.0(2)
C(7)-C(8)-C(9)	117.2(2)
C(12)-C(9)-C(8)	110.45(18)
C(12)-C(9)-C(15)	109.31(19)
C(8)-C(9)-C(15)	110.30(18)
C(12)-C(9)-S(2)	113.34(16)
C(8)-C(9)-S(2)	103.99(15)
C(15)-C(9)-S(2)	109.34(16)
C(7)-C(10)-C(11)	123.4(2)
C(7)-C(10)-H(10A)	118.3
C(11)-C(10)-H(10A)	118.3
O(2)-C(11)-C(10)	104.33(19)
O(2)-C(11)-C(13)	112.4(2)
C(10)-C(11)-C(13)	111.2(2)
O(2)-C(11)-C(12)	110.2(2)
C(10)-C(11)-C(12)	110.06(19)
C(13)-C(11)-C(12)	108.6(2)
O(3)-C(12)-C(9)	109.69(18)
O(3)-C(12)-C(11)	112.19(19)
C(9)-C(12)-C(11)	107.88(19)
O(3)-C(12)-H(12A)	109.0
C(9)-C(12)-H(12A)	109.0
C(11)-C(12)-H(12A)	109.0
C(11)-C(13)-C(14)	112.1(2)
C(11)-C(13)-H(13A)	109.2
C(14)-C(13)-H(13A)	109.2
C(11)-C(13)-H(13B)	109.2
C(14)-C(13)-H(13B)	109.2
H(13A)-C(13)-H(13B)	107.9
C(13)-C(14)-C(15)	112.2(2)

C(13)-C(14)-H(14A)	109.2
C(15)-C(14)-H(14A)	109.2
C(13)-C(14)-H(14B)	109.2
C(15)-C(14)-H(14B)	109.2
H(14A)-C(14)-H(14B)	107.9
O(4)-C(15)-C(14)	106.9(2)
O(4)-C(15)-C(9)	111.5(2)
C(14)-C(15)-C(9)	112.6(2)
O(4)-C(15)-H(4O)	26.4(13)
C(14)-C(15)-H(4O)	133.0(13)
C(9)-C(15)-H(4O)	98.5(19)
O(4)-C(15)-H(15A)	108.6
C(14)-C(15)-H(15A)	108.6
C(9)-C(15)-H(15A)	108.6
H(4O)-C(15)-H(15A)	92.7
C(17)-C(16)-C(21)	121.8(3)
C(17)-C(16)-Br(2)	116.9(2)
C(21)-C(16)-Br(2)	121.4(2)
C(18)-C(17)-C(16)	120.0(3)
C(18)-C(17)-H(17A)	120.0
C(16)-C(17)-H(17A)	120.0
C(17)-C(18)-C(19)	119.7(3)
C(17)-C(18)-H(18A)	120.2
C(19)-C(18)-H(18A)	120.2
C(20)-C(19)-C(18)	120.1(3)
C(20)-C(19)-H(19A)	119.9
C(18)-C(19)-H(19A)	119.9
C(19)-C(20)-C(21)	120.9(3)
C(19)-C(20)-H(20A)	119.6
C(21)-C(20)-H(20A)	119.6
C(16)-C(21)-C(20)	117.5(2)
C(16)-C(21)-S(2)	122.2(2)
C(20)-C(21)-S(2)	119.9(2)

Symmetry transformations used to generate equivalent atoms:

Table 42. Anisotropic displacement parameters ($\text{\AA}^2 \times 10^3$) for **2.37**. The anisotropic displacement factor exponent takes the form: $-2p^2[h^2 a^{*2}U^{11} + \dots + 2 h k a^* b^* U^{12}]$

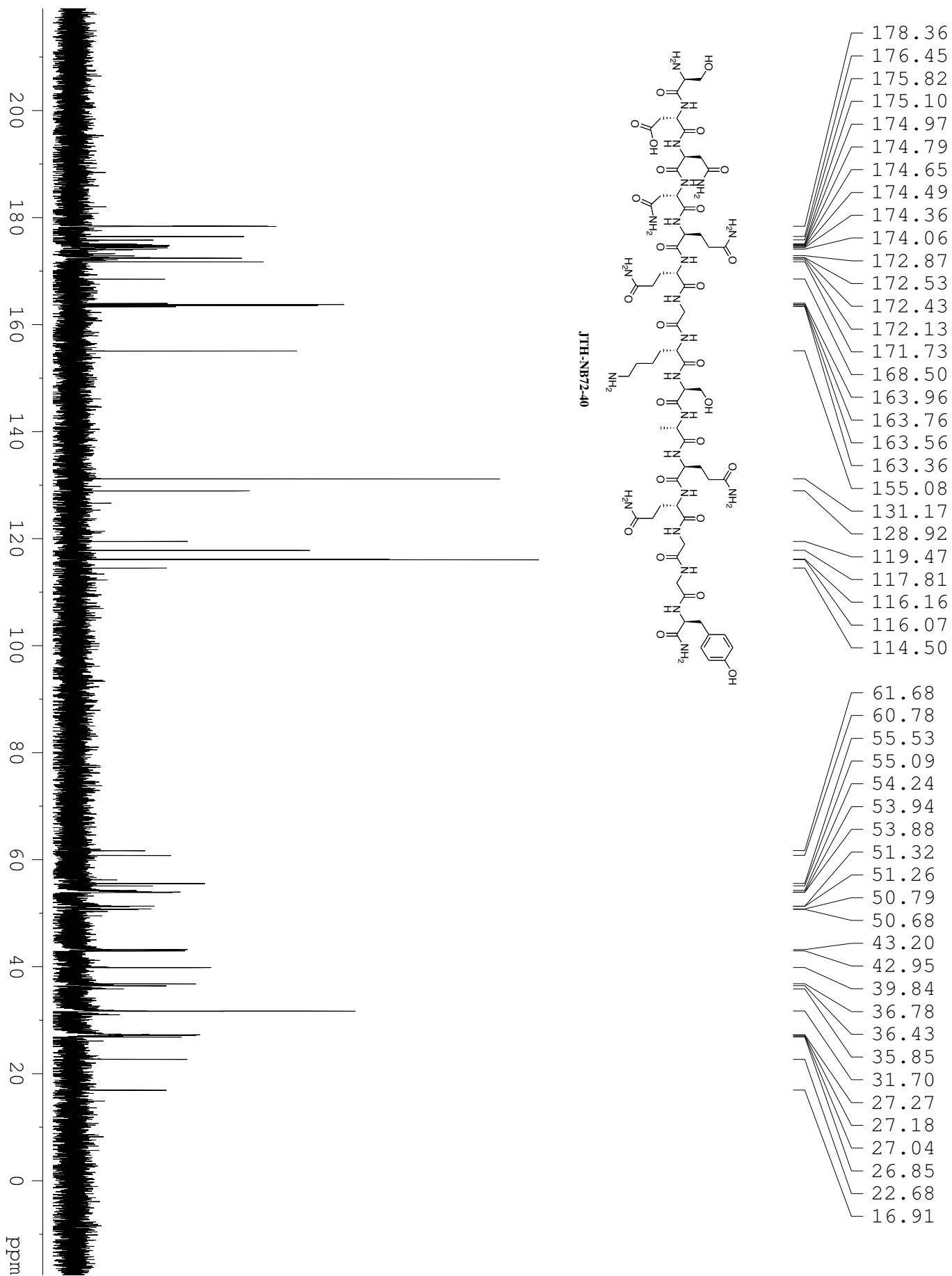
	U ¹¹	U ²²	U ³³	U ²³	U ¹³	U ¹²
Br(1)48(1)	30(1)	60(1)	-1(1)	10(1)	-3(1)	
Br(2)42(1)	48(1)	52(1)	6(1)	19(1)	-12(1)	
S(1)26(1)	49(1)	24(1)	0(1)	0(1)	6(1)	
S(2)25(1)	37(1)	28(1)	-6(1)	9(1)	-2(1)	
O(1)34(1)	40(1)	26(1)	5(1)	8(1)	8(1)	
O(2)31(1)	44(1)	21(1)	4(1)	2(1)	-4(1)	
O(3)32(1)	27(1)	23(1)	1(1)	6(1)	-1(1)	
O(4)48(1)	29(1)	56(1)	3(1)	25(1)	-1(1)	
C(1)27(1)	30(1)	34(1)	5(1)	2(1)	2(1)	
C(2)34(1)	44(2)	42(2)	4(1)	10(1)	11(1)	
C(3)37(1)	60(2)	60(2)	21(2)	16(1)	1(1)	
C(4)44(2)	42(2)	70(2)	11(2)	7(2)	-12(1)	
C(5)38(1)	39(1)	51(2)	-1(1)	-1(1)	1(1)	
C(6)23(1)	38(1)	32(1)	5(1)	-1(1)	2(1)	
C(7)23(1)	32(1)	26(1)	1(1)	2(1)	2(1)	
C(8)24(1)	23(1)	27(1)	1(1)	5(1)	3(1)	
C(9)23(1)	26(1)	25(1)	-3(1)	8(1)	0(1)	
C(10)23(1)	35(1)	25(1)	-1(1)	4(1)	1(1)	
C(11)24(1)	34(1)	22(1)	-1(1)	5(1)	-1(1)	
C(12)22(1)	28(1)	21(1)	-2(1)	3(1)	0(1)	
C(13)31(1)	40(1)	30(1)	-11(1)	10(1)	-2(1)	
C(14)36(1)	28(1)	46(1)	-9(1)	18(1)	-2(1)	
C(15)31(1)	26(1)	41(1)	-7(1)	13(1)	-2(1)	
C(16)28(1)	36(1)	38(1)	-9(1)	13(1)	-6(1)	
C(17)26(1)	46(2)	49(2)	-13(1)	9(1)	-6(1)	
C(18)27(1)	59(2)	50(2)	-10(2)	5(1)	5(1)	
C(19)34(1)	45(2)	50(2)	5(1)	11(1)	9(1)	
C(20)28(1)	32(1)	44(1)	-3(1)	12(1)	3(1)	
C(21)23(1)	34(1)	33(1)	-7(1)	11(1)	-1(1)	

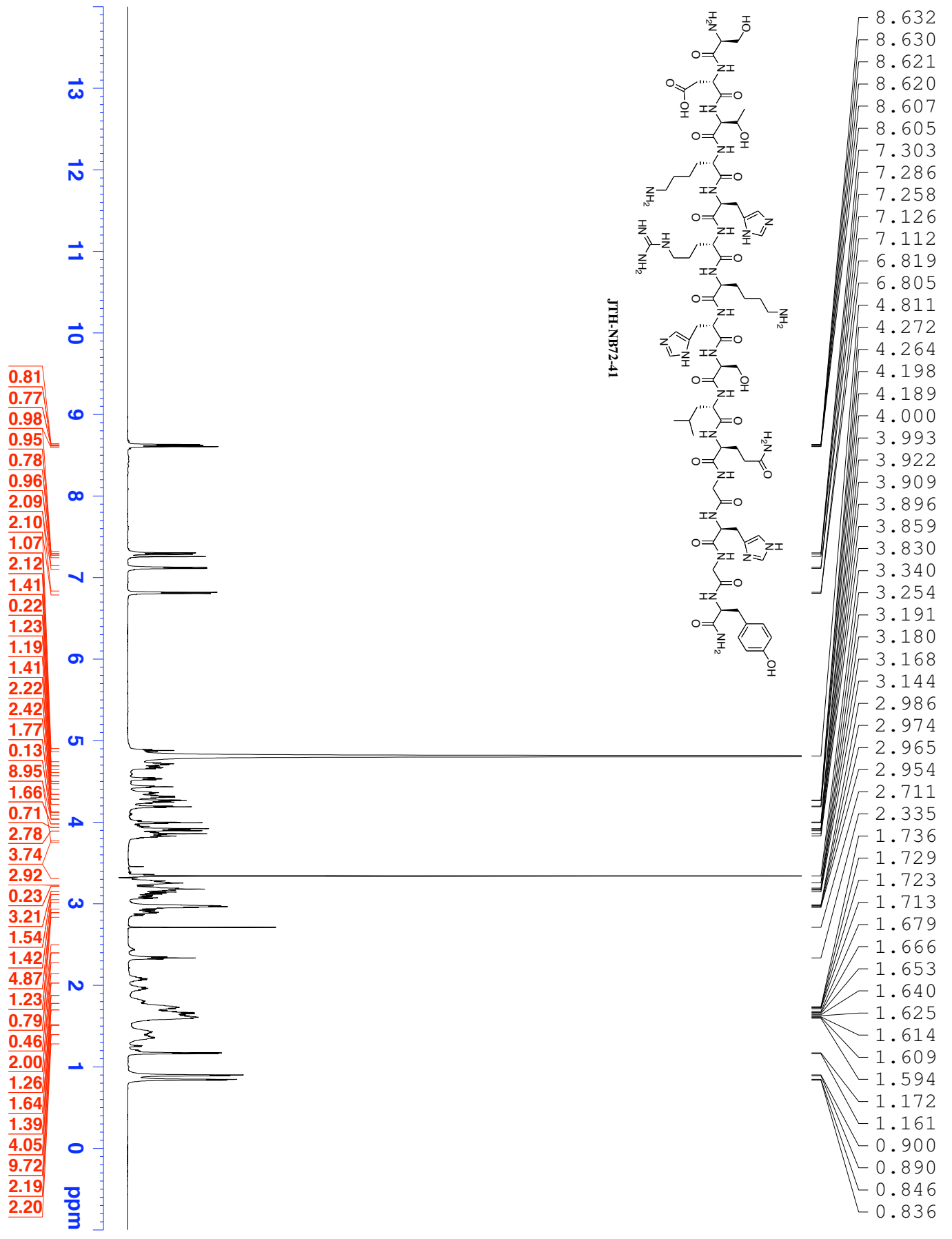
Table 43. Hydrogen coordinates ($\times 10^4$) and isotropic displacement parameters ($\text{\AA}^2 \times 10^3$) for **2.37**.

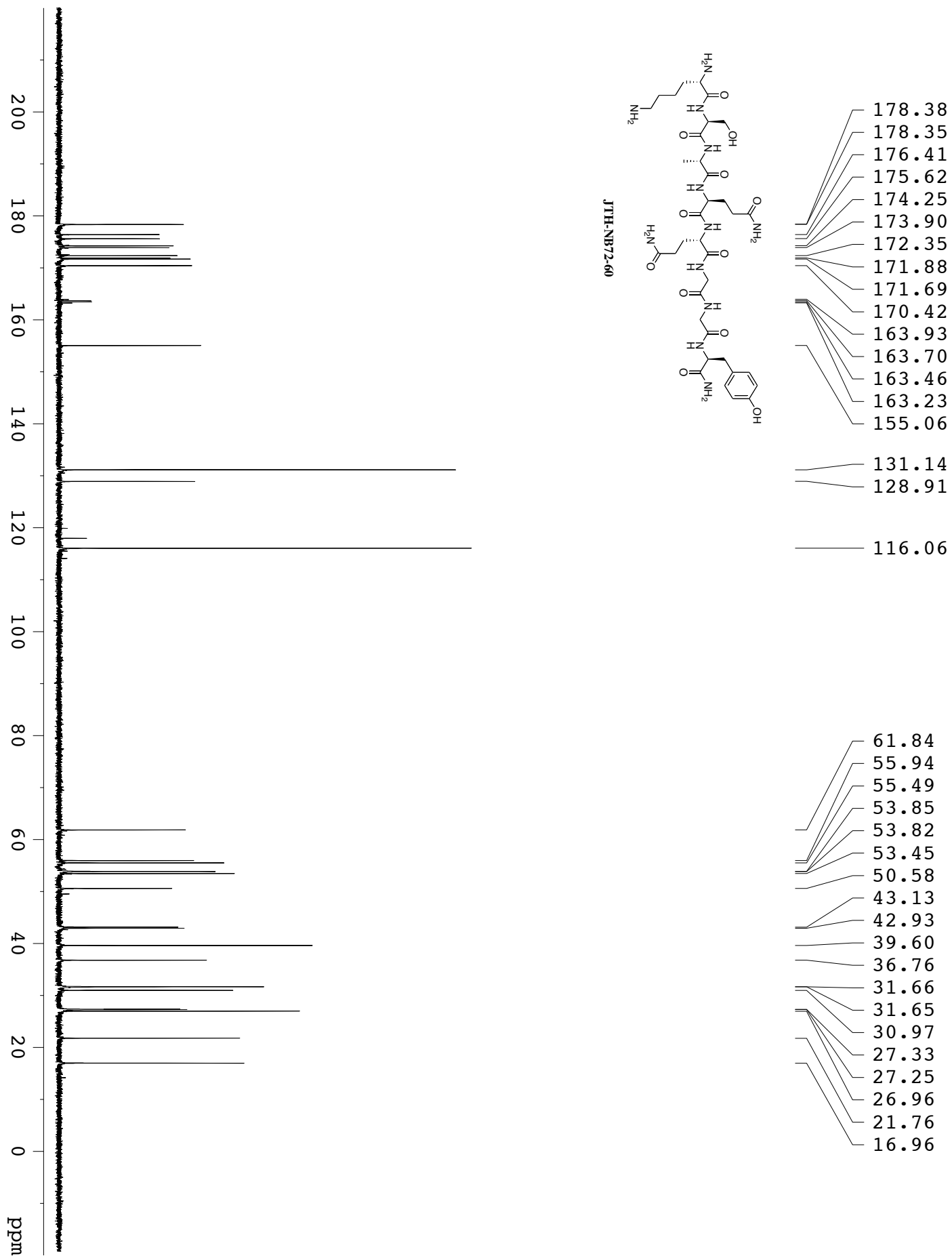
	x	y	z	U(eq)
H(2O)	1400(30)	4440(30)	4390(40)	40(10)
H(3O)	1100(20)	5360(30)	6760(40)	35(10)
H(4O)	170(30)	2140(40)	8990(70)	84(19)
H(2A)	5195	2658	6941	48
H(3A)	5817	4076	6763	62
H(4A)	5378	5313	7974	63
H(5A)	4306	5162	9368	53
H(10A)	2903	3923	6917	33
H(12A)	293	4139	6037	28
H(13A)	1846	2704	4976	40
H(13B)	865	2954	4664	40
H(14A)	1746	2106	7259	42
H(14B)	1005	1664	6111	42
H(15A)	-14	2565	6873	38
H(17A)	-2834	2988	6539	48
H(18A)	-3016	4229	4969	55
H(19A)	-1956	5350	5167	51
H(20A)	-723	5205	6898	41

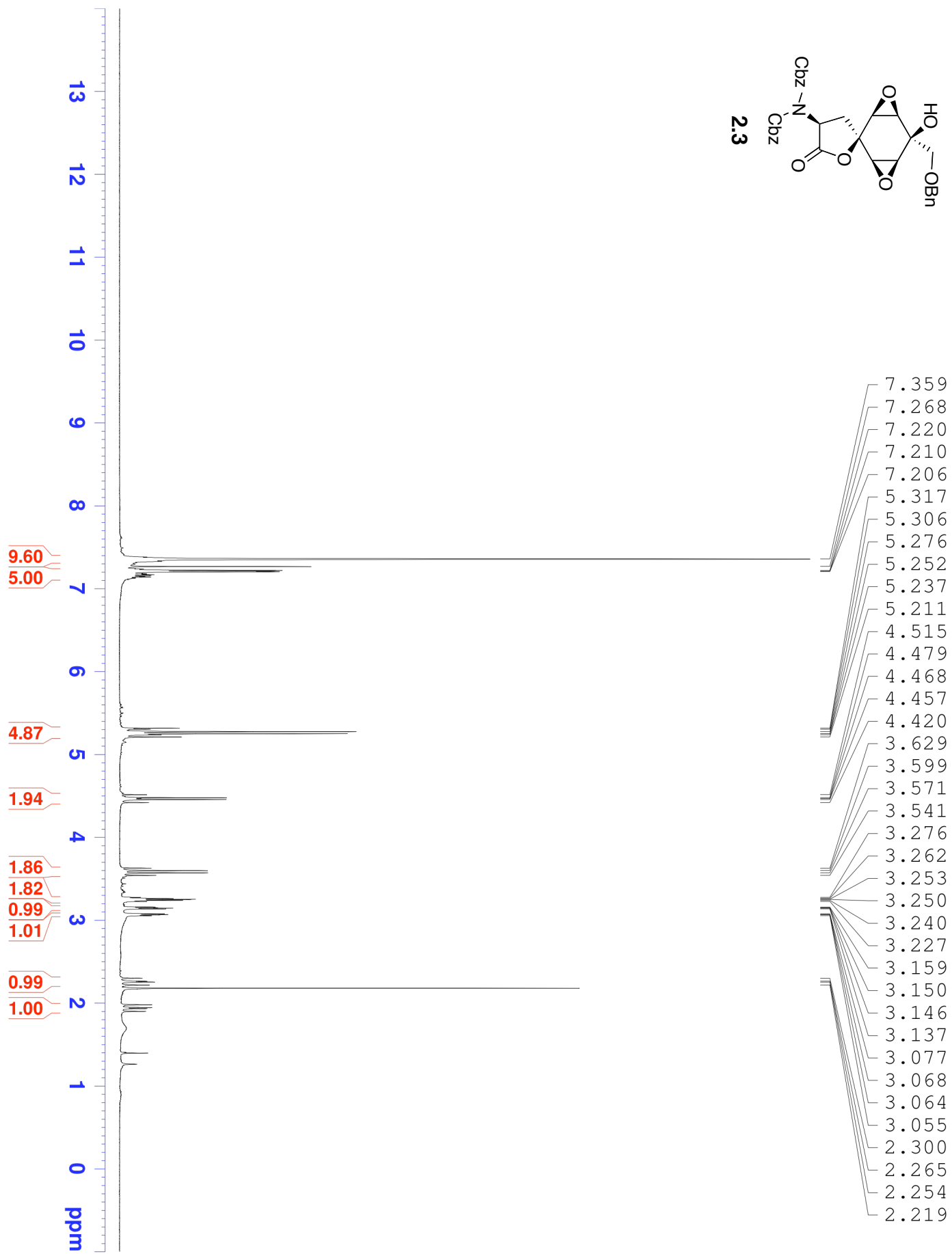
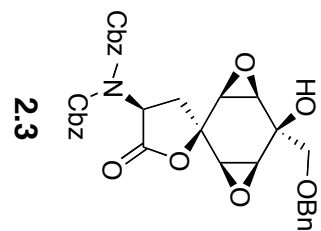
APPENDIX C

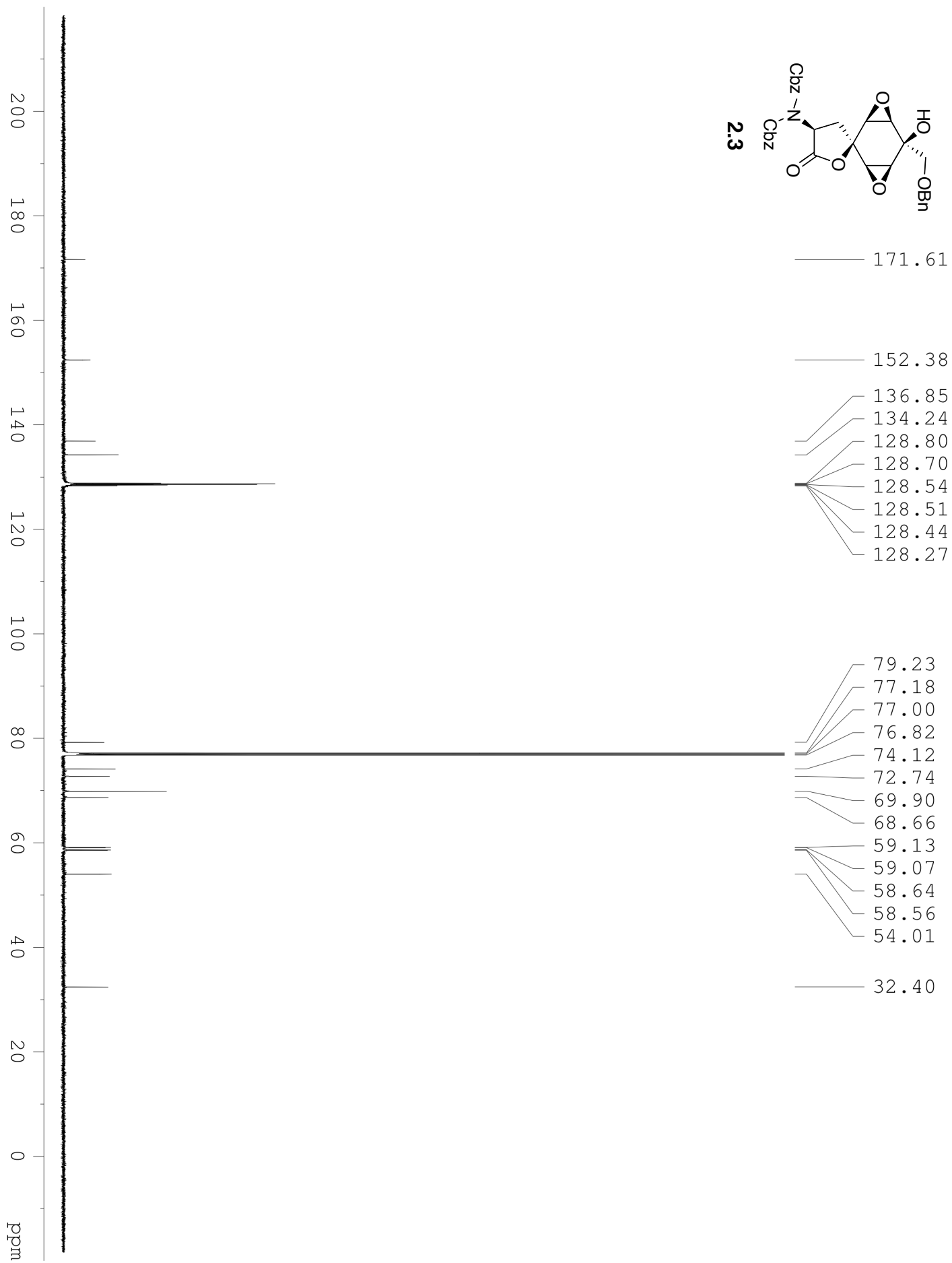
Selected NMR Spectra:

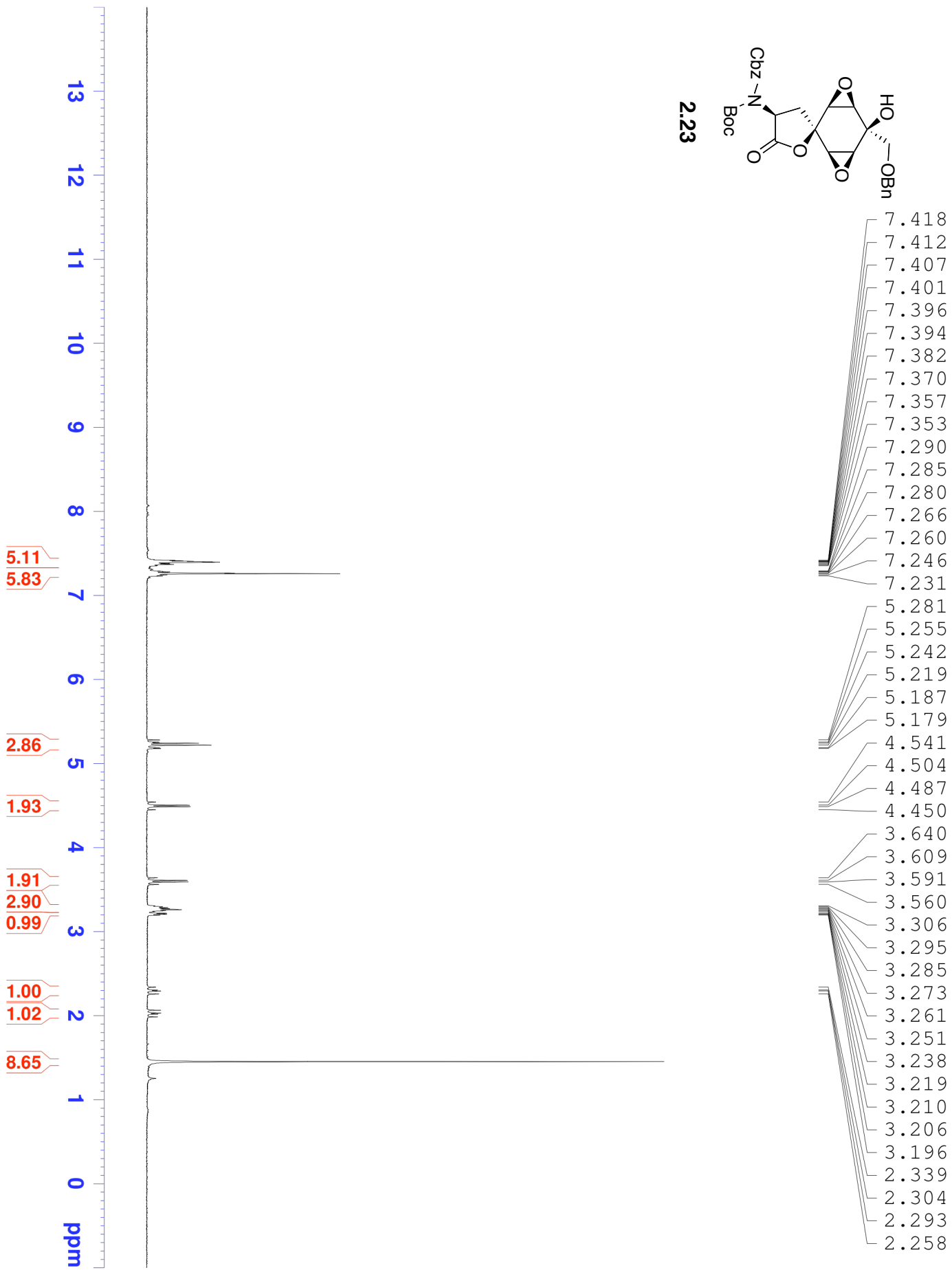




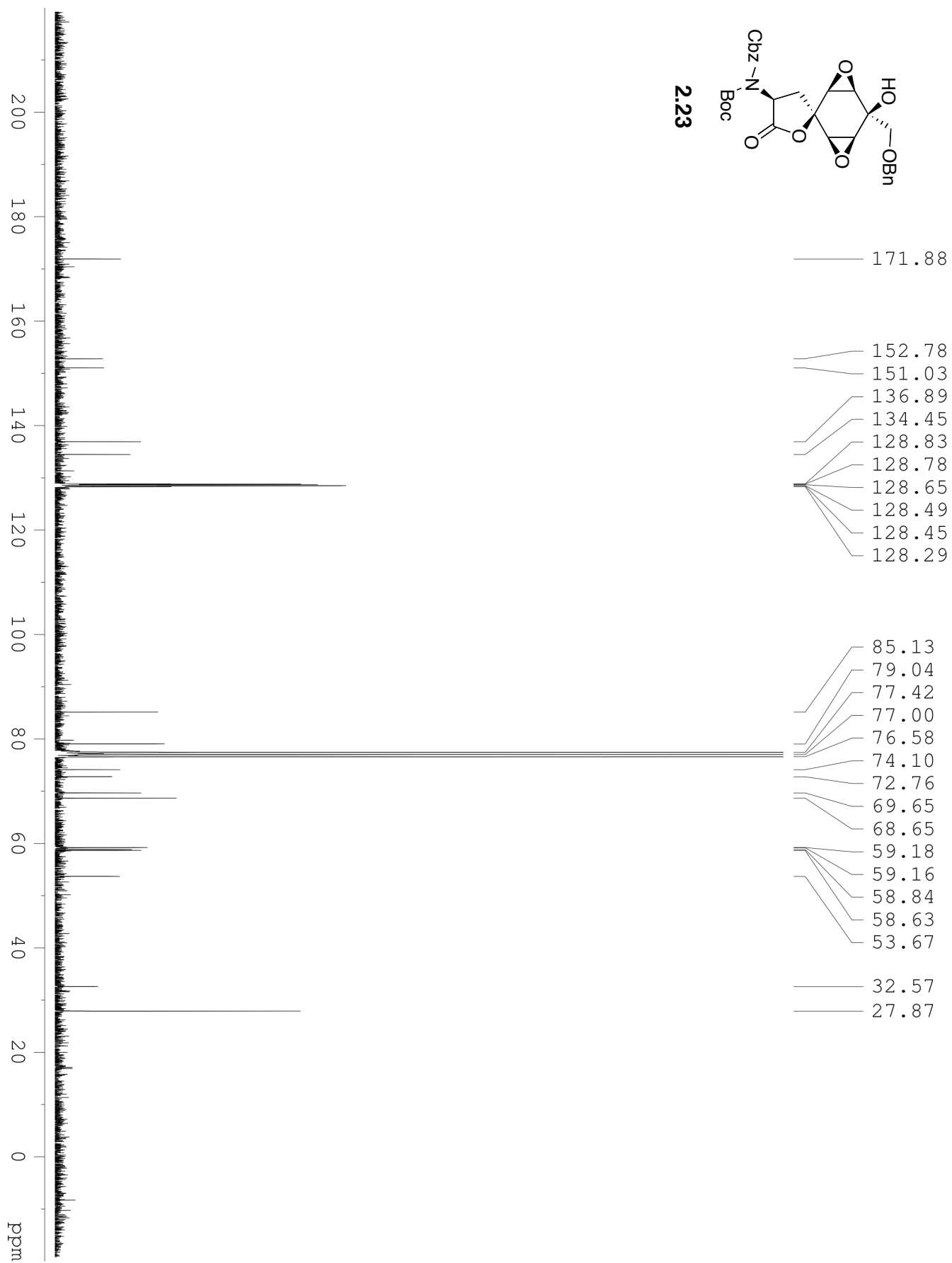
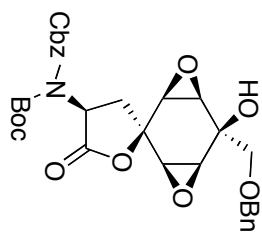


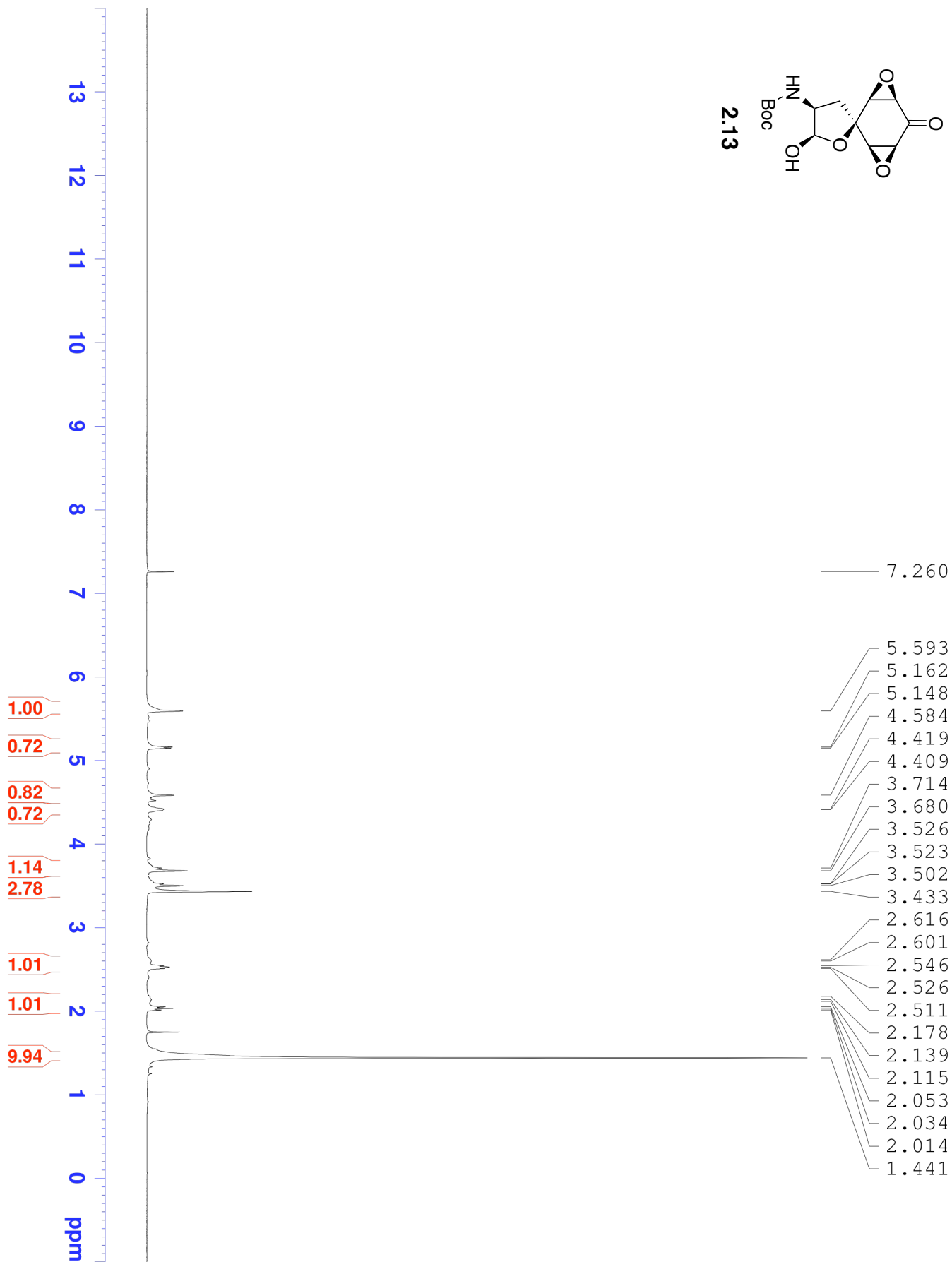
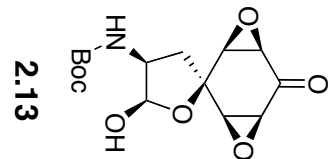


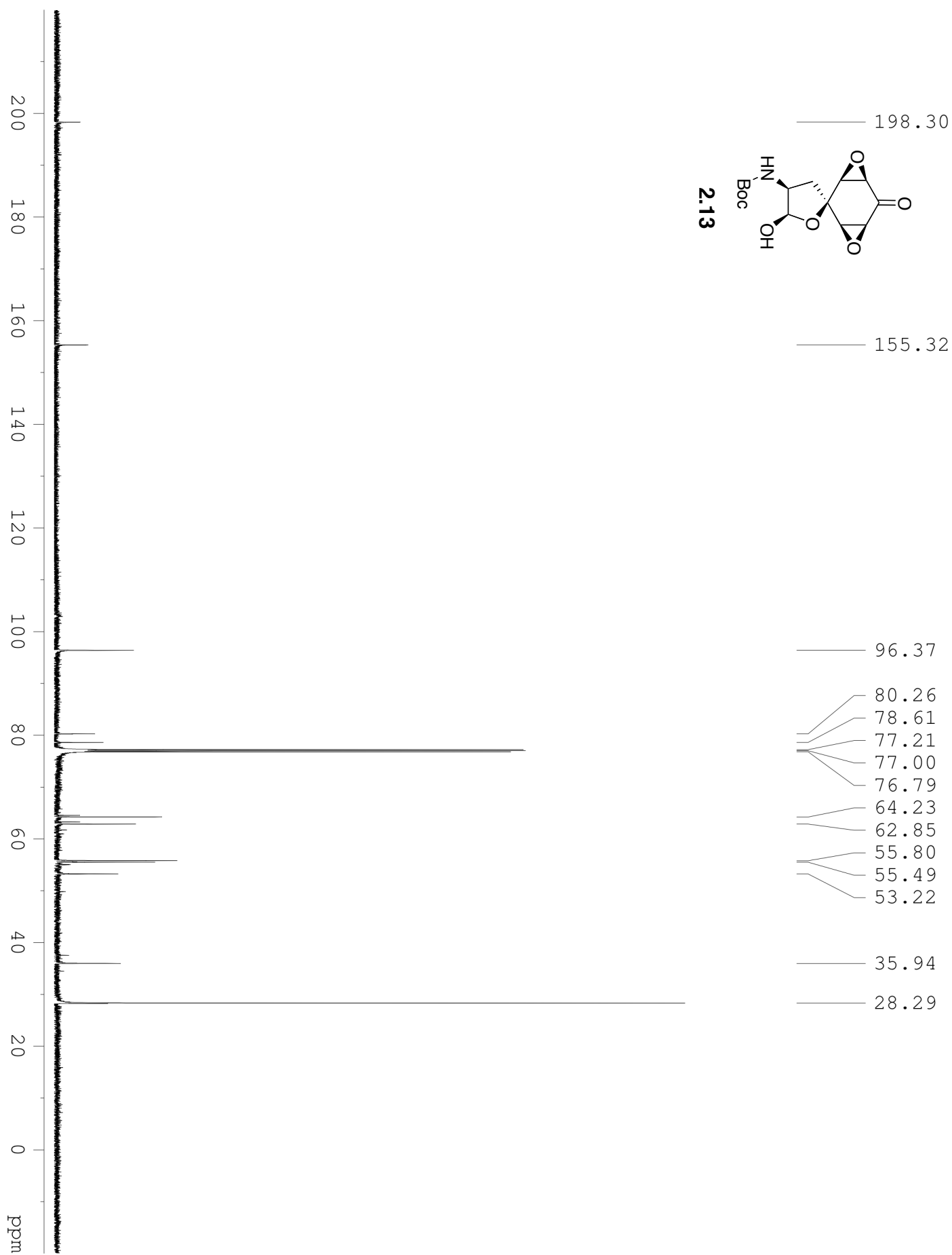


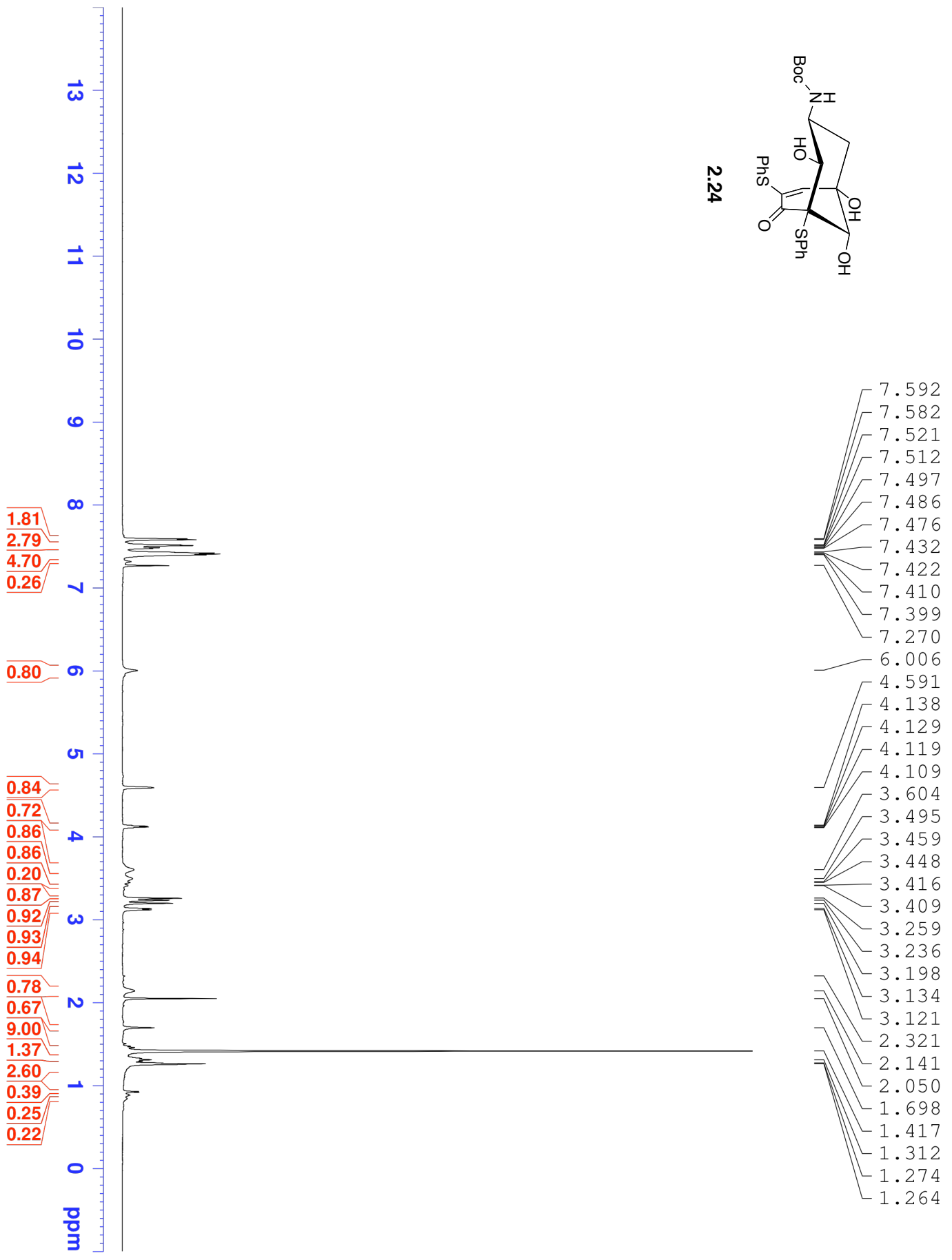
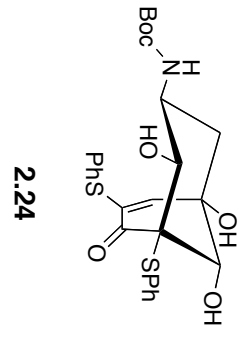


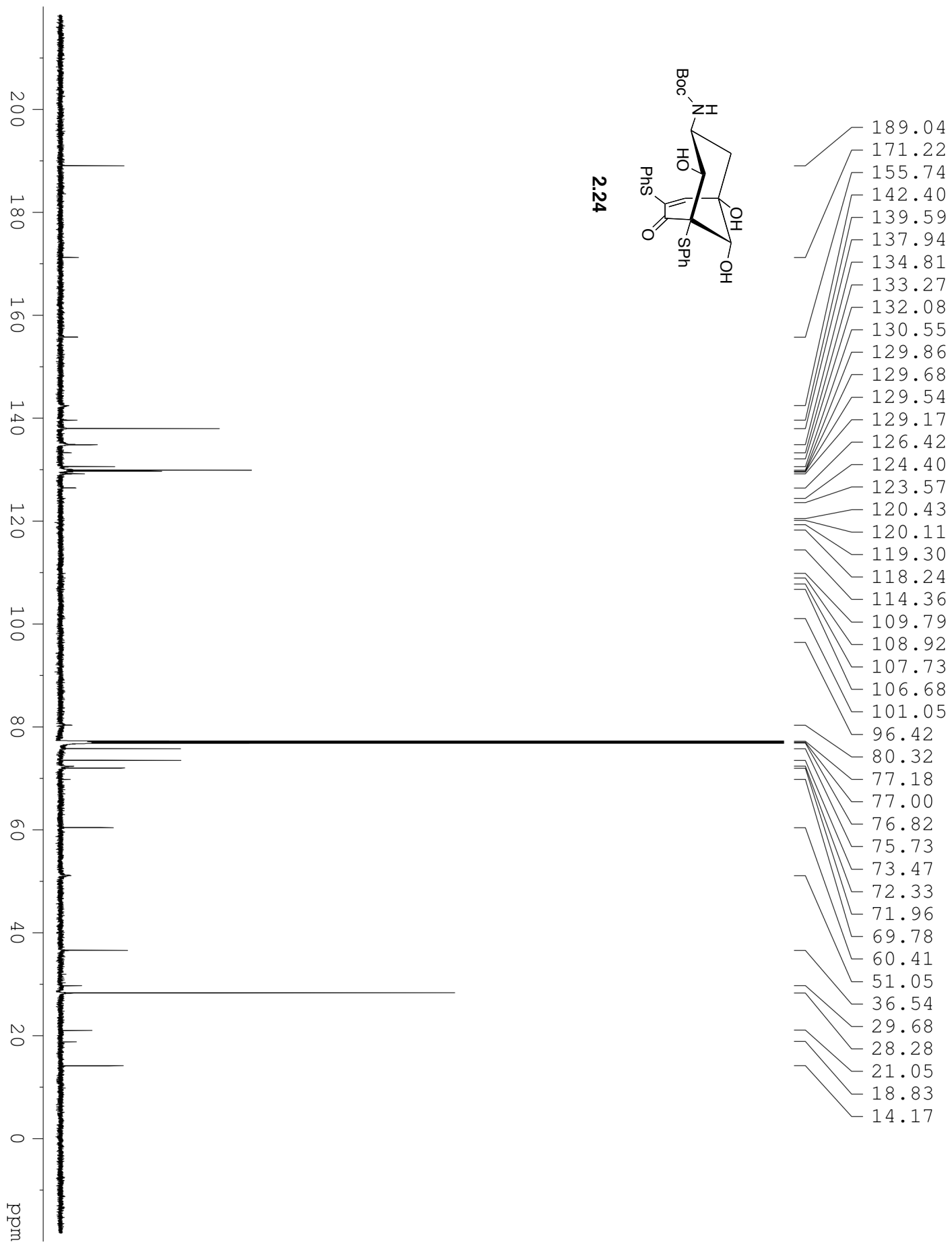
2.23

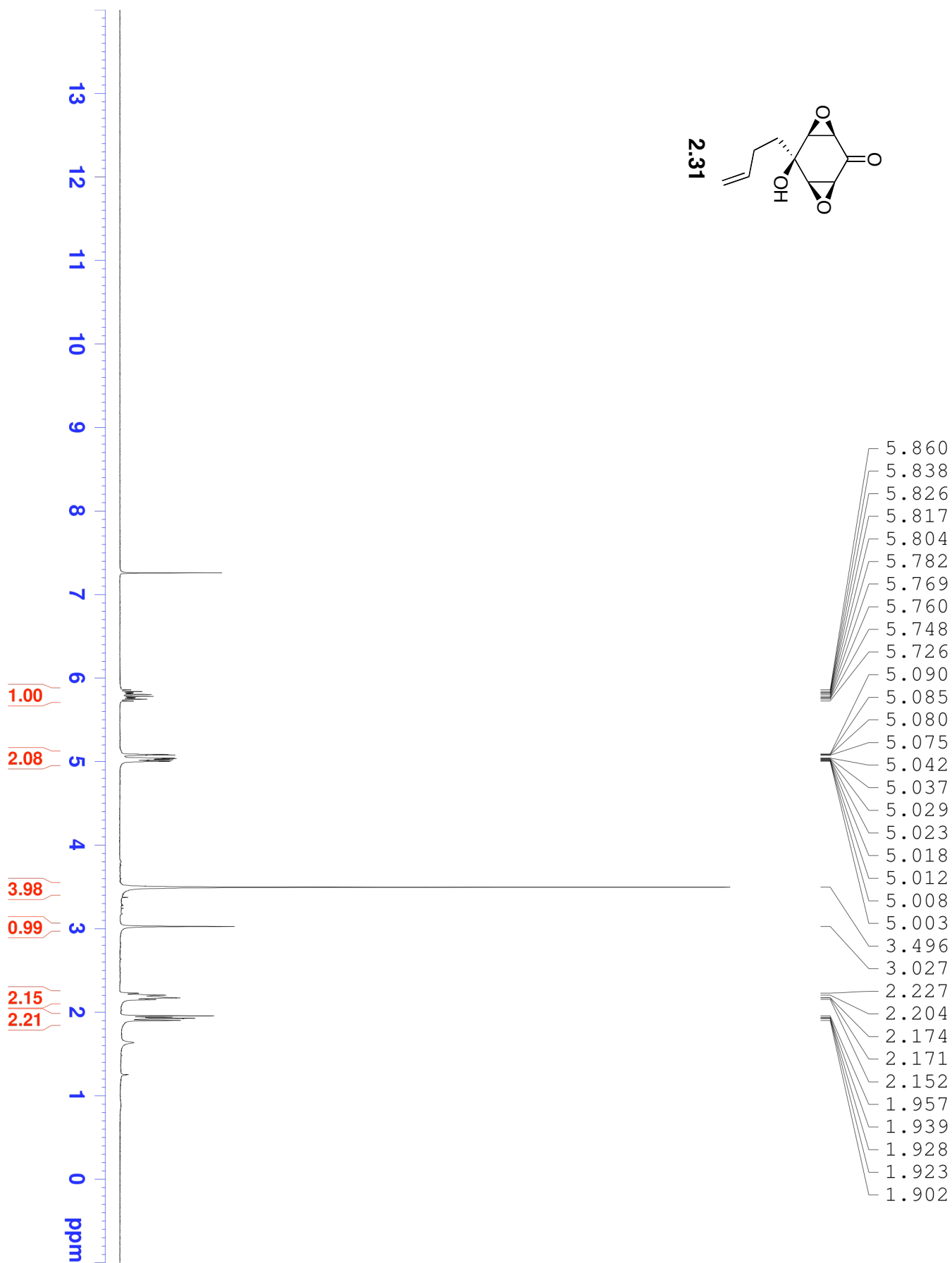
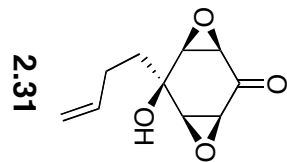


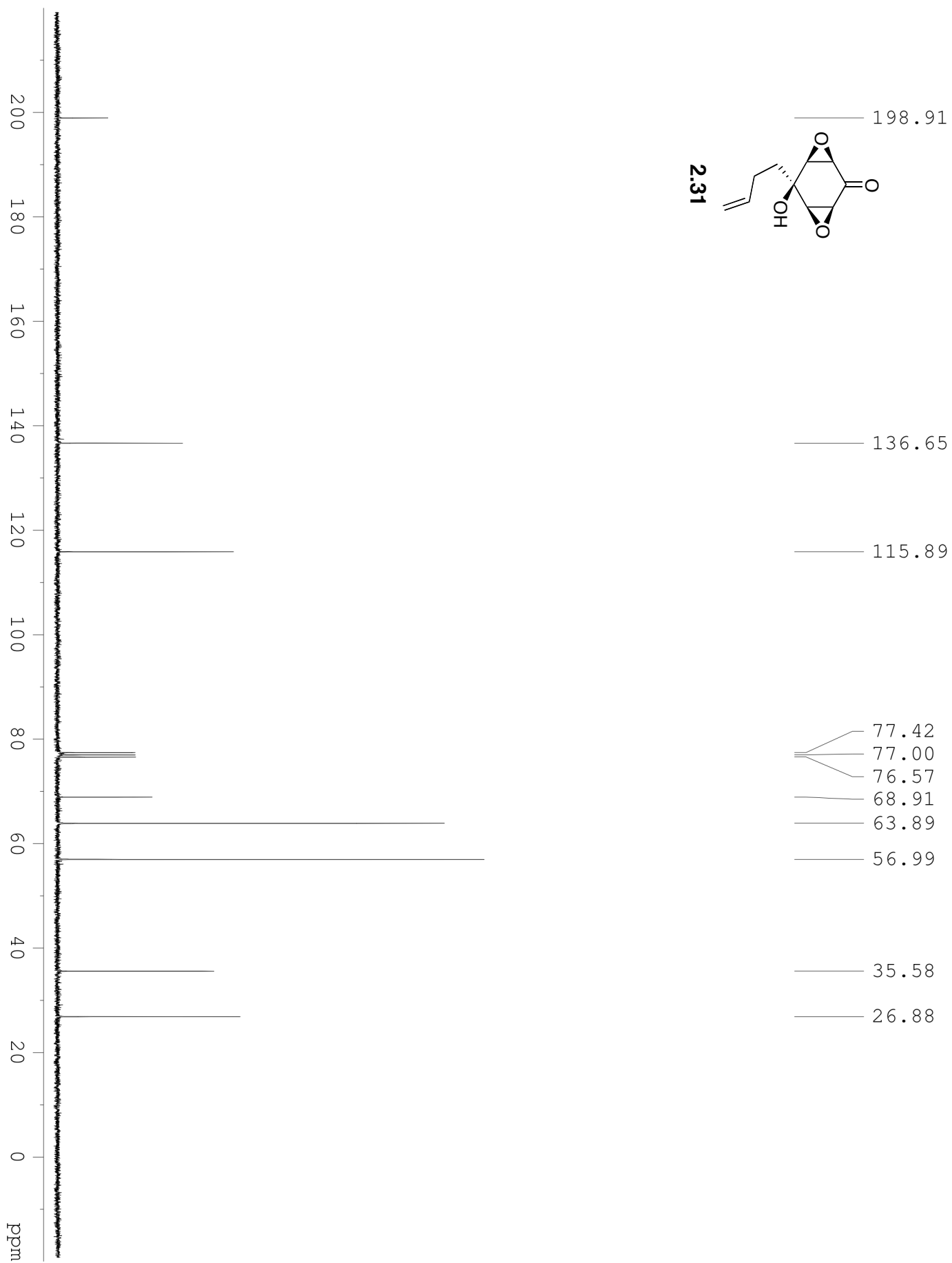


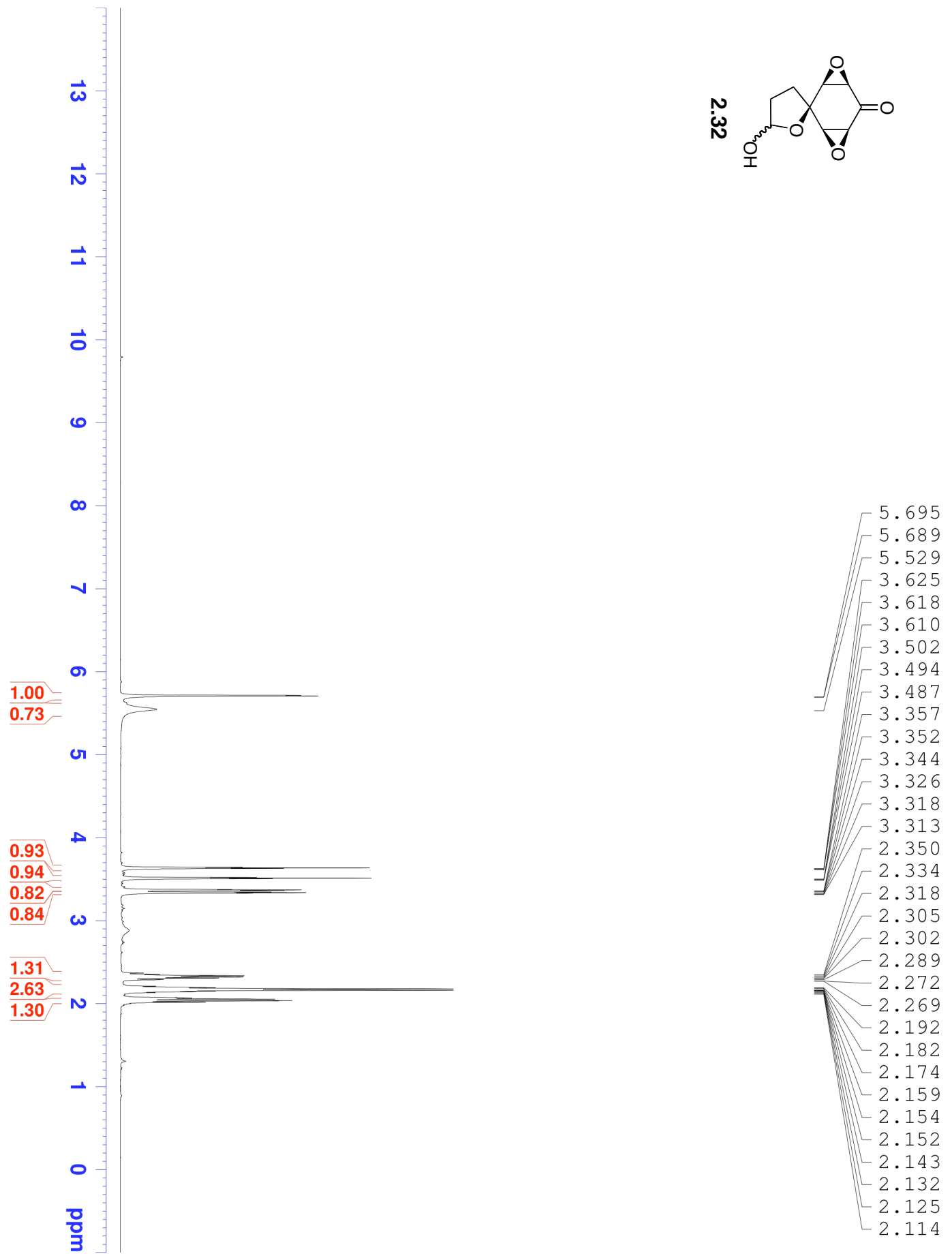
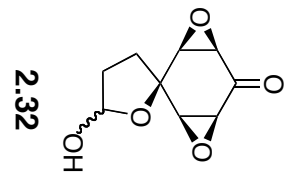


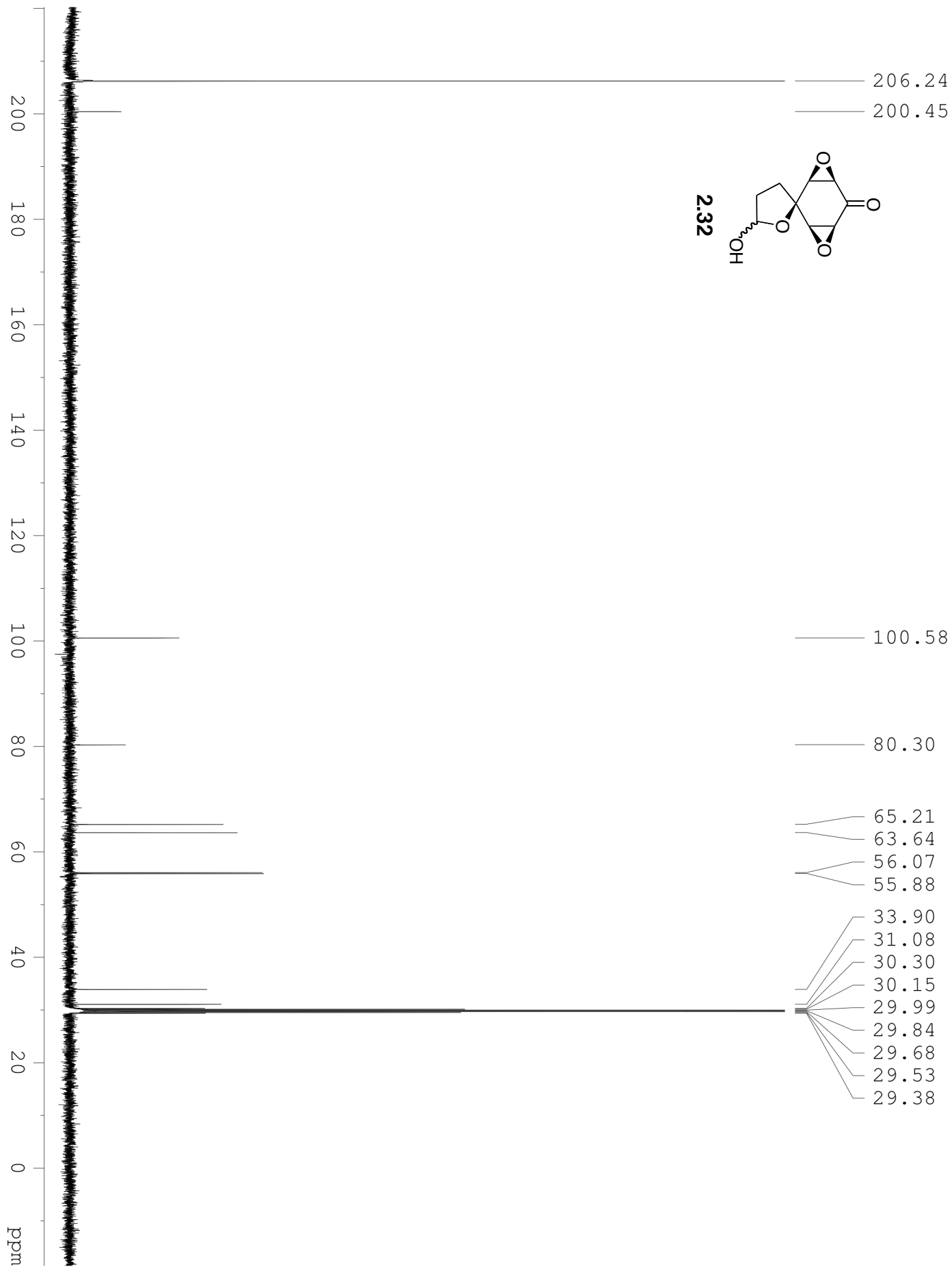


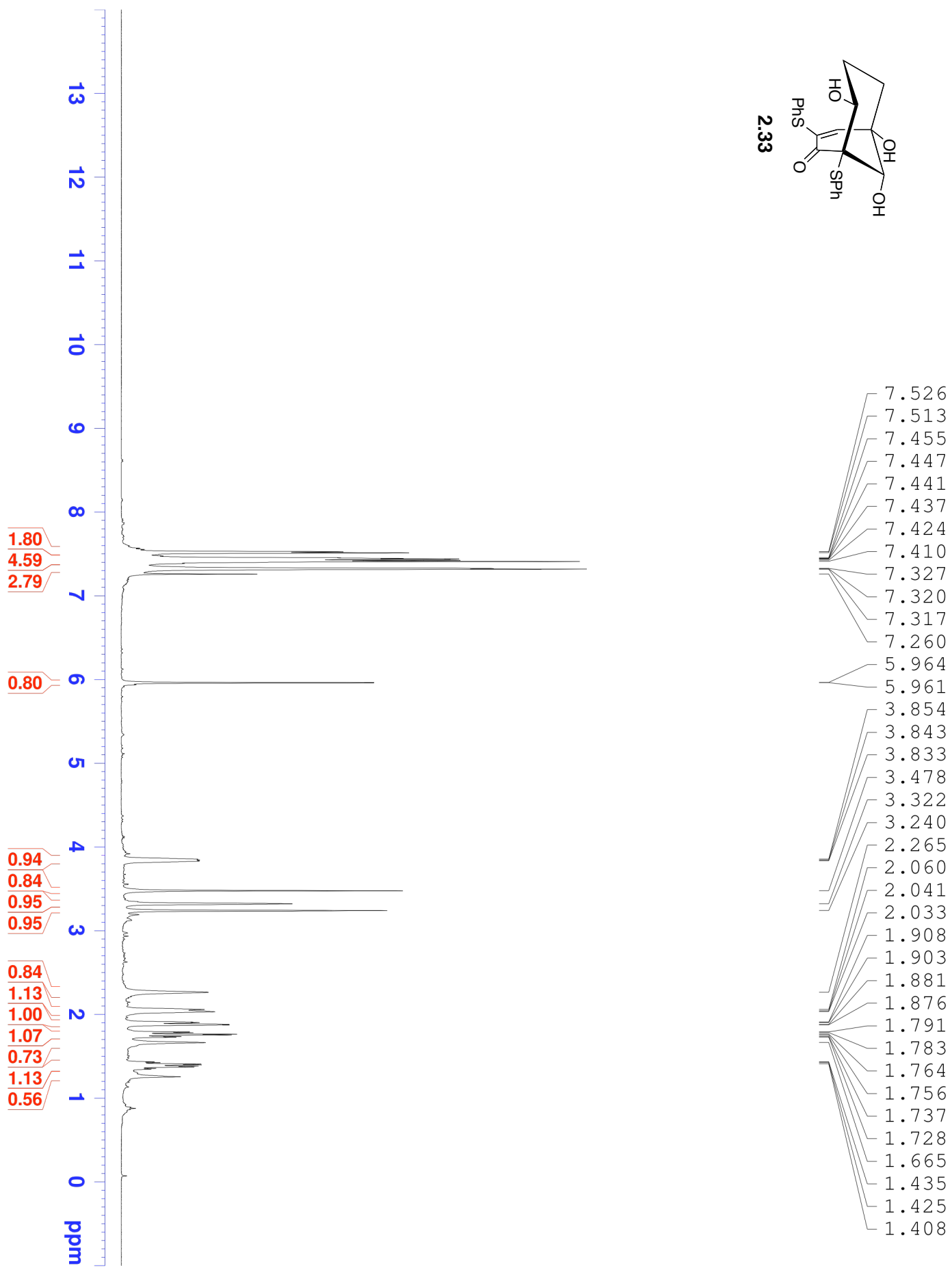
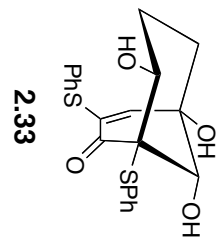


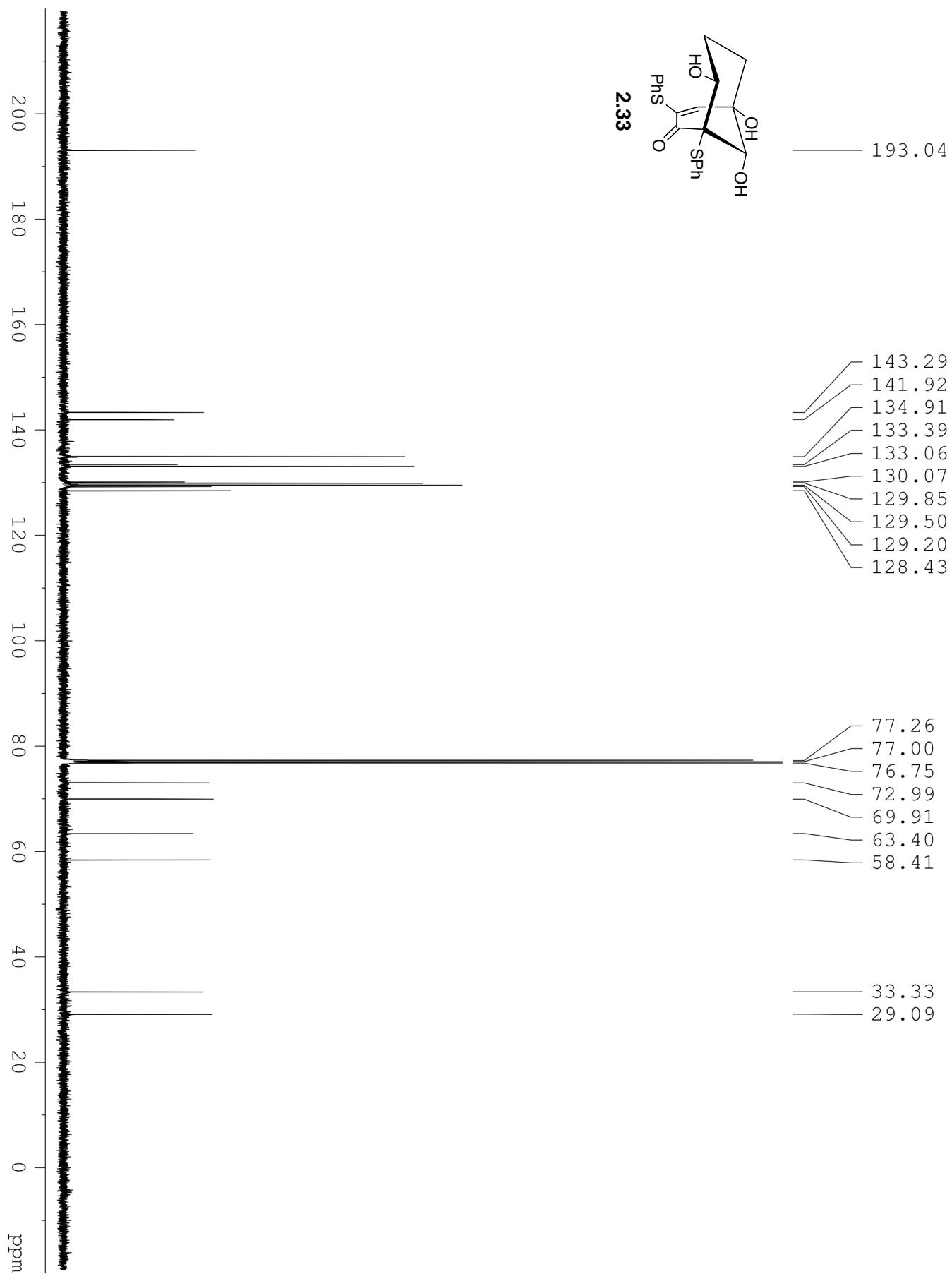


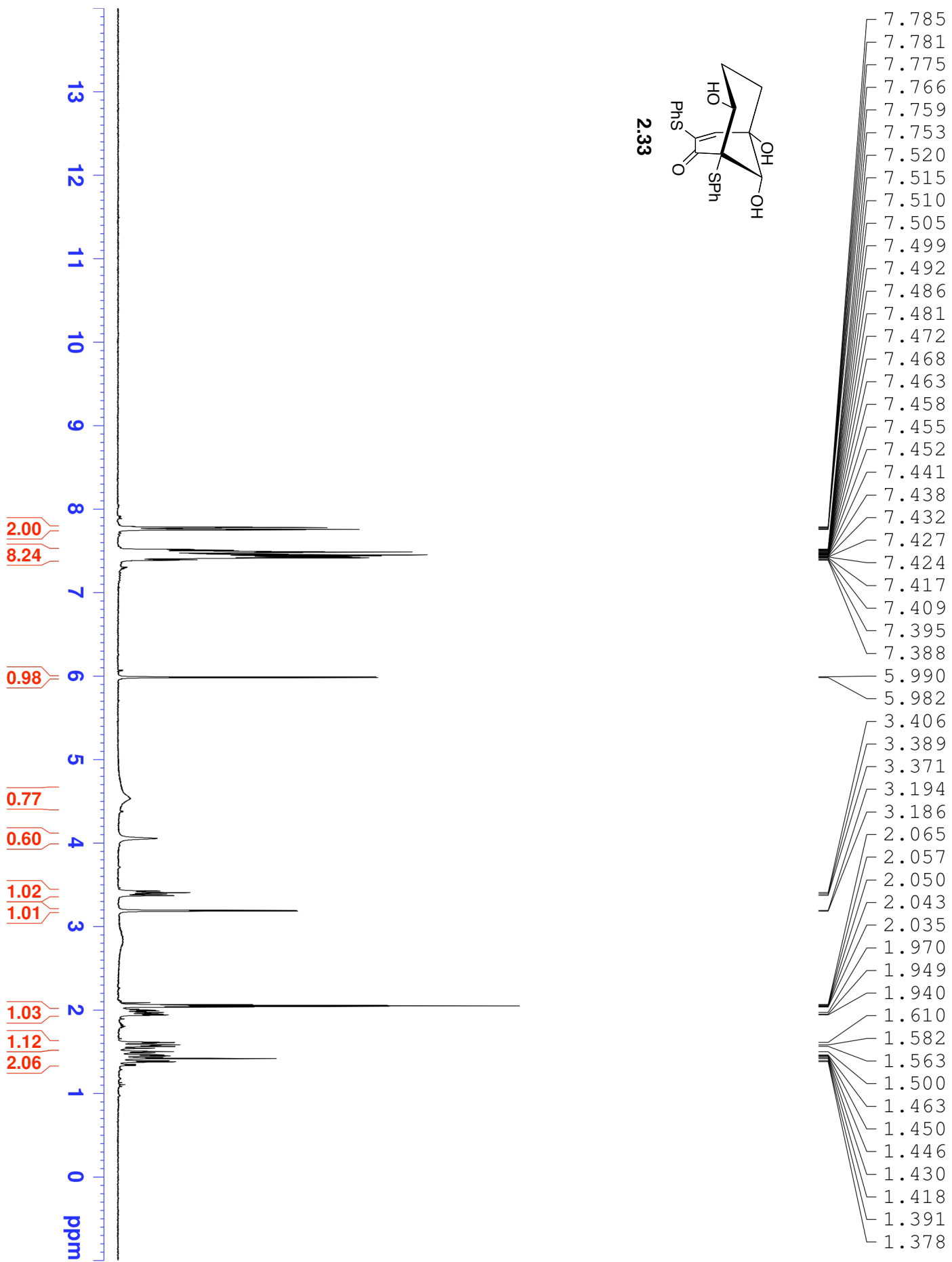
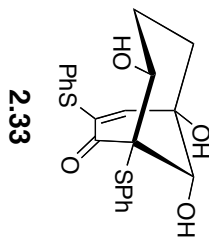


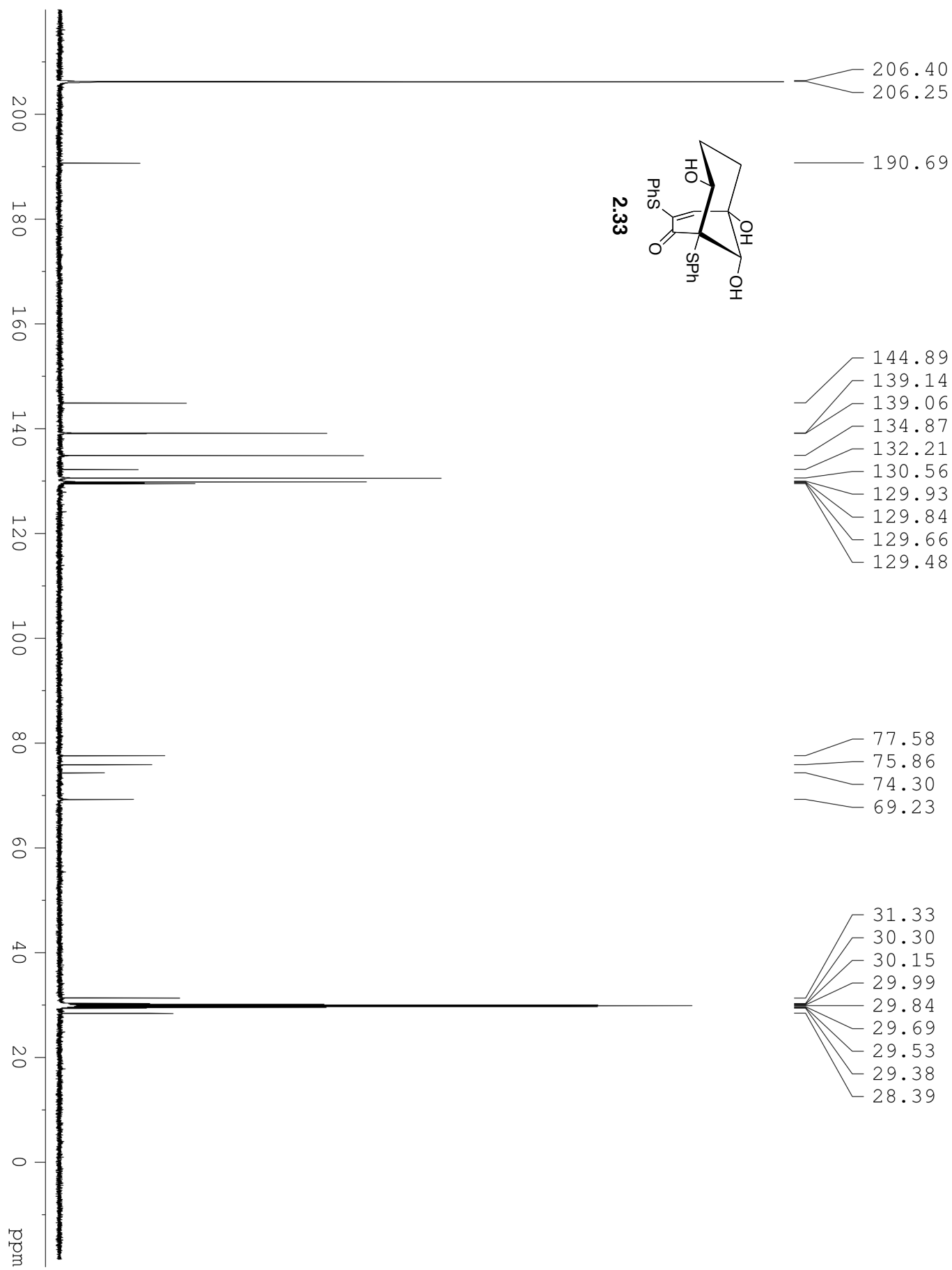


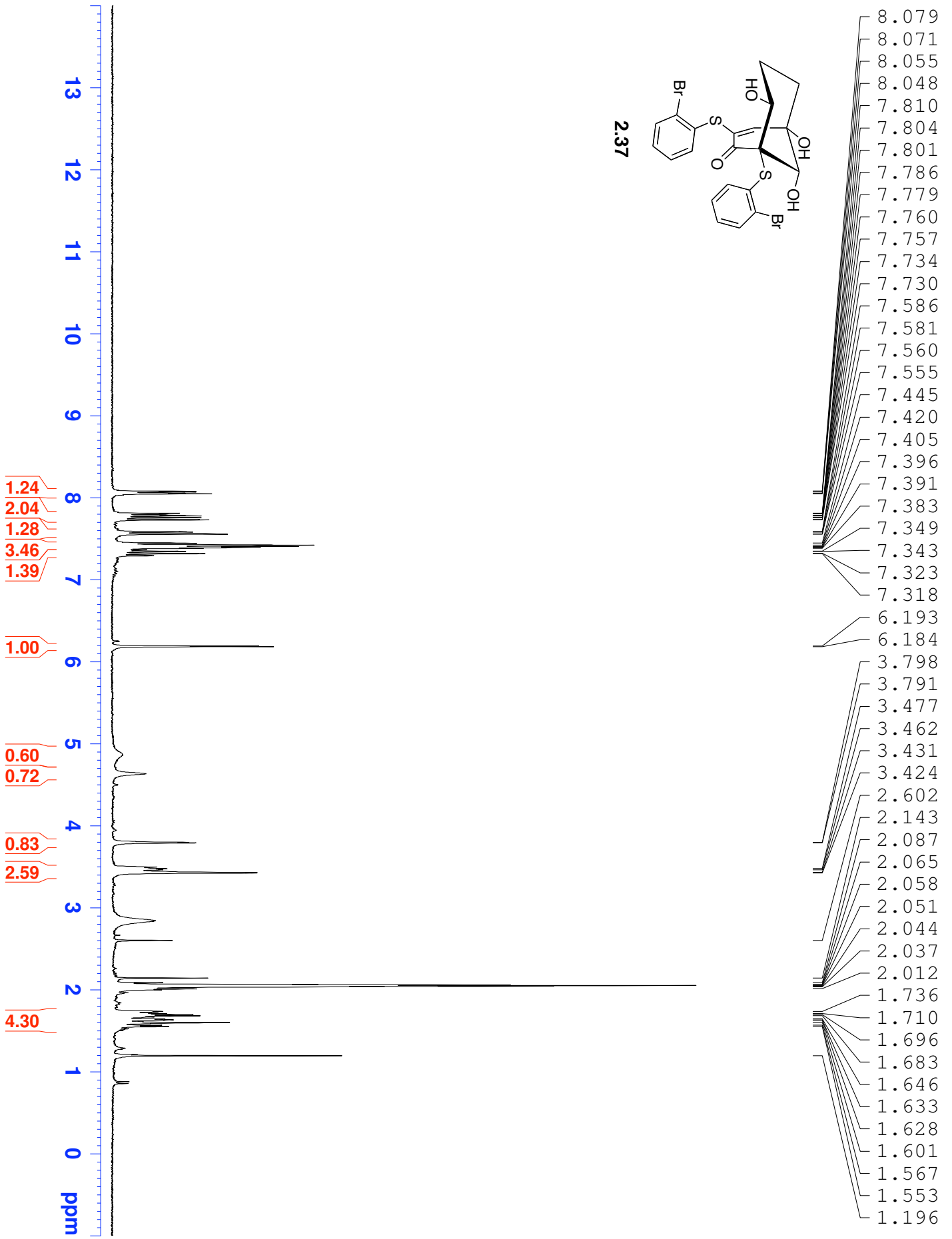


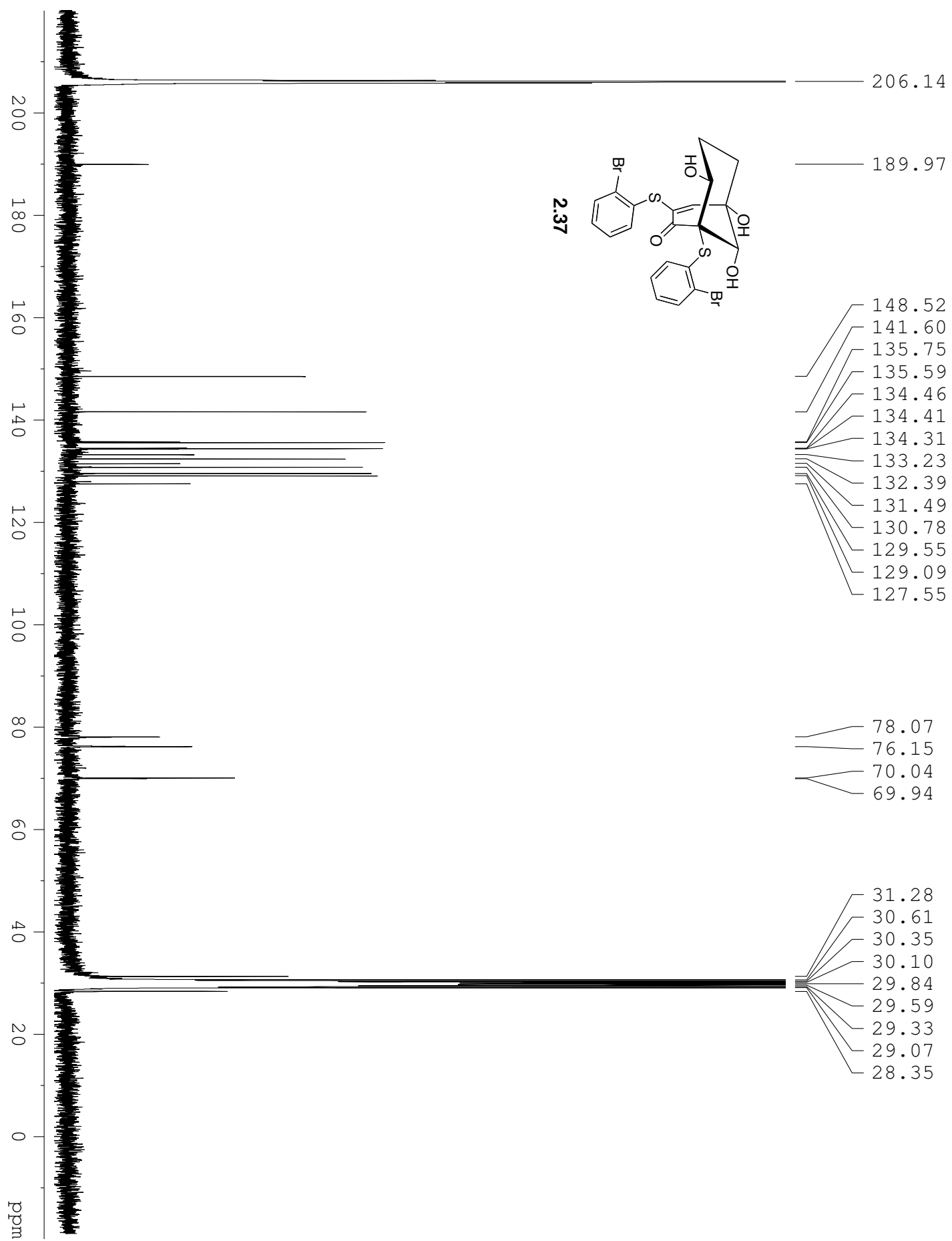


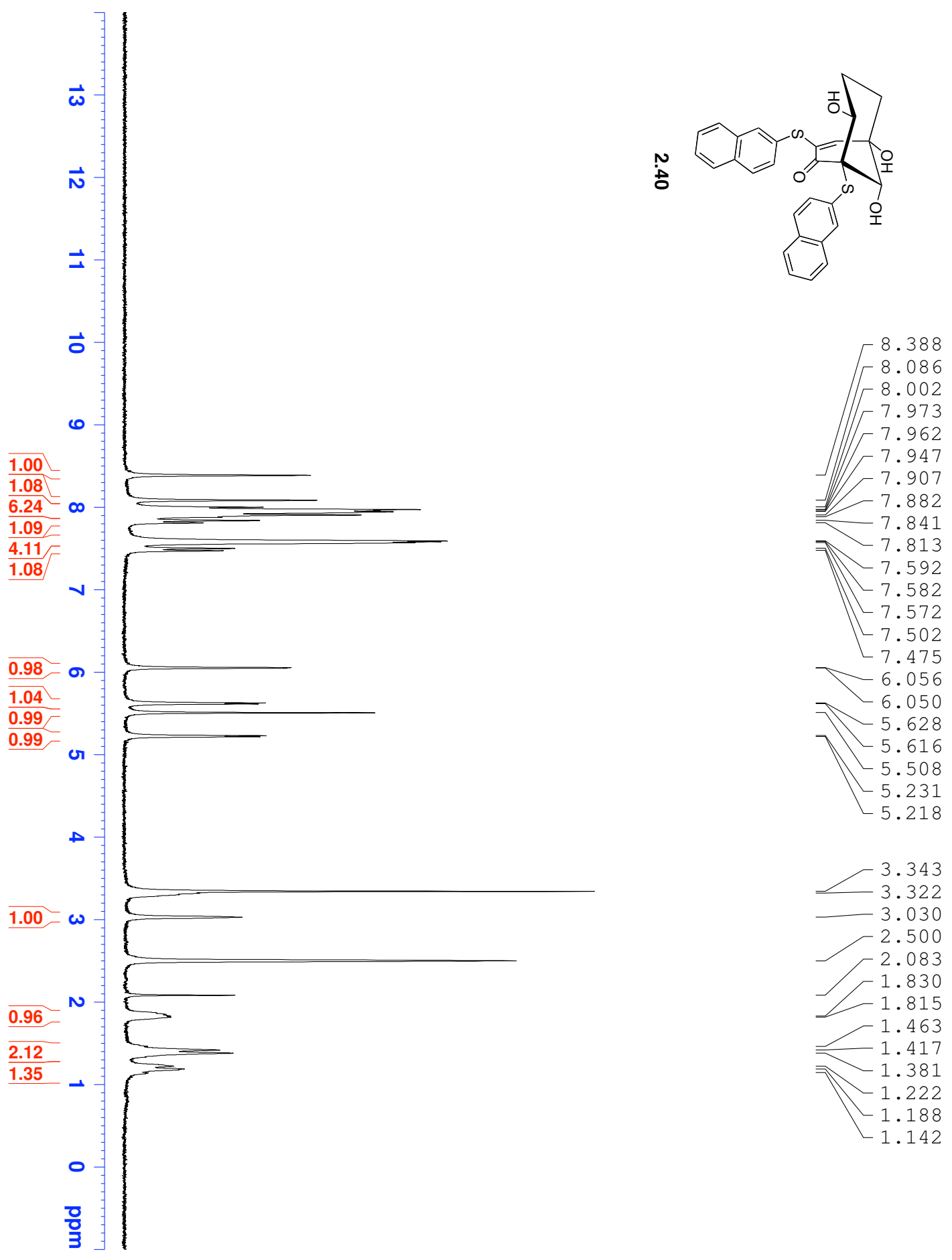
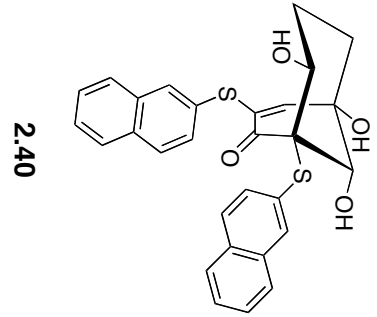


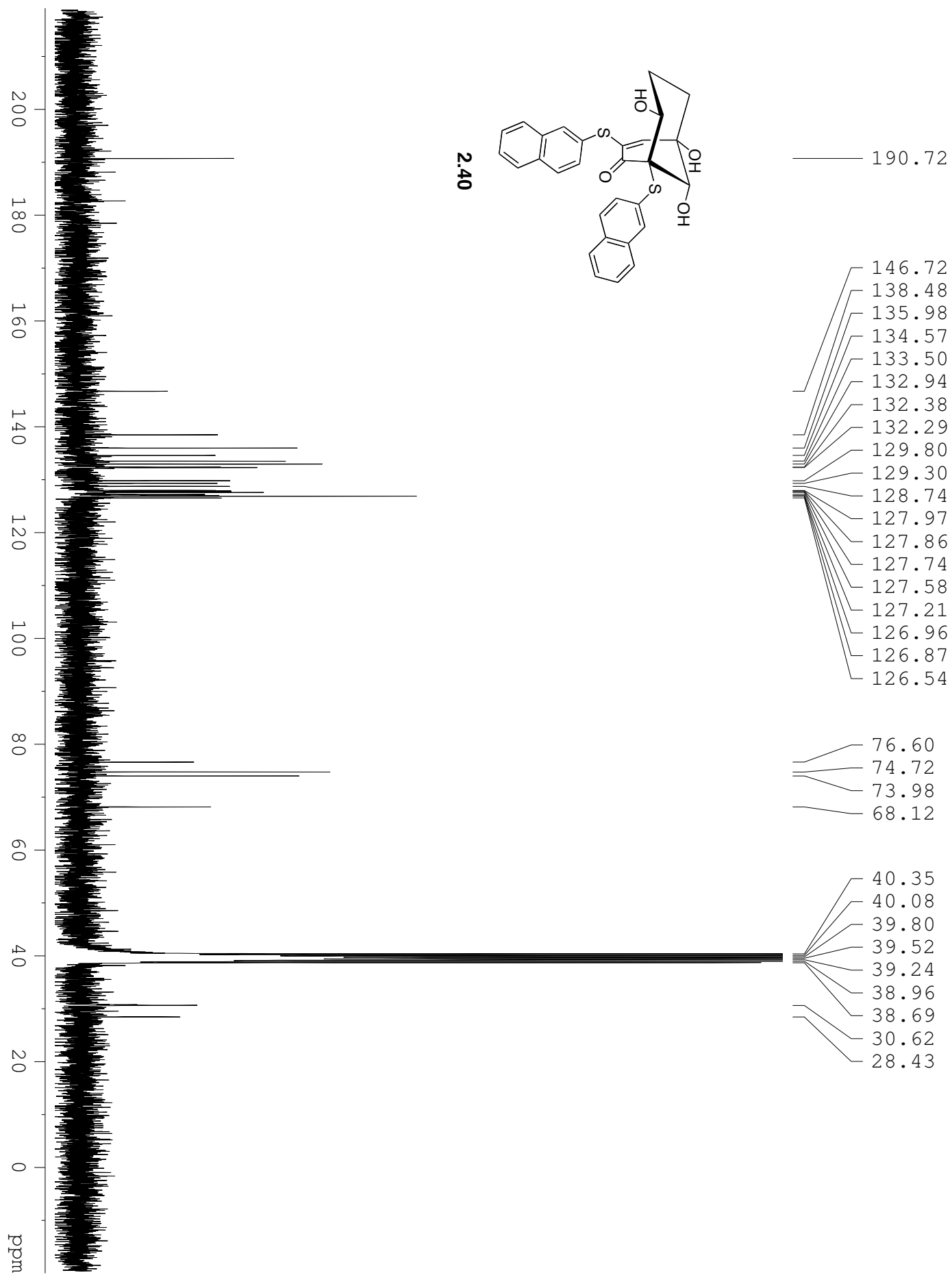




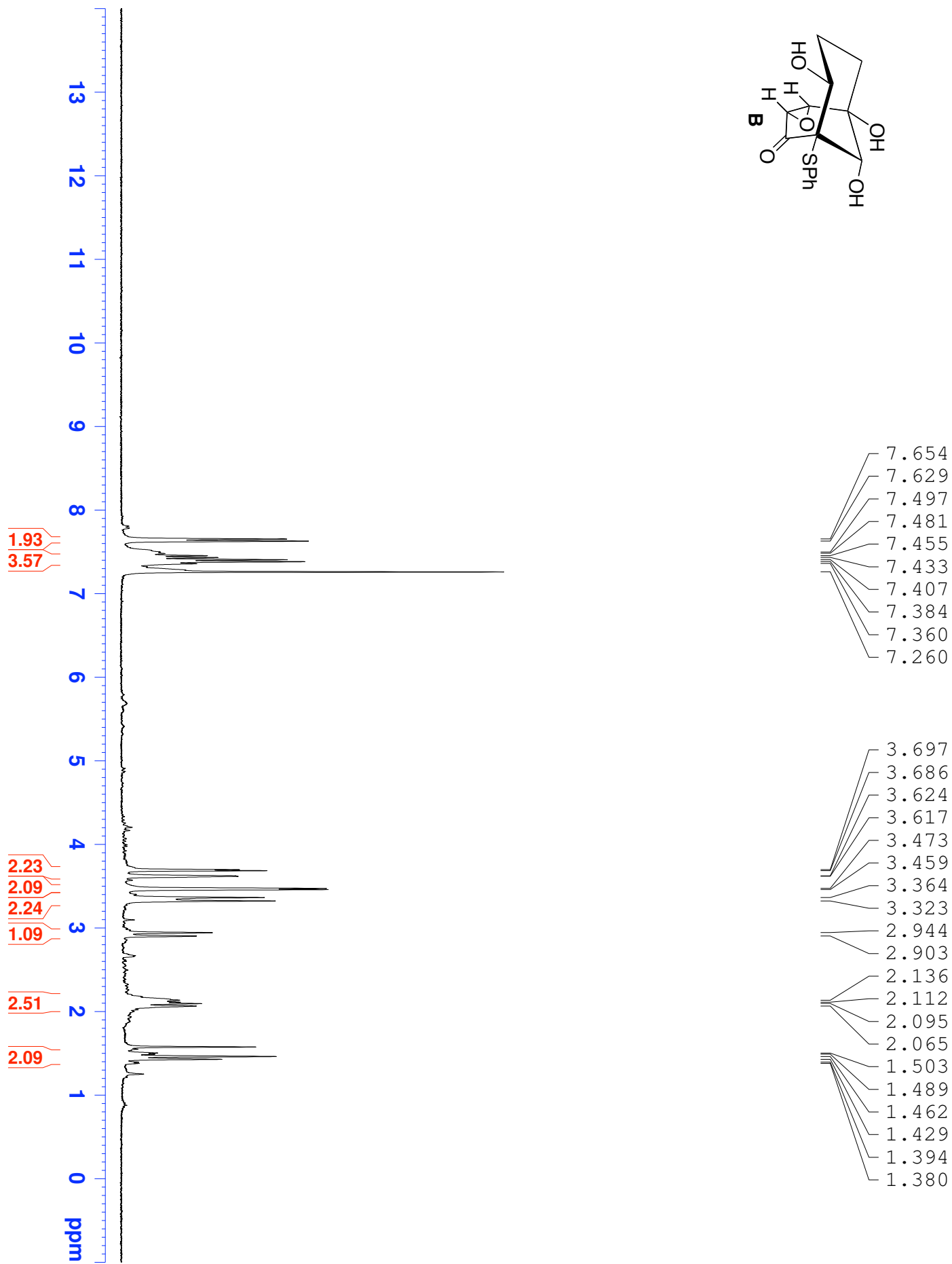
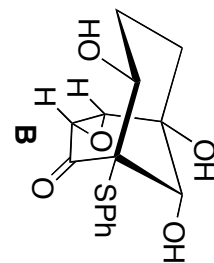


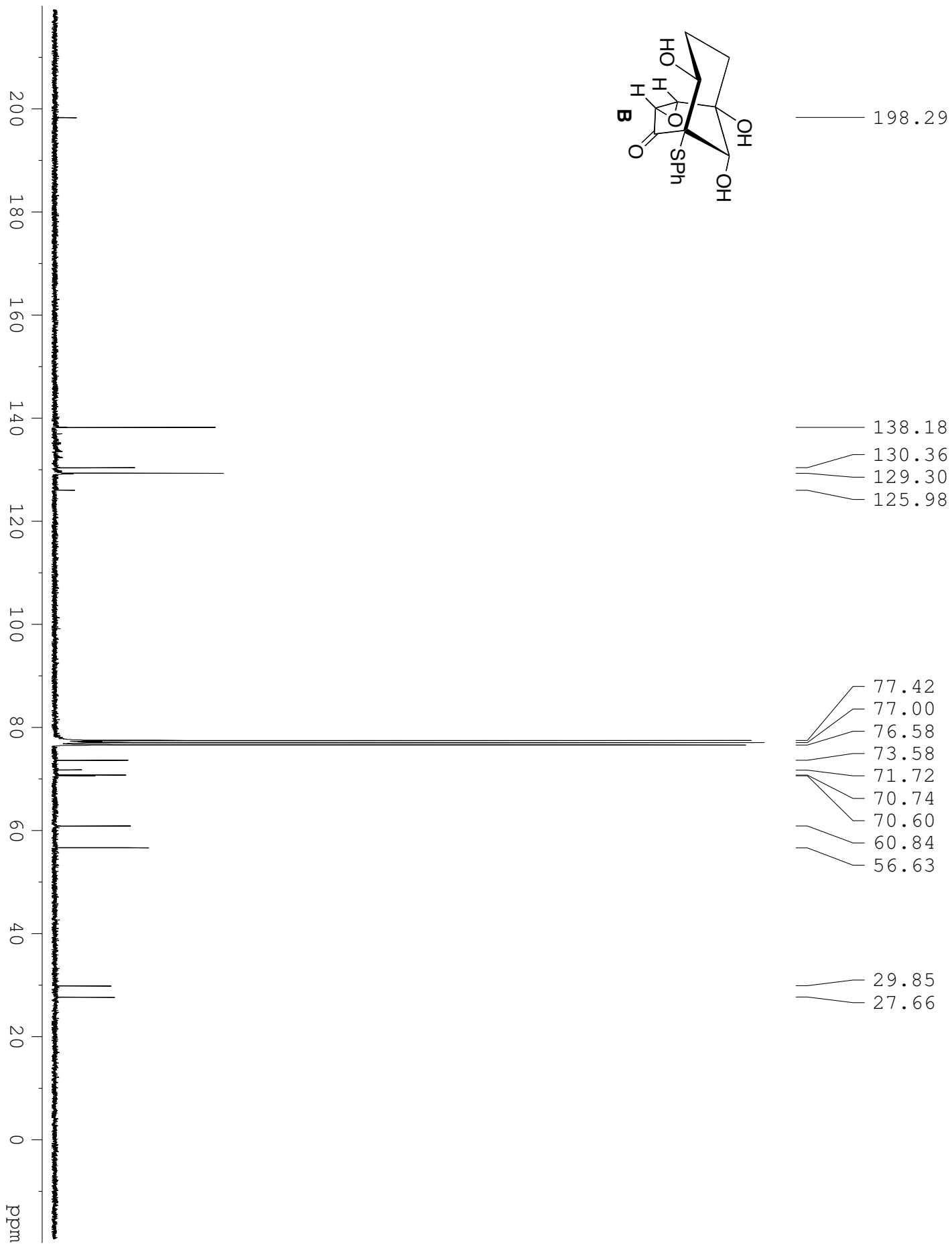


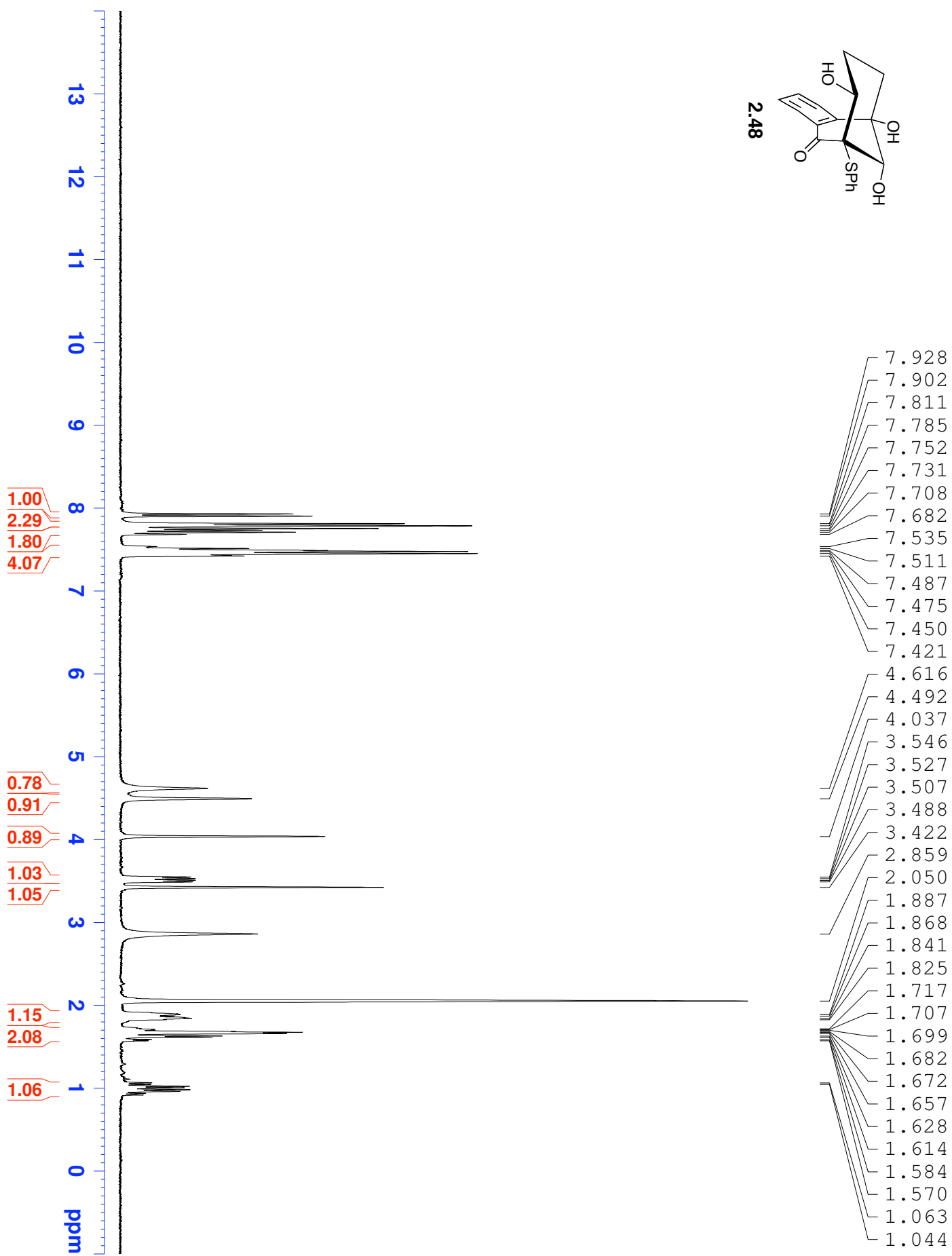
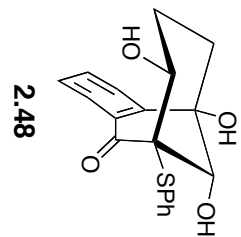


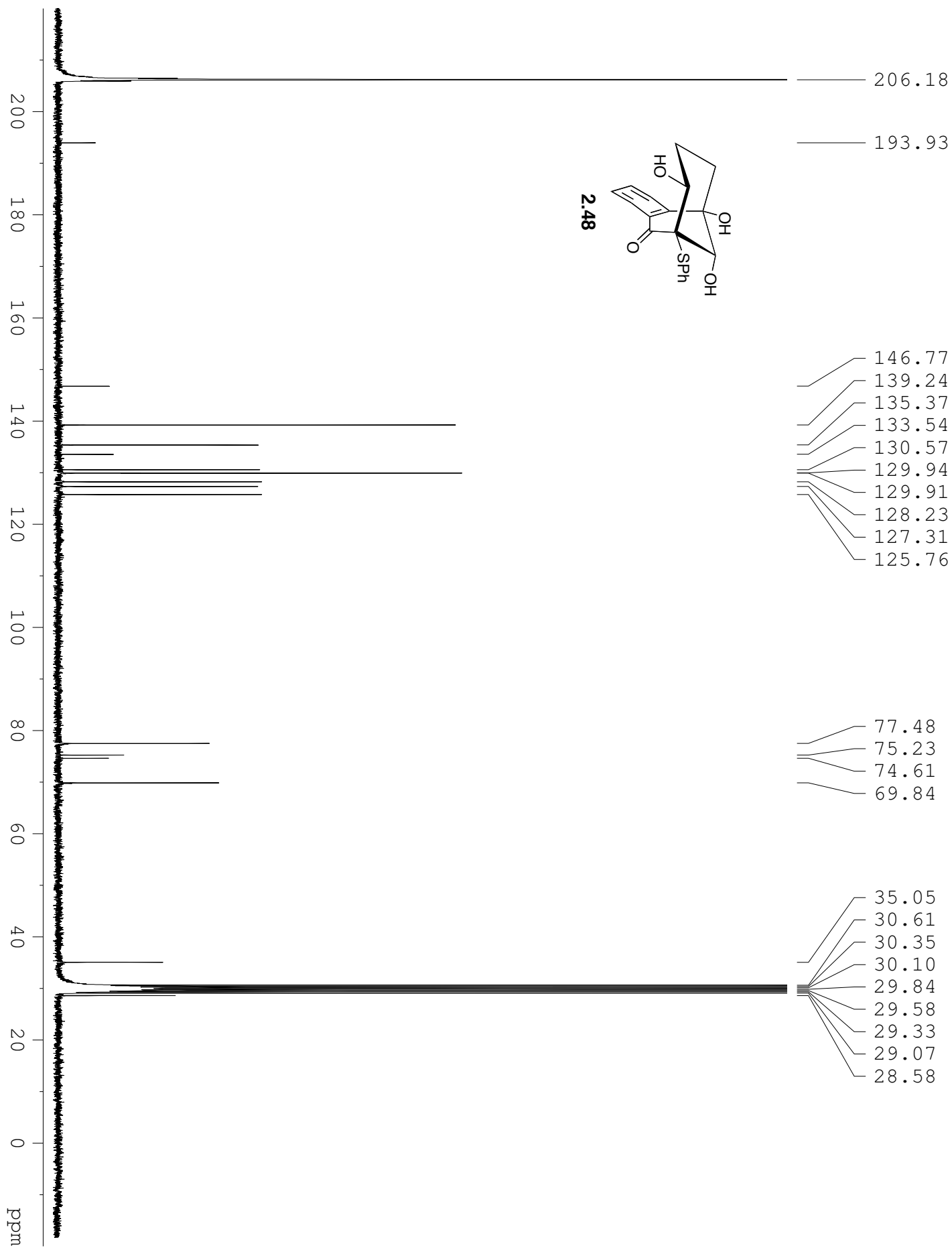


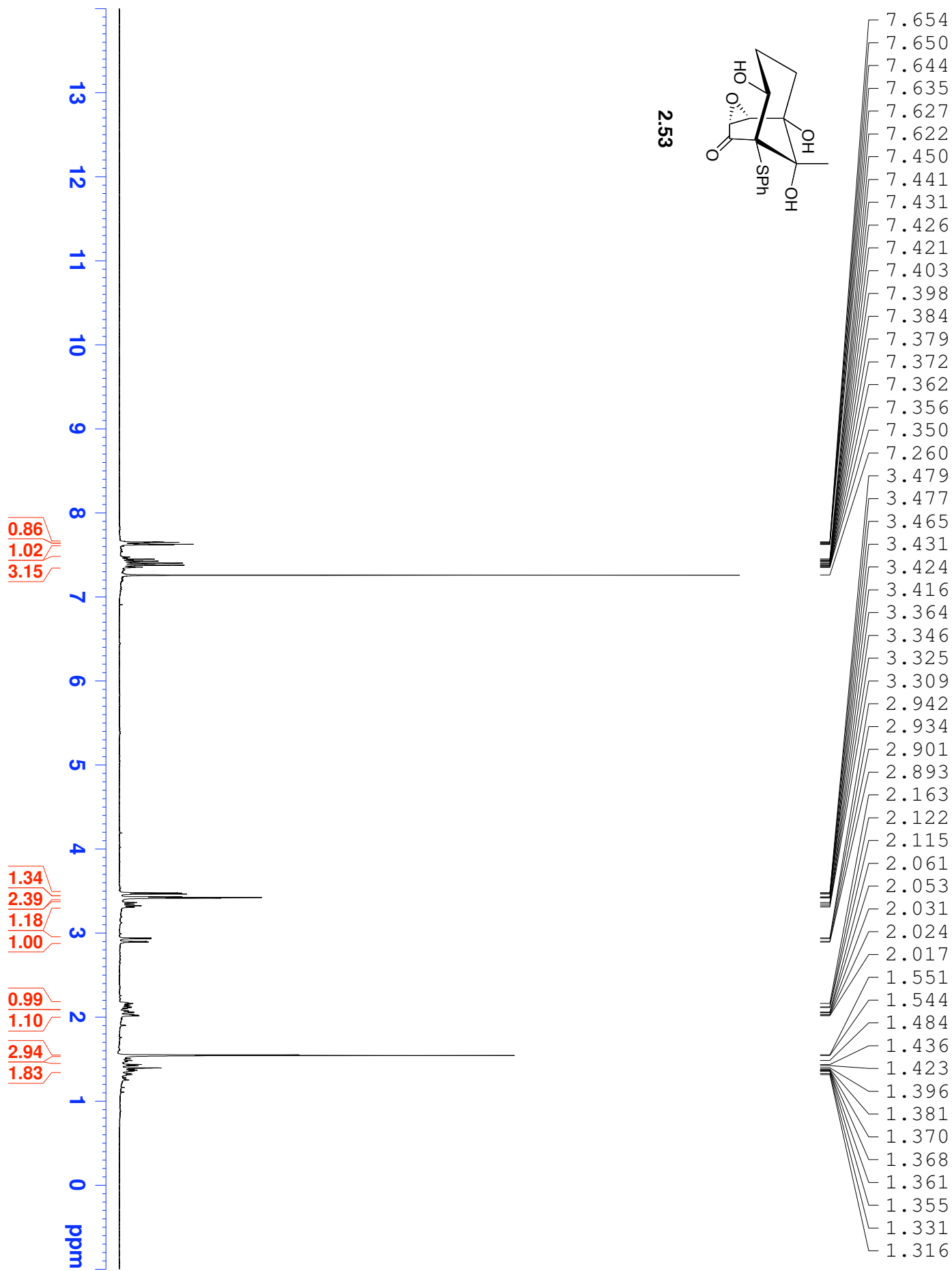
2.40

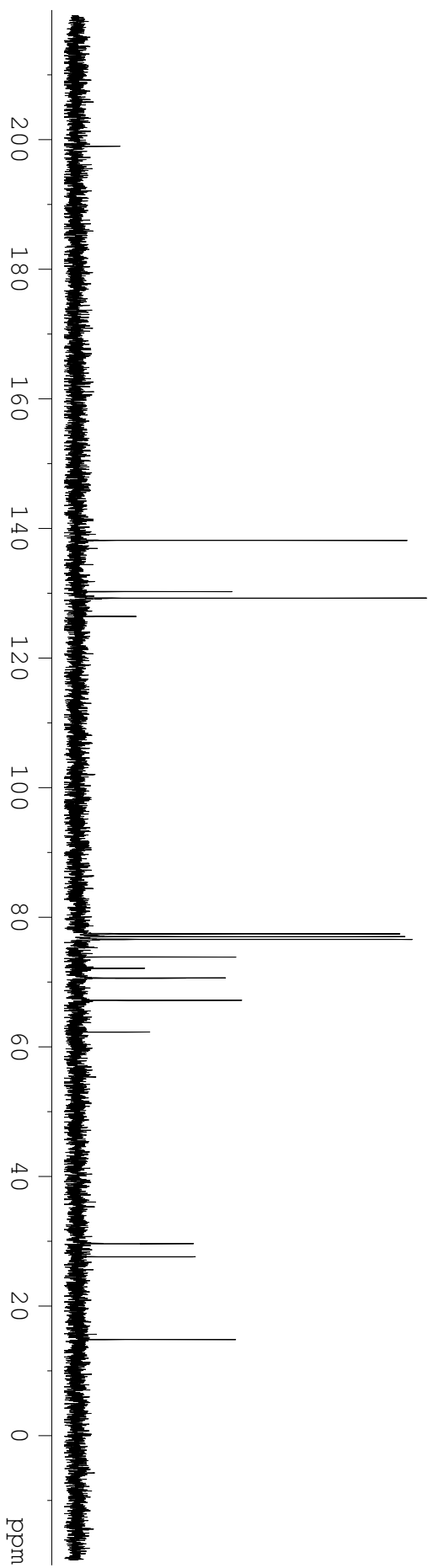




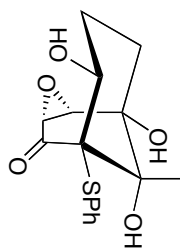








2.53



198.98

138.16

130.24

129.24

126.43

77.42

77.00

76.57

73.85

72.11

70.62

70.57

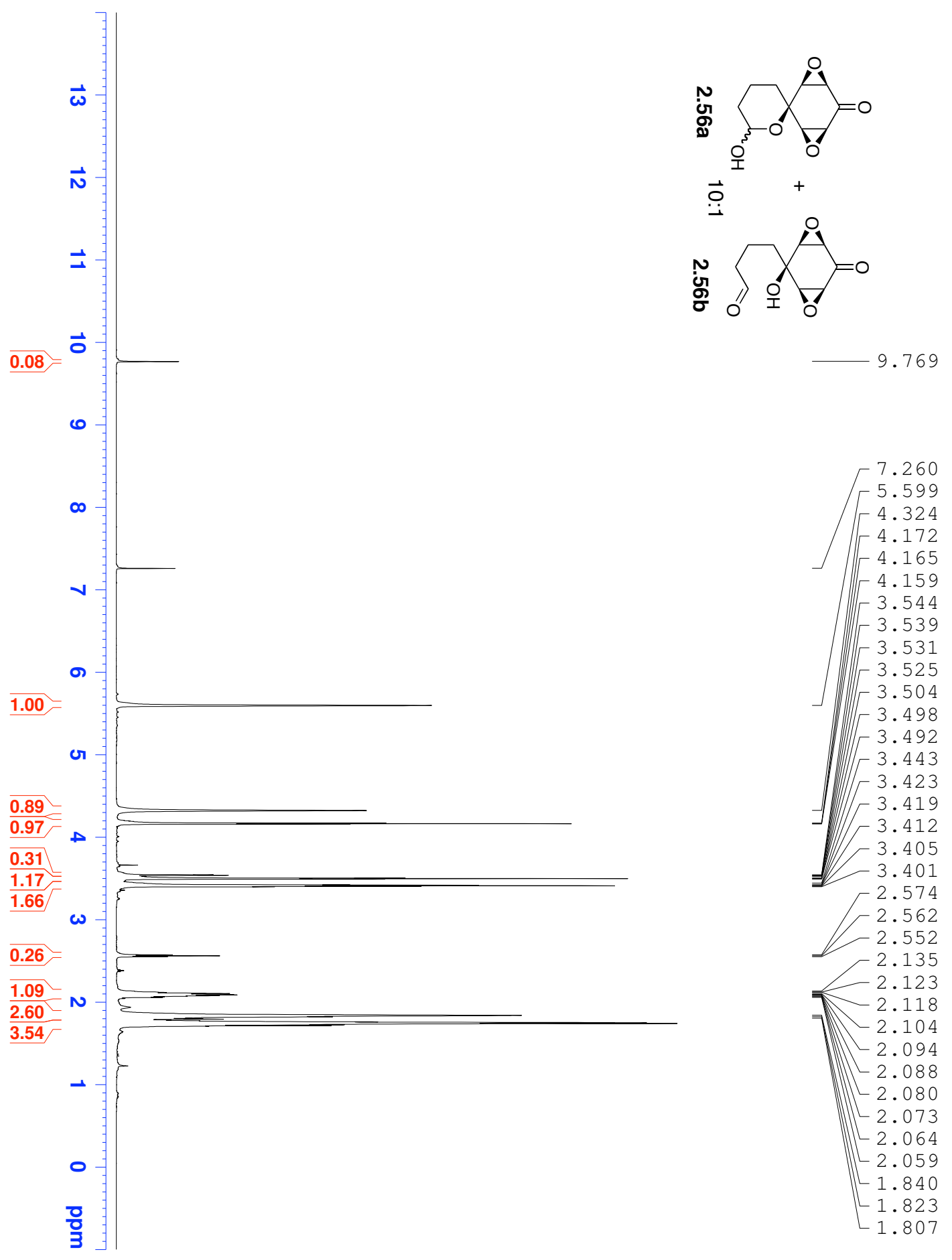
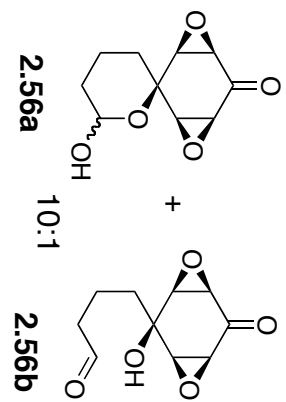
67.17

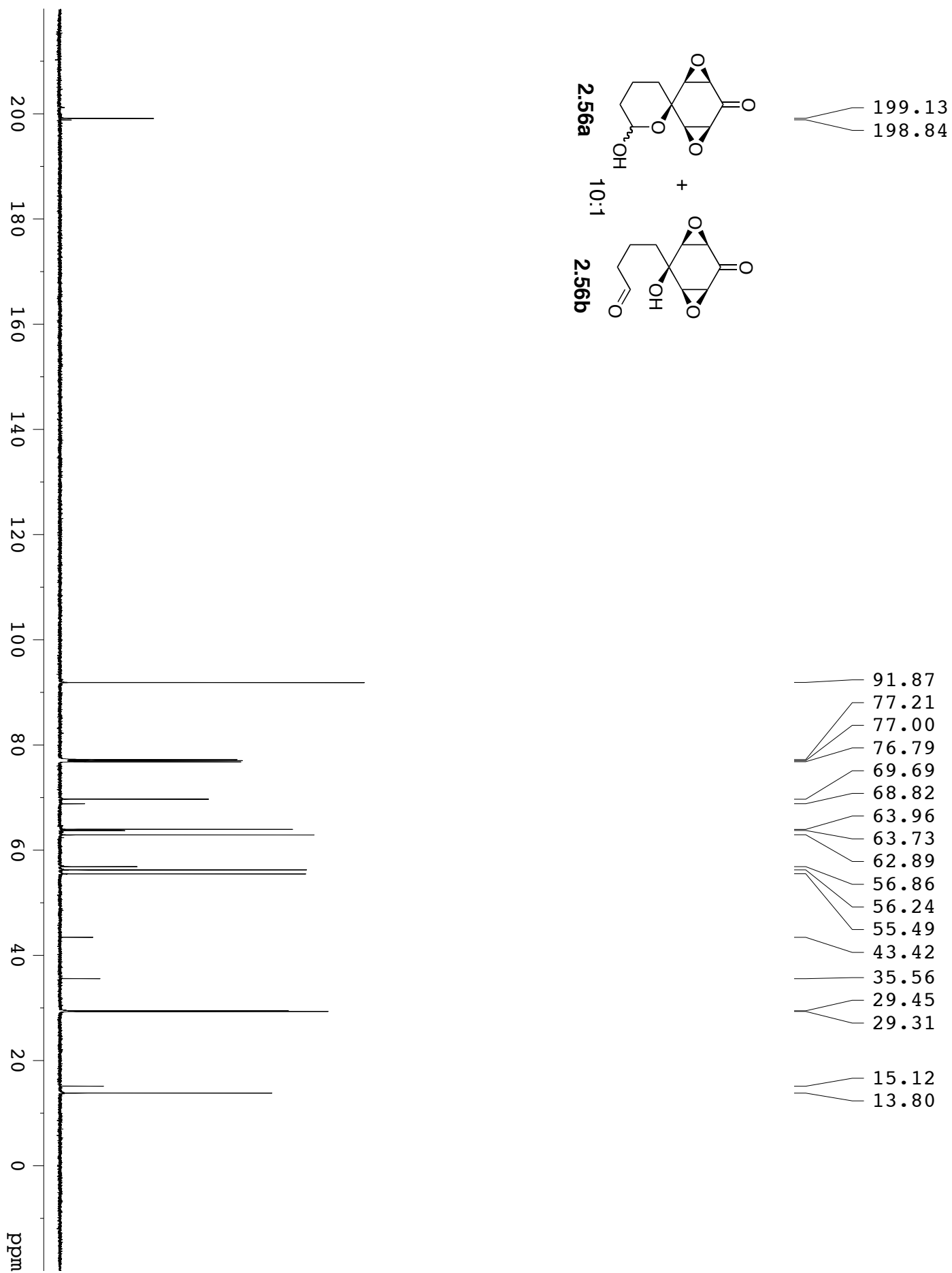
62.26

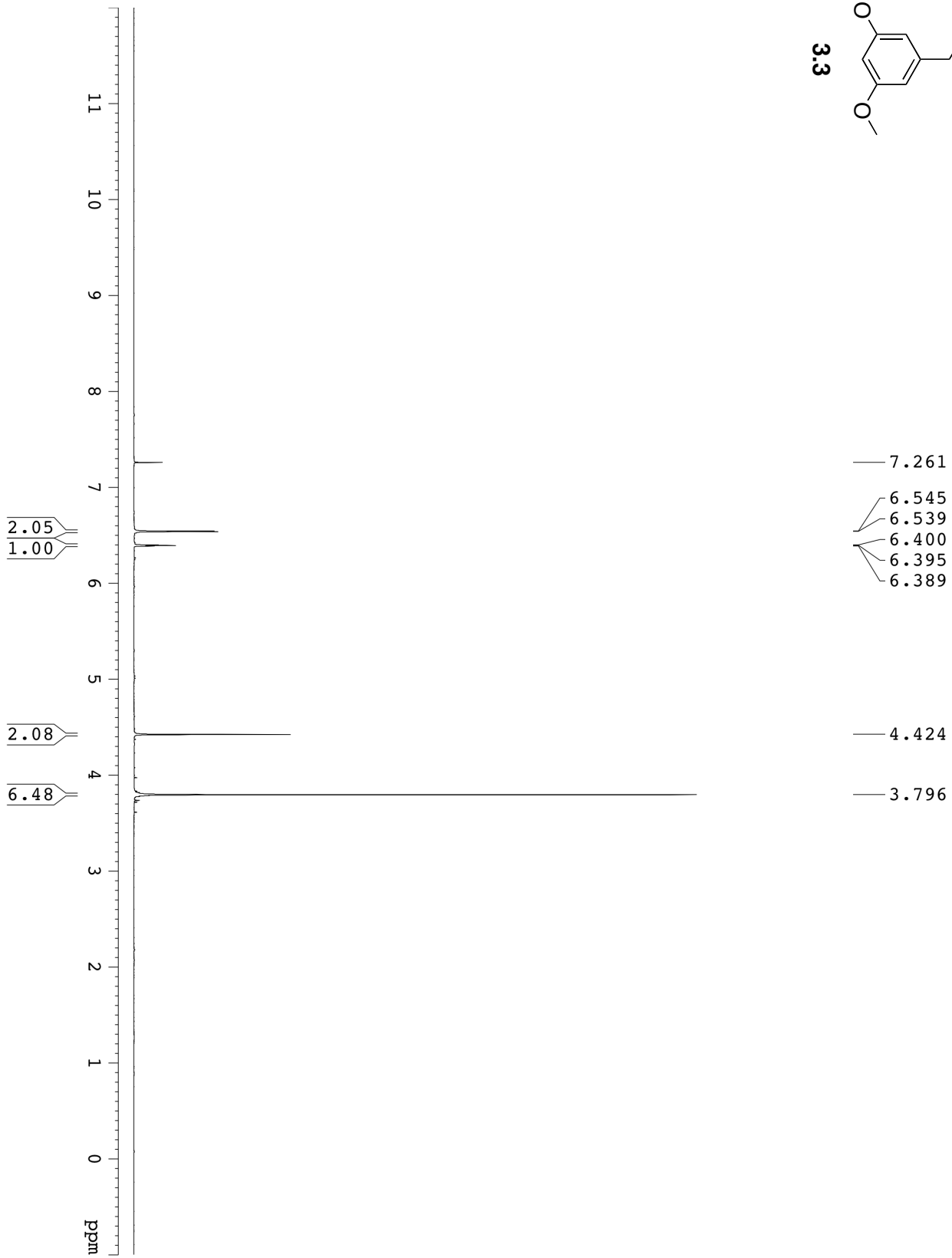
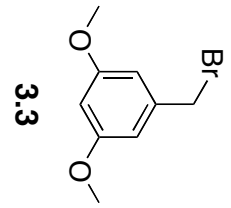
29.60

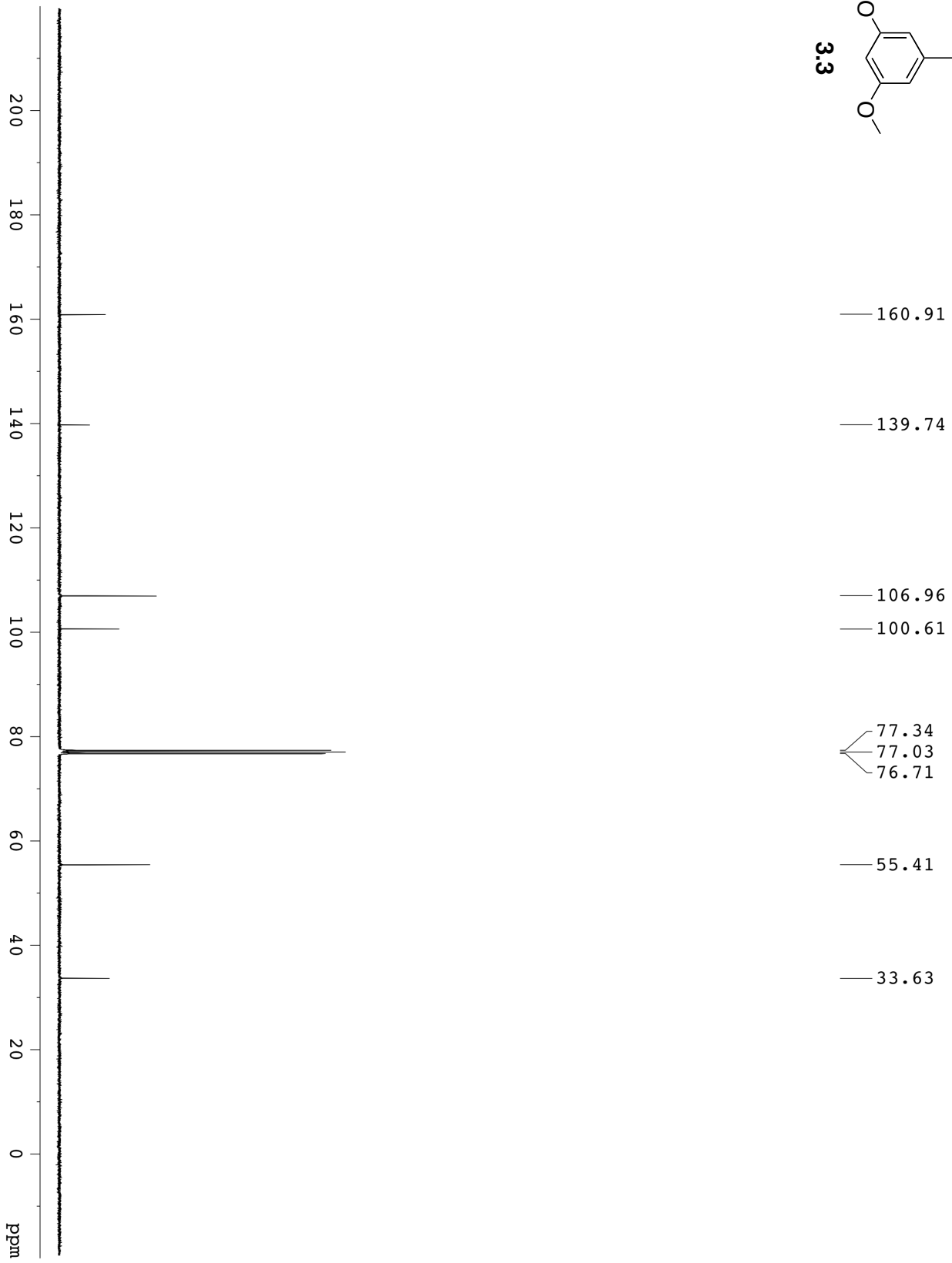
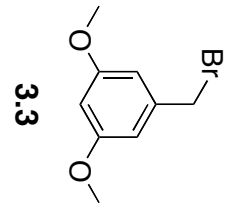
27.58

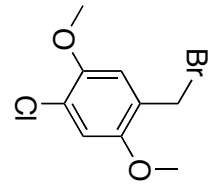
14.81



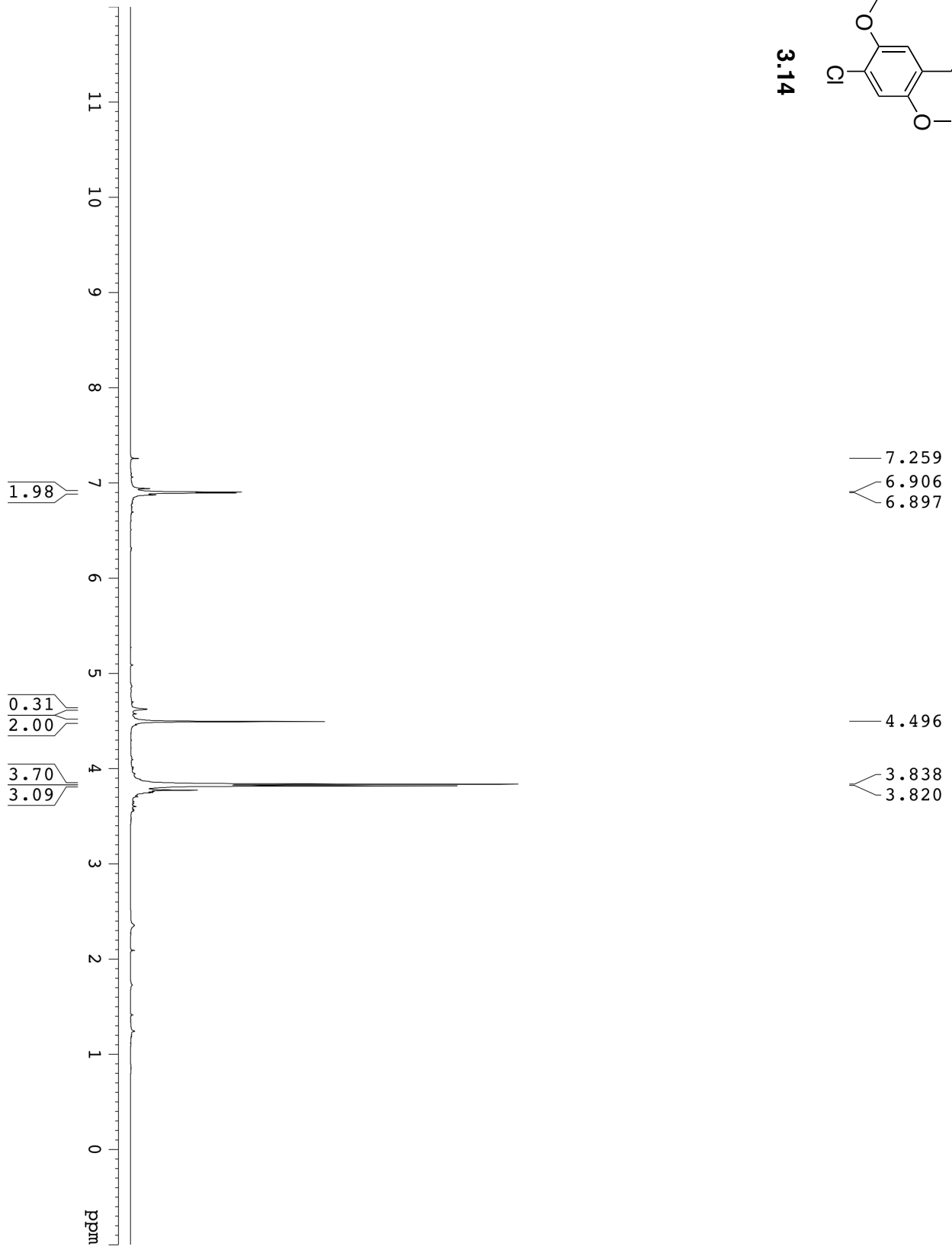


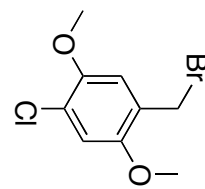






3.14





3.14

151.30
148.85

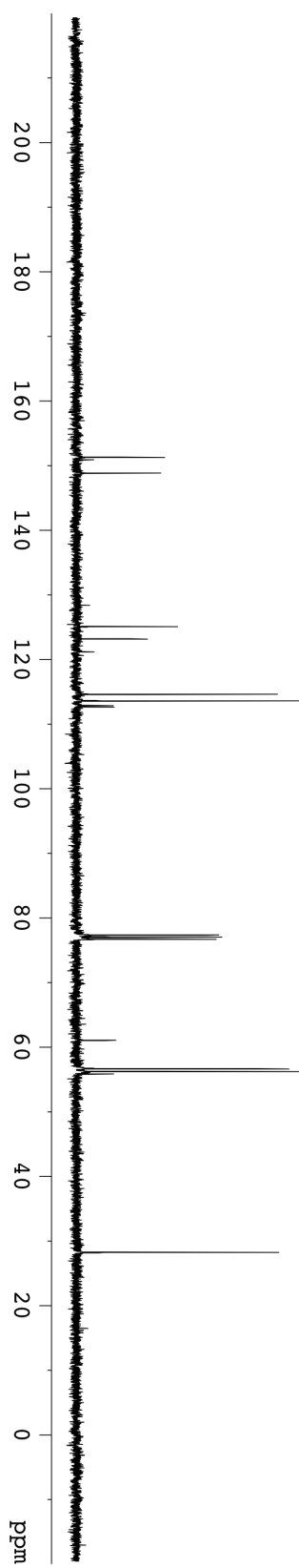
125.07
123.18

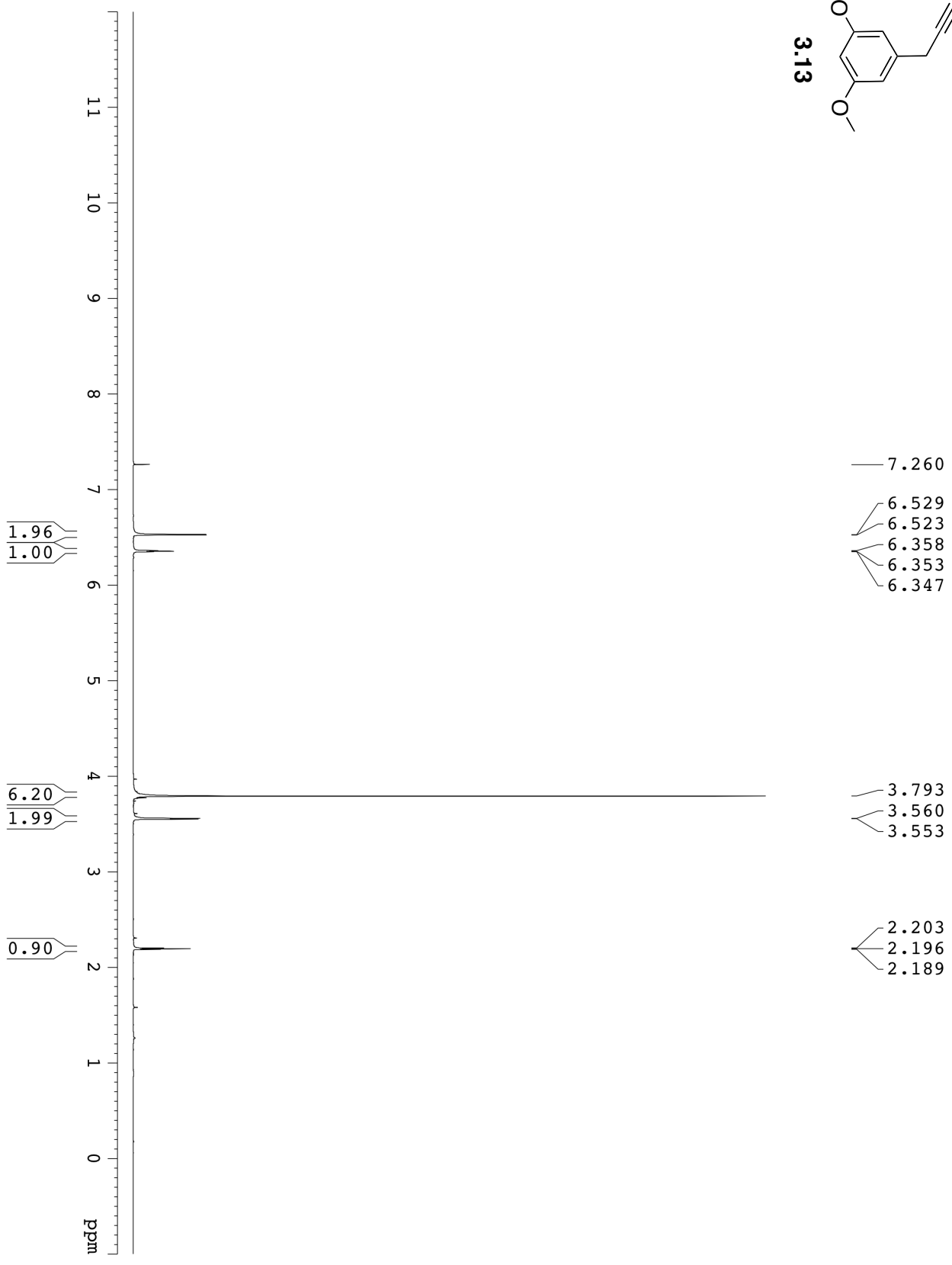
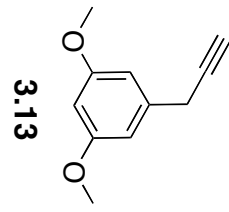
114.60
113.58

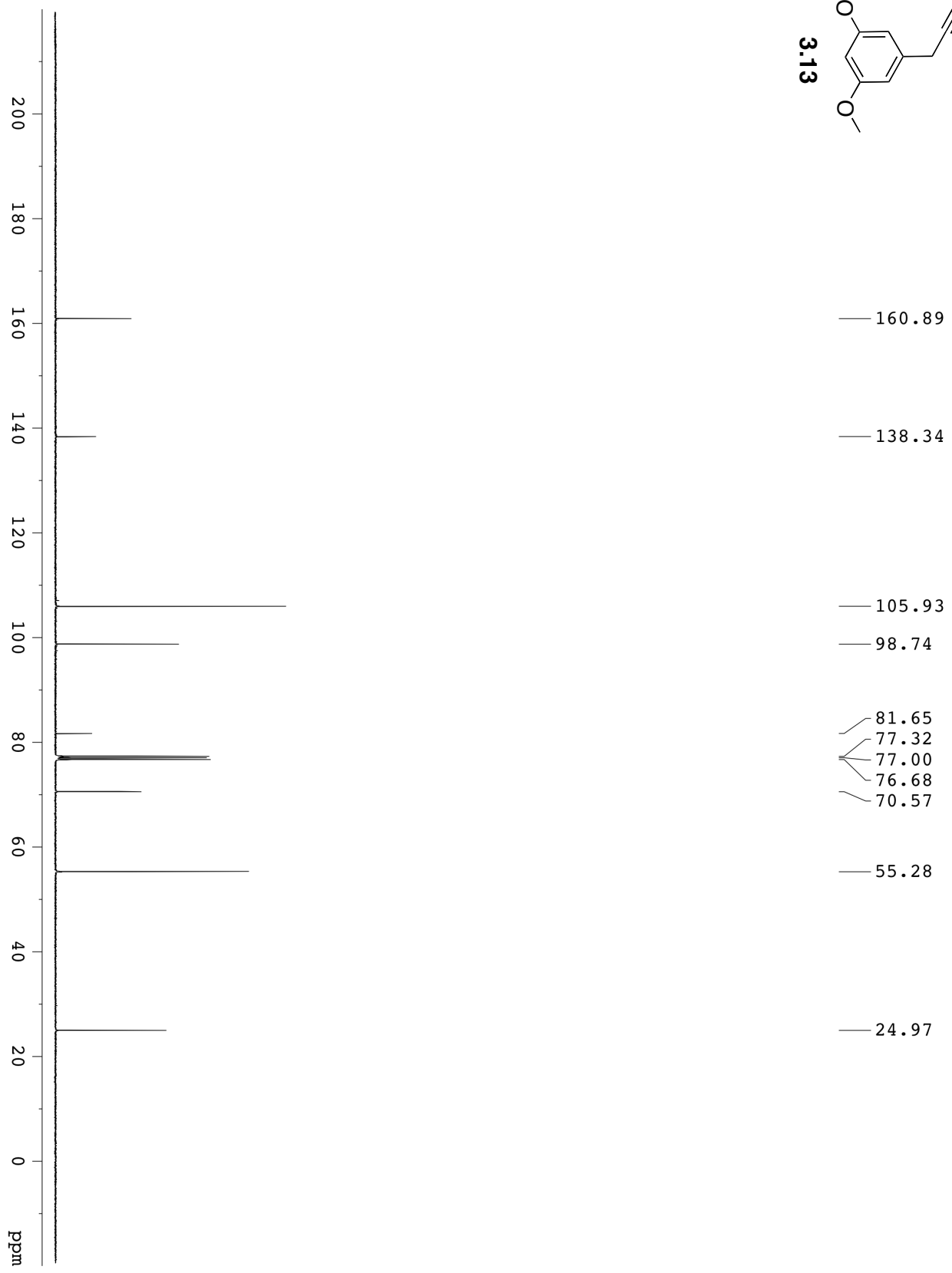
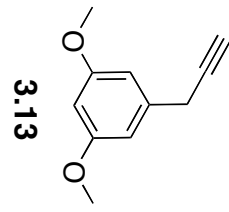
77.32
77.00
76.68

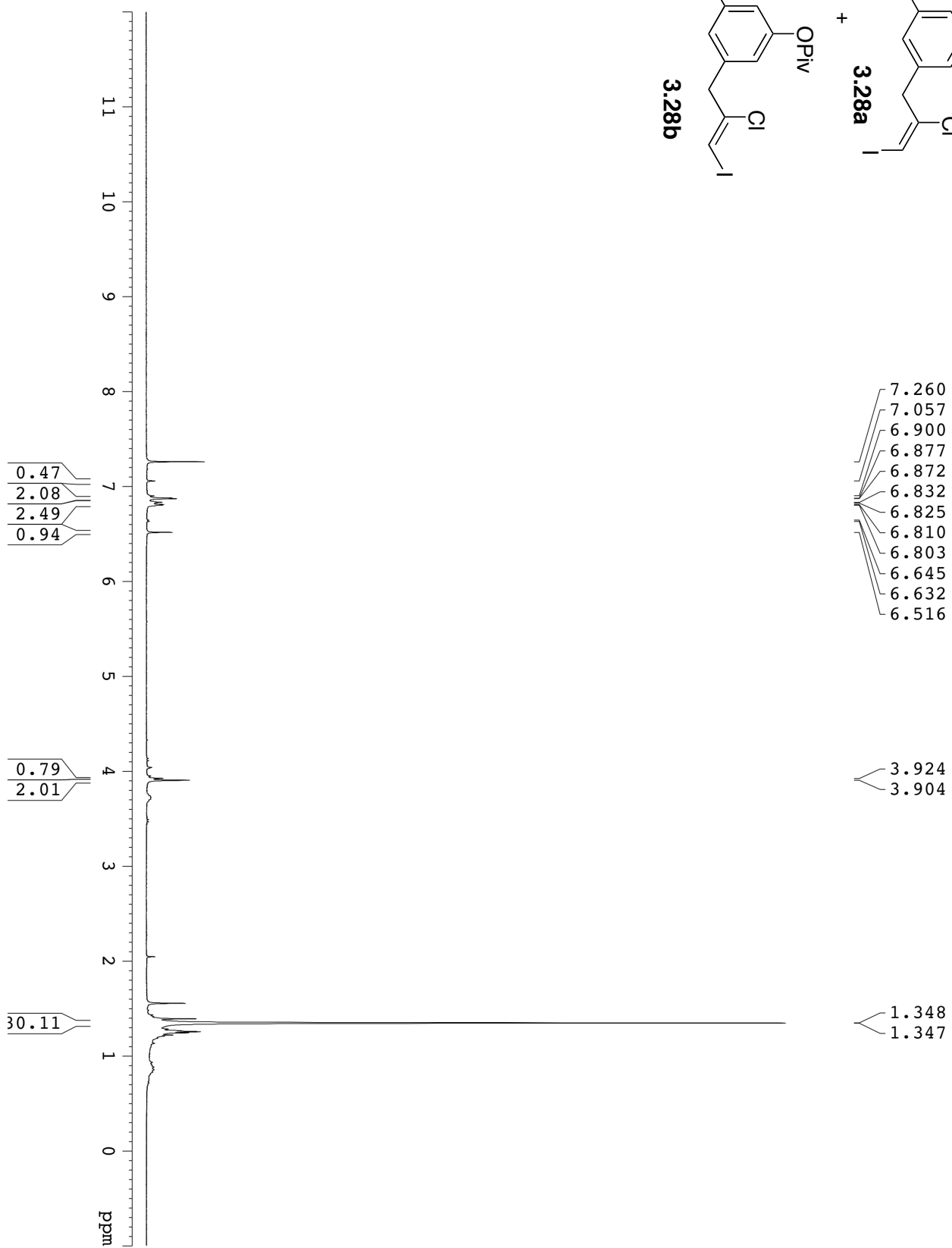
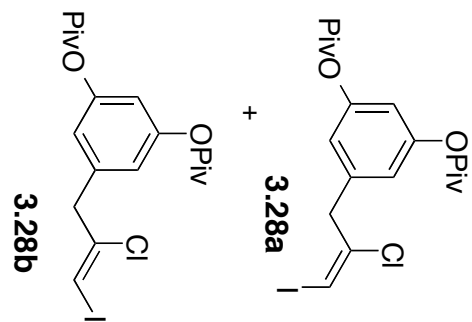
56.62
56.20

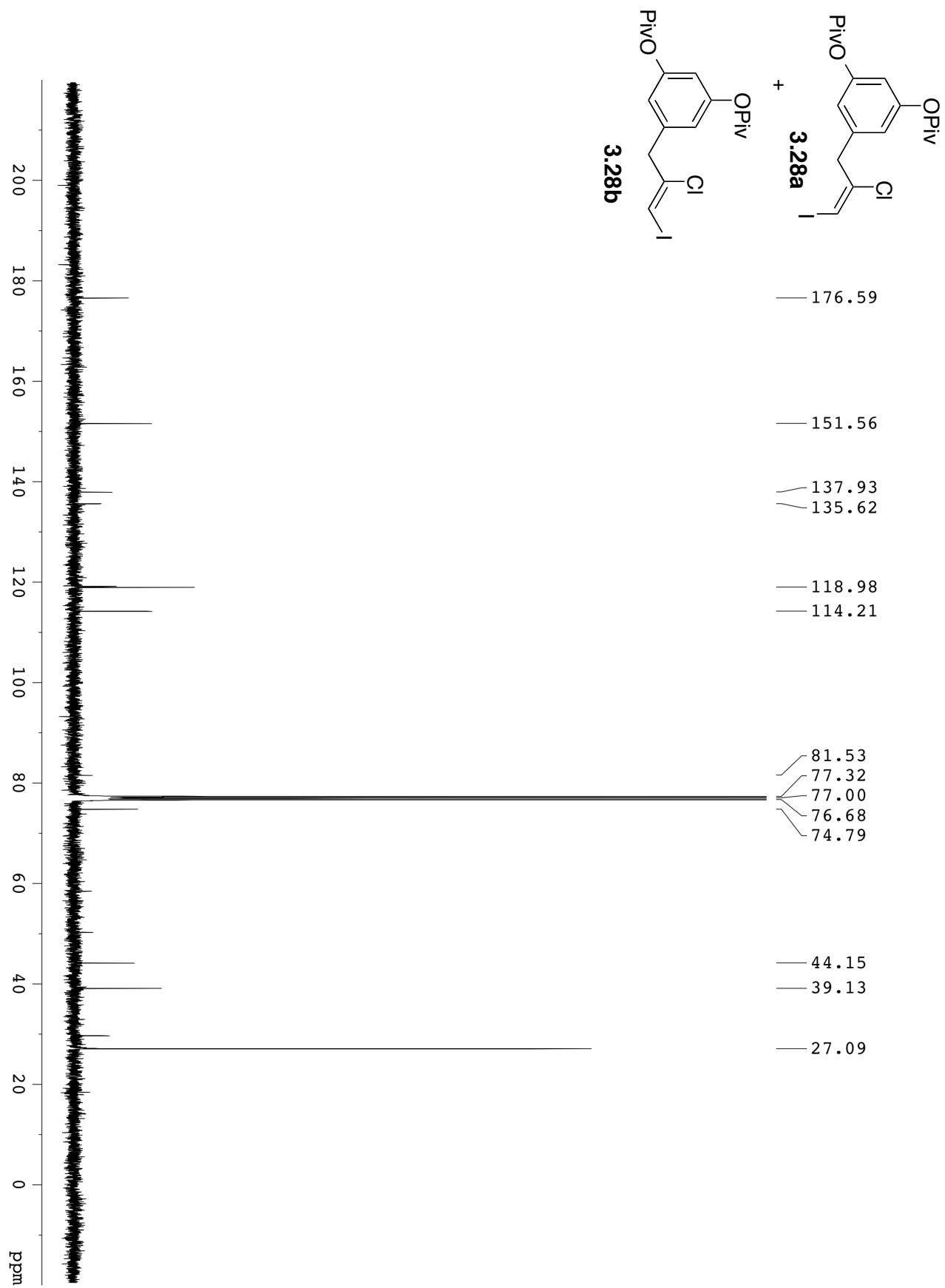
28.19

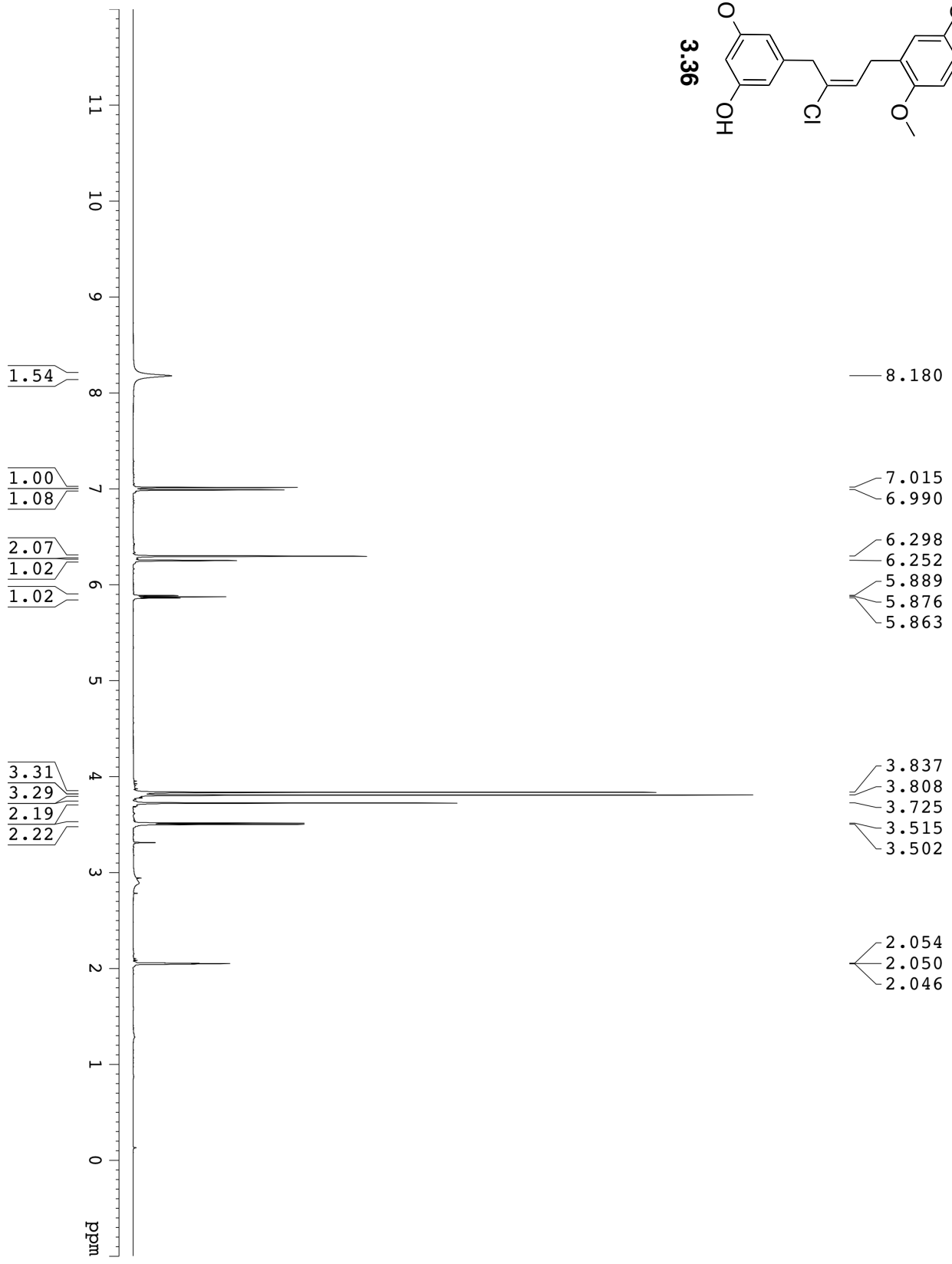
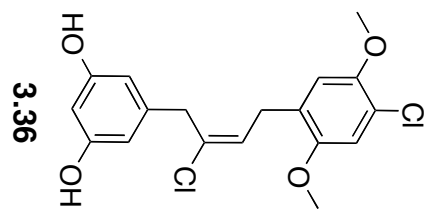


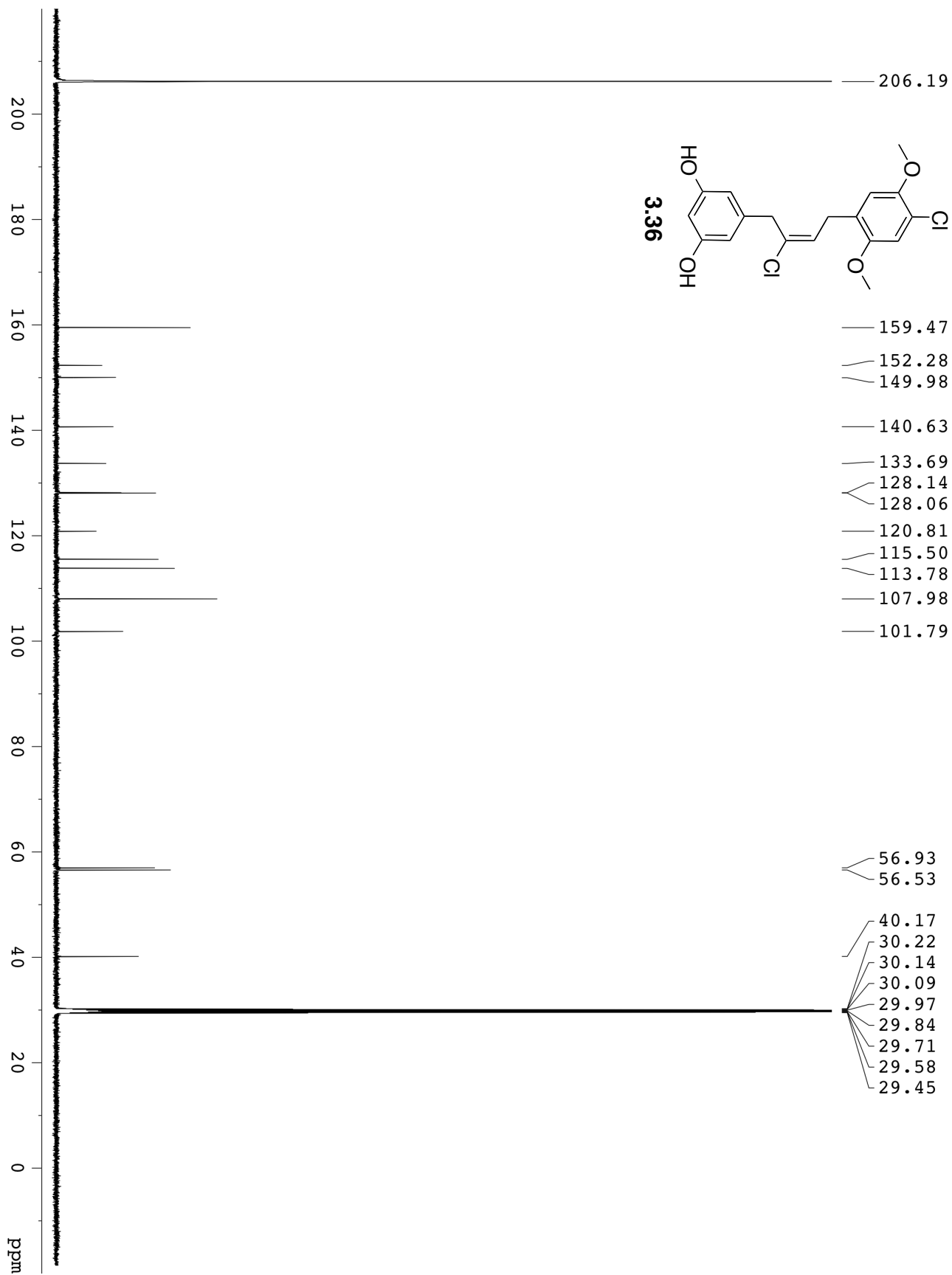


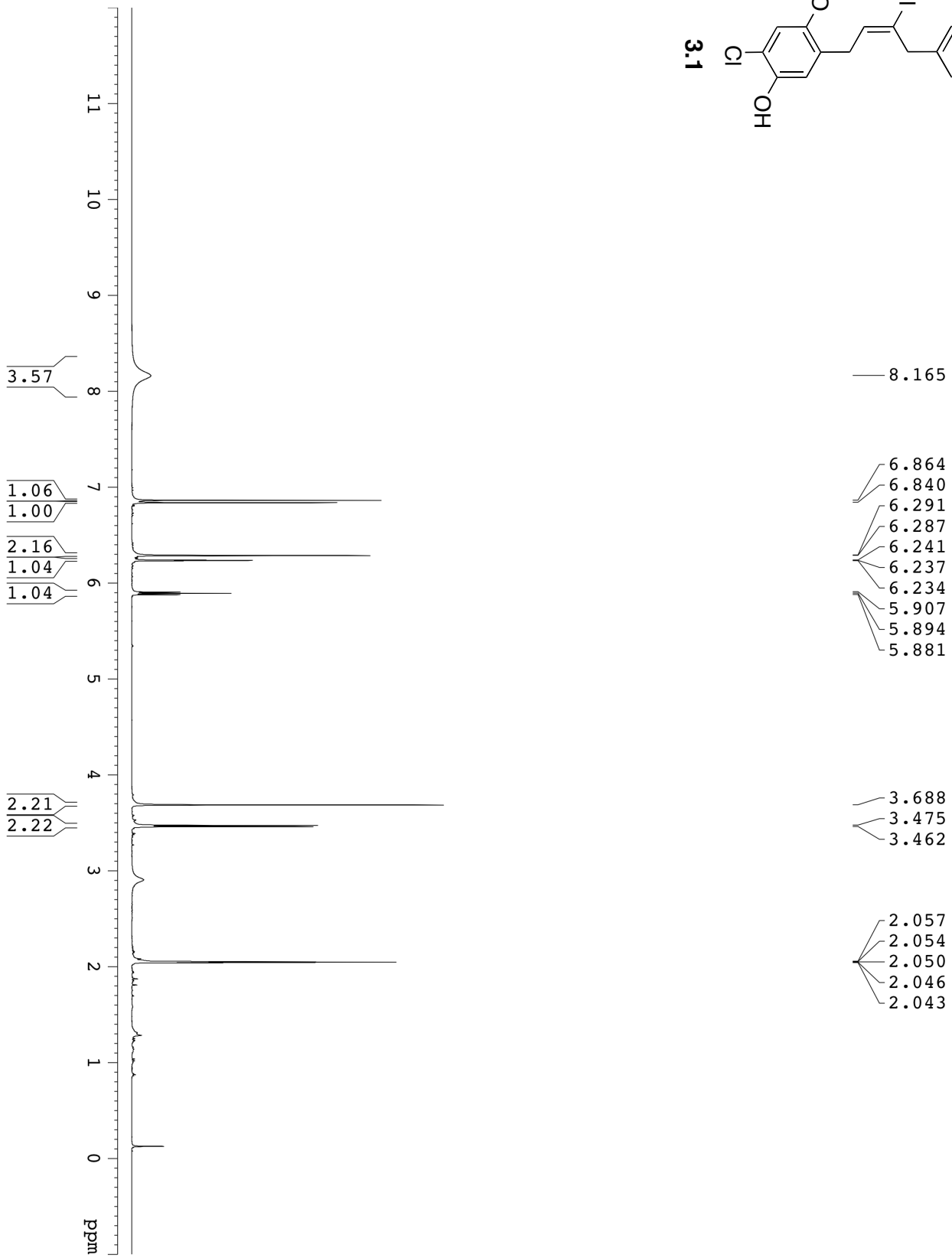
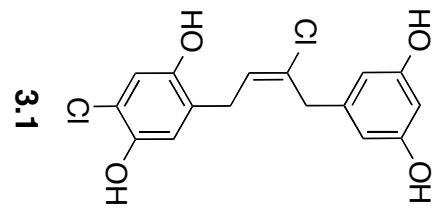


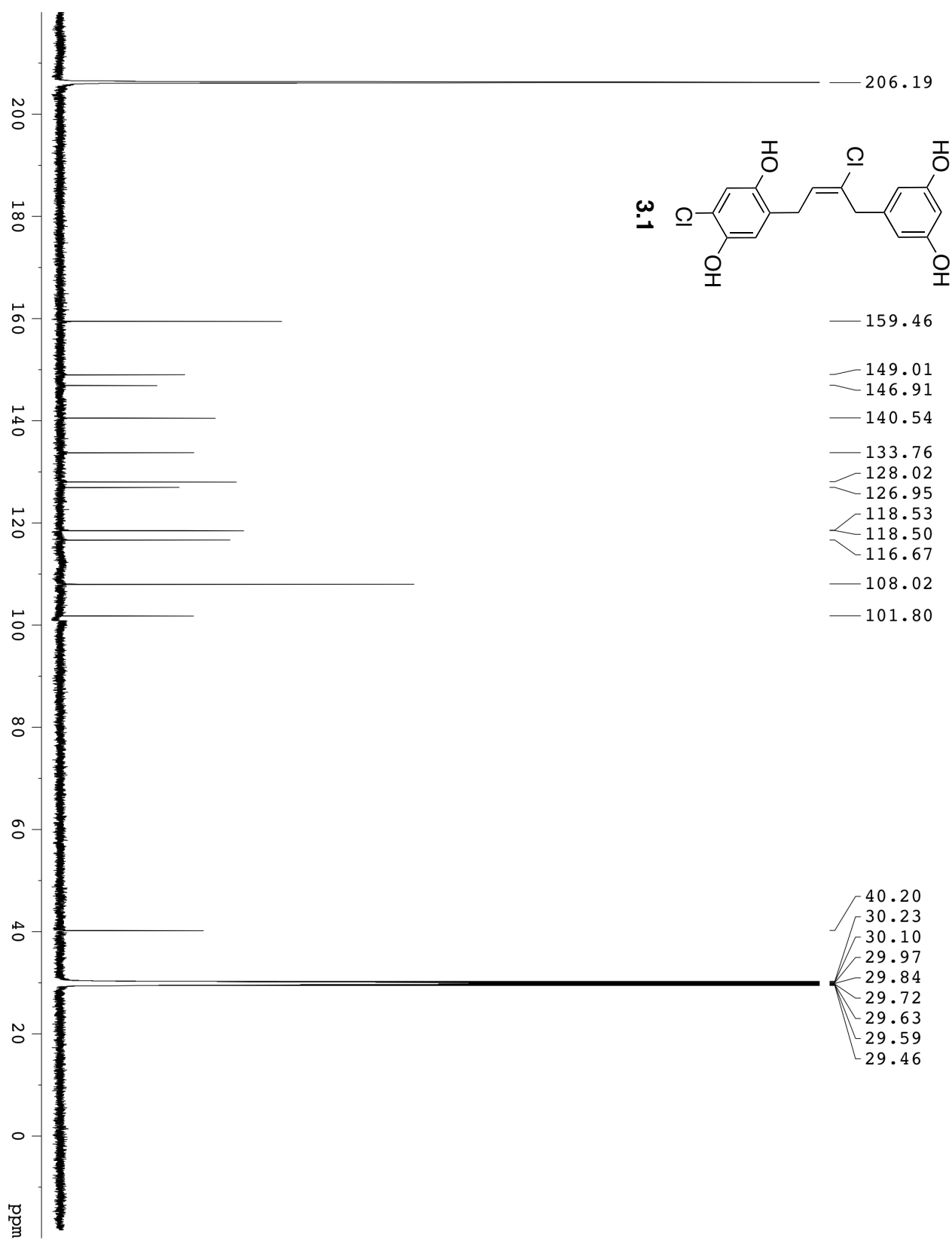


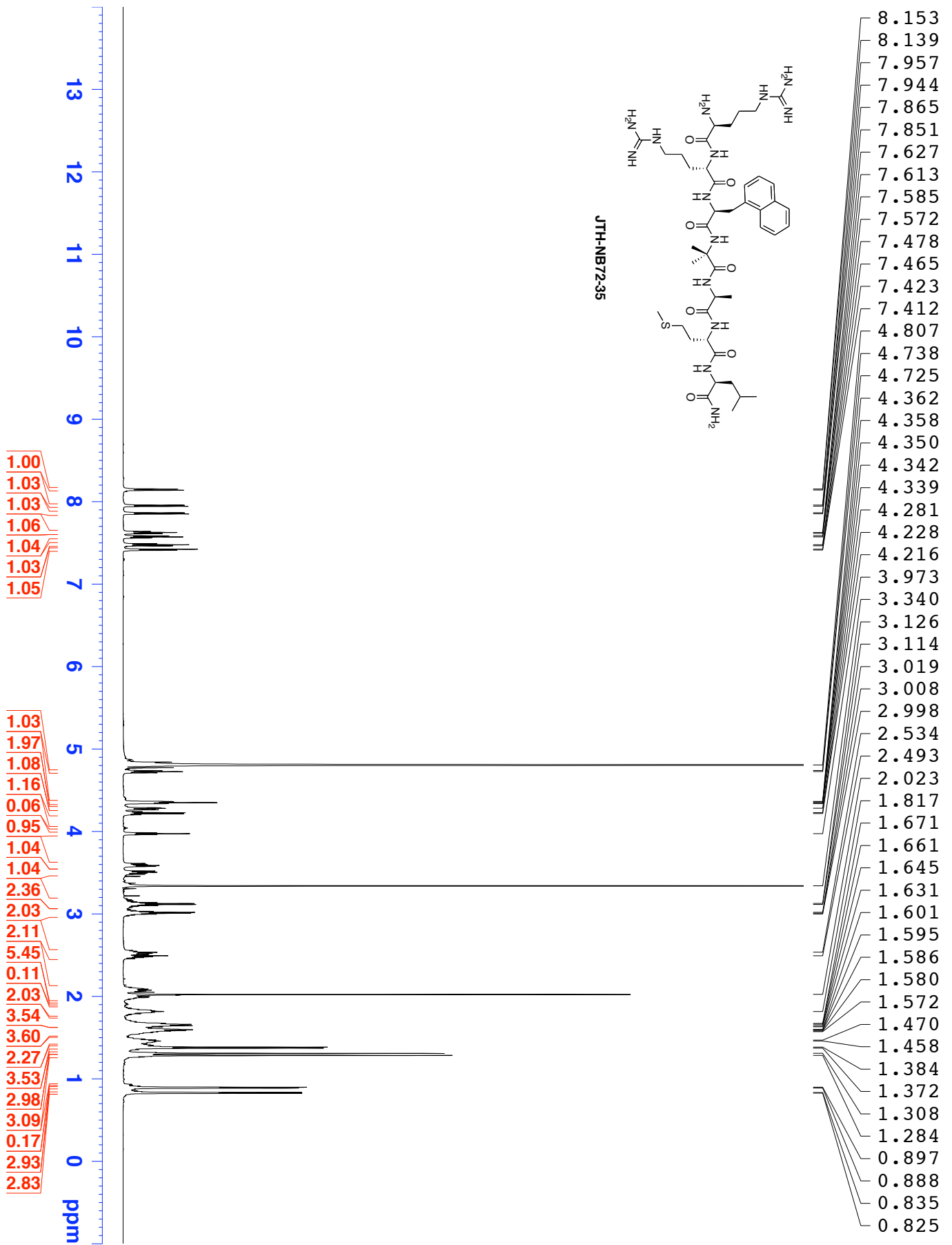


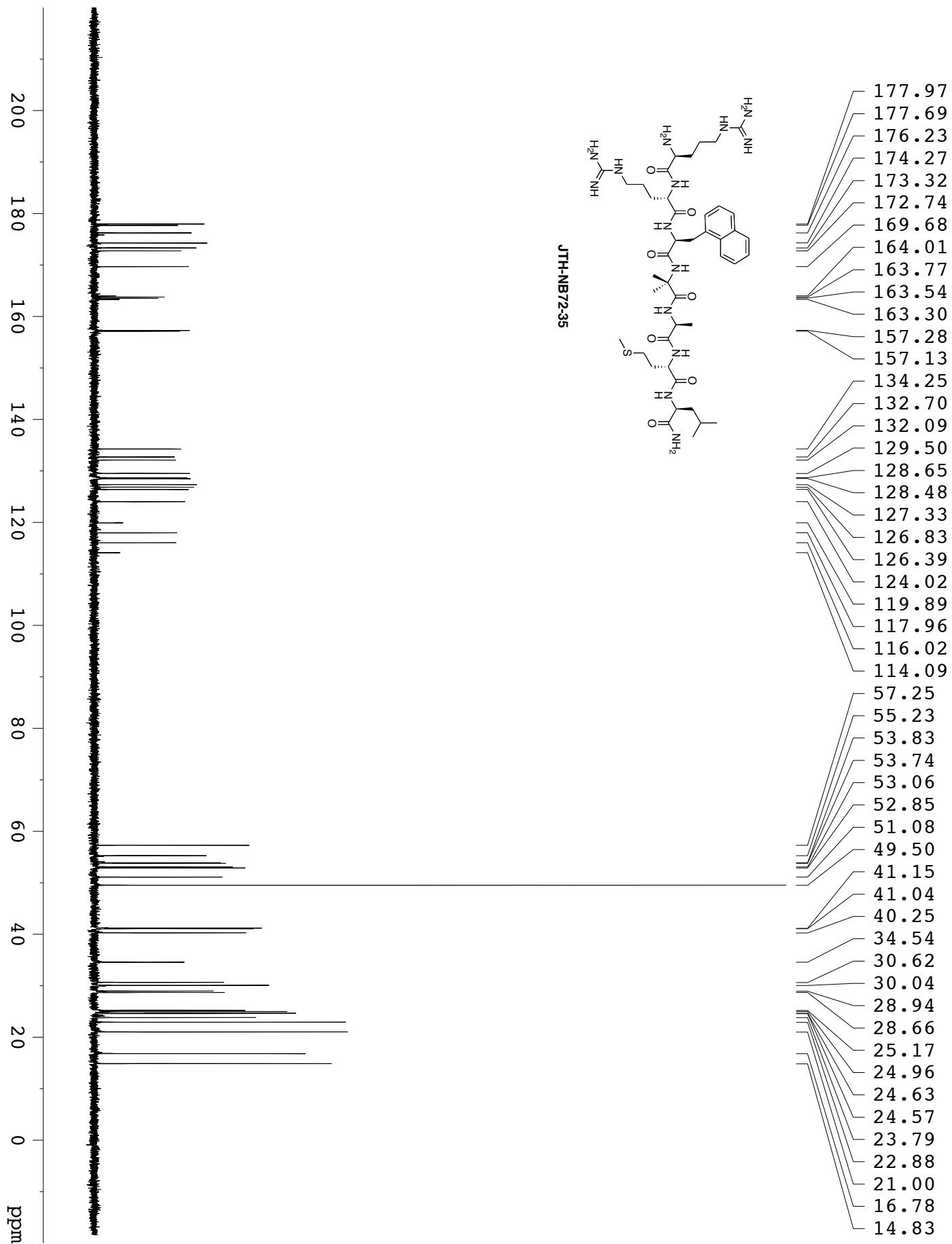


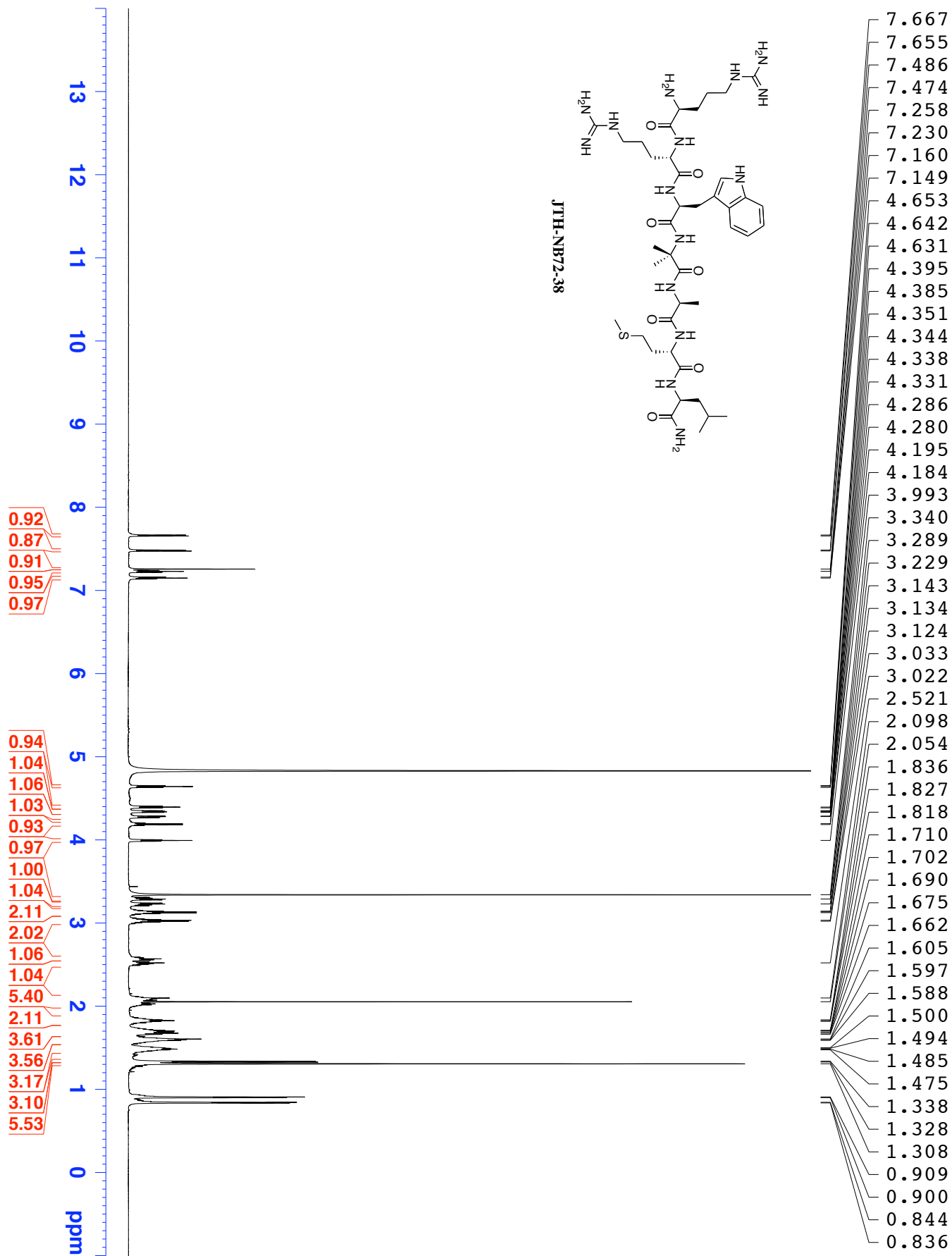


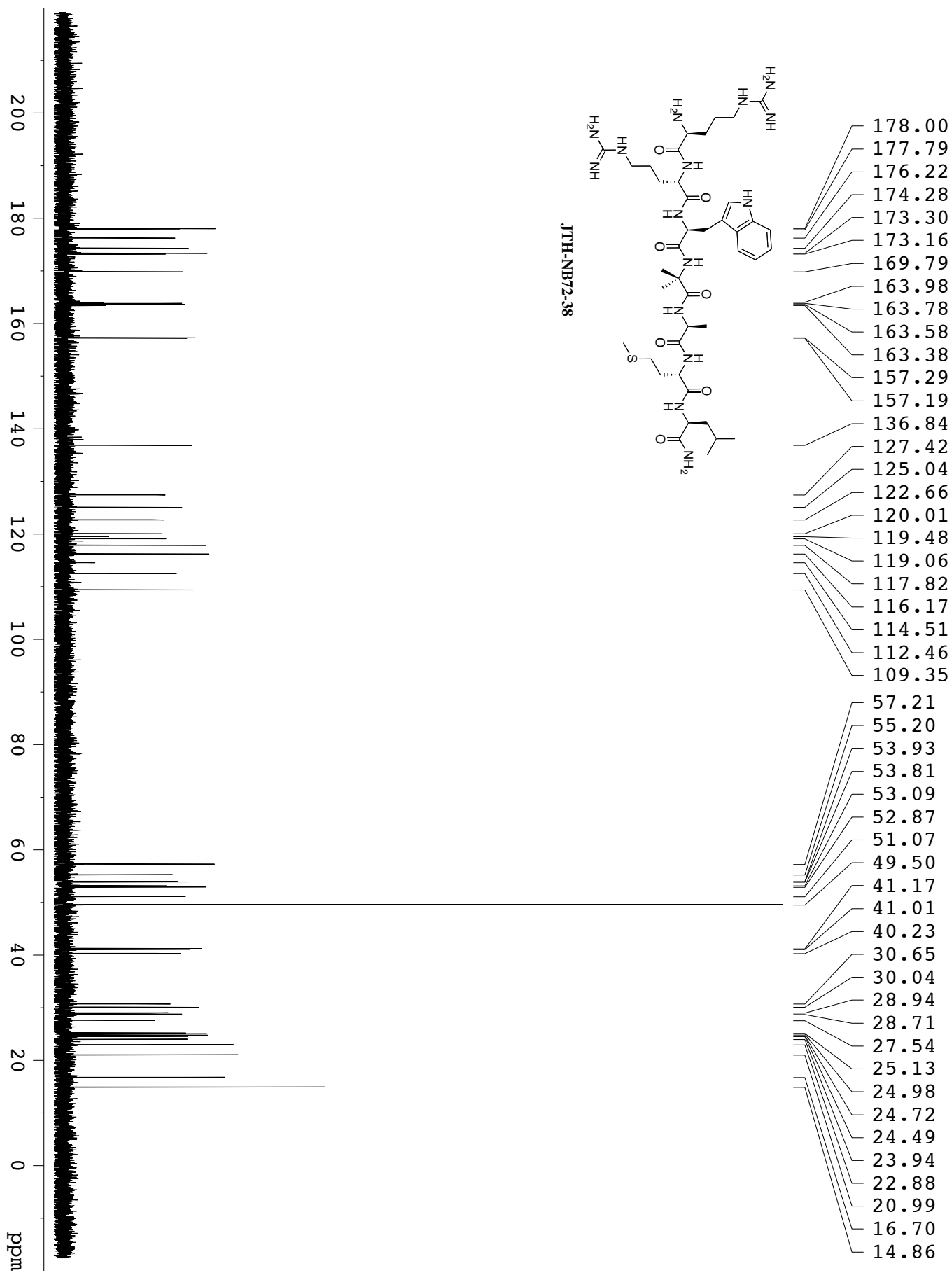


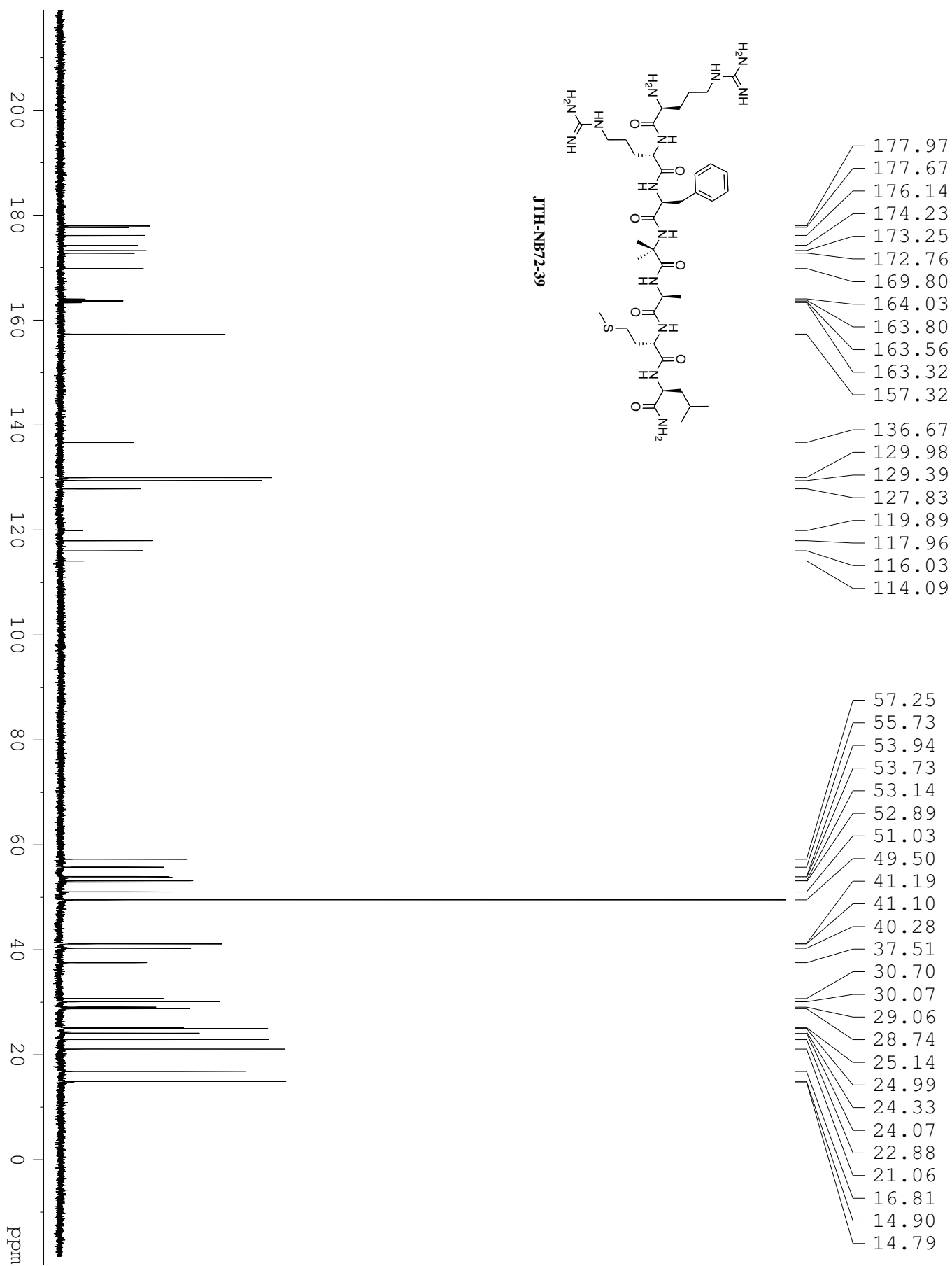


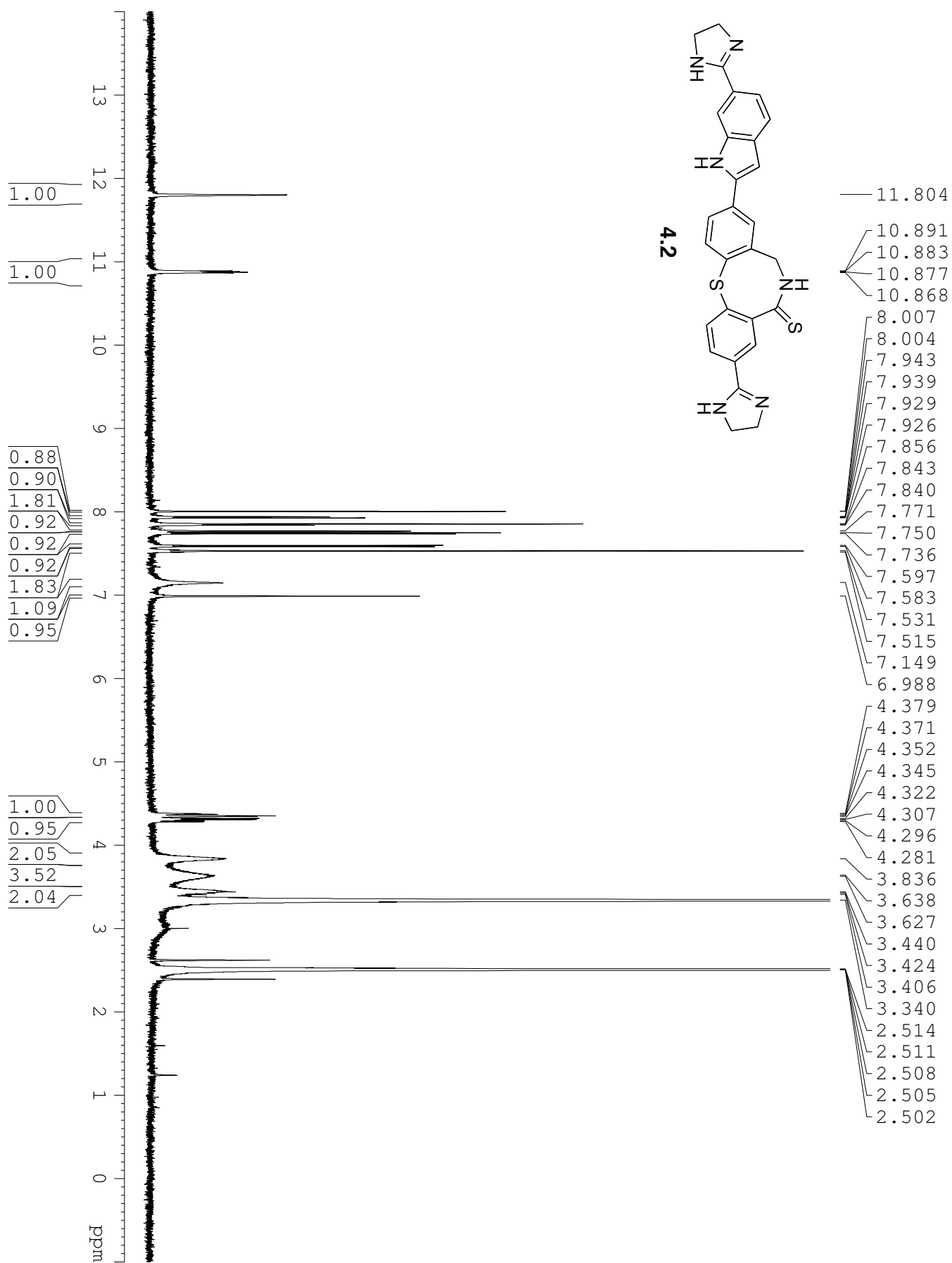
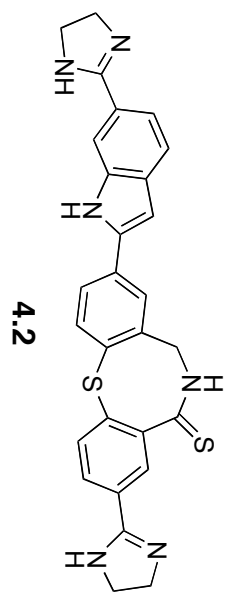


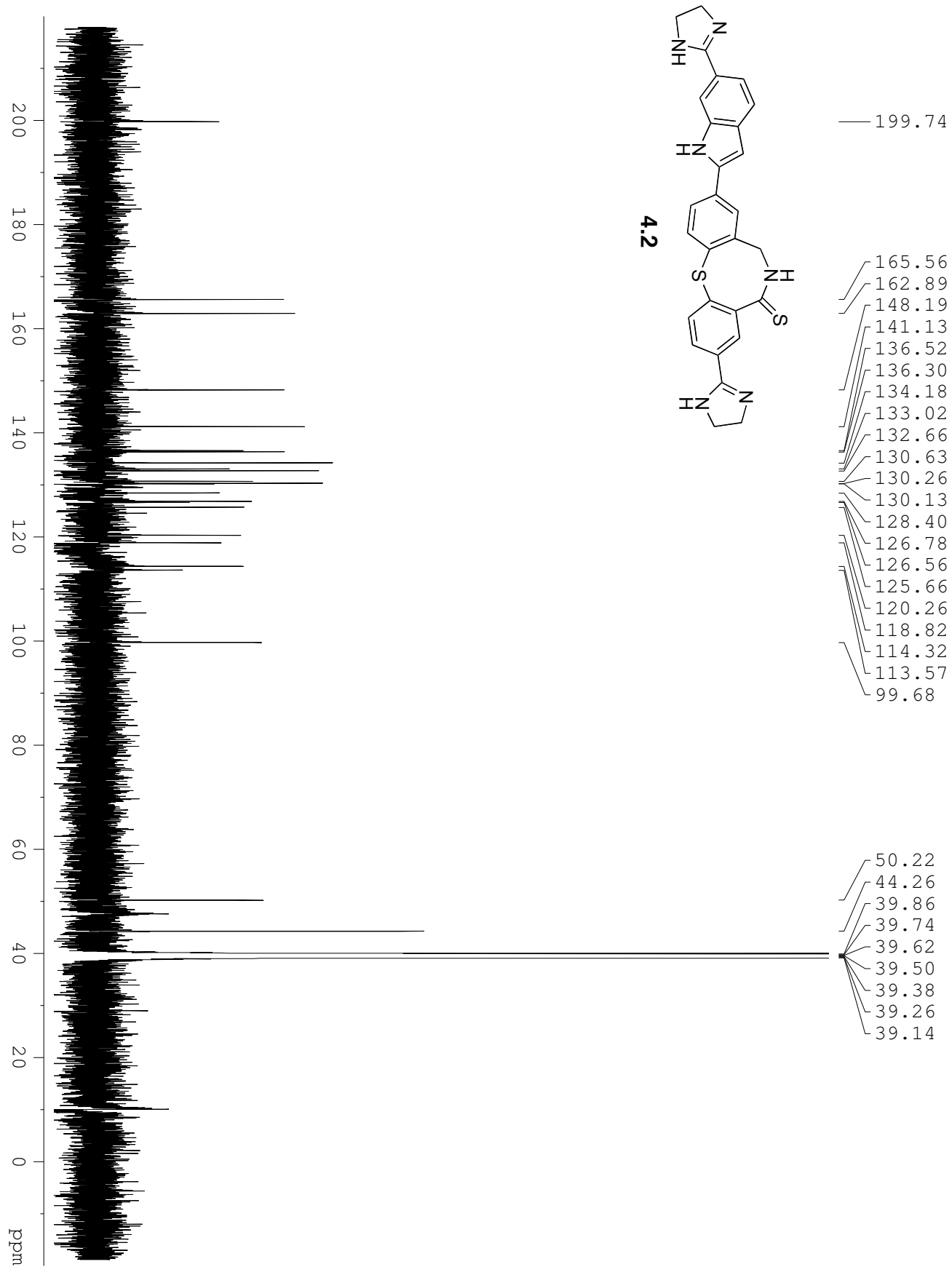


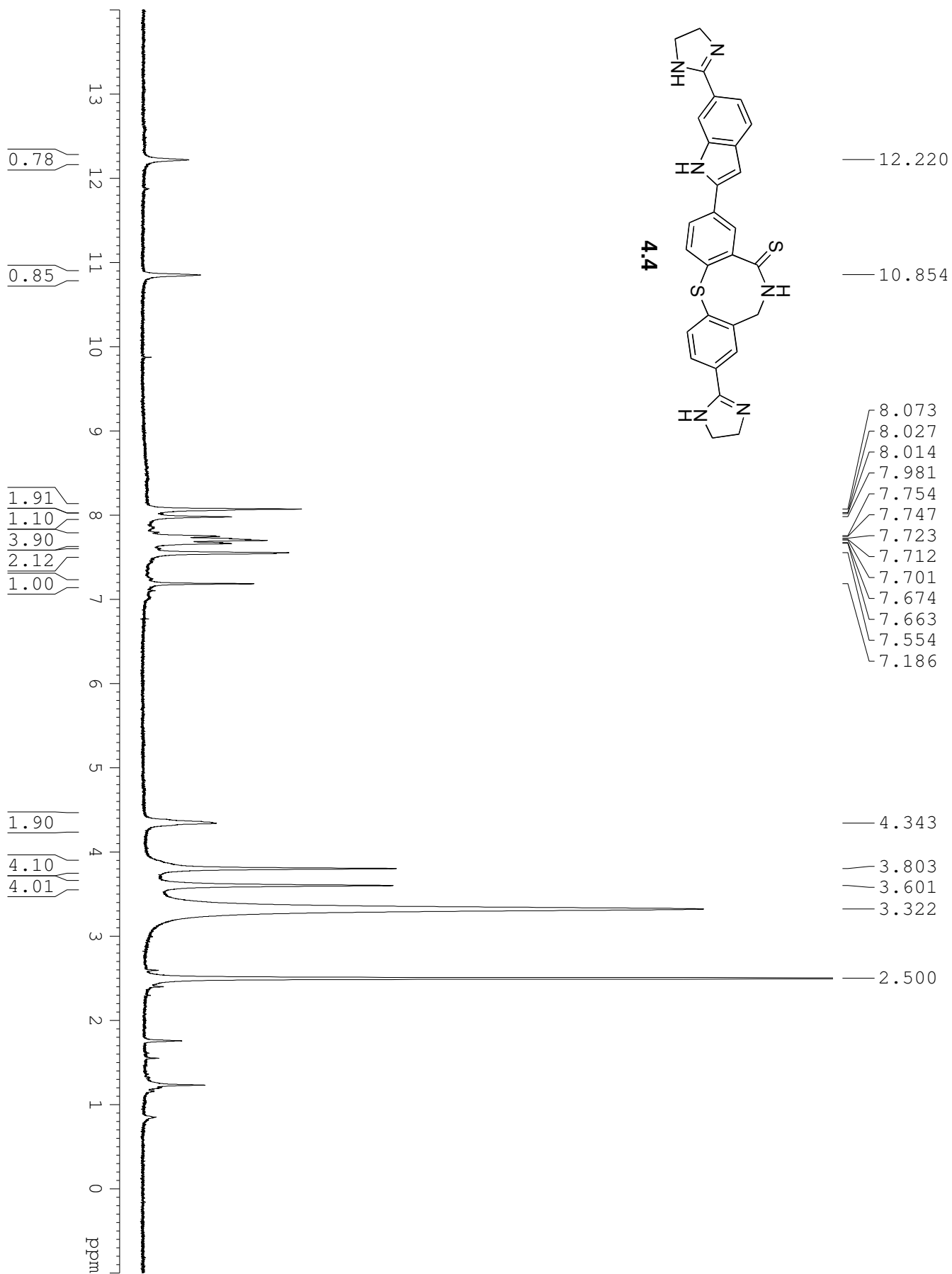


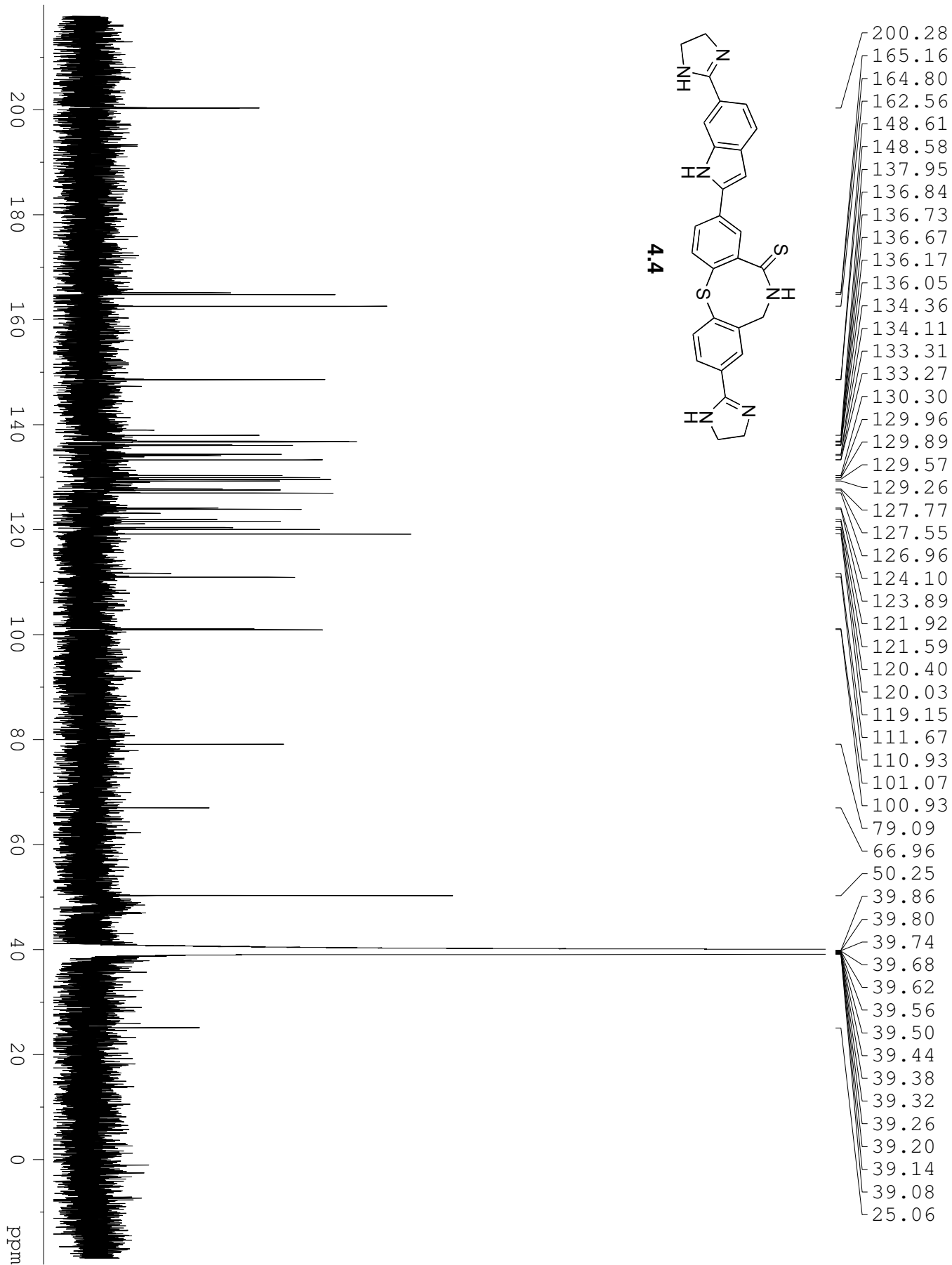












5.0 REFERENCES

- (1) Coin, I.; Beyermann, M.; Bienert, M. *Nat. Protoc.* **2007**, *2*, 3247-3256.
- (2) Fischer, E.; Fourneau, E. *Ber. Deutsch. Chem. Ges.* **1901**, *34*, 2868-2877.
- (3) du Vigneaud, V.; Ressler, C.; Swan, J. M.; Roberts, C. W.; Katsoyannis, P. G. *J. Am. Chem. Soc.* **1954**, *76*, 3115-3121.
- (4) Merrifield, R. B. *J. Am. Chem. Soc.* **1963**, *85*, 2149-2154.
- (5) Sheehan, J. C.; Hess, G. P. *J. Am. Chem. Soc.* **1955**, *77*, 1067-1068.
- (6) Valeur, E.; Bradley, M. *Chem. Soc. Rev.* **2009**, *38*, 606-631.
- (7) Montalbetti, C. A. G. N.; Falque, V. *Tetrahedron* **2005**, *61*, 10827-10852.
- (8) Benoiton, N. L. *Chemistry of peptide synthesis*; Taylor & Francis/CRC Press: Boca Raton, 2006.
- (9) Merrifield, R. B. *J. Am. Chem. Soc.* **1964**, *86*, 304-305.
- (10) Carpino, L. A. *J. Am. Chem. Soc.* **1957**, *79*, 98-101.
- (11) Merrifield, R. B. *Biochemistry* **1964**, *3*, 1385-1390.
- (12) Merrifield, R. B. *J. Org. Chem.* **1964**, *29*, 3100-3102.
- (13) Carpino, L. A.; Han, G. Y. *J. Org. Chem.* **1970**, *37*, 3404-3409.
- (14) Chang, C. D.; Meienhofer, J. *Int. J. Pept. Protein Res.* **1978**, *11*, 246-249.
- (15) Amblard, M.; Fehrentz, J.; Martinez, J.; Subra, G. *Mol. Biotech.* **2005**, *33*, 239-254.
- (16) Gedye, R.; Smith, F.; Westaway, K.; Ali, H.; Baldisera, L.; Laberge, L.; Rousell, J. *Tetrahedron Lett.* **1986**, *27*, 279-282.
- (17) Giguere, R. J.; Bray, T. L.; Duncan, S. M.; Majetich, G. *Tetrahedron Lett.* **1986**, *27*, 4945-4948.
- (18) Lidstrom, P.; Tierney, J.; Wathey, B.; Westman, J. *Tetrahedron* **2001**, *57*, 9225-9283.
- (19) Yu, H. M.; Chen, S. T.; Wang, K. T. *J. Org. Chem.* **1992**, *57*, 4781-4784.
- (20) Chen, S. T.; Chiou, S.; Wang, K. T. *J. Chin. Chem. Soc.* **1991**, *38*, 85-91.

- (21) Kremsner, J. M.; Stadler, A.; Kappe, C. O. *The Scale-Up of Microwave-Assisted Organic Synthesis*; Springer Berlin / Heidelberg: Berlin, 2006; Vol. 266.
- (22) Verlander, M. *Int. J. Pept. Protein. Res. Ther.* **2007**, *13*, 75-82.
- (23) Gerard, R. *Sci. Am.* **1950**, *189*, 118-126.
- (24) Katz, J. J.; C., H. W. *Comp. Psychol. Monogr.* **1950**, *20*, 1-38.
- (25) Setlow, B. *J. Hist. Neurosci.* **1997**, *6*, 181-192.
- (26) Fjerdingsstad, E. J.; Nissen, T.; Roigaard-Petersen, H. H. *Scand. J. Psychol.* **1965**, *6*, 1-6.
- (27) Babich, F. R.; Jacobson, A. L.; Bubash, S. *Proc. Natl. Acad. Sci. U.S.A.* **1965**, *54*, 1299-1302.
- (28) Reinis, S. *Activ. Nerv. Super.* **1965**, *7*, 167-168.
- (29) Unger, G.; Ocegüera-Navarro, C. *Nature* **1965**, *207*, 301.
- (30) Unger, G. *Persp. Biol. Med.* **1968**, *Winter*, 217-232.
- (31) Unger, G.; Galvan, L.; Clark, R. H. *Nature* **1968**, *217*, 1259-1261.
- (32) Gay, R.; Raphelson, A. *Psychon. Sci.* **1967**, *8*, 369-370.
- (33) Bryant, R. C.; Santos, N. N.; Byrne, W. L. *Science* **1972**, *177*, 635-636.
- (34) Satake, N.; Morton, B. E. *Pharmacol., Biochem. Behav.* **1979**, *10*, 449-456.
- (35) Malin, D. H.; Guttman, H. N. *Science* **1972**, *178*, 1219-1220.
- (36) Irwin, L. N. *Perspect. Biol. Med.* **1978**, *21*, 476-491.
- (37) Chauvet, M. T.; Hurpet, J. C.; Acher, R. *Proc. Natl. Acad. Sci. U.S.A.* **1983**, *80*, 2839-2843.
- (38) "enkephalin." *Encyclopædia Britannica*. 2009. *Encyclopædia Britannica Online*. 27 Oct. 2009 <<http://www.britannica.com/EBchecked/topic/188420/enkephalin>>.
- (39) Strand, F. L. *Eur. J. Pharmacol.* **2000**, *405*, 3-12.
- (40) Wilson, D. *Nature* **1986**, *320*, 313-314.
- (41) Ebner, K.; Singewalk, N. *Amino Acids* **2006**, *31*, 251-272.
- (42) Ellis, C. *Nat. Rev. Drug Discov.* **2004**, *3*, 575, 577-626.
- (43) Dorsam, R. T.; Gutkind, J. S. *Nat. Rev. Cancer.* **2007**, *7*, 79-94.
- (44) Rink, H. *Tetrahedron Lett.* **1987**, *28*, 3787-3790.
- (45) Coste, J.; Le-Nguyen, D.; Castro, B. *Tetrahedron Lett.* **1990**, *31*, 205-208.
- (46) Koenig, W.; Geiger, R. *Chem. Ber.* **1970**, *103*, 788-798.

- (47) Lloyd-Williams, P.; Albericio, F.; Giralt, E. *Chemical Approaches to the Synthesis of Peptides and Proteins*; CRC Press: Boca Raton, 1997.
- (48) Albericio, F.; Cases, M.; Alsina, J.; Triolo, S. A.; Carpino, L. A.; Kates, S. A. *Tetrahedron Lett.* **1997**, *38*, 4853-4856.
- (49) Carpino, L. A.; Imazumi, H.; El-Faham, A.; Ferrer, F. J.; Zhang, C.; Lee, Y.; Foxman, B. M.; Henklein, P.; Hanay, C.; Mugge, C.; Wenschuh, H.; Klose, J.; Beyermann, M.; Bienert, M. *Angew. Chem., Int. Ed. Engl.* **2002**, *41*, 441-445.
- (50) Coste, J.; Frerot, E.; Jouin, P.; Castro, B. *Tetrahedron Lett.* **1991**, *32*, 1967-1970.
- (51) Li, H.; Jiang, X.; Ye, Y.-h.; Fan, C.; Romoff, T.; Goodman, M. *Org. Lett.* **1999**, *1*, 91-94.
- (52) Huang, H.; Rabenstein, D. L. *J. Pept. Res.* **1999**, *53*, 548-553.
- (53) Sole, N. A.; Barany, G. *J. Org. Chem.* **1992**, *57*, 5399-5403.
- (54) Banerjee, A.; Sergienko, E.; Vasile, S.; Gupta, V.; Vuori, K.; Wipf, P. *Org. Lett.* **2009**, *11*, 65-68.
- (55) Pangalos, M. N.; Davies, C. H. *Understanding G protein-coupled receptors and their role in the CNS*; Oxford University Press: Oxford ; New York, 2002.
- (56) Crawford, K. W.; Bowen, W. D. *Cancer Res.* **2002**, *62*, 313-322.
- (57) Ki determinations were generously provided by the National Institute of Mental Health's Psychoactive Drug Screening Program, Contract # HHSN-271-2008-00025-C (NIMH PDSP). The NIMH PDSP is Directed by Bryan L. Roth MD, PhD at the University of North Carolina at Chapel Hill and Project Officer Jamie Driscoll at NIMH, Bethesda MD, USA.
- (58) Ki determinations were generously provided by the National Institute of Mental Health's Psychoactive Drug Screening Program, Contract # HHSN-271-2008-00025-C (NIMH PDSP). The NIMH PDSP is Directed by Bryan L. Roth MD, PhD at the University of North Carolina at Chapel Hill and Project Officer Jamie Driscoll at NIMH, Bethesda MD, USA.
- (59) Ki determinations were generously provided by the National Institute of Mental Health's Psychoactive Drug Screening Program, Contract # HHSN-271-2008-00025-C (NIMH PDSP). The NIMH PDSP is Directed by Bryan L. Roth MD, PhD at the University of North Carolina at Chapel Hill and Project Officer Jamie Driscoll at NIMH, Bethesda MD, USA.

- (60) Ayala, J. E.; Chen, Y.; Banko, J. L.; Sheffler, D. J.; Williams, R.; Telk, A. N.; Watson, N. L.; Xiang, Z.; Zhang, Y.; Jones, P. J.; Lindsley, C. W.; Olive, M. F.; Conn, P. J. *Neuropsychopharmacology* **2009**, *34*, 2057-2071.
- (61) Schmid, S.; Fendt, M. *Neuropharmacology* **2006**, *50*, 154-164.
- (62) Ki determinations were generously provided by the National Institute of Mental Health's Psychoactive Drug Screening Program, Contract # HHSN-271-2008-00025-C (NIMH PDSP). The NIMH PDSP is Directed by Bryan L. Roth MD, PhD at the University of North Carolina at Chapel Hill and Project Officer Jamie Driscoll at NIMH, Bethesda MD, USA.
- (63) Y., S.; M., M.; Appl., P. I., Ed. 2005.
- (64) Fehlhaver, H. W.; Kogler, H.; Mukhopadhyay, T.; Vijayakumar, E. K. S.; Ganguli, B. N. *J. Am. Chem. Soc.* **1988**, *110*, 8242-8244.
- (65) Fehlhaver, H. W.; Kogler, H.; Mukhopadhyay, T.; Vijayakumar, E. K.; Roy, K.; Rupp, R. H.; Ganguli, B. N. *J. Antibiot.* **1988**, *41*, 1785-1794.
- (66) Wipf, P.; Kim, Y.; Fritch, P. C. *J. Org. Chem.* **1993**, *58*, 7195-7203.
- (67) McKillop, A.; McLaren, L.; Watson, R. J.; Taylor, R. J. K.; Lewis, N. *Tetrahedron Lett.* **1993**, *34*, 5519-5522.
- (68) Wipf, P.; Kim, Y. *J. Am. Chem. Soc.* **1994**, *116*, 11678-11688.
- (69) Kishi, Y.; Aratani, M.; Tanino, H.; Fukuyama, T.; Goto, T.; Inoue, S.; Sugiura, S.; Kakoi, H. *J. Chem. Soc., Chem. Commun.* **1972**, *2*, 64-65.
- (70) Kim, Y. Ph.D. Thesis, University of Pittsburgh, 1995.
- (71) Kupchan, S. M.; Fessler, D. C.; Eakin, M. A.; Giacobbe, T. J. *Science* **1970**, *168*, 376-378.
- (72) Dinkova-Kostova, A. T.; Massiah, M. A.; Bozak, R. E.; Hicks, R. J.; Talalay, P. *Proc. Natl. Acad. Sci. U.S.A.* **2001**, *98*, 3404-3409.
- (73) Kunakbaeva, Z.; Carrasco, R.; Rozas, I. *J. Mol. Struct.* **2003**, *626*, 209-216.
- (74) Caron, M.; Sharpless, K. B. *J. Org. Chem.* **2002**, *50*, 1557-1560.
- (75) Behrens, C. H.; Sharpless, K. B. *J. Org. Chem.* **2002**, *50*, 5696-5704.
- (76) Wipf, P.; Jeger, P.; Kim, Y. *Bioorg. Med. Chem. Lett.* **1998**, *8*, 351-356.

- (77) The diastereomer shown was later confirmed by x-ray analysis and is in agreement with the structure shown in Wipf, P.; Jeger, P.; Kim, Y., *Biorg. Med. Chem. Lett.* **1998**, *8*, 351-356. but not with that shown in Kim, Y. Ph.D. Thesis, University of Pittsburgh, 1995.
- (78) Hammill, J. T.; Contreras-Garcia, J.; Virshup, A. M.; Beratan, D. N.; Yang, W.; Wipf, P. *Tetrahedron* **2010**, *66*, 5852-5862.
- (79) Newman, D. J.; Cragg, G. M. *J. Nat. Prod.* **2007**, *70*, 461-477.
- (80) Tan, D. S. *Nat. Chem. Biol.* **2005**, *1*, 74-84.
- (81) Amagata, T.; Minoura, K.; Numata, A. *J. Nat. Prod.* **2006**, *69*, 1384-1388.
- (82) Amagata, T.; Tanaka, M.; Yamada, T.; Minoura, K.; Numata, A. *J. Nat. Prod.* **2008**, *71*, 340-345.
- (83) Still, W. C. *J. Am. Chem. Soc.* **1978**, *100*, 1481-1487.
- (84) Macrae, C. F.; Bruno, I. J.; Chisholm, J. A.; Edgington, P. R.; McCabe, P.; Pidcock, E.; Rodriguez-Monge, L.; Taylor, R.; van de Streek, J.; Wood, P. A. *J. Appl. Cryst.* **2008**, *41*, 466-470.
- (85) Di Bussolo, V.; Fiasella, A.; Romano, M. R.; Favero, L.; Pineschi, M.; Crotti, P. *Org. Lett.* **2007**, *9*, 4479-4482.
- (86) Porter, M. J.; Skidmore, J. *Chem. Comm.* **2000**, *14*, 1215-1225.
- (87) Diez, D.; Nunez, M.; Garcia, A.; Garrido, N. M.; Marcons, I.; Basabe, P.; Urones, J. G. *Curr. Org. Syn.* **2006**, *5*, 186-216.
- (88) Rama Rao, A. V.; Gurjar, M. K.; Sharma, P. A. *Tetrahedron Lett.* **1991**, *32*, 6613-6616.
- (89) Rama Rao, A. V.; Gurjar, M. K.; Sharma, P. A. *Tetrahedron Lett.* **1991**, *32*, 6613-6616.
- (90) McKillop, A.; Taylor, R.; Watson, R.; Lewis, N. *J. Chem. Soc.* **1992**, 1589-1591.
- (91) McKillop, A.; Taylor, R. J. K.; Watson, R. J.; Norman, L. *Synlett* **1992**, 1005-1006.
- (92) Shao, Y.; Molnar, L. F.; Jung, Y.; Kussmann, J.; Ochsenfeld, C.; Brown, S. T.; Gilbert, A. T. B.; Slipchenko, L. V.; Levchenko, S. V.; O'Neill, D. P.; DiStasio Jr., R. A.; Lochan, R. C.; Wang, T.; Beran, G. J. O.; Besley, N. A.; Herbert, J. M.; Lin, C. Y.; Van Voorhis, T.; Chien, S. H.; Sodt, A.; Steele, R. P.; Rassolov, V. A.; Maslen, P. E.; Korambath, P. P.; Adamson, R. D.; Austin, B.; Baker, J.; Byrd, E. F. C.; Dachsel, H.; Doerksen, R. J.; Dreuw, A.; Dunietz, B. D.; Dutoi, A. D.; Furlani, T. R.; Gwaltney, S. R.; Heyden, A.; Hirata, S.; Hsu, C.-P.; Kedziora, G.; Khalliulin, R. Z.; Klunzinger, P.; Lee, A. M.; Lee, M. S.; Liang, W. Z.; Lotan, I.; Nair, N.; Peters, B.; Proynov, E. I.; Pieniazek,

- P. A.; Rhee, Y. M.; Ritchie, J.; Rosta, E.; Sherrill, C. D.; Simmonett, A. C.; Subotnik, J. E.; Woodcock III, H. L.; Zhang, W.; Bell, A. T.; Chakraborty, A. K.; Chipman, D. M.; Keil, F. J.; Warshel, A.; Hehre, W. J.; Schaefer, H. F.; Kong, J.; Krylov, A. I.; Gill, P. M. W.; Head-Gordon, M. *Phys. Chem. Chem. Phys.*, **2006**, *8*, 3172.
- (93) Casadei, M. A.; Galli, C.; Mandolini, L. *J. Amer. Chem. Soc.* **1984**, *106*, 1051-1056.
- (94) Rosen, J.; Lovgren, A.; Kogej, T.; Muresan, S.; Gottfries, J.; Backlund, A. *J. Comput.-Aided Mol. Des.* **2009**, *23*, 253-259.
- (95) Lipinski, C. A.; Lombardo, F.; Dominya, B. W.; Feeney, P. *J. Adv. Drug Delivery Rev.* **1997**, *23*, 3.
- (96) Wang, Y.; Xiao, J.; Suzek, T. O.; Zhang, J.; Wang, J.; Zhou, Z.; Han, L.; Karapetyan, K.; Dracheva, S.; Shoemaker, B. A.; Bolton, E.; Gindulyte, A.; Bryant, S. H. *Nucleic Acids Res.* **2012**, *40*, D400-D412.
- (97) Bolton, E. E.; Wang, Y.; Thiessen, P. A.; Bryant, S. H.; Ralph, A. W.; David, C. S. In *Annual Reports in Computational Chemistry*; Elsevier: 2008; Vol. Volume 4, 217-241.
- (98) Seyferth, D.; Brian Andrews, S. *J. Organomet. Chem.* **1971**, *30*, 151-166.
- (99) Pelter, A.; Elgendy, S. *Tetrahedron Lett.* **1988**, *29*, 677-680.
- (100) Rasko, D. A.; Sperandio, V. *Nat. Rev. Drug Discov.* **2010**, *9*, 117-128.
- (101) Payne, D. J. *Science* **2008**, *321*, 1644-1645.
- (102) Levy, S. B.; Marshall, B. *Nat. Med.* **2004**, *10*, S122.
- (103) Lock, R. L.; Harry, E. J. *Nat. Rev. Drug Discov.* **2008**, *7*, 324-338.
- (104) Matsui, T.; Yamane, J.; Mogi, N.; Yamaguchi, H.; Takemoto, H.; Yao, M.; Tanaka, I. *Acta Crystallogr., Sect. D* **2012**, *68*, 1175-1188.
- (105) Margalit, D. N.; Romberg, L.; Mets, R. B.; Hebert, A. M.; Mitchison, T. J.; Kirschner, M. W.; RayChaudhuri, D. *Proc. Natl. Acad. Sci.* **2004**, *101*, 11821-11826.
- (106) Fabiano, R. J.; Tu, A. T. *Biochemistry* **1981**, *20*, 21-27.
- (107) Wang, J.; Galgoci, A.; Kodali, S.; Herath, K. B.; Jayasuriya, H.; Dorso, K.; Vicente, F.; González, A.; Cully, D.; Bramhill, D.; Singh, S. *J. Biol. Chem.* **2003**, *278*, 44424-44428.
- (108) Hufford, C. D.; Lasswell, W. L., Jr. *Lloydia* **1978**, *41*, 156-160.
- (109) Anam, E. M. *Ind. J. Chem., Sect. B.* **1994**, *33B*, 1009-1011.
- (110) Urgaonkar, S.; La Pierre, H. S.; Meir, I.; Lund, H.; RayChaudhuri, D.; Shaw, J. T. *Org. Lett.* **2005**, *7*, 5609-5612.

- (111) Beuria, T. K.; Santra, M. K.; Panda, D. *Biochemistry* **2005**, *44*, 16584-16593.
- (112) Stokes, N. R.; Sievers, J. r.; Barker, S.; Bennett, J. M.; Brown, D. R.; Collins, I.; Errington, V. M.; Foulger, D.; Hall, M.; Halsey, R.; Johnson, H.; Rose, V.; Thomaides, H. B.; Haydon, D. J.; Czaplewski, L. G.; Errington, J. *J. Biol. Chem.* **2005**, *280*, 39709-39715.
- (113) Haydon, D. J.; Stokes, N. R.; Ure, R.; Galbraith, G.; Bennett, J. M.; Brown, D. R.; Baker, P. J.; Barynin, V. V.; Rice, D. W.; Sedelnikova, S. E.; Heal, J. R.; Sheridan, J. M.; Aiwale, S. T.; Chauhan, P. K.; Srivastava, A.; Taneja, A.; Collins, I.; Errington, J.; Czaplewski, L. G. *Science* **2008**, *321*, 1673-1675.
- (114) White, E. L.; Suling, W. J.; Ross, L. J.; Seitz, L. E.; Reynolds, R. C. *J. Antimicrob. Chemoth.* **2002**, *50*, 111-114.
- (115) Plaza, A.; Keffer, J. L.; Bifulco, G.; Lloyd, J. R.; Bewley, C. A. *J. Am. Chem. Soc.* **2010**, *132*, 9069-9077.
- (116) Nicotra, S.; Intra, A.; Ottolina, G.; Riva, S.; Danieli, B. *Tetrahedron: Asym.* **2004**, *15*, 2927-2931.
- (117) Chen, A. Y.; Lee, A. J.; Jiang, X.-R.; Zhu, B. T. *J. Med. Chem.* **2007**, *50*, 5372-5381.
- (118) Tanabe, T.; Ogamino, T.; Shimizu, Y.; Imoto, M.; Nishiyama, S. *Bioorg. Med. Chem.* **2006**, *14*, 2753-2762.
- (119) Geib, N.; Woihte, K.; Zerbe, K.; Li, D. B.; Robinson, J. A. *Bioorg. Med. Chem. Lett.* **2008**, *18*, 3081-3084.
- (120) Woihte, K.; Geib, N.; Zerbe, K.; Li, D. B.; Heck, M.; Fournier-Rousset, S.; Meyer, O.; Vitali, F.; Matoba, N.; Abou-Hadeed, K.; Robinson, J. A. *J. Am. Chem. Soc.* **2007**, *129*, 6887-6895.
- (121) Pouyegu, L.; Deffieux, D.; Quideau, S. P. *Tetrahedron* **2010**, *66*, 2235-2261.
- (122) Eickhoff, H.; Jung, G. N.; Rieker, A. *Tetrahedron* **2001**, *57*, 353-364.
- (123) Leutbecher, H.; Conrad, J. r.; Klaiber, I.; Beifuss, U. *Synlett* **2005**, *20*, 3126-3130.
- (124) Sue, D.; Kawabata, T.; Sasamori, T.; Tokitoh, N.; Tsubaki, K. *Org. Lett.* **2009**, *12*, 256-258.
- (125) Cotellet, P.; Vezin, H. *Tetrahedron Lett.* **2003**, *44*, 3289-3292.
- (126) Kozłowski, M. C.; Dugan, E. C.; DiVirgilio, E. S.; Maksimenka, K.; Bringmann, G. *Adv. Synth. Cat.* **2007**, *349*, 583-594.

- (127) Li, S.; Qu, H.; Zhou, L.; Kanno, K.-i.; Guo, Q.; Shen, B.; Takahashi, T. *Org. Lett.* **2009**, *11*, 3318-3321.
- (128) Davies, K. A.; Abel, R. C.; Wulff, J. E. *J. Org. Chem.* **2009**, *74*, 3997-4000.
- (129) Stone, M. T.; Anderson, H. L. *J. Org. Chem.* **2007**, *72*, 9776-9778.
- (130) Gopalsamuthiram, V.; Wulff, W. D. *J. Am. Chem. Soc.* **2004**, *126*, 13936-13937.
- (131) Trost, B. M.; Pinkerton, A. B. *J. Am. Chem. Soc.* **1999**, *121*, 1988-1989.
- (132) Satoh, T.; Itoh, N.; Onda, K.-i.; Kitoh, Y.; Yamakawa, K. *Tetrahedron Lett.* **1992**, *33*, 1483-1484.
- (133) Trost, B. M.; Pinkerton, A. B. *J. Am. Chem. Soc.* **2002**, *124*, 7376-7389.
- (134) Uemura, S.; Okazaki, H.; Onoe, A.; Okano, M. *J. Chem. Soc. Perkin Trans. I* **1977**, 676-680.
- (135) Bellina, F.; Colzi, F.; Mannina, L.; Rossi, R.; Viel, S. *J. Org. Chem.* **2003**, *68*, 10175-10177.
- (136) Al-Hassan, M. I. *J. Organomet. Chem.* **1989**, *372*, 183-186.
- (137) Barluenga, J.; Rodriguez, M. A.; Campos, P. J. *J. Org. Chem.* **1990**, *55*, 3104-3106.
- (138) Joubert, N.; Amblard, F.; Rapp, K. L.; Schinazi, R. F.; Agrofoglio, L. A. *Tetrahedron* **2008**, *64*, 4444-4452.
- (139) Ross, A. J.; Lang, H. L.; Jackson, R. F. W. *J. Org. Chem.* **2009**, *75*, 245-248.
- (140) Barder, T. E.; Walker, S. D.; Martinelli, J. R.; Buchwald, S. L. *J. Am. Chem. Soc.* **2005**, *127*, 4685-4696.
- (141) Goundry, W. R. F.; Baldwin, J. E.; Lee, V. *Tetrahedron* **2003**, *59*, 1719-1729.
- (142) Jessop, P. G. *Green Chem.* **2011**, *13*, 1391-1398.
- (143) Szczepankiewicz, B. G.; Liu, G.; Hajduk, P. J.; Abad-Zapatero, C.; Pei, Z.; Xin, Z.; Lubben, T. H.; Trevillyan, J. M.; Stashko, M. A.; Ballaron, S. J.; Liang, H.; Huang, F.; Hutchins, C. W.; Fesik, S. W.; Jirousek, M. R. *J. Amer. Chem. Soc.* **2003**, *125*, 4087-4096.
- (144) Oswald, C. L.; Carrillo-Marquez, T. S.; Caggiano, L.; Jackson, R. F. W. *Tetrahedron* **2008**, *64*, 681-687.
- (145) Keffer, J. L.; Hammill, J. T.; Lloyd, J. R.; Plaza, A.; Wipf, P.; Bewley, C. A. *Mar. Drugs* **2012**, *10*, 1103-1125.

- (146) Iwakuma, T.; Yonemitsu, O.; Kanamaru, N.; Kimura, K.; Witkop, B. *Angew. Chem., Int. Ed. Engl.* **1973**, *12*, 72-73.
- (147) Sahin, H.; Nieger, M.; Bräse, S. *Eur. J. Org. Chem.* **2009**, *2009*, 5576-5586.
- (148) Kametani, T.; Fukumoto, K. *Synthesis* **1972**, *12*, 657-674.
- (149) Evano, G.; Blanchard, N.; Toumi, M. *Chem. Rev.* **2008**, *108*, 3054-3131.
- (150) Xing, X.; Padmanaban, D.; Yeh, L.-A.; Cuny, G. D. *Tetrahedron* **2002**, *58*, 7903-7910.
- (151) Maumy, M.; Capdevielle, P. *J. Mol. Cat. A: Chem.* **1996**, *113*, 159-166.
- (152) Jung, M. E.; Jachiet, D.; Rohloff, J. C. *Tetrahedron Lett.* **1989**, *30*, 4211-4214.
- (153) Huang, W.-J.; Singh, O. V.; Chen, C.-H.; Lee, S.-S. *Helv. Chim. Acta* **2004**, *87*, 167-174.
- (154) Pelter, A.; Elgendy, S. M. A. *J. Chem. Soc. Perkin Trans. I* **1993**, 1891-1896.
- (155) Ncanana, S.; Baratto, L.; Roncaglia, L.; Riva, S.; Burton, S. G. *Adv. Synth. Cat.* **2007**, *349*, 1507-1513.
- (156) Kong, Z.-L.; Tzeng, S.-C.; Liu, Y.-C. *Bioorg. Med. Chem. Lett.* **2005**, *15*, 163-166.
- (157) Zerbe, K.; Woithe, K.; Li, D. B.; Vitali, F.; Bigler, L.; Robinson, J. A. *Angew. Chem., Int. Ed. Engl.* **2004**, *43*, 6709-6713.
- (158) Montero, A.; Alonso, M.; Benito, E.; Chana, A.; Mann, E.; Navas, J. M.; Herradan, B. *Bioorg. Med. Chem. Lett.* **2004**, *14*, 2753-2757.
- (159) Uyama, H.; Kobayashi, S. *J. Mol. Cat. B: Enzymatic* **2002**, *19-20*, 117-127.
- (160) Pezzella, A.; Lista, L.; Napolitano, A.; d'Ischia, M. *J. Org. Chem.* **2004**, *69*, 5652-5659.
- (161) Monnier, F.; Taillefer, M. *Angew. Chem., Int. Ed. Engl.* **2009**, *48*, 6954-6971.
- (162) Sawyer, S. J. *Tetrahedron* **2000**, *56*, 5045-5065.
- (163) Kunz, K.; Scholz, U.; Ganzer, D. *Synlett* **2003**, *14*, 2428-2439.
- (164) Frlan, R.; Kikelj, D. *Synthesis* **2006**, *14*, 2271-2285.
- (165) Ma, D.; Cai, Q. *Org. Lett.* **2003**, *5*, 3799-3802.
- (166) Wolter, M.; Nordmann, G.; Job, G. E.; Buchwald, S. L. *Org. Lett.* **2002**, *4*, 973-976.
- (167) Marcoux, J.-F. O.; Doye, S.; Buchwald, S. L. *J. Am. Chem. Soc.* **1997**, *119*, 10539-10540.
- (168) Olivera, R.; SanMartin, R.; Churruca, F.; Dominguez, E. *J. Org. Chem.* **2002**, *67*, 7215-7225.
- (169) Buck, E.; Song, Z. J.; Tschaen, D.; Dormer, P. G.; Volante, R. P.; Reider, P. J. *Org. Lett.* **2002**, *4*, 1623-1626.
- (170) Maiti, D.; Buchwald, S. L. *J. Org. Chem.* **2010**, *75*, 1791-1794.

- (171) Trost, B. M.; Shen, H. C.; Dong, L.; Surivet, J.-P.; Sylvain, C. *J. Am. Chem. Soc.* **2004**, *126*, 11966-11983.
- (172) Jung, M. E.; Lazarova, T. I. *J. Org. Chem.* **1997**, *62*, 1553-1555.
- (173) Mizufune, H.; Irie, H.; Katsube, S.; Okada, T.; Mizuno, Y.; Arita, M. *Tetrahedron* **2001**, *57*, 7501-7506.
- (174) Cristau, H.-J.; Cellier, P. P.; Hamada, S.; Spindler, J.-F.; Taillefer, M. *Org. Lett.* **2004**, *6*, 913-916.
- (175) Zhang, S.; Zhang, D.; Liebeskind, L. S. *J. Org. Chem.* **1997**, *62*, 2312-2313.
- (176) Thasana, N.; Worayuthakarn, R.; Kradanrat, P.; Hohn, E.; Young, L.; Ruchirawat, S. *J. Org. Chem.* **2007**, *72*, 9379-9382.
- (177) Sperotto, E.; van Klink, G. P. M.; van Koten, G.; de Vries, J. G. *Dalton Trans.* **2010**, *39*, 10338-10351.
- (178) Jalalian, N.; Ishikawa, E. E.; Silva, L. F.; Olofsson, B. *Org. Lett.* **2011**, *13*, 1552-1555.
- (179) Bigot, A.; Williamson, A. E.; Gaunt, M. J. *J. Am. Chem. Soc.* **2011**, *133*, 13778-13781.
- (180) Weist, S.; Kittel, C.; Bischoff, D.; Bister, B.; Pfeifer, V.; Nicholson, G. J.; Wohlleben, W.; Sussmuth, R. D. *J. Am. Chem. Soc.* **2004**, *126*, 5942-5943.
- (181) Snyder, S. A.; Zografos, A. L.; Lin, Y. *Angew. Chem., Int. Ed. Engl.* **2007**, *46*, 8186-8191.
- (182) Bloomer, J. L.; Stagliano, K. W.; Gazzillo, J. A. *J. Org. Chem.* **1993**, *58*, 7906-7912.
- (183) Trepanier, V. E.; Fillion, E. *Organometallics* **2007**, *26*, 30-32.
- (184) Irgartinger, H.; Skipinski, M. *Eur. J. Org. Chem.* **1999**, *1999*, 917-922.
- (185) Bloomer, J. L.; Gazzillo, J. A. *Tetrahedron Lett.* **1989**, *30*, 1201-1204.
- (186) Mandal, P. K.; McMurray, J. S. *J. Org. Chem.* **2007**, *72*, 6599-6601.
- (187) Li, P.; Li, J.; Arikan, F.; Ahlbrecht, W.; Dieckmann, M.; Menche, D. *J. Org. Chem.* **2010**, *75*, 2429-2444.
- (188) Devine, S. K. J.; Van Vranken, D. L. *Org. Lett.* **2007**, *9*, 2047-2049.
- (189) Green, J.; McHale, D.; Marcikiewicz, S.; Mamalis, P.; Watt, P. R. *J. Chem. Soc.* **1959**, 3362-3373.
- (190) Srebnik, M.; Mechoulam, R.; Yona, I. *J. Chem. Soc. Perkin Trans I* **1987**, *7*, 1423-1427.
- (191) Altman, R. A.; Nilsson, B. L.; Overman, L. E.; Read de Alaniz, J.; Rohde, J. M.; Taupin, V. *J. Org. Chem.* **2010**, *75*, 7519-7534.

- (192) Steinbess, S. *J. Anal. Appl. Pyrolysis* **2005**, *75*, 19-26.
- (193) Wang, P.; Zhang, Z.; Yu, B. *J. Org. Chem.* **2005**, *70*, 8884-8889.
- (194) Godfrey, I. M.; Sargent, M. V.; Elix, J. A. *J. Chem. Soc. Perkin Trans I* **1974**, 1353-1354.
- (195) Mo, F.; Yan, J. M.; Qiu, D.; Li, F.; Zhang, Y.; Wang, J. *Angew. Chem., Int. Ed. Engl.* **2010**, *49*, 2028-2032.
- (196) Montecuccio, C.; Molgo, J. *Curr. Opin. Pharmacol.* **2005**, *5*, 274-279.
- (197) Erbguth, F. *J. Mov. Disord.* **2004**, *19 Suppl 8*, S2-6.
- (198) Arnon, S. S.; Schechter, R.; Inglesby, T. V.; Henderson, D. A.; Bartlett, J. G.; Ascher, M. S.; Eitzen, E.; Fine, A. D.; Hauer, J.; Layton, M.; Lillibridge, S.; Osterholm, M. T.; O'Toole, T.; Parker, G.; Perl, T. M.; Russell, P. K.; Swerdlow, D. L.; Tonat, K. *JAMA* **2001**, *285*, 1059-1070.
- (199) Lacy, D. B.; Tepp, W.; Cohen, A. C.; DasGupta, B. R.; Stevens, R. C. *Nat. Struct. Biol.* **1998**, *5*, 898-902.
- (200) Willis, B.; Eubanks, L. M.; Dickerson, T. J.; Janda, K. D. *Angew. Chem., Int. Ed.* **2008**, *47*, 8360-8379.
- (201) Kumaran, D.; Rawat, R.; Ludivico, M. L.; Ahmed, S. A.; Swaminathan, S. *J. Biol. Chem.* **2008**, *283*, 1883-1891.
- (202) Eubanks, L. M.; Dickerson, T. J.; Janda, K. D. *Chem. Soc. Rev.* **2007**, *36*, 458-470.
- (203) Burnett, J. C.; Schmidt, J. J.; Stafford, R. G.; Panchal, R. G.; Nguyen, T. L.; Hermone, A. R.; Vennerstrom, J. L.; Mcgrath, C. F.; Lane, D. J.; Sausville, E. A.; Zaharevitz, D. W.; Gussio, R.; Bavari, S. *Biochem. Biophys. Res. Commun.* **2003**, *310*, 84.
- (204) Zuniga, J. E.; Schmidt, J. J.; Fenn, T.; Burnett, J. C.; Arac, D.; Gussio, R.; Stafford, R. G.; Badie, S. S.; Bavari, S.; Brunger, A. T. *Structure* **2008**, *16*, 1588-1597.
- (205) Wang, C.; Widom, J.; Petronijevic, F.; Burnett, J. C.; Nuss, J. E.; Bavari, B.; Gussio, R.; Wipf, P. *Heterocycles* **2009**, *79*, 487-520.
- (206) Schmidt, J. J.; Stafford, R. G.; Bostian, K. A. *FEBS Lett.* **1998**, *435*, 61-64.
- (207) Karpen, M. E.; de Haseth, P. L.; Neet, K. E. *Protein Sci.* **1992**, *1*, 1333-1342.
- (208) Demizu, Y.; Tanaka, M.; Nagano, M.; Kurihara, M.; Doi, M.; Maruyama, T.; Suemune, H. *Chem. Pharm. Bull.* **2007**, *55*, 840-842.
- (209) Narita, M.; Ishikawa, K.; Sugasawa, H.; Doi, M. *Chem. Soc. Jap.* **1985**, *58*, 1731-1737.

- (210) Zuniga, J. E.; Hammill, J. T.; Drory, O.; Nuss, J. E.; Burnett, J. C.; Gussio, R.; Wipf, P.; Bavari, S.; Brunger, A. T. *PLoS One* **2010**, *5*, e11378.
- (211) Burnett, J. C.; Schmidt, J. J.; Stafford, R. G.; Panchal, R. G.; Nguyen, T. L.; Hermone, A. R.; Vennerstrom, J. L.; McGrath, C. F.; Lane, D. J.; Sausville, E. A.; Zaharevitz, D. W.; Gussio, R.; Bavari, S. *Biochem. Biophys. Res. Commun.* **2003**, *310*, 84-93.
- (212) Burnett, J. C.; Schmidt, J. J.; McGrath, C. F.; Nguyen, T. L.; Hermone, A. R.; Panchal, R. G.; Vennerstrom, J. L.; Kodukula, K.; Zaharevitz, D. W.; Gussio, R.; Bavari, S. *Bioorg. Med. Chem.* **2005**, *13*, 333-341.
- (213) Burnett, J. C.; Ruthel, G.; Stegmann, C. M.; Panchal, R. G.; Nguyen, T. L.; Hermone, A. R.; Stafford, R. G.; Lane, D. J.; Kenny, T. A.; McGrath, C. F.; Wipf, P.; Stahl, A. M.; Schmidt, J. J.; Gussio, R.; Brunger, A. T.; Bavari, S. *J. Biol. Chem.* **2007**, *282*, 5004-5014.
- (214) The (IPr)CuCl was prepared by Dr. Nolan Griggs and shown to facilitate both the stille and sonogashira couplings in unpublished work.